

# HUMAN MOTION ESTIMATION FOR HUMAN-ROBOT COOPERATION

**Doctoral Dissertation by  
Gizem Ateş Venås**

Thesis submitted for  
the degree of Philosophiae Doctor (PhD)  
in  
Computer Science:  
Software Engineering, Sensor Networks and Engineering Computing



Department of Computer Science,  
Electrical Engineering and Mathematical Sciences  
Faculty of Engineering and Science  
Western Norway University of Applied Sciences

September 7, 2023

©Gizem Ateş Venås, 2023

The material in this report is covered by copyright law.

Series of dissertation submitted to  
the Faculty of Engineering and Science,  
Western Norway University of Applied Sciences.

ISBN (Printed Edition): 978-82-8461-036-8

ISBN (Digital Edition): 978-82-8461-037-5

Author: Gizem Ateş Venås

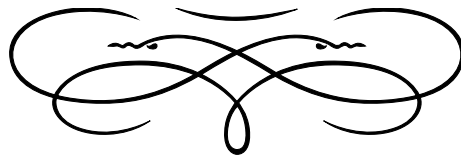
Title: Human Motion Estimation for Human-Robot Cooperation

Printed production:

Molvik Grafisk / Western Norway University of Applied Sciences

Bergen, Norway, 2023

*This thesis is dedicated to*  
***my beloved Sondre***  
*for his endless support and genuine love.*





# PREFACE

---

The author of this thesis has been employed as a PhD research fellow in the software engineering research group at the Department of Computer Science, Electrical Engineering and Mathematical Science at Western Norway University of Applied Sciences. The author has been enrolled in the PhD program in Computer Science: Software Engineering, Sensor Networks and Engineering Computing, with a specialization in robotics.

The research presented in this thesis has been developed under the *Teknoloft* project which is a business-oriented research project which is a collaboration of Western Norway University of Applied Sciences and Vestlandsforskning. This research has been funded by the Research Council of Norway through grant number 280771.

This thesis is organized into two parts. Part I presents the fundamentals that motivate the need of this thesis and discusses the state of the art and related work. It also introduces the foundational aspects and elements of this work and serves as an introduction to what is detailed in the collection of articles. Part II consists of a collection of published and peer-reviewed research articles and submitted journals.

- Paper A** Gizem Ateş & Erik Kyrkjebø. Human-Robot Cooperative Lifting using IMUs and Human Gestures. Published in Proceedings of the of *Annual Conference Towards Autonomous Robotic Systems, Part of the Lecture Notes in Computer Science book series (LNAI, volume 13054, pages 88-99)* Springer, September 8-10, 2021 DOI: [10.1007/978-3-030-89177-0\\_9](https://doi.org/10.1007/978-3-030-89177-0_9)
- Paper B** Gizem Ateş, Martin Fodstad Stølen & Erik Kyrkjebø. Force and Gesture-based Motion Control of Human-Robot Cooperative Lifting Using IMUs. Published in *HRI'22 Proceedings of the 2022 ACM/IEEE International Conference on Human-Robot Interaction (Pages 688–692)*. IEEE, March 7-10, 2022 DOI: [10.5555/3523760.3523856](https://doi.org/10.5555/3523760.3523856)
- Paper C** Gizem Ateş. Work in Progress: Learning Fundamental Robotics Concepts Through Games at Bachelor Level. Published in *International Conference on 2022 IEEE Global Engineering Education Conference (EDUCON)* IEEE, March 28-31, 2022 DOI: [10.1109/EDUCON52537.2022.9766499](https://doi.org/10.1109/EDUCON52537.2022.9766499)
- Paper D** Gizem Ateş, Martin Fodstad Stølen & Erik Kyrkjebø. A Framework for Human Motion Estimation using IMUs in Human-Robot Interaction. Published in *Proceedings of the 23rd IEEE International Conference on Industrial Technology* IEEE, August 22-25, 2022 DOI: [10.1109/ICIT48603.2022.10002746](https://doi.org/10.1109/ICIT48603.2022.10002746)
- Paper E** Gizem Ateş & Erik Kyrkjebø. Design of a Gamified Training System for Human-Robot Cooperation. Published in *Proceedings of the 2nd International Conference on Electrical, Computer, Communications and Mechatronics Engineering (ICECCME)* IEEE, November 16-18, 2022 DOI: [10.1109/ICECCME55909.2022.9988661](https://doi.org/10.1109/ICECCME55909.2022.9988661)
- Paper F** Gizem Ateş Venås, Martin Fodstad Stølen & Erik Kyrkjebø. Exploring Human-Robot Cooperation with Gamified User Training: A User Study on Cooperative Lifting. Submitted to *Frontiers in Robotics and AI* Frontiers. (Submitted)



# ACKNOWLEDGMENTS

---

It was probably the most unforeseen what-is-going-to-happen period of my life, yet now it is approaching the end with lots of gains, happiness, hopes, and accomplishments. This period officially started in September 2018 when I moved to a Norwegian town (Førde), where around 10,000 inhabitants live, from a Turkish city (İzmir), which is as big as almost the whole of Norway.

These 4 years of *philosophiae doctor* life have been a journey not only to accomplish a milestone in my academic life but also in finding myself. One can tell hundreds of stories, challenges, joys, and occasions where Murphy's law has almost been scientifically proven within a PhD period. Surely, encountering challenges is the nature of such a unique exploration but, lucky for me, it has been an enlightening, developing, evolving and amazing overall experience. There are some precious people who contributed to my journey and I would like to present my appreciation.

I would like to start with my main supervisor Erik Kyrkjebø. The best chance for a PhD student is to have a supervisor who supports, understands and guides accordingly. There were so many times that he was kinder to me than I was to myself, especially while the deadlines were approaching. The gratitude, respect and appreciation I feel have motivated me enormously to accomplish this big step in my life since the first interview we had for this PhD position on Tuesday the 26<sup>th</sup> of June 2018. Thank you so much for accepting me in the first place, giving me such a chance to explore life in Norway, and for all your support and guidance during the whole period.

My appreciation also extends to my co-supervisors Martin Fodstad Stølen and Marcello Bonfé. Their time, guidance and suggestions are significantly valuable. The comfort of them always being ready and eager to help in any challenge I have faced is inestimable.

I also would like to thank my colleagues and my friends Daniel Schäle, Raquel Motzfeldt Tirach, Laurenz Elstner and Sivert Hagelin Benjaminsen. This period would have been so unpleasant without them. Every single one of them is always genuine, helpful and supportive. Having Daniel as my fellow seatmate on this journey, Raquel with her smart and practical solutions, Laurenz's entertaining and insightful chats, and Sivert's constant positivist and humorous traits are priceless to me. Moreover, I would like to present my genuine gratitude to Eli Nummedal who is my administrative manager but feels more of a supportive-protective family member that everyone needs. She has been always there whenever I needed her, she found a way to fix it whenever there was a bureaucratic difficulty.

Speaking of family, my biggest thank-you is to my sister İzel Ateş Yıldız, my mother Ayşen Ateş and my father Bahattin Ateş. They have been the key factor in my success in many things in my life as well as in managing to be here. They are always beside me despite the thousands of kilometres of physical distance. I can feel their support and love no matter how far we get and they mean worlds to me. I would also like to express my appreciation and gratitude to my *svigermor* Inghild Marie Venås and *svigerfar* Jonny Venås from the bottom of my heart. Their kindness and love are beyond words. They embraced me the first day we met and never let me feel the physical distance between

me and my biological family during this process. I am so lucky to have them in my life.

And my precious love, Sondre... Words are not enough to describe how much he means to me and how grateful I am for everything he has done. It feels like whatever I say would diminish his contribution to realising this thesis. He stayed with me in the lab for several days, nights, and weekends until the sun rose the next day. He is my sole *pilot user* in every article produced within this thesis. He has been the cheerleader whenever I approached giving up on the day. He embraced me with kindness and lovely words whenever I was frustrated with my non-working code. As soon as the code decided to work again, he celebrated with me with a cup of coffee after sharing a Grandiosa. All the humorist details aside, thank you so much for everything. This thesis would not be possible without your endless love and support.

Finally, I would like to express my heartfelt gratitude to everyone who helped me in any way, big or small, throughout this process.

Gizem Ateş  
Førde, February 2023



# ABSTRACT

---

Human Robot Cooperation (HRC) refers to the cooperation between humans and robots to achieve a common goal or perform a task together. In HRC, the robot is designed to work alongside a human operator, providing assistance and support as needed. This collaboration can take many forms, ranging from a robot that provides physical assistance to a person with a disability, to a robot that helps workers in a factory assemble products more efficiently. HRC has many potential applications in areas such as manufacturing, healthcare, logistics, and service industries. For example, in manufacturing, robots can work alongside humans to perform repetitive or dangerous tasks, while in healthcare, robots can assist with patient care, rehabilitation and surgery.

HRC can involve the use of advanced robotics technologies such as artificial intelligence, machine learning, natural language processing, and human motion processing to enable robots to understand human intentions and communicate with people in a more natural way. Through this collaboration, humans can leverage the strength, speed, and precision of robots to perform tasks that are difficult, dangerous, or impossible for humans to do alone.

The main focus of this study is to develop a reliable Human Motion Estimation (HME) method to be used in industrial HRC applications. HME is the process of tracking and analysing human body movements with different sensory devices to determine the pose, posture, motion and/or gesture of the human. The estimated feature set is used as human input to create an action on the robot side. This thesis investigates how to choose the best motion capture system for industrial applications, how to obtain sufficiently accurate human motions and gestures, how to generate intuitive human input, and how to translate that input into a specific robot output.

HRC is a widely researched topic in robotics, including dynamics, control, motion planning, robot learning, teleoperation and machine vision among other branches. All of these branches aim to optimize the advanced interactions between robots and humans. Today, examples of HRC in the industry are limited to turn-based and low-level applications, such as simple pick-and-place tasks and interacting with buttons to start/stop a process. The integration of more complex applications has not been successful enough. An analysis of the literature revealed two key points causing this problem. The first reason is related to the accuracy, reliability, applicability, and convenience of the HME for industrial applications. There are some highly accurate HME methods presented in the literature, which mainly use visual-based motion tracking devices. However, they often fail due to occlusion, loss of line-of-sight, intolerance to lighting changes, and lack of mobility, as well as they often come with a high financial and computational cost. The second reason for the gap between HRC research and implementation in industrial applications is related to user education and the neglect of training system development. Despite the substantial amount of research in the literature, only a few studies address user training, and no studies provide a methodological approach.

Therefore, the primary motion capture system for this study is Inertial Measurement Unit (IMU) which does not suffer the aforementioned issues. The biomechanical human

body is constructed based on real-time IMU measurements and a respective human input is generated. The usability of such an estimation is tested in a cooperative lifting scenario which is a fundamental task in many HRC applications such as manufacturing, assembly, medical rehabilitation, etc. Additionally, this study investigates effective user training methods and proposes a gamified approach for HRC training.

The qualitative and quantitative results in this study show that HME based HRC is promising. IMUs are portable, affordable and reliable tools for this purpose, which makes them convenient for industry. The applicability of the proposed gamified training methodology is validated with multi-user experiments. According to the user test which is carried out at Western Norway University of Applied Sciences Campus Førde with 32 healthy adults within the age range of 20-54 years, all users show a satisfactory progression. They achieved successful cooperation with the robot after a relatively short training process regardless of age, gender, job category, gaming background and familiarity with robots, etc. While some user backgrounds affect the learning criteria in terms of how quickly, consistently and optimally the user reached a sufficient learned state, no background factor was found to be significantly advantageous or disadvantageous on overall learning achievement. In conclusion, the developed system is highly promising to be implemented in industrial applications.

# SAMMENDRAG

---

Human Robot Cooperation (HRC) er til samarbeid mellom menneske og robot for å oppnå eit felles mål eller å utføre ei felles oppgåve. I HRC er roboten utforma for å arbeide saman med ein menneskeleg operatør, og gje assistanse og støtte etter behov. Dette samarbeidet kan ta mange former. Alt frå ein robot som gjer fysisk hjelp til ein person med ei funksjonshemming, eller ein robot som bistår arbeidarar på ein fabrikk med å montere produkt meir effektivt. HRC har mange potensielle bruksområde innanfor område som produksjon, helse, logistikk og serviceindustri. Til dømes kan robotar i produksjon arbeide saman med mennesker for å utføre repetitivt eller farleg arbeid, medan dei i helsevesenet kan assistere med pasientpleie, rehabilitering og kirurgi.

HRC kan involvere bruk av avansert robotteknologi, som kunstig intelligens, maskinlæring, naturleg språkprosessering og bevegelsesanalyse, for å gjere det mogleg for robotar å forstå menneskeleg intensjon og kommunisere med mennesker på ein meir naturleg måte. Gjennom dette samarbeidet kan mennesker utnytte styrken, farta og presisjonen til robotar for å utføre oppgåver som er vanskelege, farlege eller umogleg for mennesker å gjere åleine.

Hovudfokuset til denne studien er å utvikle ein påliteleg Human Motion Estimation (HME)-metode som kan brukast i industrielle HRC-applikasjonar. HME er prosessen med å måle og analysere menneskelege kroppsrørsler med ulike sensorar for å bestemme posisjon, haldning, rørsle og/eller gester frå mennesket. Den estimerte rørsla blir brukt som menneskeleg input for å skape ei handling frå roboten si side. Oppgåva undersøker korleis ein kan velje det beste rørslerestimeringsystemet for industrielle applikasjonar, korleis ein kan få målt tilstrekkeleg nøyaktige menneskerørsler og gester, korleis ein kan generere intuitiv menneskeleg input, og korleis ein kan oversette denne inputen til ei spesifikk robotrørsle.

HRC er eit hyppig studert tema innan robotikk. Mellom anna dynamikk, kontroll, rørsleplanlegging, robotlæring, teleoperasjon og maskinsyn er vanlege greiner innanfor HRC. Alle desse greinene har som mål å optimalisere dei avanserte interaksjonane mellom robot og menneske. I dag er døma på HRC i industrien avgrensa til tur-baserte og låg-nivå applikasjonar, som enkle plukk-og-plasser oppgåver og interaksjon med knappar for å starte/stoppe prosessar. Integreringa av meir komplekse applikasjonar har ikkje vore tilstrekkeleg vellykka. Ein analyse av litteraturen avslørte to nøkkelpunkt som moglege årsaker til dette problemet. Den første årsaka er knytt til nøyaktigheita, pålitsgraden, bruksverdien og brukarvenlegheita til HME for industrielle applikasjonar. Det finst nokre svært nøyaktige HME-metodar presentert i litteraturen, som hovudsakleg brukar visuelt baserte rørslesporingsutstyr. Desse mislykkast ofte grunna okklusjon, tap av synslinje, intoleranse for lysendringar og manglande mobilitet, samt at dei ofte kjem med ein høg kostnad eller er sterkt begrensa av behov for tekniske/digitale resursar. Den andre årsaken til gapet mellom HRC-forsking og implementering i industrielle applikasjonar er knytt til brukaropplæring og neglisjering av å utvikle eit opplæringsystem. Til tross for den store mengda forskning i litteraturen, adresserer berre få studiar brukaropplæring, og ingen studiar

presenterer ei metodisk tilnærming.

Difor er Inertial Measurement Unit (IMU) hovudrørslesporingsystemet valgt for denne studien. Dette vert ikkje påverka av dei førnemnde problemstillingane. Den biomekaniske menneskekroppen blir konstruert basert på sanntids IMU-målingar og gjev eit representativt menneskeinput. Bruksevna til ein slik estimasjon blir testa i eit samarbeidsløftescenario som er ei grunnleggjande oppgåve i mange HRC-applikasjonar som produksjon, samansetjing, medisinsk rehabilitering osv. I tillegg undersøker denne studien effektive brukaropplæringsmetodar og foreslår ein spelifisert metode for HRC-opplæring.

Kvalitative og kvantitative resultat i denne studien viser at HME-basert HRC er lovande. IMU-ar er portable, kostnadseffektive og pålitelege verktøy for dette føremålet. Dette gjer dei godt eigna for industrien. Nytteverdien til den foreslåtte spelifiserte opplæringsmetoden er validert gjennom eit fleirbrukareksperiment med 32 friske vaksne i aldersgruppa 20-54 år, med ulike yrker. I følgje brukartesten som utført på Høgskulen på Vestlandet Campus Førde viste alle brukarane ein tilfredsstillande framgang og oppnådde vellykka samarbeid med roboten etter ein relativt kort opplæringsprosess, uavhengig av alder, kjønn, yrkeskategori, spelerfaring og kjennskap til robotar, osv. Medan nokre brukarbakgrunnar påverkar læringskriteria med tanke på kor raskt, konsistent og optimalt brukaren når ein tilstrekkeleg lært tilstand, vart det ikkje funne noko bakgrunnsfaktor som var eit vesentleg føremon eller ei ulempe for total læringssuksess. Konklusjonen er at det utvikla systemet er svært lovande for å bli implementert i industrielle applikasjonar.

# Contents

<b>Preface</b>	<b>i</b>
<b>Acknowledgments</b>	<b>iii</b>
<b>Abstract</b>	<b>v</b>
<b>Sammendrag</b>	<b>vii</b>
<b>I FUNDAMENTALS</b>	<b>1</b>
<b>1 Introduction</b>	<b>3</b>
1.1 Human-Robot Interaction . . . . .	3
1.2 Collaborative Robots . . . . .	4
1.3 Cooperative Lifting . . . . .	7
1.4 Human Motion Estimation . . . . .	9
1.5 Research Area, Motivation and Challenges . . . . .	10
1.5.1 On Literature . . . . .	10
1.5.2 On Inertial Measurement Units . . . . .	11
1.5.3 On Human Modelling . . . . .	12
1.5.4 On User Training . . . . .	14
1.5.5 Research Questions . . . . .	16
1.6 About Teknoløft . . . . .	17
1.7 Summary of Papers . . . . .	18
1.8 Contributions . . . . .	20
1.9 Dissertation Outline . . . . .	21
<b>2 State of the Art</b>	<b>23</b>
2.1 Narrative Approach on the HME Methods and MoCap Technologies . . . . .	24
2.1.1 Understanding Human Motions . . . . .	24
2.1.2 Applications of HME . . . . .	27
2.1.3 Motion Capture Systems . . . . .	32
2.1.4 Different Methods in HME using IMU . . . . .	42
2.2 Systematic Approach on the IMU Usage and User Training . . . . .	45
2.2.1 Status of IMUs in HRI . . . . .	47
2.2.2 Status of User Training in HRI . . . . .	48
<b>3 Background</b>	<b>51</b>

3.1	Fundamentals of Kinematics . . . . .	51
3.1.1	Parametrizing Rotation . . . . .	52
3.1.2	Rotation Vector (Axis-Angle) . . . . .	57
3.1.3	Arm Kinematics . . . . .	66
3.1.4	Quaternions and ROS TF package . . . . .	68
3.2	Fundamentals of Probability Theory . . . . .	70
3.2.1	Fundamental Definitions . . . . .	71
3.2.2	Bayes Filters . . . . .	76
3.2.3	State Estimation . . . . .	82
3.3	IMU Measurement Model . . . . .	84
3.3.1	Orientation-based HME with IMUs . . . . .	86
3.3.2	Position-based HME with IMUs . . . . .	90
3.4	Biomechanical Modelling of Human Body . . . . .	92
3.4.1	Human Arm Kinematic Calculation . . . . .	94
3.4.2	Types of Human Body Movements . . . . .	94
3.5	Statistics for User Experiments . . . . .	97
3.5.1	Selection of Statistical Test . . . . .	99
3.5.2	T-test Implementation . . . . .	100
3.5.3	Confidence Interval and Significance Level . . . . .	101
3.5.4	Effect Size . . . . .	102
<b>4</b>	<b>Methods</b>	<b>103</b>
4.1	IMU Calibration . . . . .	104
4.1.1	Digital Filters . . . . .	106
4.1.2	Noise Elimination . . . . .	108
4.1.3	Bias Elimination . . . . .	109
4.2	Sensor-to-Body Calibration . . . . .	110
4.3	Human-Robot Motion Mapping . . . . .	112
4.3.1	Mapping Methods . . . . .	112
4.3.2	Proposed HRC States and Roles in Cooperative Lifting . . . . .	116
4.4	Designing Human-Robot Experiments . . . . .	119
4.4.1	Design Methods . . . . .	121
4.4.2	Risk Assessment and Consent . . . . .	122
<b>5</b>	<b>Discussion</b>	<b>125</b>
5.0.1	HME in HRC Applications . . . . .	125
5.0.2	The Use of IMUs in HME . . . . .	126
5.0.3	Serious Games and Gamification in HRC . . . . .	127
5.0.4	Human-Robot Experiments . . . . .	128
<b>6</b>	<b>Conclusion</b>	<b>133</b>
	<b>Bibliography</b>	<b>137</b>

<b>II ARTICLES</b>	<b>175</b>
Paper A: Human-Robot Cooperative Lifting using IMUs and Human Gestures	177
Paper B: Force and Gesture-based Motion Control of Human-Robot Cooperative Lifting Using IMUs	189
Paper C: Work in Progress: Learning Fundamental Robotics Concepts Through Games at Bachelor Level	197
Paper D: A Framework for Human Motion Estimation using IMUs in Human-Robot Interaction	203
Paper E: Design of a Gamified Training System for Human-Robot Cooperation	215
Paper F: Exploring Human-Robot Cooperation with Gamified User Training: A User Study on Cooperative Lifting	225
<b>APPENDIX</b>	<b>255</b>
Auxiliary Document A: Consent Form	257
Auxiliary Document B: User Surveys	263
Auxiliary Document C: Users' Motion Data	277

## List of Tables

2.1	Leading prior work . . . . .	36
2.2	Systematic literature review results in 4 electronic databases . . . . .	48
3.1	Main characteristics or parameterization of rotation . . . . .	52
3.2	Human arm DH parameters . . . . .	94
3.3	Parametric statistical tests . . . . .	99
3.4	Non-parametric statistical tests . . . . .	100
3.5	Errors in statistical decision-making . . . . .	101
4.1	Expected and measured IMU readings when it is stable . . . . .	109
4.2	Human-UR5e joint mapping table . . . . .	114
4.3	Risk assessment matrix . . . . .	123
4.4	The list of risk factors . . . . .	124

5.1	The change in user anticipation about robot technology before and after they are involved in a human-robot research study . . . . .	131
-----	---	-----

## List of Figures

1.1	Human-centric classification of HRI . . . . .	4
1.2	Classification scheme for pHRI based on proximity . . . . .	5
1.3	Common cobots in the market today . . . . .	7
1.4	The full-cycle of co-lift task and its states (APPROACH, CO-LIFT and RELEASE) . . . . .	8
1.5	MVN system which consist of 17 IMUs by the Xsens company . . . . .	11
1.6	Demonstration of drift error . . . . .	12
1.7	Modeling human arm as 7Degrees of Freedom (DoF)s . . . . .	13
1.8	The overview of scientific articles included in this thesis . . . . .	18
2.1	Degrees of freedom in full body . . . . .	26
2.2	Example use case of HME in robotics: Teleoperation tasks . . . . .	27
2.3	Active robotic endoscope holder system controlled by human finger motions . . . . .	28
2.4	A sample of the multiple human pose estimation using OpenPose . . . . .	29
2.5	Given exemplary external wrench realized by three different effort policies . . . . .	31
2.6	An example use case of IMUs in swimming motion recording . . . . .	32
2.7	Leading prior work of IMUs in HME visual map based of [1] . . . . .	35
2.8	Silhouette reconstruction of full-body human mannequin using markers and camera . . . . .	38
2.9	Leap motion controller detecting two hands . . . . .	39
2.10	Olympic and World Champion Ireen Wust wearing the IMU suit, combined with a Local Positioning System transponder . . . . .	41
2.11	Sensor fusion types in upper limb area in literature 2007-2017 and the comparison of two most common combinations over years . . . . .	42
2.12	Taxonomy of clinical applications of HMA . . . . .	43
2.13	Number of publications on HRI over the last two decades based on Google Scholar . . . . .	46
2.14	Systematic literature review search keywords and boolean combinations . . . . .	47
2.15	Number of publications in user training in HRI in the last decade . . . . .	48
3.1	Geometrical representation of Euler angles . . . . .	53
3.2	Gimbal lock example . . . . .	54
3.3	Multiple frame rotations . . . . .	56
3.4	Direction cosine angles example demonstration . . . . .	56
3.5	Demonstration of an axis-angle rotation . . . . .	58



3.6	Hamilton's complex number multiplication . . . . .	59
3.7	Two consecutive body segments . . . . .	66
3.8	Homogeneous transformation example using two frames . . . . .	67
3.9	Interconnection of the links and assignment of the link frames using unit vectors using DH convention . . . . .	68
3.10	Uniform - Gaussian - Exponential distribution functions . . . . .	73
3.11	Kalman equations . . . . .	78
3.12	Why KF does not work in nonlinear systems . . . . .	80
3.15	How EKF works . . . . .	81
3.16	Linearization problem in highly nonlinear systems . . . . .	82
3.17	Orientation vs position-based human pose estimation . . . . .	83
3.18	Tilt measurement by accelerometer . . . . .	87
3.19	Tilt in 2 axes . . . . .	87
3.20	Human arm joint angles and positions . . . . .	88
3.21	Orientation estimate system diagram . . . . .	89
3.22	Human arm joint angles and positions . . . . .	91
3.23	Position estimate system diagram . . . . .	92
3.24	14 DoF Human body visualized in ROS Rviz . . . . .	93
3.25	The major anatomical planes of human motion, and axes of rotation . . . . .	95
3.26	Forearm anatomy for flexion/extension and abduction/adduction . . . . .	96
3.27	Upperarm anatomy for pronation/supination . . . . .	97
3.28	One-tailed and two-tailed rejection regions of a statistical test . . . . .	98
4.1	The map of this thesis and how the pillars in fundamental chapters are connected . . . . .	103
4.2	World Magnetic Model (2020) . . . . .	105
4.3	Low pass filter impulse and frequency responses . . . . .	106
4.4	Basic implementation of an FIR filter . . . . .	107
4.5	Accelerometer raw and filtered (gravity eliminated) data in a stable position . . . . .	108
4.6	Accelerometer raw and filtered (gravity not eliminated) data during 2 pitch motion . . . . .	109
4.7	Accelerometer raw data, noise eliminated data and noise+gravity eliminated data during 2 pitch motion . . . . .	110
4.8	IMU attachment on the body on T-pose calibration . . . . .	111
4.9	Running nodes and active topics in real-time teleoperation of 6-Degrees of Freedom (DoF) robotic arm with 7-Degrees of Freedom (DoF) human arm model in Gazebo . . . . .	114
4.10	Human vs. UR5e arm poses, respectively, using joint space mapping . . . . .	115
4.11	HRC roles and states in the experimental co-lift scenario . . . . .	117
4.12	Predefined-command cooperation in the active lifting phase (i.e. COLIFT state) . . . . .	118
4.13	Labeled zones on human body based on pain severeness in case of a collision . . . . .	123
5.1	User scores on each trial in human-robot experiments . . . . .	129



# ABBREVIATIONS

---

<b>CDF</b>	Cumulative Distribution Function
<b>CF</b>	Complementary filter
<b>co-lift</b>	Cooperative Lifting
<b>cobot</b>	Collaborative Robot
<b>DoF</b>	Degrees of Freedom
<b>EEG</b>	Electroencephalogram
<b>EKF</b>	Extended Kalman filter
<b>EMG</b>	Electromyography
<b>F/T</b>	Force/Torque
<b>FK</b>	Forward Kinematics
<b>GPS</b>	Global Positioning System
<b>GWN</b>	Gaussian White Noise
<b>HCI</b>	Human-Computer Interaction
<b>HME</b>	Human Motion Estimation
<b>HRC</b>	Human Robot Cooperation
<b>HRI</b>	Human-Robot Interaction
<b>HTM</b>	Homogenous Transformation Matrix
<b>IK</b>	Inverse Kinematics
<b>IMU</b>	Inertial Measurement Unit
<b>JSM</b>	Joint Space Mapping
<b>KDL</b>	Kinematics and Dynamics Library
<b>KF</b>	Kalman filter
<b>LIDAR</b>	Light Detection and Ranging
<b>LPF</b>	Low-pass Filter
<b>MEMS</b>	Micro Electro-mechanical System
<b>MoCap</b>	Motion Capture

**PDF** Probability Density Function

**pHRC** physical Human-Robot Cooperation

**pHRI** physical Human-Robot Interaction

**r.v.** Random variable

**RGBD/RGB-D** Red Green Blue Depth

**ROS** Robot Operating System

**SGG** Serious Games and Gamification

**STA** Soft Tissue Artifact

**TCP** Tool Center Point

**TF** Transform

**TSM** Task Space Mapping

**URDF** Universal Robot Description Format

**UWB** Ultra-wide Band

**VR** Virtual Reality

# MATLIST

---

$\otimes$  Quaternion multiplication

$\times$  Matrix multiplication

$q^*$  Quaternion conjugation

$q_i^{A,B}$  Quaternion from frame A to frame B of the  $i^{\text{th}}$  inertial measurement unit

$R_i^{A,B}$  Rotation matrix from frame A to frame B of the  $i^{\text{th}}$  inertial measurement unit

$H_{(P_a P_b)}^{(A,B)}$  Homogenous Transformation Matrix rotating from frame A to frame B and translating from  $P_a$  to  $P_b$

$\vec{a}^G$  3D vector represented in the global frame

$\bar{a}^G$  [3x1] column vector (or [4x1] if quaternion) represented in the global frame

$\hat{u}^{(B/A)}$  Unit vector of frame B represented in frame A

$f_s$  Sampling frequency

$h(t)/H[n]$  Filter response in time domain and in frequency domain

$\hat{x}_t^-/\hat{x}_t^+/H[n]$  aprior/ a posterior estimated state

$\mathcal{F}|_B$  Body Frame: The coordinate frame of the moving body part

$\mathcal{F}|_S$  Sensor Frame: The coordinate frame of the moving IMU

$\mathcal{F}|_G$  Global Frame: The coordinate frame of the world/ground/base frame

$\mathcal{F}|_I$  Initial Frame: The coordinate initially coincident with the global frame. The initial frame is stationary whereas the global frame rotates with the Earth



# Part I

## FUNDAMENTALS





## INTRODUCTION

---

### 1.1 Human-Robot Interaction

The need to combine human and robot skills to their fullest potential has given rise to the field of Human-Robot Interaction (HRI). The birth of this field lies back in the mid-1990s and early years of the 2000s [2]. It combines the fundamental robotics and control theory subjects with psychology, cognitive sciences and social science to achieve this interaction as 'natural' as possible. From a social perspective, humans learn new communication methods to interact with robots and it shapes society towards a shift. Interacting with robots in public is a part of the *new normal* and will be more common in the future. For children to learn how to read, to order and be delivered food in a restaurant or be welcomed by a robot at a hospital is not only a science-fiction movie any longer.

The HRI has various application fields such as search and rescue, assistive robotics, military and police, edutainment, entertainment, space, home and industry [2, 3]. Some of the areas are intertwined with each other such as assistive robotics covers a wide range of examples in the rehabilitation field. Similarly, search and rescue robotics has big contributions to remote science and exploration studies in space. All those fields commonly aim to improve individuals' lives either directly by supporting them in daily activities or introducing a reforming step to solve a dangerous/challenging operation. The human-centric classification of HRI is given in Fig. 1.1.

Robots and humans can be co-located in a workspace with or without contact. If there is no contact between the human operator and the robot, it is generally considered as a *teleoperated* case. On the other hand, if there is direct or indirect contact (through an object) between a human and a robot, then these cases are within the pHRI field. The level of HRI based on proximity can be summarized as in Fig. 1.2.

A physical contact may occur intentionally and/or unintentionally. Moreover, the expected contact can be lost during collaboration. To know the level of physical contact with some certainty is important. A very coarse way of defining physical contact is that some parts of the human body take space on the same point in the coordinate system as some parts of the robot. If this contact is desired and required for the task (for example carrying an object together), the robot should continue executing the required set of actions to keep the contact available. On the other hand, if such a contact is not demanded (a collision or a crash case), then the robot should take a different set of actions so that such a contact could not occur.

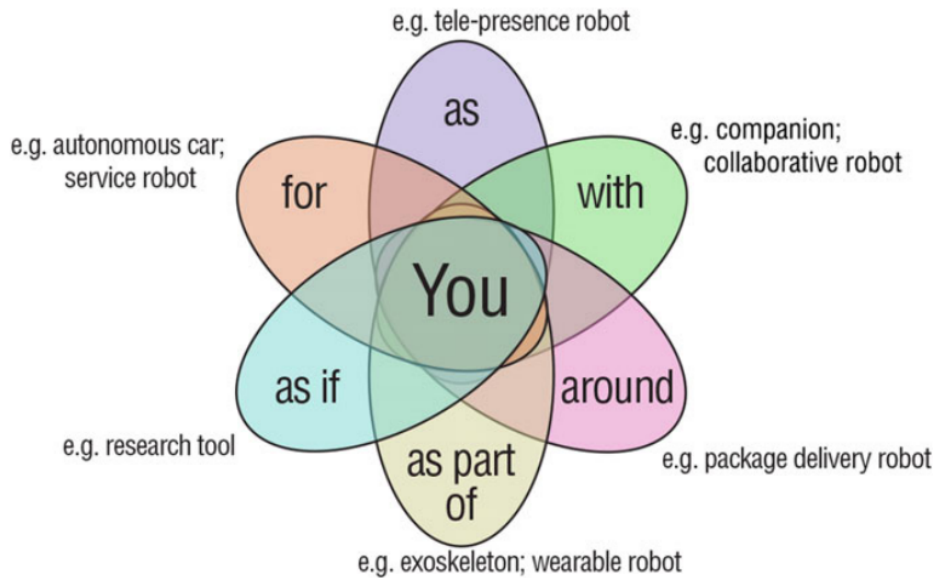


Fig. 1.1: Human-centric classification of HRI [3]

HRI is researched in two main directions; social science majors (psychology, political science, economics, sociology etc.) and technical sciences (natural science, computer science, engineering etc.). Those two directions have been doing their research independently most of the time. The HRI community is getting together [5] and there is a new era in HRI has started where the vast amount of research in the two perspectives (i.e. the technical and social aspects of HRI) is merging.

## 1.2 Collaborative Robots

Since the first usage of the "robot" term in 1920 by the Czech writer Karel Capek in his science fiction R.U.R. (Rossum's Universal Robots), humans were seeking a "thing" which does some programmed actions to make life easier for humans. After about 30 years of research, in 1954, the first industrial robot arm called a "Programmed Article Transfer" [6] device is patented by George Devol at General Motors.

Throughout robot history, they have been acknowledged as they were scary and dangerous machines. Therefore from the very early examples of robots, we can see them behind the cages, doing predefined tasks which are mostly mass-production related. They were quite powerful parts of the whole procedure that's why they were gaining more interest every day yet still behind the cages.

Acknowledging the fact that robots would move out of their cages one day, the robotics field has been a focus of interest in literary works and movies. Isaac Asimov, an American writer who is known mainly for his "robotic series" (which is a set of 37 science fiction short stories and six novels about robotics), set three rules in his short story named *Runaround*. These rules are:

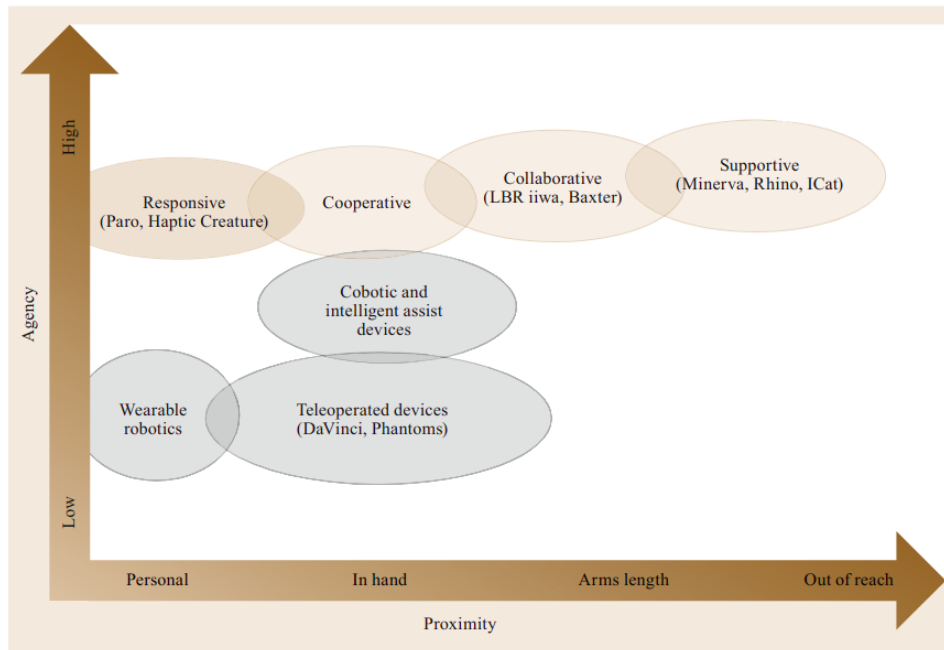


**Fig. 1.2:** Classification scheme for physical Human-Robot Interaction based on proximity [4]

**Law 1:** A robot may not injure a human being or, through inaction, allow a human being to come to harm.

**Law 2:** A robot must obey the orders given it by human beings except where such orders would conflict with **Law 1**.

**Law 3:** A robot must protect its own existence as long as such protection does not conflict with the **Law 1** or **Law 2**.

Even though these rules are from a science fiction work, they are adopted by robot scientists and engineers in their studies as a rule of thumb. Eventually, the emerging technology and the necessities in various fields lead humans to think beyond borders; robots do not have to operate standalone, instead, they can work "with" humans. This idea is presented for the first time in 1999 as a patent by defining *cobot* (i.e. Collaborative Robot) with these words: "an apparatus and method for direct physical integration between a person and a general-purpose manipulator controlled by a computer." This definition then shades off into what we would call today an Intelligent Assist Device (IAD), which can be considered as the earliest ancestor of cobots [7]. The first step of moving the robots to our side of the cage has been accomplished.

Afterwards, a German company called KUKA<sup>1</sup> announced its first cobot LBR3 in 2004. This robot is registered as the first cobot manipulator. Meanwhile, a Danish company called Universal Robots<sup>2</sup> was also working on collaborative robots and in 2008 they made a sale to Linatex, a Danish supplier of technical plastics and rubber for industrial applications. This company did something extraordinary and instead

<sup>1</sup><https://www.kuka.com/>

<sup>2</sup><https://www.universal-robots.com/>

## *Introduction*

of setting up the robot behind safety cages, they installed it right alongside their employees. They showed the possibility of robots being able to operate safely alongside people. This usage is registered as the first industrial human-robot-work-together example in the HRC history.

Those big steps lead other robot manufacturers to direct their studies to the collaboration of robots with humans. Today, there are more than 150 cobots available in the market[8]. In 2019, ABI Research [9] analyzed 12 leading collaborative robot vendors and listed as:

- ABB (Switzerland)
- Aubo Robotics (USA)
- Automata (UK)
- Doosan Robotics (South Korea)
- FANUC (Japan)
- Franka Emika (Germany)
- Kuka AG (Germany)
- Precise Automation (USA)
- Productive Robotics (USA)
- Techman Robot (*Quanta Group*) (USA)
- Universal Robots (Denmark)
- Yaskawa Motoman (Japan)

The automation industry grows exponentially and will keep growing at a similar pace in the coming years [10]. On top of the USD 191.89 billion market in 2021, the market is projected to grow from USD 205.86 billion in 2022 and is estimated to increase 9.8% compound annual growth rate until 2029 and reach almost USD 400 billion. This gross estimation applies to big, small and medium-sized enterprises (SMEs) companies. However, it is also stated in the same report that high upfront costs and unpredictable returns on automation investment make small and medium-sized enterprises (SMEs) hesitant to adopt the benefit of the technology. Therefore, collaborative robotics technology becomes a more profitable solution for companies in which mass production is not applicable. Cobots enable the HRC to be applicable in the production state, keeping the decision skills of the experienced human operator in the chain while introducing the benefits of the precision and repetition skills of the robot.

Today the term the robot is under the influence of a paradigm shift [4]. The intuition of calling a device or a machine a robot seems to be more of how it looks rather than how actually it functions conceptually. Moreover, the robotics field has been fed by the methods and facts of *the good old* control theory, mechanisms and machine theory, for so long. As the robotics field grew, newer fields such as machine learning,



**Fig. 1.3:** Common cobots in the market today. From top left to bottom right: **ABB YUMI**, **AUBO i5**, **Doosan A0509**, **FANUC CRX**, **Productive Robotics OB7**, **Franka Production 3**, **KUKA LBR iiwa**, **Techman Robot TM14**, **Universal Robots UR5e**, **Yaskawa HC20DTP**

human-computer interaction etc. are incorporated more and the robotics field has become a portal of older fundamental engineering subjects and newer shaping the future fields. This shift is relatively quick such that our social-linguistic adaptation lags behind. To distinguish between a machine and a computer was rather easy in the '90s. Today we are confused if our self-driving car is a machine or a computer. As of today, it is easier to call these so-called confusing devices robots in a popular science talk despite the fact that many roboticists would disagree. This paradoxical and dissonant discussion is surely interesting yet not within the scope of this study. Therefore, the definitions in this work are reconcilable to the ISO definitions [11]: a robot is a device that is reprogrammable in two or more axes.

### 1.3 Cooperative Lifting

Cooperative Lifting (co-lift) is a common task in collaborative, cooperative and/or supportive examples of HRI. It requires balance, coordination, power distribution and sufficient communication between robot(s) and human(s). In a broad perspective, co-lift is interested in the interaction dynamics that exist among humans, workpieces and robots to optimize the picking, carrying and placing sub-tasks.

Co-lift is a rather general term which is involved in several tasks in various application areas. For instance, in an industrial setting, integrating co-lift in material

## Introduction

manipulation is opportune. The material manipulation applications (e.g. handling, positioning, polishing etc.) constitute more than 20% in the manufacturing industry [12]. Co-lift, and HRC in general, provide speed and efficiency so that the tasks can be performed relatively easily via collaborative robots and supportive technologies. Moreover, the developments co-lift are useful in rehabilitation in which the robot helps the patient regain the mobility of a body part after an accident.

Co-lift is a relatively new field and sometimes addressed in the literature as *collaborative carrying* [13, 14]. It generally includes only the active carrying part such that pre- and post-phases are not mentioned. However, it causes a considerable gap between the academic co-lift studies and successful industrial implementation. Therefore, the co-lift term covers the whole HRC task from picking up the object, carrying it from point-A to point-B and placing it as shown in Fig. 1.4

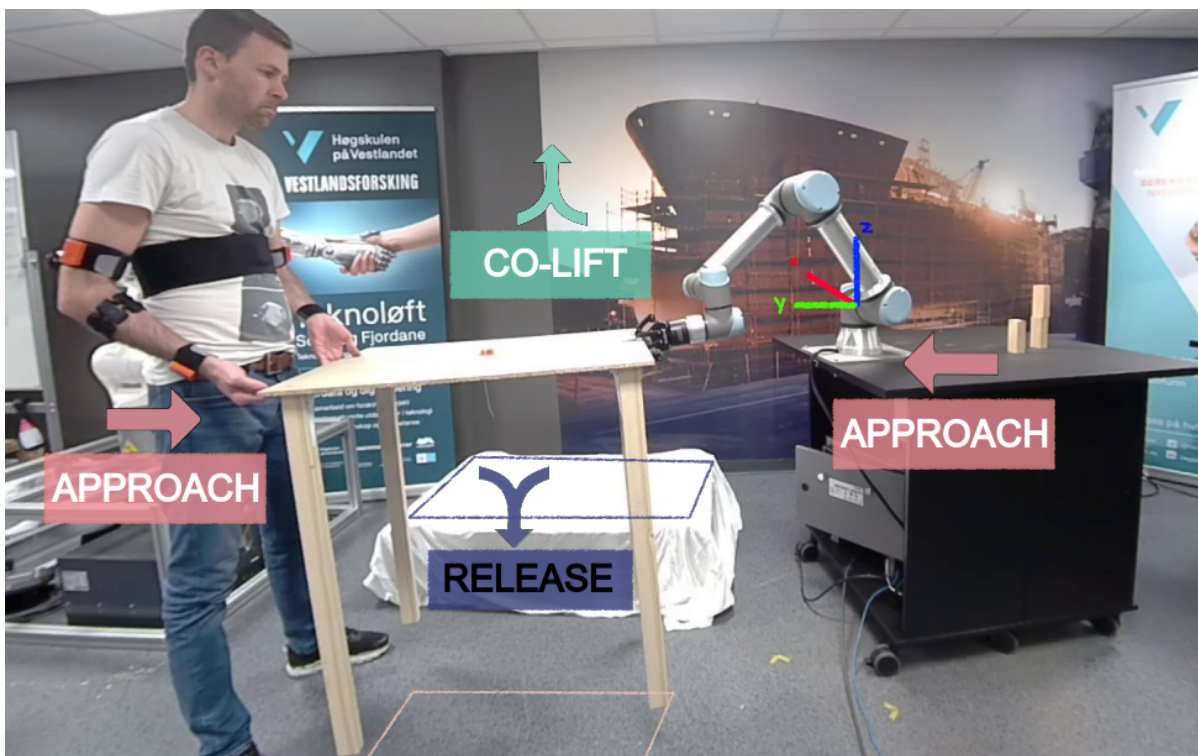


**Fig. 1.4:** The full-cycle of co-lift task and its states (APPROACH, CO-LIFT and RELEASE) and the pick and place locations of the common object [15].

The lack of implementation of advanced HRC developments in the actual industrial settings has been addressed in the literature and deeply discussed in Chapter 2. I would like to mention two particular references here to explain why co-lift is the central application of this study. According to [12]: "No hand gesture and other sophisticated communication means have been identified to be in use in current manufacturing floors." This is a rather dismal finding regarding the current status of HRC in real applications. There are several successful and sophisticated studies in the HRC yet they often fail in being an actual product/service. The second reference is [16]. The researchers remark the current collaboration of humans and robots is not a *real collaboration* but more of a sequence of turn-based actions. The main advancements in involving cobots are not in the enhancement of the collaboration between humans and robots but simply in

removing the safety cages of the robots. They indicate the underlying reason for this situation is the lack of educational technologies that facilitate effective worker-cobot interaction.

Considering the two references given above, a deep focus on co-lift gives a convenient canvas to test and improve real collaboration, sophisticated communication between the human and the robot and the user training perspective of the HRC. Additionally, the technical trips to small and mid-size manufacturing companies organized by HVL Robotics in the Western Norway region illuminate the potential of implementing the co-lift technologies.

### 1.4 Human Motion Estimation

The focus of Human Motion Estimation (HME) is to capture human motions with some certainty using sensors and analyse them using various models and algorithms. HME is often used to send the required information to the robot such as the pose, motion, and gesture of the human within the HRI field. Moreover, if the collaborated robot understands human intentions, it can provide necessary support and assistance during the whole process or at an appropriate moment.

In human motion tracking and prediction, the first step is to define the human model which is a mathematical representation of the human in the system. This model can be a silhouette as in [17, 18] or a biomechanical model as in [19–21]. The human body can be defined as a kinematic chain similar to robot modelling. However, human joints and links (i.e. soft tissue with ligaments and tendons) are more complex than the generic modelling elements in robotics (prismatic/revolute joints and rigid links). It is difficult to establish a complete kinematic model of the human body because it is a very complicated and correlated system.

As a result of that, the total Degrees of Freedom (DoF) of the human model is not exact. The DoF of this model changes according to the motion of interest (i.e. full-body, upper body, gait etc). For example, the human arm is modelled as 4 DoF in [22], 9 DoF in [23] and 7 DoF in [24] and in general applications. Modelling the human body and estimating the motions according to that model depends on the application. Increasing the DoF would result in more accurate estimation yet it would exponentially increase the computational cost. Particularly in HRC applications, the real-time capability of the developed system may play a vital role. Therefore, carefully identifying the requirements is as important as developing a precise method for human motion estimation for HRC.

Another important parameter in human motion estimation is the Motion Capture (MoCap) technology. Human motions can be tracked by cameras, wearable sensors or a combination of them. Each MoCap system has advantages and disadvantages. For example, cameras or visual-based tracking systems are widely used, providing relatively precise and accurate results if the tracking environment is ideal. However, they often come with a higher financial cost and require higher computational resources. The wearable systems may consist of different sensory equipment, often more affordable yet cannot provide as accurate results as their visual-based counterpart. Particularly, Inertial Measurement Unit (IMU)s are good options and reported to be superior for industrial use in many aspects such as compatibility with lightweight microcontrollers using

low-frequency sampling rates, providing more optimized data gathering algorithm and low-power communication protocol, a smaller impact on performance due to varying lighting conditions and body pose etc. [25]. Considering the efficiency, reliability in various industrial settings and mobility, a wearable inertial system is used as the main MoCap system in this study. This debate is an important part of this study and a detailed literature survey is provided in Section 2.1.3.

### **1.5 Research Area, Motivation and Challenges**

The emerging side of HRC in the industrial and medical applications is the main motivation of this study. Despite the substantial amount of research in the literature, there is still a gap in real HRC applications. A recent survey conducted with nine experts shows that contrary to the envisioned use of cobots, most cobot applications are only low-level interactions such as pressing the start/stop buttons etc. [16]. Additionally, experts feel traditional robotics skills are needed for collaborative and flexible interaction with cobots.

#### **1.5.1 On Literature**

The literature survey takes a big part in this study since there are several studies presented so far in HME, HRC, motion tracking using IMUs, etc. However, very few of them are applicable in a scenario where all the keywords are included. For instance, HME studies computed in the medical area are generally elaborated in an optimal laboratory environment. The application of such a system in the industrial area is most likely to fail due to electromagnetic noises, dust, required dressing rules and so on. Moreover, motion tracking using IMUs either suffers from drift in longer periods, which is not safe for pHRI or they process data using computationally expensive optimization algorithms and eliminate the drift error considerably but they often not applicable in real-time HRC applications.

Therefore, the research process started with the exploration and selection of an optimal methodology in the literature. As mentioned before, it is aimed to utilize IMUs for pose estimation for pHRI and HRC. When it is investigated in the literature, there are various approaches; selection of the optimal number of the sensors to be used, selection/definition of the human model, possible sensor fusion algorithms both using only IMUs and combination of other MoCap systems as multi-system, etc. All approaches have a small or big impact on HME quality. We are looking for the effects of those approaches and how big an impact they have on the quality of HME. In this manner, calibration-related improvements (in Section 4.1) and different methods (in Section 4.3) take part in this study.

The communication media plays a fundamental role in HRC. It is important both to let know the robot about human commands and intentions and also to avoid undesired collisions during the collaboration. Investigating the optimal communication media between humans and robots for particular tasks and developing a realistic system to be used in the industry is the main challenge. The valley of death is a growing issue from research to innovation [26] and it is regrettably a big challenge in HRI field [3]. Therefore, this study aims to define the problems in the technical aspect of the



human-motion-based HRI development, propose an affordable and realistic solution for the industrial applications and validate it with multiple user tests. Each step of this sequence is defined as a standalone challenge of this study.

### 1.5.2 On Inertial Measurement Units



**Fig. 1.5:** MVN system which consist of 17 IMUs by the Xsens company  
Source: [19]

In IMU-based HME, the procedure is such that one (or more number of) IMU is attached on different body sections as shown in Fig. 1.5. The 3D estimation of the position and/or estimation of individual IMUs is elaborated with the biomechanical constraints of the human body in calculating human posture, pose, position etc. The drift problem is by far the most mentioned challenge in using IMUs in the literature (see details in Chapter 2). Basically, the drift problem occurs in any kind of time-dependent signal measured in the real world (i.e. continuous) and transferred into the computer world (i.e. the digital world). Signals have to be processed digitally and any 'actual' signal change in the continuous world in between each consecutive time step is lost in the discrete world. To fill this missing information in the discrete world, there are various interpolation methods in the scientific calculation field to reconstruct the actual signal. However, no matter how good the signal processing is after capturing a continuous signal in the digital world, it will never be reconstructed *exactly* the same. The error between the actual and the reconstructed signal will accumulate over time and the problem will occur as we call the "drift" problem. Specifically for IMUs, the drift problem addresses the accumulated integration error over time as well as the error in reconstructing velocity/acceleration signal in the discrete world as shown in Fig. 1.6.

Researchers have been looking for an IMU based drift-free MoCap system for more than a decade. There are proposed different methods today to reduce or limit this error type by improving integration techniques and filtering techniques. However, filtering techniques are reported to somewhat slow down the error accumulation process, but

not completely eliminate it [27]. Also, even very recent and sophisticated integration methods aimed at IMU drift reduction [28] suffer from drift in a few seconds according to [29]. Therefore, since IMU output is in velocity and acceleration level, the drift problem in state estimation in the position and orientation level based on integration is inevitable [30, 31].

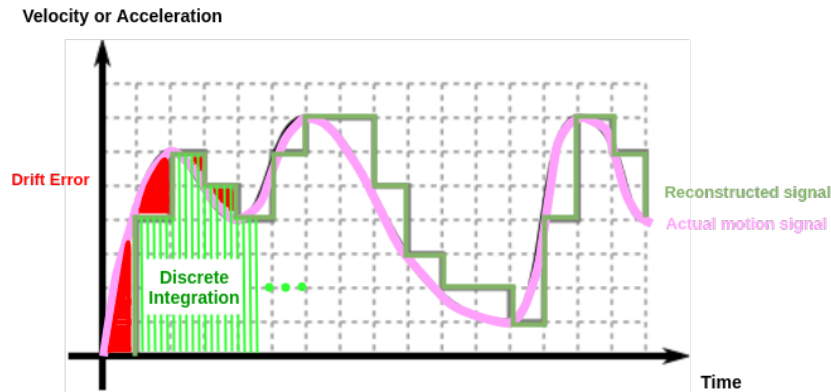


**Fig. 1.6:** Demonstration of drift error: The pink continuous signal is the actual motion signal and the green staircase signal is the reconstructed (i.e. sampled) signal. As the discrete integration is implemented, the accumulated integration error (shown as red region) grows. This is referred to as *drift error*.

To eliminate the drift error in the estimation phase, various algorithms have been presented in the literature (see Section 2.1.4) and the Bayesian filtering approach is one of the most promising. The IMUs which are being used through this study are MTw Awinda by the Xsens company. The orientation of the MTw is computed by Kalman filter (KF) in 3 DoF [32]. Nonetheless, the drift error is there and some other methodological approaches must be applied to obtain safe human inputs in pHRI applications. This has been processed in the human-robot motion mapping step in this study.

### 1.5.3 On Human Modelling

Modelling the human body and estimating human motions fast and reliably enough is a fundamental step of HME. The real-time capabilities of an HRC system affect its usability in the industry. It is much easier to run resource-demanding algorithms using today's technology at a research level. However, the financial cost of the system is a substantial parameter within our criteria. Therefore, to develop a simple yet efficient human biomechanical model for HRC, suitable motion tracking and estimation algorithms are important. Moreover, the representation of models is as important as choosing them. For instance, rotations can be represented as Euler sequences, rotation matrices, quaternions or other methods such as Rodrigues rotation, special orthogonality etc. In addition to that, translations can be represented as vectors+Euler angles, Homogenous Transformation Matrix (HTM) or dual-quaternions or other methods like the twist/wrench method, screw theory etc. The selection of representation plays a fundamental role in computation cost. It is decided to use quaternions for rotations and HTM for pose calculations. The selection process and reasoning are explained in detail in Section 3.1.

Another challenge is related to modelling errors. The human model can be a silhouette as in [17, 18] or a biomechanical model as in [19–21]. Since the human body contains more complex joints and links than ordinary actuators and link elements, it is not possible to model the human body with 100% accuracy. As a result of that, the total Degrees of Freedom (DoF) of the human model is not exact. For example, the human arm is modeled as 4 DoF in [22], 9 DoF in [23] and 7 DoF in [24]. Although the most common approach is to define the human arm as 7 DoF the distribution of this DoFs through the shoulder to wrist is tricky (see Fig. 1.7).

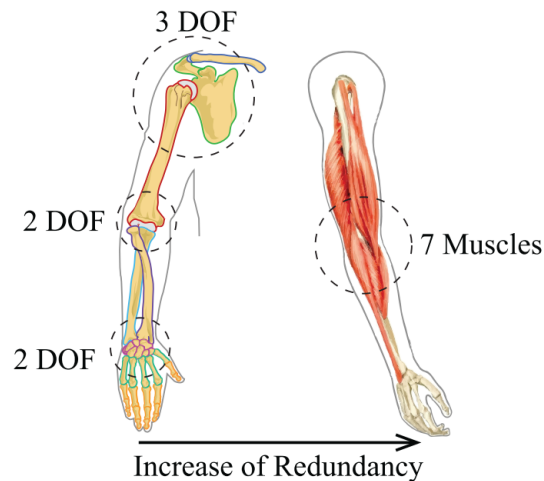


**Fig. 1.7:** Modeling human arm as 7DoFs  
Source:[24].

Previous studies elaborated on different parts of the body and got satisfying results which does not necessarily mean that the method is applicable to all human segments. For example, upper body motion estimation has a higher complexity than gait analysis. The reasons can be listed as:

1. No contact force detection periodically to correct errors in inertial measurements,
2. Shoulder and wrist joints are more sophisticated than ankle joints,
3. In contrast to gait for the lower limb, there are no standard activities for the arm,

In this study, the focus is on upper body motion estimation. Therefore, a rich literature on gait analysis, activity tracking or fall detection-related studies are inspiring but it should be noted that their methods are not necessarily applicable to this study.

Soft Tissue Artifact (STA) is another challenge on every type of wearable human motion capture systems [33, 34]. Body marker-based, IMU based, wearable strain gauge-based systems are some examples which suffer from soft tissue artifacts. Basically, STA refers to the relative motion of the wearable sensors attached to the skin with respect to the bone. Since the soft tissue (i.e. muscles and ligament) moves around the bones during motion and they have a soft materialistic property, the displacement error caused is called STA.

### **1.5.4 On User Training**

The training aspect of a developed system is a part of this research. Although HRC has been researched for a couple of decades, cooperating with robots is still a new phenomenon for both employees and employers in the industry. The implementation of new technology in the industry has always been challenging. Two major reasons for this challenge addressed in the literature are perceptions of the technology's ease of use and perceptions of the technology's usefulness [35]. Training is important not only to facilitate learning about how to use new technology but also to manage employee perceptions and attitudes about the new technology [36]. Particularly in an HRC extension of the ongoing production, the operators are hesitant to be integrated into such a novel field. The clear benefit and usability of the HRC should be both qualitatively and quantitatively verified.

As a daily life example, driving a car is a relevant human-machine interaction. People would need a relatively tedious training procedure to qualify to get a driving license. The effectiveness of the training process makes the cars an indispensable piece of our daily lives, otherwise, the cars could be killing machines. For a new beginner, the concept of gas, brake, clutch, gears and signals could be perceived a lot even before the traffic rules are presented. Obviously, the concept of clutch and gear change is cumbersome for some and as time goes on, the hassling aspects of car technology are being eliminated, and people have been benefiting from the cars for decades. The training procedure for driving has been developing with the technology itself such that the technology benefits humanity as it is being improved. If we waited for cars to be perfect before started using them, and disregarded the potential of user training, humanity could not have come that far.

In everyday life, a prominent example of human-machine interaction can be observed in the act of driving a car. Even today, individuals are required to undergo a comprehensive training process to obtain a driving license, which is crucial for ensuring the safe and effective operation of vehicles. This training process plays a pivotal role in transforming cars from potentially dangerous machines into indispensable tools that facilitate our daily activities. For novice drivers, the multitude of concepts such as gas, brake, clutch, gears, and signals can initially appear overwhelming, even before the intricacies of traffic rules are introduced. As automotive technology continues to advance, with the introduction of features such as automatic gear shifting and the emergence of self-driving cars, certain complexities associated with operating vehicles are gradually diminishing.

The training procedures for driving have evolved in tandem with technological advancements, ensuring that the benefits of these innovations are effectively harnessed by humanity. If society had waited for cars to achieve perfection before embracing their use, disregarding the potential of user training, our progress as a civilization would have been severely hindered. Therefore, it is imperative to recognize the significance of training programs in enabling individuals to navigate the complexities of human-robot interactions, ultimately enhancing the overall safety and efficiency of our interactions with technology.

Unfortunately, user training is not addressed sufficiently in the context of HRC and only a few studies suggested methodologies for user training in HRI. One approach

to improving human-machine interfaces (HMIs) for industrial machines and robots is through the use of adaptive methodologies [37]. This involves assessing the user's capabilities, adjusting the information displayed in the HMI, and providing training to the user. The goal of this approach is to tailor the interface to the specific needs and abilities of the user, thereby reducing cognitive workload and enhancing the user's interaction with the robot.

Another approach employed in the field of human-robot interaction is the Wizard-of-Oz (WoZ) technique. This methodology involves the utilization of a control interface by a remote supervisor (i.e. wizard) to operate the robot, thereby creating the illusion of an artificially intelligent entity or a fully functioning system whose missing services are supplemented by a hidden wizard [38, 39]. It allows researchers and designers to study and refine the interaction between humans and robots in a controlled environment. By using a human operator to control the robot's behaviour, researchers can observe and analyze how users interact with the robot and gather valuable insights into user preferences, expectations, and challenges. This technique is particularly useful in the early stages of human-robot interaction design, as it allows for iterative testing and refinement of the system based on user feedback. While this approach brings a valuable contribution to user training in HRI, it is not fully adapted and the examples are still limited. They are mostly focused on the social aspect and linguistic communication of HRI [40–42] and designed with the main purpose is to improving the current design rather than training the human users [43]. Moreover, there are still fundamental concerns about using WoZ since it is more of a human-human interaction via a robot rather than a real human-robot interaction [42].

Another pattern seen in user training in HRI related studies is that they vastly focus on the safety and trust factors. In [44], the researchers found that user training influences the occurrence of involuntary motion which is linked to trust. In [45], compulsory training/licensing is suggested in their evaluation of trust and safety in HRI since they found that human-robot trust directly affects people's willingness to cooperate with the robot. Those studies increase awareness and surely contribute to the user training aspect of HRI studies; however, the functionality and efficiency training of the system are lacking. Cross-training refers to a collaborative planning approach where a human and a robot engage in an iterative process of role-switching to acquire a mutual understanding and develop a shared plan for a task. This method is suggested by Nikolaidis et al. [46]. Its main focus is on optimizing the robot motions and the results are significantly better than reinforcement learning, yet the user is also aimed to be trained meanwhile.

When we look at other methods in user training in various fields Serious Games and Gamification (SGG), gamification and game-based learning approaches appear to be significantly effective. These methods can be used to create supplemental learning tools that engage with interactive learning opportunities and make the learning objectives be translated into knowledge easier [47–49]. Serious games provide users with a safe and simulated environment where they can practice skills and strategies without real-world consequences. This allows users to make mistakes and learn from them without facing any negative outcomes. The interactivity and engagement of gameplay in serious games help reinforce learning and improve knowledge retention [50]. On the other hand, gamification applies game elements such as scoring, rewards, challenges, and

## Introduction

player progression to training contexts. By incorporating these elements, gamification aims to increase motivation and engagement in the training process. Both serious games and gamification make the training process more enjoyable and engaging while still achieving real training outcomes [51].

Applying these approaches to HRI user training could potentially enhance the efficiency and comprehensiveness of the training compared to traditional instruction alone. The increased engagement and interactivity offered by serious games and gamification can aid in knowledge retention and allow users to develop practical skills through simulated practice. This is particularly relevant in the context of HRI systems, where functionality and efficiency training are crucial [51–53]

In conclusion, serious games, gamification, and game-based learning approaches have shown promise in enhancing user training in various fields. Their application in HRC user training can potentially improve the efficiency and comprehensiveness of the training process. By engaging users in interactive learning opportunities and providing a safe environment for practice, these methods can facilitate the translation of learning objectives into knowledge and help users develop practical skills.

### 1.5.5 Research Questions

The fundamental research question is *how to reliably measure and interpret human motions and translate them into meaningful robot actions in an HRC scenario?* Around this main question, there are some subquestions which are investigated in this thesis. They can be listed as follows:

- How can human motions be captured with sufficient accuracy for HRC applications?
- Is it possible to develop a sufficiently precise and accurate HRC model or a system which is computationally cheap and operates smoothly for real-time industrial usage?
- What type of MoCap systems are available today? What are the advantages and disadvantages of choosing one over another in HME?
- Which techniques are presented within HME so far? What are the advantages and disadvantages of these techniques in terms of efficiency, real-time capability, industrial applicability, reliability etc.?
- How can human motions and gestures be translated into something meaningful for the robotic system(s)?
- In a human-robot team, which one performs superior so that one can lead the collaboration? What does this superiority depend on; is it static or changes during the task being executed? How can the most efficient leadership roles be dynamically assigned in an HRC application?
- What are the bottlenecks in HRC research for it to be effectively used in the industry? What kind of methodological approach can be utilized?

- Is training an important factor in imparting HRC research into real innovation? If so, what are the most effective methods and how to implement them?

As a result of a detailed literature survey, many studies have been found related to HME. The majority are within the rehabilitation, entertaining and animation fields yet very few of them are readily applicable in robotics, particularly in HRC and pHRI. Therefore, this study targets to fill a gap in the literature as well as support industrial needs. The motivation and the effective area of this study are highly linked to the Teknoløft project, which is briefly explained in Section 1.6.

### 1.6 About Teknoløft

Teknoløft is a business-oriented research project with the collaboration of Western Norway University of Applied Sciences and Vestlandforskning. It aims to increase capacity and competence within automation and robotics, digitization and big data by making the research and development environment more relevant to the business community in the west of Norway.

The project aims to increase the business community's use of research for development and innovation, and stimulate collaboration with new national and international partners. The main initiatives in the project are to facilitate more step-by-step automation with robots in small and medium-sized companies and to develop a strong competence within Big Data that can make the business community better able to use existing data for innovation and change. The initiative will increase top competence in the R&D environment, and train new doctoral fellows on business-relevant issues. The project will develop new continuing and further education offers and a new master's degree in robotics and digitalisation to increase the supply of relevant and competent labour for the business community in Norway.

Within the automation and robotics branch, three PhD students (including me) have enrolled to develop some research on pHRI so that the results can be used in small/mid-scale companies mainly in the west of Norway and the whole country. For this purpose, **HVL Robotics Lab** has been established in late 2018 under the Teknoløft project in Western Norway University of Applied Sciences Campus Førde. Three main work packages are conducted:

- **Human Motion Estimation:** Analyze human motions by inertial motion tracking systems and estimate human behaviour for pHRI applications.
- **Human-Robot Interaction Control:** Develop a safe cooperative interaction control scheme for pHRI.
- **Human-Robot Cooperative Learning:** Develop a cooperative human-robot learning scheme for pHRI in a shared workspace.

This thesis is shaped around the work package-1 of the Teknoløft project.

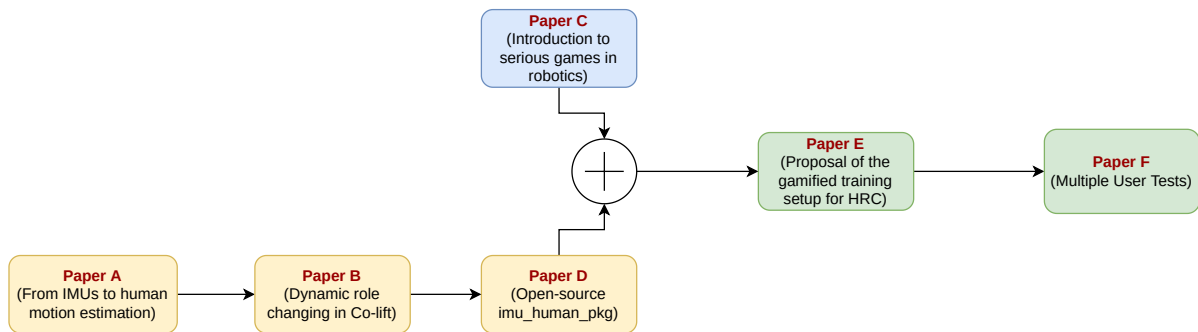


Fig. 1.8: The overview of scientific articles included in this thesis

## 1.7 Summary of Papers

During the period of this thesis, 6 peer-reviewed articles have been produced. The first focal point and the first paper were to model an optimal biomechanical representation of the human upper body and obtain sufficiently accurate human motions using inertial measurement units. In the second paper, this idea is improved by including compliant force and designing a dynamic role allocation in a co-lift scenario. The implementation of the proposed HRC system is presented as an open-source ROS package with the addition of a teleoperated scenario. In addition, training methodologies in robotics have been researched. A serious game was developed to teach fundamental robotics topics to bachelor's degree students. Although this paper was not directly linked to the HRC applications, it shed a light on further research. A gamified training setup is developed and it is also published as open-source. Finally, all the components have been put together in an extensive user study. 5 of the papers have been published and presented, and one paper was recently submitted to one of the leading IEEE journals in HRI field and is under review. The overall map of the scientific articles and how they are connected within this thesis are given in Fig. 1.8.

### **PAPER A: HUMAN-ROBOT COOPERATIVE LIFTING USING IMUs AND HUMAN GESTURES.**

This is the first paper produced during this thesis period. It is published in Springer proceedings of the Lecture Notes in Computer Science book series (LNAI, volume 13054) and the work is presented at TAROS 2021: Towards Autonomous Robotic Systems. It creates a baseline for how upper-body human motions and gestures are captured using IMUs. A novel co-lift task assessment is presented as a full cycle and improved towards actual industrial use. Our preliminary soft real-time experimental setup is presented in this paper which includes a human operator, a common object (i.e. a table) and a UR5e cobot. Human and robot are assigned leader roles based on the stage of the task. The results of the motion data regarding human inputs and robot end-effector pose output were successful but the system usability was not sufficient. It requires a lot of effort to use the system, which reduces its usability. Therefore, these aspects were improved in **Paper B**.

**PAPER B: FORCE AND GESTURE-BASED MOTION CONTROL OF HUMAN-ROBOT COOPERATIVE LIFTING USING IMUs** : This paper is published in HRI'22 Proceedings of the 2022 ACM/IEEE International Conference on Human-Robot Interaction and presented at its



respective conference which is one of the leading conferences in the HRI field. This paper is an improved version of Paper-A where the main purpose was to improve the system's usability. In addition to the IMU-based human motion input, a compliant force interaction is introduced as a communication channel. Particularly in the active lifting part the user and the robot became more in harmony. Pure human motion commands are used in the manipulating and grasping phase of the table by providing a *goal pose* to the end-effector and in the active lifting phase the robot produces its compliant force. This is a breakthrough in conceptual design because human is no longer the sole leader. Three dynamically allocated leadership roles are presented and validated on a real-world task. The improved usability is also validated by measurements taken from an IMU attached to the table.

**PAPER C: WORK IN PROGRESS: LEARNING FUNDAMENTAL ROBOTICS CONCEPTS THROUGH GAMES AT BACHELOR LEVEL** : This paper is published and presented at the 2022 IEEE Global Engineering Education Conference which is a profound conference held since 2010 on research and industrial collaboration on global engineering education. The paper takes upon a feeder road role in this thesis. It is the first paper in this thesis where SGG is introduced as an efficient training/learning mechanism in robotics. After a relatively deep literature survey, it is found that SGG are actively used for educational purposes in various fields. In this paper, a serious game is developed to teach fundamental robotic subjects at the bachelor level. Although, the serious game used in this paper is not directly towards HRI, the methodology and implementation tools used in developing this game made a way for Paper-E and Paper-F.

**PAPER D: A GENERIC FRAMEWORK FOR HUMAN-ROBOT INTERACTION BY IMU-BASED HUMAN MOTIONS AND GESTURES** : This paper is published and presented at 23rd IEEE International Conference on Industrial Technology, which is one of the flagship conferences of the IEEE Industrial Electronics Society, devoted to the dissemination of new ideas, research and works in progress within the fields of intelligent and computer control systems, robotics, factory communications and automation, flexible manufacturing, data acquisition and signal processing, vision systems, and power electronics. The paper is about an open-source ROS package which is developed on top of what is proposed in Paper-A and Paper-B. The main idea is to provide an easy-to-use human-motion-based robot control framework. Both teleoperation and pHRI cases are covered. Additionally, this study is awarded as the "BEST PAPER PRESENTATION" at ICIT 2022 conference.

**PAPER E: DESIGN OF A GAMIFIED TRAINING SYSTEM FOR HUMAN-ROBOT COOPERATION** : This paper is published and presented at IEEE 2022 International Conference on Electrical, Computer, Communications and Mechatronics Engineering (ICECCME). The paper presents an open-source gamified modular training design for HRC applications. It is where the proposed IMU-based HRC system merged with the gamified training concept. It shows how the user can be trained in/for an HRC system using a gamified approach, what game elements can be utilized and how the learning curve of the user can be measured as a game parameter to evaluate the usability and efficiency.

**PAPER F: EXPLORING HUMAN-ROBOT COOPERATION WITH GAMIFIED USER TRAINING: A USER STUDY ON COOPERATIVE LIFTING** : This paper has been submitted to *Frontiers Robotics and AI Journal* and is currently under the review process. It is a conclusion paper where the developed HRC system is tested and validated on 40 users which is considered quite a large study for HRI standards [54, 55]. It is found that a successful collaboration is plausible for everyone yet training is a vital step. The duration of the training and the level of expertise slightly vary between people. It is found that some parameters such as age, gender, occupation, programming background and anticipation of robots are relevant in learning. However, the purpose of this paper is not to reach a strict conclusion between a personal background parameter with a learning criteria. Its target is to observe the learning process of individuals and investigate rigorously what parameters might play a role in learning. Evidently, this study elucidates how to train employees with different backgrounds to increase the effectiveness of the training in the implementation of an HRC system in the industry as well as which parameters should be considered in future human-robot experiments design.

### **1.8 Contributions**

There are several theoretical and practical contributions made during this study. First of all, an effective use of IMUs in the HRC field is presented and validated. Since IMU-based motion tracking solutions are considerably cheaper than the visual-based ones [25], this real-world experimental validation plays a substantial role in turning the research into industrial innovation. The presented novel HRC system does not require to have long calibration procedure in each environment and for each user, it is rather a plug-and-play solution.

The human-motion estimation problem for HRC applications is taken as a methodological issue rather than a sole estimation problem. The effect of estimation errors in absolute positioning is more critical. The presented human-robot motion mapping suggests an algorithmic solution. Since the human-robot motion mapping is computed as relative motion mapping, the minor position estimation errors of the human body could be neglected. Eventually, a natural and intuitive control mechanism using the human body is designed.

Another methodological approach is to take the co-lift task as a whole rather than a part of a random HRC task. There are several interesting and promising solutions to the co-lift problem in the literature [56–58] yet they present solutions only in the active carrying phase. Therefore, the actual implementation of the proposed solution in an industrial setting is not addressed. There is still a gap between the research and actual innovation, which I deliberately focused to narrow in all the papers included in this thesis. In the proposed system, the human operator can activate/deactivate the robot, and transit between different HRC states only with gestures. Additionally, the system is designed as a full cycle that can automatically restart without any interrupts.

The design of quality research studies for use in HRI applications with results that are verifiable, reliable, and reproducible is reported to be a major challenge [3, 59, 60]. Therefore, all codes used in developing this study are published as open-source in

the HVL Robotics' GitHub page<sup>3</sup>. The main development environment is ROS on top of Ubuntu, both of which are free to use all around the world. Therefore, technically everything presented in this thesis is free to access/use/implement. I genuinely believe in the importance of collaboration and contributing to it to the best ability. Currently, some of the articles are not publicly available yet due to copyright restrictions but they are in the process of getting permission.

Game development is a relatively uncommon concept in the ROS environment. The user interface is mainly a black/purple terminal where the only interaction is via scripting codes. Although one might claim that there are a sprinkling of game elements in ROS, particularly around the "turtle" notion such as *Turtlesim*<sup>4</sup>, *Turtlebot*<sup>5</sup>, it is not a common matter overall. Our developed games and gamified training system are in the ROS environment.

Similarly, SGG and gamified training is not a common merge with HRC. There are more studies in the social sciences mainly regarding communication improvement where SGG is involved, however, it is scarcely researched from the technical perspective. For context, a broad search result in the IEEE Xplore Digital Library for (*"All Metadata":serious game\**) AND (*"All Metadata":human-robot interaction*) OR (*"All Metadata":hri*) ) returns only 31 publications (29 conference papers and 2 journals) where the majority are related to the social sciences. A literature gap is discovered in this study and relevant validated results are produced.

It is reported that real-world experiments with multiple users are scarce in HRI, particularly non-social HRI topics [3]. As mentioned before, a relatively large user study is conducted within this thesis in a real-world co-lift task. A part of the data collected in the experimental procedure is presented in Paper F and some yet unpublished data is mentioned in Section 5.0.4.

Finally, the dataset collected during the user experiments described in Paper F is made publicly available on DataverseNO as an open-access resource [61].

## 1.9 Dissertation Outline

This thesis is organized into two main parts. Part I introduces the study, presents the state-of-the-art, provides background about technical requirements to build the methodology, the methods used in developing this study and the discussion of the findings.

Part II consists of a collection of six articles, where five of which have been published [15, 62–65] and one is currently under review. These papers are summarized in Section 1.7.

**CHAPTER 1: INTRODUCTION** — This section introduces the study, defines the key concepts and problems, gives a brief overview of the current status of the field, the challenges and the summary of the solutions I provided in this study.

<sup>3</sup><https://github.com/frdedynamics>

<sup>4</sup><http://wiki.ros.org/turtlesim>

<sup>5</sup><https://learn.turtlebot.com/>

## *Introduction*

**CHAPTER 2: STATE OF THE ART** — A detailed literature search and strategy are given in this chapter. The literature review is carried out using both systematic and narrative methods. The gap in the literature and the direction of this study through closing the gap are highlighted.

**CHAPTER 3: BACKGROUND** — The scientific background is given in this section. It contains relevant subjects about human biomechanical modelling, robot kinematics, probability theory and statistics.

**CHAPTER 4: METHODOLOGY** — This section uses the fundamentals in Chapter 3 and presents how the scientific contributions in Part II are made. Initial sensor calibration, from sensor to human body calibration, the proposed human motion estimation methods, HRC states and roles, and the design of the human-robot experiments are given in this chapter.

**CHAPTER 5: DISCUSSION** — In this section, the general findings are discussed and the published articles are reviewed. Additional data analysis of the non-published data is also discussed in this chapter in Section 5.0.4.

**CHAPTER 6: CONCLUSION** — It is the final chapter of this thesis where the key findings are winded up. The recommendations for relevant stakeholders are presented and new questions for further research are revealed.

## STATE OF THE ART

---

For many decades, robots had been considered dangerous machines that can be harmful if there is any contact during operation. They were operated behind cages, and the process had to be stopped before any physical interaction occurred due to safety reasons. Recent advances in the robotics field have led robots to be involved in human life in various ways: from production lines to surgery rooms, from rehabilitation purposes to house cleaning purposes. Although those fields may appear to be quite different areas, they all share the same need: robots need to be out of their cages.

As the robots started to be taken out of their cages and operate in the same environments as the humans work and live *Human-Robot Interaction (HRI)* has become an increasingly important field in research. The proximate interaction between a robot and a human can be *supportive, collaborative* and *cooperative* depending on the task and the design of the system.

Supportive robotics refers to robots that provide assistance to humans in a task without actively collaborating with them. These robots may be used to lift heavy objects, perform repetitive tasks, or provide assistance to individuals with disabilities. Supportive robots typically operate autonomously but can be programmed to respond to certain human inputs or environmental conditions.

Collaborative robotics refers to robots that work alongside humans in a shared workspace to accomplish a shared task. These robots are designed to be safe and efficient when working in close proximity to humans. Collaborative robots may be used in manufacturing, healthcare, or other industries where humans and robots work together to achieve a common goal. Collaborative robots may be controlled by humans, but also have the ability to work autonomously.

Cooperative robotics refers to robots and humans working together to accomplish their individual tasks but sharing their strengths and complementing each other's weaknesses. These robots are designed to be adaptable to human behaviour and preferences and can adjust their actions based on the feedback they receive from humans. Cooperative robots may be used in settings such as education, rehabilitation, or emergency response, where humans and robots need to work closely together to achieve a specific outcome.

In summary, supportive robots provide assistance to humans, collaborative robots work alongside humans, and cooperative robots actively collaborate with humans. In the literature, *collaboration* and *cooperation* terms are sometimes used interchangeably.

However, it is important to underline that the methodology in this literature review

hardly differs in either case (supportive/ collaborative/ cooperative). Therefore in order not to bother the reader with detailed terminology and distract them from the main target of this study, the HRI term is used to define all *Supportive Robotics*, *Human Robot Collaboration (HRC)*, *Human Robot Cooperation (HRC)*, *Human Robot Interaction (HRI)* cases through this section since it covers a wider literature.

The literature review consists of two parts. In Section 2.2 a systematic approach is presented and aimed to show the importance of this study in the field. Afterwards, the gaps in the first survey have been filled in Section 2.1 to collect necessary studies to understand the literature before shaping and building up a reliable methodology.

## **2.1 Narrative Approach on the HME Methods and MoCap Technologies**

After a systematic literature survey, the results were examined in detail. An overall finding is that a big portion of these studies do not present human motion capture and analysis methods. There are a number of studies about the ethical aspects, social robotics and system design proposal in the results of the systematic literature survey. These topics are not necessarily related to the core of the methodology of this study yet important studies to construct the objectives. On the other hand, there are some studies that did not appear in those results yet are pretty relevant for the methodology of this study for example motion capture-related studies including IMUs but not necessarily include "human" motions. However, including all those keywords lead to a lot more confusing results since there would be many unrelated studies included as well. Hence, after a systematic literature review, a traditional literature survey is presented in this section.

This section is constructed such that it starts by understanding human motions and presents some important resources in human motion analysis in Section 2.1.1. Afterwards, different applications of HME in today's human life is presented in Section 2.1.2. In the third subsection Section 2.1.3, the most useful human motion capture system for this study is discussed by presenting different types of sensors and systems. As the last part of this section, different estimation methods are discussed in Section 2.1.4.

### **2.1.1 Understanding Human Motions**

The human body has a very sophisticated mechanical model. There is a whole field called kinesiology, specifically focusing on the mechanics of movement. As a sub-field of kinesiology, biomechanics is the science of the movement of a living body, including how muscles, bones, tendons, and ligaments work together to produce movement. The history of biomechanics goes back a very long in human history [66]. Human biomechanics reaches back to 15<sup>th</sup> century with Leonardo da Vinci's studies and animal biomechanics are even longer back to 4<sup>th</sup> century B.C. to Aristotle's book "De Motu Animalium" (On the Movement of Animals) defined animals' bodies where the mechanical systems and the actions of the muscles are described as well as they are subjected to geometric analysis for the first time. As such, there are numerous amount

of studies in the literature about human body modelling.

The most important thing for robotics is not only understanding the anatomical reasons and results of human motions but also translating these semantics into usable data for the robotics field so that human motions can be used in humanoids development, exoskeleton developments, new robotic structures development or HRC purposes as in this case. What we are dealing with biomechanics in this study is to estimate human motions and short future intentions. Therefore in a HRC scenario, the robot can plan its motion according to human intentions.

In human motion tracking and prediction, the first step is to define the human model. This model can be a silhouette as in [17, 18] or a biomechanical model as in [19, 21, 67]. In robotics, the biomechanical model is represented as a kinematic chain. However, the human body has a quietly sophisticated model chain. Despite the ordinary actuators which are used in mechanics, the motion of the human body occurs by contraction and relaxation of the muscles which are wind around the bones. The largest percentage of muscles in the muscular system consists of skeletal muscles, which are attached to bones and enable voluntary body movements. There are over 600 skeletal muscles in the human body [68]. Some muscle contractions create holonomic motion and it is very hard to distinguish all the individual muscle movements' effects. Therefore, it is not possible to model the human body as a kinematic chain the perfect biomechanical model of a human using general actuators available in the market today.

As a result of that, the total Degrees of Freedom (DoF) of the human model is not exact. The DoF of this model changes according to the motion of interest (i.e. full-body, upper body, gait etc). As the complexity of the model increases, the DoF increases, as well. For example, Madapura et al. modelled the full human body as 25DoF for their 3D articulated human body tracking study, Chung et al. modelled as 36DoF for animating human walk and Van Den Bogert used 47 markers to model 44DoF human model to investigate 300 muscle length changes and forces to the biomechanical analysis of human movements [69].

The Fig. 2.1 shows how the degrees of freedom is distributed in which parts of the human body in Cazzola et al's study. They used 43DoF *Rugby* model to analyze the spinal loading after cervical spine injuries and investigate cervical spine injury mechanisms during rugby activities.

Depending on the interest of motion in different studies, some human parts might be modelled very detail in one study whereas it is not modelled in another study at all. For example, compared to 0 DoF in [70], George Elkoura and Karan Singh modelled the human hand as 27 DoF in their hand simulation study.

The general approach in human body modelling in robotics and mechanics is that if the study requires a rough approximation, then the DoF of the model decreases for optimization reasons. On the other hand, although the total number of DoF is the same in some studies, their distribution might differ. For example, human arm is modeled as 4 DoF in [22], 9 DoF in [23] and 7 DoF in [24]. Moreover, the DoF might be the same as in two studies but the distribution of these DoFs differs. As an example for this case, in Ashitava Ghosal's study on analyzing the resolution of redundancy in robots and in a human arm, he used the 3-2-2 arm model (3 DoF on shoulder joint, 2 DoF on elbow joint, 2 DoF on wrist joint) whereas Shintemirov et al. used 3-1-3 arm model in their human arm motion-tracking study. The main reason is again the difference between

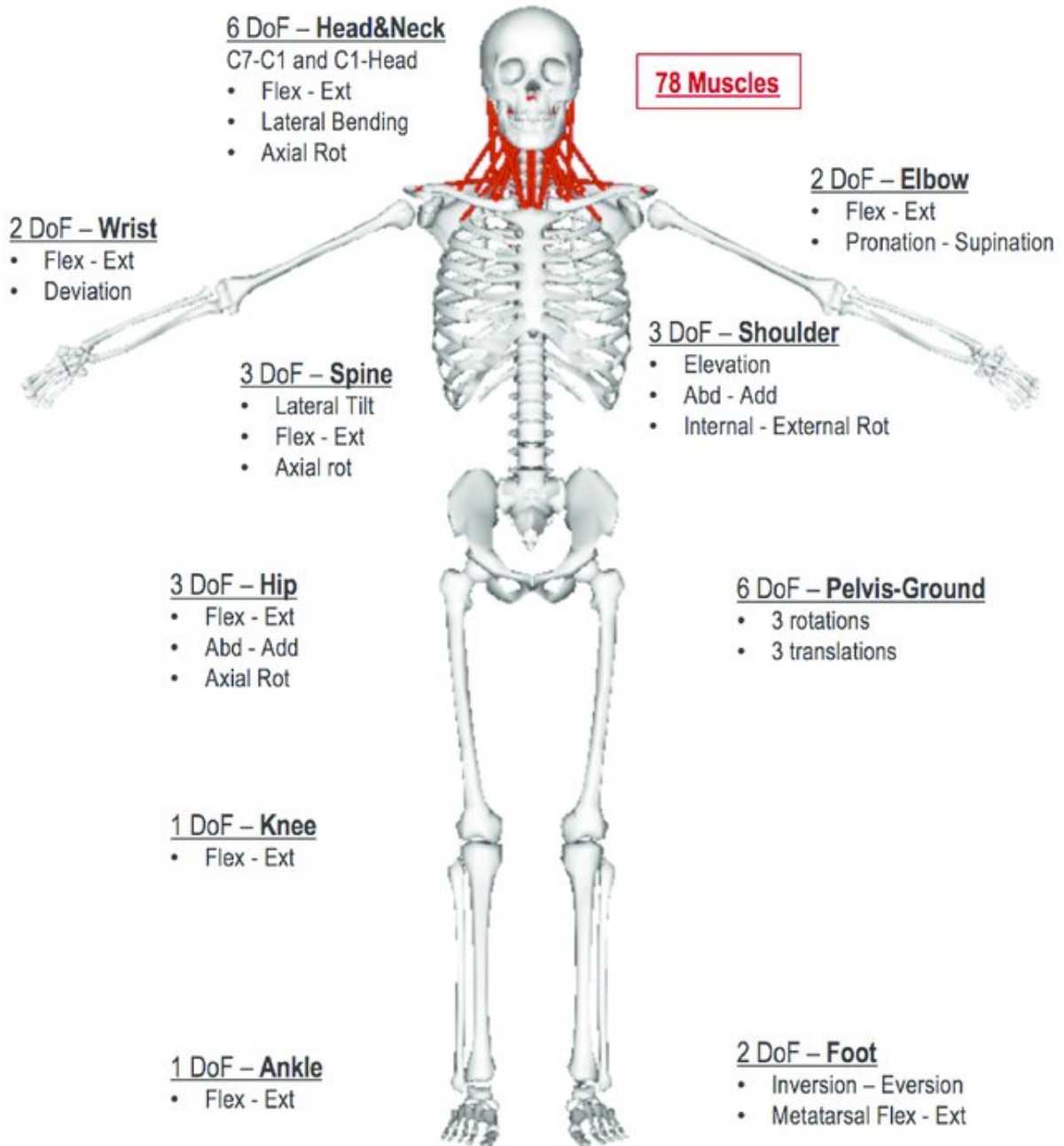


Fig. 2.1: Degrees of freedom in full body  
Source: [70]



how human motions are created by muscle contractions anatomically and how robot actuators work in real life. Since the focus of our study is upper body motion/intention estimation, the rest of the body for modelling does not take a part in this literature survey.

### 2.1.2 Applications of HME

As mentioned before, human motion analysis and estimation studies go far back in history. Therefore, the studies resulted in successful applications in various fields as shown in Fig. 2.2. Some previous studies are presented and discussed in this section.

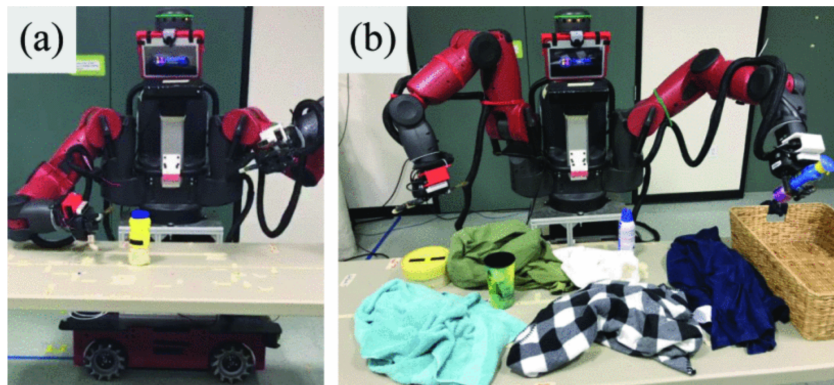


**Fig. 2.2:** Example use case of HME in robotics: Teleoperation tasks (a) reaching-to-grasp an individual object; (b) collecting multiple objects in a cluttered counter workspace. Source: [71]

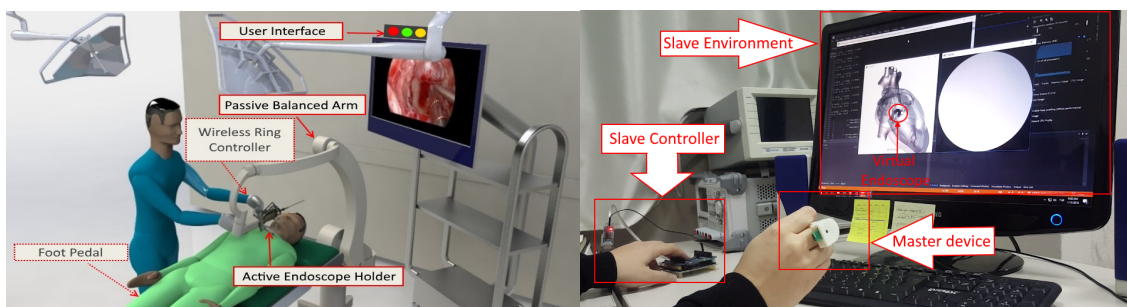
**Rehabilitation:** Medical applications lead in other categories since HME is an important process not only in a healing process but also in distinguishing healthy and abnormal human motions. Rehabilitation purposes take a big part of this cake. According to [72] Human motion tracking for rehabilitation has been an active research topic since the 1980s. For instance, Zhou et al. developed a wearable system using Inertial Measurement Unit (IMU)s to track arm motions of after-stroke patients in home-based rehabilitation [73]. Moreover, a physiotherapy exercise recognition study was carried out by [74] using RGB-D Human skeleton using a camera system (ASUS Xtion). The human model that they used has 15 DoF: 2 joints/leg, 2 joints/hand, 6 for the torso and 1 for the head. Nine predefined motions are given to subjects and the authors successfully distinguish them in live capture mode. A study by Lin and Kulic [75] was performed for human pose recovery on 20 subjects. The authors proposed an algorithm for estimating lower body pose based using 3 IMU; 1 on the lower leg, 2 on the upper leg, and 1 on the belt. Their method can estimate knee pose with an average 4.3 cm error. The authors reported that their system was valid in a clinical setting for joint replacement patients undergoing physiotherapy.

**Patience Assistance:** Besides healing purposes in rehabilitation, there are some studies that are developed to help those patients who require assistance to do daily stuff during the rehabilitation period. Tsung-Chi, Achyuthan and Li mapped human motions for teleoperation assistance [71]. They conducted a user study on muscle effort to compare physical effort, task completion time and the number of errors. They

conclude that such an aiding increases the users' preference in the acceptance of teleoperated robot technology.

**Detecting impairment:** Gait analysis is also a very trendy topic in HME, especially orthopaedics. In the clinical gait assessment study of Andreas Kranzl, impairment in walking is observed using 2D video capture [76] and [77] used wireless body sensors to diagnose abnormalities in gait. Since gait analysis is an important tool for diagnosing disease and evaluating disease progression, there are several studies in this field as nicely discussed in [78]. However, there is an important note worth mentioning here about our study. As it was mentioned in Chapter 1, we focused on upper body motion analysis and estimation. In this manner, upper body motion estimation is considerably harder than gait analysis for several reasons: 1) No contact force detection periodically to correct errors in inertial measurements, 2) shoulder and wrist joints are more sophisticated than ankle joints in contrast to gait for the lower limb, 3) there are no standard activities for the arm as in walking, etc.

**Robotic Surgery:** Another field of using HME in medical is in surgeries. Especially, robotic surgeries gain an enormous interest in the last 2 decades after ZEUS and da Vinci went on to dominate the field of robotic surgery although the history of robotics in surgery begins with the Puma 560, a robot used in 1985 by Kwoh et al. to perform neurosurgical biopsies with greater precision [79–82]. A HRC example of robotic surgeries using human motions can be seen in the design of a teleoperation scheme with a wearable master for minimally invasive surgery by [83, 84]. In their study, they control the position/velocity of an endoscope holder robotic arm which is controlled by a ring-shape IMU sensor in pituitary surgeries (Fig. 2.3). Moreover, another wearable device for controlling a robot gripper with fingertip contact, pressure, vibrotactile, and grip force feedback is developed by [85].



(a) Overall system controlled by human finger motions (b) Ring-shaped master controller

**Fig. 2.3:** Active robotic endoscope holder system controlled by human finger motions  
Source: [84]

**Entertainment:** Entertainment is also a famous use case for HME and HME studies. As an extra on commercial game systems, human motion sensing allows the user to engage in entertaining motor games using gross body movements that are not bound by the limits of a mouse, joystick or game-pad interface animation purposes. Some commercially available examples can be given as EyeToy games <sup>1</sup> by Sony's

<sup>1</sup>[https://sonycorporation.fandom.com/wiki/SIE\\_London\\_Studio](https://sonycorporation.fandom.com/wiki/SIE_London_Studio)

## 2.1 Narrative Approach on the HME Methods and MoCap Technologies

London Studio for PlayStation, Kinect games<sup>2</sup> by Microsoft for Xbox, animated avatars (i.e. Memoji<sup>3</sup>) by Apple etc. Furthermore, there are other commercial products for animation and filmmakers such as Xsens<sup>4</sup> is a Dutch company which is famous for their miniature inertial sensors for human motion tracking and MVN Animate [86] is the motion capture system for creating animation. Definitely, animation techniques, particularly based on human motions are important for HRC user studies. Schulz, Torresen and Herstand analyzed animation techniques in HRI cases and systematically reviewed the previous studies from animation to move a robot [87]. Their study is an important guideline showing the possibilities of this study as a use-case in animation for/with pHRI. Another comprehensive study is carried out by Hoffman and Ju in [88]. They presented four movement-centric designs (including character animation sketches, video prototyping, and interactive movement explorations) which could be used in real-world feasibly in HRC studies. This study is relevant and useful for this research because not all robots have an anthropomorphic mechanical structure yet well-designed robot motion can communicate, engage, and offer dynamic possibilities, and hence, give clues to its human friend.



**Fig. 2.4:** A sample of the multiple human pose estimation using OpenPose  
Source:[89]

**Serious game industry:** Serious games can be categorized outside of entertainment. Motion Rehab AVE 3D was published by Trombetta et al. as a game for post-stroke rehabilitation [90]. It is a VR-based exergame using a Kinect camera and Oculus Rift VR glass and Unity game engine. All of the 10 subjects in this study were between 61 and 75 years old and all the participants classified the interaction process "as interesting and amazing for the age", presenting a good acceptance. Moreover, Aguilar-Lazcano et al. developed a serious game for performance analysis for finger rehabilitation [91]. They used a Leap motion controller to detect finger movements and their study could be used in lighting environments ranging from 43 to 392 lux whereas most of the camera

<sup>2</sup><http://xboxaddict.com/xbox-360-kinect-game-list/>

<sup>3</sup><https://support.apple.com/en-us/HT208986>

<sup>4</sup><https://www.xsens.com/products/mvn-animate>

systems do have not this wide tolerance to lightning changes.

**Mechanical Design in Robotics:** Many of the mechanical structures of robots are influenced by human and animal anatomy. Therefore understanding human motions, reliable tracking and analysing them is essential. Festo is a famous robotic company which also gained even more reputation with its bionic robots such as BionicOpter, BionicKangaroo, BionicANT, BionicFinWave<sup>5</sup> etc. Unquestionably, one of the most useful cases in this field is humanoid development. For instance, [92] studied on dynamic leg motion generation of a humanoid robot based on human motions. Their aim is to design humanoid leg motion with high stability and similarity with the human actor. The effectiveness of the proposed method has also been experimented with successfully on the robot BHR-2. In [93], they moved one step forward and using human walking motion primitives, they developed an online path planning for humanoids. Humanoids are not only expected to achieve as much as human-like motions due to their similar shape to the human body but also they are expected to overcome the shortcomings of the human body. A comparative study between humans and humanoid robots is presented by [94]. Their study shows the different joint limits between humans and 6 different humanoid robots. Therefore, some kinematic singularities of the human body are possible configurations for some humanoid robots. Of course, there are many skills that the human body can achieve with no hassle whereas it is still impossible for a humanoid robot. In [95], the authors discuss optimization and imitation problems for humanoid robots. Nevertheless, those studies show that there is still a long way to understanding and using human motions in mechanical robotic designs.

**Industrial HRC:** Another field gaining interest in HRC where understanding human motions play a fundamental role in manufacturing applications. There are many reasons for using not only robots or humans alone in manufacturing but using those two powerful 'components' together. For instance, even a small company can focus on customer demands and offer a product for a lower price. Robots' repeatable positioning accuracy and ability to keep working for longer periods provide better quality yet can require post-processing and quality control.

The applications in this area are only limited to human imagination. From carrying an object together [96], to collaborative screwing application [97], collaborative sealant application on a white goods production line [98], in mining industry [99], human-robot interactive agricultural operations [100], or industrial service applications [101]. Every day a new use case is presented from all over the world. If we look at some of the given examples in a bit more detail, in [96] the authors analyze the effects of dynamic role allocation for a physical robotic assistant in an experimental setup where a human and a robot are collaboratively carrying a robot in 2-D x-y plane. The human motions are observed in 2 axes by a wrench sensor which is attached to the table where the human grasp the table. An identical wrench sensor is also attached on the robot's holding side and the information from both wrench sensors is used to detect the voluntary effect in the effort policies as shown in Fig. 2.5.

In [97], the researchers presented a collaborative screwing application where a projector-camera-based system was used to prevent collision and display interaction and safety-related information during the task. In [98], the authors presented a wearable

---

<sup>5</sup>[www.festo.com/us/en/e/journal/bionics-id\\_9229-66/](http://www.festo.com/us/en/e/journal/bionics-id_9229-66/)

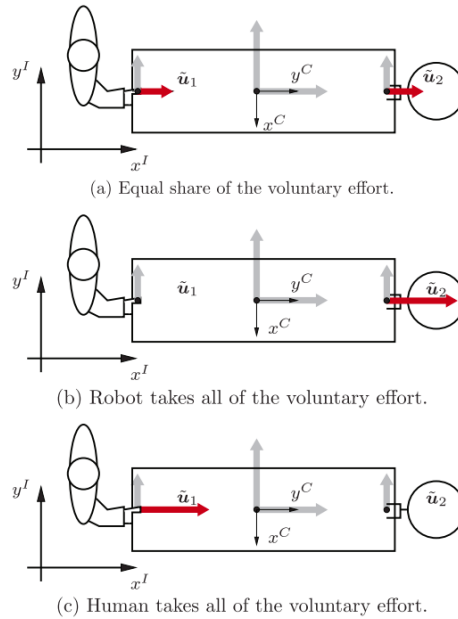


**Fig. 2.5:** Given exemplary external wrench realized by three different effort policies. Source:[96]

AR-based interface safety system. The wearable AR provides virtual instructions on how to execute the current task in the form of textual information or 3D model representation of the parts and a wristwatch is used for controlling the steps of the shared task as well as some other feature selections.

Safety reasons are also important to reliably follow human motions in human-robot coexisted environments. De Gea Fernández et al. [102] and Magrini et al. [103] used different motion capture systems (IMU, RGB-D and laser) to standardize the control and communication architecture for safe HRC. Human actions and intentions were estimated through hand gestures and the systems experimented with a real industrial task in the automotive industry. Another example study related to automotive manufacturing operations is from Ji and Piovesan about the validation of inertial-magnetic wearable sensors for full-body motion tracking [104]. The authors tested the wearable systems for HME in a manufacturing environment with compared to camera systems despite the shortcomings of both systems. Also, Czech car manufacturer Skoda demonstrated how the system supports the training of assembly workers and quality assurance in the assembly [105] based on human motions. They concluded that wearable assistance provided online instructions to the trainees about upcoming assembly steps, thereby streamlining the training.

Besides being productive, human motions are useful to assess ergonomics and work risks. A human postures inertial tracking system for ergonomic assessments is presented by [106]. The system allows for an estimation of the orientation of body segments and to assess the postures during the working tasks. The proposed system is composed of 4 independent modules in full-body configuration, each one made of 3 or 4 inertial units to increase mobility. In [107], the authors proposed a novel wearable system for the online assessment of risk for biomechanical load in repetitive efforts. Moreover, Maurice et al. published a thorough dataset of human motions in industry-like activities [108]. They collected full-body kinematics data using both wearable

inertial sensors and marker-based optical motion capture from thirteen participants who performed several series of activities, such as screwing and manipulating loads in different conditions, resulting in more than 5 hours of data.

**Sport:** As the last example use case which is touched upon in this literature review is in sports activities. Wearable systems and cameras are widely used in monitoring the workload, performance and motion efficiency of sportspersons as well as their safety in performing certain actions. In [109], the internal and external workload of the athletes is monitored using wearable sensors. Magalhaes et al.[110] used wearable inertial and magnetic sensors in swimming motion analysis (Fig. 2.6). Their study includes both front crawls and breaststroke swimming styles and all joint degrees of freedom modelled (shoulder, elbow and wrist) are analyzed. Moreover, we can see HME is studied in the sports area not only for analyzing purposes but also for teaching purposes in the literature. In [111, 112] sportspersons' motions are animated after capturing with video devices. The research group animated athletes' body motions in the first study [111] and they animated divers' body motions in their following study [112]. In a recent and well-cited study ([113]) IMUs are used together with a visual system to monitor hitting load in tennis using machine learning algorithms.



**Fig. 2.6:** An example use case of IMUs in swimming motion recording  
Source: [110]

### 2.1.3 Motion Capture Systems

In the previous section, we categorized the relevant studies based on their purpose of development. As can be seen, many studies used the same motion capture system although they are in considerably different fields such as wearable sensors are used both in [109] for swimming motion monitoring and [83] in robotic surgeries. Therefore, it is also useful to categorize the relevant studies based on used Motion Capture (MoCap) systems in the HME process. This kind of categorization will give a more methodological point of view/approach to solving the defined research problems. Another advantage of such a classification is that virtues and deficiencies of different MoCap systems become more insightful.

**Inertial Measurement Unit (IMU):** An IMU is a device that contains an accelerometer to measure linear acceleration and a gyroscope to measure the angular velocity of the body/object to which the sensor is attached. Moreover, today many IMU devices contain magnetometers to measure the magnetic field and its direction in the

environment. In some resources [114–116] IMUs are named as *m-IMU* or *magnetic and inertial measurement unit*. However, considerably many of the examples in the literature [19, 31, 117, 118] do not underline this distinction even though magnetometers do not measure an inertial property but an external property. To be consistent with the most used way in the terminology, IMU term includes all three elements (accelerometer, gyroscope, magnetometer) in this study.

Based on Muro-de-la-Herran et al's research [78], 40% of the reviewed articles published in late 2012 and 2013 on gait analysis methods were related to non-wearable systems, 37.5% presented inertial sensor-based systems, and the remaining 22.5% corresponded to other wearable systems. An increasing number of research works demonstrate that the IMU based HME is a promising method for human motion analysis.

In fact, IMUs are acknowledged as "low-cost motion sensors" [119, 120] and increased in popularity in the past few years. Accelerometers, gyroscopes and/or magnetometers can be found in most available smartphones and gaming controllers. The Apple® iPhone, Nintendo Wii and the PlayStation EyeToy are just a few examples where such technology is used to provide a more natural interaction with people's devices. A number of HME methods and use cases have been presented using IMUs such as:

- full body [19, 104, 121],
- upper body [34, 122],
- lower body [123–125]
- arm [126–129]
- joint specific [130, 131];
  - elbow [114, 132, 133],
  - finger [83],
  - shoulder [134]
  - hip and knee specific [135]

The advantages of using IMUs in HME are enumerated as being low-cost, portable, available in daily devices (such as smartphones) and computationally efficient. Compared to image and video processing, position and orientation estimation based on IMUs is possible even on basic microcontrollers [136]. On the other hand, there are some challenges also using IMUs in position and orientation estimate. Since IMU output is in velocity and acceleration level, the drift problem (i.e. accumulation of integration error) in state estimation in the position and orientation level is inevitable [30, 31]. Also, fast motion tracking is a challenging concept for IMU based HME studies [130, 137].

Magnetic disturbances, electronic devices, motors etc are some of the biggest enemies of IMU-based position/orientation estimation. Magnetometers are highly sensitive ferromagnetic materials and magnetic field changes around them. Therefore, the heading (i.e. yaw motion) estimate is more challenging as it is stated in [138, 139]. There are studies in which magnetometer-free estimation algorithms are developed

[140–142]. Such an approach increases the required number of IMUs for tracking the same amount of DoFs in the human body. For instance, [30] uses 4 IMUs for 2 joint estimations (hip and knee). Another approach is to use an external magnet to ensure the magnetic field direction in a small environment as in [143] yet a proper calibration might overcome magnetic disturbances at some level [139, 144].

Looking at the HME applications using IMUs, we see some advantages of using them instead of visual-based systems. For example, home-based rehabilitation applications are considerably easier and cheaper. Sara Oliveira's study enables using IMUs for knee rehabilitation at home [145]. Moreover, Pereira et al [146] accomplished a feasibility study on home rehabilitation. The patient wears one or two IMU devices depending on the exercise type. They propose 6 different exercises; shoulder flexion and extension, shoulder adduction and abduction, hip flexion and extension, hip adduction and abduction, knee flexion and extension, and elbow flexion and extension. They compared the results with marker-based video tracking software Kinovea and they reported that the results were reliable compared to the reference system. In [147], researchers introduced low-cost motion-tracking for virtual rehabilitation.

The number of IMU sensors used in motion tracking depends on the complexity of the human model. For example, [19] used 17 IMUs for full-body motion tracking whereas [148] used only 3+2 IMUs for their walking and running activity tracking study and [149] used 7 IMUs on upper body motion estimation. Obviously, as the number of IMUs decreased, the complexity and the cost of the overall system reduces. In this manner, [150] proposed a novel approach to reducing the number of sensing units for wearable gait analysis systems.

There is an important fact about the difference between the motion types (pitch-yaw-roll) and how human anatomy allows computing these motions. Especially, joint angle estimation is a very challenging subject as it is stated in [146]. The coupling effect (i.e. the inability of computing one axis angle independently of other axes), soft tissue artefact and translational motions in revolute-modelled joints increase the estimated joint angles error. Another big challenge is the drift problem (i.e. accumulation of integration error) and speed issue in IMU-based position and orientation estimate. Those problems and different algorithms to overcome the listed issues are presented in Section 2.1.4 in detail.

A more detailed look at using IMUs in HME can be carried out using visual literature review tools such as "Connected Papers"<sup>6</sup>. The *Survey of motion tracking methods based on inertial sensors: A focus on upper limb human motion* is a literature-leading survey article in this field and for this study, [1]. Taking this paper as the seed, the major articles about using IMUs in HME as shown in Fig. 2.7 and the list of 10 leading articles related to this search is given in Table 2.1.

These are the papers that were most commonly cited by the papers in the graph. This usually means that they are important seminal works in this field and it could be a good idea to get familiar with them. Selecting a prior work will highlight all graph papers referencing it, and selecting a graph paper will highlight all referenced prior work.

Lastly, it is important to mention the strong and weak points of the most used MoCap systems; visual-based and IMU-based systems. According to [151] accuracy

---

<sup>6</sup><https://www.connectedpapers.com/>



## 2.1 Narrative Approach on the HME Methods and MoCap Technologies

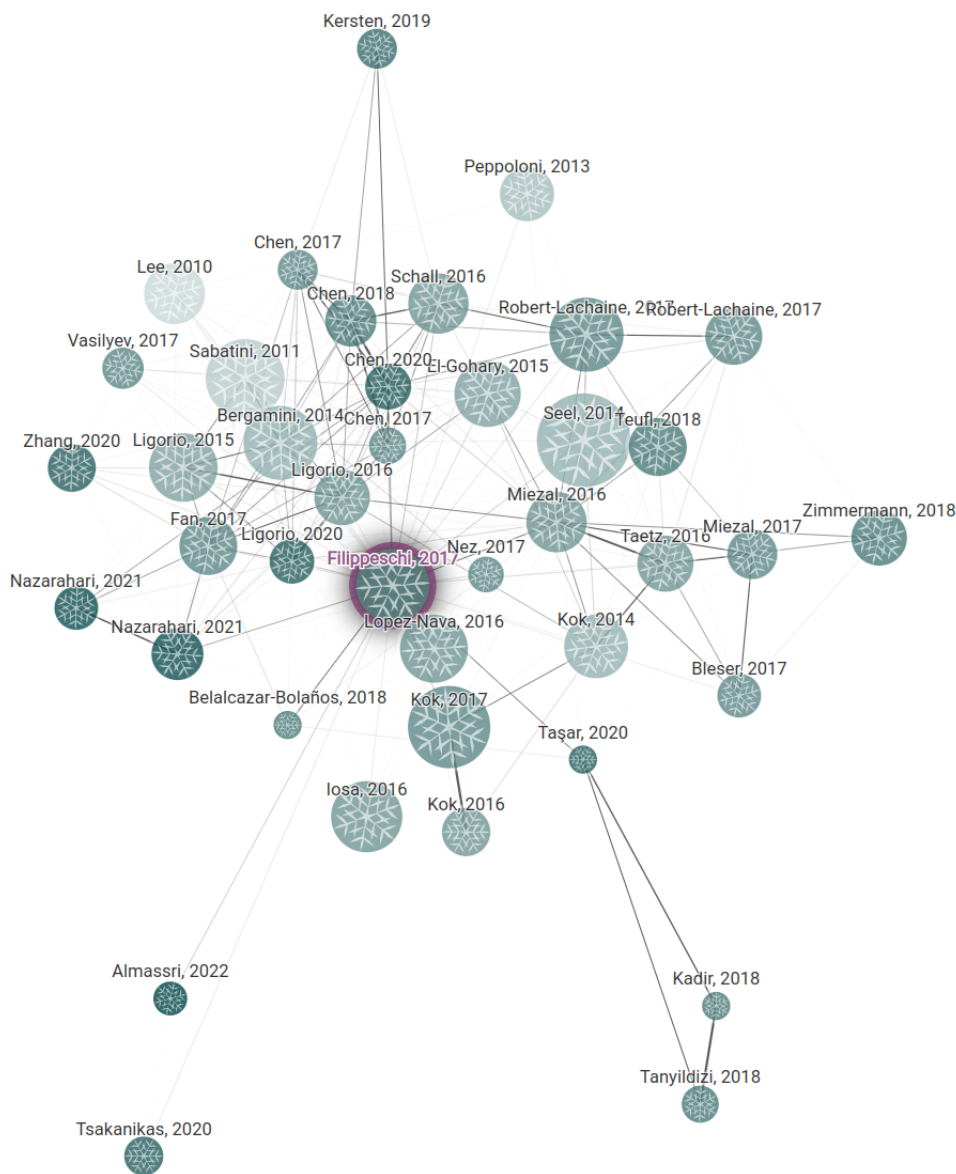


Fig. 2.7: Leading prior work of IMUs in HME visual map based of [1]

between optical and inertial motion capture systems for assessing trunk speed during preferred gait and transition periods is fair during walking, but the accuracy was reduced in the transition periods (i.e stops and waits due to IMUs drift problem.) Visual-based systems are detailed in the following subsection.

**Camera and Depth Sensors:** Visual-based systems (i.e video or image capture devices) are one of the most used human motion capture devices. One reason is undoubted that the sense of seeing feels like the most reliable among all 5 senses of humans although it is not correct 100% of the time. Therefore, eye-like sensing devices in principle "feel" more reliable. Another important reason is that since the sense of seeing is so superior in human life, the environment is also developed towards this direction; labelled signs, light indications and even human-human interactions.

Camera systems are extensively used in HME related tasks and studies. A survey of advances in vision-based human motion capture and analysis explored over 350

**Table 2.1:** Leading prior work

Title	First Author	Year	Citation
Quaternion-based extended Kalman filter for determining orientation by inertial and magnetic sensing	A. Sabatini	2006	795
Compensation of magnetic disturbances improves inertial and magnetic sensing of human body segment orientation	D. Roetenberg	2005	534
Ambulatory measurement of arm orientation.	H. Luinge	2007	346
Design, implementation, and experimental results of a quaternion-based Kalman filter for human body motion tracking	X. Yun	2005	588
Xsens MVN: Full 6DOF human motion tracking using miniature inertial sensors	D. Roetenberg	2009	761
A simplified quaternion-based algorithm for orientation estimation from earth gravity and magnetic field measurements	X. Yun	2008	307
Magnetic distortion in motion labs, implications for validating inertial magnetic sensors.	W. D. de Vries	2009	236
Ambulatory measurement of shoulder and elbow kinematics through inertial and magnetic sensors	A. Cutti	2008	264
Estimation of IMU and MARG orientation using a gradient descent algorithm	Sebastian Madgwick	2011	1650
Shoulder and elbow joint angle tracking with inertial sensors	M. El-Gohary	2012	217

studies in years between 2000-2006 [152]. Clearly, this amount is even higher today. Visual-based motion tracking systems are based on four main components, namely a camera system, a body model, the image features used and the algorithms that determine the shape, pose and location of the model itself [153]. Some of these studies are based on object tracking, some are human body tracking and some of them are outside of both these two categorizations. Since the interest is on HME for HRC-related studies, only studies that track human motions are examined. The studies selected for mention here also include some fundamental concepts of object tracking as a side topic.

The objective of using cameras in HME can be to track or estimate some body parts of the human body such as hand pose and/or motion tracking [154, 155], elbow angle estimation [156], gait analysis [157], eye gaze tracking for estimating facial expression [158] or the camera systems can be used full-body human pose and/or motion tracking and estimation purposes such as in [159–161]. Those studies commonly use a single camera to estimate human motion or for dynamic human modelling as in [162].

In limited conditions where the lightning is appropriate for cameras to detect colours correctly, where there is no obstacle between the camera and the human, where there is no occlusion on the camera lens, where the human has proper clothing or is relatively naked the camera systems work outstandingly successful in a limited workspace (i.e. total camera recording scene). Even not with average commercial camera options, it is possible to obtain sufficient results. Microsoft Kinect<sup>7</sup> is one of the most used relatively low-cost RGBD cameras in the literature on human motion tracking [163] (note that Microsoft has discontinued the Kinect sensor itself in the Fall of 2017 [164]). Asteriadis et al. used multiple Kinect cameras for estimating full-body human motion in [165] while Tian et al. [166] used it for upper body motion estimation and Chang et al. used them for physical rehabilitation purposes in [167]. Although the various possibilities of use even with a not-sophisticated camera system, in real-life applications the restrictions of camera systems are quite challenging. Also using a single RGB camera is lack depth information.

<sup>7</sup><https://en.wikipedia.org/wiki/Kinect>

The general approach to overcome the mentioned challenges in visual systems is to use one or more extra cameras. There are advantages of using camera systems, especially in position estimation in GPS-denied environments [168]. For example in [169] used two cameras for real-time hand gesture recognition. The authors tracked the hand motions based on stereo images and obtained successful results. Also, [170] used two cameras for animation purposes. In [171] the researchers used stereo-Kinect for accurate, low-risk occlusion in full-body motion capture. Still requires a dedicated camera-suitable environment for reliable results. Moreover, [172] uses three RGBD cameras for indoor human motion tracking, in [173] uses high-speed RGB cameras for full-body motion estimation and in [165] the researchers used multiple Kinect cameras, as well. Some studies are using several cameras to increase reliability and accuracy. For instance, [174] used 8-16 cameras for full-body motion tracking.

The bottleneck in scenarios where multiple cameras are used, they have to be synchronized with each other and the processing computer. There are camera networks to satisfy this necessity such as in [175] the researchers used VICON<sup>8</sup> for 3D gait analysing. Moreover, Malaguti et al. developed a methodology using RGBD Camera Networks in [176] for real-time tracking-by-detection of Human Motion.

Using multiple camera systems to increase the workspace, and reduce the sight-loss and occlusion problems is feasible yet expensive. To reduce the cost, some studies mounted the camera on the body as in [177] or some mirror systems as in [178] to track arm segments on both sides or a wheelchair user by two still-cameras (Canon T90) and a mirror.

Despite some rare examples such as in [177], visual-based motion tracking systems are generally rigidly attached to a wall or a still platform. As it is mentioned in [76] in their clinical gait assessment, the visual systems are very intolerant of any small changes in the tracking environment or the tracked body such as lightning and the clothes of the human and it requires very much pre-calibration before each use.

Another challenge is when there are multiple bodies to be tracked in the environment, especially those bodies are at a close distance to each other whereas some other MoCap systems do not have such an issue even in the beginning such as Ultra-wide Band (UWB) or IMU based system. There are some studies which are developed novel algorithms for visual-based systems to solve this problem and provide more reliable motion tracking and estimation such as in [161] where the researchers used a single RGB camera for real-time multi-person 3D motion capture. Elhayek et al. proposed a fully automatic multi-person human motion capture method for VR applications [179].

**Markers with visual systems:** To enhance the quality of the visual-based motion tracking systems, a set of small objects are attached to the human body parts as shown in Fig. 2.8. Some of the problems can be adequately solved by using markers or tags on some body segments or tools which is held/attached to the human. For instance, [21] uses 22 markers to obtain a kinematic model in 3D for full-body human motion capture. In [180], the researchers used reflective markers for a fast motion capture system for optical sensors. As an early example [181], the arm model is obtained by a marker-based optical tracking system.

One biggest disadvantages is that to obtain a fault-tolerant and reliable marker-based optical tracking system, it is necessary to use more than sufficient markers [182]. This

---

<sup>8</sup><https://www.vicon.com/>

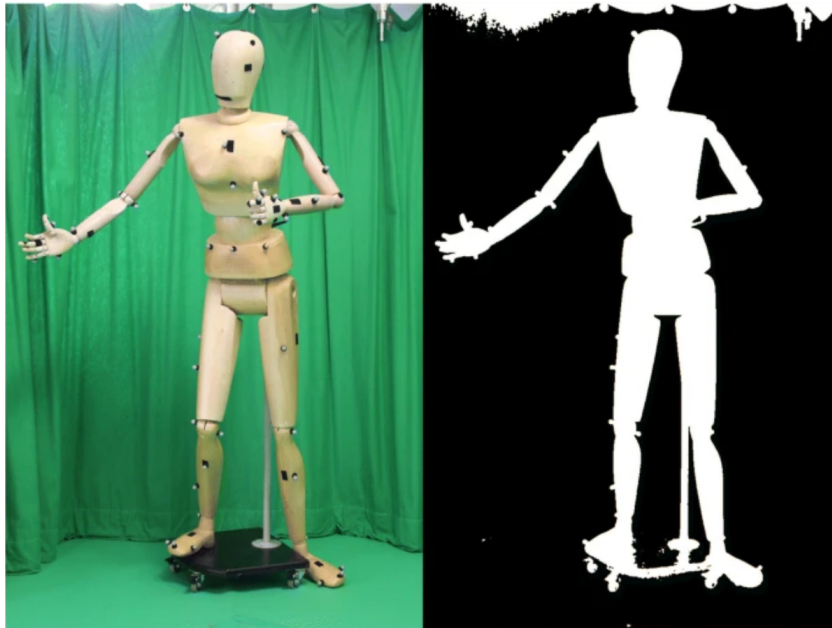


**Fig. 2.8:** Silhouette reconstruction of full-body human mannequin using markers and camera

Source: [153]

fact increases the complexity of the system and therefore the calibration process and the algorithm.

Despite some advantages and disadvantages over each other, marker-based and markerless visual human motion tracking methods are reported similar results in 3D joint angle estimation in [183]. However, for highly dynamic motion tracking, such as running, markerless solutions are acknowledged as advantageous [184].

**Point cloud and laser systems (depth sensors):** Point cloud and laser systems (or depth sensors/cameras) have similar advantages and disadvantages to the camera systems yet the procedure behind them is different. Instead of capturing the motion as an image or a video, it is captured as a set of depth information of body segments [185]. In [186], real-time full-body motion capture with high accuracy is accomplished by using a single depth sensor. Also in [187], the authors captured full-body motion using the surface geometry properties of the body. The experiments show that their method enables increasingly denoised, detailed, and complete surface reconstruction. Zhang et al. used multiple depth cameras for real-time full-body motion tracking [188]. As well as the full-body motion capture, there are some studies which focused on some parts of the body such as [189] used a depth sensor to estimate upper-body human pose in real-time.

LIDAR sensors are very common MoCap devices which can be categorized under this section. The studies [190–192] show that LIDAR sensors are possible to be used in body motion tracking. Moreover, some studies record multiple human tracking is achievable using 360-degree LIDAR sensors [193]. A successful HRC example using LIDARs in human motion tracking is by [194]. They developed a person-following shopping support robot based on human pose skeleton data and LIDAR sensor.

## 2.1 Narrative Approach on the HME Methods and MoCap Technologies

Leap motion controller<sup>9</sup> is a common and affordable depth sensor that uses a laser system to track hand motions (see Fig. 2.9). There are some studies using Leap motion controller such as for finger motion tracking [195] and finger rehabilitation [91].

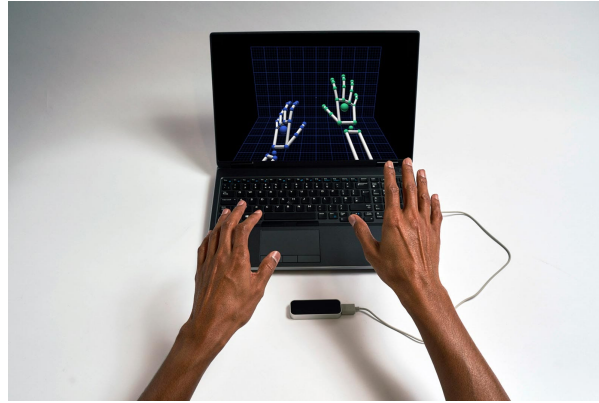


**Fig. 2.9:** Leap motion controller detecting two hands  
Source: [196]

Ultrasonic sensors can also be classified under this category since the motion detection is carried out by depth information. In [197], the researchers used a wireless ultrasonic sensor network to follow foot trajectory and in [198], the researchers used an ultrasound-based motion analyzer to determine the spatial position of the human shoulder.

Some of these MoCap systems are also tested in work conditions. In [199], analyzed depth cameras in real industrial conditions for human motion analysis. The authors recorded that this technology is quite promising yet it is not precise enough for joint angle estimation and it suffers from similar challenges as in RGB camera systems. Although depth sensors are powerful in human motion tracking and there are successful examples in certain conditions, they are still not reliable enough. Therefore, these systems are encountered as an aiding system in human motion tracking to an actual MoCap system such as camera [155, 200] or Inertial Measurement Unit (IMU) [201, 202].

**Bio-signals:** Biosensors are tools which are used to detect biological activities, mainly based on electrical or chemical changes in a human (or on a microorganism in general). They consist of three parts: a component that recognizes the bioelectrical/biochemical activities, a signal transducer, and a processing device. There are different biosensors used in laboratories and hospitals for disease diagnosis. Some are also used in HRC related research by predicting human motions and intentions.

Electromyography (EMG) is a technique for evaluating the electrical activity produced by skeletal muscles by sending and receiving weak electric signals. The muscle character (electro-permeability) changes as the muscle contracts or releases [203]. EMG devices are widely used in hospitals to diagnose different diseases for a long time. Also, EMG signals are studied in HME related studies. The same research group that was mentioned in home-based rehabilitation using IMU has also achieved another home-based rehabilitation technique using EMG [204]. Their system corrects the exercises using EMG.

<sup>9</sup><https://www.ultraleap.com/product/leap-motion-controller/>

We mostly see EMG based motion estimation not necessarily in a pose or orientation estimation but more in control-based, correction related or motor intention prediction in HRC studies [205–208]. For example, in [209] the contraction on biceps and triceps are measured by a couple of EMG sensors to estimate human intention and achieve human-robot collaborative lifting. Also, there are some studies which map EMG signals muscle-to-muscle to some robots which have custom-engineered mechanical designs [210].

Electroencephalogram (EEG) is another widely used bio-sensor which records the electrical activity of the brain by attaching a set of electrodes on the scalp. Despite its being used often in hospitals for diagnoses of different diseases like EMG, it is also widely used in human-computer interface-related studies [211]. Human-computer interface-related studies opens up the EEG signals in HRC as well. There is not any registered studies in the literature on full-body motion/pose/intention estimation using EEG based HME studies yet there are some HRC examples such as driving a mobile robot [212] and correcting robot mistakes in real-time using EEG signals [213].

**Uncategorized:** As it seems, there are a number of different MoCap systems available both in markets and under investigation in the researchers' world. Some systems have gained more interest than others as it is discussed. There are relatively less popular yet quite interesting systems that are worth mentioning. For example, a recent study [214] used radio-frequency (RF) signals to detect human motions even behind the wall. Moreover, goniometers and exoskeletons are used in body motion tracking. Carbonaro et al. used goniometers in hand motion tracking [215] and Kramer et al. developed a goniometer-based body-tracking device [216]. The device is composed of several body-attached/worn parts which are basically resistive bend sensors. As the body bends on some joints, the resistance changes on those bands and enables full-body motion tracking. This type of resistive bands are also called *membrane potentiometers* and they are used in robotic arm control through human arm movement in [217]. Song and Guo developed a real-time upper limb motion tracking exoskeleton device for active rehabilitation[218]. They presented the reliability of their system compared to IMU-based results on elbow joint angle tracking. The result shows a similar characteristic in both systems. Strain gauges are used in HME, as well. In [219], super-stretchable, transparent carbon nanotube-based capacitive strain sensors and in [220], an extremely elastic wearable carbon nanotube fiber strain sensor is used for human motion detection. Lastly, UWB based systems recently gained interest in HME studies. UWB is an RF technology which has a very low energy level for short-range and high-bandwidth communications in frequencies ranging from 3.1 to 10.5 GHz in the RF-spectrum[221]. By short pulses sending and receiving time comparison, it enables precise real-time indoor positioning and GPS-denied environments. A novel biomechanical UWB and IMU-based lower body motion capture method are presented in [222]. An experimental investigation is also presented for 3-D human body localization using wearable ultra-wideband antennas in [223].

**Multi systems:** Among all these MoCap systems, there is not a "perfect" solution for *every use*. To design the most optimal MoCap method and overcome unreliability as much as possible for the relative study, researchers use more than one MoCap system (see Fig. 2.10). For instance, Tian et al. proposed a fusion strategy using a Kinect camera and IMU using the unscented Kalman filter. According to their results, the proposed

## 2.1 Narrative Approach on the HME Methods and MoCap Technologies

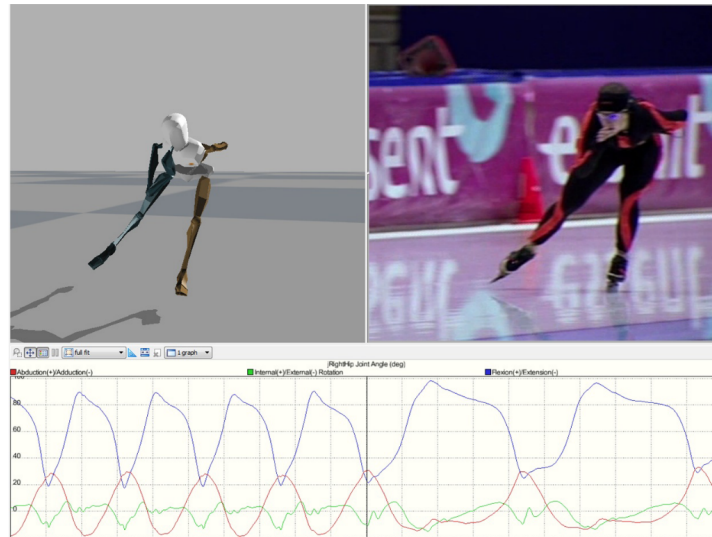


**Fig. 2.10:** Olympic and World Champion Ireen Wust wearing the IMU suit, combined with a Local Positioning System transponder. The lower graphs illustrate the right hip joint angles. Courtesy of University of Groningen. Source: [19]

method provides a drift-free upper body motion estimation method. The results were also compared with only IMU by double integration of the linear acceleration signal and only Kinect-based estimation methods. It is recorded as more robust and accurate than the other two systems.

The combination of camera and IMU systems is not unique, contrarily, it is a quite widely used method as investigated in [224, 225]. Since the IMU system gives sufficient and accurate results in orientation estimation but is often unreliable in position estimation, and the camera systems are reliable in position estimation yet loss-of-sight is a big problem, the general approach is to merge the stronger sides of both systems in position+orientation (i.e. pose) estimation. Such a combination provides quite accurate results yet it is also open to improvements such as in robustness [30], increases dynamics [226] and reducing the cost of the overall system. For the cost issue, there are some other sensors used in absolute position/distance measurement. For instance, in [222] IMU systems are merged with UWB antenna system, [120] used 3-axis flow meters and in [227–229] the researchers used depth sensors together with IMUs. For instance, in [230], the authors proposed a real-time teleoperation system to control a mobile robot's hand arm by the vision and IMU.

Since this study is focused on IMU-based motion estimation, the presented examples in this section are towards this purpose. However, the possibility of merging two MoCap systems is various. A very nice comprehensive survey by [231] shows that IMU+EMG systems and IMU+camera multi-systems cover more than half of the studies in 2007-2017 on sensor fusion in upper limb area. Other systems and their portions are given in Fig. 2.11.

We can list some examples as follows:

- IMU and camera in [230, 232],
- IMU and EMG in [233]

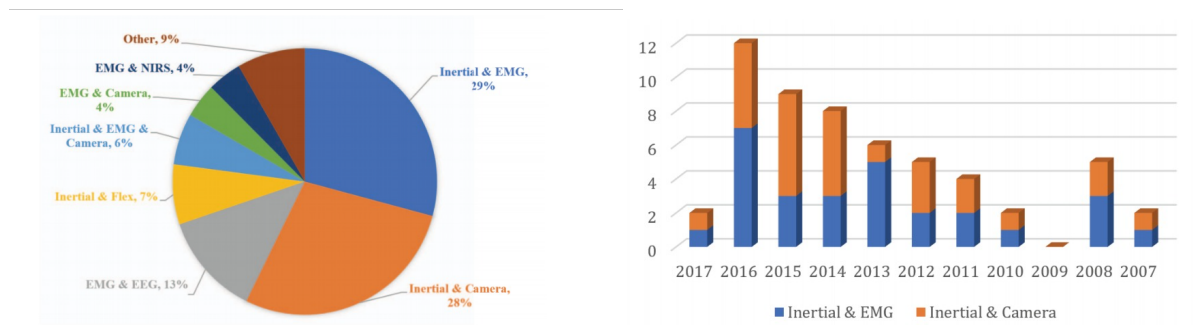


**Fig. 2.11:** Sensor fusion types in upper limb area in literature 2007-2017 and the comparison of two most common combinations over years

Source: [231]

- IMU and depth sensors in [234, 235]
- Camera and depth sensors [169, 236],
- Leap motion controller and flex sensors in [195],
- IMU, vision, UWB and GPS in [237],
- IMU and UWB in [238],
- IMU and optical fiber sensors [239],

#### 2.1.4 Different Methods in HME using IMU

Motion capturing, tracking and generation have gained interest from many researchers in various fields for years. There are several methods to track and estimate motion based on different sources of information. As the MEMS technology has improved, the inertial systems received more attention. Since the IMU based motion tracking systems have fundamentally overcome two challenges; occlusion and limited workspace, which are the biggest limitations of visual-based MoCap systems as the most preferred in the literature. Therefore, researchers insisted on improving IMU based motion capture and estimation techniques also considering the fact that they are cost-efficient.

In this manner, there has been established several companies which are working on IMU based motion tracking systems, such as; Invensense<sup>10</sup> (Invensense, San Jose, CA, USA), Trivisio<sup>11</sup> (Trivisio, Trier, Germany), Microstrain<sup>12</sup> (Lord Microstrain, Williston, VT, USA) and XSens<sup>13</sup> (Xsens Technologies B.V., Enschede, The Netherlands) and many start-ups. Their target varies from navigation in automated robot cars to attitude estimation for drones and human motion reconstruction. Regardless of the aim, the techniques used in motion estimation based on IMUs should be investigated to plan a path in our study for HME for HRC.

One interesting conjunction between the selected method and application area is the complexity of the motion tracking algorithm. For instance, stability and activity

<sup>10</sup><https://invensense.tdk.com/>

<sup>11</sup><https://www.trivisio.com/inertial-motion-tracking>

<sup>12</sup><https://www.microstrain.com/inertial/IMU>

<sup>13</sup><https://www.xsens.com/>



recognition related studies have simpler algorithms and fewer sensors than human model reconstruction according to [1].

Algorithms vary based on the sensor fusion technique such as filters/observers with Complementary filter (CF), KF, EKF; learning algorithms hidden markov models, neural networks,  $k$ -nearest neighbour, discriminant analysis, random forest etc. Even studies differ from each other although they use the same algorithm yet differ in how the parameters of the algorithms are set. The section of algorithms highly depends on the sensors used; some of them exploit IMUs, but magnetometer signals are not always used and one method requires a visual reference for tracking human upper limbs etc. Moreover, as explained in Section 2.1.1 the complexity of the selected kinematic model of the human body varies a lot. Hence, the selected kinematic model plays a big role, as well. Some studies use Euler angles, some use the Denavit Hartenberg convention and others use quaternions. Finally, they differ in how the constraints of the kinematic chain are considered.

Particularly on human motion analysis using wearable sensors, [119] categorized the techniques based on the focus of the human body as shown in Fig. 2.12. In their comprehensive review study, the researchers classified HME techniques based on the data extraction method and selected algorithm.

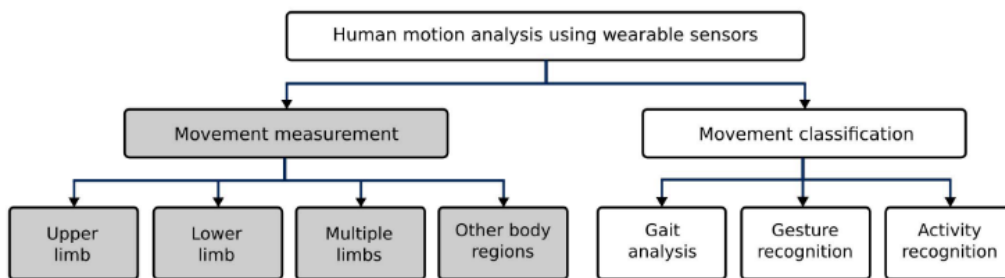


**Fig. 2.12:** Taxonomy of clinical applications of HMA  
Source:[119]

According to [119], 880 HME studies are extracted from databases with keywords: *group 1 ("human motion" OR "human movement") and group 2 ("wearable sensors" OR "inertial sensors" OR "wearable system")*. After a screening process of these 880 publications 37 of them were selected which fully explains the authors' 5 review criteria:

1. the sensor used for the measurement,
2. the measuring motion unit,
3. the sensor fusion algorithms,
4. the evaluation system, and
5. the subjects of study.

According to these 37 publishes selected in [119], (14/37) of them the orientation of a joint was estimated [119] whereas only one study (1/37) estimated individually

the position of a segment and no studies were reported on an individual estimation of the position of a joint. Moreover, (6/37) studies are reported as both position and orientation estimation of a segment or a joint and only one study (1/37) reported both position and orientation estimation for both segments and joints. An outcome of this classification to my study is that orientation estimation of joints and/or segments rather than positions is a good starting point. Also, besides being good per se, estimating the orientation is fundamental in the strap-down approach to position estimation according to [240]. In fact, the orientation solution allows gravity to be cancelled from the acceleration signals so that the inertial acceleration is double-integrated for position estimation (gravity compensation).

Another classification of HME studies is based on the selected algorithm. In [52], six attitude estimation methods using IMUs are compared. It is seen that the Kalman filter, complementary filter and observer theories occupy a big space in this type of estimation problem. Also in [1], 5 different HME techniques are presented and compared based on the accuracy (how reliable the estimated results are with respect to actual values), correlation (indicates whether the estimated position follows the real pattern of the performed movement), the capability of fast motions and source of error.

On the other hand, machine learning algorithms have also gained a substantial reputation in HME studies. For the completeness of the detailed literature review, it is important to highlight them. For instance, in [113], six different machine learning algorithms are compared in which the data is IMU-based wrist load measurement of tennis athletes. They concluded that the combination of miniature inertial sensors and machine learning offers a practical and automated method.

According to these well-categorized in-depth review articles [1, 113, 119], one of the most cited technical reports on using inertial sensors for position and orientation estimation [117] and the studies reviewed through this literature survey in other subsections of this study, some of the most used methods in motion estimation in HME are listed below:

- Algorithm:
  - Estimators:
    - \* Complementary Filter [241–243]
    - \* Kalman Filter [19, 117, 244–248]
    - \* Extended Kalman Filter [31, 117, 249–251]
    - \* Unscented Kalman Filter [166, 252, 253]
    - \* Particle Filter [254, 255]
    - \* Riccati observers [256–258]
  - Learning Algorithms:
    - \* Markov chain [259, 260]
    - \* Hidden Markov Model (Note: derived from Markov chains) [261–263]
    - \* Support Vectors [260, 264]
    - \* Neural networks [265, 266]
    - \* Discriminant analysis [267–269]

## 2.2 Systematic Approach on the IMU Usage and User Training

- \* Support vector machine [260, 262]
- \*  $k$ -nearest neighbor [121, 270]
- \* Random forest [271, 272]
- \* Gaussian mixture model [273]
- Estimators + Learning Algorithms merged [274, 275]
- Mathematical Model:
  - QUEST [276]
  - TRIAD [252]
  - Simple integration [19, 83, 117]
- Representation:
  - Euler-based [277, 278]
  - Rotation matrix based/ DH parameters [279–281]
  - Quaternion based [241, 244, 247, 249, 251, 276, 282]
  - Lie/Euclidean groups [242, 256, 257]

The list above shows that numerous methods exist for HME using IMU. If attention is paid to the dates of the example works, it can be seen that most of them have been published in the last 5 years, which indicates that this field is still open to improvements. A trade-off exists between complexity and efficiency. Often, these two terms change proportionally, such that a more complex system provides better accuracy. However, complexity reduces efficiency and applicability. Since the aim is to use the system for industrial purposes, a system that is as simple as possible, yet highly reliable is sought after.

## 2.2 Systematic Approach on the IMU Usage and User Training

The systematic literature review is conducted to answer the status of HRI in two major aspects:

1. Status of IMUs in HRI
2. Status of training in HRI

The birth of Human-Robot Interaction (HRI) field lies back in the mid-1990s and early years of the 2000s [2]. Therefore, the broad literature search covers the last 30 years. It is aimed to have the first insight into the status of HRI over years, including the subtle aspect of MoCap system used in the human motion tracking/estimation part. Although Google Scholar is not an ideal tool for complex search terms, it is still useful to have an overview of the number of publications in certain domains.

The first set of search keywords are "*human robot*" for exact match and *interaction cooperation collaboration* is at least one match in the advanced search option in Google Scholar. Since we are interested in the status of IMUs in the field and how it is compared

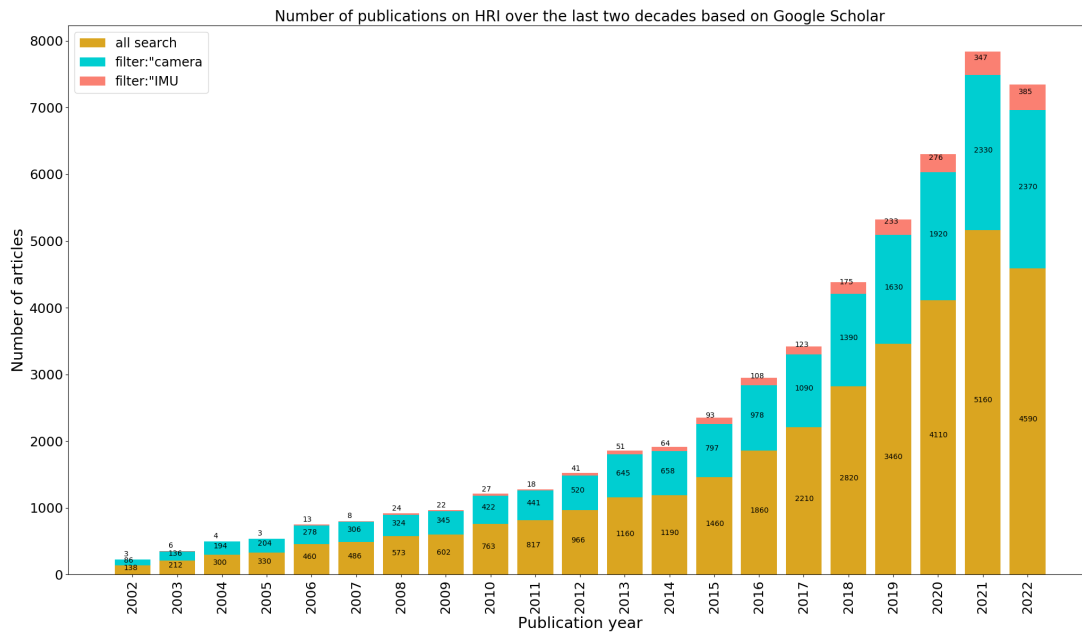


**Fig. 2.13:** Number of publications on HRI over the last two decades based on Google Scholar. The filter keywords are categorized as yellow is unfiltered, blue: camera and pink: IMU. The three numbers in each column show the number of publications in each category respectively.

to the camera-based ones, the search is filtered by adding *imu* and *camera* keyword filters to focus on the MoCap perspective. The number of publications based on these keywords and filters is given in Fig. 2.13.

It is evident that there were not many publications in the early years of the 2000s, and IMUs were barely introduced in this field, as shown in pink colour in Fig. 2.13. Despite the fact that the history of IMU in motion estimation dates back earlier than 2002 (i.e., about 6,310 results are returned by a simple search on *IMU in motion estimation* before 2002), it was not commonly used in the HRI field for quite a long time. A small jump in the number of HRI publications including IMUs was observed around 2015; however, it is still clear that IMUs have never been as popular as cameras in this field. If the focus is readjusted on the camera-included publications in the HRI field (shown in pink colour in Fig. 2.13), it can be seen that the interest in cameras has grown at a similar pace to the total number of publications.

It should be noted that a few publications in the yellow zone of each category are likely to belong to the pink or blue zones, such as publications that use "inertial\*" instead of IMU or "visual\*" instead of the camera. However, these keywords are not as common as the selected ones, so if the publication does not mention the common ones, it will not be captured in our filters. The main purpose of this section is evidently to provide an overview rather than a detailed systematic literature review.

Patents and theses are included in this search, but citations are not. The reason why the number of publications in 2022 is lower than the trend line is that several publications are still under review, as the date of the last update of this literature search was January 9, 2023.

2.2.1 Status of IMUs in HRI

In this section, the methodology of the systematic search and the results are presented. The literature analysis has been computed using 4 electronic library databases until 2022: IEEE Xplore, Web of Science, Scopus and Engineering Village. The main purpose of this section is to have a deeper look at the status of IMU in human motion estimation in HRI field.

The selection of keywords is divided into 3 sub-categories. The first subcategory is related to *human motion/intention estimation*, the second is *robot interaction/collaboration/cooperation/teleoperation*, and the third is *imu/inertial measurement unit*. Additionally, we investigated the pHRI case with *physical* keyword since this is an important criterion for this study. The overall systematic review approach with the applied keywords and boolean combinations are as shown in Fig. 2.14.

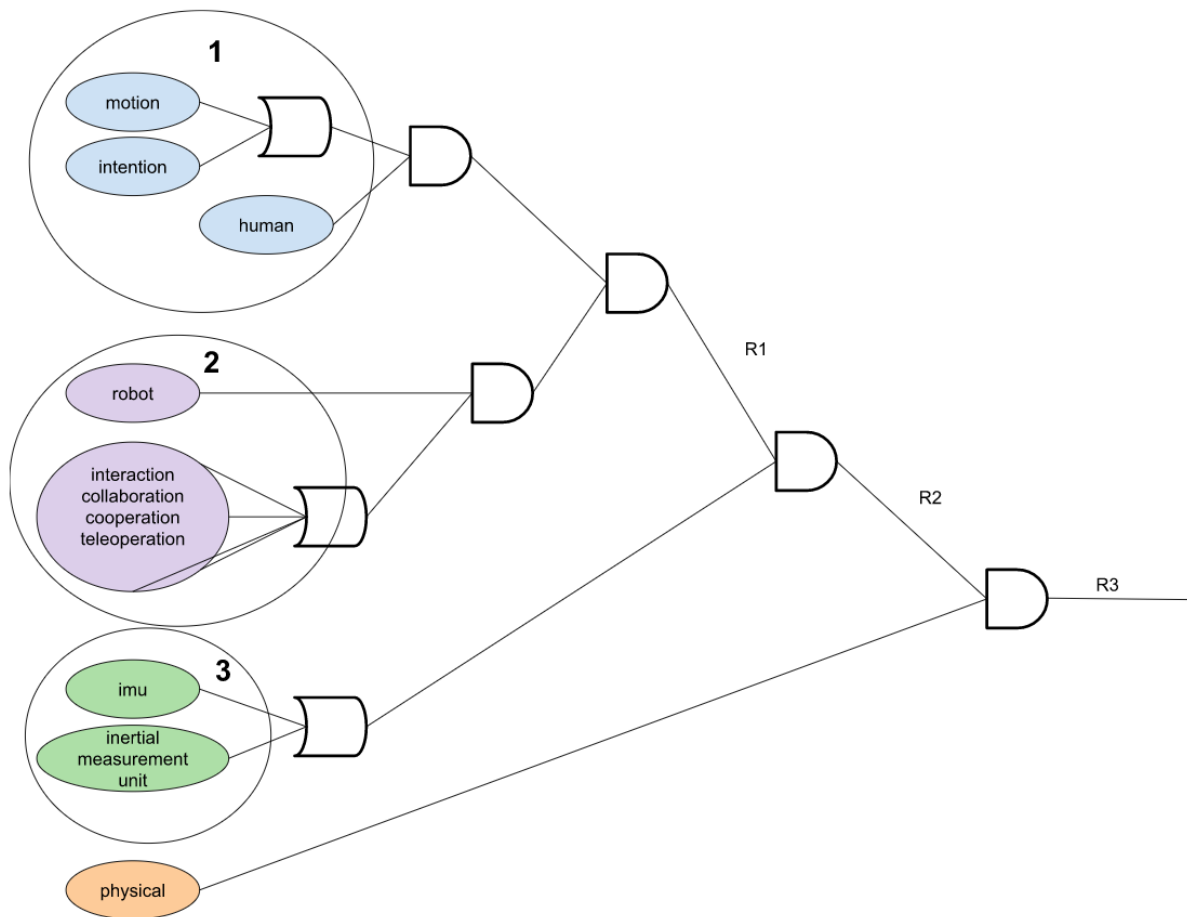


Fig. 2.14: Systematic literature review search keywords and boolean combinations

There are many studies for those individual main fields. First of all, the common studies of human motion estimation/tracking/analysis and HRI are investigated. The results are collected under RESULT-1 (R1). Also for the second part, as it is explained in Chapter 2 in detail, we are interested in IMUs for motion estimation and these are under the RESULT-2 (R2). Finally, the narrowed-down studies where the human and robot are in physical contact are under the RESULT-3 (R3). The number of studies in each result is as shown in Table 2.2.

**Table 2.2:** Systematic literature review results in 4 electronic databases

Library	First found study (year)	Number of studies		
		R1	R2	R3
IEEE Xplore	2007	6579	105	15
Web of Science	2012	2647	47	7
Scopus	2004	8777	144	18
Engineering Village	2008	13264	144	35

### 2.2.2 Status of User Training in HRI

Another research question is related to the status of user training and/or system training. As it is mentioned in Section 1.5, the lack of user training plays a fundamental role in the gap between the HRI research and the successful innovation. In this section, the status of training in this field is investigated. The literature search is performed using three keyword sets.

- 1. The status of training and Serious Games and Gamification (SGG) in the HRI field.** The used keyword set: "human robot" and training as the exact terms match, gamification "game based learning" "serious games" are at least one match.
- 2. The status of all types of user training in the HRI field.** The used keyword set: "human robot" and "user training" as the exact terms match.
- 3. The status of SGG-related user training in the HRI field.** The used keyword set: "human robot" and "user training" as the exact terms match, gamification "game based learning" "serious games" are at least one match.

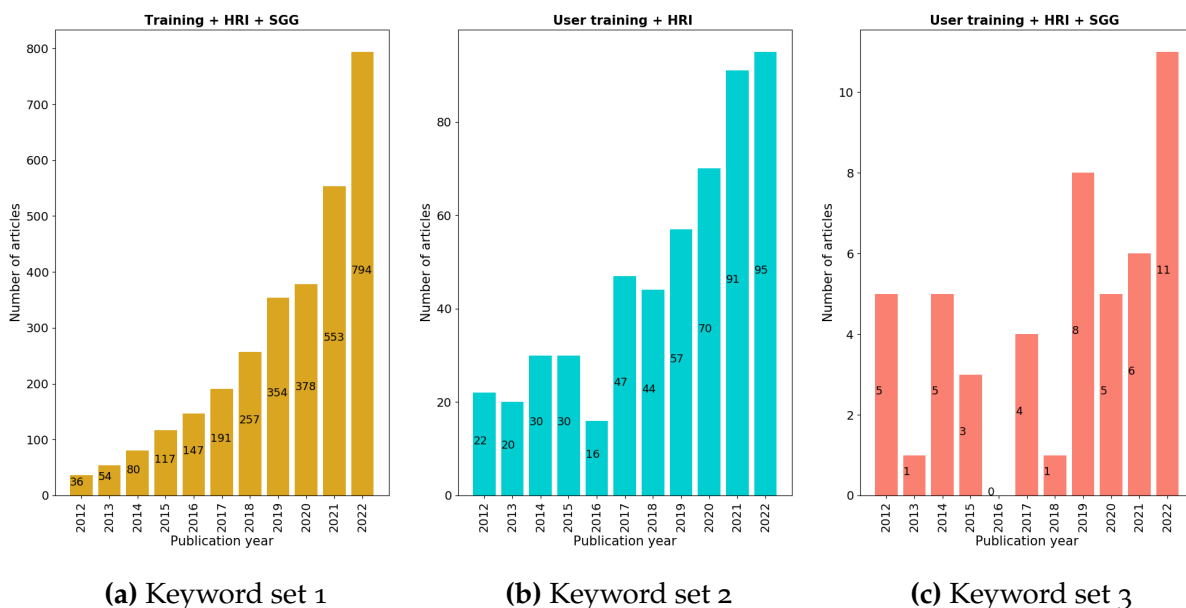


**Fig. 2.15:** Number of publications in user training in HRI in the last decade

## 2.2 Systematic Approach on the IMU Usage and User Training

The results are given in Fig. 2.15.

There is an ambiguity in referring to "training" in the literature. There are three main training concepts related to HRI field which showed up in Fig. 2.15a. One is what we are interested in where the humans are trained in learning the functionality of the developed HRI system. The second is related to training humans in learning new skills using robots and serious games such as rehabilitation, education with robots, assessing and improving autism spectrum disorder etc. The third is related to the training of a machine learning algorithm in developing the HRI system. By adding the filter related to SGG, a big portion of the third category is eliminated but it is still the first and second category is blended. Although the first subplot in Fig. 2.15 does not give many relevant numbers on what we are looking for, it is still important to have an overview of the number of publications where HRI and SGG fields are merged and a learning evaluation is computed in some sort of training concept. The numbers are not very high compared to a well-researched field until around 2017/2018 but the increase is promising in the last 5 years. This trend shows us it is a hot topic in academia, currently.

When the search is narrowed down to user training, the numbers drop drastically. Although the numbers until around 2016 are close between Fig. 2.15a and Fig. 2.15b, they diverge significantly. An important conclusion is that other types of training concepts (such as skill training, system algorithm training etc.) gained comparably more interest than the actual user training of the system. This divergence clearly shows that user training is a gap in the HRI field.

Particularly with the usage of SGG and game-based learning, there is only a scarce amount of publications. SGG is reported to be an effective and often better training experience than the conventional methods in various fields such as in health [283, 284], language and culture training [285], business [286], military [287] etc.

Serious Games and simulations can be used to create supplemental learning tools that are engaging with interactive learning opportunities and can provide visualization of the concepts that make them easier to translate knowledge [48, 49]. It is statistically proven that serious games are more effective than conventional instruction methods [53]. Developing technology makes the game-making process easier, and the produced games become more realistic, immersive, engaging, effective etc.

For objectiveness, it is important to highlight the drawbacks of the SGG. A well-cited review article about SGG in various fields presents the advantages and disadvantages of these teaching methods [47, 288]. The main advantages are listed as improving psychomotor skills, visual selective attention, motivated learning experience and better improvement compared to conventional methods whereas the main disadvantages are the violence in games, the cost of developing serious games and the current unreliable evaluation methods of effectiveness. For instance, one study scientifically proves that learning via serious games depends on the culture ( $r=0.667$  strong), ethnicity ( $r=0.842$  very strong), native language ( $r=0.754$  strong), motivation to learn ( $r=0.752$  strong) [289]. On the other hand, [286] found no significant difference in gender or ethnicity in learning via SGG but only the age factor has significance such that those who are younger than 40 scores significantly higher. Ryan Wang et. al presented earnest concerns of serious games in training health care professionals mainly due to the cost and unreliable effectiveness measures.[290].

## *State of the Art*

To sum up, SGG is a highly interdisciplinary and intricate area. There is not a concrete enough methodology to develop serious games and evaluate their effectiveness. Each field might require its own approach in involving SGG in the most effective way. The main reason for the concerns and the contradictions in the publications are related to this. Therefore, it is indigent for proper research in HRI training.



## BACKGROUND

---

In this chapter, it is aimed to provide a sufficient background related to what is presented in methodology (Chapter 4) and the published papers for the readers to grasp the ideas clearly. The aim of this chapter is not to "teach" anything new, it is a brief reminder of theoretical concepts.

In the first section, robot kinematics are explained. Both the human model and the robot model are defined as kinematic chains. Since the developed methodology is on real-time bases, it is important to know the different approaches to select the optimal and most reliable method.

The second section describes the human motion types in general terms. Afterwards, it explains how the human body can be defined using terms in the robotics field so that a meaningful human input can be generated for HRC.

The third section is about probability theory which draws an important baseline for both HME and human-robot experiments. The most fundamental terms are explained such as random variable, expected value, distribution function, mean and variance. These terms are then used in explaining Bayes filters and statistical tests.

In the fourth section, statistical testing methods are described. It is highlighted how a statistical test is chosen based on the data type and the most common statistical tests are explained.

### 3.1 Fundamentals of Kinematics

*Kinematics* is the study in robotics that finds a mathematical relationship between each link's position, velocity and acceleration of a robot. The connection points between the two links are called *joints*. Those joints can be actuated (by a motor), passive (free to move in at least one direction/axis) or rigid (no motion is allowed). Therefore, the aim of kinematics is that by knowing the link lengths and the properties of the joints robot motion planning and control can be computed.

Two main terms in robot kinematics are *translation* and *rotation*. The translation is the position change of the robot without changing its heading direction. On the other hand, rotation is the orientation change of the robot without changing the location. In an action of a robot, those two motion types generally occur synchronously. Kinematics seeks a solution of the link relations which is valid for the whole of the action time.

A *pose* is a term which is used to describe the position and the orientation of the robot, or just a part of the robot. In three-dimensional space, 6 independent variables

## Background

are required to be able to fully define the pose. In robotics, three of those 6 independent variables are related to the position of the robot and the other three are related to the orientation with respect to an origin frame (reference frame).

To completely describe the pose of a rigid object in a 3-dimensional world, 6 parameters are needed: 3 to describe its position and 3 to describe its orientation. Orientation changes by rotational motion, and position changes by translational motion. As a result, *pose* change is observed. So the pose change has two components: rotation and translation.

The position and orientation of the end-effector of a robot manipulator with respect to its base frame have to be calculated for every task. The robot is defined as a *kinematic chain* and using link lengths and joint angles, the respective pose of the end-effector is calculated.

The human body can be considered a sophisticated kinematic chain. It can be modelled as if it was a robotic structure which has revolute and/or linear actuators on the joints and consists of rigid links as body parts despite some modelling error. The human arm, for example, can be considered a robot manipulator. In fact, a lot of the robotic designs as well as many scientific improvements are bio-inspired (See Festo's bionic robots<sup>1</sup>).

### 3.1.1 Parametrizing Rotation

The main target of this study is those who have general knowledge of mechanics in physics. Therefore, the definition of position, velocity, acceleration, jerk, force, torque etc. and the relationship between those terms are assumed to be known. A more comprehensive knowledge can be obtained in [291] mainly in section 2.8.

Motion creates pose changes. The pose change is defined as a change with respect to a *reference frame*. The representation of this change varies. This section explains how rotations and translations are defined and used in robotics. For roboticists, Euler sequences, rotation vectors, and rotation matrices are quite familiar representations. The quaternion representation may be less familiar and intuitive than the others. Due to this reason and the fact that quaternions are the most used representation type in this study, the emphasis is more on quaternions than the other representations.

There are a number of different representations of rotations and translations [292]. It is useless to touch upon all of them in this chapter. The main features of the parametrizations that take a place in this study to represent an orientation are summarized in Table 3.1

**Table 3.1:** Main characteristics or parameterization of rotation

Representation	# of parameters	Continuous	Non-Singular
Euler Sequences	3	✗	✗
Rotation Matrix	9	✓	✓
Axis-Angle	4-6	✗	✗
Unit Quaternion	4	✓	✓

<sup>1</sup><https://www.festo.com/group/en/cms/10156.htm>

### 3.1.1.1 Rotation using Euler Sequences

Orientation in 3D space requires at least 3 independent parameters to be fully defined. The orientation of an object can be defined as a rotation around 3 orthogonal axes with respect to an initial frame. Euler angles, which are first presented by Leonhard Euler in 1775 to define a spherical geometry, are a set of three angles to represent a full rotation about these three orthogonal axes respectively. The geometrical representation of Euler angles are presented in Fig. 3.1.

The consecutive order in which the three rotations are done is important. The general terminology of defining an Euler sequence is such that:

1. about the  $x$ ,  $y$ , or  $z$ -axis of the fixed frame or the  $x'$ ,  $y'$ , or  $z'$  of the mobile frame, by  $\alpha$  (or  $\theta$ ) degrees,
2. about the  $x$ ,  $y$ , or  $z$  axis of the fixed frame or the  $x'$ ,  $y'$ , or  $z'$  of the mobile frame, by  $\beta$  (or  $\phi$ ) degrees,
3. about the  $x$ ,  $y$ , or  $z$  axis of the fixed frame or the  $x'$ ,  $y'$ , or  $z'$  of the mobile frame, by  $\gamma$  (or  $\psi$ ) degrees.

According to that, there are 216 ( $6^3$ ) possible ways. For instance,  $x \rightarrow y \rightarrow z$ ,  $y \rightarrow y \rightarrow z$ ,  $z \rightarrow y \rightarrow z$ ,  $x' \rightarrow y \rightarrow z$ ,  $y' \rightarrow y \rightarrow z$ ,  $z' \rightarrow y \rightarrow z$ , and so on. Some of those sequences do not define a full orientation (i.e. rotation about the same axis consecutively). Therefore only 12 meaningful ordered Euler sequences exist to describe a general orientation:  $XYX$ ,  $XYZ$ ,  $XZX$ ,  $XZY$ ,  $YXY$ ,  $YXZ$ ,  $YZX$ ,  $YZY$ ,  $ZXY$ ,  $ZXZ$ ,  $ZYX$ ,  $ZYZ$ .

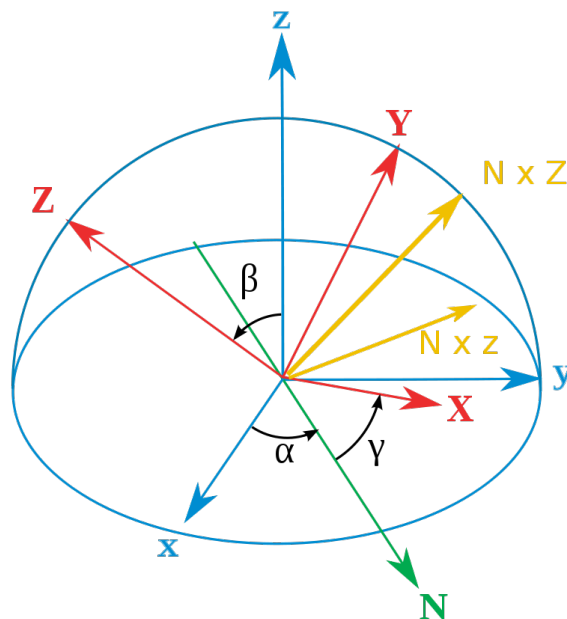


Fig. 3.1: Geometrical representation of Euler angles  
Source:[293]

Some Euler sequences are used more than others for consistency in the field. In robotics XYZ (roll-pitch-yaw) or in aerospace ZYZ sequences are mostly used. In fact, neither of the Euler sequences is better than the other in performance. However, one can be preferred over the others in some cases. This is mostly when a system's structure allows rotation in all 3 axes for all angles  $[-\pi, \pi]$ .

## Background

Let's think about the case where there is a mobile robot on a z-axis normal plane. Also, let's assume that the orientation of the mobile robot (i.e. the frame of its body) is represented in the ZYX Euler sequence. Assuming that a B- frame is rotated by  $(\psi, \theta, \phi)$  with respect to the A-frame, the sequence is expressed as:

$$\begin{aligned} R^{A,B} &= R^{A,B}(\bar{u}_1, \phi) R^{A,B}(\bar{u}_2, \theta) R^{A,B}(\bar{u}_3, \psi) \\ &= \begin{bmatrix} 1 & 0 & 0 \\ 0 & \cos \phi & \sin \phi \\ 0 & -\sin \phi & \cos \phi \end{bmatrix} \begin{bmatrix} \cos \theta & 0 & -\sin \theta \\ 0 & 1 & 0 \\ \sin \theta & 0 & \cos \theta \end{bmatrix} \begin{bmatrix} \cos \psi & \sin \psi & 0 \\ -\sin \psi & \cos \psi & 0 \\ 0 & 0 & 1 \end{bmatrix} \end{aligned} \quad (3.1)$$

where the following definitions of the unit vectors  $\mathcal{F}|_A$  are:

$$\bar{u}_1 = [1 \ 0 \ 0]^T, \quad \bar{u}_2 = [0 \ 1 \ 0]^T, \quad \bar{u}_3 = [0 \ 0 \ 1]^T.$$

Using Euler sequences is probably the most intuitive way of representing a rotation. However, there is an inevitable problem in using Euler sequences in full rotation: Gimbal lock. See Fig. 3.2[294]. It is a demonstration of what is mathematically explained above. The red circle shows pitch rotation, the green circle shows yaw rotation and the blue shows the roll rotation. At the time when the yaw rotation reaches  $\frac{\pi}{2}$  or  $-\frac{\pi}{2}$ , the red and green circles coincide. Therefore, any rotation either on pitch or roll will give the same results. This is a singularity point of this system, which is widely named as *Gimbal Lock*.

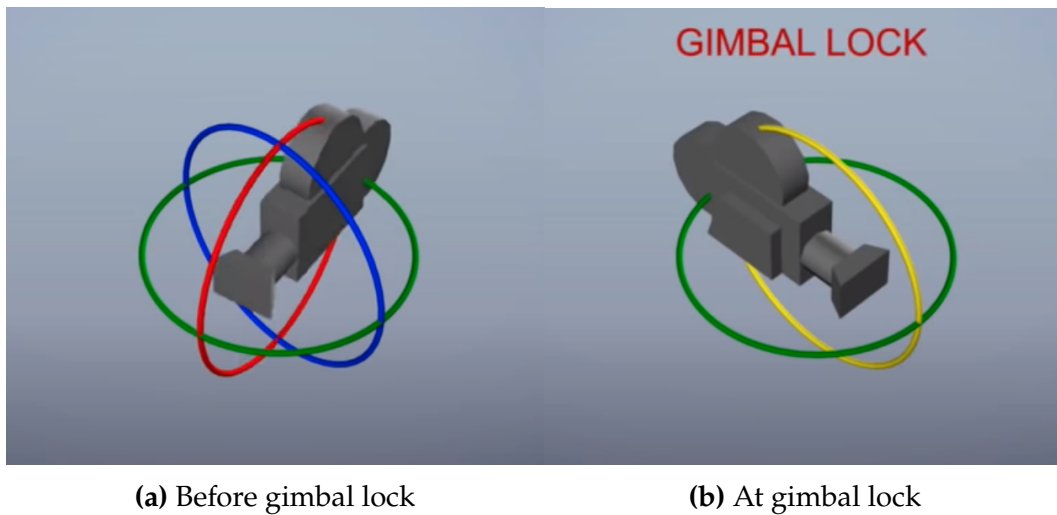


**Fig. 3.2:** Gimbal lock example  
Source: [294]

The Gimbal lock is inevitable in 3D rotation representation using Euler sequences. Based on the system, it can be tweakable. The rule of thumb in using Euler sequences in the representation of rotation is that one should always choose the middle axis as the less likely to compute full rotation in  $[-\pi, \pi]$ . In the case where the gimbal lock is shown in Fig. 3.2, it is more likely that the camera has a horizontal shot than a vertical shot. I.e the camera would less likely have a full rotation around X than Y or Z.

Therefore, any Euler sequence which doesn't set the X-axis as the middle axis would perform without a gimbal lock.

Three ways of quitting the gimbal lock are; one to use a redundant gimbal axis (a fourth axis) which is actively driven by a motor to maintain a large angle between roll and yaw gimbal axes as in the aviation field. Secondly is to lock the system or warn the user when it is approaching a gimbal lock. And third is not to use Euler sequences in systems where a gimbal lock is likely on all 3 axes.

### 3.1.1.2 Rotation Matrix

The rotation matrix is a mapping function of one coordinate frame rotated with respect to another coordinate frame. We have already encountered rotation matrices in explaining Euler sequences. The Eq. (3.1) is, in fact, the multiplication of three rotation matrices. As a definition, a rotation matrix,  $R$  is a  $3 \times 3$  which is a special orthogonal group  $SO(3)$  and thereby has the following special properties:

$$RR^T = R^T R = I_3, \quad \det[R] = 1 \quad (3.2)$$

Multiplication of two or more rotation matrices gives another rotation matrix. Following the Euler sequence expression, the result of Eq. (3.1) is:

$$\begin{aligned} R_{ZYX} &= \\ R^{A,B} &= \begin{bmatrix} \cos \theta \cos \psi & \cos \theta \sin \psi & -\sin \theta \\ \sin \phi \sin \theta \cos \psi - \cos \phi \sin \psi & \sin \phi \sin \theta \sin \psi + \cos \phi \cos \psi & \sin \phi \cos \theta \\ \cos \phi \sin \theta \cos \psi + \sin \phi \sin \psi & \cos \phi \sin \theta \sin \psi - \sin \phi \cos \psi & \cos \phi \cos \theta \end{bmatrix} \\ &= \begin{bmatrix} r_{11} & r_{12} & r_{13} \\ r_{21} & r_{22} & r_{23} \\ r_{31} & r_{32} & r_{33} \end{bmatrix} \end{aligned} \quad (3.3)$$

where  $r_{11}, \dots, r_{33}$  are the indexes of  $R$ .

Different from Euler sequences, rotation matrices can represent any angle rotation about any real axis using a single  $3 \times 3$  matrix. That's why rotation matrices do not suffer from Gimbal lock.

#### Multiple Rotations:

In a motion, when the rotation does not compute only in a single axis and there is a cascaded rotation, or if there is a kinematic model that frames are connected to each other as a chain, any situation as shown in Fig. 3.3, the resultant rotation matrix  $R^{A,C}$  is a matrix multiplication:

$$R^{A,C} = R^{A,B} R^{B,C} \quad (3.4)$$

There are various ways of creating a rotation matrix. The two most common ways are using the multiplication of Euler sequences and using direction cosines. The Euler sequence method is already explained. The transformation from rotation matrix to Euler angles is by using the equivalence of two matrices in Eq. (3.3). Each index of

## Background

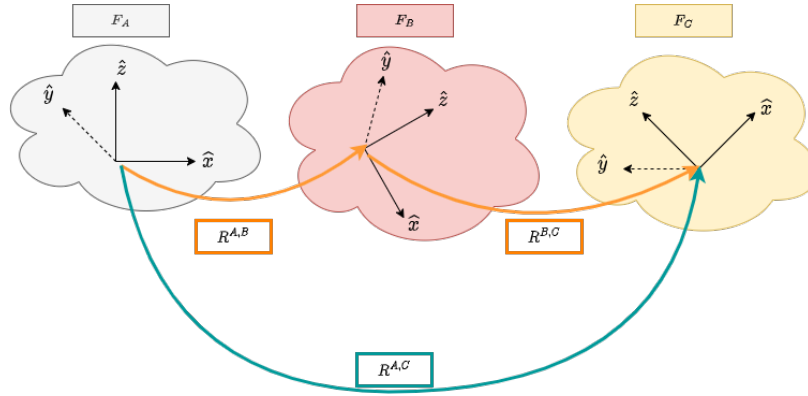


Fig. 3.3: Multiple frame rotations.  $\mathcal{F}|_A$

the rotation matrix  $r_{11}, \dots, r_{33}$  has an equivalent trigonometric relation of the rotation angles based on the Euler sequence used. Thereby the rotation order has to be known. Since ROS tf . transformations (ROS TF) library is used for Euler angles  $\Leftrightarrow$  rotation matrix, the calculation details are outside the scope of this study.

Direction cosines, on the other hand, create the *columns* of the rotation matrix in regard to the basis vectors of the stable and rotating frames.

Let's think about two frames,  $\mathcal{F}|_A$  and  $\mathcal{F}|_B$  which are initially coincident and their unit vectors are  $\hat{u}_1^A, \hat{u}_2^A, \hat{u}_3^A$  and  $\hat{u}_1^B, \hat{u}_2^B, \hat{u}_3^B$ , on axes x-y-z respectively. A rotation about the y-axis is applied as shown in Fig. 3.4.

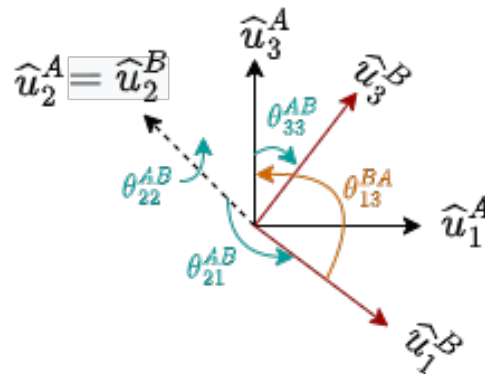


Fig. 3.4: Direction cosine angles example demonstration

where the element in the  $i^{\text{th}}$  row and the  $j^{\text{th}}$  column represents the angle between the axis- $i$  of the reference frame and the axis- $j$  of the body frame.

$$R^{A,B} = \begin{bmatrix} \cos \theta_{11}^{A,B} & \cos \theta_{12}^{A,B} & \cos \theta_{13}^{A,B} \\ \cos \theta_{21}^{A,B} & \cos \theta_{22}^{A,B} & \cos \theta_{23}^{A,B} \\ \cos \theta_{31}^{A,B} & \cos \theta_{32}^{A,B} & \cos \theta_{33}^{A,B} \end{bmatrix} = [\bar{u}_1^{(B/A)} \mid \bar{u}_2^{(B/A)} \mid \bar{u}_3^{(B/A)}] \quad (3.5)$$

where  $\cos \theta_{ij}^{A,B}$  is the cosine of the angle between  $i^{\text{th}}$  axis of frame A and  $j^{\text{th}}$  axis of

frame B. Moreover,  $\mathbf{u}_i^{(B/A)}$  is the unit vector of frame B, represented in frame A.

Lastly, to find the angle between two axes in frames, the necessary unit vectors are pre-multiplied and post-multiplied by the rotation matrix:

$$\theta_{ij}^{A,B} = \arccos(\bar{\mathbf{u}}_i^T \mathbf{R}^{A,B} \bar{\mathbf{u}}_j) \quad (3.6)$$

### Zero Rotation

Zero rotation is defined by  $3 \times 3$  identity matrix.

$$\mathbf{R}^{A,A} = \begin{bmatrix} 1 & 0 & 0 \\ 0 & 1 & 0 \\ 0 & 0 & 1 \end{bmatrix} \quad (3.7)$$

that satisfies:

$$\mathbf{R}\mathbf{R}^{-1} = \mathbf{R}\mathbf{R}^T = \mathbf{R}^{A,B}\mathbf{R}^{B,A} = \mathbf{I}_3 \quad (3.8)$$

### Rotating a Vector:

The bar representation of vector  $\vec{\mathbf{v}}$  in  $\mathcal{F}|_A$  is  $\bar{\mathbf{v}}^A$  defined in frame A. It is expressed in reference frame B by pre-multiplying the vector by the rotation matrix  $\mathbf{R}^{A,B}$  as:

$$\bar{\mathbf{v}}^B = \mathbf{R}^{A,B}\bar{\mathbf{v}}^A \quad (3.9)$$

•Note that rotation matrix representation is one of the most used orientation representations in robotics. It is both intuitive and non-singular. However, there are many redundant matrix elements which are not used for any calculations. Therefore, they are not the most computationally efficient method.

### 3.1.2 Rotation Vector (Axis-Angle)

The most famous axis-angle rotation formula is derived by Olinde Rodrigues known as *Rodrigues' rotation formula*. It says that if  $\vec{\mathbf{v}}$  is a vector in 3D space and  $\vec{\mathbf{k}}$  is a unit vector describing an axis of rotation about which rotates by an angle  $\theta$  according to the right-hand rule (see Fig. 3.5), the Rodrigues formula for the rotated vector  $\vec{\mathbf{v}}_{\text{rot}}$  is:

$$\vec{\mathbf{v}}_{\text{rot}} = \vec{\mathbf{v}} \cos \theta + (\vec{\mathbf{k}} \times \vec{\mathbf{v}}) \sin \theta + \vec{\mathbf{k}}(\vec{\mathbf{k}} \cdot \vec{\mathbf{v}})(1 - \cos \theta) \quad (3.10)$$

Angle-axis representation is more useful when two vectors defining a plane are involved. In this study, this representation is not used in the methodology, that's why details in deviation are not given here. However, it is important to mention them to understand the quaternion representation better in the following subsection.

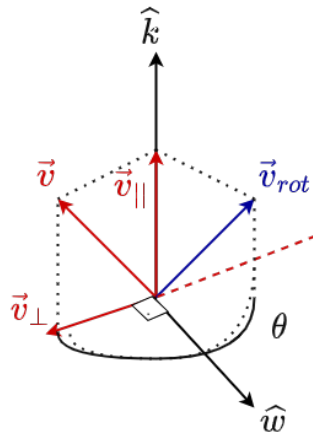


Fig. 3.5: Demonstration of an axis-angle rotation

### 3.1.2.1 Rotation with Quaternions

Every morning in the early part of October 1843, on my coming down to breakfast, your brother William Edwin and yourself used to ask me: "Well, Papa, can you multiply triples?" Whereto I was always obliged to reply, with a sad shake of the head, "No, I can only add and subtract them."

*from a letter Hamilton wrote to his son Archibald*

Quaternions are a number system proposed as an extension of complex numbers. In the 1800s, William Rowan Hamilton, an Irish mathematician, was looking for symmetry in the mathematical operations of complex numbers. The fact that the points in space can be represented, added and subtracted easily in 3D space but the multiplication operation was missing.

According to [295], on October 16, 1843, Hamilton was enlightened on his walk with his wife. He got the idea that the multiplication of "triples" was not possible. Instead, they *had to be* "quadruples". Then he wrote his famous quote (Fig. 3.6) attaching his brilliant idea on Brougham Bridge, Dublin:

*Here as he walked by on the 16th of October 1843 Sir William Rowan Hamilton in a flash of genius discovered the fundamental formula for quaternion multiplication*

$$i^2 = j^2 = k^2 = ijk = -1$$

*cut it on a stone of this bridge. (See Fig. 3.6)*

This finding has opened a door in theoretical and applied algebra. Quaternions have been started to be used in pure mathematics and applied mathematics. Thereby, they gained fame, particularly for calculations involving three-dimensional rotations. The advantages over Euler sequences are that they do not suffer from Gimbal lock, over rotation matrices that they are more computationally efficient (rotation matrix has 9 parameters to describe a full rotation whereas quaternions need only 4) and over rotation vectors the computation is faster since fewer steps are required.





Fig. 3.6: Hamilton's complex number multiplication  
Source: [295]

The following part of this section is to provide the reader with the necessary knowledge about quaternions to comprehend this study. More can be found in [296, 297].

#### Representation:

A quaternion is represented using 4 parameters:

$$q = q_4 + q_1\hat{i} + q_2\hat{j} + q_3\hat{k} = \begin{bmatrix} q_4 \\ \vec{q} \end{bmatrix} \quad (3.11)$$

where the parameter  $q_4$  is called as the *real* or *scalar* part, and  $q_1\hat{i} + q_2\hat{j} + q_3\hat{k} = \vec{q}$  is called as the *imaginary* or *vector* part of the quaternion. All 4 parameters of a quaternion are correlated with the following rule:

$$\vec{q} = \begin{bmatrix} k_x \sin\left(\frac{\theta}{2}\right) \\ k_y \sin\left(\frac{\theta}{2}\right) \\ k_z \sin\left(\frac{\theta}{2}\right) \end{bmatrix} = \hat{k} \sin\left(\frac{\theta}{2}\right), \quad q_4 = \cos\left(\frac{\theta}{2}\right) \quad (3.12)$$

#### Unit Quaternion:

Unit quaternions can be used to represent a rotation. A quaternion can be any number in a 4D space yet not all quaternions are directly used in orientation representation. In a rotation, the size of the vector must remain the same. So, a quaternion is a unit quaternion if it satisfies:

## Background

$$|\bar{q}| = \sqrt{\bar{q}^T q} = \sqrt{|q|^2 + q_4^2} \quad (3.13)$$

### Identity Quaternion:

Based on the definition of unit quaternion, the *identity quaternion* corresponds to "no rotation" whose magnitude is also equal to  $|q_1| = 1$ :

$$q_1 = 1 + 0\hat{i} + 0\hat{j} + 0\hat{k} \quad (3.14)$$

### Pure Quaternion:

Pure quaternions are used in representing a 3D vector in the 4D space. It has no component in the real part and the vector value represents the imaginary part of the quaternion. Assuming a vector in 3D space defined as  $\vec{v} = a\hat{x} + b\hat{y} + c\hat{z}$ , the quaternion representation of this vector  $\vec{v}$ :

$$q_x = 0 + a\hat{i} + b\hat{j} + c\hat{k} \quad (3.15)$$

### Quaternion Multiplication:

Assuming  $\bar{q}$  and  $\bar{p}$  are quaternions. The quaternion multiplication is defined as:

$$\begin{aligned} q \otimes p &= (q_4 + q_1\hat{i} + q_2\hat{j} + q_3\hat{k})(p_4 + p_1\hat{i} + p_2\hat{j} + p_3\hat{k}) \quad (3.16) \\ &= q_4p_4 - q_1p_1 - q_2p_2 - q_3p_3 + (q_4p_1 + q_1p_4 - q_2p_3 + q_3p_2)\hat{i} \\ &\quad + (q_4p_2 + q_2p_4 - q_3p_1 + q_1p_3)\hat{j} + (q_4p_3 + q_3p_4 - q_1p_2 + q_2p_1)\hat{k} \\ &= \begin{bmatrix} q_4p_1 + q_3p_2 - q_2p_3 + q_1p_4 \\ -q_3p_1 + q_4p_2 + q_1p_3 + q_2p_4 \\ q_2p_1 - q_1p_2 + q_4p_3 + q_3p_4 \\ -q_1p_1 - q_2p_2 - q_3p_3 + q_4p_4 \end{bmatrix} \end{aligned}$$

The quaternion multiplication can alternatively be written in matrix form. For this, the matrix notation for the cross-product using the skew-symmetric matrix operator  $[q \times]$ , defined as:

$$[q \times] = \begin{bmatrix} 0 & -q_3 & q_2 \\ q_3 & 0 & -q_1 \\ -q_2 & q_1 & 0 \end{bmatrix} \quad (3.17)$$

Then the cross-product can be written as:

$$\mathbf{q} \otimes \mathbf{p} = \begin{vmatrix} \hat{i} & \hat{j} & \hat{k} \\ q_1 & q_2 & q_3 \\ p_1 & p_2 & p_3 \end{vmatrix} = \begin{bmatrix} p_2 p_3 & -q_3 p_2 \\ q_3 p_1 & -q_1 p_3 \\ q_1 p_2 & -q_2 p_1 \end{bmatrix} = \begin{bmatrix} 0 & -q_3 & q_2 \\ q_3 & 0 & -q_1 \\ -q_2 & q_1 & 0 \end{bmatrix} \begin{bmatrix} p_1 \\ p_2 \\ p_3 \end{bmatrix} = [\mathbf{q} \times] \mathbf{p} \quad (3.18)$$

Therefore, the quaternion multiplication is:

$$\begin{aligned} \mathbf{q} \otimes \mathbf{p} &= \begin{bmatrix} q_4 & q_3 & -q_2 & q_1 \\ -q_3 & q_4 & q_1 & q_2 \\ q_2 & -q_1 & q_4 & q_3 \\ -q_1 & -q_2 & -q_3 & q_4 \end{bmatrix} \begin{bmatrix} p_1 \\ p_2 \\ p_3 \\ p_4 \end{bmatrix} \\ &= \underbrace{\begin{bmatrix} q_4 \mathbf{I}_{3 \times 3} - [\bar{\mathbf{q}} \times] & \bar{\mathbf{q}} \\ -\mathbf{q}^T & q_4 \end{bmatrix}}_{\mathcal{L}(\mathbf{q})} \underbrace{\begin{bmatrix} \bar{\mathbf{p}} \\ p_4 \end{bmatrix}}_{\bar{\mathbf{p}}} \end{aligned} \quad (3.19)$$

or equivalently:

$$\begin{aligned} \mathbf{q} \otimes \mathbf{p} &= \underbrace{\begin{bmatrix} q_4 \mathbf{I}_{3 \times 3} - [\bar{\mathbf{q}} \times] & \bar{\mathbf{q}} \\ -\mathbf{q}^T & q_4 \end{bmatrix}}_{\mathcal{R}(\mathbf{p})} \underbrace{\begin{bmatrix} \bar{\mathbf{p}} \\ p_4 \end{bmatrix}}_{\bar{\mathbf{q}}} \\ &= \begin{bmatrix} p_4 & -p_3 & p_2 & p_1 \\ p_3 & p_4 & -p_1 & p_2 \\ -p_2 & p_1 & p_4 & p_3 \\ -p_1 & -p_2 & -p_3 & p_4 \end{bmatrix} \begin{bmatrix} q_1 \\ q_2 \\ q_3 \\ q_4 \end{bmatrix} \end{aligned} \quad (3.20)$$

Hence;

$$\mathcal{L}(\mathbf{q})\bar{\mathbf{p}} = \mathcal{R}(\mathbf{p})\bar{\mathbf{q}}$$

also  $\mathcal{L}$  and  $\mathcal{R}$  has the property:

$$\begin{aligned} \mathcal{L}(\mathbf{q}^{-1}) &= \mathcal{L}^T(\mathbf{q}) \\ \mathcal{R}(\mathbf{p}^{-1}) &= \mathcal{R}^T(\mathbf{p}) \end{aligned}$$

•Note that quaternion multiplication is not commutative.

### Quaternion Inverse:

After defining the identity quaternion and the multiplication operation in quaternions, we can define the inverse of a quaternion. In any number system, the inverse of a number over a defined operation in this system is the number that returns the identity element. It works exactly the same in quaternions.

## Background

$$q \otimes q^{-1} = q^{-1} \otimes q = q_I$$

Instead of getting into complex calculations to find  $q^{-1}$  for unit quaternions, we can consider the definition of quaternions in an intuitive way. A quaternion has a vectorial and a non-vectorial part; similar to axis-angle representation. Different than axis-angle representation  $(\theta, \vec{v})$  or  $[(\theta_x, \theta_y, \theta_z), (v_x, v_y, v_z)]$ , the parameters in quaternions depend on each other. That's why the *rotation axis* in units and the *rotation angle* in radians are not clear. Nevertheless, it is there. Let's have a look at the quaternion representation:

$$q = \begin{bmatrix} q_4 \\ \bar{q} \end{bmatrix} = \begin{bmatrix} \cos\left(\frac{\theta}{2}\right) \\ \bar{k} \sin\left(\frac{\theta}{2}\right) \end{bmatrix} \quad (3.21)$$

This definition is more clear to see that the quaternion  $q$  defines  $\theta$  radians rotation about axis  $\hat{k}$ . Here it is represented in bar form  $\bar{k}$ . A rotation in the opposite direction to such a rotation *has to* give the inverse of the quaternion  $q$ . Therefore, either taking the axis  $\hat{k}$  in the opposite direction or defining the rotation as  $-\theta$  radians must give  $\bar{q}^{-1}$ .

$$q^{-1} = \begin{bmatrix} q_4 \\ -\bar{q} \end{bmatrix} = \begin{bmatrix} \cos\left(-\frac{\theta}{2}\right) \\ \bar{k} \sin\left(\frac{\theta}{2}\right) \end{bmatrix} = \begin{bmatrix} \cos\left(\frac{\theta}{2}\right) \\ \bar{k}(-\sin\left(\frac{\theta}{2}\right)) \end{bmatrix} = \begin{bmatrix} \cos\left(\frac{\theta}{2}\right) \\ -\bar{k} \sin\left(\frac{\theta}{2}\right) \end{bmatrix} = q_4 - q_1 \hat{i} - q_2 \hat{j} - q_3 \hat{k} \quad (3.22)$$

To simplify the quaternion inverse for robotics is vital. Since a vector rotation using quaternions require both left and right multiplication in each rotation, the inverse of a quaternion *has to* be used in every rotation process.

Similar to rotation matrix inverse property as its transpose  $C^{-1} = C^T$ , the inverse of a unit quaternion is also represented as its *conjugate*:

$$q^{-1} = q^* \quad (3.23)$$

The simplified path to find the inverse of a quaternion is valid only for unit quaternions. In the general approach, the magnitude of the quaternion must be considered in finding its inverse:

$$q^{-1} = \frac{q^*}{|q|} = \frac{q_4 - q_1 \hat{i} - q_2 \hat{j} - q_3 \hat{k}}{\sqrt{q_4^2 + q_3^2 + q_2^2 + q_1^2}} \quad (3.24)$$

**Rotating a Vector via Quaternions:**

A vector in three-dimensional space can be expressed as a pure quaternion as mentioned. Assuming the quaternion  $q^R$  with the additional requirement that its norm  $|q^R|$  be equal to 1 represents a rotation. A rotation of a vector  $\vec{v}_A = (v_x, v_y, v_z)$  from one coordinate frame  $A \mathcal{F}|_A$  to another frame  $B \mathcal{F}|_B$  is given by the conjugation operation:

$$q^B = q^R q^A q^{R*} \tag{3.25}$$

where  $q^A$  is a pure quaternion derived from  $\vec{v}^A$  such that  $q^A = 0 + v_x \hat{i} + v_y \hat{j} + v_z \hat{k}$ . Therefore,

$$\begin{aligned} q^R q^A q^{R*} &= (q_0 + q_1 \hat{i} + q_2 \hat{j} + q_3 \hat{k})(x \hat{i} + y \hat{j} + z \hat{k})(q_0 - q_1 \hat{i} - q_2 \hat{j} - q_3 \hat{k}) \tag{3.26} \\ &= (v_x(q_0^2 + q_1^2 - q_2^2 - q_3^2) + 2v_y(q_1 q_2 - q_0 q_3) + 2v_z(q_0 q_2 + q_1 q_3)) \hat{i} + \\ &\quad (2v_x(q_0 q_3 + q_1 q_2) + y(q_0^2 - q_1^2 + q_2^2 - q_3^2) + 2v_z(q_2 q_3 - q_0 q_1)) \hat{j} + \\ &\quad (2v_x(q_1 q_3 - q_0 q_2) + 2v_y(q_0 q_1 + q_2 q_3) + v_z(q_0^2 - q_1^2 - q_2^2 + q_3^2)) \hat{k} \end{aligned}$$

- Note that quaternion multiplication does not require the computation of trigonometric functions, only the addition and multiplication of real numbers. Therefore, quaternion-based orientation is computationally efficient.
- Note that the resultant quaternion  $q^B$  has no real component, i.e.  $q^B$  is also a pure quaternion. It can be directly used in the vector notation simply by omitting the 0 valued real part.

**Multiple Rotations with Quaternions:**

In a motion, when the rotation does not compute only in a single axis and there is a cascaded rotation, the quaternion representation of such a case is pretty similar to how it is in other representations. Assuming  $q^{GA}$  defined the rotation from global frame to  $\mathcal{F}|_A$  and  $q^{GB}$  defined the rotation from global frame to  $\mathcal{F}|_B$ . The orientation of  $\mathcal{F}|_B$  with respect to  $\mathcal{F}|_A$  is defined as:

$$q^{A,B} = q^{G,A*} \otimes q^{G,B} \tag{3.27}$$

**From Quaternions to X Transformation:**

From quaternion to vector transformation for a pure quaternion is straightforward, as mentioned. However, it is not that simple to transform a quaternion into a rotation matrix or an Euler rotation. Since ROS tf. transformations library is used when it is needed in implementation, derivations of all the steps are not given in detail here. Just the results are given here for easy-to-look-up for future works and relevant readers. Detailed validation is available in [296, 297] and [298].

## Background

Taking the quaternion  $q$  defines  $\theta$  radians rotation about axis  $\hat{k}$ .

→ General quaternion representation:  $q = q_4 + q_1\hat{i} + q_2\hat{j} + q_3\hat{k}$

→ Quaternion to Euler angles:

$$q = \begin{bmatrix} \cos(\theta/2) \\ \bar{k} \sin(\theta/2) \end{bmatrix} = e^{\hat{k}\theta} \quad (3.28)$$

→ Quaternion to rotation matrix:

$$R^{L,G}(q) = I_3 - 2q_4 [q \times] + 2 [q \times]^2 \quad (3.29)$$

OR

$$R^{L,G}(q) = \exp(-[\bar{k} \times] \theta) \quad (3.30)$$

→ Quaternion to axis-angle:

$$R(q) = (2 \cos^2(\theta/2) - 1) \cdot I_3 - 2 \cos(\theta/2) \sin(\theta/2) [\hat{k} \times] + (2 - \sin^2(\theta/2)) \hat{k} \hat{k}^T \quad (3.31)$$

### Quaternion Derivative:

Quaternion derivative is important in the transition from orientation to the angular velocity. In angular motion, the derivative in a very basic way defined as *how much* rotated in a unit of time. Therefore, the derivative quaternion  $\bar{q}^{L(t),L(t+\Delta t)}$  describes the rotation of reference frame  $L(t)$  to reference frame  $L(t + \Delta t)$  in terms of the rotation angle  $\theta$  and the axis of rotation  $\hat{k}$ . In infinitesimal time difference  $\Delta t$ , using first-order Taylor expansion of cosine and sine coefficients in our general quaternion column vector representation:

$$\bar{q}^{L(t),L(t+\Delta t)} = \begin{bmatrix} \cos(\theta/2) \\ \hat{k} \sin(\theta/2) \end{bmatrix} \approx \begin{bmatrix} 1 \\ \hat{k}\theta/2 \end{bmatrix} = \begin{bmatrix} 1 \\ \frac{1}{2} \cdot \delta\theta \end{bmatrix} \quad (3.32)$$

The vector  $\delta\theta$  has the direction of the axis of rotation and the magnitude of the angle of the rotation. Dividing this vector by  $\Delta t$  will yield, in the limit, the angular velocity:

$$\omega = \lim_{\Delta t \rightarrow 0} \frac{\delta\theta}{\Delta t} \quad (3.33)$$

We are now ready to derive the quaternion derivative as:

$$\begin{aligned}
 \bar{q}^{(G,L(t))}(t) &= \lim_{\Delta t \rightarrow 0} \frac{1}{\Delta t} (\bar{q}^{(G,L(t+\Delta t))} - \bar{q}^{(G,L(t))}) & (3.34) \\
 &= \lim_{\Delta t \rightarrow 0} \frac{1}{\Delta t} (\bar{q}^{(L,L(t+\Delta t))} \otimes \bar{q}^{(G,L(t))} - \bar{q}_I \otimes \bar{q}^{(G,L(t))}) \\
 &\approx \lim_{\Delta t \rightarrow 0} \frac{1}{\Delta t} \left( \begin{bmatrix} 1 & \\ & \frac{1}{2} \cdot \delta\theta \end{bmatrix} - \begin{bmatrix} 1 \\ 0 \end{bmatrix} \right) \\
 &= \frac{1}{2} \begin{bmatrix} 0 \\ \omega \end{bmatrix} \otimes \bar{q}^{(G,L(t))} \\
 &= \frac{1}{2} \Omega(\omega) \bar{q}^{(G,L(t))}
 \end{aligned}$$

where  $\Omega(\omega)$  is:

$$\Omega(\omega) = \begin{bmatrix} 0 & \omega_z & -\omega_y & \omega_x \\ -\omega_z & 0 & \omega_x & \omega_z \\ \omega_y & -\omega_x & 0 & \omega_z \\ -\omega_x & -\omega_y & -\omega_z & 0 \end{bmatrix} \quad (3.35)$$

### Quaternion Integral:

Often we need to integrate the angular velocity obtained from the gyroscope to find orientation. Integrating a quaternion is equivalent to solving the first-order differential equation which is just explained in Eq. (3.34).

$$\dot{\bar{q}}^{(G,L(t))}(t) = \frac{1}{2} \Omega(\omega) \bar{q}^{(G,L(t))} \quad (3.36)$$

The solution to this differential equation has the general form:

$$\bar{q}^{(G,L(t))}(t + \Delta t) = \Theta(t + \Delta t, t) \bar{q}^{(G,L(t))}(t) \quad (3.37)$$

If  $\omega(t) = \omega$  is constant over the integration period  $\Delta t$ , the matrix  $\Omega$  does not depend on time. Therefore,

$$\Theta(t + \Delta t, t) = \Theta(\Delta t) = \exp\left(\frac{1}{2} \Omega(\omega) \Delta t\right) \quad (3.38)$$

Hence,

$$\bar{q}^{(G,L(t))}(t + \Delta t) = \exp\left(\frac{1}{2} \Omega(\omega) \Delta t\right) \bar{q}^{(G,L(t))}(t) \quad (3.39)$$

---

•Note that quaternions are numbers that belong to a large number system. It is impossible and useless to touch upon all the properties of the quaternions. It is aimed only to summarize enough knowledge to show how quaternions are used in related papers. Nevertheless, quaternions are extremely useful as much as they are beautiful. For better understanding, good references about quaternions: [296, 297] and [299].

### 3.1.3 Arm Kinematics

A robot arm is a sequence of links and joints, mostly connected in a serial configuration, to be used in manipulation. A robot arm can be a simple 2 DoF serial link chain or it can have higher DoF which contains both revolute and linear actuators. The arm kinematic model is a cascade multiplication equation of joint poses. It can be simplified considering two consecutive links where an IMU is attached on each link as shown in Fig. 3-7. Those body parts can be considered as upper and lower arm segments.

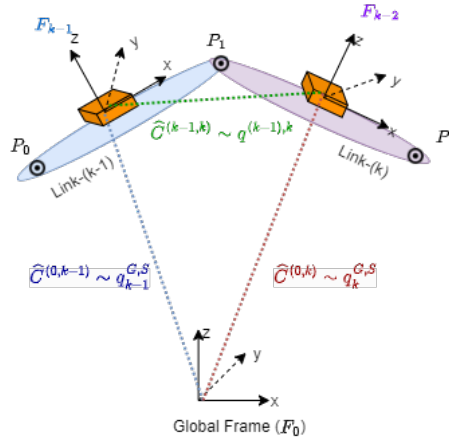


Fig. 3-7: Two consecutive body segments where all joints are simplified as revolute and rotation axes are through the page

As a general approach, the end-effector pose is calculated with Homogenous Transformation Matrix (HTM)s as in Section 3.1.3.1. Additionally, some kinematic and dynamic library functions allow automating this process such as in the ROS TF package, in which the procedure is explained in Section 3.1.4.

Arm kinematics is important for modelling both the human arm and the robot arm in this study. The comparative explanation of HTM and the quaternion+ROS TF approach is given in this section.

The following part of this section is to provide the reader the necessary knowledge about arm kinematics to comprehend this study. More can be found in [291] in chapter 4 and [300] in chapter 7.

#### 3.1.3.1 Homogeneous Transformation Matrix

The Homogenous Transformation Matrix (HTM)  $H$  is an extended version of the rotation matrix  $R$  including a vectorial translation part  $\bar{r}$  [291, 300]. HTM is a  $4 \times 4$  matrix and defined as:

$$H^{A,B} = \begin{bmatrix} R^{A,B} & \bar{r}^A \\ \bar{0}^T & 1 \end{bmatrix} \quad (3.40)$$

where  $H^{A,B}$  describes the transformation from frame A to frame B in which the rotation is defined with  $C^{A,B}$  and the translation is defined with  $\bar{r}^A$  as shown in Fig. 3.8. Therefore, transformed  $\bar{v}^B$  vector from vector  $\bar{v}^A$  using the HTM  $H^{A,B}$  will be represented as:



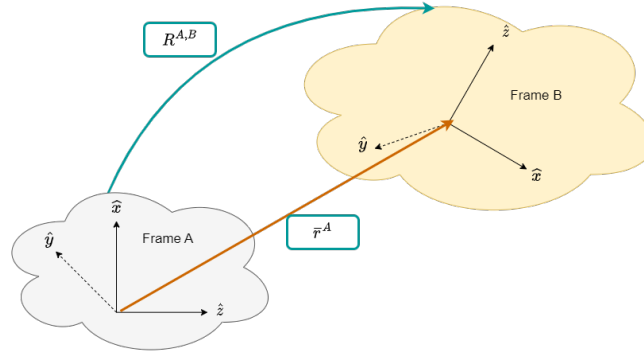


Fig. 3.8: Homogeneous transformation example using two frames

$$\begin{bmatrix} \vec{v}^B \\ 1 \end{bmatrix} = H^{(A,B)} \begin{bmatrix} \vec{v}^A \\ 1 \end{bmatrix} \quad (3.41)$$

On a link chain, the frames A and B in Fig. 3.8 are named enumerated and the rotation matrices and translation vectors are calculated iteratively (i.e.  $\mathcal{F}|_{(k-1)}$  and  $\mathcal{F}|_{(k)}$ ). The most common approach is to use DH (Denavit-Hartenberg) convention. Referring to Fig. 3.9, joint frames are defined with three unit vectors:  $\vec{u}_1^{(k)}$  is the common normal between two consecutive joint axes,  $\vec{u}_3^{(k)}$  joint axis and the  $\vec{u}_2^{(k)} = \vec{u}_3^{(k)} \times \vec{u}_1^{(k)}$  so that the frame is right-handed. Therefore, the four parameters of DH convention are  $\alpha_k$  is the rotation around the common normal  $\vec{u}_1^{(k)}$ ,  $\theta_k$  is the joint variable which is the rotation around the joint axis  $\vec{u}_1^{(k)}$  for revolute joints,  $a_k$  is the effective link length which is the distance from the proximal joint center  $O_{k-1}$  to current joint center  $O_k$  along the common normal, and the joint offset  $d_k$  is the distance from the proximal joint center  $O_{k-1}$  to current joint center  $O_k$  along the joint axis. For the prismatic joints, the joint variable  $\theta_k$  becomes  $S_k$  which is the displacement along the joint axis.

The transformation from  $\mathcal{F}|_{(k-1)}$  to  $\mathcal{F}|_{(k)}$  by rotation matrix and translation vector is defined as.

$$\mathbf{R}^{k-1,k} = e^{\vec{u}_3 \theta_k} e^{\vec{u}_1 \alpha_k} \quad (3.42)$$

$$= e^{\vec{y}_k \theta_k} \quad (3.43)$$

and

$$\vec{r}_{(P_{k-1}P_k)}|_{F_{k-1}} = s_k \vec{u}_3 + a_k e^{\vec{u}_3 \theta_k \vec{u}_1} \quad (3.44)$$

$$(3.45)$$

## Background

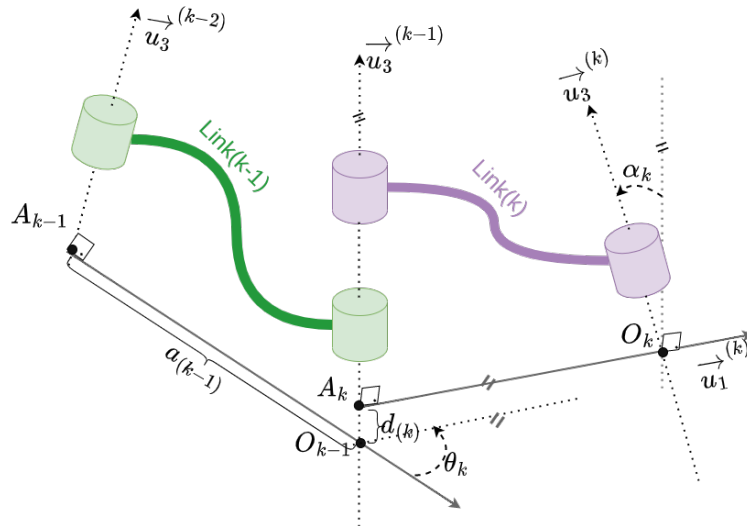


**Fig. 3.9:** Interconnection of the links and assignment of the link frames using unit vectors using DH convention

Hence the HTM from  $P_0$  to  $P_2$  in Fig. 3.7 will be:

$$\begin{aligned} \therefore H_{(P_{k-1}P_k)}^{(k-1,k)} &= \begin{bmatrix} R^{k-1,k} & \bar{r}_{(P_{k-1}P_k)} \Big|_{F_{k-1}} \\ \bar{0}^T & 1 \end{bmatrix} & (3.46) \\ H_{(P_0P_1)}^{(0,1)} \cdot H_{(P_1P_2)}^{(1,2)} &= \begin{bmatrix} R^{0,1} & \bar{r}_{(P_0P_1)} \Big|_{F_0} \\ \bar{0}^T & 1 \end{bmatrix} \cdot \begin{bmatrix} R^{1,2} & \bar{r}_{(P_1P_2)} \Big|_{F_1} \\ \bar{0}^T & 1 \end{bmatrix} \\ H_{(P_0P_2)}^{(0,2)} &= \begin{bmatrix} R^{0,2} & \bar{r}_{(P_0P_2)} \Big|_{F_0} \\ \bar{0}^T & 1 \end{bmatrix} \end{aligned}$$

This method is used in calculating the end-effector of regular robotic arms. Each robot arm manufacturer provides the DH parameters (or a sufficient kinematic model to obtain the DH parameters) of their robots. UR5e robot is the one used in the scientific papers of this thesis. The derivation of the DH parameters of UR5e (and other UR cobots) are provided in the manufacturer's website<sup>2</sup>.

### 3.1.4 Quaternions and ROS TF package

The raw orientation data from the IMU (or estimated orientation) is  $q_i^{G,S}$  where  $i$  is the IMU number. Each IMU provides orientation information with respect to global frame  $F_0$ . If the link-( $k-1$ )'s frame of reference is called  $F_{k-1}$  and link- $k$ 's frame of reference is called  $F_k$ , the rotation from the global frame to sensor frames will be  $q_{k-1}^{G,S}$  and  $q_k^{G,S}$  respectively. To calculate the joint angles in between two links the rotation  $q_{k-1,k}$  should be obtained. From quaternion multiplication:

<sup>2</sup><https://www.universal-robots.com/articles/ur/application-installation/dh-parameters-for-calculations-of-kinematics-and-dynamics>

$$\mathbf{q}_{k-1,k} = (\mathbf{q}_{k-1}^{G,S})^* \otimes \mathbf{q}_k^{G,S} \quad (3.47)$$

where  $\mathbf{q}^{k-1,k}$  gives the solid angle between link  $k-1$  and  $k$  in global frame. This can be defined respective to the rotation matrix and position vector representation in Eq. (3.42) and Eq. (3.44) as

$$\begin{aligned} \mathbf{R}^{k-1,k} &= e^{\bar{u}_3 \theta_k} e^{\bar{u}_1 \alpha_k} \\ &= e^{\bar{y}_k \theta_k} \rightarrow \mathbf{q}_y = \cos\left(\frac{\theta_k}{2}\right) + \hat{j} \sin\left(\frac{\theta_k}{2}\right) \end{aligned} \quad (3.48)$$

and

$$\begin{aligned} \bar{\mathbf{r}}_{(P_{k-1}P_k)} \Big|_{F_{k-1}} &= s_k \bar{u}_3 + a_k e^{\bar{u}_3 \theta_k \bar{u}_1} \\ &= s_k \bar{y}_k + a_k (\cos \theta_k \bar{x}_k + \sin \theta_k \bar{y}_k) \\ &= a_k \cos \theta_k \bar{x}_k + (s_k + a_k \sin \theta_k) \bar{y}_k \end{aligned} \quad (3.49)$$

where  $s_k$  and  $a_k$  are DH-parameters of link- $k$ .

After obtaining the rotation between two links, quaternion to Euler transformation (in ROS transform library) gives the Euler angles with respect to one previous body link.

At this step, for simulation reasons, quaternion-to-Euler conversion is needed. It gives us the Euler angles about each axis. From Section 3.1.2.1 we know that quaternions are representations of a full 3D rotation as a combination of about 3 orthogonal axes. In order to calculate Euler angles, first an Euler sequence should be decided. For a ZYX rotation (yaw-pitch-roll) they can be represented as:

$$\bar{\mathbf{q}} = \begin{bmatrix} \cos(\psi/2) \\ 0 \\ 0 \\ \sin(\psi/2) \end{bmatrix} \begin{bmatrix} \cos(\theta/2) \\ 0 \\ \sin(\theta/2) \\ 0 \end{bmatrix} \begin{bmatrix} \cos(\phi/2) \\ \sin(\phi/2) \\ 0 \\ 0 \end{bmatrix} \quad (3.50)$$

Therefore after necessary calculations, the Euler angles can be calculated such that:

$$\begin{bmatrix} \phi \\ \theta \\ \psi \end{bmatrix} = \begin{bmatrix} \text{atan2}(2(q_w q_x + q_y q_z), 1 - 2(q_x^2 + q_y^2)) \\ \text{asin}(2(q_w q_y - q_z q_x)) \\ \text{atan2}(2(q_w q_z + q_x q_y), 1 - 2(q_y^2 + q_z^2)) \end{bmatrix} \quad (3.51)$$

The reason why Euler angles are needed at the last step is that Rviz<sup>3</sup> is the visualization and Gazebo<sup>4</sup> for simulation tool in the ROS environment. Both of these software packages accept a file format called URDF<sup>5</sup> which is used to describe the robot model. It contains links, joints and basic material information about each part of the robot. We can only provide joint angles as Euler angles. Therefore as the last

<sup>3</sup><http://wiki.ros.org/rviz>

<sup>4</sup><http://gazebo.org/>

<sup>5</sup><http://wiki.ros.org/urdf/Tutorials>

step, a conversion from quaternions into Euler angles is computed. These Euler angles are mapped into movements as defined in Section 3.4.2. Example visualization on the human frames is shown in Fig. 3.24.

### 3.2 Fundamentals of Probability Theory

It is never possible to predict a physical occurrence with unlimited precision.

---

Max Planck

It is remarkable that a science which began with the consideration of games of chance should have become the most important object of human knowledge.

---

Pierre-Simon Laplace

When the *probability* name is pronounced, many people think about rolling some dice, tossing a few coins, picking colourful balls from a bag, picking a few cards from a deck with some order etc. Those are how we perceive probability theory and how to understand this nondeterministic world in an intuitive way. In robotics, on the other hand, we do not deal with colourful balls, cards and coins yet probability theory plays a fundamental role in the robotics field. Especially in navigation and localization, sensor readings, pose estimation, motion planning, robot learning and safety in robotics are the main studies where probability theory takes a considerable part.

In robotics, everything works on signals. IMU, camera, laser, F/T sensors, encoder readings, driver inputs and outputs motors etc. can be imagined as "information" signals. There is one thing that we are sure about the signals that *we can never be sure about the signals themselves*. Due to the true nature of how signals are produced and transmitted, they are exposed to noise, distortions, measurement and calculation errors. The physical world we are living in is a collection of continuous information and the world in which we are processing data (i.e. PC, microcontroller, robot's controller unit etc.) are discrete environment. At the very least, there is always a conversion error from our continuous world to the robot's discrete world and vice versa.

Every actual value is exposed to some distortions during measurement. Also sometimes it is not possible to measure the actual value directly but we can measure some other values and find a mathematical relation to obtaining whatever property is desired to be measured. If that's the case, then there will be additional modelling errors on the measured value as well as the aforementioned uncertainties.

Although we cannot 100% accurately measure a property, we can measure or calculate it with some uncertainty. Within this uncertainty range, using some probabilistic approaches it is possible to determine the *most likely* value of this state with acceptable confidence. Based on different scenarios, seeking the most correct value of a state is a state estimation problem.

According to [301] uncertainty in robotics arises from five different factors:

- **Environment:** Dynamic properties about the physical world.
- **Sensors:** Any limitations on the measurement devices for perceiving the robot or the environment such as resolution, noise etc.
- **Robots:** Uncertainties about actuators due to noise, signal ripples and wear-and-tear.
- **Models:** Inaccuracies and lack of precision in the robot model and environment model.
- **Computation:** Although robots are running in a continuous physical world in real-time, the data is processed in a discrete and close-to-real-time environment.

The role of probability theory in robotics is quite big. However, in this section the aim is not to teach probability in robotics; it is aimed to remind some bases which are related to orientation estimation from IMU signals in Section 3.2.2 and understanding some statistical approaches in Section 3.5. More about the theorems used in the following section can be found [302] throughout chapters 2-6.

### 3.2.1 Fundamental Definitions

The *most* we can know is in terms of probabilities.

---

Richard Feynman

Some fundamental definitions of the probability theory are given. Since probability theory is an enormous branch of mathematics, only the topics related to this study are explained in this subsection. The details about the equations and derivations in this chapter is found in [302].

#### 3.2.1.1 Probability Density Function (PDF) and Cumulative Distribution Function (CDF)

Probability Density Function (PDF) is a mathematical function that shows a *random variable's* all possible values as well as which values it can take in which probability. A r.v.,  $X$ , is a variable whose value is subject to variations that can take on a set of possible different values, each with an associated probability. In robotics, it can be the position or the orientation of a robot, or a sensor reading. It can be a *continuous* if the data can take infinitely many values or it can be *discrete* if the data can take a countable number of values.

PDF is represented as  $\rho(x)$  for continuous  $X$  and  $P(x)$  for discrete  $X$ . The sum of the probabilities of all values in a PDF is equal to one (see Eq. (3.54)). If instead of the probability of a r.v. to be equal to a certain value but the probability of the r.v. to be *higher* or *lower* than some certain value is demanded, then CDF is considered. Cumulative Distribution Function (CDF) is the accumulation of all the probabilities of a r.v. from the less probable possibility to the highest possibility. It is represented as  $C(x)$  for both continuous and discrete  $X$ . The relation between PDF and CDF is such that

## Background

the integral of the  $\rho(x)$  (or the sum of  $P(x)$  if  $X$  is a discrete r.v.) is equal to its  $C(x)$ . The mathematical representation of this relationship is shown in Eq. (3.55).

PDF is defined for continuous r.v. as:

$$\Pr(x \in I) = \int_I \rho(x) dx \quad (3.52)$$

and for discrete r.v. as:

$$P(x) = \begin{cases} 0 & x \leq a \\ P(X = x) & \text{if } x \in [a, b] \\ 0 & x \geq b \end{cases} \quad (3.53)$$

where  $I$  is a subset of  $[a, b]$ ,  $\rho(x)$  and  $P(x)$  defined on the interval  $[a, b]$  with  $a \leq b$  also with the fact that:

$$\rho(x) = \int_a^b \rho(x) dx = 1 \quad (3.54)$$

The cumulative distribution  $f \Pr(X \leq x)$  then defined as:

$$C(x) = P(X \leq x) = \int_a^x \rho(\xi) d\xi = \sum_{X=a}^x P(x) \quad (3.55)$$

PDF varies depending on the distribution character of a r.v.. For instance, if we pick a number between 0 and 10, the probability of choosing any random number is equal for all numbers in  $[0,10]$  (i.e. uniform distribution). On the other hand, if we chose a person in a group of 100 people, there is a higher chance of him/her being around 170 cm height than being around 200 cm height (i.e. Normal (Gaussian) distribution). Another example could be the expectation of an earthquake if it is expected in a location. If it hasn't occurred yet, every day there is a higher chance to occur (i.e. exponential distribution). There are many more different distribution types that yield different characteristics on PDF but they are not very common in robotics. The uniform distribution is important because generally the initial values of a state are distributed uniformly unless extra information is given. Most of the estimated states under some constraints perform a normal distribution where the calculations give certain values whereas noise adds Gaussian uncertainty. Or exponential distribution becomes important when it is concerned with the amount of time until some specific event occurs.

The comparative PDFs of these three distribution types are given in Fig. 3.10.

### 3.2.1.2 Gaussian (Normal) Distribution

The representation of Gaussian PDF is  $X \sim \mathcal{N}(\mu, \sigma^2)$ . where  $\mu$  is the mean and  $\sigma^2$  is the variance of the distribution. This representation is given by the following Gaussian function for a one-dimensional r.v.:

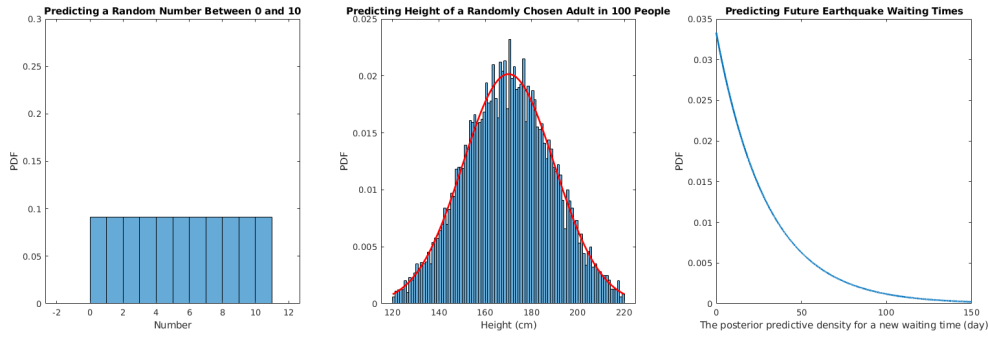


**Fig. 3.10:** Uniform - Gaussian - Exponential distribution functions

$$\rho(x) = (2\pi\sigma^2)^{\frac{1}{2}} \exp\left\{-\frac{1}{2} \frac{(x - \mu)^2}{\sigma^2}\right\} \quad (3.56)$$

Furthermore, if a r.v. is a *multivariate* vector, then the Gaussian function is represented as:

$$\rho(x) = \det(2\pi\Sigma) \exp\left\{-\frac{1}{2}(x - \mu)^T \Sigma^{-1}(x - \mu)\right\} \quad (3.57)$$

where  $\mu$  is the mean vector and  $\Sigma$  is a positive semi-definite symmetric matrix called *covariance matrix*.

### 3.2.1.3 Conditional Probability

Another important term in probabilistic robotics is the *joint distribution* or two random variables  $X$  and  $Y$ . This type of distribution is considered when it is calculated that the probability of two events happened to be true together. The representation of joint distribution of two events where the r.v.  $X$  takes on the value  $x$  and r.v.  $Y$  takes on the value  $y$  is given by:

$$\rho(x, y) = \rho(X = x \wedge Y = y) \quad (3.58)$$

if these random variables are independent then the joint distribution of these two events is equal to the multiplication of each event's PDF:

$$\rho(x, y) = \rho(x)\rho(y) \quad (3.59)$$

However, in most cases, random variables carry some information about other random variables. In such cases, the probability of  $X$  to take the value  $x$  when  $\Pr(Y = y)$  is given is different than no information given about  $Y$ . This type of dependence is called *conditional probability* and it is defined as:

$$\rho(x | y) = \frac{\rho(x, y)}{\rho(y)} = \rho(x) \quad (3.60)$$

## Background

### 3.2.1.4 Bayes Rule

This relation between two random variables leads us to one of the most predominant concepts in the probability theory; *Bayes Rule*. This rule allows us to calculate multiple beliefs.

$$\rho(x|y) = \frac{\rho(y|x)\rho(x)}{\rho(y)} = \frac{\rho(y|x)\rho(x)}{\int \rho(y|x')\rho(x')dx'} \quad (\text{continuous}) \quad (3.61)$$

$$P(x|y) = \frac{P(y|x)P(x)}{P(y)} = \frac{P(y|x)P(x)}{\sum_{x'} P(y|x')P(x')} \quad (\text{discrete}) \quad (3.62)$$

Bayes rule or *Bayes theorem* is undoubtedly the most used fact in the probability theory. Especially in robotics, thanks to Bayes theorem the probability of a r.v. (i.e. state of a system) can be calculated depending on both sensor measurements and the *prior* probabilities of this state. If  $x$  is a quantity that is to be inferred from  $y$ , the probability  $\rho(x)$  will be referred to as *prior probability distribution*, and  $y$  is called the *data* (e.g., a sensor measurement). The probability  $\rho(x|y)$  is called the *posterior probability distribution* over  $X$ . Therefore Bayes rule gives the opportunity to calculate a posterior  $\rho(x|y)$  using the "inverse" conditional probability  $\rho(y|x)$  as well as the prior probability  $\rho(x)$ . In other words *acknowledging* that the sensor measurement  $Y$  has  $y$  values since the state variable  $X$  causes it to be so, and therefore the posterior state can be calculated based on this acknowledgement.

Another useful outcome of Bayes rule is that the denominator  $\rho(y)$  does not depend on the state variable  $X$ , which means that  $\rho^{-1}(y)$  is the same for any value  $x$  in the posterior  $\rho(x|y)$ . Therefore the equation can be rearranged as in Eq. (3.63).

$$\rho(x|y) = \eta \rho(y|x)\rho(x) \quad (3.63)$$

where  $\eta$  is mostly referred as *normalizer* variable in robotics since it normalizes the final result of  $\rho(x|y)$  to 1.

### 3.2.1.5 Expected Value and Covariance

Since after overall calculations a result to be used is needed, the *final decision* of a distribution of a r.v. is called as *expected value* of this r.v.. The expected value of r.v.  $X$  is given by:

$$E[X] = \int x\rho(x)dx \quad (\text{continuous}) \quad (3.64)$$

$$E[X] = \sum_x x\rho(x) \quad (\text{discrete}) \quad (3.65)$$

and the covariance of  $X$  is obtained as:

$$\text{Cov}[X] = E[X - E[X]]^2 = E[X^2] - E[X]^2 \quad (3.66)$$



3.2.1.6 Generalization on Multivariate Cases

As a conclusion of basic concepts in probability, it is perfectly fine to condition any of the rules discussed so far on arbitrary other random variables, such as the variable  $Z$ . For example,  $\Pr(Z = z)$  conditioning on Bayes rule gives us:

$$\rho(x | y, z) = \frac{\rho(y | x, z) \rho(x | z)}{\rho(y | z)} \tag{3.67}$$

if  $x$  and  $y$  are independent on  $z$  then the joint distribution of these variables holds such that:

$$\rho(x, y | z) = \rho(x | z) \rho(y | z) \tag{3.68}$$

therefore the *conditional independence* can be observed:

$$\begin{aligned} \rho(x | z) &= \rho(x | z, y) \\ \rho(y | z) &= \rho(y | z, x) \end{aligned} \tag{3.69}$$

However, conditional does not imply absolute independence.  $x$  and  $y$  can be independent on  $z$  yet they can be dependent on each other. Also, absolute independence does not imply conditional independence.

$$\begin{aligned} \rho(x, y | z) = \rho(x | z) \rho(y | z) &\not\Rightarrow \rho(x, y) = \rho(x)\rho(y) \\ \rho(x, y) = \rho(x)\rho(y) &\not\Rightarrow \rho(x, y | z) = \rho(x | z) \rho(y | z) \end{aligned} \tag{3.70}$$

3.2.1.7 Probability vs Likelihood

Supposing a stochastic process which takes  $X$  as a r.v.. Let the observed outcomes  $\mathcal{O}$  and the set of parameters that describe this stochastic process as  $\theta$ . As it is seen so far, the probability of the observation  $\mathcal{O}$  given  $\theta$  is  $P(\mathcal{O} | \theta)$ .

However, it is hardly possible to perfectly define all the model parameters  $\theta$  in real life. Then the problem becomes such that the observation  $\mathcal{O}$  and then the goal is to arrive at an estimate for  $\theta$  which would yield a satisfying choice given the observed outcomes  $\mathcal{O}$ . It is known that at a given value of  $\theta$  the probability of observing  $\mathcal{O}$  is  $P(\mathcal{O} | \theta)$ . Therefore a *likelihood* problem seeks the best probability of the parameter values  $\theta$  to maximize the chance of observing  $\mathcal{O}$ . The mathematical description of such a function is:

$$L(\theta | \mathcal{O}) = P(\mathcal{O} | \theta) \tag{3.71}$$

In continuous cases, this approach is not applicable as it is since it is obvious that the probability of observation for a specific parameter value  $P(\mathcal{O} | \theta)$  is zero. Adapting the concept into continuous cases, a specific value of a state is no longer the concern but the PDF is associated with the observed outcomes  $\mathcal{O}$ . Therefore, the likelihood problem in continuous case problem seeks the best PDF of  $\theta$  to maximize the chance of observing  $\mathcal{O}$ . The mathematical description of such a function is then:

$$L(\theta | \mathcal{O}) = p(\mathcal{O} | \theta) \quad (3.72)$$

### 3.2.2 Bayes Filters

In robotics, at every time step, new data is collected through sensors and a set of actions is taken that updates the robot's state. Therefore, the uncertain robot states have to be updated recursively based on both prior states and the current sensor inputs. Such a process which takes the current measurements, as well as the prior estimates of the system state, is called recursive state estimation.

It is explained that the Bayes rule allows us to calculate multiple beliefs (i.e. in robotics prior knowledge of robot states and the current sensor measurements). There are different algorithms to filter undemanded signal residuals, estate estimators and observers which are developed on the Bayes rule. Depending on the purpose of the algorithm, similar approaches can be named as those terms interchangeably, the root from the same principle. Therefore those types of algorithms are a type of Bayes Filter.

Bayes filters, both named as an observer or a filter, have two main steps: *prediction* and *correction*. The correction step can be named as *innovation* or *update* in different resources. For consistency, the "correction" term is used for the step where the predicted states are *corrected* according to prior knowledge.

There are many different forms of Bayes filters. Kalman filter (KF), Extended Kalman filter (EKF), Unscented Kalman Filter, Particle Filter and many well-used estimation and learning algorithms can be given as an example. In this section, the principle on KF and how the prediction and correction steps are calculated are presented. Although neither KF nor EKF is manually calculated in the presented papers in Part-II, it is still an essential step in understanding the position and orientation estimation linked to this study.

The following part of this section is compiled from the online lecture notes from Cyrill Stachniss [303] and in [304].

#### 3.2.2.1 Kalman filter (KF)

Kalman filter (KF) is the equivalent form of Bayes filter when the variables are normally distributed and the transition is linear. It is known as the best/most optimal state estimator in linear systems [304], and therefore, one of the most common estimation algorithms for linear systems. It produces estimates of imponderable states of a system based on past estimations and current measurements. In other words, it is an estimator (and observer). Using the linear system model reduces the estimation error in every iteration. In a case where angular velocity and linear acceleration can be measured but orientation can not, then the orientation is an imponderable state.

Every linear time-invariant (LTI) system can be modelled as:

$$\begin{aligned} \bar{\hat{x}}_t &= \mathbf{A} \cdot \bar{\hat{x}}_{t-1} + \mathbf{B} \cdot \bar{u}_t + \bar{w}_t \\ \bar{y}_t &= \mathbf{C} \cdot \bar{\hat{x}}_t + \bar{v}_t \end{aligned} \quad (3.73)$$

Where  $\bar{x}_t$  is the estimated **system state vector**,  $\bar{u}_t$  is the **input vector** and  $\bar{y}_t$  is the **measurement vector** at time  $t$ .

- **A**: system matrix ( $n \times n$ ) (relates the current states to the next states)
- **B**: input matrix ( $n \times l$ ) (relates inputs to the next states)
- **C**: output matrix ( $k \times n$ ) (system states to the measured/observed states)
- $\bar{w}_t$ : process noise ( $\mathcal{N} \sim (\mu = 0, \sigma_w^2 = Q)$  where  $Q$  is ( $n \times n$ ))
- $\bar{v}_t$ : measurement noise ( $\mathcal{N} \sim (\mu = 0, \sigma_v^2 = R)$  where  $R$  is ( $k \times k$ ))
- $\bar{x}_t$ : estimated state vector
- $\bar{y}_t$ : measurement vector (observation vector)

Simply, in a linear motion model under Gaussian noise, KF seeks the solution of the problem  $\rho(\bar{x}_t | \bar{u}_t, \bar{x}_{t-1})$  in the representation of Bayes filter. In other words, if the system states vector  $\bar{x}_t$  holds the position or orientation states of the robot, the KF estimates the most likely values of the robot states considering the past states  $\bar{x}_{t-1}$  and the current sensor measurements  $\bar{u}_t$  which yields the observations  $\bar{y}_t$ .

**Note:** Column vector notation  $\bar{x}_t$  is omitted for brevity from now on.  $x_t$  represents all of the states, not a single value.

The linear motion under Gaussian noise looks like this:

$$\rho(x_t | u_t, x_{t-1}) = \det(2\pi R_t)^{-\frac{1}{2}} \exp\left(-\frac{1}{2}(x_t - A_t x_{t-1} + B_t u_t)^T R_t^{-1} (x_t - A_t x_{t-1} + B_t u_t)\right) \quad (3.74)$$

where  $R_t$  represents the noise of the motion. The same representation for a linear observation model looks like this:

$$\rho(z_t | x_t) = \det(2\pi R_t)^{-\frac{1}{2}} \exp\left(-\frac{1}{2}(z_t - C_t x_t)^T R_t^{-1} (z_t - C_t x_t)\right) \quad (3.75)$$

where  $Q_t$  represents the noise of the observation/measurement. As explained in Since everything is Gaussian, given an initial Gaussian belief, the belief is always Gaussian (derivation in [305]):

$$\begin{aligned} \overline{\text{bel}}(x_t) &= \int \rho(x_t | u_t, x_{t-1}) \text{bel}(x_{t-1}) dx_{t-1} \\ \text{bel}(x_t) &= \eta \rho(z_t | x_t) \overline{\text{bel}}(x_{t-1}) \end{aligned} \quad (3.76)$$

Kalman Filter is based on modelling the process noise. As well, the Kalman filter provides a prediction of the future system state by prediction. How this process is applied using the mathematical system model is as follows:

## Background

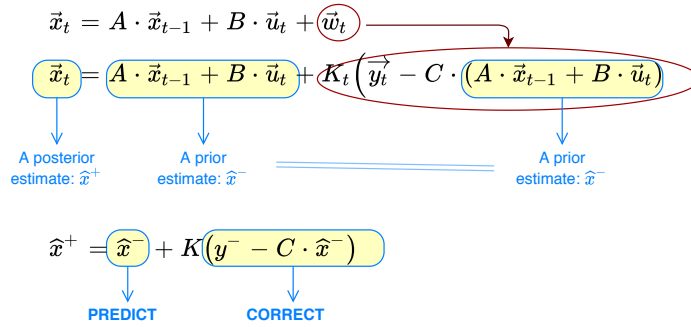


**Fig. 3.11:** Kalman equations

In the prediction step, the system model is used in the calculation of error covariance matrix  $\mathbf{P}$  as in Eq. (3.77):

$$\begin{aligned}\bar{\hat{x}}_t &= \mathbf{A} \cdot \bar{\hat{x}}_{t-1} + \mathbf{B} \cdot \bar{u}_t \\ \mathbf{P} &= \mathbf{A} \cdot \mathbf{P} \cdot \mathbf{A}^T + \mathbf{Q}\end{aligned}\quad (3.77)$$

Then, this error covariance matrix is used in updating the Kalman gain  $\mathbf{K}$  as in Eq. (3.78):

$$\begin{aligned}\tilde{y}_t &= \bar{y}_t - \mathbf{C} \cdot \bar{\hat{x}}_{t+1} \\ \mathbf{S} &= \mathbf{C} \cdot \mathbf{P} \cdot \mathbf{C}^T + \mathbf{R} \\ \mathbf{K} &= \mathbf{P} \cdot \mathbf{C}^T \cdot \mathbf{S}^{-1} \\ \bar{\hat{x}}_t &= \bar{\hat{x}}_t + \mathbf{K} \cdot \tilde{y}_t \\ \mathbf{P} &= (\mathbf{I} - \mathbf{K} \cdot \mathbf{C}) \cdot \mathbf{P}\end{aligned}\quad (3.78)$$

where,

- $\mathbf{K}$  is the Kalman gain,
- $\mathbf{P}$  is the error covariance,
- $\mathbf{Q}$  is covariance matrix of the process noise,
- $\mathbf{R}$  is covariance matrix of the measurement noise,
- $\tilde{y}_t$  is error between the actual measurement and the estimated.

**VALIDATION OF KF** According to Eq. (3.77) and Eq. (3.78), the Kalman gain  $\mathbf{K}$  is adapted based on  $\mathbf{Q}$  and  $\mathbf{R}$ . Principally, KF estimates a *posterior* states depending on the reliability of the model prediction (*a prior estimate*) and the observation prediction, i.e. lower variance in measurement noise ( $\lim_{\mathbf{R} \rightarrow 0}$ ) makes the Kalman gain  $\mathbf{K}$  closer to 1 and posterior estimates will be more based on the measurements.

It can be mathematically proven like that:

$$\lim_{\mathbf{R} \rightarrow 0} \mathbf{K} = \frac{\mathbf{P}^- \cdot \mathbf{C}^T}{\mathbf{C} \cdot \mathbf{P}^- \cdot \mathbf{C}^T + (\mathbf{R} = 0)} \rightarrow \mathbf{K} = \mathbf{C}^{-1}\quad (3.79)$$

If Eq. (3.79) is substituted into the a posterior estimation in Fig. 3.11:

$$\begin{aligned}
 \hat{x}^+ &= \hat{x}^- + \mathbf{K} \cdot (\mathbf{y}^- - \mathbf{C} \cdot \hat{x}^-) & (3.80) \\
 &= \hat{x}^- + \mathbf{C}^{-1} \cdot (\mathbf{y}^- - \mathbf{C} \cdot \hat{x}^-) \\
 &= \hat{x}^- + \mathbf{C}^{-1} \cdot \mathbf{y}^- - \mathbf{C}^{-1} \cdot \mathbf{C} \cdot \hat{x}^- \\
 &= \mathbf{C}^{-1} \cdot \mathbf{y}^-
 \end{aligned}$$

and  $\mathbf{C}^{-1}$  is equal to 1 in general case. Therefore the estimated value only depends on the measured value, not prior estimates. Hence:

$$\hat{x}^+ = \mathbf{y}^- \quad (3.81)$$

In the opposite case, lower variance in prior estimate covariance converges to zero ( $\lim_{\mathbf{P}^- \rightarrow 0}$ ), then only prior estimates contribute to our current estimation.

$$\lim_{\mathbf{P}^- \rightarrow 0} \mathbf{K} = \frac{(\mathbf{P}^- = 0) \cdot \mathbf{C}^T}{\mathbf{C} \cdot (\mathbf{P}^- = 0) \cdot \mathbf{C}^T + \mathbf{R}} \rightarrow \mathbf{K} = \frac{0}{\mathbf{R}} = 0 \quad (3.82)$$

If Eq. (3.82) is substituted into the a posterior estimation in Fig. 3.11:

$$\hat{x}^+ = \hat{x}^- + \mathbf{K} \cdot (\mathbf{y}^- - \mathbf{C} \cdot \hat{x}^-) \quad (3.83)$$

$$= \hat{x}^- + \mathbf{0} \cdot (\mathbf{y}^- - \mathbf{C} \cdot \hat{x}^-) \quad (3.84)$$

Therefore the estimated value only depends on the prior estimates, not measurements. Hence:

$$\hat{x}^+ = \hat{x}^- \quad (3.85)$$

### 3.2.2.2 Extended Kalman filter (EKF)

The Kalman filter is only applicable in casual, linear and time-invariant systems. If the system model does not satisfy these three conditions, then another type of filter/estimator/observer or a different variation of the Kalman filter should be implemented.

For not-highly nonlinear systems, an Extended Kalman filter (EKF) can be implemented. In this case, the system matrix is not a function of the non-linear states but also it may be a function of states and inputs that cannot be separated linearly. On the other hand, the non-linearity might appear in the measurement part. Therefore, the system equations must be formulated as the following equation set:

$$\hat{x}_t = f(x_{t-1}, u_t) + w_t \quad (3.86)$$

$$y_t = h(x_t) + v_t \quad (3.87)$$

In such a case, with arbitrary functions,  $f$  and  $h$ , the belief is no longer a Gaussian. The system model does not behave linearly to all the states therefore the behaviour of

## Background

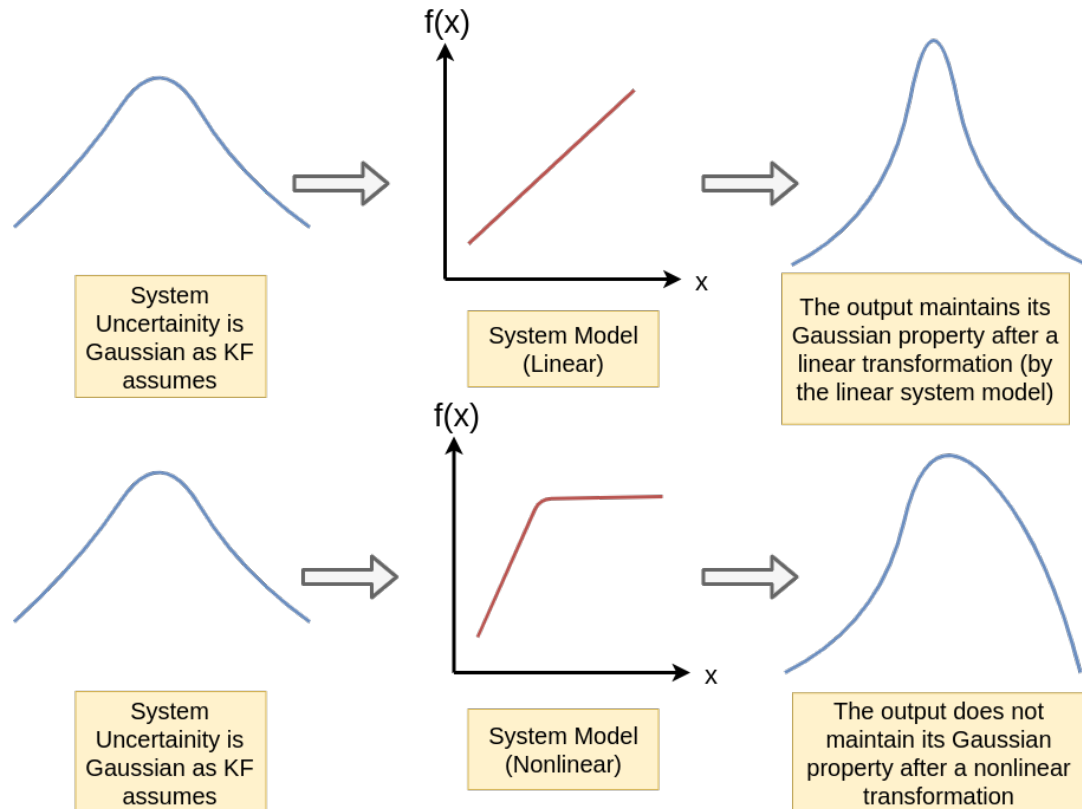


**Fig. 3.12:** Why KF does not work in nonlinear systems: The KF assumes the system is linear and the character of system uncertainty is Gaussian. Therefore, the output system maintains its Gaussian properties. However, the Gaussian property breaks down at the output and it causes big errors in estimated properties.

the output states does not reflect a Gaussian property as shown in Fig. 3.12. The figure shows on state function  $f(x)$  but the same case is valid in the measurement function  $h(x)$ , as well.

Therefore, in the EKF process local linearization processes are applied. The nonlinear functions are linearized in each time step, and afterwards, the same prediction+correction steps are applied as in KF. The Fig. 3.13a shows how the local linearization affects the output differently than what is shown in Fig. 3.12.

The EKF calculates an approximation to the true belief. The representation is pretty much the same as linear KF whereas  $f$  replaces the matrices  $A$  and  $B$ , and  $h$  replaces the matrix  $C$ .

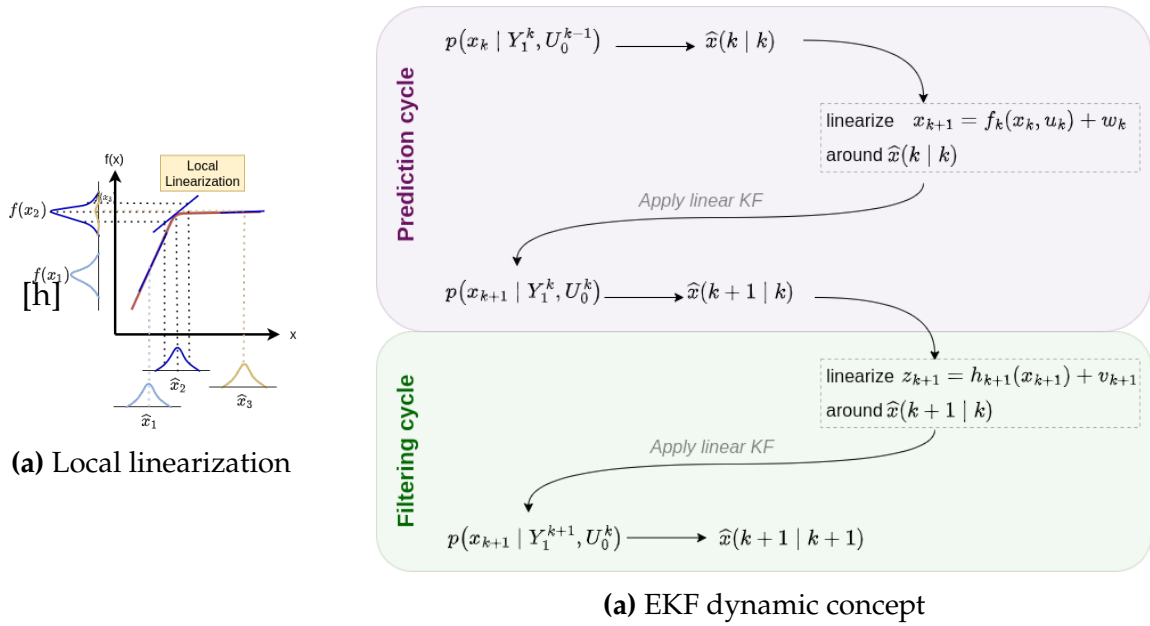


**Fig. 3.15:** How EKF works: The system model is linearized in each prediction cycle to apply linear KF predict state, then the observer model is linearized in the filtering cycle to apply linear KF correction state.

The EKF linearizes the system dynamics and measurement dynamics in every time step (see Fig. 3.15). Then, apply the KF steps as if everything is linear and has Gaussian characteristics.

One most common way to do it is to use Taylor expansion to approximate the  $f$  and  $h$  functions around the working point i.e. a tangent line to the function at the mean of the Gaussian as shown in Fig. 3.13a. These linearized functions  $F$  and  $H$  respectively are also called Jacobians. The Jacobian functions of the system and measurement function using  $2^{\text{nd}}$  degree Taylor expansion would be as in Eq. (3.88).

$$\mathbf{F} = \left. \frac{\partial f}{\partial \mathbf{x}} \right|_{\hat{\mathbf{x}}_{k-1}, \mathbf{u}_k} = f(\hat{\mathbf{x}}_{k-1}, \mathbf{u}_k) + f_{\mathbf{x}}(\hat{\mathbf{x}}_{k-1}, \mathbf{u}_k)(\mathbf{x} - \hat{\mathbf{x}}_{k-1}) + f_{\mathbf{u}}(\hat{\mathbf{x}}_{k-1}, \mathbf{u}_k)(\mathbf{u} - \mathbf{u}_k) \quad (3.88)$$

$$+ \frac{f_{\mathbf{x}\mathbf{x}}(\hat{\mathbf{x}}_{k-1}, \mathbf{u}_k)}{2}(\mathbf{x} - \hat{\mathbf{x}}_{k-1})^2 + f_{\mathbf{x}\mathbf{u}}(\hat{\mathbf{x}}_{k-1}, \mathbf{u}_k)(\mathbf{x} - \hat{\mathbf{x}}_{k-1})(\mathbf{u} - \mathbf{u}_k)$$

$$+ \frac{f_{\mathbf{u}\mathbf{u}}(\hat{\mathbf{x}}_{k-1}, \mathbf{u}_k)}{2}(\mathbf{u} - \mathbf{u}_k)^2$$

$$\mathbf{H} = \left. \frac{\partial h}{\partial \mathbf{x}} \right|_{\hat{\mathbf{x}}_k} = h(\hat{\mathbf{x}}_k) + h'(\mathbf{x})(\mathbf{x} - \hat{\mathbf{x}}_k) + \frac{h''(\hat{\mathbf{x}}_k)}{2}(\mathbf{x} - \hat{\mathbf{x}}_k)^2$$

where  $f_{\mathbf{x}}$  and  $f_{\mathbf{u}}$  are the first derivatives,  $f_{\mathbf{x}\mathbf{x}}$ ,  $f_{\mathbf{u}\mathbf{u}}$  and  $f_{\mathbf{x}\mathbf{u}}$  are the second derivatives of the system function with respect to system states vector  $\mathbf{x}$  and inputs vector  $\mathbf{u}$ , respectively;  $h'$  and  $h''$  are the first and second derivatives of the measurement function's first and second derivatives with respect to system states vector  $\mathbf{x}$ . Then the linearized system becomes:

## Background

$$\begin{aligned}\Delta(x_k, u_k) &\cong \mathbf{F}\Delta(x_{k-1}, u_k) + w_k \\ \Delta y_k &\cong \mathbf{H}\Delta x_k + w_k\end{aligned}\quad (3.89)$$

The functions  $\mathbf{F}\Delta(x_{k-1}, u_k)$  and  $\mathbf{H}\Delta x_k$  are linear functions are linear KF procedures can be safely applied as in Fig. 3.14a.

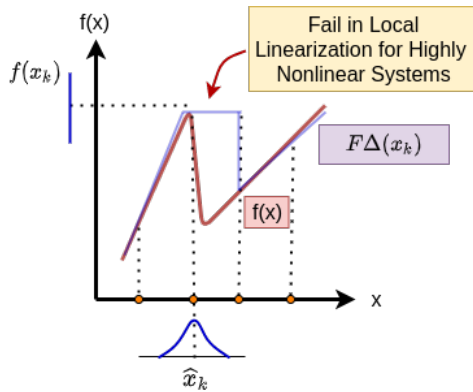


**Fig. 3.16:** Linearization problem in highly nonlinear systems

The EKF is a very useful approach to applying Bayes filter-based optimal state estimation. Compared to the KF, the EKF is computationally more expensive because the Jacobians have to be calculated in every step. Moreover, the EKF is only applicable to systems that have a differentiable model.

However, the EKF is not optimal if the system is highly nonlinear. As shown in Fig. 3.16, if high nonlinearity occurs in between time steps, they are missed in the linearization process and return faulty  $\mathbf{F}\Delta(x_{k-1}, u_k)$  and/or  $\mathbf{H}\Delta x_k$ . Therefore, different nonlinear state estimators should be used.

### 3.2.3 State Estimation

States are system parameters which are used in a model. There is a mathematical model and any variable changing in time can be a system state.

There are two common approaches in HME state estimation [119]: orientation-based and position based. One can either directly use orientation estimate and find joint angles and then joint+end point positions (shoulder, elbow, wrist, hand), or one can do position estimation to find out each joint+end point respective positions to a fixed point (chest), calculate joint angles, and then using human body model to find out joint angles. The differences in the processes are summarized in Fig. 3.17.

States in robotics are generally the position/orientation/heading/tilt/joint position information of a robot. In this case, the human body is treated as a robot model i.e a kinematic chain. The general approach behind the state estimation is to use a mathematical model and calculate/predict states based on this model, and after, to correct them by some observable states if needed. In every time step, new data is collected through sensors and a set of actions is taken that updates the robot's state. If the uncertain states have to be updated recursively based on both prior states and the current sensor inputs. Such a process which takes the current measurements, as well as the prior estimates of the system state, is called recursive state estimation.

Bayes filter is one of the most used recursive state estimation methods in robotics. It uses the measured states in given input values as well as the prior estimates to find out the desired output states. It is such a game-changer method that even the basis of machine learning and some different filter bases of the Bayes filtering approach.



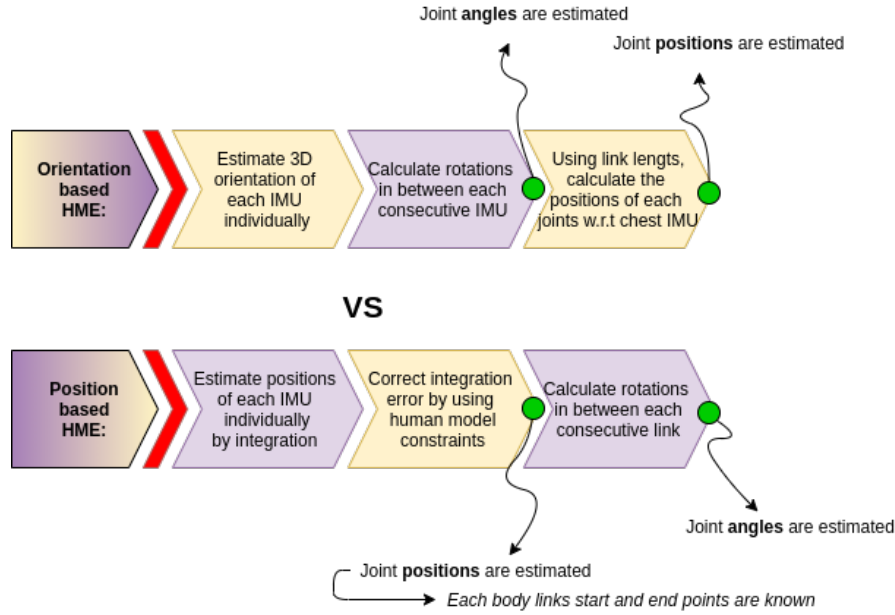


Fig. 3.17: Orientation vs position-based human pose estimation

Kalman filter is one of them. Kalman filter is the best possible linear estimator in the minimum mean-square-error sense [304].

Recently machine learning, deep learning, artificial intelligence, convolutional neural networks, hidden markov, etc. are used in state estimation in robotics. This study focuses on HME using Kalman Filter. As the basic principle, the Kalman filter (in general a Bayes filter) adaptively updates the Kalman gain  $K_t$  to reduce the observation error  $y_t - H\hat{x}_t^-$  based on aprior estimates of the system states  $\hat{x}_t^-$ , and calculate a posterior estimate  $\hat{x}_t^+$  as shown in Eq. (3.90).

$$\begin{aligned} \hat{x}_t^+ &= \hat{x}_t^- + k_t(y_t - h\hat{x}_t^-) && \text{(continuous)} && (3.90) \\ \hat{x}_k^+ &= \hat{x}_k^- + \mathbf{K}_k(y_k - \mathbf{C}\hat{x}_k^-) && \text{(discrete)} && \end{aligned}$$

The general approach in using IMUs in the state estimation is either integrating the gyroscope values to obtain the orientation and then correcting the calculation with accelerometer and magnetometer readings or double integration of the accelerometers to obtain the position and then correcting the calculation with gyroscope and magnetometer (an more commonly using some other external sensors) [117]. All these methods are also called *sensor fusion*. In HME using IMUs, there are some extra observable states for aiding state estimation by using IMUs than using them in free space. Commonly in IMU-based HME problems, the IMUs are used in the mathematical model as inputs, body constraints and/or external sensors (such as cameras, lasers, strain gauges, etc.) are used in the correction step as observable states.

The estimation of the *position* of the human is investigated in 2 categories; local HME and global HME. This study uses only local HME.

In local HME, the aim is to estimate the correct orientation between each body links (i.e. correct joint angle). It is based on only IMUs without any external sensors. It is fundamental in the strap-down approach to position estimation. In one point of view,

## Background

orientation estimation can be superior since allows the gravity to be cancelled from the acceleration signals yet it is inferior since the orientation estimate accepts the human joints as pure rotational joints. This acknowledgement causes orientation estimation to be less powerful for soft tissue artifacts and translational motion on the human joints.

On the other hand, in global HME, the aim is to estimate the position of the human in the environment as well as the position of the body links with respect to the human reference frame. To eliminate long-term drift, generally, external sensors are involved. It is most likely to use the external sensors to estimate the **global position** of the human such as GPS, depth sensor, leap motion, camera, force sensor etc. Position estimation requires perfect determination of the center of rotation and determination of the axis of rotation of a rigid body.

Although, in the end, no stochastic state estimation was manually applied in this study, it occupies quite a big portion of this study. Instead of manual KF implementation, the Xsens Awinda IMU orientation output is used, which is estimated using KF [32] by the firmware.

### 3.3 IMU Measurement Model

IMU has 3 distinct measurement devices in it; a gyroscope for angular velocity measurement, an accelerometer for linear acceleration measurement and a magnetometer to measure the magnetization in the environment. This subsection explains how those measurements are mathematically modelled. While the majority of the mathematical models delineated in this section are not straightforwardly employed in any of the papers introduced in Part II, comprehending this section is critical for grasping how the entire system functions and the rationale behind choosing the presented methodologies.

Before getting into the details about the orientation and position estimate there are 4 main coordinate frames which play fundamental roles:

- $\mathcal{F}|_S$  is the coordinate frame of the moving IMU,
- $\mathcal{F}|_B$  The coordinate frame of the moving body part,
- $\mathcal{F}|_G$  is the the coordinate frame of the world; Ground/Base frame,
- $\mathcal{F}|_I$  The coordinate initially coincident with the *Global frame*. Contrary to  $\mathcal{F}|_G$ , the initial frame is stationary whereas the global frame rotates with the earth.

There is also *navigation frame* which is a local geographic frame to be navigated. However, the difference between the navigation frame and the global frame is negligible at small distances. It is important in aviation but not HME.

A pose is defined as a combination of the *orientation* and the *position* of an object. Orientation defines the **direction** or the object whereas position defines the **location**, both with respect to a reference frame. The distinction between the initial frame and

the global frame is important in long periods of usage; like a few years. This is mostly because of the magnetometer challenges explained in Section 4.1.

To utilize a state estimation using IMUs, it is important to mathematically describe the data which is obtained from an IMU.

**Angular velocity measurement model:**

The gyroscope measures the angular velocity of the sensor frame with respect to the inertial frame, expressed in the global frame. It is denoted as  $\omega_S^G$  expressed as [117]:

$$\bar{\omega}_S^G = R^{S,G} \bar{\omega}_S + R^{I,G} \cdot \bar{\omega}_I \tag{3.91}$$

where  $\omega_{IG}^I$  is our planet's angular velocity around its own z-axis in 23.9345 hours with respect to the Sun according to [306] represented in  $\mathcal{F}_I$ . Hence, the earth rate is approximately  $7.29 \times 10^{-5}$  rad/s. This is negligible in our case. Hence, the angular velocity of a sensor in the sensor frame [117]:

$$\bar{\omega}_S^G = R^{G,S}(\bar{\omega}_S^S) \tag{rotation matrix representation} \tag{3.92}$$

$$\Omega_S^G = q^{G,S} \otimes \Omega_S^G \otimes q^{G,S*} \tag{quaternion representation} \tag{3.93}$$

where  $\Omega_S^G$  is the quaternion representation of the vector  $\vec{\omega}$ , defined as a pure quaternion  $\Omega = (0, \vec{\omega}_S^G) = (0, \omega_x, \omega_y, \omega_z)^T$  and represented in  $\mathcal{F}_G$ .  $q^{S,G}$  is the quaternion represents the rotation from sensor frame to global frame,  $q^{S,G*}$  is the conjugate of the  $q^{S,G}$ . Both  $q^{S,G}$  and  $q^{S,G*}$  are unit quaternions.

The measurement vector from the gyroscope at time  $t$  including the noise effect  $\sigma$  is:

$$\bar{y}_{\omega,t} = \bar{\omega}_t^S + \sigma_{\omega,t} \tag{3.94}$$

**Linear acceleration measurement model:**

The accelerometer measures the specific force  $\vec{F}$  in the sensor frame  $\mathcal{F}_S$ . This can be expressed as [117]:

$$\bar{s}^S := R^{S,G}(\bar{a}^S - \bar{g}^S) \tag{rotation matrix representation} \tag{3.95}$$

$$f^S := q^{S,G} \otimes (a^S - g^S) \otimes q^{S,G*} \tag{quaternion representation} \tag{3.96}$$

where the same notation rules are valid as in angular velocity expression.

The measurement vector from the accelerometer at time  $t$  including the noise effect  $\sigma$  is:

$$\bar{y}_{a,t} = R_t^{S,G}(\bar{a}^S - \bar{g}^S) + \sigma_{a,t} \tag{3.97}$$

**Environment magnetization measurement model:**

Magnetometers measure the local magnetic field, consisting of both the Earth’s magnetic field and the magnetic field due to the presence of magnetic material. The (local) Earth’s magnetic field is denoted  $m^n$ . The ratio between the horizontal and vertical components depends on the location on the earth. The angle between the *needle* and the horizontal plane is the inclination angle; the angle between the *needle* and the true north is the declination angle. These two angles make a solid angle so-called dip angle  $\alpha$ . The dip angle and the magnitude of the Earth’s magnetic field are accurately known from geophysical studies. Similar to the tilt calculation from known gravity value, heading (i.e yaw) calculation from the known magnetization direction of the location can be computed.

Magnetometers provide information about the heading in all locations on the earth except on the magnetic poles, where the local magnetic field  $m^n$  is vertical. Orientation can be estimated based on the *direction* of the magnetic field. The *magnitude* of the field is irrelevant. Because of this, without loss of generality, the Earth’s magnetic field can be modelled as [117]:

$$m^n = (\cos \alpha \quad 0 \quad \sin \alpha)^T \tag{3.98}$$

assuming that  $|m|_2 = 1$  and the magnetometer only measures the local magnetic field, its measurements  $y_{m,t}$  can be modeled as:

$$\bar{y}_{a,t} = R_t^{G,S}(m^S) + \sigma_{m,t} \tag{3.99}$$

**3.3.1 Orientation-based HME with IMUs**

The orientation estimation from an IMU has been studied widely [117]. A simple integration of the angular velocity is computed by integration of gyroscope data as in Eq. (3.100).

$$\begin{aligned} \text{roll} \rightarrow \hat{\phi}^G &= \int_{t_0}^t \omega_x \Delta t = \int y_{\omega_x,t}^G dt &= \phi_{k-1} + \vec{\omega}_k \cdot dt \\ \text{pitch} \rightarrow \hat{\theta}^G &= \int_{t_0}^t \omega_y \Delta t = \int y_{\omega_y,t}^G dt &= \theta_{k-1} + \vec{\omega}_k \cdot dt \\ \text{yaw} \rightarrow \hat{\psi}^G &= \int_{t_0}^t \omega_z \Delta t = \int y_{\omega_z,t}^G dt &= \psi_{k-1} + \vec{\omega}_k \cdot dt \end{aligned} \tag{3.100}$$

$$\tag{3.101}$$

This mathematical expression is our system model in the KF where the gyroscope readings are the system inputs in Eq. (3.77).

For the correction step of the KF, observable states must be expressed mathematically by system states. Accelerometer readings can be used for roll and pitch correction, magnetometer readings can be used for yaw correction.

Accelerometers are sensitive to both linear acceleration and the local gravitational field (Eq. (3.97)). If the linear acceleration on the body is negligible, then assume that

the only acceleration exerted on the body is gravity. In our case, as the body stays still, the gravitational acceleration is measured only by the z-axis of the IMU (see Fig. 3.18). If the IMU is rotated, let's say  $\theta$  angles around the y-axis, then the gravity vector is expressed by x and z components on the IMU readings.

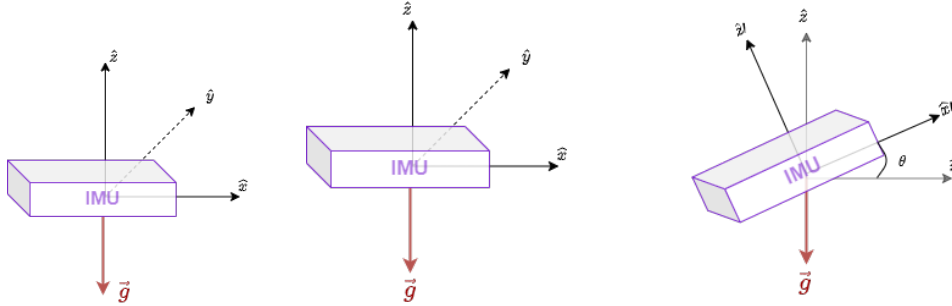


Fig. 3.18: Tilt measurement by accelerometer

Generally, rotations are not only around one axis. If the IMU is rotated around both x and y axes, by  $\theta$  and  $\phi$  angles respectively:

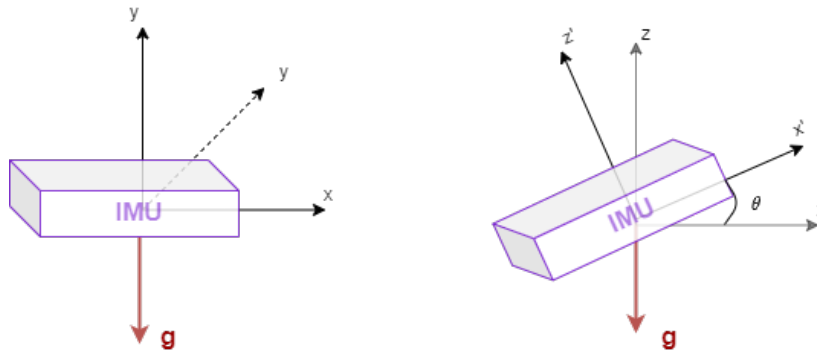


Fig. 3.19: Tilt in 2 axes

where the  $\theta$  and  $\phi$  angles are found by the following formula:

$$\tan(\phi) = -\frac{a_y}{\tilde{a}_z} = -\frac{a_y}{\sqrt{(a_x^2 + a_z^2)}} \quad (3.102)$$

$$\tan(\theta) = \frac{a_x}{\tilde{a}_z} = \frac{a_x}{\sqrt{(a_y^2 + a_z^2)}}$$

and the  $\psi$  angle is found by:

$$H_x = m_x \cos \theta + m_y \sin \theta \sin \phi + m_z \sin \theta \cos \phi \quad (3.103)$$

$$H_y = m_y \cos \phi - m_z \sin \phi$$

$$\psi = \arctan \left( \frac{H_y}{H_x} \right)$$

## Background

Eq. (3.102) and Eq. (3.103) can now be used in the KF where the accelerometer and magnetometer readings are the measurements in Eq. (3.78).

Since the orientations of each IMU are obtained, the orientation based HME can begin. Fig. 3.7 shows the poses of two consecutive links in which the orientation of each IMU is *estimated* by the KF at this point. Also, the HME gives us the kinematic chain representation of the human body. The Eq. (3.104) maps the IMU sensor orientations into body link orientations.

$$q^{G,B} = q^{G,S} \otimes q^{B,S^*} \quad (3.104)$$

where  $\otimes$  denotes the quaternion multiplication and  $*$  the complex conjugate of the quaternion. Neglecting the STA,  $q^{S,B}$  is a constant value. Hence,  $q^{G,B}$  gives the orientation of each link with respect to  $\mathcal{F}_G$ .

$q_i^G$  represents the orientation of link  $i$  and the quaternion  $q_{i+1}^G$  represents the orientation of link  $i + 1$  with respect to  $\mathcal{F}_G$ . Then, the rotation from link  $i$  to  $i + 1$  is represented as:

$$q^{i,i+1} = q_i^{G*} \otimes q_{i+1}^G \quad (3.105)$$

$q^{i,i+1}$  is the rotation between link  $i$  and  $i + 1$ . According to Fig. 3.20, three joint angles  $\theta_s, \theta_e, \theta_w$  denoting shoulder, elbow and wrist angles in 3-axes respectively calculated by this process.

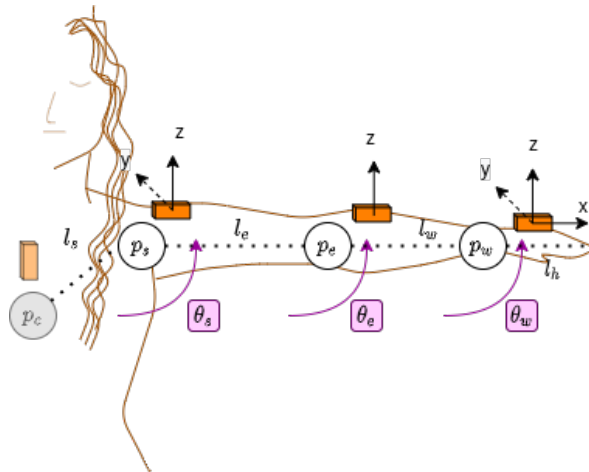


Fig. 3.20: Human arm joint angles and positions

$p_c, p_s, p_e, p_w$  and  $p_h$  denotes the joint (and end effector) positions as frame origins,  $l_s, l_e, l_w, l_h$  are the body link lengths of the (chest), shoulder, elbow, wrist and hand respectively.  $p_c$  is assumed stationary as well as the chest IMU is used as the body frame. Therefore, any undemanded motions caused by the torso and affecting the arm motion are eliminated. The rest of the positions are calculated by multiplying the joint angles with their respective body links as shown in Eq. (3.106).

$$p_c^G = (0, 0\hat{i}, 0\hat{j}, 0\hat{k}) \tag{3.106}$$

$$p_s^G = p_c^G + q_s^G \otimes l_s \Big|_{\mathcal{F}_s} \otimes q_s^{G*}$$

$$p_e^G = p_s^G + q_e^G \otimes l_e \Big|_{\mathcal{F}_e} \otimes q_e^{G*}$$

$$p_w^G = p_e^G + q_w^G \otimes l_w \Big|_{\mathcal{F}_w} \otimes q_w^{G*}$$

$$p_h^G = p_w^G + q_I \otimes l_h \Big|_{\mathcal{F}_w} \otimes q_I^* \tag{3.107}$$

where  $p_i^G$  is the position of link- $i$  in the global frame,  $q_i^G$  is the orientation of the link- $i$  with respect to the global frame,  $l_i \Big|_{\mathcal{F}_i}$  is the link length of the link- $i$  represented in its own frame and  $q_I$  is the unit quaternion which represents the null rotation  $(1, 0\hat{i}, 0\hat{j}, 0\hat{k})$ .

To sum up, in orientation based HME, the system is modelled such that a rotation input is given and orientation is tried to be estimated. Orientation in 3-axes, therefore, is the system states  $\hat{x}$ , accelerometer and/or velocity are the observable states  $\bar{y}$ . Hence, the mathematical model in which the relation between rotation input and acceleration/velocity output relation is defined gives us the possibility of comparing the outputs of the physical model and the mathematical model. By eliminating the difference between observable states, the Kalman gain updates itself and reduces the error in unobservable states i.e. reduces the estimated orientation error. The diagram of such an approach would be as in Fig. 3.21

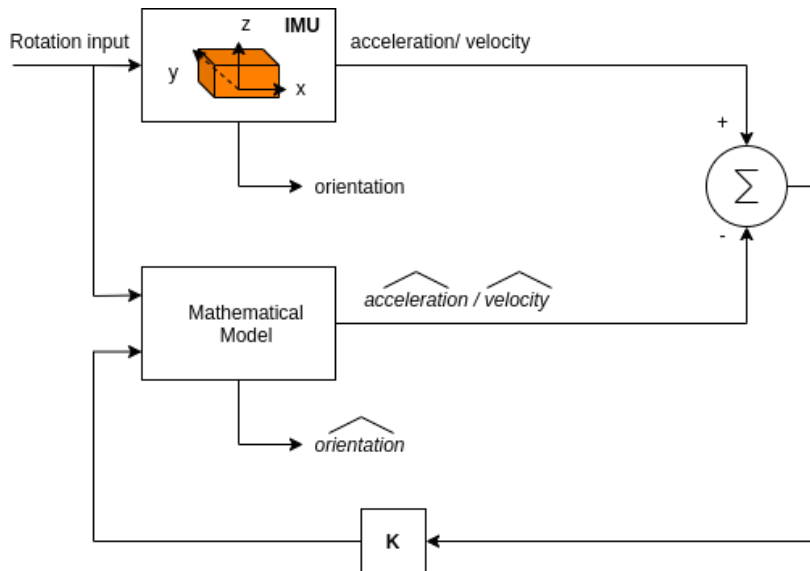


Fig. 3.21: Orientation estimate system diagram

After the orientation of each IMU is estimated, their joint angles are calculated using kinematic relations. Finally, using link lengths, the position of each joint and the end effector are calculated.

### 3.3.2 Position-based HME with IMUs

In orientation-based HME, there are some assumptions such as rigid body link lengths, neglecting the linear acceleration of the body, etc. that cause errors in state estimation. To remedy these deficiencies, position-based HME is proposed. The method is derived from the studies proposed in [19, 117].

Orientation of each IMU is either calculated as in Section 3.3.1 or directly from the raw orientation data which is provided by Xsens Awinda IMUs. For manual calculation of the orientation, the approach from Kok et. al. [117] is used to obtain the orientation by integration:

$$\dot{q}_t^{G,S} = \frac{1}{2} q_t^{G,S} \otimes \Omega_t \quad (3.108)$$

Hence,

$$q_{t+1}^{G,S} = q_t^{G,S} \otimes \exp_q\left(\frac{T}{2}(\mathbf{y}_{\omega,t} - \sigma_{\omega,t})\right) \quad (3.109)$$

where  $\exp_q$  is the *exponential map*,  $\exp_q : \mathbb{R}^3 \rightarrow \mathbf{q} \in \mathbb{R}^4 : \|\mathbf{q}\|_2 = 1$ , from a corresponding Lie algebra (SO(3)). However, the process explained in this chapter does not depend on *how* the orientation of IMUs are obtained, so we will not explain further.

If the orientation of the sensor  $q_t^{G,S}$  is known, the linear acceleration at time  $t$  of the body in the global frame is obtained by:

$$\mathbf{a}_t^G - \mathbf{g}^G = q_t^{G,S} \otimes (\mathbf{a}_t^S - \mathbf{g}^S) \otimes q_t^{G,S*} \quad (3.110)$$

where  $\mathbf{a}_t^G$  and  $\mathbf{g}^G$  are linear acceleration and gravity in global frame in quaternion form. Note that they are pure quaternions.

The process starts with double integrating the accelerometer measurements in 3-axes. After removing the gravity component, the acceleration  $\mathbf{a}_t$  can be integrated once to velocity  $\mathbf{v}_t$  and twice to position  $\mathbf{p}_t$ , all in the global frame:

$$\ddot{\mathbf{p}}_t^G = \mathbf{a}_t^G \quad (3.111)$$

$\mathbf{p}_t^G$  is the position of the IMU. The relation which is used as a system model is based on that. Since the position is updated discretely and every time step, using Newton's equations of motion [307], the velocity and position vectors can be described as:

$$\begin{aligned} \mathbf{p}_{k+1}^G &= \mathbf{p}_k^G + T\mathbf{v}_k^G + \frac{T^2}{2}\mathbf{a}_k^G \\ \mathbf{v}_{k+1}^G &= \mathbf{v}_k^G + T\mathbf{a}_k^G \end{aligned} \quad (3.112)$$

where  $T$  is the time between two samples. In some approaches, the dynamics of the orientation is also mathematically described and the system state vector contains all position, orientation angular+linear velocity as well as the linear acceleration as in [117]. However, it is better to simplify the system equation since the process has to be repeated in every time step. Hence, the state vector only contains the positions of each joint origins.

The offsets where the IMUs are placed with respect to their belonging joint origins



are shown in Fig. 3.22 denoted as  $d_s, d_e, d_w$  for shoulder, elbow and wrist joints, respectively. The offsets are assumed to be rigid for simplicity neglecting the bone-to-skin motion of the human body limbs. However, if the effect of STA needed to be considered, these offsets are also supposed to be adaptively parametrized.

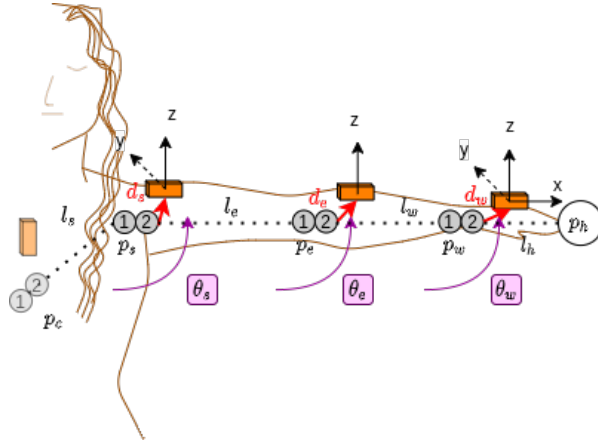


Fig. 3.22: Human arm joint angles and positions

As Fig. 3.22 implies, the joint origins are expressed as two points; 1 and 2 for each joint. The notation 1 is used where the previous link ends and 2 is used where the next link starts. In my assumption, I choose point-2s as the joint origin. Neglecting the joint clearance, point-1 and point-2 belong to the same joint and are coincident. However, these points are separated due to the drift error during position estimation. Therefore, the positions of each body link are estimated individually in the KF predict step and the kinematic constraints are used in the correct step.

Let  $p_{i_1, k+1}$  represent the position of the origin of the  $i_1^{\text{th}}$  link at  $k+1$  and Let  $p_{i_2, k+1}$  represent the position of the origin of the  $i_2^{\text{th}}$  link, the system model is based on these equations:

$$p_{i_1, k+1} = p_{i_1, k} + \overbrace{T \vec{v}_{i_1, k}^G}^{\text{integral}} + \frac{T^2}{2} a_{i_1, k}^G \quad (3.113)$$

$$p_{i_2, k+1} = p_{i_2, k} + T \vec{v}_{i_2, k}^G + \frac{T^2}{2} a_{i_2, k}^G \quad (3.114)$$

$$p_{i_2, k} = p_{i_1, k} + \overbrace{q_{i_1, k}^{G, S} \otimes l_1^B \otimes q_{i_1, k}^{G, S^*}}^{\text{rotation}} \quad (3.115)$$

and our observable states are:

$$p_{i_1, k} - p_{i_2, k} = 0 \quad (3.116)$$

$$p_{i_1, k+1} - p_{i_2, k+1} = 0 \quad (3.117)$$

If Eq. (3.115) is substituted into Eq. (3.113), the KF steps will be:

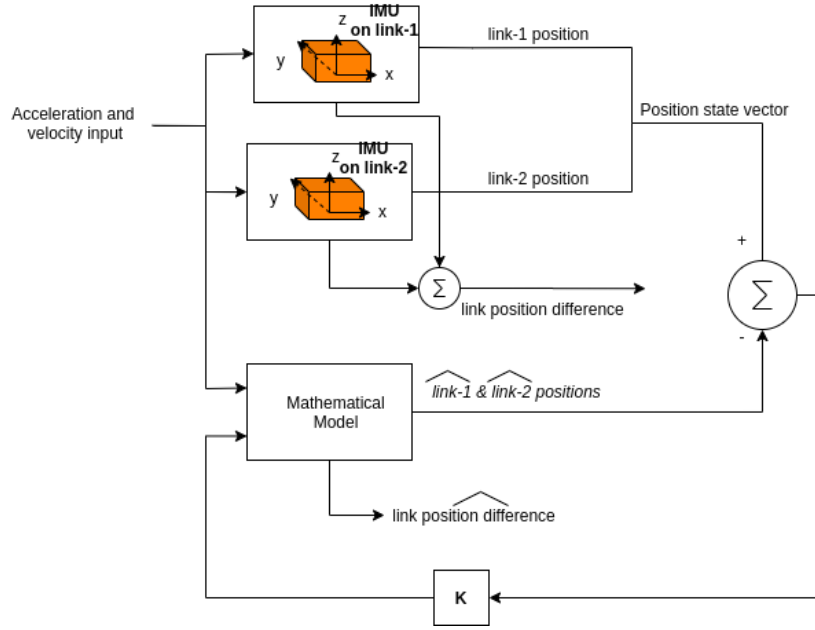


Fig. 3.23: Position estimate system diagram

**Predict step:**

$$p_{i_1,k+1} = p_{i_2,k} - q_{i_1,k}^{G,S} \otimes l_1^B \otimes q_{i_1,k}^{G,S*} - T \vec{v}_k^G + \frac{T^2}{2} a_k^G \quad (3.118)$$

$$p_{i_2,k+1} = p_{i_2,k} + T \vec{v}_k^G + \frac{T^2}{2} a_k^G \quad (3.119)$$

where  $p$ ,  $\vec{v}$  and  $a$  are pure quaternions as the representation of 3D vectorial position, velocity and acceleration respectively.

**Correct step:**

$$q_{i_1,k}^{G,S} \otimes l_1^B \otimes q_{i_1,k}^{G,S*} = p_{i_1,k} - p_{i_2,k} \quad (3.120)$$

$$q_{i_1,k+1}^{G,S} \otimes l_1^B \otimes q_{i_1,k+1}^{G,S*} = p_{i_1,k+1} - p_{i_2,k+1} \quad (3.121)$$

where  $q_{i,k}^{G,S}$  is the rotation from the  $i^{\text{th}}$  sensor to global frame at time step  $k$ . Hence, the system state vector  $x_k$  holds the positions of two consecutive link origins.

$$x_k = \begin{bmatrix} p_{i_1,k} \\ p_{i_2,k} \end{bmatrix}$$

The KF representation of this process is summarized in Fig. 3.23.

### 3.4 Biomechanical Modelling of Human Body

Achieving a human-like motion is one of the most interesting areas in the robotics field. Most of the serial industrial manipulators are inspired by the human arm in their design procedure. From the mechanical design to control the robot, from the

interaction level of the robot to social skills there are different ways to increase the anthropomorphism of the robots.

Biomechanical modelling of the human body is the first step in motion and gesture-based HRC. In robotics, the biomechanical model is represented as a kinematic chain. However, the human body has a sophisticated model chain. Despite the ordinary actuators which are used in mechanics, the motion of the human body occurs by contraction and relaxation of the muscles which are wind around the bones. The largest percentage of muscles in the muscular system consists of skeletal muscles, which are attached to bones and enable voluntary body movements. There are over 600 skeletal muscles in the human body [68]. Some muscle contractions create holonomic motion and it is very hard to distinguish all the individual muscle movements' effects.

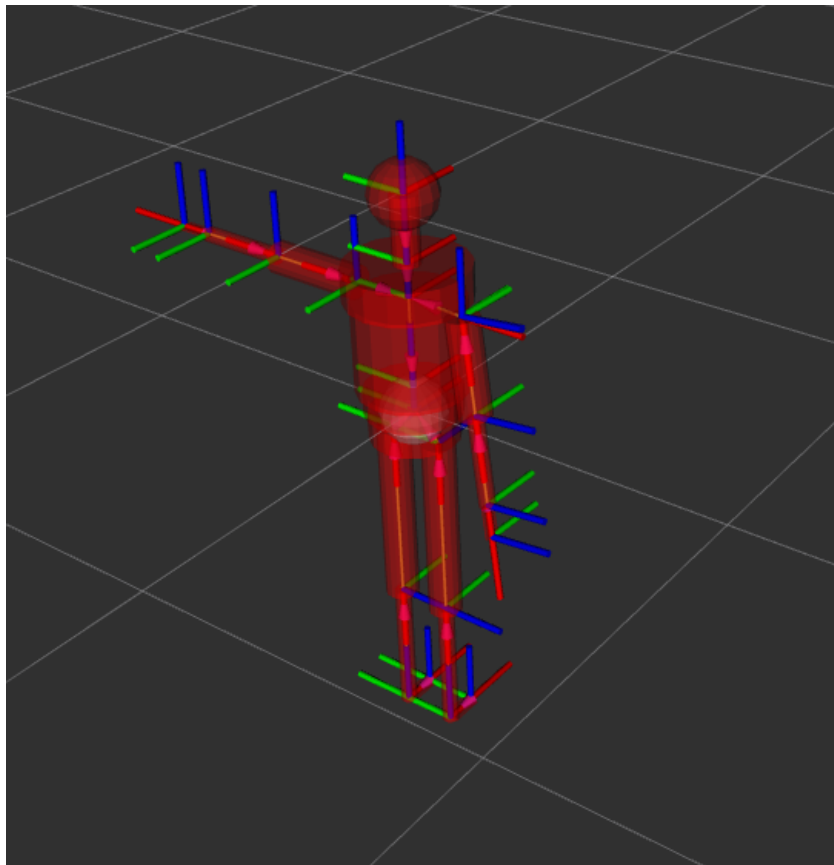


**Fig. 3.24:** 14 DoF Human body visualized in ROS Rviz. The left shoulder is up, respective axis colours are RGB:xyz

In Fig. 3.24, the model has 7 DoF on the right arm and 7 DoF on the left. The left arm is shown in its initial pose. The DoF distribution for this upper body model is that the shoulder joint has 3 DoF, the elbow has 1 DoF and the wrist has 3 DoF on each side of the human model. The methodology is the same for both arms, therefore, the explanation is going to be only for the left side.

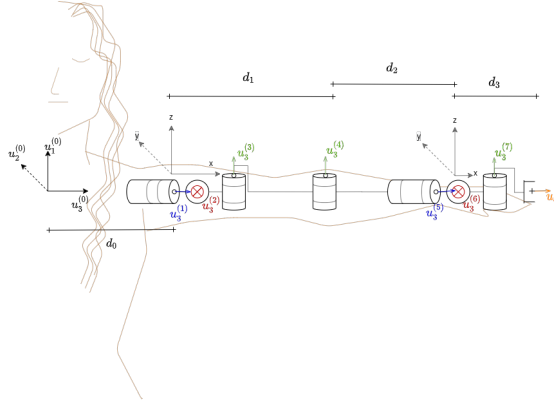
The model varies depending on the field of interest of the study. Less number of joints allows simpler computation but gives more vague information about the human pose. Increasing the DoF would result in more accurate estimation yet it would exponentially increase the computation cost. Particularly in HRC applications, the real-time capability of the developed system might play a vital role. Therefore, carefully

## Background

identifying the requirements is as important as developing a precise method for human motion estimation for HRC.

### 3.4.1 Human Arm Kinematic Calculation

The 7 DoF human arm can be modelled by DH parameters as follows:



	$\theta_k$	$s_k$	$a_k$	$\alpha_k$
1	$\theta_1$	0	0	0
2	$\theta_2$	0	0	$+\frac{\pi}{2}$
3	$\theta_3$	0	0	$-\frac{\pi}{2}$
4	$\theta_4$	0	$d_1$	0
5	$\theta_5$	0	$d_2$	$+\frac{\pi}{2}$
6	$\theta_6$	0	0	$+\frac{\pi}{2}$
7	$\theta_7$	0	0	$-\frac{\pi}{2}$
Hand (EE)	0	0	$d_3$	$+\frac{\pi}{2}$

**Table 3.2:** Human arm DH parameters

If it is applied Eq. (3.47) from link-0 (chest to shoulder) to link-4 (wrist to hand), an arm posture of a human based on orientation based HME is obtained.

In order to find the rotation from the global frame to the wrist frame, the kinematic chain for such a human model from the base (chest) to the tip (hand) can be written in quaternion form as:

$$q^{G,W} = q^{G,C} \otimes q^{C,S} \otimes q^{S,E} \otimes q^{E,W} \quad (3.122)$$

$$q^{G,E} = q^{G,C} \otimes q^{C,S} \otimes q^{S,E} \quad (3.123)$$

$$q^{G,S} = q^{G,C} \otimes q^{C,S} \quad (3.124)$$

where  $q^{G,W}$ ,  $q^{G,E}$ ,  $q^{G,S}$  are the quaternions that represent the orientation from the global frame to the wrist, elbow, and shoulder frames respectively. Those values are *measurements* of IMUs after calibration.  $G, C, S, E, W$  indices represents **global** → **chest** → **shoulder** → **elbow** → **wrist**, respectively. Each quaternion in this chain is the orientation from the previous body link to the next one. In other words, quaternion representation of each joint.

**Note:**  $q^{G,C}$  is a fixed orientation and it is equal to  $1+0\hat{i}+0\hat{j}+0\hat{k}$  to reduce the error on the base frame (i.e chest frame) in this study.

### 3.4.2 Types of Human Body Movements

Human motions are provided by muscle contractions and relaxations. Human anatomy can be translated into robotics terminology as such that the actuators of the human body are the muscles, and the links are the limbs of the body.

Since the muscles are wrapped around the bones, the actuation does not occur at a single point on the joint contrary to what we are used to in robotics. Furthermore, the contraction and relaxation of the muscles change the link lengths as well as the ligament displacement (soft tissue artifact). Therefore, even anatomically well-defined

human motions can be hardly translated into the robotics world. Moreover, having numerous different muscles leads to the fact that the human biomechanical model has quite high DoF yet it can hardly be modelled by current methods in robotics. Therefore there has not been a conclusion about the exact independent/non-holonomic DoF of a human body in the literature yet. However, according to the focus of the study, the biomechanical model of the human body is simplified and widely used in the robotics field.

Human motions are defined with respect to three anatomical planes which are shown in Fig. 3.25. Although for almost every body limb the naming for certain motion types differs in anatomical terminology, there is a simplified naming convention for general motion types according to these three planes [308].

- **Flexion/extension** refers to a decrease/increase in joint angle in the sagittal plane.
- **Abduction/adduction** is the motion of a segment away from/towards the midline in the frontal plane.
- **Internal/external rotation** is the joint motion in the transverse plane.

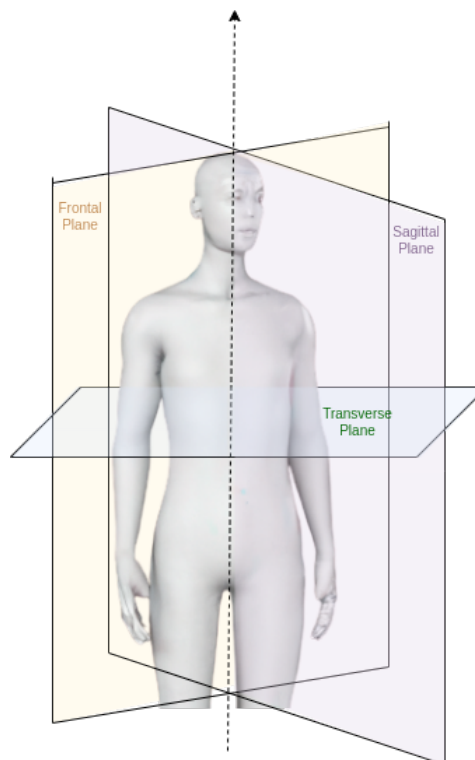


**Fig. 3.25:** The major anatomical planes of human motion, and axes of rotation

As well as this general recognition, during the motion, the relative motion of the body limbs' planes changes. Therefore, there are many other naming conventions for different joint motions for clarification. **Pronation** and **Supination** is also important to mention in this manner. These two terms are used for the complex triplanar action of the subtalar joint (on the ankle) and the radioulnar joint (on the forearm) and they are important to define the roll motion of the hand and foot. This motion can be mapped

## Background

as the roll motion in robotics if the body limb axes are taken as the x-axis in the body frame.

Within this study, the main focus is upper-body motions. According to [309], the upper limb is composed of six body segments (thorax, clavicle, scapula, humerus, forearm, and hand) and three main joints (shoulder, elbow, and wrist).

Human joints are mostly underactuated and holonomic. This issue is addressed as *coupling pronlem*. In particular, the shoulder and wrist joints are complex. For instance, on the wrist joint, executing only a roll motion without imposing any yaw motion is extremely hard due to the biomechanical structure of the human wrist.

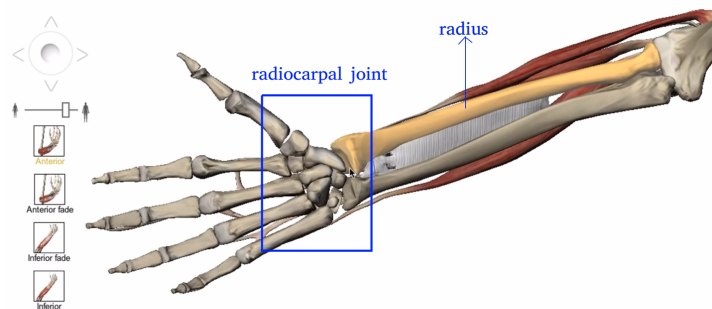


**Fig. 3.26:** Forearm anatomy for flexion/extension and abduction/adduction  
source: *Visible Body - Muscle Premium 2*

The wrist is an ellipsoidal (condyloid) type synovial joint, allowing for movement along two axes (flexion/extension, abduction/adduction). Those two motions are the pitch and yaw motions in robotic terminology. They are performed in the radiocarpal joint (where indicated as wrist, which consists of 7 small carpal bones on the hand and one long bone named radius on the lower arm) by the muscles of the forearm as shown in Fig. 3.26.

The pronation/supination (or the roll motion) on the other hand is performed by distal biceps brachii which is placed on the upper arm and attached to the radius on the elbow end. As the distal biceps brachii contracts and relaxes, it affects the forearm position so that it pronates and supinates and therefore changes the radiocarpal joint's orientation as shown in Fig. 3.27.

In the robotics field, one way of representing the whole set of 3D motions in orientation is pitch-yaw-roll angles. The respective equivalents of those motions in the human wrist are flexion/extension, abduction/adduction and pronation/supination.

The fact that the muscles of the upper arm generate the actuation of the roll motion of the wrist joint whereas the muscles of the forearm generate the pitch and the yaw motion causes some problems in mirroring human wrist motions by generic industrial manipulators intuitively. Most of them have a spherical wrist structure and the roll motion is mostly the last joint on the manipulator contrary to the human wrist (which is the 'first' one in this case). This fact makes it harder to control/mimic the wrist motion in joint space. It gives undesired results for direct joint-to-joint mapping and unnatural motion for one-to-one end effector mirroring.

The explanation of the human-to-robot motion mapping problem related to complex human anatomy is exemplified in the wrist joint. However, each human joint is unique

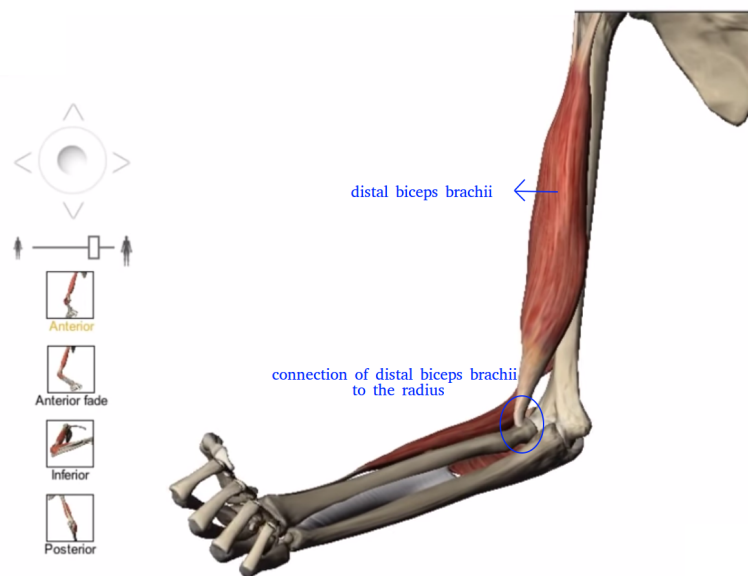


**Fig. 3.27:** Upperarm anatomy for pronation/supination  
*source: Visible Body - Muscle Premium 2*

and each creates the motion with a different set of muscle contraction/relaxation procedures.

However, the details of each joint's motion are not in the scope of this study. The definitions in this section will be referred for shoulder, elbow, and wrist joint motions are discussed in the following chapters.

### 3.5 Statistics for User Experiments

Even if you are not normal, your average is normal.

*Josh Starmer*

Statistics is a branch of collecting and analysing data using quantified models and representations as a whole from those in a representative sample. Generally, no individual data is clean and useful but more of it reveals a meaningful conclusion.

The statistical process in scientific research starts with a hypothesis, which is called the null hypothesis  $H_0$ , and its mutually exclusive alternative statements  $H_i$  [302]. The null hypothesis and the alternative hypotheses must complement 1 in total probability distribution for the test to be valid. For simplicity, the focus is only two mutually exclusive statements, so there is only one alternative hypothesis  $H_1$ .

Based on the selected null and alternative hypotheses, the test of the hypothesis is decided. It can be one-tailed where the rejection region is either on the left or on the right side of the test's bell curve as shown in Fig. 3.28, or it can be two-tailed where the rejection region is both the left and the right regions. For example, in a test scenario where it is stated that the average IQ of adults is 100 ( $H_0 : \mu = 100$ ) but if it is believed that it is *lower*, then it is a left one-tailed test ( $H_1 : \mu < 100$ ). Oppositely, if the belief is the average adult IQ is *higher*, then the alternative hypothesis ( $H_1 : \mu > 100$ ), which

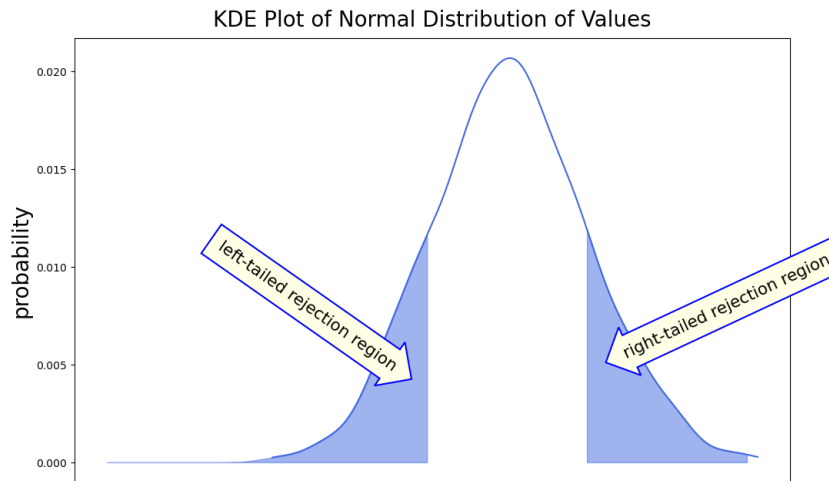


**Fig. 3.28:** One-tailed and two-tailed rejection regions of a statistical test

leads the test to be computed right one-tailed. The two-tailed test is mostly used when two group means are compared. The null hypothesis states that two group means are equal ( $H_0 : \mu_1 = \mu_2$ ) and the alternative hypothesis becomes true if the means are significantly different *lower or higher* ( $H_1 : \mu_1 \not\approx \mu_2$ ).

The region of the one-tailed or two-tailed test is calculated corresponding to the confidence level of the test. The respective test table is used to find out the critical test score.

Afterwards, a data collection process starts. Depending on the hypothesis, the collected data might be numerical or categorical. The applied scientific test differs based on the data type - not all statistical tests are applicable to all types of data. Finally, a proportional result is obtained regarding the null and alternative hypotheses.

However, a statistical test does not mean much without knowing the confidence interval and the effect size of the findings. A confidence interval is the mean of the estimate plus and minus the variation in that estimate. An effect size is the standardized mean difference which tells us how meaningful the relationship between variables is or the difference between groups. It indicates the practical significance of a research outcome, or in other words, how meaningful is the significance.

There are three common assumptions in the implementation of a statistical test:

1. **Gaussian distribution:** The qualitative data follows a normal (Gaussian) distribution.
2. **Independent observations:** The observations/variables are independent among different test subjects - although the variables are not independent within the subject.
3. **Homogeneity of variances:** The variance of each group being tested is similar enough not to limit the test's effectiveness.

In this section, different statistical tests based on the data type, confidence interval and effect size calculations are briefly explained to understand the findings in multi-user human-robot cooperative lifting experiments.



The following part of this section is compiled from the online lecture notes from Josh Starmer [310] and in [302] throughout chapters 8-12.

### 3.5.1 Selection of Statistical Test

There are two types of data: numerical (quantitative) and categorical (qualitative). Also, those data types are divided into sections within each other. The numerical data can be continuous (i.e. can be divided into units and have a decimal value e.g. 0.5N force) or discrete (i.e cannot be divided into the decimation of units, represent counts e.g. 2 times a day). The categorical data can be ordinal (ranking-based), nominal (representation name-based) or binary. It is important to analyse the data properly before applying a statistical test otherwise, the results may not point to the correct implication.

**PARAMETRIC VS NON-PARAMETRIC TESTS** These types of tests are strict in implementation and they are able to make stronger interference from the data. The most common parametric tests are regression tests, comparison tests and correlation tests. The regression tests look for a cause-and-effect relationship, comparison tests look for differences among group means, and correlation tests check whether the variables are related without concluding if there is a cause-and-effect relationship. The usage of those tests is summarized in the Table 3.3:

**Table 3.3:** Parametric statistical tests

Test Type		Observed variable	Outcome	Example research question
Regression Tests	Simple linear regression	- Continuous - 1 observed variable	- Continuous - 1 outcome	What is the effect of user height on learning score?
	Multiple linear regression	- Continuous - 2 or more observed variables	- Continuous - 1 outcome	What is the effect of the user height and age on learning score?
	Logistic regression	- Continuous	- Binary	What is the effect of gender on learning score?
Comparison Tests	Paired t-test	- Categorical - 1 observed variable	- Numerical - groups from the same population	What is the effect of two different training methods on average learning score?
	Independent t-test	- Categorical - 1 observed variable	- Numerical - groups from different populations	What is the difference in average learning score for users tested on two different training setups?
	ANOVA	- Categorical - 1 or mote observed variable	- Numerical - 1 outcome	What is the difference in average learning score for users tested on three different training setups?
	MANOVA	- Categorical - 1 or mote observed variable	- Numerical - 2 or more outcomes	What is the effect of the user's occupation on leaning category-1, learning category-2 and learning category-3.
Correlation Tests	Pearson's $r$	- 2 continuous variables	- Ratio in $[-1,1]$	How is the user's age related to the learning score?

## Background

Non-parametric tests can be used where one or more common assumptions are violated. They are not suggested to be used as long as the parametric test is applicable because the inferences they make are not as strong as with parametric tests. Some of the alternative non-parametric tests with their respective parametric test are given in Table 3.4.

**Table 3.4:** Non-parametric statistical tests

Test	Observed variable	Outcome	Example research question
Spearman's $r$	Numerical	Numerical	Pearson's $r$
Chi <sup>2</sup>	Categorical	Categorical	Pearson's $r$
Sign Test	Categorical	Numerical	One-sample t-test
Kruskal-Wallis $H$	Categorical 3 or more groups	Numerical	ANOVA
ANOSIM	Categorical 3 or more groups	Numerical 2 or more outcomes	MANOVA
Wilcoxon Rank-Sum Test	Categorical 2 groups	Numerical groups from different populations	Independent t-test
Wilcoxon Signed-rank Test	Categorical 2 groups	Quantitative groups from the same population	Paired t-test

### 3.5.2 *T-test Implementation*

The independent t-test is the most applicable test which is suitable for our research questions. It is also called one-way ANOVA among two independent variables and it is very similar to z-test. However, the z-test requires the mean and standard deviation of the whole population in the calculation steps, it is used seldom.

The simplest t-test score calculation is computed with the following formula:

$$t = \frac{m - \mu}{\frac{s}{\sqrt{n}}} \quad (3.125)$$

$$df = n - 1 \quad (3.126)$$

where  $t$  is the t-score (to reject or fail to reject the null hypothesis),  $m$  is the mean of the sample,  $\mu$  is the hypothetical mean,  $s$  is the standard deviation and  $n$  is the group size.

The degrees-of-freedom (df) has a slightly different meaning in statistics than it has in robotics. **Degrees of freedom** in statistics, often represented by  $v$  or  $df$ , is the number of independent pieces of information used to calculate a statistic. It's calculated as the sample size minus the number of restrictions if the sample sizes of the two groups are equal and standard deviations are close enough. If not, the following formula should be used:

$$t = \frac{(\bar{x} - \bar{y}) - (\mu_x - \mu_y)}{\sqrt{\frac{s_x^2}{n_x} + \frac{s_y^2}{n_y}}} \quad (3.127)$$

$$df = \frac{\left(\frac{s_x^2}{n_x}\right)^2}{n_x - 1} + \frac{\left(\frac{s_y^2}{n_y}\right)^2}{n_y - 1} \quad (3.128)$$

where  $\bar{x}$ ,  $\bar{y}$  are the calculated means,  $s_x$ ,  $s_y$  are the standard deviations and  $n_x$ ,  $n_y$  are the size of the sample- $\mathcal{X}$  and sample- $\mathcal{Y}$ . The term  $(\mu_x - \mu_y)$  is the difference of hypothetical means of two samples, which is equal to zero in this case based on our selection of null hypothesis ( $H_0 : \mu_x = \mu_y$ ). The denominator is the estimated standard deviation, which is the denominator of Eq. (3.127) ( $SE_{\bar{x}-\bar{y}}$ ) of the distribution of differences between independent sample means to for unequal variances.

There are alternative versions of correcting the standard deviation differences (e.g. Asprin Welch's standard error calculation) and df calculation of different group sizes (e.g. Satterthwaite's correction) but so far the explained calculation steps for the t-test are sufficient for this study.

### 3.5.3 Confidence Interval and Significance Level

The confidence interval reveals how much uncertainty there is with any particular statistic. With the sample data the null hypothesis might be rejected but it is most likely not 100% correct for every sample in the world. Different random samples drawn from the same population are likely to produce slightly different intervals.

The confidence level is the percentage of the intervals that contain the parameter. For 95% confidence intervals, an average of 19 out of 20 includes the population parameter right. The **p-value** is the most common representation of confidence level.

While the confidence level measures how confident we are that our conclusions are correct. In contrast, the significance level (also called  $\alpha$  value) is the probability of rejecting the null hypothesis when it is true.

This type of error is called a false positive (i.e. Type I error). A similar failure in a test result is a false negative (i.e. Type-II error) when the null hypothesis is not rejected when it is false. The visualization of errors in statistical decision-making is given in Table 3.5. In other words,  $\alpha = \text{Prob}(\text{Type I error})$ ,  $\beta = \text{Prob}(\text{Type II error})$ .

**Table 3.5:** Errors in statistical decision-making

	$H_0$ rejected	Fail to reject $H_0$
$H_0$ false	Correct	Type II error
$H_0$ true	Type I error	Correct

In summary, if the p-value is less than alpha, the null hypothesis is rejected. If it is greater than the alpha, the null hypothesis fails to be rejected.

### 3.5.4 Effect Size

Effect size tells how meaningful the relationship between variables or the difference between groups is. It is an indication of the practical significance of a research outcome. A large effect size means that a research finding has practical significance, while a small effect size indicates limited practical applications. For example, assume that a statistical test result shows female students have better mathematics grades than male ones with 95% confidence ( $\alpha = 0.05$ ). The effect size compares the differences between means within the standard deviations. If the mean of the mathematics grades of female students is 89/100 and for the male students it is 87/100, then the difference is statistically significant but not an effective conclusion is made.

Two common effect size calculation methods are using Cohen's  $d$  and Hedge's  $g$ . Cohen's  $d$  is used when the standard deviations of two samples are similar enough.

$$d = \frac{(\bar{x} - \bar{y})}{\sqrt{\frac{s_x^2 + s_y^2}{2}}} \quad (3.129)$$

Hedge's  $g$  is the extended version of Cohen's  $d$ , where the standard deviation differences of two samples are considered in the effect size calculation.

$$g = \frac{(\bar{x} - \bar{y})}{\sqrt{\frac{((n_x - 1) \cdot s_x^2 + (n_y - 1) \cdot s_y^2)}{n_x + n_y - 2}}} \quad (3.130)$$

## METHODS

This chapter provides a detailed account of the methods utilized in conducting this study. The focus is on techniques for upper-body 3D human pose and gesture estimation using wearable inertial measurement units (IMUs). This enables the estimated poses and gestures to be applied in a dynamic cooperative task. Figure Fig. 4.1 visually summarizes the overall study. Chapter Chapter 3 characterizes the problem, provides the necessary background, and takes initial steps to implement proposed solutions. Specifically, a biomechanical model of the human upper body is constructed by fusing orientation data from a network of IMUs worn on the body and merging it with upper-body kinematics.

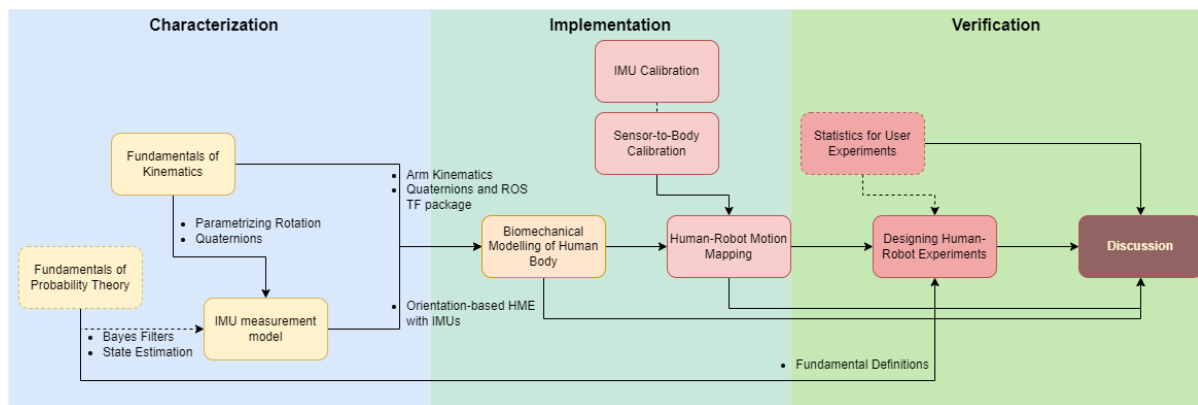


**Fig. 4.1:** The map of this thesis and how the pillars in fundamental chapters are connected. The straight-line-framed pillars indicate the main focus of the study and the dashed-framed pillars indicate them as supplementary yet essential pillars. The coloured background with 3 subdivisions indicates the state of the work in the pipeline

To enable a reliable model, the first critical step is obtaining clean measurement data, which requires calibration. Filtering is the most important aspect of calibration. In particular, noisy accelerometer data is nearly useless without proper filtering. A digital low-pass filter is ideal for eliminating high-frequency GWN and outlier measurements that appear as glitches in the IMU signals. Applying a cascaded median filter further smooths the signals, preparing them for subsequent usage.

Another critical calibration step is sensor-to-body calibration, which involves setting a reference origin for each IMU on the body. Properly establishing the alignment between each IMU sensor frame and the anatomical frame of the corresponding

body segment is essential for accurate pose and gesture estimation. This calibration transforms the raw sensor measurements into biomechanically meaningful joint angles and segment orientations.

Common calibration procedures include precisely locating bony landmarks through manual palpation or using an external measurement system. The joint centers and segment axes defined by these landmarks provide the anatomical coordinate frame. The calibration protocol then assigns the predefined rotation matrix and offset that transforms the initial arbitrary IMU frame to the anatomically aligned one. Some advanced methods even estimate these calibration parameters during live motion using kinematic constraints, however, such an implementation does not take part in this study.

At this stage, reliable measurements of human upper-body pose and gestures have been obtained. The next step is to generate a robot trajectory based on human motions. It is important to note that the estimated poses are relative, not absolute. This implies two key points. First, the processed arm motions are defined with respect to the human's own frame of reference, not the global world frame. Second, the initial human-fixed frame of reference is set at  $t = 0$  and arbitrarily changes upon restarts. A few methods are presented to translate human motions into meaningful robot motions in terms of robot action type, motion mapping type and mapping space selection. After a thorough evaluation and back-and-forth experimental processes, adequate human-robot motion mapping methods are selected for each sub-task of the proposed Cooperative Lifting (co-lift) scenario.

The procedures summarized above correspond with the implementation piece of Fig. 4.1. The verification step starts with designing user experiments and it is handled in the final section of this chapter. The methodology of how user experiments should be designed within the HRI field, the interpretation of the collected data according to Cohen's kappa and the risk assessment of human-robot experiments are covered. The rest of the verification step is wrapped up in Chapter 5.

### 4.1 IMU Calibration

An IMU is a device that contains an accelerometer to measure linear acceleration and a gyroscope to measure the angular velocity of the body/object to which the sensor is attached. Moreover, today many IMU devices contain magnetometers to measure the magnetic field and its direction in the environment. In some resources, those IMUs are named as *m-IMU* or *inertial-magnetic measurement*. However, most of the examples in the literature do not underline this distinction even though magnetometers do not measure an inertial property but an external property. To be consistent with the most used way in the terminology, IMU term includes all three elements (accelerometer, gyroscope, magnetometer) in this study.

An IMU provides the linear acceleration, angular velocity, and magnetic field information in 3 orthogonal axes, which provide 9 independent parameters in the measurement. Therefore those types of IMU devices are acknowledged as 9DoF inertial navigation devices.

For a reliable sensor fusion, all measurement parts of IMU should be calibrated. The main reasons for an IMU not to give reliable results can be listed such that:

- **Gyroscope:** Offset (sensor bias).
- **Accelerometer:** bias and high-frequency noise
- **Magnetometer:** By far the most effort required for magnetometer calibration. The distortions can be listed below:
  - (a) hard-iron offset (magnetometer bias)
  - (b) highly dependent on the location on Earth (tilt due to the shape of the Earth, magnetic field magnitude) as well as the attitude. The needle does not show direct north. It has a tilt (angle of dip or inclination angle),
  - (c) time (the magnetic pole is drifting toward Russia with an average speed of 40km/year[311], it is updated every 5 years) and the ferromagnetic materials in the environment. Here is the picture of the isometric lines showing the same magnetic field strength in 2022,
  - (d) ferromagnetic (Hard iron) distortion: If there is iron it is bad. It is created by objects that produce a magnetic field, such as magnetized iron,
  - (e) soft iron distortion stretches or distorts the magnetic field and is caused by metals such as nickel and iron.

Also, the calibration of the magnetometer tends to distort quite easily. Therefore, researchers try to find better sensor fusion algorithms without using magnetometers [114, 142].

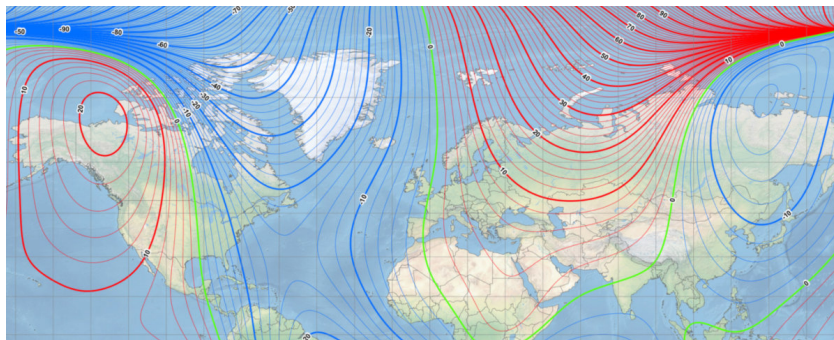


**Fig. 4.2:** World Magnetic Model (2020) developed by NCEI and the British Geological Survey, with support from the Cooperative Institute for Research in Environmental Sciences (CIRES)

Source: [311]

Those are the main things to adjust before using an IMU in a sensor fusion process. In addition to measurement calibration, sensor-to-body calibration is also required where IMU systems are used for human motion analysis purposes. This calibration can be executed in static and/or dynamic predefined positions.

According to [32], there are several different data available in the Xsens Awinda wireless IMU sensors such as 3D orientation, wireless network properties, sample counter, etc. as well as accelerometer, gyroscope, and magnetometer data as expected from an IMU. Depending on which output data type is used, calibration steps change.

## Methods

When accelerometer, gyroscope or magnetometer raw data directly used, an IMU calibration step is required afterwards. However, the 3D orientation output is provided by an internal sensor fusion algorithm, and it is factory-calibrated; the Sensor-to-body calibration step follows as next. This raw 3D orientation data is also more robust to drift than regular lower cost IMU since it corrects the orientation data with the internal barometer data [32].

### 4.1.1 Digital Filters

In electronics, a filter is a piece of hardware and/or software that eliminates unwanted components of a signal. According to input and output signal types, filters are divided into 2 categories: digital filters and analog filters. In analog filters, the input signal is a continuous signal. Since the processing of the analog signal does not involve any sampling step, the output signal is also a continuous signal. On the other hand, a digital filter takes the input signal and takes samples in each sampling period ( $1/f_s$ ).

Filtering is the most important part of the calibration. As specified in [32], Xsens Awinda has its own analog and digital filtering process before it outputs the data. However, some extra noise is also attached to the output data, especially on the accelerometer data. Therefore, a digital filter needs to be designed before using the IMU data for estimation.

As explained in bias and noise elimination, 2 different cascaded digital filters are used. One is a low-pass filter with a cutoff frequency of 10 Hz and sampling frequency of 512 Hz for an input accelerometer signal, which is obtained in 100 Hz. The second digital filter that is a moving median filter with 51 samples of window size and 512 Hz sampling frequency. In both implementations, `scipy.signal` library is used.

The working principle of these two filters can be simplified as follows:

**Low-pass Filter:** It eliminates any components which have a higher frequency than the filter's cutoff frequency of an input signal. A digital low-pass filter has impulse and frequency responses as shown in Fig. 4.3.

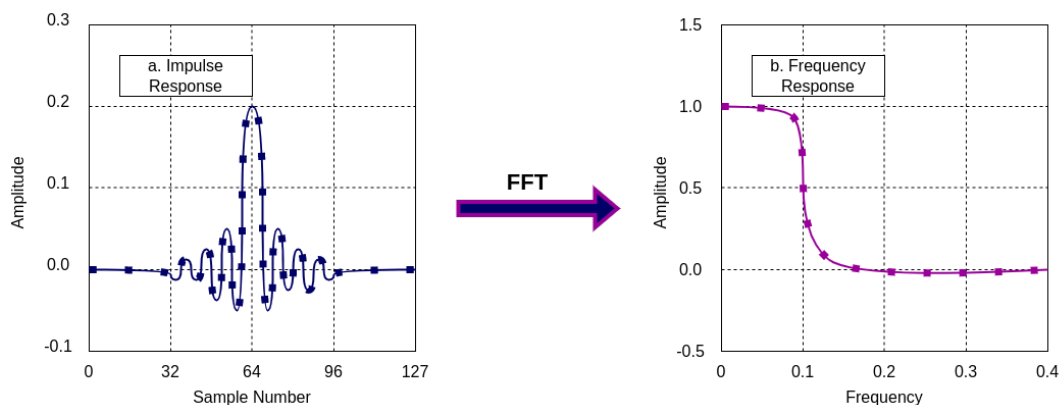


Fig. 4.3: Low pass filter impulse and frequency responses

The general representation of the transfer function of a filter in the time domain is  $h(t)$  and in the frequency domain is  $H[n]$  where  $t$  is the time and  $n$  is the sample step [312]. For a digital input signal  $x[n]$  (or  $X[n]$  in the frequency domain), the output



signal  $y[n]$  can be found by convolution of the signal with the filter transfer function  $h[n]$  in the time domain.

$$x[n] \otimes h[n] = y[n] \quad (4.1)$$

$$\forall n, h[n] \Rightarrow (x \otimes h)[n] = \sum_{k=-\infty}^{\infty} h_{\infty}[k].x_{\infty}[n - k] \quad (4.2)$$

However, in the implementation of convolution, is it not possible to have all the samples in  $-(\infty, \infty)$  so the filter function has to be truncated. After the truncation, the transfer function and expanding it in a Fourier representation to find the coefficients of the filter. The number of samples after the truncation is the filter order. The bigger is the filter order, the slower get the filter. In an example of a 3<sup>rd</sup> order low-pass filter then:

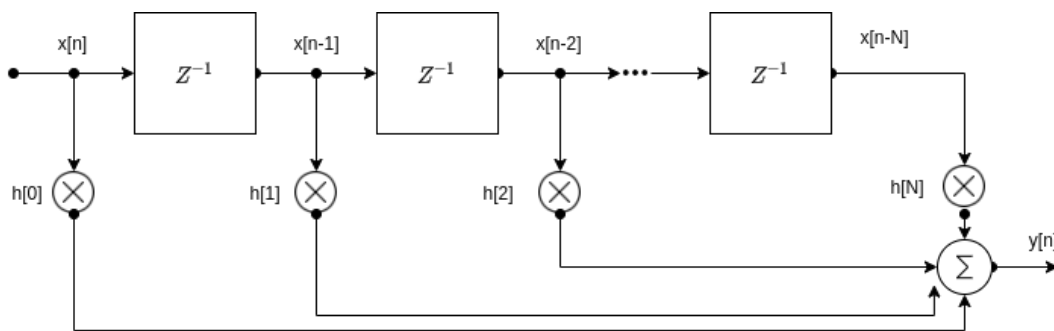


**Fig. 4.4:** Basic implementation of an FIR filter

This implementation is the same for both the moving median filter and low-pass filter with a finite impulse response. The coefficients of the low-pass filter can be calculated by the Fourier transformation yet for moving the median filter, this step is not needed. For a median filter that has a window size =  $N$ , the required number of coefficients is  $N+1$  as shown in Fig. 4.4. To keep the magnitude of the signal the same, the summation of all the coefficients used in the filter should be equal to 1. To make each sample of input signal behave/contribute the same, all the coefficients must be equal to each other in the median filter.

$$\begin{aligned} h[0] = h[1] = h[2] = \dots = h[N] \wedge h[0] + h[1] + h[2] + \dots + h[N] &= 1 \\ \therefore h[0] = h[1] = h[2] = \dots = h[N] &= \frac{1}{N+1} \end{aligned} \quad (4.3)$$

Hence, the implementation is

$$y[n] = h[0] \cdot x[n] + h[1] \cdot x[n - 1] + h[2] \cdot x[n - 2] + \dots + h[N] \cdot x[n - N] \quad (4.4)$$

$$= \frac{1}{N + 1} \cdot x[n] + \frac{1}{N + 1} \cdot x[n - 1] + \frac{1}{N + 1} \cdot x[n - 2] + \dots + \frac{1}{N + 1} \cdot x[n - N] \quad (4.5)$$

$$= \frac{1}{N + 1} [x[n] + x[n - 1] + x[n - 2] + \dots + x[n - N]] \quad (4.6)$$

### 4.1.2 Noise Elimination

Noise can be defined as any unwanted additional signal added to the actual measurement in signal processing. Noise in a measurement device can occur for many reasons. In general, in any sensor measurement, additive noise occurs due to electrons' motion in capturing, storing, or processing the signal. The character of this noise is mostly undetermined so its uncertainty is accepted as it has a Gaussian distribution. This term is also "white noise" or "Gaussian White Noise (GWN)".

The noise effect on different sensors is different. In some cases, it can be neglected. For instance, in this case, we see a high-frequency noise added to the raw data of the accelerometer (see Fig. 4.5 and Fig. 4.6), yet we do not see a big effect on the raw gyroscope data. It is well known that accelerometer readings have a white noise due to the electronic noise of the circuitry that converts the motion into a voltage signal and the mechanical noise of the sensor itself [313].

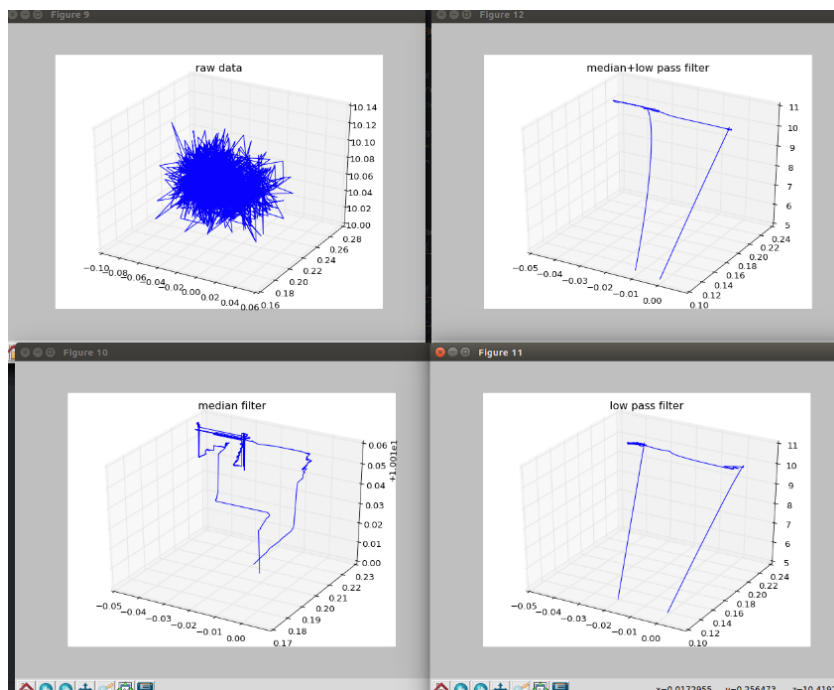
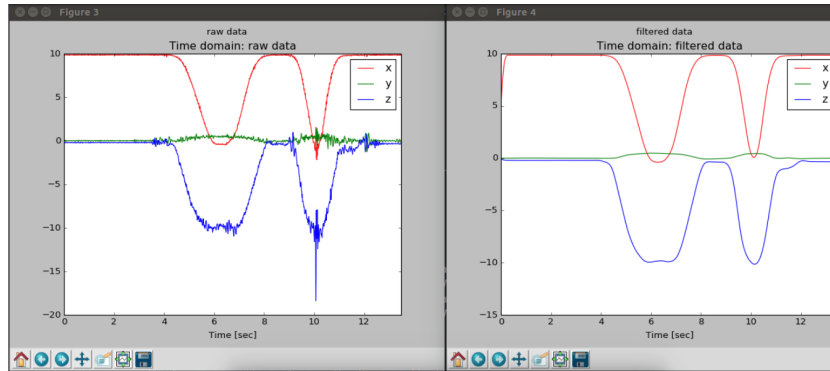


Fig. 4.5: Accelerometer raw and filtered (gravity eliminated) data in a stable position

The character of the additive noise in the accelerometer data is GWN, which has high frequency. The use of a low-pass filter with a sampling frequency of 512 Hz and a cut-off frequency of 10 Hz is adequate to eliminate this GWN. It is safe to use such a



**Fig. 4.6:** Accelerometer raw and filtered (gravity not eliminated) data during 2 pitch motion

low cut-off frequency because relatively slow motions are computed.

### 4.1.3 Bias Elimination

Bias, or in another terminology sensor offset, is the nonzero reading when the IMU stays stable. The bias elimination is computed simply by removing these offset values before the actual measurement starts.

At any place, the MEMS magnetic needle in the IMU points in the direction of the resultant intensity of Earth's magnetic field and the accelerometer measures the gravity vector at the place. The direction of this needle and the inclination angle can be converted into compass headings of the magnetometer's x-y-z axis as in [314]. Those expected readings of the magnetometer and the accelerometer are accepted as zero readings in a stable pose. Gyroscope, on the other hand, should return numerical zero values when the IMU is stable.

**Table 4.1:** Expected and measured IMU readings when it is stable at the location of HVL Robotics in Førde (Latitude:61.459145 N, Longitude:5.835823 E) when the IMU's x-axis is directed to the north

Device	Axis	Expected	Measured	Error
Gyroscope (deg/sec)	x	0	0.001536	-0.001536
	y	0	0.003052	-0.003052
	z	0	-0.00049	0.00049
Accelerometer (m/s <sup>2</sup> )	x	0	-0.025217	0.025217
	y	0	-0.053239	0.053239
	z	9.820306	9.835812	-0.015506
Magnetometer ( $\mu$ T)	x	$51.485\mu\text{T} \cdot \cos(73.37) \cdot \cos(1.5)$	70.0	-55.27
	y	$51.485\mu\text{T} \cdot \cos(73.37) \cdot \sin(1.5)$	2.4	-2.01
	z	$51.485\mu\text{T} \cdot \sin(73.37)$	30.9	18.43

These values in Table 4.1 are fluctuating over time. Instead of treating the offset as a constant, they are measured before each use and bias elimination is computed dynamically on the site. The result of the noise elimination and the bias elimination on accelerometer raw data is shown in Fig. 4.7.

As explained, bias and noise are the biggest problems in using IMUs for pose estimation. The residuals, sensor-to-motion axis misalignment and integration errors cause non-neglectable errors. This step is vital for sure but more calibration and

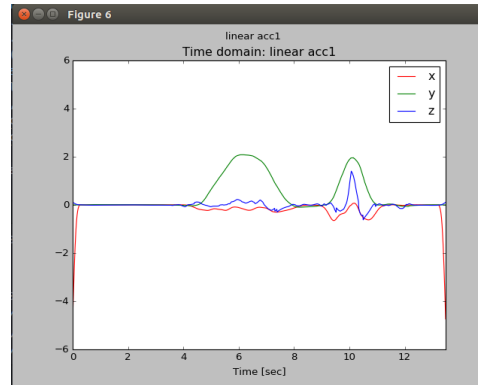


**Fig. 4.7:** Accelerometer raw data, noise eliminated data and noise+gravity eliminated data during 2 pitch motion

different human-to-robot motion mapping methods are needed to reliably use IMUs in HRC applications.

## 4.2 Sensor-to-Body Calibration

Sensor-to-body calibration is to position the sensors with respect to the body frame and remove the zero-error; this refers to when the sensor records a small angle even though it is totally level. It is required in every type of MoCap system. For a camera system, the position of the cameras and the position of the human with respect to each camera has to be calibrated before HME. Moreover, marker-based systems need to be calibrated as camera-based systems as well as IMU based systems because body-attached markers have the sensor-to-body displacement problem as IMU systems. Since the scope of this study is using IMU in HME, IMU calibration is focused on in this section.

This calibration step is not a part of the internal calibration of IMU but it is a part of the calibration process before human motion analysis and estimation. The purpose of this calibration is to provide information to the system about the initial pose of the human. Moreover, during the action, the defined position of the sensors is displaced due to anatomical reasons such as soft tissue artifacts, joint clearances etc.

The calibration can be static calibration; performing some predefined poses, and/or dynamic calibration; performing some predefined motions. Static calibration is for eliminating the initial orientation/position offsets on each individual sensor. In this study, only static calibration is performed in the results, dynamic calibration is only researched. Therefore, this section only focuses on static calibration.

N-pose is the natural human pose in which the human is standing up, arms are naturally released on the sides. T-pose is the two-arms-up pose in which the human is standing up, arms are lifted as if the body makes a T-shape (see Fig. 4.8). An initial pose is when the calibration pose is the same as the initial pose of the HRC system start. During different processes of the study, different calibration poses are used such as N-pose, T-pose or initial pose calibration. Since the T-pose is the easiest to illustrate and the one used in this study at most, the sensor-to-body calibration methods are explained via this pose. The process is the same in each pose, just the given human angles set to a different IMU initial reading. However, the initial pose calibration gave

better usage in the end.

The rotation angle between each consecutive IMU corresponds to a joint angle. The 7 IMUs placement on the human body for measuring chest, shoulder, elbow and wrist joint angles from the torso and two arms respectively. The process of calculating the joint angles is given in Chapter 4 with details.

The human body frame is defined such that it is concentric as the IMU-0's sensor frame. The axes are defined as x: towards to head, y: towards to right shoulder, z: out of the chest. According to this assumption, the initial orientation of each IMU in Fig. 4.8 can be listed as:

- IMU-0 initial:  $R(0) = \hat{I}_{3 \times 3}$  or  $q_I$
- IMU-1,2,3 initial:  $\left( R_x(-\frac{\pi}{2}) \times R_z(-\frac{\pi}{2}) \right)$  or  $q^{(-\frac{\pi}{2}, x)} \otimes q^{(-\frac{\pi}{2}, z)}$
- IMU-4,5,6 initial:  $\left( R_x(-\frac{\pi}{2}) \times R_z(\frac{\pi}{2}) \right)$  or  $\left( q^{(-\frac{\pi}{2}, x)} \otimes q^{(\frac{\pi}{2}, z)} \right)$

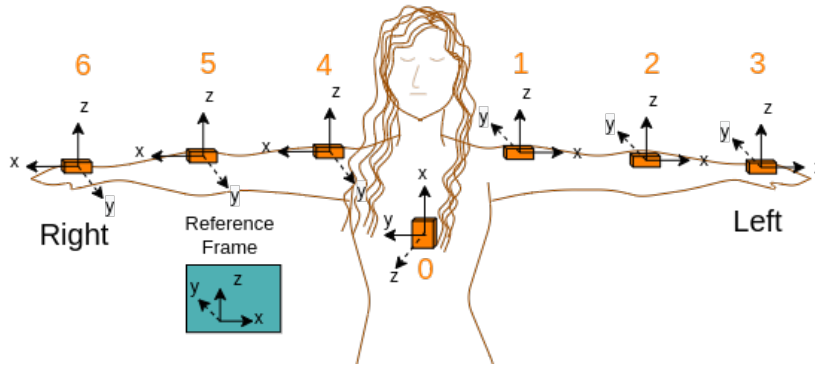


Fig. 4.8: IMU attachment on the body

All measurement data is in the sensor frame. The quaternion  $q_i^{G,S}$  represents the rotation from the global frame to the sensor frame of respected  $i^{th}$  IMU. The quaternion  $q_i^{B,S}$  represents the rotation from the body frame to the sensor frame of respected  $i^{th}$  IMU (i.e  $q_0^{B,S}$  is for IMU-0). For simplicity, the method is explained on the left arm but the procedure is the same for the right arm.

Therefore the orientation of the body on which the  $i^{th}$  IMU is attached with respect to the global frame is then:

$$q_i^{G,B} = q_i^{G,S} \otimes q_i^{B,S*} \quad (4.7)$$

If we analyze the Eq. (4.7) component-wise,  $q_i^{G,B}$  is what we want to find,  $q_i^{G,S}$  is what we read from the IMU and  $q_i^{B,S}$  is what we initially set.

An important point is that the sensor gets misaligned during the action due to skin motion with respect to the underlying bone. This issue is known as soft tissue artifact. To overcome this problem an adaptive calibration process can be implemented or it can be considered as noise in the pose estimation process. The misalignment can be examined by dissolving  $q_i^{B,S}$  as in Eq. (4.8).

$$q_i^{B,S} = q_{i,accurate}^{B,S} \otimes q_{i,distortion}^{B,S} \quad (4.8)$$

## Methods

where  $q_{i,accurate}^{B,S}$  is the accurate sensor-to-body orientation.  $q_{i,distortion}^{B,S}$  can be determined adaptive and  $q_{i,accurate}^{B,S}$  can be updated as  $q_i^{B,S}$  during the experiment/usage. However, this misalignment issue is eliminated in the human-robot motion mapping step in this study.

### 4.3 Human-Robot Motion Mapping

The methodology of motion mapping between the human and the robot is as important as estimating the human motions. The intuitiveness of the system is highly connected to the selected human-robot motion mapping mode. The teleoperation of a 6 DoF manipulator is one of the basic methods to extend people's capabilities in a wide variety of applications [315]. One of the key challenges in robotic imitation is kinematics mapping, especially across dissimilar bodies and the captured sensor data may not be able to directly map the actual human motions [315, 316]. To eliminate the kinematic mismatch and human motion estimation errors, there are various human-robot motion mapping methods are presented in the literature.

This step in HRC using human motions as human input of the system is particularly important. So far, it has been discussed how to obtain the estimated human motions, presented various approaches in the methodology, and quantitatively compared in detail the advantages and disadvantages of different methods. The focus of optimizing human motion and gesture-based HRC has been *only* on the human motion estimation side. However, the environment and applications enable new parameters to be used in the system.

*A motivating example:* A generic PC mouse has a limited range of input methods - two press buttons, one rotating button and an optical sensor that detects motions on a 2D surface. Yet, the aptitude for things that can be done with a generic PC mouse is vast. The range of functionalities that can be assigned to those inputs improves the usability range. Human motion mapping methods influence the HRC application/system the same. The intricacy of the human body is not even comparable to a regular PC mouse. The opportunity to use human body motions as an input method to interact with a robot is bizarre.

Human-robot motion (and gesture) mapping methods are related to improving the intuitiveness and efficiency of the HRC system. The HME errors can be eliminated and new functionalities can be assigned to different poses, gestures and the sequence of these.

Additionally, human-robot motion mapping is not necessarily unilateral. It is not straightforward to assign a leader to a human-robot team to achieve the task in the most optimal way. When the robot takes over a non-passive role, the human-robot motion mapping paradigm shifts. In this section, different motion mapping methods and dynamic role allocations between human(s) and robot(s) are discussed.

#### 4.3.1 Mapping Methods

When the *motion mapping* term is used in between humans and robots, a mimic behaviour is imagined by many people. However, there are several variations of motion mapping between a human and a robot. A deterministic real-time human-to-robot motion

mapping procedure using wearable sensors can be divided into three methodological categories: action type, motion mapping type and mapping space selection.

1. Robot action type
  - (a) Active-command cooperation
  - (b) Predefined-command cooperation
2. Motion mapping type
  - (a) Absolute mapping
  - (b) Relative mapping
3. Mapping space selection
  - (a) human joint space  $\rightarrow$  robot joint space
  - (b) human joint space  $\rightarrow$  robot task space
  - (c) human task space  $\rightarrow$  robot joint space
  - (d) human task space  $\rightarrow$  robot task space
  - (e) Other

The **robot action type** is related to the response level of the robot. The robot can either follow the given human commands simultaneously (active-command cooperation) or it can process a given human command - for instance, a gesture or a haptic input - and execute a predefined function (predefined-command cooperation). The predefined-command cooperation (also referred to as task-based approach in the literature [317, 318]) has the advantage of requiring less bandwidth yet the online liberty to achieve other tasks is limited. In this study, both action types are used based on the task state and how to select the action type is explained in Section 4.3.2 in detail.

The **motion mapping type** predicates how the frame of origin of the command from the human and the frame of origin of the execution by the robot are handled during the motion translation. Since motion can be defined as the act of changing the position and/or orientation of an object or a part of the object with respect to time, it is necessary to define a reference frame to translate the motion from human to robot. In absolute mapping, they share one fixed reference frame. The absolute pose of the human arm with respect to the fixed reference frame is used in calculating the goal pose of the robot. On the other hand in relative mapping, the translated human motion is not the absolute position of the arm with respect to a fixed reference frame but the displacement of the human arm with respect to a predefined reference frame. It can be an internal frame on the human body, an external frame in the task environment, a robot-fixed frame or it can be dynamic. Regardless of the selection of the reference frame, the initial poses of the human arms are registered at time  $t = 0$  and the pose change (relative pose) of the human arm is translated into robot motion. The human and the robot may or may not share a common reference frame for securing safety and avoiding collisions but their absolute poses are not used in motion translation. The intuitiveness is highly linked to the mapping reference frame. In [319], the results on teleoperated grasping with iCub humanoid robot via 7 DoF arm motions are reported

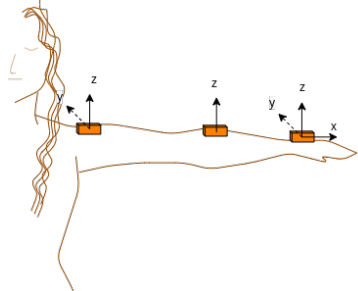
## Methods

to be worse when the user when operator was facing the robot, due to the confusing point-of-view.

Joint space and task space regulations are two common control schemes for robot manipulators [320]. The **motion space selection** deals with the scheme to be mapped between the human and the robot. 4 combinations of such a selection are given above, some of which are more common than others. Additionally, there are some examples of parameter mapping other than pose mappings such as force, torque, velocity and acceleration. Those are under the *other* category.

The most common motion mapping types between a human and a robot manipulator are Joint Space Mapping (JSM) (human joint space  $\rightarrow$  robot joint space) Task Space Mapping (TSM) (human task space  $\rightarrow$  robot joint space). In the JSM method the human joint angles are mapped to a respective robot joint angle set.

The limitation of this type of mapping scheme is the kinematics dissimilarities. The robot's and human body-limb's kinematic structure should be similar enough as shown in Table 4.2. One of the DoFs in the human shoulder (about x-axis) is not mapped to any joints on the UR5e side. The rest of the joints are mapped as listed:



Human	UR5e
shoulder-y	shoulder pan
shoulder-x	shoulder lift
elbow-z	elbow
wrist-y	wrist-1
wrist-x	wrist-2
wrist-z	wrist-3

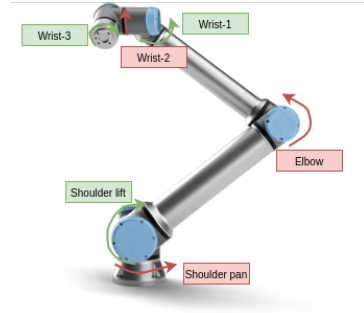


**Table 4.2:** Human-UR5e joint mapping table

In the early stage of this study, the JSM is tested out between the human arm and the UR5 robot arm at simulation level as shown in Fig. 4.10. Human joint angles are published as Euler angles and the robot controller subscribes to this topic. The active topics and nodes are presented in Fig. 4.9. According to this presentation, /awindamonitor publishes each IMUs orientations in quaternion as  $q_i^{G,S}$  where  $i = \text{shoulder, elbow, wrist}$  to /IMU\_to\_human\_joints node. It is where IMU orientations are transformed into human joints as explained above. The human joints are published as joint\_states to /arm\_controller. The controller sets the required actuation for the simulated UR5e and sends them to /gazebo and the robot state is published in real-time.

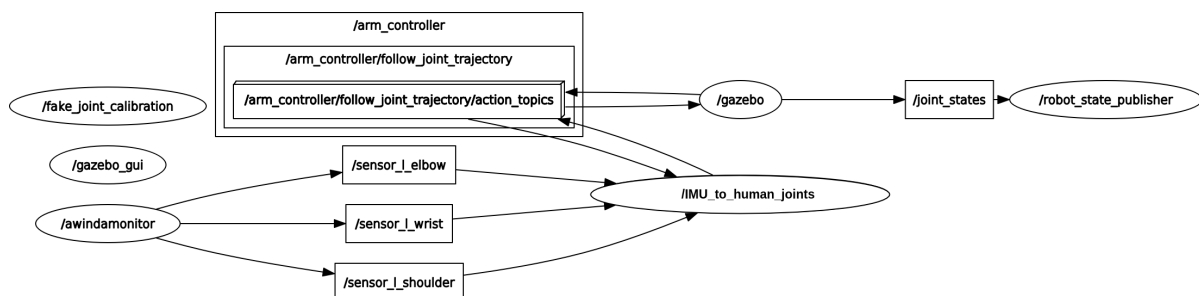


**Fig. 4.9:** Running nodes and active topics in real-time teleoperation of 6-DoF robotic arm with 7-DoF human arm model in Gazebo



This method is common and useful both on simple joint mappings such as gait, elbow, and head motions and with highly anthropomorphic designs such as hand and fingers, humanoids etc. However, it has limitations, especially across dissimilar bodies [316] such as between a generic robotic manipulator and a human arm. Therefore TSM comes in hand.

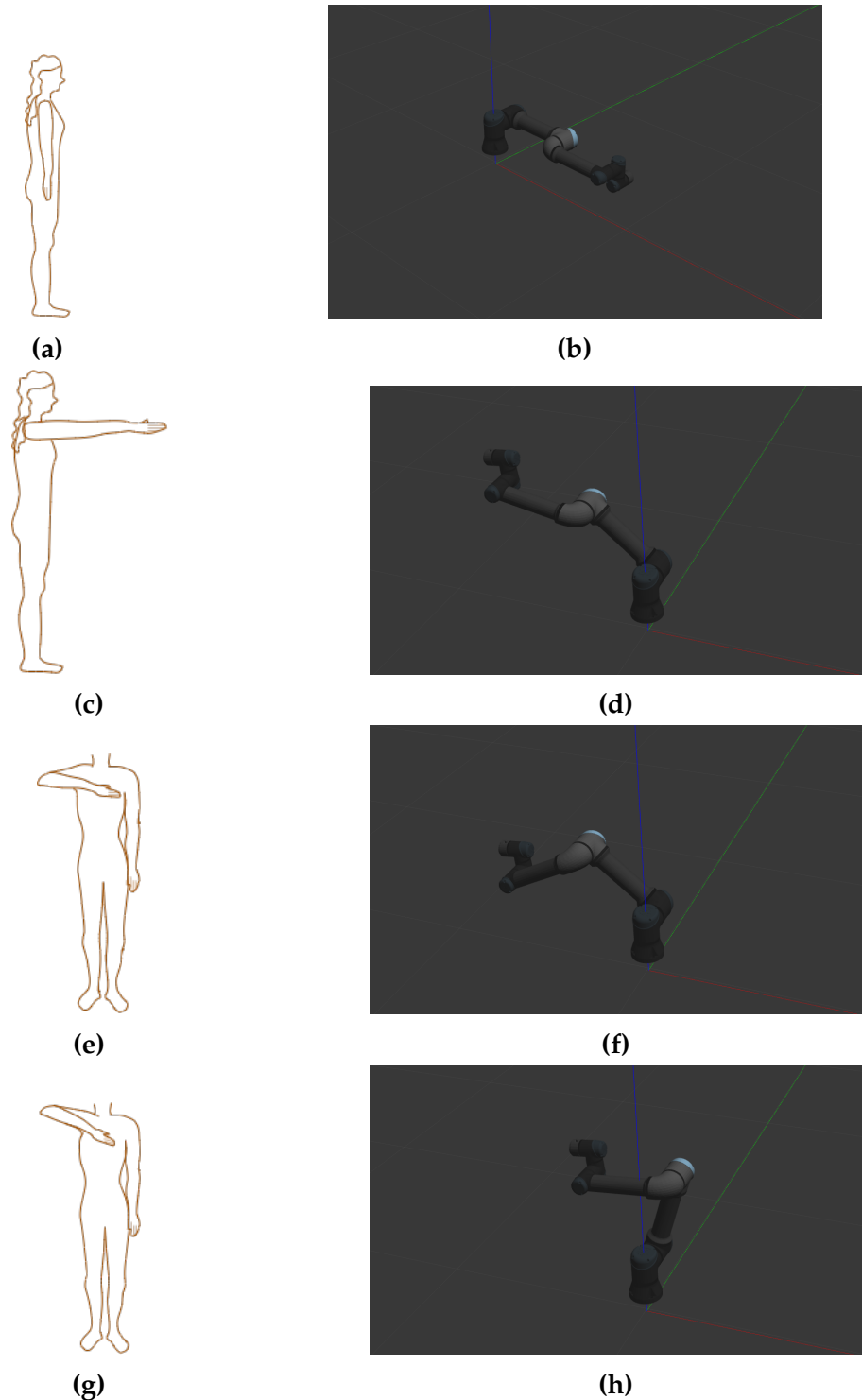


Fig. 4.10: Human vs. UR5e arm poses, respectively, using joint space mapping

## Methods

In TSM human's end point of the body limb (i.e. hand for human arm, foot for human leg, etc.) is mapped to the robot's end-effector pose. If we focus on the human arm to robot manipulator TSM mapping scenario, first the human joint angles are calculated, then using the human body limb sizes, the human hand pose is calculated using FK with respect to a fixed frame (i.e. chest, human base, world etc.). The hand pose is then sent to the robot as an end-effector goal pose. The necessary IK calculations are computed and the respective robot joint angles are set. With this method, the kinematic dissimilarities between the robot and the human can be relatively suppressed; however, new issues can show up. Two of the issues that are experienced and solved in this study are given below.

- Singularities <sup>1</sup>
- Real-time issues <sup>2</sup>

Singularity can be defined as configurations in which the robot end effector becomes blocked in some directions. It can occur when either two actuated axes become parallel during a motion or the robot arm gets to the workspace limits. In these circumstances, the robot's motion capabilities are restricted. If the end-effector goal pose causes a singularity, the IK solver still finds a solution but with a different kinematic configuration. Often, this *alternative* configuration is computed via the elbow joint. The robot end-effector can still reach the requested pose, but it can jump between two different elbow configurations during the motion, which is unacceptable for a co-lift scenario.

Therefore, either each singularity pose should be handled specially or motion planners should be used in TSM mapping. Motion planning is a large research field within robotics and several parameters are considered based on the task requirements. In this scenario, obtaining a continuous motion path is vital. Generally, the motion planner optimizes the path either by the shortest path or by minimum power requirement on one or one set of the joint(s). However, if the optimization for real-time use cases is not handled properly, it will not be useful in real-time co-lift scenarios. There are methods to improve TSM on the robot side with respect to how the robot handles end-effector pose commands in real-time, such as visual servoing.

There are **other** motion mapping types which are mentioned in the literature. For example, robot and human dynamics can be mapped [319], poses can be functionally mapped, where commanding human body parts and robot are placed in a number of similar functional poses, and a relationship between each robot and human joint is calculated [321], or the mapping can be object-specific [322]. However, the details of these methods are out of the scope of this study.

### 4.3.2 Proposed HRC States and Roles in Co-lift

In total four different states are defined for the whole HRC co-lift operation: IDLE, APPROACH, CO-LIFT, and RELEASE, and the 3 different roles of cooperation as **Human Leading**, **Robot Leading**, and **Shared Control**. The states and roles of the system are demonstrated in Fig. 4.11.

---

<sup>1</sup><https://youtu.be/p28DdWnTDew>

<sup>2</sup><https://youtu.be/faqxhQmiAB0>

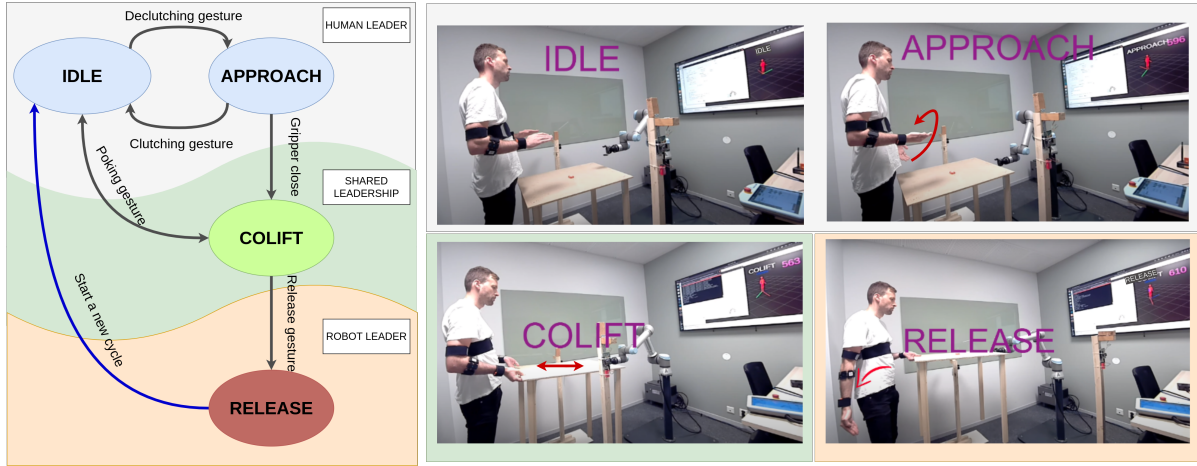


Fig. 4.11: HRC roles and states in the experimental co-lift scenario.[323]

**HUMAN LEADING ROLE** The human is the sole leader of the HRC systems. The states defined under this role are

**IDLE:** This is a safety state that the human can enter with the clutching gesture at any time. No motion command is sent to the robot, and the robot stays at rest in the initial position.

**APPROACH:** A merged hands motion - a combined pose parameter of the two hand poses with an adjustable scale - is actively calculated and sent as servo control commands to the robot. The robot follows the merged hand's motion. This type of human-to-motion mapping is referred to in the previous subsection as *active-command cooperation*. The initial merged hand pose is calculated in every IDLE→APPROACH transition.

To create the merged hand's motion, the relative motions of both human arms are merged and translated into a single goal pose for the robot as introduced in [62]. Pose calculations are computed using  $4 \times 4$  Homogenous Transformation Matrix (HTM). The merged hands pose is calculated based on the relative motions of each arm. Two arms of the human are referred to as the motion arm and steering arm. The steering arm is also responsible for clutching and state transitions. For the current setup, the steering arm is the right arm but it can be changed in the open-source code easily.

$$\hat{P}_{h,t}^- = \hat{s} \cdot (\hat{P}_{hm,t=0}^{-1} \times \hat{P}_{hm,t}) + \hat{k} \cdot (\hat{P}_{hs,t=0}^{-1} \times \hat{P}_{hs,t}) \quad (4.9)$$

where  $\hat{P}_{h,t}^-$  is the merged hand pose at  $t = 0^-$ ,  $\hat{P}_{hm,t=0}$  is the motion hand's pose,  $\hat{P}_{hs,t=0}$  is the steering hand's pose. The multiplication with their inverse respectively at  $t = 0$  simply sets the pose readings to zero for relative motion mapping.

Also, different weights for each arm motion can be defined by the scaling factors  $\hat{s}$  and  $\hat{k}$  in Eq. (4.9) in the code but for these experiments, they both set to the same multiplier.

The robot goal pose based on the merged hand pose is

$$\hat{H}(t) = \hat{P}_{h,t=0}^{-1} \times \hat{P}_{h,t} \quad \hat{P}_{r,t} = \hat{P}_{r,t=0} \times \hat{H}(t) \quad (4.10)$$

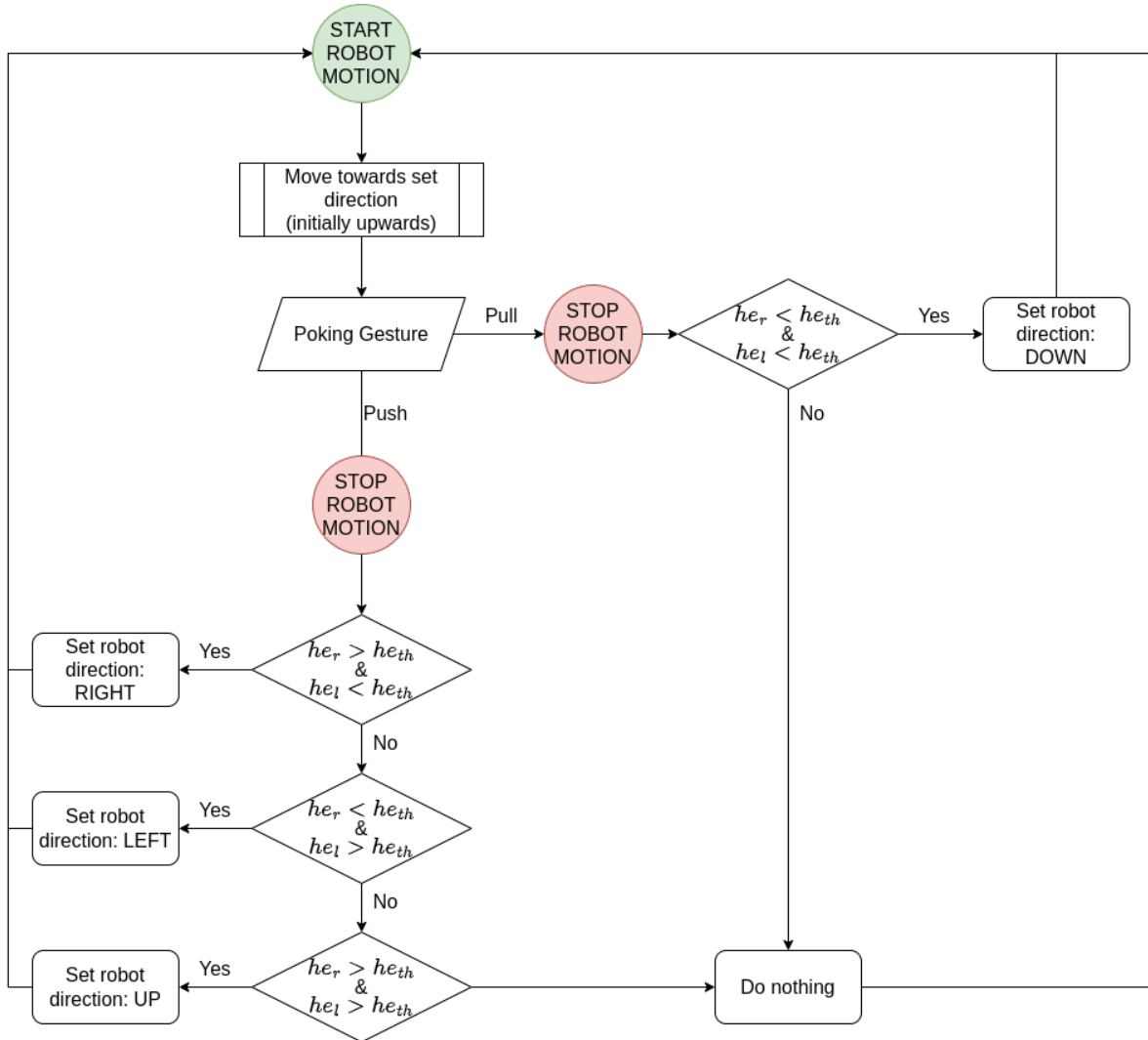


**Fig. 4.12:** Predefined-command cooperation in the active lifting phase (i.e. COLIFT state) [323]

where  $\hat{P}_{r,t=0}$  is the initial pose of the robot and  $\hat{P}_{r,t}$  is the current pose of the robot. The  $\hat{H}$  is set as target pose in `servoL` command[324] with 0.1s look-ahead time to smoothen the trajectory.

**SHARED CONTROL ROLE** The human and the robot share the leadership of the HRC systems. The state defined under this role is

**CO-LIFT:** The robot applies a directional-compliant force. The direction is determined by the human elbow heights (rather than direct hand motion mapping as in [62] due to the restrictions on hand movements during holding an object). The robot is actively leading the cooperation until an external force is applied by the human to the object. When the human force input is detected by the robot, the compliant force is adjusted based on the elbow configuration as shown in Fig. 4.12.

If both elbows are higher than a threshold, the direction is set UP. If the left elbow is higher than the threshold and the right elbow is lower than the threshold, the direction is set LEFT, or vice-versa. If both elbow heights are lower than the threshold when the human external force is applied, the robot generates no directional compliant

force (direction is set to NULL). This behaviour is computed by using the `forceMode` command[324] where the compliance is set in the end-effector frame with 170 mm maximum allowed deviation on non-compliant axes and 30 N force applied with 0.5m/s maximum end-effector speed on the compliant axis.

**ROBOT LEADING ROLE** The robot is the sole leader of the HRC systems. The state defined under this role is

**RELEASE:** The robot takes the lead in the operation, and moves to a predefined pose. The human follows the robot's motions.

*Note that the defined states can be expanded under these three roles according to different HRC tasks.*

### 4.4 Designing Human-Robot Experiments

The design of quality research studies for use in HRI applications with results that are verifiable, reliable, and reproducible is reported to be a major challenge [3, 60]. To increase the reliability of the user studies in HRI, multiple metrics should be measured from the five primary methods of evaluation methods: (1) self-assessment, (2) observational or behavioural measures, (3) psychophysiology measurements, (4) interviews, and (5) task performance metrics [325–328], tested on a sufficient sample size and not conduct studies using a convenience sample of college-aged students. The highlights in this section are important methods/points in designing HRI experiment design.

The collected data from 32 users in this study is relatively large and comparatively diverse according to [3, 55]. The data collection is performed by various methods (i.e. sensor measurements and user surveys), and all the code required to reproduce the experiment setup is open-source to improve the verify-ability and reliability. For further research or for other researchers who focus on relevant studies, the following section aims to provide a methodological approach to designing human-robot experiments.

**HISTORY OF HRI EXPERIMENT DESIGN** Some social scientists are working to establish methodological approaches for HRI [329]. There is an urgent need to examine extended studies in real-world settings to move studies away from laboratory settings with college-aged students and practical samples [330, 331].

Despite this contribution, it appears that the HRI community still needs more focus on evaluation methods. For example, in [332] evaluation methods are investigated and recommendations are made for design experiments. They suggested possible hybrids of HRI methods should be applied according to the research questions. The study [333] highlighted methodological problems in scenario-based evaluation, arguing that scenario media characteristics influence robot user acceptance and attitudes and that *human-computer interaction* methods may not be applicable to HRI. They suggested five guidelines to help select the most appropriate storyline media for evaluation purposes, recognizing that media could introduce significant bias. Furthermore, a virtual robot does not produce the same effect as a real robot, because humans can identify more with a physical robot than with a simulated robot [334]. It is important for the proposal

## Methods

of a reproducible HRI experimental design (to induce empathy towards robots in the laboratory) and an empathy measurement tool that would allow researchers to reproduce the same result.

**PROBLEMS OF CURRENT HRI EXPERIMENT EVALUATION METHODS** It is difficult to compare robotic systems which are designed for different tasks so it is important to establish benchmarks for effective and ethical HRI[335]. Currently, it does not seem feasible to compare results across studies due to the lack of a respective methodology. In the reviewed literature, almost no standardized research tools have been used, implying that the research field of assistive robotics is still in an "exploratory" state in which qualitative methods and subjective measurements predominate [336].

Impact measurements such as measurements of the user's quality of life (perceived safety) or user care were carried out as part of short-term user trials in a living lab situation. Effects are usually measured in long-term studies using pre-post measures, as reported in [337] and [338]. It seems that the question remains open whether impact factors measured in the short term can provide valuable information about subsequent long-term effects on the ground.

**SUGGESTIONS** The field of user experience (or UX) is a particularly relevant field for designing interactions between robot agents and human agents. It proposes to consider and anticipate the experiences (real or imaginary) that individuals have with technical objects such as robots. Moreover, social influence refers to an individual's attitudes and/or behaviours being influenced by others, whether implicit or explicit, such that persuasion and compliance gaining are instances of social influence [339, 340]. In human-human interaction (HHI), the desire to understand compliance and maximise social influence for persuasion can lead to the development of theory and resulting strategies one can use in an attempt to leverage HRI through social influence.

Cohen's kappa is used to measure the level of agreement between two qualitative data; both for it is transcription data and behavioural data. Many statistical analysis software packages can be used to perform this statistical test and there are also online calculators available (for example: <https://idostatistics.com/cohen-kappa-free-calculator/>). It is commonly agreed that a Cohen's Kappa score of 0.60 or greater indicates satisfactory reliability [326]. It is important to perform this evaluation and report it as part of the HRI studies which involve qualitative data. The scale to evaluate Cohen's Kappa and reliability is:

- 0.01–0.20 slight agreement
- 0.21–0.40 fair agreement
- 0.41–0.60 moderate agreement
- 0.61–0.80 substantial agreement
- 0.81–1.00 almost perfect or perfect agreement

### 4.4.1 Design Methods

There are three broad design approaches, each of which may be valid depending on the context and intended goals: human-centered design, robot-centered design, and symbiotic design [3].

#### 4.4.1.1 Human-centered design (HCD)

Human-centered design (HCD) is the central paradigm of HCI and therefore a large part of HRI design. It aims to involve the intended user population in most phases of development, including identifying needs and requirements, brainstorming, conceptualizing, creating solutions, testing and refining prototypes through an iterative design process [341].

In the HRI context, the main assumption is that humans have their own communication mechanisms and unconsciously expect robots to follow human social communication modalities, rules, conventions, and protocols. Important aspects of the robot behaviour and embodiment design that play a strong role in terms of the human's perception of the interaction include physical presence [342], size [343], embodiment [344, 345], effective behaviours [346], role expectations [347], just to cite a few. From an evaluation point of view, HCD relies a lot on subjective self-reports of users to measure their perceptions, and complement more objective measures such as task performance.

There are many HCD approaches that exist particularly for social robots. An interesting observation is treating robots as expressive characters, i.e. robots with the ability to express identity, emotion, and intent during autonomous interaction with human users [348] via animation elements. Designing for expressivity can be achieved for example by bringing professional animators to work side by side with robotic and AI programmers. The idea is to utilize concepts of animation developed over several decades and apply them to robotic platforms [349–351].

#### 4.4.1.2 Robot-centered design (RCD)

Historically, robots were developed solely by engineers who carried little concern about the human beyond the interface. While the focus in HRI has now shifted to a more human-centered approach as was discussed in the previous section, HCD as a general design paradigm has been criticized by many researchers who consider it to be harmful in some aspects [352, 353]. For example, it has been criticized for its focus on usability (how easy it is to use) as opposed to usefulness (what benefits it provides) and its focus on incremental contributions based on human input conditioned by current technologies, which prevents it from pushing technological boundaries. Additionally, adapting the technology to the user may sometimes be more costly than having the user adapt to the technology.

Therefore, there are instances where a more RCD approach may work best. Overfitting robots with humans can lead to lower performance, high development costs, or unmet expectations. It is important to realize that in some cases it may be better to ask the human to adapt to the robot (possibly through training) in order to achieve better long-term performance. Humans are much better at adapting than robots and it is crucial to know when robots should not adapt, as it would be more efficient to

ask or expect humans to do so [353]. In many cases, the robot may have needs that impose immediate costs on humans but result in better future performance. It can be that the robot asks people for help if they encounter limitations [354] or teach the robot to perform a certain task so that it can better perform relevant tasks. An RCD approach can also involve modifying our environments to make them suitable for robots.

### 4.4.1.3 *Symbiotic Design*

Considering the advantages and disadvantages of HCD and RCD, a merged approach is also possible. It is important to carefully identify the strengths and weaknesses of each part and design for increased symbiosis between the human(s) and the robot(s). One way to achieve this symbiosis is to take a holistic view that focuses on the overall behaviour of the system based on robots, humans, and the environment[355].

## 4.4.2 *Risk Assessment and Consent*

In human-robot experiment design, there are some bureaucratic steps which must be followed. Two of the most important ones are related the user risk assessment and consent. In this subsection, the procedure is briefly explained according to Norwegian Centre for Research Data (NSD)<sup>3</sup> regulations.

### 4.4.2.1 *Risk Assessment*

Risk assessment is a systematic process of evaluating the potential risks that may be involved during the experiment (or a project in general). It is an essential step, especially in pHRI experiments where there are collision risks. There are various evaluation methods such as quantitative, qualitative, semi-quantitative, asset-based, vulnerability-based, or threat-based [356]. Each methodology can evaluate an organization's risk posture, but they all require trade-offs. We evaluated a vulnerability-based risk assessment due to the limited resources in the literature in this regard.

Risk analysis provides answers to these three questions [356]:

1. What can go wrong?
2. What is the likelihood of that happening?
3. What are the consequences?

First of all, the risk factors of the experiment are defined. In the co-lift experiment, the risk factors are related to fatigue and possible collisions of the robot (or the carried object) with the different parts of the human body. Hence, the severeness of such collisions is determined as in Fig. 4.13.

---

<sup>3</sup><https://www.nsd.no/>



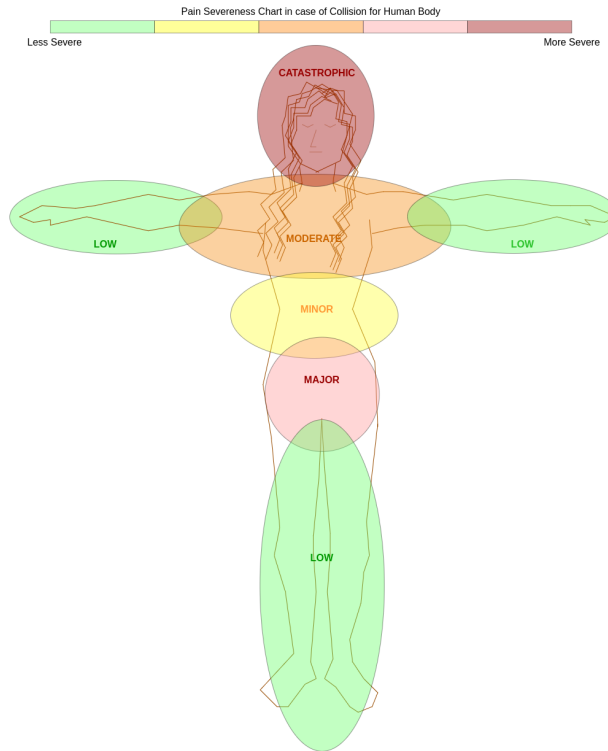


Fig. 4.13: Labeled zones on human body based on pain severeness in case of a collision

Afterwards, the risk assessment matrix is created as in Table 4.3. It is a relatively common severity vs likelihood matrix but modified according to the application. The probability scale can also be modified depending on the risk and severity resolutions.

Table 4.3: Risk assessment matrix

Risk Probability		Severity of Harm						
		Negligible	Minor	Moderate	Serious	Catastrophic		
	5	Almost Certain	5	10	15	20	25	<div style="background-color: red; color: white; padding: 2px;">Extreme [15+)</div> <div style="background-color: orange; color: white; padding: 2px;">High [9,15)</div> <div style="background-color: yellow; color: black; padding: 2px;">Moderate [5,9)</div> <div style="background-color: green; color: black; padding: 2px;">Low [0, 5)</div>
Likelihood	4	Likely	4	8	12	16	20	
	3	Moderate	3	6	9	12	15	
	2	Unlikely	2	4	6	8	10	
	1	Hardly Ever	1	2	3	4	5	

Finally, the list of possibilities is calculated based on the risk assessment matrix as shown in Table 4.4.

4.4.2.2 User Consent and Data Collection

The type of users, the collected data type, the procedure of how the data is collected, who has access and how long it will be stored must be reported to the user and NSD before the experiments. The relevant consent form related to the multiple user experiments in Paper F is provided as an appendix in Appendix-A.

In human-robot experiments, the collected data varies. It can be via sensor measurements, self-reporting methods, user surveys etc. [3]. The collected data must be verifiable and anonymous if possible. The sensor measurements and the methodology of the process of collecting the respective data are explained in each paper.

**Table 4.4:** The list of risk factors

Risk Factor	Likelihood	Severity	Risk Zone
Fatigue	5	1	5
Arm Pain	4	2	8
Hit by the robot at LOW zone	1	2	2
Hit by the robot at MINOR zone	1	3	3
Hit by the robot at MODERATE zone	1	3	3
Hit by the robot at MAJOR zone	1	4	4
Hit by the robot at CATASTROPHIC zone	1	5	5
Hit by the table at LOW zone	2	2	4
Hit by the table at MINOR zone	3	3	9
Hit by the table at MODERATE zone	1	3	3
Hit by the table at MAJOR zone	2	4	8
Hit by the table at CATASTROPHIC zone	1	5	5

The vast portion of the collected data comes from the experimental procedure of [Paper F](#). The quantitative measurements of each user from the sensors are provided as an appendix in [Appendix-C](#) and the accommodated surveys are presented in [Appendix-B](#).

## DISCUSSION

---

In this chapter, the general findings are discussed. Additional data analysis of the non-published data is also reviewed in Section 5.0.4.

### 5.0.1 HME in HRC Applications

Human Motion Estimation (HME) is a fundamental step in interacting with a robot through postures, motions, and gestures. The anthropomorphic inspiration in robot design makes it more convenient in many applications. Through this study, different techniques for obtaining accurate and reliable human motions are investigated both in selection of the optimal motion tracking solution, and in implementation for industrial use.

Overall, the human body is a good communication tool for HRC. When attempting to solve HME as a part of an HRC system rather than a standalone estimation problem, efficiency increases significantly. HRC enables more observable and controllable parameters in the system model, making pose, motion, and gesture more successful and reliable. For example, relative motion mapping between the human and the robot is one of the main novel methodological implementations in this study, which significantly contributed to eliminating HME errors when HME is used in generating the robot's target pose.

The possible set of human input data to an HRI system can be vast. I would like to elaborate on this claim with an example: *imagine how much you can achieve with three buttons on a 2D surface (i.e. with a computer mouse)*. As long as a meaningful equivalent functionality is well-defined on the computer side such as selecting, copying, dragging etc., the amount of work you can achieve is enormous – as humankind has been doing for decades. The human body, in this regard, has infinitely more potential control surfaces. Postures, gestures, and the sequences of these can be translated into a goal for various types of robots in an HRI system. Different functionalities can be assigned to each and every single human limb motion. Therefore, research on HME in HRI investigates not only the mathematical aspect of an estimation problem but also discovers the intuitive translation of motions between a human and a robot.

When there is a human-robot team, it is not straightforward who is supposed to be the leader for achieving the task in the most efficient way. Furthermore, the sole leadership from either part does not result in universal efficiency in every task. Therefore, a dynamic leadership switching scheme in the HRI applications is handy.

The HME-based HRI systems enable this switching step smoothly and intuitively. This concept is demonstrated in [Paper A](#), [Paper B](#) and [Paper D](#) extensively. The smooth and intuitive leadership switching is another important advantage of using human motions in HRI applications.

### 5.0.2 The Use of IMUs in HME

One main design criterion of an HME-based HRC is the selection of the MoCap technology. As it is thoroughly discussed in Section 2.1.3, there are various tools in the motion estimation field, and each technology has its own advantages and disadvantages. The vision-based technologies are the most common ones in HME when it comes to accuracy and precision, but they suffer from occlusion, loss of line-of-sight, light changes, often require long and tedious calibration procedures and are less portable. These bottlenecks affect their efficient and safe use in HRC applications. Among the non-vision-based technologies, IMUs offer solutions to each of the aforementioned problems.

Although the motion estimation algorithms using IMUs are still in debate due to the drift problem, the current solutions are thoroughly investigated in this study. Unfortunately, there is no drift-free position estimation method using only IMUs in the literature, but several methods exist to minimize it. Starting from manual sensor fusion methods [117, 139], several approaches have been tested to obtain the most reliable position estimate from IMUs. What is found in the end is that the IMUs that provide a filtered absolute orientation output are the most convenient ones for this use. Since the noise elimination, signal filtering, and tuning of the orientation estimator (often the Kalman Filter or the Extended Kalman Filter) are carried out at the hardware level, the estimated orientation is less prone to drift. Some examples IMUs that can be used for this purpose and are available in the market today are Xsens MTw Awinda, Infineon CY8CKIT-062S2-43012, and BOSCH BNO055. Particularly, Xsens MTw Awinda uses an additional barometer and claims that they provide a 3D drift-free orientation output [32]. However, the drift elimination quality is not a part of this study, and no quantitative evaluation is computed in this regard. It is only stated for guidance to the relevant stakeholders.

The question is then, can this drift be minimized such that IMUs can reliably be used in HRI applications? For example, if the drift is minimized sufficiently, then the usage of IMUs is suitable. IMUs are already reported as superior in several aspects for industrial HRI [25]. In this study, the feasibility of IMUs in HME for HRI applications is validated. In this study, using Xsens Awinda raw orientation output and implementing a relative motion mapping algorithm from the human to robot eliminate the drift problem sufficiently. The user is calibrated before each trial by staying stable for 4 seconds in N-pose (details can be found in [Paper B](#) and [Paper D](#)). No major errors are recorded during the experimental studies regarding the drift problem.

The final point of using IMUs in HME studies and applications is related to calibration. In this study, there are several calibration points in the process of estimating human motions and translating them into robot commands (see [Paper A](#)), the first of which is IMU calibration. The only calibration methods applied in this study on IMUs are static bias elimination and noise filtering (see Section 4.1). The developed

system allows a quick calibration option that takes only 3 seconds. The IMUs can be recalibrated at any step. However, I believe that dynamic IMU calibration methods can give better results, which is important to highlight as a recommendation for future studies.

### 5.0.3 *Serious Games and Gamification in HRC*

Serious Games and Simulations (SSGs), Game-Based Learning (GBL), and gamification are used to create supplemental learning tools that are engaging. They allow for translating knowledge into skills in a more intuitive way. They have been widely used in several fields for over two decades; however, HRC is not a common one. In this study, the investigation of SSGs, GLB, and gamification started with [Paper C](#) and focused more on HRC training in [Paper E](#) and [Paper F](#).

User training is an essential step in developing an HRC system. Gamified training is a promising method for this purpose. Based on the observations and quantitative results during the experimental procedure in [Paper F](#), gamification and game score-based learning evaluation triggered user learning positively. Users stated amusement both verbally during the physical experimental procedure and in the relevant questions in the surveys. It is observed that a gamified training methodology rather than a conventional reading-the-manual approach is preferred by the users. Nonetheless, the effectiveness of the two main approaches should be quantitatively evaluated by a dedicated experimental study if more general conclusions are to be drawn.

On the other hand, it is observed that the gamification aspect of the training setup triggered competitive users to learn unconventionally. This is something referred in [Paper F](#) to as "reverse learning". This type of behaviour is observed more in users with competitive traits and those who have another acquaintance enrolled in the experiment. As the user feels more comfortable using the system, they tend to ask/request more risky execution options, such as if the robot could do something faster, or trying to develop new strategies in different states of the task, to pass their individual best scores, which sometimes results in worse scores. It is more likely to be observed in a gamified training setup than in a conventional training method. Therefore, the adequate proportion of motivational vs risky competitiveness of gamification in the design of a training setup should be carefully considered. However, there is not enough data to conclude a correlation between personality traits and gamified learning.

The use of virtual reality (VR) in SSG is rather common. In this study, a regular screen is used in giving visual feedback to the users during the experiments instead of a VR goggle. Since there is physical contact between the robot and the human, either directly or through an object, the mental involvement of the user should be in the current state for safety reasons. Therefore, VR technology is not suggested/planned to be the focal point in future studies in gamified training methodology in HRC. VR technology might add unnecessary complexity, but augmented reality (AR) or mixed reality (MR) technologies are more suitable in this regard.

Finally, in the current setup, the gamified training system is supervised by a human expert and the system is not in a fully-developed game format. The users were informed that they could ask questions but the supervisor could not reveal any answers which could cause unfairness between users. As a future work, the system can be modified

towards a version which can provide more clear feedback and guidance. However, there is still a debate about this in development of SSGs for education and training purposes due to the overall effort in developing games. Therefore, the cost vs effectiveness of a fully-developed serious game should be evaluated beforehand.

### 5.0.4 Human-Robot Experiments

The experiments involving humans and robots in this study can be divided into three categories. The first category consists of only one user during the development of the system, the second category refers to the pilot users who are mainly the members of *HVL Robotics Lab* and experienced in the robotics field, and the third category refers to the regular users whose age varies between 20 and 54 and those who might or might not have experience in the robotics field. The most significant category is the third one because it is the biggest and randomly selected to represent the average end-user the most adequately.

A total of 8 pilot users and 32 actual users took a part in the human-robot experiments. The pilot data are used in optimizing the system parameters and the actual user data are used in hypothesis testing. The experiment consists of 4 stages: pre-survey, video tutorial, physical experiment and post-survey. The pre-survey and post-survey are provided as in Appendix-B and the training setup code is open-source<sup>1</sup>. The technical details of the training setup are explained in Paper E and the collected user data are reviewed in Paper F. The procedure of the physical experiment is summarized in Section 4.3.2, which was repeated 10 times for each user.

The presented results in Paper F focus on the usability and learnability of an HRC system and the paper covers only parts of the collected data. Some additional user perspective-related data are also presented and discussed in this section.

#### 5.0.4.1 Measures From Physical Experimental Procedure

The overall user results are given in Fig. 5.1. Although the experiment is designed for 10 trials, some users would like/agree to continue trials due to curiosity, eagerness, competitiveness and desire to achieve their personal best. The comparative discussions are made only for the first 10 trials for all users but the results of all trials are given here for complete reference. The majority of the users within 10 trials and almost all users at the end seem to reach a very good learning state.

Note that some users reach a decent learning state within 10 trials but experience worse results afterwards. This paradigm is addressed as "reverse learning" in Paper F and in Section 5.0.3 and is often observed as a result of risk-taking behaviour as user comfort increases.

In total, 9 motion metrics related to the HRC system from 32 users are presented as an appendix in Appendix-C. At a glance, it is clear that all users have some unique behaviours as well as common ones. For instance, the user score is considerably increased from the 1<sup>st</sup> to the 10<sup>th</sup> trial in every user. The average score of the first trial is 503 points whereas the last is 659 points. The Paper F discusses the effect of each user

---

<sup>1</sup>[https://github.com/frdedynamics/hrc\\_training](https://github.com/frdedynamics/hrc_training)

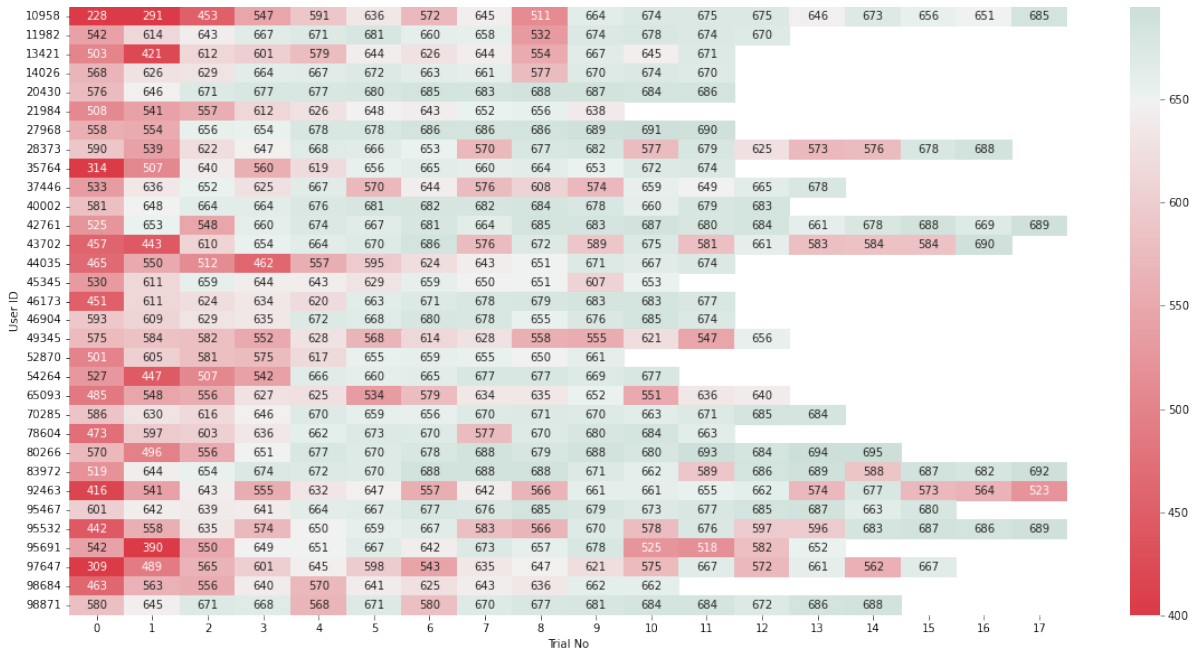


**Fig. 5.1:** User scores on each trial in human-robot experiments. The results are colour-coded from red to green to visualize the training results from low to high. [323]

background parameter with respect to 6 different learning criteria. Therefore, I will only briefly discuss the highlights between users and comment on the overall system.

One of the most distinct behaviours between users was how they interacted with the robot during the IDLE and APPROACH states. After the first IDLE to APPROACH transition, some users preferred staying in the APPROACH state until the COLIFT starts - without any human-robot motion mapping reset - (i.e. ID:42761, ID:46173, ID:46904), some users used the human-robot motion mapping resetting quite often by transiting between IDLE and APPROACH (i.e ID:44035 trials [5-9], ID:45345, ID:70285, ID:10958) and some started with the resetting behaviour until they reach to the learned plateau (i.e. ID:52870, ID:65092). Similarly, some users used both left and right hands actively (i.e. ID:80266, ID:83972, ID:95467), and some used only one hand motion (ID:70285, ID:78604, ID:95691). All users show significant progress, nonetheless, there are interesting user behaviours which can be investigated later to compare progression.

Another distinct behaviour is related to the number of poking attempts during the COLIFT state and the magnitude of poking force over trials. In the first trials, there are notably more poking attempts than in the last trials. The poking force is either well above the threshold (i.e. ID:10958 trials [2-3], ID:11982 trial 1, ID:14026, ID:20430) or well below (i.e. ID:10958, ID:21984). Some users applied both excessive and non-sufficient forces throughout their training which can be related to the uncertainty of the system responsiveness. However, it is seen that almost all users converged to the same level of interaction force which is around 30-40 Newton and the same number of poking gestures which are often 7 times, sometimes 8 times and rarely different numbers. Even though the level of the interaction force and attempts do not imply any universal conclusion outside of this setup, the process of reaching it by several user data shows clear progress in learning about human-robot interactions and how humans can develop a common strategy.

## Discussion

The changes in the duration of the IDLE+APPROACH and COLIFT states are another point to highlight. The duration of the IDLE+APPROACH state shows how comfortably the user controls the robot's motion using two arm motions when the user is the sole leader of the system. For the user ID:35764 for instance, the first attempt to grab the table took around 160 seconds whereas the user managed to reduce it to under 10 seconds in the last trials. Moreover, the duration of the COLIFT state shows two things: 1) how comfortably the user controls the robot's motion using instant gestures when the user is not the sole leader any longer, and 2) how well the grasping is succeeded. In default, the robot moves upwards after grasping the table is completed. If the grasping is too harsh, the robot will not automatically start moving upwards (as seen in trials 1,2, 5 and 10 of user ID:35764) because it registers an initial poking gesture. The user needs to adjust the elbows' poses adequately and poke the robot so that the initial upward motion starts again.

It is important to highlight that it is the first version of the proposed HRC system except for moderate tuning based on the pilot studies with 8 users. I made the majority of the critical design choices only based on my initial intuition such as which motion types will be mapped (i.e. two arms merged motion in APPROACH state and elbow heights in COLIFT state), which gesture types during the state transitions are applied, which feedback will be given to user via screen etc. However, after observing the users during the experiments, I can see some design choices are better than expected and some are worse. For example, the usage of two arms instead of only one arm in the APPROACH state, the right-hand rotation gesture for transition IDLE↔APPROACH, the initial upwards motion of the robot when the COLIFT starts and the poking gesture in the COLIFT state are commented on positively by the many users whereas several people complained the COLIFT→RELEASE gesture (releasing the right arm downwards) because they triggered the RELEASE state unintentionally while they are trying to lift the table in the COLIFT state. Another interesting observation is related to the *mirror motion* behaviour of the robot instead of *mimic motion*. Many users who often play computer games found it counter-intuitive whereas many other users stated completely opposite. The human-robot experiments revealed many interesting human-robot interactions during a complex collaboration as well as validated the system's usability. In conclusion, there is still room for improvement in investigating the most optimal and intuitive gestures.

Finally, the soft-real time response of the system is superb and the robot's end effector follows the merged hand's motion satisfactorily.

### 5.0.4.2 User Surveys

The users answered 23 pre-survey questions and 33 post-survey questions. The aim of the pre-survey is to obtain relevant user background and the aim of the post-survey is to get user feedback. Some of the variables from 56 data points from the surveys are used in [Paper F](#) but there are still possible correlations to be investigated.

For instance, there is a section in both pre-survey and post-survey containing the same questions which measures the user anticipation about the robot technology. This section is to observe if there are any changes in the user's perception, expectation, fear and hope about robotics before they carry out the physical experimental procedure



and after. The findings are interesting and quite positive in terms of triggering positive anticipation via human-robot studies.

The questions are in the fom of 7-point Likert scale items between *Completely disagree* and *Completely agree*. The answers are quantified between -100 and +100. The mean of the 32 answers to each common question from the pre-survey and post-survey are compared. The change in user anticipation is given in Table 5.1. The change value is expected to be 0 for all questions if taking part in this human-robot experiment does not have any effects.

**Table 5.1:** The change in user anticipation about robot technology before and after they are involved in a human-robot research study

Question	Change
I think robotics technology has developed a lot and it amuses me.	19.35
I think robotics technology has developed a lot and it scares me.	-12.10
I think robots will take over human jobs and THEREFORE many people will be unemployed.	-13.71
I think robots will take over human jobs BUT many new job opportunities will be formed.	3.23
I think robots will take over heavy human jobs and the average life quality will increase.	17.74

As seen in Table 5.1, the overall user perception of the positive opinions about robotics technology such as amusement, increasing job opportunities and increasing life quality increased whereas the negative opinions such as fear and worry of unemployment reduced.



## CONCLUSION

---

This is the final chapter of this thesis. The purpose, methods and key findings are summarized and some recommendations are provided for relevant stakeholders.

This study focuses on estimating human motion and gestures reliably for safe Human Robot Cooperation (HRC). The intended usage is in the production, manufacturing and machining processes in small/medium-scale industries which acquire sufficient profit, efficiency, and performance in neither fully atomized nor manual solutions and require more modular solutions. Additionally, this study aims to open up possibilities of HME-based HRC applications in the medical field.

An intensive literature search revealed two major gaps: one is related to the need for a reliable, cost-efficient, and intuitive-to-use interaction method for HRC that is suitable for industrial applications. While many highly precise and accurate motion-tracking solutions have been found to work well in ideal research setups, they often fail when implemented in an actual industrial environment. The other gap is related to the lack of user/operator training. The absence of methodological user training in HRC causes successfully researched and promising HRC solutions not to be implemented in a real application, which widens the valley of death between research and successful innovation.

The proposed Human Motion Estimation (HME) solution in this study is computed using several Inertial Measurement Unit (IMU)s which are low in the cost scale of motion capture devices. They do not suffer from issues such as occlusion, loss of line of sight, light changes etc. and require substantially fewer computational resources than their common alternatives visual-based sensory devices, which makes them favourable in industrial applications. Additionally, the selected HME method is orientation-based motion estimation which was found to be the most suitable with the chosen motion tracking sensors.

First sufficiently reliable poses and gestures of the human are obtained in real-time. The remaining tracking and estimation errors are eliminated by appropriate human-robot motion mapping methods. Two key findings are:

- IMUs are low-cost devices which satisfactory real-time HME results can be obtained with. The modularity allows them to be convenient in industrial HRC applications.
- *HME for HRC* is a broad concept rather than a mere tracking/estimation problem. Obtaining accurate and precise pose estimation is a fundamental step, but it

## Conclusion

is not the whole picture. The system (including the robot) and environmental parameters should also be carefully considered. Various algorithms for mapping human-robot motion are effective in achieving this goal.

The HRC implementation in this study is shaped around a fundamental task which is called *Cooperative Lifting (co-lift)*. Different methods are provided for three HRC roles - human leading, robot leading and shared leadership - and endorsed with real-world experiments to deeply investigate the *leadership* roles. The proposed methodology and implementation are validated with a relatively large user test. Four key findings related to human-robot leadership and user training are:

- The robot and the human excel in different skills so the HRC system should be either designed or dynamically assigning the most efficient leadership roles between the human and the robot. While humans are good at problem-solving and decision-making, robots are more efficient if the task requires precision, accuracy and repeatability.
- *Everyone* can cooperate with robots regardless of age, gender, occupation and body size. However, there are some differences in the learning process and the type of learning based on different user background factors.
- Training is fundamental. As engineers, we are responsible not only for developing solutions to meet society's needs but also for providing adequate educational techniques so that the solutions can be used effectively. This is particularly important in the field of HRI.
- The anticipation of the user towards robots and collaborative tasks is important for efficient HRC. Moreover, this change can be achieved through proper training and interaction with robots, as discussed earlier. This finding is significant because there is hesitancy among a non-negligible portion of the industry to implement HRC in their manufacturing or production processes. An interactive training opportunity would enable HRC solutions to be more positively considered by the industry.

Moreover, this study supports the open-source community and all the codes related to this study can be found under HVL Robotics Github page<sup>1</sup>. This study provides a free-of-charge HME solution which otherwise would be relatively expensive.

In conclusion, research is a never-ending process in which findings reveal new questions. Although this study fulfilled the research questions, it also led to more curiosity. These questions are not presented as *future work* of this study but rather the beginning of new chapters. For instance, the methodology implemented in this study can be expanded to the full body. Additional sensory devices, such as cameras for precision-critical positioning tasks or F/T sensors for sense-critical tasks, can enhance the proposed methodological approach and increase the variations of possible HRC tasks. Moreover, the user training part is a big research area that should be focused more on in HRC studies. In this study, a novel gamified training setup was developed

---

<sup>1</sup><https://github.com/frdedynamics>

and tested. However, diverse methods of user training (i.e. documents, tutorial videos, games, etc.), as well as different methods of gamified/game-based learning, should be compared. For instance, the effectiveness of a fully developed serious game might be different from a supervised gamified training setup. Additionally, the different application areas of this system might be investigated. Medical applications, service industries, and home use are areas where HRC has potential, and the proposed methodological approach can be useful.



# BIBLIOGRAPHY

---

- [1] Alessandro Filippeschi, Norbert Schmitz, Markus Miezal, Gabriele Bleser, Emanuele Ruffaldi, and Didier Stricker. Survey of Motion Tracking Methods Based on Inertial Sensors: A Focus on Upper Limb Human Motion. *Sensors (Switzerland)*, 17(6):1–40, 2017. ISSN 14248220. doi: 10.3390/s17061257. ([document](#)), [2.1.3](#), [2.7](#), [2.1.4](#), [2.1.4](#)
- [2] Michael A. Goodrich and Alan C. Schultz. Human-Robot Interaction: A Survey. *Foundations and Trends in Human-Computer Interaction*, 1(3):203–275, 2007. doi: 10.1561/1100000005. URL <https://doi.org/10.1561/1100000005>. [1.1](#), [2.2](#)
- [3] Celine Jost, Brigitte Le Pevedic, Tony Belpaeme, Cindy Bethel, Dimitrios Chrysostomou, Nigel Crook, Marine Grandgeorge, and Nicole Mirnig, editors. *Human-robot interaction*. Springer Series on Bio- and Neurosystems. Springer Nature, Cham, Switzerland, 1 edition, May 2020. doi: 10.1007/978-3-030-42307-0. URL <https://doi.org/10.1007/978-3-030-42307-0>. [1.1](#), [1.1](#), [1.5.1](#), [1.8](#), [4.4](#), [4.4.1](#), [4.4.2.2](#)
- [4] Bruno Siciliano and Oussama Khatib. Physical Human-Robot Interaction. In *Springer Handbook of Robotics*, chapter 69, pages 1835–1874. Springer, 2016. [1.2](#), [1.2](#)
- [5] Leila Takayama. Putting Human-Robot Interaction Research into Design Practice. In *2022 17th ACM/IEEE International Conference on Human-Robot Interaction (HRI)*. IEEE, March 2022. doi: 10.1109/hri53351.2022.9889659. URL <https://doi.org/10.1109/hri53351.2022.9889659>. [1.1](#)
- [6] Jr George C Devol. Programmed Article Transfer, 1954. US2988237A. [1.2](#)
- [7] James E. Colgate and Michael A. Peshkin. COBOTS, 14 Sept 1999. [1.2](#)
- [8] Cobotics-World. Cobotics World Cobot List - More than 150 Collaborative Robots. <https://www.coboticsworld.com/cobots-list/>, (Accessed on 10 Oct 2020). (Accessed on 10 Oct 2020). [1.2](#)
- [9] ABI-Research. Collaborative Robotics. <https://www.abiresearch.com/market-research/product/1027365-collaborative-robotics/>, 2017. (Accessed on 10 Oct 2020). [1.2](#)
- [10] Fortune Business Insight. Industrial Automation Market Size, Share COVID-19 Impact Analysis, by Component (Hardware, Software), by Industry (Discrete Automation, Process Automation), and Regional Forecast, 2022-2029, 2022. URL <https://www.fortunebusinessinsights.com/industry-reports/industrial-automation-market-101589>. [1.2](#)
- [11] International Organization for Standardization. ISO 10218-1:2011 Robots and robotic devices, 2012. URL <https://www.iso.org/standard/51330.html>. [1.2](#)

## BIBLIOGRAPHY

- [12] Pablo Segura Parra, Odette Lobato Calleros, and Alejandro Ramirez-Serrano. Human-Robot Collaboration Systems: Components and Applications. In *Int. Conf. Control. Dyn. Syst. Robot*, volume 150, pages 1–9, 2020. doi: 10.11159/cdsr20.150. URL <https://doi.org/10.11159/cdsr20.150>. 1.3, 1.3
- [13] Tamim Asfour, Lukas Kaul, Mirko Wächter, Simon Ottenhaus, Pascal Weiner, Samuel Rader, Raphael Grimm, You Zhou, Markus Grotz, Fabian Paus, et al. Armar-6: A Collaborative Humanoid Robot for Industrial Environments. In *2018 IEEE-RAS 18th International Conference on Humanoid Robots (Humanoids)*, pages 447–454. IEEE, 2018. doi: 10.1109/HUMANOIDS.2018.8624966. URL <https://doi.org/10.1109/HUMANOIDS.2018.8624966>. 1.3
- [14] Don Joven Agravante, Andrea Cherubini, Alexander Sherikov, Pierre-Brice Wieber, and Abderrahmane Kheddar. Human-Humanoid Collaborative Carrying. *IEEE Transactions on Robotics*, 35(4):833–846, 2019. doi: 10.1109/TRO.2019.2914350. URL <https://doi.org/10.1109/TRO.2019.2914350>. 1.3
- [15] Gizem Ateş, Martin Fodstad Stølen, and Erik Kyrkjebø. Force and Gesture-based Motion Control of Human-Robot Cooperative Lifting Using IMUs. In *2022 17th ACM/IEEE International Conference on Human-Robot Interaction (HRI)*. IEEE, March 2022. doi: 10.1109/hri53351.2022.9889450. URL <https://doi.org/10.1109/hri53351.2022.9889450>. 1.4, 1.9
- [16] Joseph E. Michaelis, Amanda Siebert-Evenstone, David Williamson Shaffer, and Bilge Mutlu. Collaborative or Simply Uncaged? Understanding Human-Cobot Interactions in Automation. In *Proceedings of the 2020 CHI Conference on Human Factors in Computing Systems, CHI '20*, page 1–12, New York, NY, USA, 2020. Association for Computing Machinery. ISBN 9781450367080. doi: 10.1145/3313831.3376547. URL <https://doi.org/10.1145/3313831.3376547>. 1.3, 1.5
- [17] Behzad Dariush. Human Motion Analysis for Biomechanics and Biomedicine. 14 (4):202–205, sep 2003. doi: 10.1007/s00138-002-0108-8. URL <https://doi.org/10.1007/s00138-002-0108-8>. 1.4, 1.5.3, 2.1.1
- [18] G. R. Bradski and J. Davis. Motion Segmentation and Pose Recognition With Motion History Gradients. *Proceedings of IEEE Workshop on Applications of Computer Vision*, 2000-Janua(2002):238–244, 2000. ISSN 21583986. doi: 10.1109/WACV.2000.895428. URL <https://doi.org/10.1007/s001380100064>. 1.4, 1.5.3, 2.1.1
- [19] Daniel Roetenberg, Henk Luinge, and Per Slycke. Xsens MVN : Full 6DOF Human Motion Tracking Using Miniature Inertial Sensors. *Hand, The*, (January 2009):1–7, 2009. doi: 10.1.1.569.9604. 1.4, 1.5, 1.5.3, 2.1.1, 2.1.3, 2.10, 2.1.4, 3.3.2
- [20] H. Luinge and P.H. Veltink. Inclination Measurement of Human Movement Using a 3-D Accelerometer With Autocalibration. *IEEE Transactions on Neural Systems and Rehabilitation Engineering*, 12(1):112–121, March 2004. doi: 10.1109/tnsre.2003.822759. URL <https://doi.org/10.1109/tnsre.2003.822759>. 1.4, 1.5.3



- [21] P. Cerveri, A. Pedotti, and G. Ferrigno. Kinematical Models to Reduce the Effect of Skin Artifacts on Marker-Based Human Motion Estimation. *Journal of Biomechanics*, 38(11):2228–2236, 2005. ISSN 00219290. doi: 10.1016/j.jbiomech.2004.09.032. URL <https://doi.org/10.1016/j.jbiomech.2004.09.032>. 1.4, 1.5.3, 2.1.1, 2.1.3
- [22] Michail Theofanidis, Alexandros Lioulemes, and Fillia Makedon. A Motion and Force Analysis System for Human Upper-limb Exercises. *Petra* 2016, 03 2016. URL <http://dx.doi.org/10.1145/2910674.2910698>. 1.4, 1.5.3, 2.1.1
- [23] Dung Phan, Bipasha Kashyap, Pubudu Pathirana, and Aruna Seneviratne. A Constrained Nonlinear Optimization Solution for 3D Orientation Estimation of the Human Limb. pages 1–4, 08 2017. doi: 10.1109/BMEiCON.2017.8229138. URL <https://doi.org/10.1109/BMEiCON.2017.8229138>. 1.4, 1.5.3, 2.1.1
- [24] Ashitava Ghosal. Resolution of Redundancy in Robots and in a Human Arm. *Mechanism and Machine Theory*, 125:126–136, 2018. ISSN 0094-114X. doi: 10.1016/j.mechmachtheory.2017.12.008. URL <https://doi.org/10.1016/j.mechmachtheory.2017.12.008>. 1.4, 1.5.3, 1.7, 2.1.1
- [25] Luis Roda-Sanchez, Celia Garrido-Hidalgo, Arturo S. García, Teresa Olivares, and Antonio Fernández-Caballero. Comparison of RGB-d and IMU-based gesture recognition for human-robot interaction in remanufacturing. *The International Journal of Advanced Manufacturing Technology*, October 2021. doi: 10.1007/s00170-021-08125-9. URL <https://doi.org/10.1007/s00170-021-08125-9>. 1.4, 1.8, 5.0.2
- [26] John Hudson and Hanan F Khazragui. Into the Valley of Death: Research to Innovation. *Drug Discovery Today*, 18(13-14):610–613, 2013. doi: 10.1016/j.drudis.2013.01.012. URL <https://doi.org/10.1016/j.drudis.2013.01.012>. 1.5.1
- [27] Cheng Xu, Jie He, Xiaotong Zhang, Xinghang Zhou, and Shihong Duan. Towards Human Motion Tracking: Multi-sensory IMU/TOA Fusion Method and Fundamental Limits. *Electronics (Switzerland)*, 8(2):1–22, 2019. ISSN 20799292. doi: 10.3390/electronics8020142. URL <https://doi.org/10.3390/electronics8020142>. 1.5.2
- [28] Patrick Esser, Helen Dawes, Johnny Collett, and Ken Howells. IMU: Inertial sensing of vertical CoM movement. *Journal of Biomechanics*, 42(10):1578–1581, July 2009. doi: 10.1016/j.jbiomech.2009.03.049. URL <https://doi.org/10.1016/j.jbiomech.2009.03.049>. 1.5.2
- [29] Qilong Yuan and I. Ming Chen. Localization and velocity tracking of human via 3 IMU sensors. *Sensors and Actuators, A: Physical*, 212:25–33, 2014. ISSN 09244247. doi: 10.1016/j.sna.2014.03.004. URL <http://dx.doi.org/10.1016/j.sna.2014.03.004>. 1.5.2
- [30] Yawen Chen, Chenglong Fu, Winnie Suk, Wai Leung, and Ling Shi. Drift-Free and Self-Aligned IMU-Based Human Precision and Robustness. 5(3):4671–4678,

## BIBLIOGRAPHY

2020. doi: 10.1109/LRA.2020.3002203. URL <https://doi.org/10.1109/LRA.2020.3002203>. 1.5.2, 2.1.3, 2.1.3
- [31] A. R. Jimenez, F. Seco, J. C. Prieto, and J. Guevara. Indoor Pedestrian Navigation using an INS/EKF Framework for yaw Drift reduction and a Foot-mounted IMU. *Proceedings of the 2010 7th Workshop on Positioning, Navigation and Communication, WPNC'10*, (April):135–143, 2010. ISSN 1536-1268. doi: 10.1109/WPNC.2010.5649300. URL <https://doi.org/10.1109/WPNC.2010.5649300>. 1.5.2, 2.1.3, 2.1.4
- [32] Xsens. MTw Awinda User Manual Document MW0502P, Revision L. (May), 2018. URL [https://www.xsens.com/hubfs/Downloads/Manuals/MTw\\_Awinda\\_User\\_Manual.pdf](https://www.xsens.com/hubfs/Downloads/Manuals/MTw_Awinda_User_Manual.pdf). 1.5.2, 3.2.3, 4.1, 4.1.1, 5.0.2
- [33] Niccolo M. Fiorentino, Penny R. Atkins, Michael J. Kutschke, Justine M. Goebel, K. Bo Foreman, and Andrew E. Anderson. Soft Tissue Artifact Causes Significant Errors in the Calculation of Joint Angles and Range of Motion at the Hip. *Gait & Posture*, 55:184–190, June 2017. doi: 10.1016/j.gaitpost.2017.03.033. URL <https://doi.org/10.1016/j.gaitpost.2017.03.033>. 1.5.3
- [34] Mahdi Zabat, Amina Ababou, Nouredine Ababou, and Raphaël Dumas. IMU-Based Sensor-to-Segment Multiple Calibration for Upper Limb Joint Angle Measurement—a Proof of Concept. *Medical and Biological Engineering and Computing*, 57(11), 2019. ISSN 17410444. doi: 10.1007/s11517-019-02033-7. URL <https://doi.org/10.1007/s11517-019-02033-7>. 1.5.3, 2.1.3
- [35] Janet H Marler, Xiaoya Liang, and James Hamilton Dulebohn. Training and Effective Employee Information Technology Use. *Journal of Management*, 32(5): 721–743, 2006. URL <https://doi.org/10.1177/0149206306292388>. 1.5.4
- [36] Lesa Huber and Carol Watson. Technology: Education and Training Needs of Older Adults. *Educational Gerontology*, 40(1):16–25, September 2013. doi: 10.1080/03601277.2013.768064. URL <https://doi.org/10.1080/03601277.2013.768064>. 1.5.4
- [37] Valeria Villani, Lorenzo Sabattini, Julia N. Czerniaki, Alexander Mertens, Birgit Vogel-Heuser, and Cesare Fantuzzi. Towards Modern Inclusive Factories: A Methodology for the Development of Smart Adaptive Human-Machine Interfaces. In *2017 22nd IEEE International Conference on Emerging Technologies and Factory Automation (ETFA)*. IEEE, September 2017. doi: 10.1109/etfa.2017.8247634. URL <https://doi.org/10.1109/etfa.2017.8247634>. 1.5.4
- [38] Hamish Tennent, Wen-Ying Lee, Yoyo Tsung-Yu Hou, Ilan Mandel, and Malte Jung. PAPERINO. In *Companion of the 2018 ACM Conference on Computer Supported Cooperative Work and Social Computing*. ACM, October 2018. doi: 10.1145/3272973.3272994. URL <https://doi.org/10.1145/3272973.3272994>. 1.5.4

- [39] Daniel Salber and Joëlle Coutaz. Applying the Wizard of Oz technique to the study of multimodal systems. In *Lecture Notes in Computer Science*, pages 219–230. Springer Berlin Heidelberg, 1993. doi: 10.1007/3-540-57433-6\_51. URL [https://doi.org/10.1007/3-540-57433-6\\_51](https://doi.org/10.1007/3-540-57433-6_51). 1.5.4
- [40] Katie Winkle, Emmanuel Senft, and Séverin Lemaignan. LEADOR: A method for end-to-end participatory design of autonomous social robots. *Frontiers in Robotics and AI*, 8, December 2021. doi: 10.3389/frobt.2021.704119. URL <https://doi.org/10.3389/frobt.2021.704119>. 1.5.4
- [41] Pedro Sequeira, Patricia Alves-Oliveira, Tiago Ribeiro, Eugenio Di Tullio, Sofia Petisca, Francisco S. Melo, Ginevra Castellano, and Ana Paiva. Discovering social interaction strategies for robots from restricted-perception Wizard-of-Oz studies. In *2016 11th ACM/IEEE International Conference on Human-Robot Interaction (HRI)*. IEEE, March 2016. doi: 10.1109/hri.2016.7451752. URL <https://doi.org/10.1109/hri.2016.7451752>. 1.5.4
- [42] Laurel Riek. Wizard of Oz Studies in HRI: A systematic review and new reporting guidelines. *Journal of Human-Robot Interaction*, pages 119–136, August 2012. doi: 10.5898/jhri.1.1.riek. URL <https://doi.org/10.5898/jhri.1.1.riek>. 1.5.4
- [43] Ganesh Pai, Sarah Widrow, Jaydeep Radadiya, Cole D. Fitzpatrick, Michael Knodler, and Anuj K. Pradhan. A Wizard-of-Oz Experimental Approach to Study The Human Factors of Automated Vehicles: Platform and Methods Evaluation. *Traffic Injury Prevention*, 21(sup1):S140–S144, August 2020. doi: 10.1080/15389588.2020.1810243. URL <https://doi.org/10.1080/15389588.2020.1810243>. 1.5.4
- [44] Robin Jeanne Kirschner, Lisa Burr, Melanie Porzenheim, Henning Mayer, Saeed Abdolshah, and Sami Haddadin. Involuntary Motion in Human-Robot Interaction: Effect of Interactive User Training on the Occurrence of Human Startle-Surprise Motion. In *2021 IEEE International Conference on Intelligence and Safety for Robotics (ISR)*. IEEE, March 2021. doi: 10.1109/isr50024.2021.9419526. URL <https://doi.org/10.1109/isr50024.2021.9419526>. 1.5.4
- [45] Maha Salem and Kerstin Dautenhahn. Evaluating Trust and Safety in Hri: Practical Issues and Ethical Challenges. *Emerging Policy and Ethics of Human-Robot Interaction*, 2015. URL <http://hdl.handle.net/2299/16336>. 1.5.4
- [46] Stefanos Nikolaidis and Julie Shah. Human-Robot Cross-Training: Computational Formulation, Modeling and Evaluation of a Human Team Training Strategy. In *2013 8th ACM/IEEE International Conference on Human-Robot Interaction (HRI)*. IEEE, March 2013. doi: 10.1109/hri.2013.6483499. URL <https://doi.org/10.1109/hri.2013.6483499>. 1.5.4
- [47] Tarja Susi, Mikael Johannesson, and Per Backlund. Serious games: An overview. 2007. 1.5.4, 2.2.2

## BIBLIOGRAPHY

- [48] Ar Anil Yasin and Asad Abbas. Role of Gamification in Engineering Education: A Systematic Literature Review. In *2021 IEEE Global Engineering Education Conference (EDUCON)*. IEEE, April 2021. doi: 10.1109/EDUCON46332.2021.9454038. URL <https://doi.org/10.1109/EDUCON46332.2021.9454038>. 1.5.4, 2.2.2
- [49] Alexandros Kleftodimos and Georgios Evangelidis. Augmenting Educational Videos With Interactive Exercises and Knowledge Testing Games. In *2018 IEEE Global Engineering Education Conference (EDUCON)*. IEEE, April 2018. doi: 10.1109/EDUCON.2018.8363322. URL <https://doi.org/10.1109/EDUCON.2018.8363322>. 1.5.4, 2.2.2
- [50] David R Michael and Sandra L Chen. Serious Games: Games That Educate, Train, and Inform. In *Muska & Lipman/Premier-Trade*, 2005. URL <https://dl.acm.org/doi/10.5555/1051239>. 1.5.4
- [51] Sebastian Deterding, Dan Dixon, Rilla Khaled, and Lennart Nacke. From Game Design Elements to Gamefulness: Defining "Gamification". In *Proceedings of the 15th international academic MindTrek conference: Envisioning future media environments*, pages 9–15, 2011. doi: 10.1145/2181037.2181040. URL <https://dl.acm.org/doi/abs/10.1145/2181037.2181040>. 1.5.4
- [52] Thibaud Michel, Hassen Fourati, Pierre Geneves, and Nabil Layaida. A comparative analysis of attitude estimation for pedestrian navigation with smartphones. *2015 International Conference on Indoor Positioning and Indoor Navigation, IPIN 2015*, 2015. doi: 10.1109/IPIN.2015.7346767. URL <https://doi.org/10.1109/IPIN.2015.7346767>. 1.5.4, 2.1.4
- [53] Pieter Wouters, Christof van Nimwegen, Herre van Oostendorp, and Erik D. van der Spek. A meta-analysis of the cognitive and motivational effects of serious games. *Journal of Educational Psychology*, 105(2):249–265, May 2013. doi: 10.1037/a0031311. URL <https://doi.org/10.1037/a0031311>. 1.5.4, 2.2.2
- [54] Tony Belpaeme. Advice to New Human-Robot Interaction Researchers. In *Springer Series on Bio- and Neurosystems*, pages 355–369. Springer International Publishing, 2020. doi: 10.1007/978-3-030-42307-0\_14. URL [https://doi.org/10.1007/978-3-030-42307-0\\_14](https://doi.org/10.1007/978-3-030-42307-0_14). 1.7
- [55] Marlena R. Fraune, Iolanda Leite, Nihan Karatas, Aida Amirova, Amélie Legeleux, Anara Sandygulova, Anouk Neerincx, Gaurav Dilip Tikas, Hatice Gunes, Mayumi Mohan, Nida Itrat Abbasi, Sudhir Shenoy, Brian Scassellati, Ewart J. de Visser, and Takanori Komatsu. Lessons Learned About Designing and Conducting Studies From HRI experts. *Frontiers in Robotics and AI*, 8, January 2022. doi: 10.3389/frobt.2021.772141. URL <https://doi.org/10.3389/frobt.2021.772141>. 1.7, 4.4
- [56] Paul Evrard, Elena Gribovskaya, Sylvain Calinon, Aude Billard, and Abderahmane Kheddar. Teaching Physical Collaborative Tasks: Object-Lifting Case Study With a Humanoid. In *2009 9th IEEE-RAS International Conference on Humanoid Robots*. IEEE, December 2009. doi: 10.1109/ichr.2009.5379513. URL <https://doi.org/10.1109/ichr.2009.5379513>. 1.8

- [57] Ye Gu, Anand Thobbi, and Weihua Sheng. Human-Robot Collaborative Manipulation Through Imitation and Reinforcement Learning. In *2011 IEEE International Conference on Information and Automation*. IEEE, June 2011. doi: 10.1109/icinfa.2011.5948979. URL <https://doi.org/10.1109/icinfa.2011.5948979>. 1.8
- [58] Bojan Nemec, Nejc Likar, Andrej Gams, and Aleš Ude. Human Robot Cooperation With Compliance Adaptation Along the Motion Trajectory. *Autonomous Robots*, 42(5):1023–1035, November 2017. doi: 10.1007/s10514-017-9676-3. URL <https://doi.org/10.1007/s10514-017-9676-3>. 1.8
- [59] Christoph Bartneck, Dana Kulić, Elizabeth Croft, and Susana Zoghbi. Measurement Instruments for the Anthropomorphism, Animacy, Likeability, Perceived Intelligence, and Perceived Safety of Robots. *International Journal of Social Robotics*, 1(1):71–81, November 2008. doi: 10.1007/s12369-008-0001-3. URL <https://doi.org/10.1007/s12369-008-0001-3>. 1.8
- [60] Cindy L. Bethel and Robin R. Murphy. Review of Human Studies Methods in HRI and recommendations. *International Journal of Social Robotics*, 2(4):347–359, July 2010. doi: 10.1007/s12369-010-0064-9. URL <https://doi.org/10.1007/s12369-010-0064-9>. 1.8, 4.4
- [61] Gizem Ateş Venâs. Replication Data for: Exploring Human-Robot Cooperation with Gamified User Training: A User Study on Cooperative Lifting, 2023. URL <https://doi.org/10.18710/CZGZVZ>. 1.8
- [62] Gizem Ateş and Erik Kyrkjebø. Human-robot Cooperative Lifting Using IMUs and Human Gestures. In *Annual Conference Towards Autonomous Robotic Systems*, pages 88–99. Springer, 2021. doi: 10.1007/978-3-030-89177-0\_9. URL [https://doi.org/10.1007/978-3-030-89177-0\\_9](https://doi.org/10.1007/978-3-030-89177-0_9). 1.9, 4.3.2, 4.3.2
- [63] Gizem Ateş, Martin Fodstad Stølen, and Erik Kyrkjebø. A Framework for Human Motion Estimation using IMUs in human-robot interaction. In *2022 IEEE International Conference on Industrial Technology (ICIT)*. IEEE, August 2022. doi: 10.1109/icit48603.2022.10002746. URL <https://doi.org/10.1109/icit48603.2022.10002746>. 1.9
- [64] Gizem Ateş. Work in Progress: Learning Fundamental Robotics Concepts Through Games at Bachelor Level. In *2022 IEEE Global Engineering Education Conference (EDUCON)*. IEEE, March 2022. doi: 10.1109/educon52537.2022.9766499. URL <https://doi.org/10.1109/educon52537.2022.9766499>. 1.9
- [65] Gizem Ateş and Erik Kyrkjebø. Design of a Gamified Training System for Human-Robot Cooperation. In *2022 International Conference on Electrical, Computer, Communications and Mechatronics Engineering (ICECCME)*. IEEE, November 2022. doi: 10.1109/iceccme55909.2022.9988661. URL <https://doi.org/10.1109/iceccme55909.2022.9988661>. 1.9
- [66] Reinhard Klette and Garry Tee. Understanding Human Motion: A Historic Review. (May):1–22, 2008. doi: 10.1007/978-1-4020-6693-1\_1. 2.1.1

## BIBLIOGRAPHY

- [67] H. J. Luinge and P.H. H. Veltink. Measuring Orientation of Human Body Segments Using Miniature Gyroscopes and Accelerometers. *Medical & Biological Engineering & Computing*, 43(2):273–282, apr 2005. ISSN 0140-0118. doi: 10.1007/BF02345966. URL <http://link.springer.com/10.1007/BF02345966>. 2.1.1
- [68] Gregory John Stewart. Chapter 8 - Skeletal muscles. In *Skeletal and muscular systems*, page 106. Chelsea House Publishers, Philadelphia, 2004. ISBN 9781438107738-1438107730. doi: <https://doi.org/10.1016/B978-0-12-405190-4.00005-2>. URL <http://www.sciencedirect.com/science/article/pii/B9780124051904000052>. 2.1.1, 3.4
- [69] Antonie J. Van Den Bogert, Thomas Geijtenbeek, Oshri Even-Zohar, Frans Steenbrink, and Elizabeth C. Hardin. A Real-Time System for Biomechanical Analysis of Human Movement and Muscle Function. *Medical and Biological Engineering and Computing*, 51(10):1069–1077, 2013. ISSN 01400118. doi: 10.1007/s11517-013-1076-z. URL <https://doi.org/10.1007/s11517-013-1076-z>. 2.1.1
- [70] Dario Cazzola, Timothy P. Holsgrove, Ezio Preatoni, Harinderjit S. Gill, and Grant Trewartha. Cervical Spine Injuries: A Whole-Body Musculoskeletal Model for the Analysis of Spinal Loading. *PLoS ONE*, 12(1), 2017. ISSN 19326203. doi: 10.1371/journal.pone.0169329. 2.1.1, 2.1
- [71] Tsung-Chi Lin, Achyuthan Unni Krishnan, and Zhi Li. Shared Autonomous Interface for Reducing Physical Effort in Robot Teleoperation via Human Motion Mapping. In *2020 IEEE International Conference on Robotics and Automation (ICRA)*. IEEE, May 2020. doi: 10.1109/icra40945.2020.9197220. URL <https://doi.org/10.1109/icra40945.2020.9197220>. 2.2, 2.1.2
- [72] Huiyu Zhou and Huosheng Hu. Human Motion Tracking for Rehabilitation — A Survey. *Biomedical signal processing and control*, 3(1):1–18, 2008. doi: 10.1016/j.bspc.2007.09.001. URL <https://doi.org/10.1016/j.bspc.2007.09.001>. 2.1.2
- [73] Huiyu Zhou, Huosheng Hu, and Nigel D Harris. Wearable Inertial Sensors for Arm Motion Tracking in Home-Based Rehabilitation. In *IAS*, pages 930–937, 2006. 2.1.2
- [74] Csaba Kertesz. Physiotherapy Exercises Recognition Based on RGB-d human skeleton models. In *2013 European Modelling Symposium*. IEEE, November 2013. doi: 10.1109/ems.2013.4. URL <https://doi.org/10.1109/ems.2013.4>. 2.1.2
- [75] Jonathan FS Lin and Dana Kulić. Human Pose Recovery Using Wireless Inertial Measurement Units. *Physiological measurement*, 33(12):2099, 2012. 2.1.2
- [76] Andreas Kranzl. *Clinical Gait Assessment by Video Observation and 2D Techniques*, pages 473–488. Springer International Publishing, Cham, 2018. ISBN 978-3-319-14418-4. doi: 10.1007/978-3-319-14418-4\_24. URL [https://doi.org/10.1007/978-3-319-14418-4\\_{\\_}24](https://doi.org/10.1007/978-3-319-14418-4_{_}24). 2.1.2, 2.1.3

- [77] Sen Qiu, Zhelong Wang, Hongyu Zhao, Long Liu, Jinxiao Li, Yongmei Jiang, and Giancarlo Fortino. Body Sensor Network-Based Robust Gait Analysis: Toward Clinical and at Home Use. *IEEE Sensors Journal*, 19(19):8393–8401, October 2019. doi: 10.1109/jsen.2018.2860938. URL <https://doi.org/10.1109/jsen.2018.2860938>. 2.1.2
- [78] Alvaro Muro de-la Herran, Begonya Garcia-Zapirain, and Amaia Mendez-Zorrilla. Gait Analysis Methods: An Overview of Wearable and Non-Wearable Systems, Highlighting Clinical Applications. *Sensors*, 14(2):3362–3394, February 2014. doi: 10.3390/s140203362. URL <https://doi.org/10.3390/s140203362>. 2.1.2, 2.1.3
- [79] Victor B Kim, William HH Chapman Iii, Robert J Albrecht, B Marcus Bailey, James A Young, L Wiley Nifong, and W Randolph Chitwood Jr. Early Experience With Telem manipulative Robot-Assisted Laparoscopic Cholecystectomy Using Da Vinci. *Surgical Laparoscopy Endoscopy & Percutaneous Techniques*, 12(1):33–40, 2002. 2.1.2
- [80] Yik San Kwoh, Joahin Hou, Edmond A Jonckheere, and Samad Hayati. A Robot With Improved Absolute Positioning Accuracy for CT Guided Stereotactic Brain Surgery. *IEEE Transactions on Biomedical Engineering*, 35(2):153–160, 1988. 2.1.2
- [81] Anthony R. Lanfranco, Andres E. Castellanos, Jaydev P. Desai, and William C. Meyers. Robotic Surgery. *Annals of Surgery*, 239(1):14–21, January 2004. doi: 10.1097/01.sla.0000103020.19595.7d. URL <https://doi.org/10.1097/01.sla.0000103020.19595.7d>. 2.1.2
- [82] Tim Lane. A Short History of Robotic Surgery. *The Annals of The Royal College of Surgeons of England*, 100(6<sub>sup</sub>):5–7, May 2018. doi: 10.1308/rcsann.suppl1.5. URL <https://doi.org/10.1308/rcsann.suppl1.5>. 2.1.2
- [83] Gizem Ateş, Ronny Majani, and Mehmet İsmet Can Dede. Design of a Teleoperation Scheme with a Wearable Master for Minimally Invasive Surgery. In *Mechanisms and Machine Science*, pages 45–53. Springer International Publishing, September 2018. doi: 10.1007/978-3-030-00329-6\_6. URL [https://doi.org/10.1007/978-3-030-00329-6\\_6](https://doi.org/10.1007/978-3-030-00329-6_6). 2.1.2, 2.1.3, 2.1.4
- [84] Gizem Ateş and Can Dede. *Teleoperation System Design of a Robot Assisted Endoscopic Pituitary Surgery*. Master of science thesis, Izmir Institute of Technology, July 2018. URL <https://tez.yok.gov.tr/UlusalTezMerkezi/tarama.jsp>. 2.1.2, 2.3
- [85] Rebecca M Pierce, Elizabeth A Fedalei, and Katherine J Kuchenbecker. A Wearable Device for Controlling a Robot Gripper With Fingertip Contact, Pressure, Vibrotactile, and Grip Force Feedback. In *2014 IEEE Haptics Symposium (HAPTICS)*, pages 19–25. IEEE, 2014. doi: 10.1109/HAPTICS.2014.6775428. URL <https://doi.org/10.1109/HAPTICS.2014.6775428>. 2.1.2
- [86] Xsens. MVN Animate. <https://www.xsens.com/products/mvn-animate>. (Accessed on 11/16/2020). 2.1.2

## BIBLIOGRAPHY

- [87] Trenton Schulz, Jim Torresen, and Jo Herstad. Animation Techniques in Human-Robot Interaction User Studies. *ACM Transactions on Human-Robot Interaction*, 8(2):1–22, June 2019. doi: 10.1145/3317325. URL <https://doi.org/10.1145/3317325>. 2.1.2
- [88] Guy Hoffman and Wendy Ju. Designing Robots With Movement in Mind. *Journal of Human-Robot Interaction*, 3(1):89, March 2014. doi: 10.5898/jhri.3.1.hoffman. URL <https://doi.org/10.5898/jhri.3.1.hoffman>. 2.1.2
- [89] Deivid De Meyer. Robust Real-Time Pose Estimation with OpenPose. <https://medium.com/brainjar/robust-real-time-pose-estimation-with-openpose-89ae39ee05ed>, Nov 2017. (Accessed on 12/10/2020). 2.4
- [90] Mateus Trombetta, Patrícia Paula Bazzanello Henrique, Manoela Rogofski Brum, Eliane Lucia Colussi, Ana Carolina Bertoletti De Marchi, and Rafael Rieder. Motion Rehab AVE 3D: A VR-based exergame for post-stroke rehabilitation. *Computer Methods and Programs in Biomedicine*, 151:15–20, 2017. ISSN 0169-2607. doi: <https://doi.org/10.1016/j.cmpb.2017.08.008>. URL <http://www.sciencedirect.com/science/article/pii/S016926071730113X>. 2.1.2
- [91] Carlos Alberto Aguilar-Lazcano and Ericka Janet Rechy-Ramirez. Performance analysis of Leap motion controller for finger rehabilitation using serious games in two lighting environments. *Measurement*, 157:107677, June 2020. doi: 10.1016/j.measurement.2020.107677. URL <https://doi.org/10.1016/j.measurement.2020.107677>. 2.1.2, 2.1.3
- [92] Lige Zhang, Shusheng Bi, and Dengchao Liu. Dynamic Leg Motion Generation of Humanoid Robot Based on Human Motion Capture. In *Intelligent Robotics and Applications*, pages 83–92. Springer Berlin Heidelberg, 2008. doi: 10.1007/978-3-540-88513-9\_10. URL [https://doi.org/10.1007/978-3-540-88513-9\\_10](https://doi.org/10.1007/978-3-540-88513-9_10). 2.1.2
- [93] Mirko Raković, Srdjan Savić, José Santos-Victor, Milutin Nikolić, and Branislav Borovac. Human-Inspired Online Path Planning and Biped Walking Realization in Unknown Environment. *Frontiers in Neurobotics*, 13, June 2019. doi: 10.3389/fnbot.2019.00036. URL <https://doi.org/10.3389/fnbot.2019.00036>. 2.1.2
- [94] Katsu Yamane and Akihiko Murai. *A Comparative Study Between Humans and Humanoid Robots*, pages 1–20. Springer Netherlands, Dordrecht, 2016. ISBN 978-94-007-7194-9. doi: 10.1007/978-94-007-7194-9\_7-1. URL [https://doi.org/10.1007/978-94-007-7194-9\\_{\\_}7-1](https://doi.org/10.1007/978-94-007-7194-9_{_}7-1). 2.1.2
- [95] Wael Suleiman, Eiichi Yoshida, Fumio Kanehiro, Jean-Paul Laumond, and André Monin. Optimization and Imitation Problems for Humanoid Robots. In *Cognitive Systems Monographs*, pages 233–247. Springer Berlin Heidelberg, 2013. doi: 10.1007/978-3-642-36368-9\_19. URL [https://doi.org/10.1007/978-3-642-36368-9\\_19](https://doi.org/10.1007/978-3-642-36368-9_19). 2.1.2



- [96] Alexander Mörtl, Martin Lawitzky, Ayse Kucukyilmaz, Metin Sezgin, Cagatay Basdogan, and Sandra Hirche. The Role of Roles: Physical Cooperation Between Humans and Robots. *The International Journal of Robotics Research*, 31(13):1656–1674, 2012. doi: 10.1177/0278364912455366. URL <https://doi.org/10.1177/0278364912455366>. 2.1.2, 2.5
- [97] Christian Vogel, Christoph Walter, and Norbert Elkmann. Safeguarding and Supporting Future Human-robot Cooperative Manufacturing Processes by a Projection- and Camera-based Technology. *Procedia Manufacturing*, 11:39–46, 2017. ISSN 2351-9789. doi: <https://doi.org/10.1016/j.promfg.2017.07.127>. URL <http://www.sciencedirect.com/science/article/pii/S2351978917303311>. 2.1.2, 2.1.2
- [98] Christos Gkournelos, Panagiotis Karagiannis, Niki Kousi, George Michalos, Spyridon Koukas, and Sotiris Makris. Application of wearable devices for supporting operators in human-robot cooperative assembly tasks. *Procedia CIRP*, 76:177–182, 2018. ISSN 22128271. doi: 10.1016/j.procir.2018.01.019. URL <https://doi.org/10.1016/j.procir.2018.01.019>. 2.1.2, 2.1.2
- [99] Mokhinabonu Mardonova and Yosoon Choi. Review of Wearable Device Technology and Its Applications to the Mining Industry. *Energies*, 11(3):547, 2018. doi: 10.3390/en11030547. URL <https://doi.org/10.3390/en11030547>. 2.1.2
- [100] Lefteris Benos, Avital Bechar, and Dionysis Bochtis. Safety and Ergonomics in Human-Robot Interactive Agricultural Operations. *Biosystems Engineering*, 200:55–72, December 2020. doi: 10.1016/j.biosystemseng.2020.09.009. URL <https://doi.org/10.1016/j.biosystemseng.2020.09.009>. 2.1.2
- [101] Markus Aleksy, Mikko J Rissanen, Sylvia Maczey, and Marcel Dix. Wearable Computing in Industrial Service Applications. *Procedia Computer Science*, 5: 394–400, 2011. doi: 10.1016/j.procs.2011.07.051. URL <https://doi.org/10.1016/j.procs.2011.07.051>. 2.1.2
- [102] José de Gea Fernández, Dennis Mronga, Martin Günther, Tobias Knobloch, Malte Wirkus, Martin Schröer, Mathias Trampler, Stefan Stiene, Elsa Kirchner, Vinzenz Bargsten, et al. Multimodal Sensor-Based Whole-Body Control for Human–Robot Collaboration in Industrial Settings. *Robotics and Autonomous Systems*, 94:102–119, 2017. doi: 10.1016/j.robot.2017.04.007. URL <https://doi.org/10.1016/j.robot.2017.04.007>. 2.1.2
- [103] Emanuele Magrini, Federica Ferraguti, Andrea Jacopo Ronga, Fabio Pini, Alessandro De Luca, and Francesco Leali. Human-Robot Coexistence and Interaction in Open Industrial Cells. *Robotics and Computer-Integrated Manufacturing*, 61:101846, 2020. doi: 10.1016/j.rcim.2019.101846. URL <https://doi.org/10.1016/j.rcim.2019.101846>. 2.1.2
- [104] Xiaoxu Ji and Davide Piovesan. Validation of Inertial-Magnetic Wearable Sensors for Full-Body Motion Tracking of Automotive Manufacturing Operations. *International Journal of Industrial Ergonomics*, 79:103005, 2020. doi: 10.1016/j.ergon.

## BIBLIOGRAPHY

- 2020.103005. URL <https://doi.org/10.1016/j.ergon.2020.103005>. 2.1.2, 2.1.3
- [105] Thomas Stiefmeier, Daniel Roggen, Georg Ogris, Paul Lukowicz, and Gerhard Tröster. Wearable Activity Tracking in Car Manufacturing. *IEEE Pervasive Computing*, 7(2):42–50, 2008. doi: 10.1109/MPRV.2008.40. URL <https://doi.org/10.1109/MPRV.2008.40>. 2.1.2
- [106] Francesco Caputo, Alessandro Greco, Egidio D’Amato, Immacolata Notaro, Marco Lo Sardo, Stefania Spada, and Lidia Ghibaudo. A Human Postures Inertial Tracking System for Ergonomic Assessments. In *Congress of the International Ergonomics Association*, pages 173–184. Springer, 2018. doi: 10.1007/978-3-319-96068-5\_19. URL [https://doi.org/10.1007/978-3-319-96068-5\\_19](https://doi.org/10.1007/978-3-319-96068-5_19). 2.1.2
- [107] L Peppoloni, A Filippeschi, E Ruffaldi, and CA Avizzano. A Novel Wearable System for the Online Assessment of Risk for Biomechanical Load in Repetitive Efforts. *International Journal of Industrial Ergonomics*, 52:1–11, 2016. doi: 10.1016/j.ergon.2015.07.002. URL <https://doi.org/10.1016/j.ergon.2015.07.002>. 2.1.2
- [108] P. Maurice, Adrien Malaisé, Clélie Amiot, N. Paris, Guy-Junior Richard, Olivier Rochel, and Serena Ivaldi. Human Movement and Ergonomics: An Industry-Oriented Dataset for Collaborative Robotics. *The International Journal of Robotics Research*, 38:1529 – 1537, 2019. doi: 10.1177/0278364919882089. URL <https://doi.org/10.1177/0278364919882089>. 2.1.2
- [109] Dhruv R Seshadri, Ryan T Li, James E Voos, James R Rowbottom, Celeste M Alfes, Christian A Zorman, and Colin K Drummond. Wearable Sensors for Monitoring the Internal and External Workload of the Athlete. *NPJ digital medicine*, 2(1): 1–18, 2019. doi: 10.1038/s41746-019-0149-2. URL <https://doi.org/10.1038/s41746-019-0149-2>. 2.1.2, 2.1.3
- [110] F.A. Magalhães, A. Giovanardi, R. Di Michele, M. Cortesi, G. Gatta, and S. Fantozzi. Swimming Motion Analysis: 3D Joints Kinematics of the Upper Limb Using Wearable Inertial and Magnetic Sensors. 2014. doi: 10.13140/2.1.2302.6248. URL <http://rgdoi.net/10.13140/2.1.2302.6248>. 2.1.2, 2.6
- [111] Jessica K Hodgins, Wayne L Wooten, David C Brogan, and James F O’Brien. Animating Human Athletics. In *Proceedings of the 22nd annual conference on Computer graphics and interactive techniques*, pages 71–78, 1995. doi: 10.1145/218380.218414. URL <https://doi.org/10.1145/218380.218414>. 2.1.2
- [112] Wayne L Wooten and Jessica K Hodgins. Animation of Human Diving. In *Computer Graphics Forum*, volume 15, pages 3–13. Wiley Online Library, 1996. doi: 10.1111/1467-8659.1510003. URL <https://doi.org/10.1111/1467-8659.1510003>. 2.1.2

- [113] David Whiteside, Olivia Cant, Molly Connolly, and Machar Reid. Monitoring hitting load in tennis using inertial sensors and machine learning. *International Journal of Sports Physiology and Performance*, 12(9):1212–1217, 2017. ISSN 15550265. doi: 10.1123/ijsp.2016-0683. URL <https://doi.org/10.1123/ijsp.2016-0683>. 2.1.2, 2.1.4
- [114] G. Ligorio, D. Zanotto, A. M. Sabatini, and S. K. Agrawal. A Novel Functional Calibration Method for Real-Time Elbow Joint Angles Estimation With Magnetic-Inertial Sensors. *Journal of Biomechanics*, 54:106–110, 2017. ISSN 18732380. doi: 10.1016/j.jbiomech.2017.01.024. URL <http://dx.doi.org/10.1016/j.jbiomech.2017.01.024>. 2.1.3, 4.1
- [115] Bingfei Fan, Qingguo Li, Chao Wang, and Tao Liu. An Adaptive Orientation Estimation Method for Magnetic and Inertial Sensors in the Presence of Magnetic Disturbances. *Sensors (Switzerland)*, 17(5), 2017. ISSN 14248220. doi: 10.3390/s17051161. URL <https://doi.org/10.3390/s17051161>. 2.1.3
- [116] Simone A. Ludwig and Kaleb D. Burnham. Comparison of Euler Estimate using Extended Kalman Filter, Madgwick and Mahony on Quadcopter Flight Data. In *2018 International Conference on Unmanned Aircraft Systems, ICUAS 2018*, 2018. ISBN 9781538613535. doi: 10.1109/ICUAS.2018.8453465. URL [10.1109/ICUAS.2018.8453465](https://doi.org/10.1109/ICUAS.2018.8453465). 2.1.3
- [117] Manon Kok, Jeroen D. Hol, and Thomas B. Schön. Using Inertial Sensors for Position and Orientation Estimation. *Foundations and Trends in Signal Processing*, 11(1-2):1–153, 2017. doi: 10.1561/2000000094. URL <https://doi.org/10.1561/2000000094>. 2.1.3, 2.1.4, 3.2.3, 3.3, 3.3, 3.3, 3.3, 3.3.1, 3.3.2, 3.3.2, 5.0.2
- [118] S. Zihajehzadeh, D. Loh, M. Lee, R. Hoskinson, and E. J. Park. A cascaded two-step Kalman filter for estimation of human body segment orientation using MEMS-IMU. *2014 36th Annual International Conference of the IEEE Engineering in Medicine and Biology Society, EMBC 2014*, (2):6270–6273, 2014. doi: 10.1109/EMBC.2014.6945062. URL <https://doi.org/10.1109/EMBC.2014.6945062>. 2.1.3
- [119] Irvin Hussein Lopez-Nava and Munoz Melendez Angelica. Wearable Inertial Sensors for Human Motion Analysis: A review. *IEEE Sensors Journal*, PP (99):7821–7834, 2016. ISSN 1530437X. doi: 10.1109/JSEN.2016.2609392. URL <https://doi.org/10.1109/JSEN.2016.2609392>. 2.1.3, 2.1.4, 2.12, 2.1.4, 2.1.4, 3.2.3
- [120] Shiqiang Liu, Junchang Zhang, Yuzhong Zhang, and Rong Zhu. A wearable motion capture device able to detect dynamic motion of human limbs. *Nature Communications*, 2020. ISSN 2041-1723. doi: 10.1038/s41467-020-19424-2. URL <https://doi.org/10.1038/s41467-020-19424-2>. 2.1.3, 2.1.3
- [121] Frank J. Wouda, Matteo Giuberti, Giovanni Bellusci, and Peter H. Veltink. Estimation of full-body poses using only five inertial sensors: An eager or lazy learning approach? *Sensors (Switzerland)*, 16(12), 2016. ISSN 14248220. doi: 10.3390/s16122138. URL <https://doi.org/10.3390/s16122138>. 2.1.3, 2.1.4

## BIBLIOGRAPHY

- [122] Qi Wang, Panos Markopoulos, Bin Yu, Wei Chen, and Annick Timmermans. Interactive wearable systems for upper body rehabilitation: A systematic review. *Journal of NeuroEngineering and Rehabilitation*, 14(1):1–21, 2017. ISSN 17430003. doi: 10.1186/s12984-017-0229-y. URL <https://doi.org/10.1186/s12984-017-0229-y>. 2.1.3
- [123] Ive Weygers, Manon Kok, Marco Konings, Hans Hallez, Henri De Vroey, and Kurt Claeys. Inertial Sensor-Based Lower Limb Joint Kinematics: A Methodological Systematic Review. *Sensors*, 20(3):673, jan 2020. ISSN 1424-8220. doi: 10.3390/s20030673. URL <https://www.mdpi.com/1424-8220/20/3/673>. 2.1.3
- [124] Chunzhi Yi, Feng Jiang, Zhiyuan Chen, Baichun Wei, Hao Guo, Xunfeng Yin, Fangzhuo Li, and Chifu Yang. Sensor-Movement-Robust Angle Estimation for 3-DoF Lower Limb Joints Without Calibration. (October):0–10, 2019. URL <http://arxiv.org/abs/1910.07240>. 2.1.3
- [125] Mohamed Abdelhady, Antonie J. van den Bogert, and Dan Simon. A High-Fidelity Wearable System for Measuring Lower-Limb Kinetics and Kinematics. *IEEE Sensors Journal*, 19(24):12482–12493, December 2019. doi: 10.1109/jsen.2019.2940517. URL <https://doi.org/10.1109/jsen.2019.2940517>. 2.1.3
- [126] Almas Shintemirov, Tasbolat Taunyazov, Bukeikhan Omarali, Aigerim Nurbayeva, Anton Kim, Askhat Bukeyev, and Matteo Rubagotti. An Open-Source 7-Dof Wireless Human Arm Motion-Tracking System for Use in Robotics Research. *Sensors (Switzerland)*, 20(11):1–19, 2020. ISSN 14248220. doi: 10.3390/s20113082. URL <https://doi.org/10.3390/s20113082>. 2.1.3
- [127] Junghee Kim, Sungho Cho, Choongho Lee, Jaewoong Han, and Heon Hwang. Kinematic and Dynamic Analyses of Human Arm Motion. *Journal of Biosystems Engineering*, 38(2):138–148, 2013. ISSN 1738-1266. doi: 10.5307/jbe.2013.38.2.138. URL <http://dx.doi.org/10.5307/JBE.2013.38.2.138>. 2.1.3
- [128] H. J. Luinge, P. H. Veltink, and C. T.M. Baten. Ambulatory measurement of arm orientation. *Journal of Biomechanics*, 40(1):78–85, 2007. ISSN 00219290. doi: 10.1016/j.jbiomech.2005.11.011. URL <https://doi.org/10.1016/j.jbiomech.2005.11.011>. 2.1.3
- [129] Tasbolat Taunyazov, Bukeikhan Omarali, and Almas Shintemirov. A novel low-cost 4-DOF wireless human arm motion tracker. *Proceedings of the IEEE RAS and EMBS International Conference on Biomedical Robotics and Biomechatronics*, 2016-July:157–162, 2016. ISSN 21551774. doi: 10.1109/BIOROB.2016.7523615. URL <https://doi.org/10.1109/BIOROB.2016.7523615>. 2.1.3
- [130] Benedikt Fasel, Jorg Sporri, Julien Chardonens, Josef Kroll, Erich Muller, and Kamiar Aminian. Joint Inertial Sensor Orientation Drift Reduction for Highly Dynamic Movements. *IEEE Journal of Biomedical and Health Informatics*, 22(1), 2018. ISSN 21682194. doi: 10.1109/JBHI.2017.2659758. URL [10.1109/JBHI.2017.2659758](https://doi.org/10.1109/JBHI.2017.2659758). 2.1.3

- [131] Pubudu N. Pathirana, M. Sajeewani Karunaratne, Gareth L. Williams, Phan T. Nam, and Hugh Durrant-Whyte. Robust and Accurate Capture of Human Joint Pose Using an Inertial Sensor. *IEEE Journal of Translational Engineering in Health and Medicine*, 6, 2018. ISSN 21682372. doi: 10.1109/JTEHM.2018.2877980. URL <https://doi.org/10.1109/JTEHM.2018.2877980>. 2.1.3
- [132] Philipp Muller, Marc Andre Begin, Thomas Schauer, and Thomas Seel. Alignment-Free, Self-Calibrating Elbow Angles Measurement Using Inertial Sensors. *IEEE Journal of Biomedical and Health Informatics*, 21(2), 2017. ISSN 21682194. doi: 10.1109/JBHI.2016.2639537. URL <https://doi.org/10.1109/JBHI.2016.2639537>. 2.1.3
- [133] Wei Sin Ang, I. Ming Chen, and Qilong Yuan. Ambulatory measurement of elbow kinematics using inertial measurement units. *2013 IEEE/ASME International Conference on Advanced Intelligent Mechatronics: Mechatronics for Human Wellbeing, AIM 2013*, (July):756–761, 2013. ISSN 2159-6247. doi: 10.1109/AIM.2013.6584184. URL <https://doi.org/10.1109/AIM.2013.6584184>. 2.1.3
- [134] Arianna Carnevale, Umile Giuseppe Longo, Emiliano Schena, Carlo Massaroni, Daniela Lo Presti, Alessandra Berton, Vincenzo Candela, and Vincenzo Denaro. Wearable Systems for Shoulder Kinematics Assessment: A Systematic Review. *BMC Musculoskeletal Disorders*, 20(1), 2019. ISSN 14712474. doi: 10.1186/s12891-019-2930-4. URL <https://doi.org/10.1186/s12891-019-2930-4>. 2.1.3
- [135] Sarvenaz Salehi, Gabriele Bleser, Attila Reiss, and Didier Stricker. Body-IMU autocalibration for inertial hip and knee joint tracking. In *BodyNets International Conference on Body Area Networks*, 2015. doi: 10.4108/eai.28-9-2015.2261522. 2.1.3
- [136] Brandon McCarron. Low-cost IMU implementation via sensor fusion algorithms in the Arduino environment. 2013. 2.1.3
- [137] El-Gohary M. and McNames J. Human Joint Angle Estimation with Inertial Sensors and Validation with A Robot Arm. *IEEE Transactions on Biomedical Engineering*, 62(7):1759–1767, 2015. ISSN 1558-2531. URL <http://doi.org/10.1109/TBME.2015.2403368>. 2.1.3
- [138] Andrea Cereatti, Ugo Della Croce, and Angelo M. Sabatini. Three-Dimensional Human Kinematic Estimation Using Magneto-Inertial Measurement Units. *Handbook of Human Motion*, 1-3:221–244, 2018. doi: 10.1007/978-3-319-14418-4\_162. 2.1.3
- [139] Manon Kok and Thomas B. Schon. Magnetometer Calibration Using Inertial Sensors. *IEEE Sensors Journal*, 16(14), 2016. ISSN 1530437X. doi: 10.1109/JSEN.2016.2569160. URL <https://doi.org/10.1109/JSEN.2016.2569160>. 2.1.3, 5.0.2
- [140] Gabriele Ligorio, Elena Bergamini, Luigi Truppa, Michelangelo Guaitolini, Michele Raggi, Andrea Mannini, Angelo Maria Sabatini, Giuseppe Vannozzi,

## BIBLIOGRAPHY

- and Pietro Garofalo. A Wearable Magnetometer-Free Motion Capture System: Innovative Solutions for Real-World Applications. *IEEE Sensors Journal*, 14(8):1–1, 2020. ISSN 1530-437X. doi: 10.1109/jsen.2020.2983695. URL <https://doi.org/10.1109/jsen.2020.2983695>. 2.1.3
- [141] Shaghayegh Zihajehzadeh and Edward J. Park. A Novel Biomechanical Model-Aided IMU/UWB Fusion for Magnetometer-Free Lower Body Motion Capture. *IEEE Transactions on Systems, Man, and Cybernetics: Systems*, 47(6), 2017. ISSN 21682232. doi: 10.1109/TSMC.2016.2521823. URL <https://doi.org/10.1109/TSMC.2016.2521823>. 2.1.3
- [142] Daniel Laidig, Dustin Lehmann, Marc Andre Begin, and Thomas Seel. Magnetometer-free Realtime Inertial Motion Tracking by Exploitation of Kinematic Constraints in 2-DoF Joints. In *Proceedings of the Annual International Conference of the IEEE Engineering in Medicine and Biology Society, EMBS*, pages 1233–1238. Institute of Electrical and Electronics Engineers Inc., jul 2019. ISBN 9781538613115. doi: 10.1109/EMBC.2019.8857535. URL <https://doi.org/10.1109/EMBC.2019.8857535>. 2.1.3, 4.1
- [143] Henk G. Kortier, H. Martin Schepers, and Peter H. Veltink. On-Body Inertial and Magnetic Sensing for Assessment of Hand and Finger Kinematics. *Proceedings of the IEEE RAS and EMBS International Conference on Biomedical Robotics and Biomechatronics*, pages 555–560, 2014. ISSN 21551774. doi: 10.1109/biorob.2014.6913836. 2.1.3
- [144] Olli Sarkka, Tuukka Nieminen, Saku Suuriniemi, and Lauri Kettunen. A Multi-Position Calibration Method for Consumer-Grade Accelerometers, Gyroscopes, and Magnetometers to Field Conditions. *IEEE Sensors Journal*, 17(11), 2017. ISSN 1530437X. doi: 10.1109/JSEN.2017.2694488. URL <https://doi.org/10.1109/JSEN.2017.2694488>. 2.1.3
- [145] Sara Oliveira. Rehabilitation Exercises for Knee Recovery at Home. 2017. URL <https://api.semanticscholar.org/CorpusID:56441508>. 2.1.3
- [146] Ana Pereira, Vânia Guimarães, and Inês Sousa. Joint angles tracking for rehabilitation at home using inertial sensors. In *Proceedings of the 11th EAI International Conference on Pervasive Computing Technologies for Healthcare*. ACM Press, 2017. doi: 10.1145/3154862.3154888. URL <https://doi.org/10.1145/3154862.3154888>. 2.1.3
- [147] Sebastian Koenig, Aitor Ardanza, Camilo Cortes, Alessandro De Mauro, and Belinda Lange. *Introduction to Low-Cost Motion-Tracking for Virtual Rehabilitation*, pages 287–303. Springer Berlin Heidelberg, Berlin, Heidelberg, 2014. ISBN 978-3-642-38556-8. doi: 10.1007/978-3-642-38556-8\_15. URL [https://doi.org/10.1007/978-3-642-38556-8\\_{\\_}15](https://doi.org/10.1007/978-3-642-38556-8_{_}15). 2.1.3
- [148] Umran Azziz Abdulla, Ken Taylor, Michael Barlow, and Khushnood Z. Naqshbandi. Measuring Walking and Running Cadence Using Magnetometers. In

- 2013 12th IEEE International Conference on Trust, Security and Privacy in Computing and Communications. IEEE, July 2013. doi: 10.1109/trustcom.2013.176. URL <https://doi.org/10.1109/trustcom.2013.176>. 2.1.3
- [149] Ryan Sers, Steph Forrester, Esther Moss, Stephen Ward, Jianjia Ma, and Massimiliano Zecca. Validity of the Perception Neuron inertial motion capture system for upper body motion analysis. *Measurement*, 149:107024, January 2020. doi: 10.1016/j.measurement.2019.107024. URL <https://doi.org/10.1016/j.measurement.2019.107024>. 2.1.3
- [150] Arash Salarian, Pierre R Burkhard, François JG Vingerhoets, Brigitte M Jolles, and Kamiar Aminian. A Novel Approach to Reducing Number of Sensing Units for Wearable Gait Analysis Systems. *IEEE Transactions on Biomedical Engineering*, 60(1):72–77, 2012. doi: 10.1109/TBME.2012.2223465. URL <https://doi.org/10.1109/TBME.2012.2223465>. 2.1.3
- [151] M. Fleron, N. Ubbesen, Francesco Battistella, David Leandro Dejtiar, and A. Oliveira. Accuracy Between Optical and Inertial Motion Capture Systems for Assessing Trunk Speed During Preferred Gait and Transition Periods. *Sports Biomechanics*, 18:366 – 377, 2019. doi: 10.1080/14763141.2017.1409259. URL <https://doi.org/10.1080/14763141.2017.1409259>. 2.1.3
- [152] Thomas B Moeslund, Adrian Hilton, and Volker Krüger. A Survey of Advances in Vision-Based Human Motion Capture and Analysis. *Computer Vision and Image Understanding*, 104(2):90–126, 2006. ISSN 1077-3142. doi: <https://doi.org/10.1016/j.cviu.2006.08.002>. URL <http://www.sciencedirect.com/science/article/pii/S1077314206001263>. 2.1.3
- [153] Steffi L. Colyer, Murray Evans, Darren P. Cosker, and Aki I. T. Salo. A Review of the Evolution of Vision-Based Motion Analysis and the Integration of Advanced Computer Vision Methods Towards Developing a Markerless System. *Sports Medicine - Open*, 4(1), June 2018. doi: 10.1186/s40798-018-0139-y. URL <https://doi.org/10.1186/s40798-018-0139-y>. 2.1.3, 2.8
- [154] Liuha0 Ge, Zhou Ren, Yuncheng Li, Zehao Xue, Yingying Wang, Jianfei Cai, and Junsong Yuan. 3D Hand Shape and Pose Estimation From a Single RGB Image. In *Proceedings of the IEEE/CVF Conference on Computer Vision and Pattern Recognition (CVPR)*, June 2019. doi: 10.48550/arXiv.1903.00812. URL <https://doi.org/10.48550/arXiv.1903.00812>. 2.1.3
- [155] Srinath Sridhar, Antti Oulasvirta, and Christian Theobalt. Interactive Markerless Articulated Hand Motion Tracking Using RGB and Depth Data. In *Proceedings of the IEEE international conference on computer vision*, pages 2456–2463, 2013. 2.1.3, 2.1.3
- [156] Muhammad Yahya, Jawad Ali Shah, Arif Warsi, Kushsairy Kadir, Sher0z Khan, and M Izani. Real Time Elbow Angle Estimation Using Single RGB Camera, 2018. URL <https://doi.org/10.48550/arXiv.1808.07017>. 2.1.3

## BIBLIOGRAPHY

- [157] X. Gu, F. Deligianni, B. Lo, W. Chen, and G.Z. Yang. Markerless gait analysis based on a single RGB camera. In *2018 IEEE 15th International Conference on Wearable and Implantable Body Sensor Networks (BSN)*. IEEE, March 2018. doi: 10.1109/bsn.2018.8329654. URL <https://doi.org/10.1109/bsn.2018.8329654>. 2.1.3
- [158] Congyi Wang, Fuhao Shi, Shihong Xia, and Jinxiang Chai. Realtime 3D Eye Gaze Animation Using a Single RGB Camera. *ACM Trans. Graph.*, 35(4), July 2016. ISSN 0730-0301. doi: 10.1145/2897824.2925947. URL <https://doi.org/10.1145/2897824.2925947>. 2.1.3
- [159] Dushyant Mehta, Srinath Sridhar, Oleksandr Sotnychenko, Helge Rhodin, Mohammad Shafiei, Hans-Peter Seidel, Weipeng Xu, Dan Casas, and Christian Theobalt. VNect: Real-Time 3D Human Pose Estimation with a Single RGB Camera. *ACM Trans. Graph.*, 36(4), July 2017. ISSN 0730-0301. doi: 10.1145/3072959.3073596. URL <https://doi.org/10.1145/3072959.3073596>. 2.1.3
- [160] Tomoya Kaichi, Tsubasa Maruyama, Mitsunori Tada, and Hideo Saito. Resolving Position Ambiguity of IMU-based human pose with a single RGB camera. *Sensors*, 20(19):5453, September 2020. doi: 10.3390/s20195453. URL <https://doi.org/10.3390/s20195453>. 2.1.3
- [161] Dushyant Mehta, Oleksandr Sotnychenko, Franziska Mueller, Weipeng Xu, Mohamed Elgharib, Pascal Fua, Hans-Peter Seidel, Helge Rhodin, Gerard Pons-Moll, and Christian Theobalt. XNect: Real-Time Multi-Person 3D Motion Capture With a Single RGB camera. *ACM Transactions on Graphics (TOG)*, 39(4):82–1, 2020. 2.1.3
- [162] Haiyu Zhu, Yao Yu, Yu Zhou, and Sidan Du. Dynamic Human Body Modeling Using a Single RGB camera. *Sensors*, 16(3):402, March 2016. doi: 10.3390/s16030402. URL <https://doi.org/10.3390/s16030402>. 2.1.3
- [163] Roanna Lun and Wenbing Zhao. A Survey of Applications and Human Motion Recognition With Microsoft Kinect. *International Journal of Pattern Recognition and Artificial Intelligence*, 29(05):1555008, 2015. 2.1.3
- [164] Matt Weinberger. The rise and fall of Kinect: Why Microsoft gave up on its most promising product. <https://finance.yahoo.com/news/downfall-kinect-why-microsoft-gave-183900710.html>, January 2018. (Accessed on 11/17/2020). 2.1.3
- [165] Stylianos Asteriadis, Anargyros Chatzitofis, Dimitrios Zarpalas, Dimitrios S Alexiadis, and Petros Daras. Estimating human motion from multiple kinect sensors. In *Proceedings of the 6th international conference on computer vision/computer graphics collaboration techniques and applications*, pages 1–6, 2013. doi: 10.1145/2466715.2466727. URL <https://doi.org/10.1145/2466715.2466727>. 2.1.3



- [166] Yushuang Tian, Xiaoli Meng, Dapeng Tao, Dongquan Liu, and Chen Feng. Upper Limb Motion Tracking With the Integration of IMU and Kinect. *Neurocomputing*, 159:207–218, 2015. doi: 10.1016/j.neucom.2015.01.071. URL <https://doi.org/10.1016/j.neucom.2015.01.071>. 2.1.3, 2.1.4
- [167] Chien-Yen Chang, Belinda Lange, Mi Zhang, Sebastian Koenig, Phil Requejo, Noom Somboon, Alexander A Sawchuk, and Albert A Rizzo. Towards Pervasive Physical Rehabilitation Using Microsoft Kinect. In *2012 6th international conference on pervasive computing technologies for healthcare (PervasiveHealth) and workshops*, pages 159–162. IEEE, 2012. doi: <https://doi.org/10.4108/icst.pervasivehealth.2012.248714>. 2.1.3
- [168] Abraham Bachrach, Samuel Prentice, Ruijie He, Peter Henry, Albert S Huang, Michael Krainin, Daniel Maturana, Dieter Fox, and Nicholas Roy. Estimation, planning, and mapping for autonomous flight using an RGB-D camera in GPS-denied environments. *The International Journal of Robotics Research*, 31(11): 1320–1343, 2012. URL <http://hdl.handle.net/1721.1/81874>. 2.1.3
- [169] Kui Liu and Nasser Kehtarnavaz. Real-Time Robust Vision-Based Hand Gesture Recognition Using Stereo Images. *Journal of Real-Time Image Processing*, 11(1): 201–209, 2016. URL <https://doi.org/10.1007/s11554-013-0333-6>. 2.1.3, 2.1.3
- [170] Jinxiang Chai and Jessica K Hodgins. Performance Animation From Low-Dimensional Control Signals. In *ACM SIGGRAPH 2005 Papers*, pages 686–696. 2005. doi: 10.1145/1073204.1073248. URL <https://doi.org/10.1145/1073204.1073248>. 2.1.3
- [171] Zhiquan Gao, Yao Yu, Yu Zhou, and Sidan Du. Leveraging Two Kinect Sensors for Accurate Full-Body Motion Capture. *Sensors*, 15(9):24297–24317, 2015. doi: 10.3390/s150924297. URL <https://doi.org/10.3390/s150924297>. 2.1.3
- [172] Zhenbao Liu, Jinxin Huang, Junwei Han, Shuhui Bu, and Jianfeng Lv. Human Motion Tracking by Multiple RGBD cameras. *IEEE Transactions on Circuits and Systems for Video Technology*, 27(9):2014–2027, September 2017. doi: 10.1109/tcsvt.2016.2564878. URL <https://doi.org/10.1109/tcsvt.2016.2564878>. 2.1.3
- [173] Jongsung Kim and Myunggyu Kim. Motion capture with high-speed RGB-d cameras. In *2014 International Conference on Information and Communication Technology Convergence (ICTC)*. IEEE, October 2014. doi: 10.1109/ictc.2014.6983165. URL <https://doi.org/10.1109/ictc.2014.6983165>. 2.1.3
- [174] Aravind Sundaresan and Rama Chellappa. Markerless motion capture using multiple cameras. In *Computer Vision for Interactive and Intelligent Environment (CVIIE'05)*, pages 15–26. IEEE, 2005. doi: 10.1109/CVIIE.2005.13. URL <https://doi.org/10.1109/CVIIE.2005.13>. 2.1.3
- [175] Thiago Braga Rodrigues, Debora Pereira Salgado, Ciarán Ó Catháin, Noel O'Connor, and Niall Murray. Human gait assessment using a 3D markerless multimodal motion capture system. *Multimedia Tools and Applications*,

## BIBLIOGRAPHY

- 79(3-4):2629–2651, November 2019. doi: 10.1007/s11042-019-08275-9. URL <https://doi.org/10.1007/s11042-019-08275-9>. 2.1.3
- [176] Alessandro Malaguti, Marco Carraro, Mattia Guidolin, Luca Tagliapietra, Emanuele Menegatti, and Stefano Ghidoni. Real-time Tracking-by-Detection of Human Motion in RGB-d camera networks. In *2019 IEEE International Conference on Systems, Man and Cybernetics (SMC)*. IEEE, October 2019. doi: 10.1109/smc.2019.8914539. URL <https://doi.org/10.1109/smc.2019.8914539>. 2.1.3
- [177] Farid Abedan Kondori and Li Liu. 3D Active human motion estimation for biomedical applications. In *World Congress on Medical Physics and Biomedical Engineering May 26-31, 2012, Beijing, China*, pages 1014–1017. Springer, 2013. 2.1.3
- [178] HEJ Veeger, FCT Van der Helm, and RH Rozendal. Orientation of the Scapula in a Simulated Wheelchair Push. *Clinical Biomechanics*, 8(2):81–90, 1993. doi: 10.1016/S0268-0033(93)90037-I. URL [https://doi.org/10.1016/S0268-0033\(93\)90037-I](https://doi.org/10.1016/S0268-0033(93)90037-I). 2.1.3
- [179] Ahmed Elhayek, Onorina Kovalenko, Pramod Murthy, Jameel Malik, and Didier Stricker. Fully automatic multi-person human motion capture for VR applications. In *International Conference on Virtual Reality and Augmented Reality*, pages 28–47. Springer, 2018. 2.1.3
- [180] Min Ho Song and Rolf Inge Godøy. How fast is your body motion? Determining a sufficient frame rate for an optical motion tracking system using passive markers. *PLoS ONE*, 11(3):1–14, 2016. ISSN 19326203. doi: 10.1371/journal.pone.0150993. 2.1.3
- [181] X Wang. Construction of Arm Kinematic Linkage From External Surface Markers. In *Proceeding of the Fourth International Symposium on 3D Analysis of Human Movement*, pages 1–3, 1996. 2.1.3
- [182] A Kolahi, Mo Hoviattalab, Tahmineh Rezaeian, M Alizadeh, M Bostan, and Hossein Mokhtarzadeh. Design of a marker-based human motion tracking system. *Biomedical Signal Processing and Control*, 2(1):59–67, 2007. 2.1.3
- [183] Trent M Guess, Swithin Razu, Amirhossein Jahandar, Marjorie Skubic, and Zhiyu Huo. Comparison of 3D Joint Angles Measured With the Kinect 2.0 Skeletal Tracker Versus a Marker-Based Motion Capture System. *Journal of applied biomechanics*, 33(2):176–181, 2017. 2.1.3
- [184] C. Reinschmidt, A.J. van den Bogert, B.M. Nigg, A. Lundberg, and N. Murphy. Effect of Skin Movement on the Analysis of Skeletal Knee Joint Motion During Running. *Journal of Biomechanics*, 30(7):729–732, July 1997. doi: 10.1016/s0021-9290(97)00001-8. URL [https://doi.org/10.1016/s0021-9290\(97\)00001-8](https://doi.org/10.1016/s0021-9290(97)00001-8). 2.1.3
- [185] Lulu Chen, Hong Wei, and James Ferryman. A survey of human motion analysis using depth imagery. *Pattern Recognition Letters*, 34(15):1995–2006, 2013. 2.1.3

- [186] Xiaolin Wei, Peizhao Zhang, and Jinxiang Chai. Accurate Realtime Full-Body Motion Capture Using a Single Depth Camera. *ACM Transactions on Graphics (TOG)*, 31(6):1–12, 2012. URL <https://dl.acm.org/doi/10.1145/2366145.2366207>. 2.1.3
- [187] Tao Yu, Kaiwen Guo, Feng Xu, Yuan Dong, Zhaoqi Su, Jianhui Zhao, Jianguo Li, Qionghai Dai, and Yebin Liu. Bodyfusion: Real-Time Capture of Human Motion and Surface Geometry Using a Single Depth Camera. In *Proceedings of the IEEE International Conference on Computer Vision*, pages 910–919, 2017. doi: 10.1109/ICCV.2017.104. URL <https://doi.org/10.1109/ICCV.2017.104>. 2.1.3
- [188] Licong Zhang, Jurgen Sturm, Daniel Cremers, and Dongheui Lee. Real-time human motion tracking using multiple depth cameras. In *2012 IEEE/RSJ International Conference on Intelligent Robots and Systems*. IEEE, October 2012. doi: 10.1109/iros.2012.6385968. URL <https://doi.org/10.1109/iros.2012.6385968>. 2.1.3
- [189] Himanshu Prakash Jain, Anbumani Subramanian, Sukhendu Das, and Anurag Mittal. Real-Time Upper-Body Human Pose Estimation Using a Depth Camera. In *International Conference on Computer Vision/Computer Graphics Collaboration Techniques and Applications*, pages 227–238. Springer, 2011. doi: 10.1007/978-3-642-24136-9\_20. URL [https://doi.org/10.1007/978-3-642-24136-9\\_20](https://doi.org/10.1007/978-3-642-24136-9_20). 2.1.3
- [190] Ayush Dewan, Tim Caselitz, Gian Diego Tipaldi, and Wolfram Burgard. Motion-Based Detection and Tracking in 3D LIDAR Scans. In *2016 IEEE International Conference on Robotics and Automation (ICRA)*, pages 4508–4513. IEEE, 2016. doi: 10.1109/ICRA.2016.7487649. URL <https://doi.org/10.1109/ICRA.2016.7487649>. 2.1.3
- [191] Zhi Yan, Tom Duckett, and Nicola Bellotto. Online Learning for Human Classification in 3D LIDAR-Based Tracking. In *2017 IEEE/RSJ International Conference on Intelligent Robots and Systems (IROS)*, pages 864–871. IEEE, 2017. doi: 10.1109/IROS.2017.8202247. URL <https://doi.org/10.1109/IROS.2017.8202247>. 2.1.3
- [192] Masanobu Shimizu, Kenji Koide, Igi Ardiyanto, Jun Miura, and Shuji Oishi. LIDAR-Based Body Orientation Estimation by Integrating Shape and Motion Information. In *2016 IEEE International Conference on Robotics and Biomimetics (ROBIO)*, pages 1948–1953. IEEE, 2016. doi: 10.1109/ROBIO.2016.7866614. URL <https://doi.org/10.1109/ROBIO.2016.7866614>. 2.1.3
- [193] John Shackleton, Brian VanVoorst, and Joel Hesch. Tracking People With a 360-Degree LIDAR. In *2010 7th IEEE International Conference on Advanced Video and Signal Based Surveillance*, pages 420–426. IEEE, 2010. doi: 10.1109/AVSS.2010.52. URL <https://doi.org/10.1109/AVSS.2010.52>. 2.1.3
- [194] Md Matiqul Islam, Antony Lam, Hisato Fukuda, Yoshinori Kobayashi, and Yoshinori Kuno. A Person-Following Shopping Support Robot Based on Human

## BIBLIOGRAPHY

- Pose Skeleton Data and LIDAR Sensor. In *International Conference on Intelligent Computing*, pages 9–19. Springer, 2019. URL [https://doi.org/10.1007/978-3-030-26766-7\\_2](https://doi.org/10.1007/978-3-030-26766-7_2). 2.1.3
- [195] Godwin Ponraj and Hongliang Ren. Sensor Fusion of Leap Motion Controller and Flex Sensors Using Kalman Filter for Human Finger Tracking. *IEEE Sensors Journal*, 18(5):2042–2049, 2018. 2.1.3, 2.1.3
- [196] UltraLeap.com. Tracking | Leap Motion Controller | Ultraleap. <https://www.ultraleap.com/product/leap-motion-controller/>, 2020. (Accessed on 12/10/2020). 2.9
- [197] Yongbin Qi, Cheong Boon Soh, Erry Gunawan, Kay-Soon Low, and Rijil Thomas. Assessment of Foot Trajectory for Human Gait Phase Detection Using Wireless Ultrasonic Sensor Network. *IEEE Transactions on Neural Systems and Rehabilitation Engineering*, 24(1):88–97, 2015. doi: 10.1109/TNSRE.2015.2409123. URL <https://doi.org/10.1109/TNSRE.2015.2409123>. 2.1.3
- [198] Árpád Illyés and Rita M Kiss. Method for Determining the Spatial Position of the Shoulder With Ultrasound-Based Motion Analyzer. *Journal of Electromyography and Kinesiology*, 16(1):79–88, 2006. URL <https://doi.org/10.1016/j.jelekin.2005.06.007>. 2.1.3
- [199] Pierre Plantard, Hubert PH Shum, and Franck Multon. Motion Analysis of Work Conditions Using Commercial Depth Cameras in Real Industrial Conditions. In *DHM and Posturography*, pages 673–682. Elsevier, 2019. URL <https://doi.org/10.1016/B978-0-12-816713-7.00052-0>. 2.1.3
- [200] Evan Herbst, Xiaofeng Ren, and Dieter Fox. RGB-D flow: Dense 3-D Motion Estimation using Color and Depth. In *2013 IEEE international conference on robotics and automation*, pages 2276–2282. IEEE, 2013. doi: 10.1109/ICRA.2013.6630885. URL <https://doi.org/10.1109/ICRA.2013.6630885>. 2.1.3
- [201] Ashok Kumar Patil, Adithya Balasubramanyam, Jae Yeong Ryu, Pavan Kumar B N, Bharatesh Chakravarthi, and Young Ho Chai. Fusion of Multiple Lidars and Inertial Sensors for the Real-Time Pose Tracking of Human Motion. *Sensors*, 20(18):5342, September 2020. doi: 10.3390/s20185342. URL <https://doi.org/10.3390/s20185342>. 2.1.3
- [202] Zerong Zheng, Tao Yu, Hao Li, Kaiwen Guo, Qionghai Dai, Lu Fang, and Yebin Liu. HybridFusion: Real-Time Performance Capture Using a Single Depth Sensor and Sparse IMUs. *Lecture Notes in Computer Science (including subseries Lecture Notes in Artificial Intelligence and Lecture Notes in Bioinformatics)*, 11213 LNCS:389–406, 2018. ISSN 16113349. URL <https://api.semanticscholar.org/CorpusID:52956761>. 2.1.3
- [203] Altinus Lucilus Hof. EMG and Muscle Force: An Introduction. *Human Movement Science*, 3(1-2):119–153, 1984. URL [https://doi.org/10.1016/0167-9457\(84\)90008-3](https://doi.org/10.1016/0167-9457(84)90008-3). 2.1.3

- [204] Ana Pereira, Duarte Folgado, Francisco Nunes, Joao Almeida, and Ines Sousa. Using Inertial Sensors to Evaluate Exercise Correctness in Electromyography-based Home Rehabilitation Systems. In *2019 IEEE International Symposium on Medical Measurements and Applications (MeMeA)*. IEEE, June 2019. doi: 10.1109/memea.2019.8802152. URL <https://doi.org/10.1109/memea.2019.8802152>. 2.1.3
- [205] Achim Buerkle, Ali Al-Yacoub, and Pedro Ferreira. An Incremental Learning Approach for Physical Human-Robot Collaboration. In *Proceedings of The 3rd UK-RAS Conference*, 2020. URL [https://doi.org/10.1007/978-3-030-63486-5\\_33](https://doi.org/10.1007/978-3-030-63486-5_33). 2.1.3
- [206] Luzheng Bi, Aberham >Genetu Feleke, and Cuntai Guan. A review on EMG-based motor intention prediction of continuous human upper limb motion for human-robot collaboration. *Biomedical Signal Processing and Control*, 51:113–127, 2019. ISSN 1746-8094. doi: <https://doi.org/10.1016/j.bspc.2019.02.011>. URL <http://www.sciencedirect.com/science/article/pii/S1746809419300473>. 2.1.3
- [207] Yu Zhuang, Shaowei Yao, Chenming Ma, and Rong Song. Admittance Control Based on EMG-driven musculoskeletal model improves the human–robot synchronization. *IEEE Transactions on Industrial Informatics*, 15(2):1211–1218, February 2019. doi: 10.1109/tii.2018.2875729. URL <https://doi.org/10.1109/tii.2018.2875729>. 2.1.3
- [208] S. Gowtham, K. M. A. Krishna, T. Srinivas, R. G. P. Raj, and A. Joshuva. EMG-Based Control of a 5 DOF Robotic Manipulator. In *2020 International Conference on Wireless Communications Signal Processing and Networking (WiSPNET)*, pages 52–57, 2020. 2.1.3
- [209] Joseph DelPreto and Daniela Rus. Sharing the Load: Human-Robot Team Lifting Using Muscle Activity. In *2019 International Conference on Robotics and Automation (ICRA)*. IEEE, May 2019. doi: 10.1109/icra.2019.8794414. URL <https://doi.org/10.1109/icra.2019.8794414>. 2.1.3
- [210] Wan-Ting Shi, Zong-Jhe Lyu, Shih-Tsang Tang, Tsorng-Lin Chia, and Chia-Yen Yang. A bionic hand controlled by hand gesture recognition based on surface EMG signals: A preliminary study. *Biocybernetics and Biomedical Engineering*, 38(1):126–135, 2018. 2.1.3
- [211] Reza Abiri, Soheil Borhani, Eric W Sellers, Yang Jiang, and Xiaopeng Zhao. A comprehensive review of EEG-based brain–computer interface paradigms. *Journal of neural engineering*, 16(1):011001, 2019. 2.1.3
- [212] Luzheng Bi, Xin-An Fan, and Yili Liu. EEG-based brain-controlled mobile robots: A survey. *IEEE Transactions on Human-Machine Systems*, 43(2):161–176, March 2013. doi: 10.1109/tsmcc.2012.2219046. URL <https://doi.org/10.1109/tsmcc.2012.2219046>. 2.1.3

## BIBLIOGRAPHY

- [213] Andres F. Salazar-Gomez, Joseph DelPreto, Stephanie Gil, Frank H. Guenther, and Daniela Rus. Correcting robot mistakes in real time using EEG signals. In *2017 IEEE International Conference on Robotics and Automation (ICRA)*. IEEE, May 2017. doi: 10.1109/icra.2017.7989777. URL <https://doi.org/10.1109/icra.2017.7989777>. 2.1.3
- [214] Fadel Adib, Chen-Yu Hsu, Hongzi Mao, Dina Katabi, and Frédo Durand. Capturing the human figure through a wall. *ACM Transactions on Graphics (TOG)*, 34(6): 1–13, 2015. 2.1.3
- [215] Nicola Carbonaro, Gabriele Dalle Mura, Federico Lorussi, Rita Paradiso, Danilo De Rossi, and Alessandro Tognetti. Exploiting wearable goniometer technology for motion sensing gloves. *IEEE Journal of Biomedical and Health Informatics*, 18(6):1788–1795, November 2014. doi: 10.1109/jbhi.2014.2324293. URL <https://doi.org/10.1109/jbhi.2014.2324293>. 2.1.3
- [216] James F Kramer, John M Ananny, Loren F Bentley, Paul L Korff, Allen R Boronkay, and Conor McNamara. Goniometer-based body-tracking device, July 4 2006. US Patent 7,070,571. 2.1.3
- [217] Edwin Basil Mathew, Dushyant Khanduja, Bhavya Sapra, and Bharat Bhushan. Robotic Arm Control Through Human Arm Movement Detection Using Potentiometers. In *2015 International Conference on Recent Developments in Control, Automation and Power Engineering (RDCAPE)*, pages 298–303. IEEE, 2015. doi: 10.1109/RDCAPE.2015.7281413. URL <https://doi.org/10.1109/RDCAPE.2015.7281413>. 2.1.3
- [218] Zhibin Song and Shuxiang Guo. Development of a Real-Time Upper Limb’s Motion Tracking Exoskeleton Device for Active Rehabilitation Using an Inertia Sensor. In *2011 9th World Congress on Intelligent Control and Automation*, pages 1206–1211. IEEE, 2011. doi: 10.1109/WCICA.2011.5970708. URL <https://doi.org/10.1109/WCICA.2011.5970708>. 2.1.3
- [219] Le Cai, Li Song, Pingshan Luan, Qiang Zhang, Nan Zhang, Qingqing Gao, Duan Zhao, Xiao Zhang, Min Tu, Feng Yang, et al. Super-Stretchable, Transparent Carbon Nanotube-Based Capacitive Strain Sensors for Human Motion Detection. *Scientific reports*, 3(1):1–9, 2013. URL <https://doi.org/10.1038/srep03048>. 2.1.3
- [220] Seongwoo Ryu, Phillip Lee, Jeffrey B Chou, Ruize Xu, Rong Zhao, Anastasios John Hart, and Sang-Gook Kim. Extremely Elastic Wearable Carbon Nanotube Fiber Strain Sensor for Monitoring of Human Motion. *ACS nano*, 9(6):5929–5936, 2015. URL <https://doi.org/10.1021/acsnano.5b00599>. 2.1.3
- [221] Dr. Mustafa Bakr. Introduction to Ultra-Wideband (UWB) Technology - Technical Articles. <https://www.allaboutcircuits.com/technical-articles/introduction-to-ultra-wideband-uwband-technology/>, March 2020. (Accessed on 11/18/2020). 2.1.3

- [222] Shaghayegh Zihajehzadeh and Edward J Park. A Novel Biomechanical Model-Aided Imu/Uwb Fusion for Magnetometer-Free Lower Body Motion Capture. *IEEE Transactions on Systems, Man, and Cybernetics: Systems*, 47(6):927–938, 2016. doi: 10.1109/TSMC.2016.2521823. URL <https://doi.org/10.1109/TSMC.2016.2521823>. 2.1.3, 2.1.3
- [223] R. Bharadwaj, C. Parini, and A. Alomainy. Experimental Investigation of 3-D Human Body Localization Using Wearable Ultra-Wideband Antennas. *IEEE Transactions on Antennas and Propagation*, 63(11):5035–5044, 2015. doi: 10.1109/TAP.2015.2478455. URL <https://doi.org/10.1109/TAP.2015.2478455>. 2.1.3
- [224] Timo von Marcard, Roberto Henschel, Michael J. Black, Bodo Rosenhahn, and Gerard Pons-Moll. Recovering Accurate 3D human pose in the wild using IMUs and a moving camera. In *European Conference on Computer Vision (ECCV)*, volume Lecture Notes in Computer Science, vol 11214, pages 614–631. Springer, Cham, September 2018. doi: 10.1007/978-3-030-01249-6\_37. URL [https://doi.org/10.1007/978-3-030-01249-6\\_37](https://doi.org/10.1007/978-3-030-01249-6_37). 2.1.3
- [225] Charles Malleson, Andrew Gilbert, Matthew Trumble, John Collomosse, Adrian Hilton, and Marco Volino. Real-Time Full-Body Motion Capture From Video and IMUs. In *2017 International Conference on 3D Vision (3DV)*, pages 449–457. IEEE, 2017. doi: 10.1109/3DV.2017.00058. URL <https://doi.org/10.1109/3DV.2017.00058>. 2.1.3
- [226] Sheldon Andrews, Ivan Huerta, Taku Komura, Leonid Sigal, and Kenny Mitchell. Real-Time Physics-Based Motion Capture With Sparse Sensors. In *Proceedings of the 13th European conference on visual media production (CVMP 2016)*, pages 1–10, 2016. URL <https://doi.org/10.1145/2998559.2998564>. 2.1.3
- [227] Thomas Helten, Meinard Muller, Hans-Peter Seidel, and Christian Theobalt. Real-Time Body Tracking With One Depth Camera and Inertial Sensors. In *Proceedings of the IEEE international conference on computer vision*, pages 1105–1112, 2013. doi: 10.1109/ICCV.2013.141. URL <https://doi.org/10.1109/ICCV.2013.141>. 2.1.3
- [228] Bogdan Kwolek and Michal Kepski. Improving Fall Detection by the Use of Depth Sensor and Accelerometer. *Neurocomputing*, 168:637–645, 2015. URL <https://doi.org/10.1016/j.neucom.2015.05.061>. 2.1.3
- [229] Chen Chen, Roozbeh Jafari, and Nasser Kehtarnavaz. A Survey of Depth and Inertial Sensor Fusion for Human Action Recognition. *Multimedia Tools and Applications*, 76(3):4405–4425, 2017. URL <https://doi.org/10.1007/s11042-015-3177-1>. 2.1.3
- [230] Shuang Li, Jiayi Jiang, Philipp Ruppel, Hongzhuo Liang, Xiaojian Ma, Norman Hendrich, Fuchun Sun, and Jianwei Zhang. A mobile robot hand-arm teleoperation system by vision and IMU. *arXiv*, pages 1–7, 2020. 2.1.3, 2.1.3

## BIBLIOGRAPHY

- [231] Aaron Duivenvoorden, Kyungjin Lee, Maxime Raison, and Sofiane Achiche. Sensor Fusion in Upper Limb Area Networks: A Survey. In *2017 Global Information Infrastructure and Networking Symposium (GIIS)*, pages 56–63. IEEE, 2017. doi: 10.1109/GIIS.2017.8169802. URL <https://doi.org/10.1109/GIIS.2017.8169802>. 2.1.3, 2.11
- [232] Changdi Li, Lei Yu, and Shumin Fei. Real-Time 3D Motion Tracking and Reconstruction System Using Camera and IMU Sensors. *IEEE Sensors Journal*, 19(15):6460–6466, 2019. doi: 10.1109/JSEN.2019.2907716. URL <https://doi.org/10.1109/JSEN.2019.2907716>. 2.1.3
- [233] Alberto López-Delis, Andrés Felipe Ruiz-Olaya, Teodiano Freire-Bastos, and Denis Delisle-Rodríguez. A Comparison of Myoelectric Pattern Recognition Methods to Control an Upper Limb Active Exoskeleton. In *Iberoamerican Congress on Pattern Recognition*, pages 100–107. Springer, 2013. URL [https://doi.org/10.1007/978-3-642-41827-3\\_13](https://doi.org/10.1007/978-3-642-41827-3_13). 2.1.3
- [234] Yi Li, Jun Cheng, Wei Feng, and Dapeng Tao. Feature Fusion of Triaxial Acceleration Signals and Depth Maps for Human Action Recognition. In *2016 IEEE International Conference on Information and Automation (ICIA)*, pages 1255–1260. IEEE, 2016. doi: <https://doi.org/10.1109/ICInfA.2016.7832012>. URL [10.1109/ICInfA.2016.7832012](https://doi.org/10.1109/ICInfA.2016.7832012). 2.1.3
- [235] Kui Liu, Chen Chen, Roozbeh Jafari, and Nasser Kehtarnavaz. Multi-HMM Classification for Hand Gesture Recognition Using Two Differing Modality Sensors. In *2014 IEEE Dallas Circuits and Systems Conference (DCAS)*, pages 1–4. IEEE, 2014. doi: 10.1109/DCAS.2014.6965338. URL <https://doi.org/10.1109/DCAS.2014.6965338>. 2.1.3
- [236] Yejin Kim. Dance Motion Capture and Composition Using Multiple Rgb and Depth Sensors. *International Journal of Distributed Sensor Networks*, 13(2): 1550147717696083, 2017. URL <https://doi.org/10.1177/1550147717696083>. 2.1.3
- [237] Jeroen D Hol. *Sensor Fusion and Calibration of Inertial Sensors, Vision, Ultra-Wideband And GPS*. PhD thesis, Linköping University Electronic Press, 2011. URL <https://api.semanticscholar.org/CorpusID:110168300>. 2.1.3
- [238] Juan Antonio Corrales, FA Candelas, and Fernando Torres. Hybrid Tracking of Human Operators Using IMU/UWB Data Fusion by a Kalman Filter. In *2008 3rd ACM/IEEE International Conference on Human-Robot Interaction (HRI)*, pages 193–200. IEEE, 2008. doi: 10.1145/1349822.1349848. URL <https://doi.org/10.1145/1349822.1349848>. 2.1.3
- [239] Arnaldo G Leal-Junior, Laura Vargas-Valencia, Wilian M dos Santos, Felipe B A Schneider, Adriano A G Siqueira, Maria José Pontes, and Anselmo Frizera. Pof-Imu Sensor System: A Fusion Between Inertial Measurement Units and Pof Sensors for Low-Cost and Highly Reliable Systems. *Optical Fiber Technology*, 43:82–89, 2018. ISSN 1068-5200. doi: 10.1016/j.yofte.2018.04.012. URL <https://doi.org/10.1016/j.yofte.2018.04.012>. 2.1.3



- [240] Eric Foxlin. Motion Tracking Requirements and Technologies. *Handbook of virtual environment technology*, pages 163–210, 2002. URL <http://citeseerx.ist.psu.edu/viewdoc/download?doi=10.1.1.92.4384&rep=rep1&type=pdf>. 2.1.4
- [241] Alexander David Young. Use of Body Model Constraints to Improve Accuracy of Inertial Motion Capture. In *2010 International Conference on Body Sensor Networks*, pages 180–186. IEEE, 2010. doi: 10.1109/BSN.2010.30. URL <https://doi.org/10.1109/BSN.2010.30>. 2.1.4
- [242] Robert Mahony, Tarek Hamel, and Jean Michel Pflimlin. Complementary Filter Design on the Special Orthogonal Group  $So(3)$ . *Proceedings of the 44th IEEE Conference on Decision and Control, and the European Control Conference, CDC-ECC '05*, 2005(1):1477–1484, 2005. doi: 10.1109/CDC.2005.1582367. URL <https://doi.org/10.1109/CDC.2005.1582367>. 2.1.4
- [243] Ya Tian, Hongxing Wei, and Jindong Tan. An Adaptive-Gain Complementary Filter for Real-Time Human Motion Tracking With Marg Sensors in Free-Living Environments. *IEEE Transactions on Neural Systems and Rehabilitation Engineering*, 21(2):254–264, 2012. doi: 10.1109/TNSRE.2012.2205706. URL <https://doi.org/10.1109/TNSRE.2012.2205706>. 2.1.4
- [244] Xiaoping Yun and Eric R Bachmann. Design, Implementation, and Experimental Results of a Quaternion-Based Kalman Filter for Human Body Motion Tracking. *IEEE transactions on Robotics*, 22(6):1216–1227, 2006. doi: 10.1109/TRO.2006.886270. URL <https://doi.org/10.1109/TRO.2006.886270>. 2.1.4
- [245] Jung K. Lee and Edward J. Park. Minimum-Order Kalman Filter With Vector Selector for Accurate Estimation of Human Body Orientation. *IEEE Transactions on Robotics*, 25(5):1196–1201, 2009. ISSN 15523098. doi: 10.1109/TRO.2009.2017146. URL <https://doi.org/10.1109/TRO.2009.2017146>. 2.1.4
- [246] Seong Hoon Won, William Melek, and Farid Golnaraghi. Position and Orientation Estimation Using Kalman Filtering and Particle Filtering With One IMU and One Position Sensor. *IECON Proceedings (Industrial Electronics Conference)*, (April 2019):3006–3010, 2008. doi: 10.1109/IECON.2008.4758439. URL <https://doi.org/10.1109/IECON.2008.4758439>. 2.1.4
- [247] Kaiqiang Feng, Jie Li, Xiaoming Zhang, Chong Shen, Yu Bi, Tao Zheng, and Jun Liu. A New Quaternion-Based Kalman Filter for Real-Time Attitude Estimation Using the Two-Step Geometrically-Intuitive Correction Algorithm. *Sensors (Switzerland)*, 17(9), 2017. ISSN 14248220. doi: 10.3390/s17092146. 2.1.4
- [248] Chang June Lee and Jung Keun Lee. Relative Position Estimation using Kalman Filter Based on Inertial Sensor Signals Considering Soft Tissue Artifacts of Human Body Segments. *Journal of Sensor Science and Technology*, 29(4):237–242, 2020. ISSN 1225-5475. doi: 10.46670/jsst.2020.29.4.237. URL <https://doi.org/10.46670/jsst.2020.29.4.237>. 2.1.4

## BIBLIOGRAPHY

- [249] Angelo Maria Sabatini. Estimating Three-Dimensional Orientation of Human Body Parts by Inertial/Magnetic Sensing. *Sensors*, 11(2):1489–1525, 2011. ISSN 14248220. doi: 10.3390/s110201489. URL <https://doi.org/10.3390/s110201489>. 2.1.4
- [250] Min Su Lee, Hojin Ju, Jin Woo Song, and Chan Gook Park. Kinematic Model-Based Pedestrian Dead Reckoning for Heading Correction and Lower Body Motion Tracking. *Sensors (Switzerland)*, 15(11):28129–28153, 2015. ISSN 14248220. doi: 10.3390/s151128129. URL <https://doi.org/10.3390/s151128129>. 2.1.4
- [251] Xingchuan Liu, Sheng Zhang, Lizhe Li, and Xiaokang Lin. Quaternion-Based Algorithm for Orientation Estimation From MARG Sensors. *Qinghua Daxue Xuebao/Journal of Tsinghua University*, 2012. ISSN 1000054. doi: 10.1109/IROS.2001.976367. URL <https://doi.org/10.1109/IROS.2001.976367>. 2.1.4
- [252] Arash Atrsaei, Hassan Salarieh, Aria Alasty, and Mohammad Abediny. Human Arm Motion Tracking by Inertial/Magnetic Sensors Using Unscented Kalman Filter and Relative Motion Constraint. *Journal of Intelligent and Robotic Systems: Theory and Applications*, 90(1-2):161–170, 2018. ISSN 15730409. doi: 10.1007/s10846-017-0645-z. URL <https://doi.org/10.1007/s10846-017-0645-z>. 2.1.4
- [253] Eun-Hwan Shin. Estimation techniques for low-cost inertial navigation. *PhD thesis*, (20219), 2005. 2.1.4
- [254] Salma Habbachi, Mounir Sayadi, and Nasser Rezzoug. Partial Filtering for Orientation Determining Using Inertial Sensors IMU. *2018 4th International Conference on Advanced Technologies for Signal and Image Processing, ATSIP 2018*, pages 1–5, 2018. doi: 10.1109/ATSIP.2018.8364487. URL <https://doi.org/10.1109/ATSIP.2018.8364487>. 2.1.4
- [255] Gabriele Ligorio and Angelo M. Sabatini. A Particle Filter for 2D Indoor Localization Relying on Magnetic Disturbances and Magnetic-Inertial Measurement Units. *SAS 2016 - Sensors Applications Symposium, Proceedings*, (c):13–18, 2016. doi: 10.1109/SAS.2016.7479630. URL <https://doi.org/10.1109/SAS.2016.7479630>. 2.1.4
- [256] Florent Le Bras, Tarek Hamel, Robert Mahony, and Claude Samson. Observers for Position Estimation Using Bearing and Biased Velocity Information. *Lecture Notes in Control and Information Sciences*, 474:3–23, 2017. ISSN 01708643. doi: 10.1007/978-3-319-55372-6\_1. URL [https://doi.org/10.1007/978-3-319-55372-6\\_1](https://doi.org/10.1007/978-3-319-55372-6_1). 2.1.4
- [257] Tarek Hamel, Claude Samson, Tarek Hamel, Claude Samson, Tarek Hamel, and Claude Samson. Riccati Observers for Position and Velocity Bias Estimation From either Direction or Range Measurements. 2016. URL <https://doi.org/10.48550/arXiv.1606.07735>. 2.1.4

- [258] D. Metaxas and D. Terzopoulos. Shape and Nonrigid Motion Estimation Through Physics-Based Synthesis. volume 15, pages 580–591, 1993. doi: 10.1109/34.216727. URL <https://doi.org/10.1109/34.216727>. 2.1.4
- [259] Andreas M Lehrmann, Peter V Gehler, and Sebastian Nowozin. Efficient Non-linear Markov Models for Human Motion. In *Proceedings of the IEEE Conference on Computer Vision and Pattern Recognition*, pages 1314–1321, 2014. URL <https://dl.acm.org/doi/10.1109/CVPR.2014.171>. 2.1.4
- [260] Naomi T. Fitter and Katherine J. Kuchenbecker. Using IMU data to demonstrate hand-clapping games to a robot. In *2016 IEEE/RSJ International Conference on Intelligent Robots and Systems (IROS)*. IEEE, October 2016. doi: 10.1109/iros.2016.7759150. URL <https://doi.org/10.1109/iros.2016.7759150>. 2.1.4
- [261] Guangyi Shi, Yuexian Zou, Yufeng Jin, Xiaole Cui, and W.J. Li. Towards HMM based human motion recognition using MEMS inertial sensors. In *2008 IEEE International Conference on Robotics and Biomimetics*. IEEE, February 2009. doi: 10.1109/robio.2009.4913268. URL <https://doi.org/10.1109/robio.2009.4913268>. 2.1.4
- [262] Min Wang, Xinyu Wu, Duxin Liu, Can Wang, Ting Zhang, and Pingan Wang. A human motion prediction algorithm for Non-binding Lower Extremity Exoskeleton. In *2015 IEEE International Conference on Information and Automation*. IEEE, August 2015. doi: 10.1109/icinfa.2015.7279315. URL <https://doi.org/10.1109/icinfa.2015.7279315>. 2.1.4
- [263] Hongyi Liu and Lihui Wang. Human motion prediction for human-robot collaboration. *Journal of Manufacturing Systems*, 44:287–294, 2017. URL <https://doi.org/10.1016/j.jmsy.2017.04.009>. 2.1.4
- [264] H. Sidenbladh. Detecting human motion with support vector machines. In *Proceedings of the 17th International Conference on Pattern Recognition, 2004. ICPR 2004.*, volume 2, pages 188–191 Vol.2, 2004. doi: 10.1109/ICPR.2004.1334092. URL <https://doi.org/10.1109/ICPR.2004.1334092>. 2.1.4
- [265] Eric Christopher Townsend. Townsend - Master Thesis Estimating Human Intent for Physical Human-Robot Co-Manipulation. 2017. URL <http://hdl.lib.byu.edu/1877/etd9227>. 2.1.4
- [266] Hsien I. Lin, Xuan Anh Nguyen, and Wei Kai Chen. Active Intention Inference for Robot-Human Collaboration. *International Journal of Computational Methods and Experimental Measurements*, 6(4):772–784, 2018. ISSN 20460554. doi: 10.2495/CMEM-V6-N4-772-784. URL <https://doi.org/10.2495/CMEM-V6-N4-772-784>. 2.1.4
- [267] Xin Zhao, Xue Li, Chaoyi Pang, and Sen Wang. Human Action Recognition Based on Semi-supervised Discriminant Analysis With Global Constraint. *Neurocomputing*, 105:45–50, 2013. URL <https://doi.org/10.1016/j.neucom.2012.04.038>. 2.1.4

## BIBLIOGRAPHY

- [268] Adil Mehmood Khan, Y-K Lee, Seok-Yong Lee, and T-S Kim. Human Activity Recognition via an Accelerometer-Enabled-Smartphone Using Kernel Discriminant Analysis. In *2010 5th international conference on future information technology*, pages 1–6. IEEE, 2010. doi: 10.1109/FUTURETECH.2010.5482729. URL <https://doi.org/10.1109/FUTURETECH.2010.5482729>. 2.1.4
- [269] C. Sminchisescu, A. Kanaujia, Zhiguo Li, and D. Metaxas. Discriminative density propagation for 3D human motion estimation. In *2005 IEEE Computer Society Conference on Computer Vision and Pattern Recognition (CVPR'05)*, volume 1, pages 390–397 vol. 1, 2005. doi: 10.1109/CVPR.2005.132. URL <https://doi.org/10.1109/CVPR.2005.132>. 2.1.4
- [270] Sahak Kaghyan and Hakob Sarukhanyan. Activity Recognition Using K-Nearest Neighbor Algorithm on Smartphone With Tri-Axial Accelerometer. *International Journal of Informatics Models and Analysis (IJIMA), ITHEA International Scientific Society, Bulgaria*, 1:146–156, 2012. URL <https://api.semanticscholar.org/CorpusID:14991554>. 2.1.4
- [271] Gabriele Fanelli, Juergen Gall, and Luc Van Gool. Real Time Head Pose Estimation With Random Regression Forests. In *CVPR 2011*, pages 617–624. IEEE, 2011. doi: 10.1109/CVPR.2011.5995458. URL <https://doi.org/10.1109/CVPR.2011.5995458>. 2.1.4
- [272] Vahid Kazemi, Magnus Burenius, Hossein Azizpour, and Josephine Sullivan. Multi-View Body Part Recognition With Random Forests. In *2013 24th British Machine Vision Conference, BMVC 2013; Bristol; United Kingdom; 9 September 2013 through 13 September 2013*. British Machine Vision Association, 2013. doi: 10.1109/JSEN.2016.2607223. URL <https://doi.org/10.1109/JSEN.2016.2607223>. 2.1.4
- [273] Jie Kang, Kai Jia, Fang Xu, Fengshan Zou, Yanan Zhang, and Hengle Ren. Real-Time Human Motion Estimation for Human Robot Collaboration. *8th Annual IEEE International Conference on Cyber Technology in Automation, Control and Intelligent Systems, CYBER 2018*, pages 552–557, 2019. doi: 10.1109/CYBER.2018.8688348. URL <https://doi.org/10.1109/CYBER.2018.8688348>. 2.1.4
- [274] Chul Woo Kang, Hyun Jin Kim, and Chan Gook Park. A Human Motion Tracking Algorithm Using Adaptive EKF Based on Markov Chain. *IEEE Sensors Journal*, 16(24):8953–8962, 2016. doi: 10.1109/JSEN.2016.2607223. URL <https://doi.org/10.1109/JSEN.2016.2607223>. 2.1.4
- [275] X. Tong, Z. Li, G. Han, N. Liu, Y. Su, J. Ning, and F. Yang. Adaptive EKF Based on HMM Recognizer for Attitude Estimation Using MEMS MARG Sensors. *IEEE Sensors Journal*, 18(8):3299–3310, 2018. doi: 10.1109/JSEN.2017.2787578. URL <https://doi.org/10.1109/JSEN.2017.2787578>. 2.1.4
- [276] Rong Zhu and Zhaoying Zhou. A real-time articulated human motion tracking using tri-axis inertial/magnetic sensors package. *IEEE Transactions on Neural systems and rehabilitation engineering*, 12(2):295–302, 2004. doi: 10.1109/TNSRE.2004.827825. URL <https://doi.org/10.1109/TNSRE.2004.827825>. 2.1.4

- [277] Daniele Giansanti, Giovanni Maccioni, and Velio Macellari. The Development and Test of a Device for the Reconstruction of 3-D Position and Orientation by Means of a Kinematic Sensor Assembly With Rate Gyroscopes and Accelerometers. *IEEE transactions on biomedical engineering*, 52(7):1271–1277, 2005. doi: 10.1109/TBME.2005.847404. URL <https://doi.org/10.1109/TBME.2005.847404>. 2.1.4
- [278] Gabriele Bleser, Gustaf Hendeby, and Markus Miezal. Using Egocentric Vision to Achieve Robust Inertial Body Tracking Under Magnetic Disturbances. In *2011 10th IEEE International Symposium on Mixed and Augmented Reality*, pages 103–109. IEEE, 2011. doi: 10.1109/ISMAR.2011.6092528. URL <https://doi.org/10.1109/ISMAR.2011.6092528>. 2.1.4
- [279] Lorenzo Peppoloni, Alessandro Filippeschi, Emanuele Ruffaldi, and Carlo Alberto Avizzano. A Novel 7 Degrees of Freedom Model for Upper Limb Kinematic Reconstruction Based on Wearable Sensors. In *2013 IEEE 11th international symposium on intelligent systems and informatics (SISY)*, pages 105–110. IEEE, 2013. doi: 10.1109/SISY.2013.6662551. URL <https://doi.org/10.1109/SISY.2013.6662551>. 2.1.4
- [280] Andrea Giovanni Cutti, Andrea Giovanardi, Laura Rocchi, Angelo Davalli, and Rinaldo Sacchetti. Ambulatory Measurement of Shoulder and Elbow Kinematics Through Inertial and Magnetic Sensors. *Medical & biological engineering & computing*, 46(2):169–178, 2008. URL <https://doi.org/10.1007/s11517-007-0296-5>. 2.1.4
- [281] Zhi-Qiang Zhang, Wai-Choong Wong, and Jian-Kang Wu. Ubiquitous Human Upper-Limb Motion Estimation Using Wearable Sensors. *IEEE Transactions on Information technology in biomedicine*, 15(4):513–521, 2011. doi: 10.1109/TITB.2011.2159122. URL <https://doi.org/10.1109/TITB.2011.2159122>. 2.1.4
- [282] Jung Keun Lee and Woo Chang Jung. Quaternion-Based Local Frame Alignment between an Inertial Measurement Unit and a Motion Capture System. *Sensors*, 18(11):4003, November 2018. doi: 10.3390/s18114003. URL <https://doi.org/10.3390/s18114003>. 2.1.4
- [283] LD de Wit-Zuurendonk and SG Oei. Serious gaming in women’s health care. *BJOG: An International Journal of Obstetrics & Gynaecology*, 118:17–21, October 2011. doi: 10.1111/j.1471-0528.2011.03176.x. URL <https://doi.org/10.1111/j.1471-0528.2011.03176.x>. 2.2.2
- [284] M Graafland, J M Schraagen, and M P Schijven. Systematic review of serious games for medical education and surgical skills training. *British Journal of Surgery*, 99(10):1322–1330, September 2012. doi: 10.1002/bjs.8819. URL <https://doi.org/10.1002/bjs.8819>. 2.2.2
- [285] W Lewis Johnson and Shumin Wu. Assessing aptitude for learning with a serious game for foreign language and culture. In *International Conference on Intelligent Tutoring Systems*, pages 520–529. Springer, 2008. URL [https://doi.org/10.1007/978-3-540-69132-7\\_55](https://doi.org/10.1007/978-3-540-69132-7_55). 2.2.2

## BIBLIOGRAPHY

- [286] Richard Blunt. Does game-based learning work? Results from three recent studies. In *Proceedings of the Interservice/Industry Training, Simulation, & Education Conference*, pages 945–955. National Defense Industrial Association Orlando FL, 2007. URL [http://www.rickblunt.com/blunt\\_game\\_studies.pdf](http://www.rickblunt.com/blunt_game_studies.pdf). 2.2.2
- [287] Betty V Whitehill and Barbara A McDonald. Improving learning persistence of military personnel by enhancing motivation in a technical training program. *Simulation & Gaming*, 24(3):294–313, 1993. 2.2.2
- [288] Per Backlund and Maurice Hendrix. Educational Games-Are They Worth the Effort? A Literature Survey of the Effectiveness of Serious Games. In *2013 5th international conference on games and virtual worlds for serious applications (VS-GAMES)*, pages 1–8. IEEE, 2013. doi: 10.1109/VS-GAMES.2013.6624226. URL <https://doi.org/10.1109/VS-GAMES.2013.6624226>. 2.2.2
- [289] Mazeyanti Mohd Ariffin, Alan Oxley, and Suziah Sulaiman. Evaluating game-based learning effectiveness in higher education. *Procedia-Social and Behavioral Sciences*, 123:20–27, 2014. URL <https://doi.org/10.1016/j.sbspro.2014.01.1393>. 2.2.2
- [290] Ryan Wang, Samuel DeMaria, Andrew Goldberg, and Daniel Katz. A Systematic Review of Serious Games in Training Health Care Professionals. *Simulation in Healthcare: The Journal of the Society for Simulation in Healthcare*, 11(1):41–51, February 2016. doi: 10.1097/sih.000000000000118. URL <https://doi.org/10.1097/sih.000000000000118>. 2.2.2
- [291] J.J. Craig. *Introduction to Robotics: Mechanics and Control*. Addison-Wesley series in electrical and computer engineering: control engineering. Pearson/Prentice Hall, 2005. ISBN 9780201543612. URL <https://books.google.no/books?id=MqMeAQAAIAAJ>. 3.1.1, 3.1.3, 3.1.3.1
- [292] Malcolm Shuster. A survey of Attitude Representation, 1993. URL [http://www.ladispe.polito.it/corsi/Meccatronica/02JHCOR/2011-12/Slides/Shuster\\_{\\_}Pub\\_{\\_}1993h\\_{\\_}J\\_{\\_}Repsurv\\_{\\_}scan.pdf](http://www.ladispe.polito.it/corsi/Meccatronica/02JHCOR/2011-12/Slides/Shuster_{_}Pub_{_}1993h_{_}J_{_}Repsurv_{_}scan.pdf). 3.1.1
- [293] Wikipedia. Equations Angles — Wikipedia, the free encyclopedia. [https://en.wikipedia.org/wiki/Euler\\_angles](https://en.wikipedia.org/wiki/Euler_angles), 2020. [Online; accessed 19-October-2020]. 3.1
- [294] GuerrillaCG. Euler (gimbal lock) Explained. [https://www.youtube.com/watch?v=zc8b2Jo7mno&t=328s&ab\\_channel=GuerrillaCG](https://www.youtube.com/watch?v=zc8b2Jo7mno&t=328s&ab_channel=GuerrillaCG), Jan 2009. [Online; accessed 05-December-2020]. 3.1.1.1, 3.2
- [295] Wikipedia. Quaternion — Wikipedia, the free encyclopedia. <http://en.wikipedia.org/w/index.php?title=Quaternion&oldid=992483260>, 2020. [Online; accessed 08-December-2020]. 3.1.2.1, 3.6
- [296] Moti Ben-Ari. A Tutorial on Euler Angles and Quaternions. *Weizmann Institute of Science, Israel*, 524, 2014. 3.1.2.1, 3.1.2.1, 3.1.2.1

- [297] Nikolas Trawny and Stergios I Roulmeliotis. Indirect Kalman Filter for 3D Attitude Estimation A Tutorial for Quaternion Algebra Multiple Autonomous Robotic Systems Laboratory Technical Report Number 2005-002 , Rev . 57. *Engineering*, (612), 2005. URL <http://www.cs.umn.edu>. 3.1.2.1, 3.1.2.1, 3.1.2.1
- [298] Renato Zanetti. Rotations, Transformations, Left Quaternions, Right Quaternions? *The Journal of the Astronautical Sciences*, 66(3):361–381, April 2019. doi: 10.1007/s40295-018-00151-2. URL <https://doi.org/10.1007/s40295-018-00151-2>. 3.1.2.1
- [299] Anabel Navarro Morante. Universidad de Murcia. *All rights reserved. IJES*, 281(4):1–30, 2015. URL <http://nadir.uc3m.es/alejandro/phd/thesisFinal.pdf>{%}5Cn<http://scholar.google.com/scholar?hl=en{%&btnG=Search{%&q=intitle:Universidad+de+murcia{#}0>. 3.1.2.1
- [300] Peter. Corke. Robotics, Vision and Control : Fundamental Algorithms in MATLAB. *SpringerLink Books - AutoHoldings*, page 629, 10 2011. ISSN 1012-2443. doi: 10.1007/2F978-3-642-20144-8. URL <https://www.springer.com/gp/book/9783319544120>. 3.1.3, 3.1.3.1
- [301] Sebastian Thrun, Burgard Wolfram, and Fox Dieter. Probabilistic Robotics. In *Probabilistic Robotics*, chapter 1, pages 1–8. MIT Press, 2005. 3.2
- [302] Jay Devore. *Probability and Statistics for Engineering and the Sciences*. 8 edition. ISBN 978-0-538-73352-6. 3.2, 3.2.1, 3.5, 3.5
- [303] Cyrill Stachniss. Kalman Filter and Extended Kalman Filter. [https://www.youtube.com/watch?v=E-6paM\\_Iwfc](https://www.youtube.com/watch?v=E-6paM_Iwfc), 09 2023. Online Course (Accessed on 05/09/2023). 3.2.2
- [304] Dan Simon. *Optimal State Estimation -Kalman, H infinity, and Nonlinear Approaches*. Wiley, dec 2006. 3.2.2, 3.2.2.1, 3.2.3
- [305] Sebastian Thrun, Burgard Wolfram, and Fox Dieter. Probabilistic Robotics. In *Probabilistic Robotics*, chapter 3, pages 10–50. MIT Press, 2005. 3.2.2.1
- [306] NASA. Earth fact sheet. <http://nssdc.gsfc.nasa.gov/planetary/factsheet/earthfact.html>, November 2020. (Accessed on 7/12/2020). 3.3
- [307] Wikipedia. Equations of motion — Wikipedia, the free encyclopedia. <http://en.wikipedia.org/w/index.php?title=Equations%20of%20motion&oldid=986731579>, 2020. [Online; accessed 08-December-2020]. 3.3.2
- [308] Duane V. Knudson. *Fundamentals of Biomechanics*. Kluwer Academic, 2003. ISBN 9780306474743. URL [https://books.google.no/books?id=js2P\\_8lbr2wC](https://books.google.no/books?id=js2P_8lbr2wC). 3.4.2
- [309] Andrea Giovanni Cutti, Ilaria Parel, and Andrea Kotanxis. *Upper Extremity Models for Clinical Movement Analysis*, pages 583–606. Springer International Publishing, Cham, 2018. ISBN 978-3-319-14418-4. doi: 10.1007/978-3-319-14418-4\_30. URL [https://doi.org/10.1007/978-3-319-14418-4\\_30](https://doi.org/10.1007/978-3-319-14418-4_30). 3.4.2

## BIBLIOGRAPHY

- [310] Josh Starmer. StatQuest. <https://www.youtube.com/playlist?list=PLblh5JK0oLUIcdlgu78MnlATeyx4cEVeR>, 09 2023. Online Course (Accessed on 05/09/2023). 3.5
- [311] NCEI. World Magnetic Model 2020 by National Centers for Environmental Information (NCEI). <https://www.ncei.noaa.gov/news/world-magnetic-model-2020-released>, 10 2022. (Accessed on 10/01/2022). (c), 4.2
- [312] S. L. Freeny. Introduction To Digital Filters. (1):406–409, 1973. 4.1.1
- [313] FierceElectronics. Noise Measurement. <https://www.fierceelectronics.com/embedded/noise-measurement>. (Accessed on 10/04/2020). 4.1.2
- [314] Ozyagcilar Talat. Implementing a Tilt-Compensated eCompass using Accelerometer and Magnetometer Sensors. *Freescale Semiconductor Application Note*, AN4248, 2015. URL <https://www.nxp.com/docs/en/application-note/AN4248.pdf>. 4.1.3
- [315] Zihao Li, Fugui Xie, Yanlei Ye, Peng Li, and Xinjun Liu. A Novel 6-DOF force-sensed human-robot interface for an intuitive teleoperation. *Chinese Journal of Mechanical Engineering*, 35(1), November 2022. doi: 10.1186/s10033-022-00813-1. URL <https://doi.org/10.1186/s10033-022-00813-1>. 4.3
- [316] Xiaojun Zhao, Qiang Huang, Zhaoqin Peng, and Kejie Li. Kinematics mapping and similarity evaluation of humanoid motion based on human motion capture. In *2004 IEEE/RSJ International Conference on Intelligent Robots and Systems (IROS)(IEEE Cat. No. 04CH37566)*, volume 1, pages 840–845. IEEE, 2004. doi: 10.1109/IROS.2004.1389457. URL <https://doi.org/10.1109/IROS.2004.1389457>. 4.3, 4.3.1
- [317] Neal Y Lii, Zhaopeng Chen, Maximo A Roa, Annika Maier, Benedikt Pleintinger, and Christoph Borst. Toward a task space framework for gesture commanded telemanipulation. In *2012 IEEE RO-MAN: The 21st IEEE International Symposium on Robot and Human Interactive Communication*, pages 925–932. IEEE, 2012. doi: 10.1109/ROMAN.2012.6343869. URL <https://doi.org/10.1109/ROMAN.2012.6343869>. 4.3.1
- [318] Rui Li, Hongyu Wang, and Zhenyu Liu. Survey on Mapping Human Hand Motion to Robotic Hands for Teleoperation. *IEEE Transactions on Circuits and Systems for Video Technology*, 32(5):2647–2665, May 2022. doi: 10.1109/tcsvt.2021.3057992. URL <https://doi.org/10.1109/tcsvt.2021.3057992>. 4.3.1
- [319] Juergen Leitner, Matthew Luciw, Alexander Förster, and Jurgen Schmidhuber. Teleoperation of a 7 Dof Humanoid Robot Arm Using Human Arm Accelerations and EMG Signals. In *Proceedings of the International Symposium on Artificial Intelligence, Robotics and Automation in Space*, 2014. URL <https://api.semanticscholar.org/CorpusID:16097252>. 4.3.1, 4.3.1



- [320] Wen Yu. Preliminaries. In *PID Control with Intelligent Compensation for Exoskeleton Robots*, pages 1–12. Elsevier, 2018. doi: 10.1016/b978-0-12-813380-4.00001-3. URL <https://doi.org/10.1016/b978-0-12-813380-4.00001-3>. 4.3.1
- [321] Minas V. Liarokapis, Panagiotis K. Artemiadis, and Kostas J. Kyriakopoulos. Functional Anthropomorphism for Human to Robot Motion Mapping. In *2012 IEEE RO-MAN: The 21st IEEE International Symposium on Robot and Human Interactive Communication*. IEEE, September 2012. doi: 10.1109/roman.2012.6343727. URL <https://doi.org/10.1109/roman.2012.6343727>. 4.3.1
- [322] G Gioioso, G Salvietti, M Malvezzi, and D Prattichizzo. An Object-Based Approach to Map Human Hand Synergies Onto Robotic Hands With Dissimilar Kinematics. In *Robotics: Science and Systems VIII*, pages 97–104. The MIT Press Sydney, NSW, 2012. URL <https://doi.org/10.7551/mitpress/9816.003.0018>. 4.3.1
- [323] Gizem Ateş, Martin Fodstad Stølen, and Erik Kyrkjebø. Exploring Human-Robot Cooperation with Gamified User Training: A User Study on Cooperative Lifting. In *Frontiers Robotics and AI (Under review)*. Frontiers Robotics and AI, 2023. 4.11, 4.12, 5.1
- [324] Universal Robots. Real-Time Data Exchange Guide, 2021. URL <https://www.universal-robots.com/articles/ur/interface-communication/real-time-data-exchange-rtde-guide/>. 4.3.2, 4.3.2
- [325] Cindy L. Bethel, Zachary Henkel, and Kenna Baugus. Conducting Studies in Human-Robot Interaction. In *Springer Series on Bio- and Neurosystems*, pages 91–124. Springer International Publishing, 2020. doi: 10.1007/978-3-030-42307-0\_4. URL [https://doi.org/10.1007/978-3-030-42307-0\\_4](https://doi.org/10.1007/978-3-030-42307-0_4). 4.4
- [326] Jonathan Lazar, Jinjuan Heidi Feng, and Harry Hochheiser. *Research Methods in Human-Computer Interaction*. Morgan Kaufmann, 2017. URL <https://www.sciencedirect.com/book/9780128053904/research-methods-in-human-computer-interaction>. 4.4, 4.4
- [327] Jennifer Preece, Helen Sharp, and Yvonne Rogers. *Interaction Design: Beyond Human-Computer Interaction*. John Wiley & Sons, 2015. 4.4
- [328] Cory D Kidd and Cynthia Breazeal. Human-Robot Interaction Experiments: Lessons Learned. In *Proceeding of AISB*, volume 5, pages 141–142, 2005. URL <https://www.media.mit.edu/publications/human-robot-interaction-experiments-lessons-learned-2>. 4.4
- [329] Diego Compagna, Manuela Marquardt, and Ivo Boblan. Introducing a methodological approach to evaluate HRI from a genuine sociological point of view. In *Cultural Robotics: First International Workshop, CR 2015, Held as Part of IEEE RO-MAN 2015, Kobe, Japan, August 31, 2015. Revised Selected Papers 1*, pages 55–64. Springer, 2016. URL [https://doi.org/10.1007/978-3-319-42945-8\\_5](https://doi.org/10.1007/978-3-319-42945-8_5). 4.4

## BIBLIOGRAPHY

- [330] Kerstin Dautenhahn. Some brief thoughts on the past and future of human-robot interaction, 2018. 4.4
- [331] Sara Kiesler and Michael A. Goodrich. The Science of Human-Robot Interaction. *ACM Transactions on Human-Robot Interaction*, 7(1):1–3, May 2018. doi: 10.1145/3209701. URL <https://doi.org/10.1145/3209701>. 4.4
- [332] Jeremy Straub. In search of technology readiness level (TRL) 10. *Aerospace Science and Technology*, 46:312–320, 2015. 4.4
- [333] SPARC Robotics. Robotics 2020 multi-annual roadmap for robotics in Europe. *SPARC Robotics, EU-Robotics AISBL, The Hague, The Netherlands*, accessed Feb, 5:2018, 2016. URL [https://old.eu-robotics.net/cms/upload/topic\\_groups/H2020\\_Robotics\\_Multi-Annual\\_Roadmap\\_ICT-2017B.pdf](https://old.eu-robotics.net/cms/upload/topic_groups/H2020_Robotics_Multi-Annual_Roadmap_ICT-2017B.pdf). 4.4
- [334] Matthias Merten, Andreas Bley, Christof Schroeter, and Horst-Michael Gross. A Mobile Robot Platform for Socially Assistive Home-Care Applications. In *ROBOTIK 2012; 7th German Conference on Robotics*, pages 1–6. VDE, 2012. 4.4
- [335] David Feil-Seifer, Kristine Skinner, and Maja J Matarić. Benchmarks for Evaluating Socially Assistive Robotics. *Interaction Studies*, 8(3):423–439, 2007. 4.4
- [336] Tina Ganster, Sabrina C Eimler, AM Von Der Pütten, Laura Hoffmann, Nicole C Krämer, and A von der Pütten. *Methodological Considerations for Long-Term Experience With Robots and Agents*. na, 2010. doi: 10.1075/is.8.3.07fei. URL <https://doi.org/10.1075/is.8.3.07fei>. 4.4
- [337] Wafa Johal, Carole Adam, Humbert Fiorino, Sylvie Pesty, Celine Jost, and Dominique Duhaut. Acceptability of a companion robot for children in daily life situations. In *2014 5th IEEE Conference on Cognitive Infocommunications (CogInfoCom)*. IEEE, November 2014. doi: 10.1109/coginfocom.2014.7020474. URL <https://doi.org/10.1109/coginfocom.2014.7020474>. 4.4
- [338] Amedeo Cesta, Gabriella Cortellessa, Andrea Orlandini, and Lorenza Tiberio. Evaluating telepresence robots in the field. In *Agents and Artificial Intelligence: 4th International Conference, ICAART 2012, Vilamoura, Portugal, February 6-8, 2012. Revised Selected Papers 4*, pages 433–448. Springer, 2013. URL [https://doi.org/10.1007/978-3-642-36907-0\\_29](https://doi.org/10.1007/978-3-642-36907-0_29). 4.4
- [339] Robert B Cialdini and Noah J Goldstein. Social influence: Compliance and conformity. *Annu. Rev. Psychol.*, 55:591–621, 2004. URL <https://doi.org/10.1146/annurev.psych.55.090902.142015>. 4.4
- [340] Robert H Gass and John S Seiter. *Persuasion: Social influence and compliance gaining*. Routledge, 2018. 4.4
- [341] Chadia Abras, Diane Maloney-Krichmar, Jenny Preece, and William Bainbridge. Encyclopedia of human-computer interaction. *Thousand Oaks: Sage Publications*, 37:445–456, 2004. URL <https://www.interaction-design.org/literature/book/the-encyclopedia-of-human-computer-interaction-2nd-ed>. 4.4.1.1

- [342] Wilma A Bainbridge, Justin Hart, Elizabeth S Kim, and Brian Scassellati. The effect of presence on human-robot interaction. In *RO-MAN 2008-The 17th IEEE International Symposium on Robot and Human Interactive Communication*, pages 701–706. IEEE, 2008. doi: 10.1109/ROMAN.2008.4600749. URL <https://doi.org/10.1109/ROMAN.2008.4600749>. 4.4.1.1
- [343] Aaron Powers, Sara Kiesler, Susan Fussell, and Cristen Torrey. Comparing a computer agent with a humanoid robot. In *Proceedings of the ACM/IEEE international conference on Human-robot interaction*, pages 145–152, 2007. URL <https://doi.org/10.1145/1228716.1228736>. 4.4.1.1
- [344] Kwan Min Lee, Younbo Jung, Jaywoo Kim, and Sang Ryong Kim. Are Physically Embodied Social Agents Better Than Disembodied Social Agents?: The Effects of Physical Embodiment, Tactile Interaction, and People’s Loneliness in Human–Robot Interaction. *International journal of human-computer studies*, 64(10):962–973, 2006. URL <https://doi.org/10.1016/j.ijhcs.2006.05.002>. 4.4.1.1
- [345] Joshua Wainer, David J Feil-Seifer, Dylan A Shell, and Maja J Mataric. Embodiment and Human-Robot Interaction: A Task-Based Perspective. In *RO-MAN 2007-The 16th IEEE International Symposium on Robot and Human Interactive Communication*, pages 872–877. IEEE, 2007. doi: 10.1109/ROMAN.2007.4415207. URL <https://doi.org/10.1109/ROMAN.2007.4415207>. 4.4.1.1
- [346] Iolanda Leite, André Pereira, Carlos Martinho, and Ana Paiva. Are emotional robots more fun to play with? In *RO-MAN 2008-The 17th IEEE International Symposium on Robot and Human Interactive Communication*, pages 77–82. IEEE, 2008. doi: 10.1109/ROMAN.2008.4600646. URL <https://doi.org/10.1109/ROMAN.2008.4600646>. 4.4.1.1
- [347] Kerstin Dautenhahn, Sarah Woods, Christina Kaouri, Michael L Walters, Kheng Lee Koay, and Iain Werry. What is a robot companion-friend, assistant or butler? In *2005 IEEE/RSJ international conference on intelligent robots and systems*, pages 1192–1197. IEEE, 2005. doi: 10.1109/IROS.2005.1545189. URL <https://doi.org/10.1109/IROS.2005.1545189>. 4.4.1.1
- [348] Tiago Ribeiro and Ana Paiva. Animating the adelino robot with ERIK: The expressive robotics inverse kinematics. In *Proceedings of the 19th ACM International Conference on Multimodal Interaction*, pages 388–396, 2017. URL <https://doi.org/10.1145/3136755.3136791>. 4.4.1.1
- [349] Albert JN van Breemen. Animation engine for believable interactive user-interface robots. In *2004 IEEE/RSJ International Conference on Intelligent Robots and Systems (IROS)(IEEE Cat. No. 04CH37566)*, volume 3, pages 2873–2878. IEEE, 2004. doi: 10.1109/IROS.2004.1389845. URL <https://doi.org/10.1109/IROS.2004.1389845>. 4.4.1.1
- [350] Michael J Gielniak and Andrea L Thomaz. Enhancing interaction through exaggerated motion synthesis. In *Proceedings of the seventh annual ACM/IEEE international conference on Human-Robot Interaction*, pages 375–382, 2012. URL <https://doi.org/10.1145/2157689.2157813>. 4.4.1.1

## BIBLIOGRAPHY

- [351] Tiago Ribeiro and Ana Paiva. The illusion of robotic life: principles and practices of animation for robots. In *Proceedings of the seventh annual ACM/IEEE international conference on Human-Robot Interaction*, pages 383–390, 2012. doi: 10.1145/2157689.2157814. URL <https://doi.org/10.1145/2157689.2157814>. 4.4.1.1
- [352] Saul Greenberg and Bill Buxton. Usability Evaluation Considered Harmful (Some of the Time). In *Proceedings of the SIGCHI conference on Human factors in computing systems*, pages 111–120, 2008. URL <https://doi.org/10.1145/1357054.1357074>. 4.4.1.2
- [353] Donald A Norman. Human-Centered Design Considered Harmful. *interactions*, 12(4):14–19, 2005. doi: 10.1145/1070960.1070976. URL <https://doi.org/10.1145/1070960.1070976>. 4.4.1.2
- [354] Manuela Veloso, Joydeep Biswas, Brian Coltin, and Stephanie Rosenthal. Cobots: Robust symbiotic autonomous mobile service robots. In *Twenty-fourth international joint conference on artificial intelligence*, 2015. URL <https://api.semanticscholar.org/CorpusID:9653894>. 4.4.1.2
- [355] Aaron Steinfeld, Odest Chadwicke Jenkins, and Brian Scassellati. The Oz of Wizard: Simulating the Human for Interaction Research. In *Proceedings of the 4th ACM/IEEE international conference on Human robot interaction*, pages 101–108, 2009. doi: 10.1145/1514095.1514115. URL <https://doi.org/10.1145/1514095.1514115>. 4.4.1.3
- [356] Marvin Rausand. *Risk Assessment: Theory, Methods, and Applications*, volume 115. John Wiley & Sons, 2013. doi: 10.1002/9781119377351. URL <https://doi.org/10.1002/9781119377351>. 4.4.2.1

## **Part II**

# **ARTICLES**



# HUMAN-ROBOT COOPERATIVE LIFTING USING IMUS AND HUMAN GESTURES

---

Gizem Ateş & Erik Kyrkjebø

Human-Robot Cooperative Lifting using IMUs and Human Gestures. Published in Proceedings of the *Annual Conference Towards Autonomous Robotic Systems, Part of the Lecture Notes in Computer Science book series (LNAI, volume 13054, pages 88-99)* Springer, September 8-10, 2021 DOI: [10.1007/978-3-030-89177-0\\_9](https://doi.org/10.1007/978-3-030-89177-0_9)

*“Reproduced with permission from Springer Nature”*





# Human-Robot Cooperative Lifting using IMUs and Human Gestures<sup>\*</sup>

Gizem Ates<sup>[0000-0003-1717-2944]</sup> and Erik Kyrkjebø<sup>[0000-0002-5487-6839]</sup>

Department of Computer Science, Electrical Engineering and Mathematical Sciences, Western  
Norway University of Applied Sciences, Førde, Norway.  
{gizem.ates, erik.kyrkjebo}@hvl.no

**Abstract.** In physical Human-Robot Cooperation (pHRC), humans and robots interact frequently or continuously to manipulate the same object or workpiece. One of the tasks within pHRC that has the highest potential for increased value in the industry is the cooperative lifting (co-lift) task where humans and robots lift long, flexible or heavy objects together. For such tasks, it is important for both safety and control that the human and robot can access motion information of the other to safely and accurately execute tasks together. In this paper, we propose to use Inertial Measurement Units (IMUs) to estimate human motions for pHRC, and also to use the IMU motion data to identify two-arm gestures that can aid in controlling the human-robot cooperation. We show how to use pHRC leader-follower roles to exploit the human cognitive skills to easily locate the object to lift, and robot skills to accurately place the object on a predefined target location. The experimental results presented show how to divide the co-lifting operation into stages: approaching the object while clutching in and out of controlling the robot motions, cooperatively lift and move the object towards a new location, and place the object accurately on a predefined target location. We believe that the results presented in this paper have the potential to further increase the uptake of pHRC in the industry since the proposed approach do not require any pre-installation of a positioning system or features of the object to enable pHRC.

**Keywords:** physical Human-Robot Interaction · Cooperative lifting · IMUs

## 1 INTRODUCTION

In physical Human-Robot Cooperation (pHRC), humans and robots work towards a common goal in a shared workspace with physical interaction, and more examples of pHRC such as cooperative lifting and carrying, kinesthetic teaching, coordinated material handling and rehabilitation therapy are seen within industry and healthcare [16]. The introduction of collaborative robots (cobots) is particularly important for small and medium-sized enterprises since the configuration of the fully automated production for each design might take as much effort as the conventional production process when the number of product is little. Installation can be done without replanning whole factories or introducing additional safety measures such as fences or cages for the cobots.

---

<sup>\*</sup> This work was funded by the Research Council of Norway through grant number 280771.

The cooperative lifting (co-lift) operation have the potential to enable humans and robots to lift and carry long, flexible, or heavy objects together while exploiting the human cognitive skills and the robot accuracy in different parts of the task. However, to enable safe and accurate pHRC in co-lift tasks, the control system must have access to human motion data to be able to follow human motions. There are several studies on co-lift and manipulation between a human and a robot in the literature. In [11], the authors use haptic data to dynamically allocate human-robot leader roles on a co-lift scenario. A recent study using only haptic data from the robot joints without requiring external sensors is presented in [7] where the authors estimated external forces applied by the human operator during the collaborative assembly of a car engine. In [13], a human operator and a cobot on a mobile platform carry a long aluminium stick between two locations in the work environment. Cartesian impedance control is applied in the co-lift process and the localization in the environment is done by using a laser scanner. Learning algorithms are also quite popular in co-lifting and co-manipulation studies [2, ?,?]. In [12], a novel approach using the learning by demonstration for various cooperative tasks is proposed where a demonstrated trajectory is adapted through weighting factors to adjust learning speed and disturbance rejection to collaboratively transport an object. In [3] a table-lifting task performed by a human and a humanoid using programming by demonstration and in [2] the human-robot role change is assessed probabilistically using Gaussian Mixture Regression. While these studies found cover important topics for HRC and co-lift tasks, they generally only address the stages of the cooperation where the human and robot is physically interacting. There is no study found that also address the approach to the co-lift stage of the cooperation as this requires motions sensors able to detect human motions when not in contact with the object or robot directly.

To enable pHRC for a cooperative lifting task where also the approach stage is included, the control system must be able to estimate human motions both to control and to detect gestures that can enable/disable human control over the robot. Studies on human motion tracking and estimation can be categorized based on the type of the motion tracker devices used: visual-based [10, 15], and nonvisual-based [1, 4, 14], and hybrid solutions [8, 9]. Each category has its advantages and disadvantages depending on the application area. For example, visual-based solutions are dominant in motion tracking solutions since provide highly accurate human motion tracking but they often fail in industrial usage for pHRC due to occlusion, loss in line-of-sight, intolerant to lightning changes, and lack of mobility etc. IMU-based solutions are stand-alone systems without no permanent installations and can be a good alternative to address the challenges of vision-based systems at a lower cost, but are prone to drift for long term usage. While several solutions to eliminate the drift problem have been proposed [5], there are still few pHRC industrial applications using IMU-based solutions in soft real-time.

The roles in pHRC may change in different stages of a cooperative lifting task [2, 6, 11]. The human cognitive skills can be exploited in the approach stage of a co-lift task to identify the location of the object to pick up, while the robot accuracy can be used to accurately place the object on a predefined target location. In this scenario, the human takes the leader role in picking and the follower role in placing. In addition to the active stages, a passive idle stage is also needed for the user to clutch in and out of. This allows the human to disconnect from controlling the robot to re-position. Switching between roles and active/passive stages of the cooperation requires that triggers may be

identified in the operation, or that additional control signals are introduced to control the switching.

In this paper, we propose a novel approach for Human-Robot cooperative lifting in section 2, and show how we can estimate human motions using IMUs during the approach and co-lift stage of the cooperation in section 2.1. We also address the different roles of cooperation in section 2.2 by using individual human arm gestures to clutch in and out of active roles. The proposed approach is experimentally tested in section 3, and the results discussed in section 4. Conclusion and outlook is provided in section 5.

## 2 Human-Robot cooperative lifting using IMUs and gestures

In this paper, we address the problem of collaborative lifting, carrying and placing an object as a joint operation between a human and a robot to share the load of the object, and also to exploit the accuracy of the robot to place the object at a predefined target location. First, we will show how we estimate human motions and gestures using IMUs. Second, we show how leader-follower roles are defined, and how arm gestures are used to switch between active (approach, co-lift, release) and passive (idle) states.

### 2.1 Posture and Gesture Estimation

We propose to estimate 13 DoFs upper-body motions (chest, left and right arm) using 5 IMUs placed as shown in fig. 1. Note that we disregard any wrist motion in this paper.

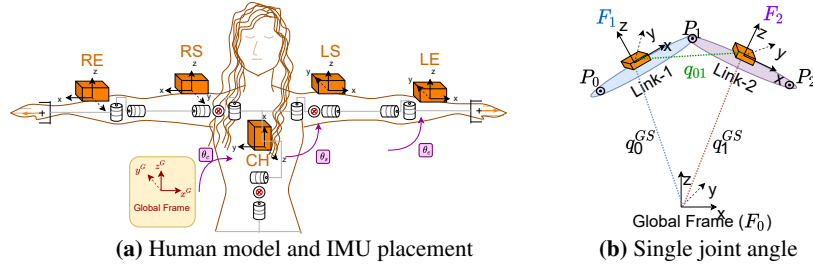


**Fig. 1:** Human model, IMU placements and joint angle definitions.

The full upper-body posture and motion estimation is a collection of estimated individual joint angles, and where a joint angle can be found by calculating the rotation between two consecutive links with attached IMUs as shown in figure fig. 1a. The illustrated body parts in fig. 1b can be considered as upper and lower arm segments.

The raw orientation data from the IMU sensor is referred as  $q_i^{GS}$  where  $i$  is the IMU number. Each IMU provides orientation information with respect to global frame  $F_0$ . If the link-1's frame of reference is called  $F_1$  and link-2's frame of reference is called  $F_2$ , the rotation from the global frame to sensor frames will be  $q_0^{GS}$  and  $q_1^{GS}$  respectively. We can find the joint angle  $q^{01}$  between two links as the rotation from  $F_1$  to  $F_2$  using quaternion multiplication as

$$q_{01} = (q_0^{GS})^* \otimes q_1^{GS} \quad (1)$$

where  $\otimes$  denotes the quaternion multiplication and  $*$  the complex conjugate of the quaternion. The term  $q_1^{GS}$  is the rotation of the IMU attached on link-1 from global to sensor frame. If we apply this process from link-0 (chest to shoulder) to link-2 (elbow to wrist), we obtain the arm posture of a human arm based on estimated IMU

orientations. One arm can be modelled as a total of 5 DoFs where 3 DoFs are on the shoulder joint and 2 DoFs are on the elbow joint as shown in fig. 1a. The kinematic chain for such a human model from the base (chest) to the tip (hand) can be written as:

$$q_c = q_{CH} \quad q_s = q_c^* \otimes q_{LS} \quad q_e = q_c^* \otimes q_s^* \otimes q_{LE} \quad (2)$$

where  $q_c$ ,  $q_s$  and  $q_e$  are the quaternions representing joint angle rotations,  $q_{CH}$ ,  $q_{LS}$  and  $q_{LE}$  are the IMU orientation from global to the sensors frame in fig. 1a - which are the raw orientation readings from the sensors. The process is identical for the second arm.

## 2.2 Cooperation roles and states in cooperative lifting

The cooperative lifting scenario can be divided into three active (APPROACH, CO-LIFT, RELEASE) and one passive (IDLE) state of the operation as shown in fig. 2.

There are two key concepts in this scenario, one is the **role** and the other is the **state**. The role is defined by *who is leading the cooperative task* and the state defines which *stage* of the task is running. There is a dynamic role change between human and the robot leader-follower roles based on the human two-arm gestures and the completion of the task, and also the state changes are triggered based on human arm gestures.

**Human leader:** This role is where the robot takes actions led by the human operator based on his/her upper-body motions. The pick position of the object is not necessarily to be known by the robot. The cognitive skills of the human can be exploited to approach the object sensibly, identify the object to pick up, and finally lift and carry it towards a target position. Within a close distance to the place position, the robot-leader role is activated by a gesture so that a precise placement is achieved.

In our proposed approach, we track both human arms individually and can use them for different purposes in human-robot cooperation. We define one arm as the *motion* arm (left) and the other as the *steering* arm (right). The motion arm is directly controlling the robot motions in the active stages when the human is the leader, while the steering arm motions are superimposed on the motion arm when applied to the robot. In this way, the human can approach and grip the object on one end using the motion hand – and the robot will mirror this motion – but also use the steering hand to adjust the robot position to the proper gripping position on the other end of the object while keeping the motion hand still. Thus, any misalignment between the starting position of the human and robot can be corrected. Furthermore, gestures from the steering hand can be used as triggers or control signals to move from one state to another in cooperation. There are 3 states in the human-leader role: idle, approach and co-lift.

In **IDLE**, no human motions are mapped into robot motions. The human can move closer to the pick-up position without moving the robot. This state is also a *safe* state which the human can switch to from any other state in the human-leading role, and thus enables the human operator to move freely at any time. In **APPROACH**, motion and

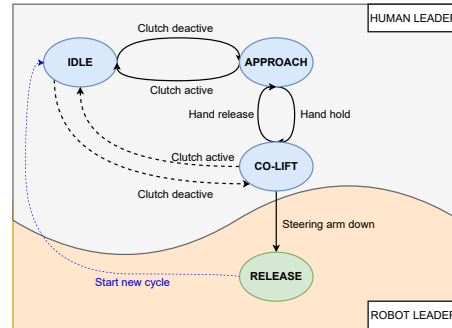


Fig. 2: HRC states and leader roles

steering arm motions are combined into a *hand* pose that controls the goal pose of the robot. The individual contribution of the two arms can be scaled through gains. Human forward/backwards and up/down motions are identical on the robot, but sideways motions are mirrored by the robot. In **CO-LIFT**, both the robot and the human is holding the common object and lifting it towards the desired target position. Only the motion hand controls the goal pose of the robot. The steering arm is free to move to help to lift, or to perform gestures. Two gestures of the steering arm are defined as "release down" and "rotate up/down" to trigger state and role changes.

There are two transition gestures and a foot pedal activated transition between states and roles. The "clutch activate/ deactivate" gesture activates and deactivates the human to robot motion mapping. The clutch is triggered by the steering hand rotating to the palm up gesture to switch from IDLE to APPROACH/CO-LIFT, and rotating to palm down gesture to switch from APPROACH/ CO-LIFT to IDLE. The "handhold/release" transition is triggered by a foot pedal to close the robot gripper so that the CO-LIFT stage can start. The option to switch from CO-LIFT to IDLE state (dashed lines in fig. 2) is included for safety reasons in case the human leader need to free the motion hand from the object. Care should be taken to support the load of the lifted object in such a scenario since the load cannot necessarily be supported by the robot alone. The last transition gesture is the "release down" gesture where the human points the steering arm downwards to trigger the role change from human leader to robot leader.

**Robot leader:** The trigger gesture "release down" switches from a human leader role strategy to a robot leader strategy where the robot can take over control of the execution to move the object to the target position while the human keeps supporting the load of the object and follows the robot motions. Only one state called RELEASE is proposed in our design, but a sequence of other tasks can be added for more complex tasks. As soon as the robot reaches the desired target position, the gripper is automatically released and the robot moves away from the object and is ready for another cycle.

### 2.3 Human-Robot Cooperative lifting of a table

The cooperation starts in the IDLE state, and is shown in fig. 3. The robot expects the clutch deactivate signal (see the rotation of the steering hand from fig. 3a to fig. 3b). At this stage, the motion hand pose  $\hat{P}_{hm}$  and steering hand pose  $\hat{P}_{hs}$  are combined into the hand pose  $\hat{P}_h$ , but the goal pose  $\hat{P}_{goal}$  is not sent to the robot in the IDLE state.

When the clutch is released the HRC system switches to an active APPROACH state as shown in fig. 3b. The human operator controls the robot, and as the human approaches to the table with the motion hand, the robot approaches the table with a scaled mimicking motion. If the motion hand reaches and grips the table, the robot can still be controlled using the steering hand to approach the appropriate grip position on the other side. Pose calculations are computed using 4x4 homogeneous transformation matrix (HTM). The robot goal pose is calculated based on the relative position change of the hand pose  $\hat{P}_{h,t}$  as shown in eq. (3).

$$\hat{P}_{h,t}^- = \hat{s} \cdot (\hat{P}_{hm,t=0}^{-1} \times \hat{P}_{hm,t}) + \hat{k} \cdot (\hat{P}_{hs,t=0}^{-1} \times \hat{P}_{hs,t}) \quad (3)$$

where  $\hat{P}_{h,t}^-$  is the merged hand pose. To get the approach response from the robot the y-axis in  $\hat{P}_{h,t}^-$  is inverted and  $\hat{P}_{h,t}$  is obtained to control the approach of the robot. The

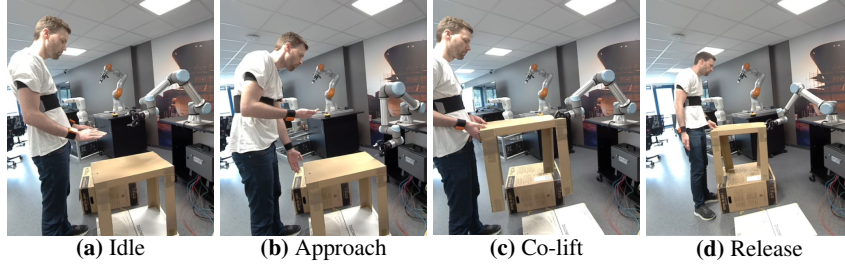


**Fig. 3:** Human and robot poses in co-lift states. **(a)** shows both the human and the robot initial poses in the IDLE state. The steering hand (right) is palm down. **(b)** shows both the human and the robot poses in action in the APPROACH state. The steering hand is palm up. **(c)** shows the CO-LIFT state where both the human and the robot is carrying the table. The steering hand does not influence motion commands, but is helping the motion hand (left) to lift the object. Finally, **(d)** shows the RELEASE state triggered by the "release down" of the steering hand, and where the robot takes control of the operation to place the object at the desired target position.

4x4 scaling matrix for the motion hand  $\hat{s}$  has the last row equal to  $[s_x, s_y, s_z, 1]$  with the rest of the elements as 1. The scaling matrix  $\hat{k}$  is defined similarly for the steering hand. The robot goal pose based on the combined hand pose is

$$\hat{H}(t) = \hat{P}_{h,t=0}^{-1} \times \hat{P}_{h,t} \quad \hat{P}_{r,t} = \hat{P}_{r,t=0} \times \hat{H}(t) \quad (4)$$

where  $\hat{H}(t)$  is the transformation of merged hand pose from initial to the current pose. The goal pose is set to initial orientation of the robot for easier cooperation.

When the system switches to the CO-LIFT state, the contribution of the steering hand is eliminated. The current pose of the motion hand is set to a new initial pose and the robot goal pose is calculated based on only the motion hand's relative position changes as in

$$\hat{P}_{h,t}^- = \hat{s}_2 \cdot (\hat{P}_{hm,t=t_{co-lift}}^{-1} \times \hat{P}_{hm,t}) \quad (5)$$

where  $\hat{P}_{hm,t=t_{co-lift}}$  is the new pose measurement of the motion hand in HTM form needed to ensure a smooth transition between states. The  $\hat{s}_2$  term is the new scaling factor for the motion hand. Finally, the y-axis measurements of  $\hat{P}_{h,t}^-$  are reversed for a mirror the human motions to obtain the new hand pose command  $\hat{P}_{h,t}$  in CO-LIFT.

When the steering hand is released down to switch to the RELEASE state, we no longer compute the human hand to robot motion mapping since the robot takes over the leading role in the RELEASE state, and the human follows the robot motions.

### 3 Experimental setup and results

The experimental test was performed as a full human-robot cooperative lifting operation as shown in fig. 3. We first present the experimental setup and the calibration steps before presenting the resulting data.

### 3.1 Setup

The human is equipped with 5 Xsens Awinda IMUs to estimate orientations output as filtered orientation raw data in quaternions. The cooperative robot as the Universal Robots UR5e cobot equipped with a Robotiq 2F-85 gripper. The data acquisition is processed in the ROS Melodic environment on two PCs. One PC is running the ROS master and the Universal Robot's ROS driver, and the other PC runs all the other ROS nodes. The UR5e is connected via Ethernet cable to the ROS Master PC, and the URCap software is started after the UR5e ROS driver is started on the ROS Master PC. The data acquisition from the IMUs runs at 100Hz whereas the UR5e controller runs at 50Hz. The inverse kinematic solver node using *ikfast* runs at 10 Hz, and scaling factors for the motion and steering hand are set to 1.

### 3.2 Calibration

The calibration process consists of three steps as following: The first step is to remove any bias on IMU orientation raw data, the second is to initialize human posture and the third is to map the human initial pose to the robot's initial pose.

**IMU Orientation Calibration:** First, we eliminated the bias and set a relative initial pose of each IMU to make sure the IMUs output zero orientation initially as

$$q_{I,abs} \otimes q_{init-rot} = q_{bias} \quad q_{I,rel} = q_{bias}^* \otimes q_{bias}. \quad (6)$$

where  $q_{I,abs}$  is the absolute initial orientation of an IMU, which is a unit quaternion, on a particular 3D orientation where the IMU axes are perfectly aligned with the global frame of reference. The  $q_{init-rot}$  is the rotation from the initial orientation to when the data acquisition starts, which is unknown. The  $q_{bias}$  is initial raw orientation data from the sensors that changes in every setup. The initial orientation is set based on recording  $q_{bias}$  for 2s in a steady T-pose (arms out), and  $q_{I,rel}$  is set to the identity quaternion.

**Human Body Calibration:** The IMU calibration is computed in a the T-pose, and all the joint angles are set to zero, and  $q_{bias}^*$  is set to identity quaternion.

**Hands to Robot Calibration:** This sets the human arm pose to the robot initial pose. The human moves to a desired initial pose and the robot move to its predefined initial pose fig. 3a. The robot initial pose  $\hat{P}_{r,t=0}$  is registered, and the computed hand pose  $\hat{P}_{h,t=0}$  is initialized to zero position and zero rotation.

### 3.3 Results

The experiment is carried out by an inexperienced user and the data is presented in fig. 4. As explained in section 3.1, the actual robot data is recorded on the ROS Master PC, and therefore the recorded data clocks are synchronized after recording. In human-leading role states, it can be seen how hand motions affect the goal position of the end-effector of the robot whereas the hand positions are not affecting the goal position in the robot-leading role state. In IDLE, we observe motions of the human arms (blue/orange), but these motions do not affect the robot goal position (red) in this state. The merged hand position (green) at the initial pose shown in fig. 3a is set to zero. When the clutch is deactivated (t=8s), the goal pose is sent to the robot based on the merged hand pose (green), and the robot starts following the same trend as the goal pose (red). Between t=15-20s, the motion hand (blue) is stable (holding the table at one end) and the steering

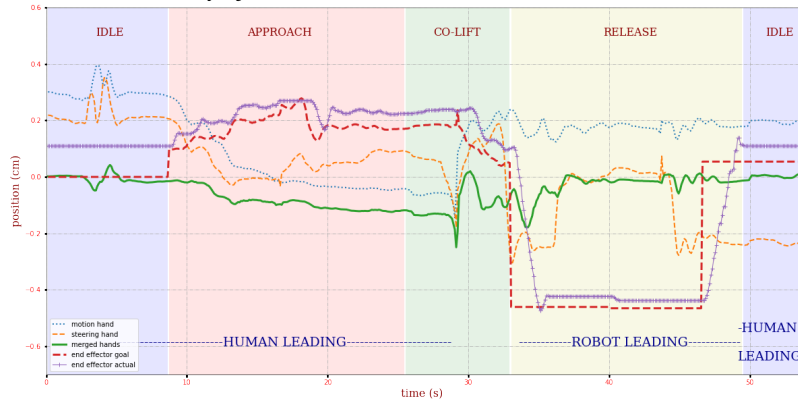


**Fig. 4:** A full cycle demo of the proposed HRC cooperative lifting scenario. The lines shows the position change on the x-axis of the motion hand (left) in **blue**, steering hand (right) in **orange**, merged hands in **green**, the goal pose to the robot's end-effector in **red** and the actual robot pose in **purple**. The states IDLE, APPROACH, CO-LIFT and RELEASE are indicated as background colours. The roles (human or robot leading) are indicated with blue texts at the bottom of the figure where human-leading role covers IDLE, APPROACH and CO-LIFT and robot-leading role covers only RELEASE.

hand (orange) keeps commanding the robot to adjust the robot position to be ready to grip the table. After the human is satisfied with the position on which the robot can grip the table, the handhold signal is sent and the CO-LIFT stage starts. In this state, only the motion hand (blue) is affecting the goal pose (red) - but inverted. The steering hand (orange) helps to lift without affecting the goal pose. After the steering hand is released down as in fig. 3d, a role changing is triggered and the RELEASE stage starts. No hand motion is sent as the goal pose in this stage. Instead, the goal pose is set to the predefined target position. When the robot reaches the target position at around  $t=40s$ , it automatically opens the gripper and pulls itself back ( $t=40$ ), and waits for input to do another cycle ( $t=49s$ ), where the goal pose is set to the robot initial pose. When the robot reaches the desired position with a small tolerance (the absolute sum of joint angle error is less than  $0.001$  rad), the system is automatically set to the IDLE and the robot wait for the clutch to deactivate for the new co-lift cycle.

#### 4 Discussion and Future Work

In this study, we demonstrated a human-robot cooperative lifting task scenario based on estimated human motions and gestures using IMUs, and we tested and validated the proposed pHRC states, roles and their transitions using a real robot in experiments.

The proposed method is a novel conceptual design that still requires some tuning based on more extensive user tests. Different learning curves are observed for different users, and also some feedback on preferences are reported which conflict between users:

**Motion mapping:** In the current setup, we take the spine-fixed frame as the human motion reference frame. It is reported as *confusing* in the beginning. After a few trials, it is reported to become *more natural*. It is still an open question for real applications and highly depends on the users' learning curve. To develop a training setup is a possibility or more intuitive frame of reference can be analyzed with more user tests - potentially using the motion arm as the frame of reference.



**Robot speed:** It is seen fig. 4 that the actual pose (purple) does not follow the goal pose (red) identically. There is no lagging or real-time during the experiments, but the robot maximum speed is set to be 30% of full speed as a safety measure. If this is increased, the robot becomes more responsive and exceeds the comfort zone of the human operator which then tries to slow the robot down, and thus we can induce harmonic motions around the desired pose. With training, the trust in the robot increases, and the speed limit can be increased.

**Contribution of the two hands:** We set the contribution of the two hands equal in the experiments based on user preferences. However, during tests in the development stage, other users reported that they preferred either the motion or steering hand to be more dominant. Also, the approach direction of the motion hand could be either *mimicked* or *mirrored* based on user preferences. These are open questions.

The pick and place positions are selected close due to the limited workspace of the robot. The `ikfast` module provides a rapid inverse kinematic (IK) solution (on the order of  $4\mu s$ ) but no limitless elbow/wrist configuration can be set. Therefore, we set joint limits in the experiments to make sure the robot works within the configuration space, but this can be extended in future versions, or changed to a recursive IK solver.

The human and robot motions are defined as relative positions with respect to the initial states. Therefore, the parameters of the human model do not play a vital role. An average human model can be used for most users. It should be noted that the behaviours on the other axes are observed; the states and the transitions correspond in all axes yet they are not presented in this paper due to the number of page limitations.

For the proposed method, the initial position of the object and its properties is unknown. The approach is lead by the human, and the release is lead by the robot. Only the target position of the object is necessary. Such a design opens up a wide range of application possibilities such as co-manipulation, co-assembly as well as co-lifting.

The real-time term describes a *soft* real-time behaviour that the human does not *feel* a delay or lagging. We have not assessed quantitatively the real-time capabilities, and we are planning to address this issue in future studies.

The IMUs are prone to drift but the filtered orientation by Xsens Awinda provides relatively stable data. For about 15 minutes of data collection period without recalibrating IMUs, no drastic drift issue is reported. However, before testing the system in real industrial applications, a quantitative drift assessment study in various magnetic disturbances should be carried out.

## 5 CONCLUSIONS

In this study, a conceptual design of human-robot cooperative lifting based on human motions and gestures captured using IMU data is presented and validated with a real-world experiment. The proposed system consists of two leading roles as human-leader and robot-leader which dynamically switches based on human gestures. The proposed roles consist of 4 different states and the human-to-robot motion mapping differs according to the system state. This study aims to open up new possibilities in pHRC for industrial applications by using IMUs as cheap, portable, and low-cost measurement systems that do not suffer from occlusion and line-of-sight loss.

## References

1. Bi, L., Genetu Feleke, A., Guan, C.: A review on EMG-based motor intention prediction of continuous human upper limb motion for human-robot collaboration. *Biomedical Signal Processing and Control* **51**, 113–127 (May 2019). <https://doi.org/10.1016/j.bspc.2019.02.011>
2. Evrard, P., Gribovskaya, E., Calinon, S., Billard, A., Kheddar, A.: Teaching physical collaborative tasks: object-lifting case study with a humanoid. In: 2009 9th IEEE-RAS International Conference on Humanoid Robots. IEEE (Dec 2009). <https://doi.org/10.1109/ichr.2009.5379513>
3. Gu, Y., Thobbi, A., Sheng, W.: Human-robot collaborative manipulation through imitation and reinforcement learning. In: 2011 IEEE International Conference on Information and Automation. IEEE (Jun 2011). <https://doi.org/10.1109/icinfa.2011.5948979>
4. Kok, M., Hol, J.D., Schön, T.B.: An optimization-based approach to human body motion capture using inertial sensors. *IFAC Proceedings Volumes (IFAC-PapersOnline)* **19**, 79–85 (2014). <https://doi.org/10.3182/20140824-6-ZA-1003.02252>
5. Kok, M., Hol, J.D., Schön, T.B.: Using Inertial Sensors for Position and Orientation Estimation (2017). <https://doi.org/10.1561/20000000094>
6. Kyrkjebø, E., Rodriguez, B.L., Ates, G., Mogster, J., Schale, D., Drewniak, M., Ziebinski, A.: The Potential of Physical Human-Robot Cooperation using Cobots on AGVs in Flexible Manufacturing. (Under review) pp. 1–13
7. Liu, S., Wang, L., Wang, X.V.: Sensorless haptic control for human-robot collaborative assembly. *CIRP Journal of Manufacturing Science and Technology* **32**, 132–144 (Jan 2021). <https://doi.org/10.1016/j.cirpj.2020.11.015>
8. Malleson, C., Gilbert, A., Trumble, M., Collomosse, J., Hilton, A., Volino, M.: Real-time full-body motion capture from video and IMUs. In: 2017 International Conference on 3D Vision (3DV). IEEE (Oct 2017). <https://doi.org/10.1109/3dv.2017.00058>
9. von Marcard, T., Henschel, R., Black, M.J., Rosenhahn, B., Pons-Moll, G.: Recovering accurate 3d human pose in the wild using IMUs and a moving camera. In: *Computer Vision – ECCV 2018*, pp. 614–631. Springer International Publishing (2018). [https://doi.org/10.1007/978-3-030-01249-6\\_37](https://doi.org/10.1007/978-3-030-01249-6_37)
10. Morato, C., Kaipa, K.N., Zhao, B., Gupta, S.K.: Toward safe human robot collaboration by using multiple kinects based real-time human tracking. *Journal of Computing and Information Science in Engineering* **14**(1) (2014)
11. Mörtl, A., Lawitzky, M., Kucukyilmaz, A., Sezgin, M., Basdogan, C., Hirche, S.: The role of roles: Physical cooperation between humans and robots. *International Journal of Robotics Research* **31**(13), 1656–1674 (2012). <https://doi.org/10.1177/0278364912455366>
12. Nemeč, B., Likar, N., Gams, A., Ude, A.: Human robot cooperation with compliance adaptation along the motion trajectory. *Autonomous Robots* **42**(5), 1023–1035 (Nov 2017). <https://doi.org/10.1007/s10514-017-9676-3>
13. Ramasubramanian, A.K., Papakostas, N.: Operator - mobile robot collaboration for synchronized part movement. *Procedia CIRP* **97**, 217–223 (2021). <https://doi.org/10.1016/j.procir.2020.05.228>
14. Roetenberg, D., Luinge, H., Slycke, P.: Xsens MVN : Full 6DOF Human Motion Tracking Using Miniature Inertial Sensors. *Hand, The* (January 2009), 1–7 (2009). <https://doi.org/10.1.1.569.9604>
15. Sheng, W., Thobbi, A., Gu, Y.: An integrated framework for human–robot collaborative manipulation. *IEEE Transactions on Cybernetics* **45**(10), 2030–2041 (Oct 2015). <https://doi.org/10.1109/tcyb.2014.2363664>
16. Siciliano, B., Khatib, O.: Physical Human-Robot Interaction. In: *Springer Handbook of Robotics*, chap. 69, pp. 1835–1874. Springer (2016)

# FORCE AND GESTURE-BASED MOTION CONTROL OF HUMAN-ROBOT COOPERATIVE LIFTING USING IMUS

---

Gizem Ateş, Martin Fodstad Stølen & Erik Kyrkjebø

Force and Gesture-based Motion Control of Human-Robot Cooperative Lifting Using IMUs. Published in *HRI'22 Proceedings of the 2022 ACM/IEEE International Conference on Human-Robot Interaction* (Pages 688–692). IEEE, March 7-10, 2022 DOI: [10.5555/3523760.3523856](https://doi.org/10.5555/3523760.3523856)

*“In reference to IEEE copyrighted material which is used with permission in this thesis, the IEEE does not endorse any of Western Norway University of Applied Sciences’s products or services. Internal or personal use of this material is permitted. If interested in reprinting/republishing IEEE copyrighted material for advertising or promotional purposes or for creating new collective works for resale or redistribution, please go to [http://www.ieee.org/publications\\_standards/publications/rights/rights\\_link.html](http://www.ieee.org/publications_standards/publications/rights/rights_link.html) to learn how to obtain a License from RightsLink. If applicable, University Microfilms and/or ProQuest Library, or the Archives of Canada may supply single copies of the dissertation.”*



# Force and Gesture-based Motion Control of Human-Robot Cooperative Lifting Using IMUs

Gizem Ateş, Martin Fodstad Stølen, Erik Kyrkjebø  
Dept. of Computer Science, Electrical Engineering and Mathematical Sciences,  
Western Norway University of Applied Sciences, Førde, Norway  
{gizem.ates, martin.fodstad.stolen, erik.kyrkjebo}@hvl.no

**Abstract**—Cooperative lifting (co-lift) is an important application of HRI with use-cases in many fields such as manufacturing, assembly, medical rehabilitation, etc. Successful industrial implementation of co-lifting requires the operations of approaching, attaching, lifting, carrying and placing the object to be handled as a whole rather than individually. In this paper, we target all stages of cooperative lifting in a holistic approach and extend previous results in [1] using IMU-based human motions estimates by introducing force-based control. We demonstrate through experiments on a UR5e robot how the force-based approach significantly improves on the position-based approach of [1]. Additionally, we improve the real-time control capabilities of the system by using a real-time data exchange communication interface. We believe that our system can be an advancing point for more human motion/gesture-based HRI applications as well as increasing the uptake of human-robot co-lifting systems in industrial settings.

**Index Terms**—Human Motion Estimation, Inertial Measurement Units (IMUs), Compliant pHRC, Cooperative Lifting.

## I. INTRODUCTION

The field of Human-Robot Interaction (HRI) covers a wide range of interactions between humans and robots coexisting in the same workspace. In an industrial context, the interactions can be supportive, collaborative or cooperative [2]. If the interaction requires continuous physical contact between a robot and a human - either directly or through an object - it can be defined as a physical Human-Robot Cooperation (pHRC).

The different strengths of human workers and robots make them excel at different tasks. While robots are durable, precise and repeatable, humans have excellent problem-solving skills and are creative in their decision-making. cooperative lifting (co-lift) is a widely studied application of pHRC where a robot and a human carry a common object from one point to another as shown in fig. 1.

Different HRI strategies and methods have been addressed in the literature for the co-lift task [3]–[5]. In [3], the authors proposed to use EMG activities on human biceps by training neural networks. In [4], a Gaussian mixture model is used on vision-based motion data. In [5], a kinesthetic teaching method is proposed to create trajectories to allow adaptive interaction both in co-manipulation and co-lifting tasks. The examples in the literature present valuable results but only focus on the co-lift stage rather than the whole pHRC cycle.

This work was funded by the Research Council of Norway through grant number 280771.



**Fig. 1:** Frame-capture from co-lift experiments using IMUs for human motion estimation and an EMG-sensor to open/close the gripper. The co-lift states of APPROACH, CO-LIFT and RELEASE, and the pick and place locations, are illustrated.

In [1], the whole pHRC cycle was addressed using human motion estimates from IMUs, and in this paper, we will extend these results by introducing compliant force interaction.

To enable cooperative lifting through pHRC, some key factors must be in place. First, human motions must be estimated using a sensor system to inform the robot of human actions. Second, the pHRC system should allow role allocation in different stages of the co-lift operation; approaching the object, lifting and placing it safely. Third, a human-robot interaction interface must allow humans and robots to communicate intentions and commands.

Human motion estimation is an active area of research for HRI. It is crucial in HRI tasks both for controlling robot motions when the human is in the leading role and for role allocations during task execution for gesture-based interaction interfaces. It can be either low-level such that human motions are directly transferred to the robot [6], [7] or semantically higher level using gestures [8]–[11]. Moreover, human motion tracking and estimation can also be categorized based on the type of the motion tracking devices used: vision-based [4], [6], non-vision based [12]–[14], and hybrid solutions [15], [16]. Depending on the application area, each category has its advantages and disadvantages. While vision-based solutions are dominant in motion tracking since they provide high accuracy, they often fail in industrial usage due to occlusions

and loss of sight, being sensible to lighting, and having lack of mobility etc. IMU-based solutions do not suffer from these issues but low-cost sensors are prone to drift when used for position estimation. However, solutions to eliminate the drift have been proposed in [17] that performs with comparable accuracy as vision-based systems [18], but there are still few pHRC industrial applications using pure IMU-based solutions.

In cooperative human-robot tasks, both the robot and the human can be assigned roles that are either static (human leader and robot follower [19], [20] or vice-versa) or dynamically changing during the task execution [21], [22]. Three different shared role schemes were proposed in [22] where the adaptive role allocation is assigned based on the necessary effort of both the robot and the human. In [7], the authors executed a role adaptation derived from the interaction force feedback. Another study [21], commits roles in two steps where in the first step the motion command is taught by a human leader, and then in the second step, the leader role is assigned.

Force and haptic interaction is an important aspect of co-lift applications [19]–[22]. A physical contact parameter can be implemented such that both robot and human share the sense of lifting and can take action accordingly. In [19], a sensor-less haptic system is developed to form a force-to-motion relationship. In [21] a haptic desktop controller is used as a haptic interface with scaled force feedback to a human leader while the robot is carrying a table with another human.

In this paper, we target the three key factors for successful human-robot cooperative lifting: 1) Estimating human motions using an IMU-based solution which can be easily applied in industrial applications, 2) role transition between human and robot during the different stages of the co-lift, and 3) employing human motion data for a gesture-based HRI interface to send commands to the robot. We compare our results to prior work in [1] to show the effects of introducing compliant force interactions between the human and robot, and also how improving the real-time data exchange capabilities can enhance the system performance significantly.

## II. METHODOLOGY

In this section, we show how human motions can be estimated from a set of individual IMUs in section II-A, and how the states and role-transitions is controlled in section II-B.

### A. Estimating Human Motions

To estimate human motions, we can equip the human partner with a set of IMU sensors on the chest, left/right upper arms, and left/right forearms as shown in fig. 2. The IMUs are used for human motion estimation for controlling robot motions, and also for gesture estimation for the HRI interface commands.

The human motion estimation follows the approach of [1]. First, the raw orientation data from each sensor in a global frame is obtained. Then, individual IMU orientations in their respective sensor frame is calculated as in eq. (1).

$$q_{joint} = (q_{prevLink}^{GS})^* \otimes q_{currentLink}^{GS} \quad (1)$$

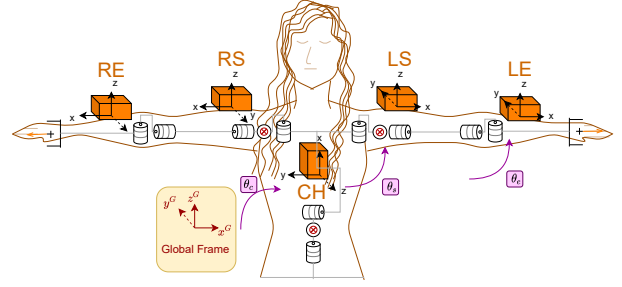


**Fig. 2:** Human model and IMU placement on right/left elbow (RE/LE), right/left shoulder(RS/LS) and chest (CH).

Further, joint angles in both arms starting from the chest to the left wrist is calculated as in eq. (2).

$$q_c = q_{CH} \quad q_{ls} = q_c^* \otimes q_{LS} \quad q_{le} = q_c^* \otimes q_{ls}^* \otimes q_{LE} \quad (2)$$

where the asterisk denote quaternion conjugate,  $q_c, q_{ls}, q_{le}$  are human joint angles;  $q_{CH}, q_{LS}, q_{LE}$  are calibrated IMU-readings of chest, left-shoulder, and left-elbow, respectively. The same calculation applies to the human right-side. Note that the human chest is modeled as a ball joint with 3 degrees of freedom (DoF)s, and each arm is modeled with 5 DoF (i.e. 3 DoF shoulder and 2 DoF elbow), while wrist motions are ignored. Finally, the biomechanical model of the human is constructed as a pair of kinematic chains for both arms using the measured body link lengths and calculated joint angles. Additionally, a low-cost EMG sensor on the right forearm is used to control gripper opening - which also changes HRC states from APPROACH to CO-LIFT (see section II-B).

There are two main reasons why two-handed motions are used as the control input to the robot rather than the motion of only one hand. First, while mapping the motions of one hand - the motion hand - as the desired motions for the robot, the second hand - steering hand - can take on a clutching function to engage or disengage the robot to follow human main-hand motions, and allow the human to move without controlling the robot. Second, the steering-hand motion inputs can be used as corrective inputs to the motions of the main hand to scale robot motions relative to human motions. This is particularly valuable in the grasping state to enable alignment of the human and robot wrists from any initial condition.

### B. Roles and States

Following [1], we define four different states of the whole HRC co-lift operation as IDLE, APPROACH, CO-LIFT, and RELEASE, and the 3 different roles of cooperation as **Human Leading**, **Robot Leading**, and **Shared Control**. The different states and roles of the system are defined in the following.

**Human Leading role:** IDLE: No motion command is sent to the robot, and the robot stays at rest in the initial position. This is a safety state that the human can enter with the clutching gesture at any time.

APPROACH: A merged hands motion - a combined pose parameter of the two hand poses with an adjustable scale as in [1] - is actively calculated and sent as servo control commands to the robot. The robot follows the merged hands

motions. The initial merged hand pose is calculated in every IDLE→APPROACH transition as

$$\left[ \hat{P}_{handLeft,t=0} \times \hat{P}_{handRight,t=0} \right]^{-1} = \hat{P}_{r,t=0} \quad (3)$$

and the desired robot command is calculated continuously as

$$\hat{H}(t) = \hat{P}_{h,t=0}^{-1} \times \hat{P}_{h,t} \Rightarrow \hat{P}_{r,t} = \hat{H}(t) \times \hat{P}_{r,t=0} \quad (4)$$

where  $\hat{P}_{handLeft,t=0}$ ,  $\hat{P}_{handRight,t=0}$  and  $\hat{P}_{r,t=0}$  are Homogeneous Transformation Matrix (HTM) representing human left hand, human right hand (i.e. motion and steering hand for this setup) and robot end-effector pose at initial, respectively.  $\hat{H}$  is a HTM mapping merged hands motion to robot pose with respect to robot's initial pose  $\hat{P}_{r,t=0}$ . The  $\hat{H}$  is set as target pose in `servoL` command [23] with 0.1s look-ahead time to smoothen the trajectory.

**Shared Control role: CO-LIFT:** The robot applies a directional compliant force. The direction is determined by the human elbow heights (rather than direct hand motion mapping as in [1] due to the restrictions on hand movements during holding an object). The robot is actively leading the cooperation until an external force is applied by the human to the object. When the human force input is detected by the robot, the compliant force is adjusted based on the elbow configuration as shown in fig. 3. If both elbows are higher than a threshold, the direction is set UP. If left elbow is higher than the threshold and right elbow is lower than the threshold, the direction is set LEFT, or vice-versa. If both elbow heights are lower than the threshold when the human external force is applied, no directional compliant force is generated by the robot (direction is set to NULL). This behaviour is computed by using the `forceMode` command [23] where the compliance is set in the end-effector frame with 170 mm maximum allowed deviation on non-compliant axes and 30 N force applied with 0.5m/s maximum end-effector speed on the compliant axis.

**Robot Leading role: RELEASE:** The robot takes the lead of the operation, and moves to a predefined pose. The human follows robot motions.

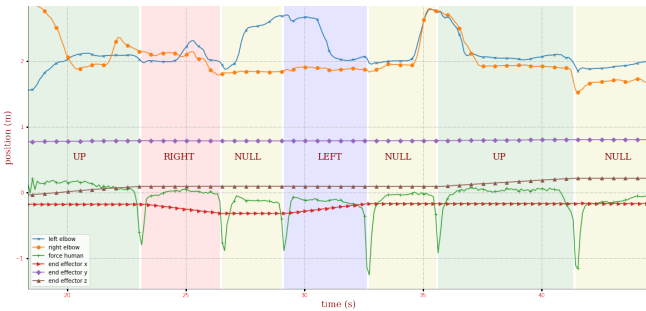


**Fig. 3:** Force profiles and elbow heights in the CO-LIFT state. Blue (left) and orange (right) lines show elbow heights, green line shows the external force input (in y-direction) and the spikes indicate where the human applied an external force. The red (x), purple (y) and brown (z) lines shows the actual end-effector pose in the world coordinate system. The background colors indicate compliant forces in different directions.

### III. EXPERIMENTAL SETUP

An experimental setup of the pHRC co-lift scenario is set up to demonstrate cooperative lifting of a table. The demonstration setup allows the human to control the robot approach (from any initial position), grip the table, and then execute a cooperative lift and carry operation, before the table is placed at a predefined release position as shown in fig. 1. In this setup, the human is utilizing his superior cognitive capabilities in understanding the task and identifying the pick-up position during APPROACH stage, while the human and robot is sharing the load while carrying in the CO-LIFT stage, and the robot is utilizing its superior accuracy when placing the table in the RELEASE stage.

In the experiments, a human user is equipped with 5 Xsens Awinda IMUs as motion sensors, and one Myo Armband for EMG-measurements as shown in fig. 1. Data acquisition is carried out at 100Hz on a Ubuntu 20.04 computer with ROS Noetic installed. The computer is connected to a UR5e robot from Universal Robots using cabled Ethernet connection transmitting servo control commands at 125 Hz while utilizing the real-time data exchange protocol [23].

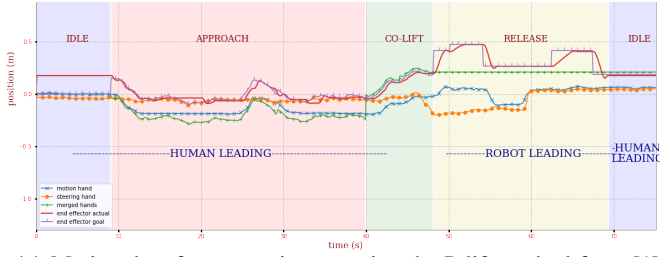
To compare our results to the results presented in [1], all parameters are set equal for the task for both experiments, and the same pick and place positions are used. The human user is trained on the same task in both version of the system until he feels comfortable in using both systems at his best. An additional IMU is attached to the table to measure the table tilt and acceleration during the process. For the experiments, the human hand and elbow poses, robot end-effector pose and force, and system state changes are recorded.

### IV. RESULTS AND DISCUSSION

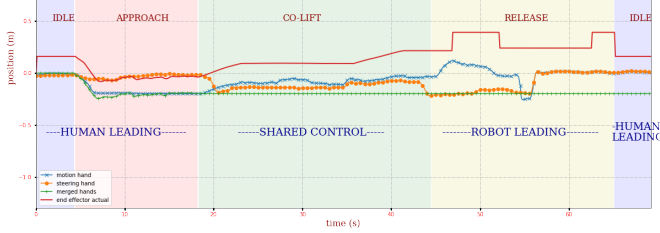
The main objective of this study is to develop a robot partner for lift-and-carry operations. The goal is that the robot should behave intuitively and smoothly, be comfortable to work with, and ultimately increase the usability of the system for industrial applications. To analyse the performance of the system towards this goal, we measured the instant jerk and tilt of the table during the co-lift operation using an extra IMU attached to the table. This also indirectly measures the real-time capabilities of the system since any time-delays resulting in conflicting control inputs from the human and robot would be apparent in the accelerometer data from the table.

The overall motion data and system states recorded from the proof-of-concept experiments are shown in fig. 4. Fig. 4a shows experimental data recorded using the position-based (P-Lift) method from [1], while fig. 4b show experimental data recorded from the force-enhanced cooperative lifting (F-Lift) method presented in this paper. The figures shows the human hand motions as well as the robot motions only for one axis due to page limitation. Note that there is no "goal pose" in the F-lift system since the robot is controlled in servo and force mode rather than in position mode (as in [1]).

The different colors of fig. 4 shows the states of the system during the data collection. Both experiments start in the IDLE state and complete the whole co-lift cycle of APPROACH,



(a) Motion data from experiments using the P-lift method from [1]



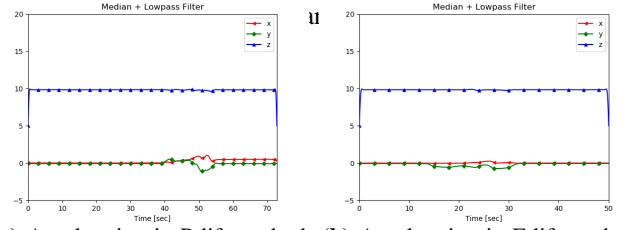
(b) Motion data from experiments using the F-lift method.

**Fig. 4:** A full cycle demo of the co-lift scenario using P-lift and F-lift methods. Lines show position change on z-axis for motion hand (blue), steering hand (orange), merged hands (green) for both plots. The goal pose of the end-effector is shown (only) in (a) in red, with the actual end-effector pose (purple). In (b), the actual end-effector pose is shown in red.

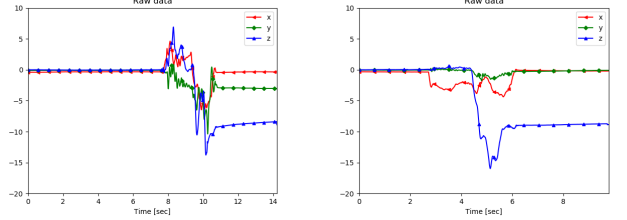
CO-LIFT, RELEASE, and move the robot back to the initial position ready for the next cycle.

The main improvements from the results presented in [1] can be seen particularly in APPROACH and CO-LIFT states. The APPROACH state in the P-lift system takes more time than using the F-lift method. The main reason is difficulties in controlling the robot to approach the table at the correct position for gripping. Joint safety limitations, and the lack of real-time response despite calculating inverse kinematic solutions in less than  $10\mu s$ , cause what is experienced as an un-natural HRC behaviour. The peak at  $t=27s$  show an unsuccessful attempt of grasping the table and the user's retry. The shorter duration of the CO-LIFT state in the P-lift system is mainly because of the difficulty in sending hand motion commands while holding a rigid object. Therefore, the user lifts the table as needed and quickly triggers the RELEASE.

Another main improvement is the introduction of the *Shared Control* role. In the P-lift method, the motion hand pose is mirrored to set a robot goal pose in CO-LIFT state, which makes the human the leader through the whole state. In the F-lift method, no hand motions are directly used in controlling the robot pose in CO-LIFT. The robot is in *force mode* where the direction of the compliant force is determined by the elbow height when the human applies a force as seen in fig. 3. The robot has the leader role in the majority of the time. When an external force (above the threshold of 30N) is applied by the human, the robot checks the elbow heights and updates the compliant force. Note that since the leader role is mostly on the robot in the CO-LIFT state in the F-lift system, and that the state which was previously a *Human Leading* role in P-lift is now a *Shared Control* role in F-lift since the human



(a) Acceleration in P-lift method (b) Acceleration in F-lift method



(c) Tilt angles and heading (blue) in P-lift method (d) Tilt angles and heading (blue) in F-lift method

**Fig. 5:** Acceleration and orientation measurements of the table

Fig. 5a and 5c shows the table acceleration and tilt angles, as well as the heading angle, for the P-lift method. Fig. 5b and 5d shows the same data for the F-lift method. The raw accelerometer data is filtered using a low-pass filter with 10Hz cutoff frequency at 512 Hz sampling rate and cascaded with a median filter with 155 window size in fig. 5a and 5b to remove the accelerometer sensor noise. Comparing the acceleration in both methods, it is seen that the magnitude of the acceleration for the P-lift method in fig. 5a is higher (and even changing direction) than the smoother behaviour of the F-lift method in fig. 5b. The fluctuation of the tilt angles for the P-lift method is related to the non-smooth trajectory and undesired behaviour. Both the results on acceleration and angle deviations suggest that the F-lift method is a significant improvement over the P-lift method for a smoother human-robot cooperative lifting operation.

## V. CONCLUSION

We presented an ongoing study on HRC co-lift with significant improvements compared to previous results in [1]. A full co-lift scenario - consisting of four states: IDLE, APPROACH, CO-LIFT, RELEASE - based on only human motion estimations (P-lift) is augmented with compliant force interaction (F-lift) as well as the real-time behaviour of the system is enhanced with the real-time data exchange protocol. By adding the force interaction, the human-robot role allocations are re-defined and the *Shared Control* role is introduced in addition to *Human Leading* and *Robot Leading* HRC roles in [1]. Improvements are experimentally validated on a UR5e robot. The tilt angles and the jerk on the carried object are monitored for quantitative comparison and a remarkable improvement is recorded. Note that only a proof-of-concept study has been performed, and future work aim for a broader user study with more participants to verify the findings.

## CREDITING AND ACKNOWLEDGMENT

GA: Conceptualization, Methodology, Investigation, Writing - original draft. MFS, EK: Conceptualization, Writing - review & editing. The authors thank Sondre Venås for help with experiments.



## REFERENCES

- [1] G. Ateş and E. Kyrkjebø, "Human-robot cooperative lifting using IMUs and human gestures," in *Towards Autonomous Robotic Systems*. Springer International Publishing, 2021, pp. 88–99. [Online]. Available: [https://doi.org/10.1007/978-3-030-89177-0\\_9](https://doi.org/10.1007/978-3-030-89177-0_9)
- [2] B. Siciliano and O. Khatib, "Physical Human-Robot Interaction," in *Springer Handbook of Robotics*. Springer, 2016, ch. 69, pp. 1835–1874.
- [3] J. DelPreto and D. Rus, "Sharing the load: Human-robot team lifting using muscle activity," in *2019 International Conference on Robotics and Automation (ICRA)*. IEEE, May 2019. [Online]. Available: <https://doi.org/10.1109/icra.2019.8794414>
- [4] W. Sheng, A. Thobbi, and Y. Gu, "An integrated framework for human-robot collaborative manipulation," *IEEE Transactions on Cybernetics*, vol. 45, no. 10, pp. 2030–2041, Oct. 2015.
- [5] B. Nemeč, N. Likar, A. Gams, and A. Ude, "Human robot cooperation with compliance adaptation along the motion trajectory," *Autonomous Robots*, vol. 42, no. 5, pp. 1023–1035, Nov. 2017.
- [6] C. Morato, K. N. Kaipa, B. Zhao, and S. K. Gupta, "Toward safe human robot collaboration by using multiple kinects based real-time human tracking," *Journal of Computing and Information Science in Engineering*, vol. 14, no. 1, 2014.
- [7] M. Arduengo, A. Arduengo, A. Colome, J. Lobo-Prat, and C. Torras, "Human to robot whole-body motion transfer," in *2020 IEEE-RAS 20th International Conference on Humanoid Robots (Humanoids)*. IEEE, Jul. 2021. [Online]. Available: <https://doi.org/10.1109/humanoids47582.2021.9555769>
- [8] S. Waldherr, R. Romero, and S. Thrun, "A gesture based interface for human-robot interaction," *Autonomous Robots*, vol. 9, no. 2, pp. 151–173, 2000.
- [9] S. Chen, H. Ma, C. Yang, and M. Fu, "Hand gesture based robot control system using leap motion," in *International Conference on Intelligent Robotics and Applications*. Springer, 2015, pp. 581–591.
- [10] K. Qian, J. Niu, and H. Yang, "Developing a gesture based remote human-robot interaction system using kinect," *International Journal of Smart Home*, vol. 7, no. 4, pp. 203–208, 2013.
- [11] A. Jackowski, M. Gebhard, and R. Thietje, "Head motion and head gesture-based robot control: A usability study," *IEEE Transactions on Neural Systems and Rehabilitation Engineering*, vol. 26, no. 1, pp. 161–170, 2017.
- [12] M. Kok, J. D. Hol, and T. B. Schön, "An optimization-based approach to human body motion capture using inertial sensors," *IFAC Proceedings Volumes (IFAC-PapersOnline)*, vol. 19, pp. 79–85, 2014.
- [13] B. Luzheng and C. Guan, "A review on EMG-based motor intention prediction of continuous human upper limb motion for human-robot collaboration," *Biomedical Signal Processing and Control*, vol. 51, pp. 113–127, May 2019.
- [14] D. Roetenberg, H. Luinge, and P. Slycke, "Xsens MVN : Full 6DOF Human Motion Tracking Using Miniature Inertial Sensors," *Hand, The*, no. January 2009, pp. 1–7, 2009.
- [15] C. Malleson, A. Gilbert, M. Trumble, J. Collomosse, A. Hilton, and M. Volino, "Real-time full-body motion capture from video and IMUs," in *2017 International Conference on 3D Vision (3DV)*. IEEE, Oct. 2017.
- [16] T. von Marcard, R. Henschel, M. J. Black, B. Rosenhahn, and G. Pons-Moll, "Recovering accurate 3d human pose in the wild using IMUs and a moving camera," in *Computer Vision – ECCV 2018*. Springer International Publishing, 2018, pp. 614–631.
- [17] M. Kok, J. D. Hol, and T. B. Schön, "Using Inertial Sensors for Position and Orientation Estimation," 2017.
- [18] A. Filipposchi, N. Schmitz, M. Miezal, G. Bleser, E. Ruffaldi, and D. Stricker, "Survey of motion tracking methods based on inertial sensors: A focus on upper limb human motion," *Sensors*, vol. 17, no. 6, p. 1257, Jun. 2017. [Online]. Available: <https://doi.org/10.3390/s17061257>
- [19] S. Liu, L. Wang, and X. V. Wang, "Sensorless haptic control for human-robot collaborative assembly," *CIRP Journal of Manufacturing Science and Technology*, vol. 32, pp. 132–144, Jan. 2021.
- [20] L. Rozo, S. Calinon, D. G. Caldwell, P. Jimenez, and C. Torras, "Learning physical collaborative robot behaviors from human demonstrations," *IEEE Transactions on Robotics*, vol. 32, no. 3, pp. 513–527, Jun. 2016. [Online]. Available: <https://doi.org/10.1109/tro.2016.2540623>
- [21] P. Evrard, E. Gribovskaya, S. Calinon, A. Billard, and A. Kheddar, "Teaching physical collaborative tasks: object-lifting case study with a humanoid," in *2009 9th IEEE-RAS International Conference on Humanoid Robots*. IEEE, Dec. 2009.
- [22] A. Mörtl, M. Lawitzky, A. Kucukyilmaz, M. Sezgin, C. Basdogan, and S. Hirche, "The role of roles: Physical cooperation between humans and robots," *International Journal of Robotics Research*, vol. 31, no. 13, pp. 1656–1674, 2012.
- [23] U. Robots. (2021) Real-time data exchange guide. [Online]. Available: <https://www.universal-robots.com/articles/ur-interface-communication/real-time-data-exchange-rtde-guide/>



# WORK IN PROGRESS: LEARNING FUNDAMENTAL ROBOTICS CONCEPTS THROUGH GAMES AT BACHELOR LEVEL

---


Gizem Ateş

Work in Progress: Learning Fundamental Robotics Concepts Through Games at Bachelor Level. Published in Proceedings of the 2022 *IEEE Global Engineering Education Conference (EDUCON)* IEEE, March 28-31, 2022 DOI: [10.1109/EDUCON52537.2022.9766499](https://doi.org/10.1109/EDUCON52537.2022.9766499)

*“In reference to IEEE copyrighted material which is used with permission in this thesis, the IEEE does not endorse any of Western Norway University of Applied Sciences’s products or services. Internal or personal use of this material is permitted. If interested in reprinting/republishing IEEE copyrighted material for advertising or promotional purposes or for creating new collective works for resale or redistribution, please go to [http://www.ieee.org/publications\\_standards/publications/rights/rights\\_link.html](http://www.ieee.org/publications_standards/publications/rights/rights_link.html) to learn how to obtain a License from RightsLink. If applicable, University Microfilms and/or ProQuest Library, or the Archives of Canada may supply single copies of the dissertation.”*



# Work in Progress: Learning Fundamental Robotics Concepts Through Games at Bachelor Level

Gizem Ateş 

Dept. of Computer Science, Electrical Engineering and Mathematical Sciences,  
Western Norway University of Applied Sciences,  
Førde, Norway

**Abstract**—Increasing amounts of robotics applications and possible job opportunities in the industry within the robotics field encourage more universities to involve robotics subject in their current programs or incorporate robotics engineering as a new department. This highlights the importance of comprehensible robotics teaching for more people with various levels of technical background. One of the major subjects at the university level in robotics education is representing the physical robot model using mathematical notations. The majority of the current teaching methods of robotics theory for undergraduate students use conventional approaches from robotics books which relies on 3D pictures and sketches for illustration. There are a few modern approaches where the book chapters are linked to supplemental videos, however, the lack of interaction diminishes the student engagement. Moreover, there are some simulators to enhance visual and interactive skills, but they are either costly or robot specific and require adequate competence of programming skills on the associated programming language. In this paper, a serious game to be used in robotics teaching for bachelor students with various technical backgrounds is presented. The game combines the traditional notations in robot modelling with a gamified approach so that the students can comprehend and imagine easier.

**Index Terms**—Robotics Education, Serious Games, Kinematics, Robot Operating System, Robot Modelling, Denavit-Hartenberg

## I. INTRODUCTION

Robotics is a subject which is taught in various engineering departments such as mechanical, electronics, computer, and automation engineering. It can also be constituted as a stand-alone engineering department in some institutes. Depending on the main focus of the parent department or the objectives of the degree, the content varies [1]. Some contents are accepted as the core subject and taught in every approach such as robot programming, modelling, or mechatronics [2].

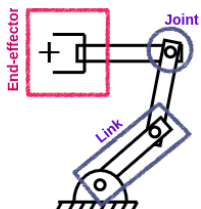


**Fig. 1:** Links and joints definitions on a robot arm

Constructing a mathematical model of a robot arm (i.e. kinematic modelling) is one of the most fundamental subjects in robotics at the bachelor level. A robot arm consists of joints and links connected sequentially from a fixed ground to the robot hand (end-effector) as shown in fig. 1. Denavit-Hartenberg (DH) notation [3] is a universally used kinematic modelling representation for robot arms. It relies on describing each joint relative to the previous one based on translations and

rotations based on 4 parameters. Those parameters are shown in fig. 2. Although kinematic modelling of a robot arm using DH-notation is methodologically straightforward, robotics students struggle to learn it, intuitively comprehend it and visually connect which mathematical representation reflects what type of design criteria and/or the motion capability.

Serious Games and Simulations (SSGs) can be used to create supplemental learning tools that are engaging with interactive learning opportunities and can provide visualization of the concepts that make them easier to translate knowledge [4]–[6]. This paper provides a potential solution that is a gamified experience of robot modelling in various configurations. It provides opportunities for students to experiment with how changing parameters affects the robot in task-based training.

## II. BACKGROUND

Robotics teaching is applied in a wide age range [1], [2], [7], [8]. It is common to use robotics as a tool in teaching STEM (Science, Technology, Engineering and Math) related subjects to increase student engagement at early ages as well as to teach robotics elements at a basic level. Tools used in primary schools and at the K-12 level such as Lego Mindstorm, Evobot and Turtlebot commonly have high human-robot interaction, focus on gamified learning and the outcomes are easy to visualize for students. The learning objectives are at a conceptual and abstract level in this group of students; trigonometric and algebraic calculations mostly do not take place.

The advanced mathematical calculations are covered at the undergraduate and graduate levels in teaching robotics. The conventional books-and-publications based methods are used at this level [2], [8]. Although the gamified approach in teaching robotics has a positive impact on early stages [9], there are few examples of it at higher levels. Moreover, it is observed that students struggle in relating the mathematical expressions with the physical meaning of the robot design and motion. Trigonometric and algebraic calculations in mathematics and classical mechanics in physics underlie robot modelling in the name of *kinematics and dynamics*. These are the most fundamental subjects of robotics at the undergraduate level. The kinematic modelling is widely taught using DH-notation [3] to represent joint poses on a robot arm with respect to the previous joint. The illustration in fig. 2 is a 3D drawing of a part of a robot arm and its *DH-table*. Although this illustration is not intuitive to relate in the real-world meaning

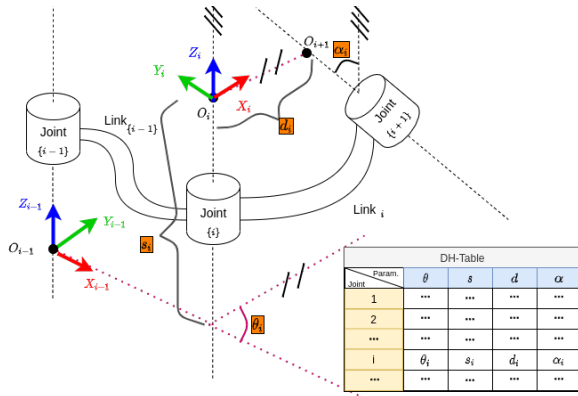


**Fig. 2:** Visualization of a robot section and DH-parameters in conventional teaching methods. Four DH-parameters for joint<sub>*i*</sub>,  $\theta_i, s_i, d_i, \alpha_i$  are highlighted with orange background.

for beginner robotics learners, it is still the most common method of teaching serial robot arms [10]–[13].

Despite the lack of serious games used in robotics teaching at the undergraduate level, there are a few simulators both for testing and development. The author of [14], provides a MATLAB Toolbox for teaching robotics using MATLAB functions [15] in addition to aiding videos referred to in his book. Robotica has a software package for robot analysis in the Mathematica environment [16]. Another interactive software, which allows modelling and simulating robot arms, is presented in [17] also comes with the implementation of a computer-vision algorithm. These software provide comprehensive designing and visualizing platforms, but they require a clear understanding of robot kinematics and dynamics also a sufficient competence of the associated programming language [18]. Additionally, there are simulators developed by the robot vendors such as KUKA, Universal Robots, ABB etc. specific for their robots, but due to high cost and low versatility, they are hardly used for teaching. RoboAnalyzer [19] and Webots [20] examples which are free-of-charge. The RoboAnalyzer is based on 3D models of robots which is developed for teaching and learning robot mechanics. Webots is a development platform focusing on modelling, programming, and simulation of mobile robots. Also, a virtual laboratory for robotics teaching is developed by [21] which allows remote control of robots in the virtual environment. Despite those platforms being useful in robotic teaching, they are either limited to certain robot types or presented as a simulator, hence they do not have a concrete learning path. The platform dependency of the software limits the developed robots to be used in further research. Although MATLAB-based development tools [15], [22] give space for additional research with the compatibility to other toolboxes, the MATLAB software itself is not free-to-use and each toolbox comes with additional cost.

The proposed game is developed in the Robot Operating System (ROS) which is an open-source meta-operating system [23]. There are two main reasons for selecting the ROS environment for developing such a game rather than using common game development engines such as Unity, GameMaker Studio, CryENGINE etc. First, ROS has a large

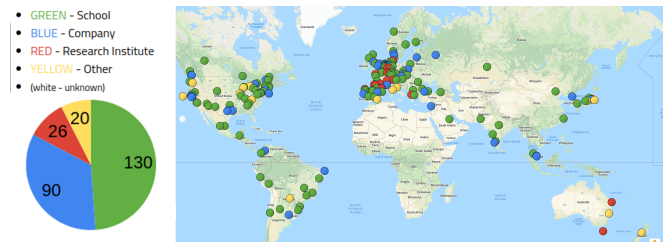


**Fig. 3:** ROS users distribution on location in December 2021  
Source: <http://metrorobots.com/rosmap.html>

user group all around the world (see fig. 3) with a rapid increase every year. There are 127.94% new users who have joined the ROS community between July 2019 - July 2020 [?]. It is getting more popular in robotics teaching in advanced topics such as motion planning, navigation, localization, robot vision, etc. in addition to kinematics and dynamics. It allows the designed custom robot in the proposed game to be used in further research. Second, it is completely open-source, which enables the developed game to be used by more users for free.

### III. METHODOLOGY

The proposed game is a *problem-solving* style of game where the player is supposed to achieve given objectives by solving problems. The game consist of three pillars: **task selection**, **robot design** and **robot interaction**. The objectives are in gradual increasing difficulty and can be selected at the beginning in the task selection. The students should design a robot arm by selecting the correct number of joints, joint types and link lengths to meet the objective requirements in the design screen. Then, the students interact with the robot and observe how the mathematical representation changes. In this section, these pillars and the game setup are explained.

1) **Task Selection:** The game starts with an introduction screen containing questionnaire as game objectives in 6 categories to understand joint types, DH parameters, DoF complexity, workspace, singularity, and optimization. Categorization is constructed in an increasing difficulty and connected to previous task. Each category has 3 to 5 questions, which makes over 700 game paths related to robot design.

2) **Robot Design:** The robot design section in fig. 4 is the first problem-solving step in the game. After selecting the task, the students should plan how many joints (or *degrees of freedom (DoF)*), which type of joints the robot should have and how long the links should be. In this step, the conceptual idea of a link and a joint with specific types is aimed to be introduced to the students. Since the objectives are increasing in difficulty, the students get familiar with the joint types and the effect of link lengths to the design before they are asked to build complex robots up to 7 DoFs in current version.

3) **Robot Interaction:** The goal in this section is to build a systematic correlation between the robot design, robot motion and mathematical expressions. The students can visualize their custom robot, the respective DH-table of the robot and interactively change the joint values as shown in fig. 5. The DH-table is automatically created. The students are supposed to achieve goals and observe the changes based on the task selection which they made at the beginning of the game.

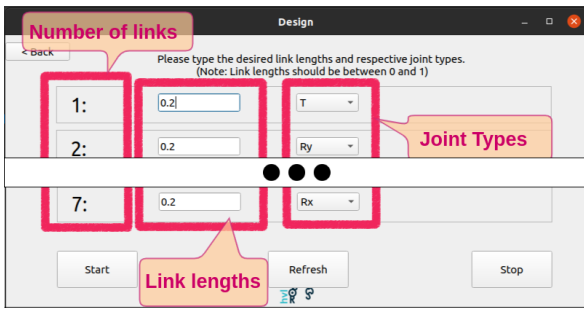


**Fig. 4:** Design: Joint types and link-lengths selection screen

A *workspace* analysis tool is also provided in this section. Every robot arm has a reachable and unreachable region around itself. It is called workspace in robotics terminology. As the number of joints increase, imagining the workspace becomes more complicates. Singularities (configurations in which the robot end-effector becomes blocked in certain directions), collisions and unreachable sub-regions within the workspace are hard to picture in the design step. To enable a visual workspace the robot they create is important to relate how their design choices affect the workspace. Only few examples presented in the literature in robotics teaching has such a feature, which signifies that there is a gap to be filled.

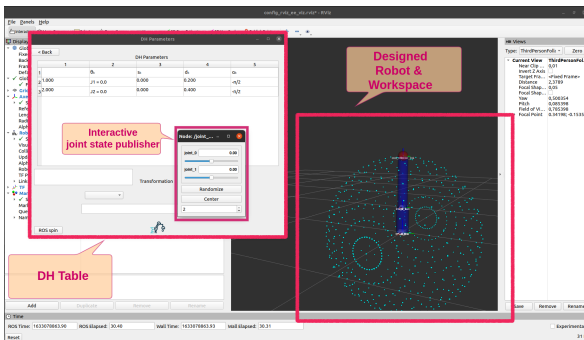


**Fig. 5:** Interact: moving the designed robot, observing mathematical representation and visualizing the workspace

The game uses the design parameters to create the robot model and operates *forward kinematics*, which is the procedure of calculating the pose of the end-effector of a robot arm with given joint values. The students seek an answer where the robot hand will be if certain joint values are set. An example, the visual workspace of a custom 2-DoF robot arm is shown in fig. 5 with light blue dots around the robot.

**GAME SETUP:** The game is developed in ROS Noetic. The graphical user interface is designed using Qt and PyQt5 binding. The task selection screen runs a *ROS node*, which is an executable Python script, to set the goal as a ROS action. A ROS client runs at the background to count score.

#### IV. CONCLUSION AND FUTURE WORK

A novel serious game in the ROS environment is developed so that the students can design various robot arms, challenge themselves with given objectives related to kinematic modelling, interactively play with the designed robot and observe the robot behaviour. The next goal is to evaluate the

effectiveness of the game qualitatively with a questionnaire to robotics lecturers in our institute and quantitatively with statistic approaches.

#### REFERENCES

- [1] A. Bredenfeld, A. Hofmann, and G. Steinbauer, "Robotics in education initiatives in europe-status, shortcomings and open questions," in *Proceedings of international conference on simulation, modeling and programming for autonomous robots (SIMPAN 2010) workshops*, 2010, pp. 568–574.
- [2] F. B. V. Benitti, "Exploring the educational potential of robotics in schools: A systematic review," *Computers & Education*, vol. 58, no. 3, pp. 978–988, Apr. 2012. [Online]. Available: <https://doi.org/10.1016/j.compedu.2011.10.006>
- [3] J. Denavit and R. S. Hartenberg, "A kinematic notation for lower-pair mechanisms based on matrices," *Journal of Applied Mechanics*, vol. 22, no. 2, pp. 215–221, Jun. 1955. [Online]. Available: <https://doi.org/10.1115/1.4011045>
- [4] T. Susi, M. Johannesson, and P. Backlund, "Serious games: An overview," 2007.
- [5] A. Anil Yasin and A. Abbas, "Role of gamification in engineering education: A systematic literature review," in *2021 IEEE Global Engineering Education Conference (EDUCON)*. IEEE, Apr. 2021.
- [6] A. Klefodimos and G. Evangelidis, "Augmenting educational videos with interactive exercises and knowledge testing games," in *2018 IEEE Global Engineering Education Conference (EDUCON)*. IEEE, Apr. 2018.
- [7] D. Scaradozzi, L. Sorbi, A. Pedale, M. Valzano, and C. Vergine, "Teaching robotics at the primary school: an innovative approach," *Procedia-Social and Behavioral Sciences*, vol. 174, pp. 3838–3846, 2015.
- [8] M. J. Mataric, "Robotics education for all ages," in *Proc. AAAI Spring Symposium on Accessible, Hands-on AI and Robotics Education*, 2004, pp. 22–24.
- [9] M. ÜÇGÜL, "History and educational potential of lego mindstorms nxt," *Mersin Üniversitesi Eğitim Fakültesi Dergisi*, vol. 9, no. 2, 2013.
- [10] K. M. Lynch and F. C. Park, "Modern robotics." Cambridge University Press, 2017, ch. Appendix-C, p. 586.
- [11] P. Corke, "Robotics, vision and control: fundamental algorithms in matlab." Springer, 2011, ch. 7.4, p. 219, [Second Edition].
- [12] B. Siciliano and O. Khatib, "Springer handbook of robotics (second edition)," B. Siciliano and O. Khatib, Eds. Springer Berlin Heidelberg.
- [13] Wikipedia, "Denavit-hartenberg parameters," [https://en.wikipedia.org/wiki/Denavit\OT1\textendashHartenberg\\_parameters](https://en.wikipedia.org/wiki/Denavit\OT1\textendashHartenberg_parameters), 2021, [Online; accessed 09-December-2021].
- [14] P. I. Corke and O. Khatib, *Robotics, vision and control: fundamental algorithms in MATLAB*. Springer, 2011, vol. 73.
- [15] P. I. Corke, "A robotics toolbox for matlab," *IEEE Robotics & Automation Magazine*, vol. 3, no. 1, pp. 24–32, 1996.
- [16] J. F. Nethery and M. W. Spong, "Robotica: A mathematica package for robot analysis," *IEEE Robotics & Automation Magazine*, vol. 1, no. 1, pp. 13–20, 1994.
- [17] C. A. Jara, F. A. Candelas, J. Pomares, and F. Torres, "Java software platform for the development of advanced robotic virtual laboratories," *Computer Applications in Engineering Education*, vol. 21, no. S1, pp. E14–E30, 2013.
- [18] S. Ivaldi, V. Padois, and F. Nori, "Tools for dynamics simulation of robots: a survey based on user feedback," *arXiv preprint arXiv:1402.7050*, 2014.
- [19] R. S. Othayoth, R. G. Chittawadigi, R. P. Joshi, and S. K. Saha, "Robot kinematics made easy using RoboAnalyzer software," *Computer Applications in Engineering Education*, vol. 25, no. 5, pp. 669–680, May 2017. [Online]. Available: <https://doi.org/10.1002/cae.21828>
- [20] O. Michel, "Cyberbotics ltd. webots™: professional mobile robot simulation," *International Journal of Advanced Robotic Systems*, vol. 1, no. 1, p. 5, 2004.
- [21] F. A. Candelas, S. T. Puente, F. Torres, F. G. Ortiz, P. Gil, and J. Pomares, "A virtual laboratory for teaching robotics," vol. 1, no. 10, 2003.
- [22] M. Flanders and R. C. Kavanagh, "Build-a-robot: Using virtual reality to visualize the denavit-hartenberg parameters," *Computer Applications in Engineering Education*, vol. 23, no. 6, pp. 846–853, 2015.
- [23] M. Quigley, J. Faust, T. Foote, J. Leibs *et al.*, "Ros: an open-source robot operating system."





# A FRAMEWORK FOR HUMAN MOTION ESTIMATION USING IMUS IN HUMAN-ROBOT INTERACTION

---

Gizem Ateş, Martin Fodstad Stølen & Erik Kyrkjebø

A Framework for Human Motion Estimation using IMUs in Human-Robot Interaction. Published in Proceedings of the 23rd IEEE International Conference on Industrial Technology (ICIT) IEEE, August 22-25, 2022 DOI:[10.1109/ICIT48603.2022.10002746](https://doi.org/10.1109/ICIT48603.2022.10002746)

*“In reference to IEEE copyrighted material which is used with permission in this thesis, the IEEE does not endorse any of Western Norway University of Applied Sciences’s products or services. Internal or personal use of this material is permitted. If interested in reprinting/republishing IEEE copyrighted material for advertising or promotional purposes or for creating new collective works for resale or redistribution, please go to [http://www.ieee.org/publications\\_standards/publications/rights/rights\\_link.html](http://www.ieee.org/publications_standards/publications/rights/rights_link.html) to learn how to obtain a License from RightsLink. If applicable, University Microfilms and/or ProQuest Library, or the Archives of Canada may supply single copies of the dissertation.”*



# A Framework for Human Motion Estimation using IMUs in Human-Robot Interaction

Gizem Ateş<sup>1</sup>, Martin Fodstad Stølen<sup>2</sup>, Erik Kyrkjebø<sup>3</sup>  
*Dept. of Computer Science, Electrical Engineering and Mathematical Sciences,  
Western Norway University of Applied Sciences, Førde, Norway*  
{<sup>1</sup>gizem.ates, <sup>2</sup>martin.fodstad.stolen, <sup>3</sup>erik.kyrkjebo}@hvl.no

**Abstract**—The field of human-robot interaction (HRI) covers a wide range of interactions between humans and robots in various settings. In most cases, both the human and the robot should know the status of each other and interchange data accordingly. Particularly, informing the robot about the human poses and gestures is critical for safe and reliable interaction. We present an open-source inertial measurement unit (IMU)-based human motion estimation framework designed for HRI applications which can be used with multiple robotic systems. The presented framework is developed as a Robot Operating System (ROS) package and takes on a bridge role between the human and the robot by utilizing the estimated human motions to produce a desired robot goal pose. Although there are different human motion tracking systems that are used in gaming, film making, industrial and medical applications today, they are either quite costly, tedious to set up or system dependent. Also, those systems have some limitations to be used in industrial environments such as suffering from occlusion and obstacles between the tracker system and the human, sensitive to light changes etc., and require long calibration steps before each use. The availability of a versatile human motion estimation framework that can be easily used in different HRI scenarios is handy for industrial applications. Some examples of usages of the proposed framework both in simulation and real-world applications are demonstrated in this paper. We aim our package to be a useful boosting tool to develop IMU-based human motion estimated HRI applications and auxiliary templates to develop more complex HRI scenarios for research and development purposes.

**Index Terms**—human-robot interaction, inertial measurement unit, human motion estimation

## I. INTRODUCTION

Robots can perform repetitive, dangerous or high-precision task without getting tired or needing sleep. They are becoming a bigger part of the industrial production processes every day [1]–[4]. Particularly, with the focus on Industry 4.0, the field of robotics have a key role in the development of new and innovative technologies and solutions [5]. Despite great advances in robot decision making by using artificial intelligence [6], [7], robots are still lacking compared to human intelligence when it comes to the replacing humans in the majority of industrial applications.

The field of Human-Robot Interaction (HRI) covers a wide range of interactions between humans and robots either coexisting in the same workspace or working together remotely. In

an industrial context, interactions between humans and robots can be supportive, collaborative or cooperative [8], [9] in the common workspace, or the robots can be remotely controlled by the humans (i.e teleoperation). Robots are excellent for precision, accuracy and repeatability; humans are excellent in decision making and problem solving. From an industrial perspective, HRI focuses on employing the best skills of both the robot and the human working together to achieve a common or shared task more efficiently. As a subcategory of HRI, Human-Robot Collaboration (HRC) is where the human and the robot work with the same objective in the same workspace, but with different leadership roles. The roles can be assigned either statically (human leader and robot follower [10], [11] or vice-versa), or dynamically changing during the task execution [12], [13]. Collaborative robots (COBOTs) are widely used in HRC applications, and have a rapidly increasing market share of new robots sold world-wide. Teleoperation is another application of HRI where the human is the operator of a master system and the robot is a part of the slave system through the whole process. The data transaction can be from human to robot only (unilateral) [14] or it can be both ways (bilateral) [15], [16]. Teleoperated systems are widely used in applications where the environment is dangerous for humans such as in search and rescue missions, military operations, or underwater explorations etc. [17]–[19], and for applications where the robot located at a physical distance from the human operator such as in surgical robotics and tele-rehabilitation [16], [20].

Human motion tracking solutions to estimate human motions and gestures for HRI can be investigated into two categories: visual-based and non-visual-based. Cameras, depth sensors, lasers etc. are common technologies in the visual-based systems, while Inertial Measurement Unit (IMU)s, Ultra-wide Band (UWB)s, radio-transceivers, wearable/attachable strain-gauge systems are part of the non-visual based motion tracking category. Although the accuracy of visual-based solutions in human tracking, especially with the aid of body markers [21], [22] is excellent in some applications, there are still several drawbacks of using them in real HRC applications such as possible obstacles between the capturing device and the tracked body, occlusions, lighting changes in the room, etc. Non-visual-based motion tracking systems do not suffer from any of these issues, but may suffer from drift or other disturbances inherent to their specific sensor

This work was funded by the Research Council of Norway through grant number 280771.

technology.

Inertial Measurement Units are popular devices for non-visual-based motion tracking solutions. There are a number of studies using IMUs as the main motion tracking system [23]–[25] as well studies combining them with different sensor systems such as cameras, UWB, laser IMU for global motion tracking [26]–[28]. In particular, acsimu-based human motion tracking solutions have recently gained popularity due to their portability and ease of setting up [23], [29], [30]. Some of the challenges in using IMUs for motion tracking are drift, sensor noise, and being prone to have big errors during fast motion etc. Nonetheless, recent studies show that IMUs can achieve as reliable results as cameras in human motion tracking [31].

In an HRI scenario, the reliability and the safety of the overall human motion tracking system is important, and the current available human motion tracking solutions have promising capabilities. However, there is not yet a 'perfect' system for every use and application. Available solutions are either environment-dependent or too system-specific, and there is a need for a versatile human motion estimation framework that can interface to several types of collaborative robots, be fast enough to be used in real-time, quick to calibrate, and robust to environmental changes. To our knowledge, there is no such available framework that can be used for both industrial and research applications that with plug-and-play functionality. Therefore, this paper aims to fill this gap by proposing an open-source framework that estimates human motions and gestures based on IMU data, and provides a robot goal pose available for a wide range of COBOTS.

The proposed framework is developed in Robot Operating System (ROS) which is an open-source meta-operating system [32]. The framework can be downloaded as a ROS package from our GitHub page<sup>1</sup>. The ROS environment is fully open-source, have a large user group around the world<sup>2</sup>, and recently approached the industrial segment through the ROS-i project. ROS also supports most robotics and control programs such as MATLAB and LabView.

The paper is structured as follows: section II covers the mathematical representation of how the IMU-based human motions are calculated, and section III shows how the motion and gesture data are processed as an action command to the robot. section IV explains the proposed package structure and how to use it, and section V and section VI demonstrate two example of using the package both for simulation and for real-life robot control. Finally, the paper is concluded and future work is presented in section VII.

Readers only interested in the functionalities and use of the framework can jump to section IV.

## II. IMU-BASED ONLINE HUMAN MOTION ESTIMATION

This section gives the mathematical background of the proposed framework. Estimating human motions is done based on body limb orientations as mentioned in a previous study

[33] rather than as joint positions. First, the individual orientation of each body limb part is obtained before the human biomechanical model is constructed. In this paper, we will use quaternions to represent body limb orientations and rotations.

### A. Quaternion Rotation

There are different ways of representing rotations and translations in robotics [34]. Quaternions provide a continuous, non-singular, and parametrically efficient representation of orientation, and are widely used in robotics. In this section, we present only the necessary background on quaternions needed to understand the basis of the calculations in the framework, and more details can be found in [35], [36].

A quaternion is a 4-dimensional number system ( $q = q_0 + q_1\mathbf{i} + q_2\mathbf{j} + q_3\mathbf{k}$ ) with a real part ( $q_0$ ) and imaginary part ( $\mathbf{q} = q_1\mathbf{i} + q_2\mathbf{j} + q_3\mathbf{k}$ ). It represents a 4D sphere. To define a rotation, it must be constrained on the unit sphere where the rotated object's (i.e. body part in this case) length remains the same. Therefore, not all quaternions represent rotation but only *unit quaternions* do. A unit quaternion  $\bar{q}$  has a magnitude equal to 1 ( $|\bar{q}| = \sqrt{\bar{q}^* \bar{q}} = \sqrt{q_0^2 + q_1^2 + q_2^2 + q_3^2} = 1$ ) and represents a full 3D orientation. The multiplication of a quaternion with its inverse  $q^{-1}$  yields the identity quaternion ( $q \otimes q^{-1} = q_I = (\bar{q}_I = 1 + 0\mathbf{i} + 0\mathbf{j} + 0\mathbf{k})$ ), which means zero rotation in robotics. The same rotation in opposite direction is defined with its *conjugate* ( $q^* = q_0 - q_1\mathbf{i} - q_2\mathbf{j} - q_3\mathbf{k}$ ), which is the same quaternion with the opposite sign for the imaginary part. For unit quaternions, the conjugate and the inverse are equal ( $\bar{q}^{-1} = \bar{q}^*/|\bar{q}| = \bar{q}^*$ ).

Quaternions can be multiplied together to form a series of rotations – similar to rotation matrices. For instance, a unit quaternion representing the rotation from frame A to frame C via frame B can be represented as  $q_{CA} = q_{CB} \otimes q_{BA}$ . This is particularly important in constructing the kinematic model of the articulated human arm as well as sensor-to-body frame representations.

### B. From Quaternions to Human Biomechanical Model

A human bio-mechanical model can be constructed with a complexity determined by its use. The proposed framework focuses on chest-to-hand motion estimation for two hands. In section III-A and III-B, we explain how the human bio-mechanical model is slightly changed based on its purpose for the particular application. Regardless of the use case, the process of building the model is the same. In this section, we give the theory of chest-to-hand motion estimation for the most comprehensive scenario. The details of the mapping in different use cases are explained in the next subsections.

The measurements from the IMUs provide the raw orientation data from each sensor in the global frame to sensor frame. The calibration process is the first step of translating the quaternion output from the IMUs into human model. It is based on eliminating the 'bias' of the sensor measurements on a fix position and assigning predefined human joint angles in a known posture. Currently, the very last sample of a 4-seconds data collected at 100 Hz is assigned as the calibration

<sup>1</sup>[https://github.com/frdedynamics/imu\\_human\\_pkg](https://github.com/frdedynamics/imu_human_pkg)

<sup>2</sup><http://metrorobots.com/rosmap.html>

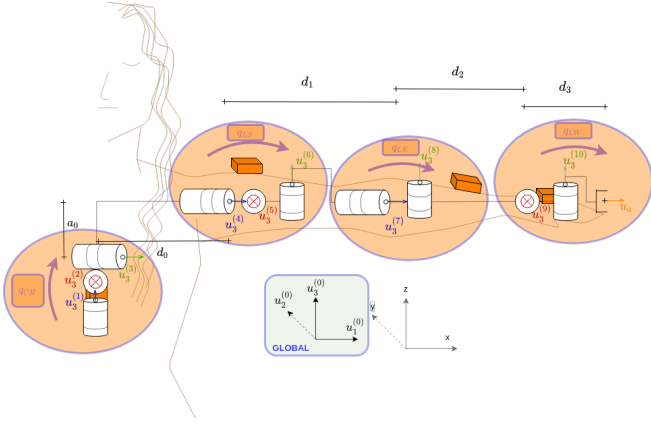


**Fig. 1:** Left arm biomechanical model with 3-DoF chest, 3-DoF shoulder, 2-DoF elbow and 2-DoF wrist. The orange cubes represents the IMUs,  $q_{XX}$  are raw orientation readings of each IMU for the respective human joint,  $d_x$  and  $a_x$  are the joint offsets. The mechanical joint illustrations are given with cylindrical shapes and each represents one revolute joint with the main axis  $u_3^F$  where F is the frame number.

quaternion yet a moving average filter implementation on using averaging quaternion [37] method is under development.

After a calibration process, a calibration quaternion from global (G) to sensor (S) frame ( $q_{GS_{cal}}$ ) is used in human joint angle calculation as in eq. (1). Each human joint angle is then calculated as a quaternion rotation between each consecutive body parts as in eq. (2).

$$q_{S(i,t)} = q_{GS_{i,t}}^* \otimes q_{GS_{i,cal}} \quad (1)$$

$$q_{joint_i} = q_{joint_{i-1}}^* \otimes q_{S_{i,t}} \quad (2)$$

where  $q_{S_{i,t}}$  is the calibrated sensor orientation at each time step,  $q_{joint_i}$  is the orientation of the  $i^{th}$  joint. The joint angles calculation starts from the chest to the wrists as described in eq. (3). Finally, the bio-mechanical model of the human is constructed as a pair of kinematic chains for both arms using measured body link lengths and calculated joint angles.

$$q_c = q_{CH} \quad (3)$$

$$q_{ls} = q_c^* \otimes q_{LS}$$

$$q_{le} = q_c^* \otimes q_{ls}^* \otimes q_{LE}$$

$$q_{lh} = q_c^* \otimes q_{ls}^* \otimes q_{le} \otimes q_{LH}$$

where the asterisk denotes the quaternion conjugate,  $q_c, q_{ls}, q_{le}, q_{lh}$  are human joint angles, and  $q_{CH}, q_{LS}, q_{LE}, q_{LH}$  are calibrated IMU readings of chest, left-shoulder, left-elbow, left-hand, respectively. The same calculation applies for right-arm joint angles.

### III. MAPPING HUMAN MOTIONS TO ROBOT GOAL POSE

Two arm motions are merged to create a robot pose. In the default use, the left-arm is assigned as the main and the right-arm as the secondary in the merge process. This assignment can be changed in the package. To generalize, we will use

*main arm/hand* and *secondary arm/hand* through the rest of the paper.

For mapping human motions to robot goal poses, we show the mapping for the two categories of HRI; teleoperation and HRC. For these two mappings, the human bio-mechanical model is calculated slightly different. In the teleoperation scenario the human teleoperates the robot to manipulate some objects on a table. In this case, both the position and the orientation of the end effector matters. The merged arm motions are mapped as robot goal position with respect to its base and the main hand orientation is assigned as end-effector orientation. In the HRC scenario, the human and the robot carries a table cooperatively. The initial orientation of the robot end-effector is kept stable unless the robot has the leader role and change its end-effector orientation itself. The combination of two arms motions are mapped as robot goal position with respect to its base and no human motion is assigned for end-effector orientation.

There are three main reasons of using two arms rather than one:

- 1) The secondary hand can be assigned a "clutching" role that triggers state changes in a HRC application. This means that while the main hand motion is mapped to be the desired robot motion, the secondary arm/hand gestures can be assigned to control different functionalities such as stopping the robot movement in case of emergency and/or changing the system state to make the robot move in with different motion characteristic.
- 2) The combination of two hands in relative motion mapping can be used as a correction of the main hand. This is particularly valuable in cooperative lifting applications. When one hand of the human is about to grasp the common object to lift, the secondary hand-motions can be used to correct the robot's position to the correct grasping point.
- 3) Since most of the commercially available robot manipulators have a different kinematic structure than the human arm anatomy, a perfect anthropomorphic motion mapping is challenging [38]. There is a trade of between joint space mapping and task space mapping due to the complexity neurobiomechanical processes underlying in object manipulation. Although, the majority of the direct control examples in the literature relies on task space mapping, the differences in robot's and human's workspace cause an additional complexity. Therefore, the combination of two-arm motions, rather than a one-to-one mapping of the human arm to robot arm motion, eliminates this anthropomorphic confusion.

We used relative chest-to-hands motion mapping to change the goal pose of the robot. By doing that, the human has more opportunities for fine adjustment than if we assigned a posture to be one particular robot goal pose statically. The mapping starts with an initial human-to-robot mapping such that the human takes a predefined posture to be set as the starting posture, and the robot moves to its *home* configuration. The

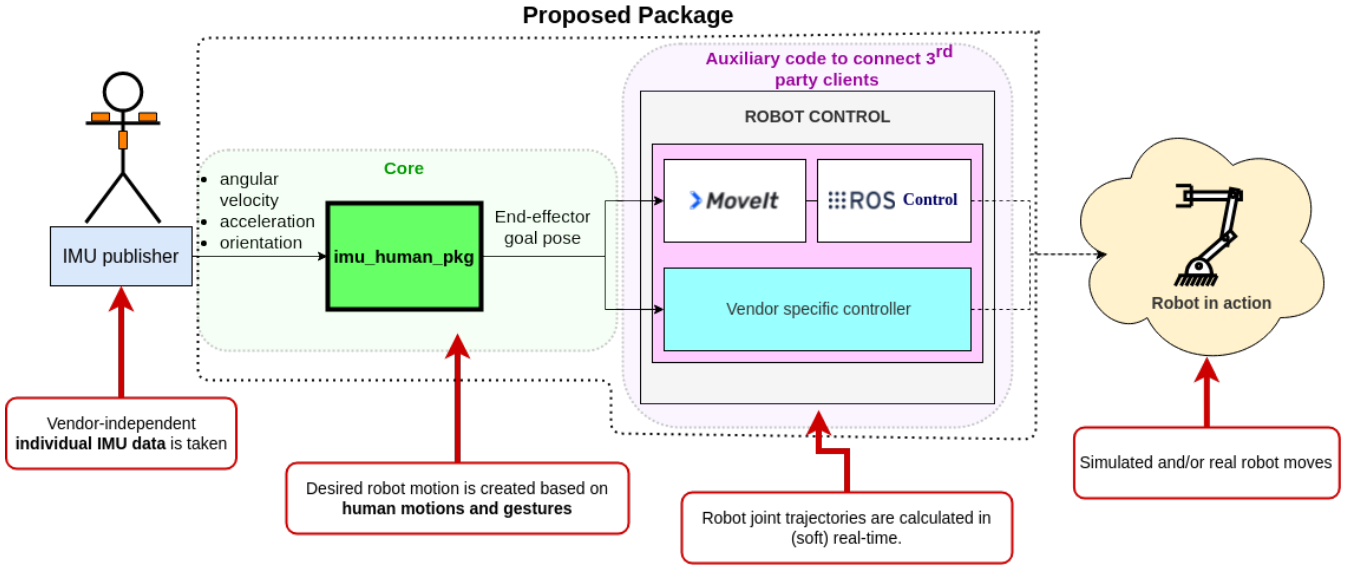


**Fig. 2:** Overview of the proposed package. The human wears the IMUs as instructed in the package. Motion parameters are obtained and processed by the core of the package. Chest-to-hands individual motions are merged and published as a single end-effector goal pose. This goal pose can be either used by ROS controllers to determine joint efforts or by a vendor-specific controller. Finally, the robot takes an action accordingly.

initial postures of both hands are then mapped as in eq. (4)

$$\left[ \hat{P}_{hm,(t=0)} \times \hat{P}_{hs,(t=0)} \right] = \hat{P}_{h,(t=0)} \quad (4)$$

where  $\hat{P}_{hm}$ ,  $\hat{P}_{hs}$  and  $\hat{P}_r$  are Homogeneous Transformation Matrix (HTM) representing human main hand, human secondary hand and robot end-effector poses, respectively. The main and secondary hand motions differ from each other by their contribution to the merged hands calculation with a scale. The robot goal pose is calculated based on the relative position change of the merged hand pose  $\hat{P}_{h,t}$ ,

$$\hat{P}_{h,t}^- = \hat{s} \cdot (\hat{P}_{hm,t=0}^{-1} \times \hat{P}_{hm,t}) + \hat{k} \cdot (\hat{P}_{hs,t=0}^{-1} \times \hat{P}_{hs,t}) \quad (5)$$

where  $\hat{P}_{h,t}^-$  is the merged hand pose. To get an approaching behaviour from the robot rather than escaping behaviour, the y-axis in  $\hat{P}_{h,t}^-$  is inverted and  $\hat{P}_{h,t}$  is used to control the approach of the robot. A 4x4 scaling matrix for the main hand  $\hat{s}$  has the last row equal to  $[s_x s_y s_z 1]$  with the rest of the elements as 1. The scaling matrix  $\hat{k}$  is defined similarly for the secondary hand. The robot goal pose based on the combined hand pose as  $\hat{H}(t)$  is

$$\hat{H}(t) = \hat{P}_{h,(t=0)}^{-1} \times \hat{P}_{h,t} \quad \hat{P}_{r,t} = \hat{P}_{r,(t=0)} \times \hat{H}(t) \quad (6)$$

We can now do human-to-robot motion mapping for two examples of HRI by changing the role of the hands in collaborative lifting and in teleoperation. In both scenarios, relative motion mapping starts with the initial mapping as in eq. (4) and then differs as shown in the following.

#### A. Teleoperation Scenario

In a teleoperation scenario, the human has full control over the robot end-effector position and orientation. The human can

make the robot manipulate objects remotely as in fig. 5. To avoid anthropomorphic confusion, the control of the orientation and position assignments are divided such that only the change of the main hand wrist motion controls the end-effector orientation and the change of merged hand position from two hands is mapped as the end-effector position as shown in eq. (7).

$$\hat{H}(t) = \left[ \begin{array}{ccc|c} \hat{P}_{hm}[0,0] & \hat{P}_{hm}[0,1] & \hat{P}_{hm}[0,2] & \hat{P}_h[0,3] \\ \hat{P}_{hm}[1,0] & \hat{P}_{hm}[1,1] & \hat{P}_{hm}[1,2] & \hat{P}_h[1,3] \\ \hat{P}_{hm}[2,0] & \hat{P}_{hm}[2,1] & \hat{P}_{hm}[2,2] & \hat{P}_h[2,3] \\ \hline 0_{(1 \times 3)} & & & 1 \end{array} \right] \quad (7)$$

where  $\hat{H}(t)$  is the transformation matrix for the robot from its initial pose to the current desired pose,  $\hat{P}_{hm}$  is the HTM of the main hand and  $\hat{P}_h$  is merged hands HTM as calculates in eq. (4) from initial to current with respect to chest, respectively.

Two arm motions are estimated using in total 6 IMUs; on chest, left/right upper arms, left/right forearms, and main hand. Secondary-hand motion is assumed to be rigid with respect to its wrist.

The teleoperation scenario is based on mimicking human motions in the most simplistic way without the complexity of task-specific states. However, often teleoperating the robot in a leader-follower (master-slave) approach is not the most efficient method of HRI, especially in industrial applications. The different strengths of human workers and robots make them good at different tasks. While robots are durable, precise and repeatable, humans have excellent problem-solving skills and are creative in their decision-making. They can change

roles in different stages of the task depending on their stronger skills. This scenario is covered in the next subsection.

### B. Human-Robot Cooperation Scenario

The field of HRC covers a wide range of cooperations between humans and robots where they can change the leadership roles during the task depending on their skill level. Cooperative lifting (co-lift) is a widely studied application of physical HRC where a robot and a human carry a common object from one point to another as shown in fig. 6. It is a versatile use case that is a part of various industrial applications as well as an example of how to change between different states of a predefined task. The co-lift scenario contains 4 states; APPROACH, COLIFT, RELEASE and IDLE [23]. The APPROACH is where human and robot approaches the common object in human leadership affiliates the human decision making skill. The COLIFT state is where the human and the robot lifts the common object and manipulate it cooperatively with shared leadership. The RELEASE state exploits the robot's precision and repeatability, and where the co-lifted object is released onto a predefined location under robot leadership. On top of that, the IDLE state is a cut-off safety state which the human can trigger at any time by using the clutching motion (secondary-hand palm rotate upwards) to stop motion mapping from human to the robot in case of emergency.

Two-arm motions are estimated using a minimum of 5 IMUs; on chest, left/right upper arms and left/right forearms. Since the orientation of the robot end-effector does not change while the human is taking the leader role, the 6<sup>th</sup> IMU on the main hand wrist which is attached in the teleoperation scenario is not needed. Both main and secondary-hand motions are assumed to be rigid with respect to their respective wrists.

Different from the teleoperation case, in a cooperative lifting scenario, we immobilize the end-effector orientation and set it to an initial orientation which can only be changed if the robot is assigned a leader role in the cooperation. It cannot be changed based on human hand orientations. Therefore, we assign a robot goal position by merging two hand positions and keeping the end-effector orientation stable as in eq. (8).

$$\hat{H}(t) = \left[ \begin{array}{ccc|c} \hat{P}_{r,t=0}[0,0] & \hat{P}_{r,t=0}[0,1] & \hat{P}_{r,t=0}[0,2] & \hat{P}_h[0,3] \\ \hat{P}_{r,t=0}[1,0] & \hat{P}_{r,t=0}[1,1] & \hat{P}_{r,t=0}[1,2] & \hat{P}_h[1,3] \\ \hat{P}_{r,t=0}[2,0] & \hat{P}_{r,t=0}[2,1] & \hat{P}_{r,t=0}[2,2] & \hat{P}_h[2,3] \\ \hline & 0_{(1 \times 3)} & & 1 \end{array} \right] \quad (8)$$

where  $\hat{P}_{r,t=0}$  is the HTM of the initial pose of the end-effector with respect to robot base.

## IV. THE PACKAGE AND FUNCTIONALITIES

The proposed `imu_human_pkg` has `imu_human_class` node as the backbone of the overall system. This node takes on a constructing role from individual IMU topics to the human body model. The human model publishes the transformation of each body link frame at 100 Hz. To map human motions to robot goal pose, a 4-second calibration

process is needed, where the user stands still in a fixed position (two arms are released down), each IMU reading is registered with the "Calibrate Human" button in the Actions Groupbox as shown in fig. 3. After the human calibration process, the "Connect to Robot" button is automatically activated and human-to-robot initial mapping is computed. This action starts the node publishing the  $\hat{H}$  transformation matrix in eq. (7) and eq. (8) depending on the type of the task (i.e. teleoperation or cooperative lifting). Different types of the robot environment (i.e. simulated or real) and the necessary robot nodes can be started at this point. The required buttons are activated in an order. Some representative robot examples are also included in the package (see fig. 2).

### A. Main Graphical User Interface (GUI)

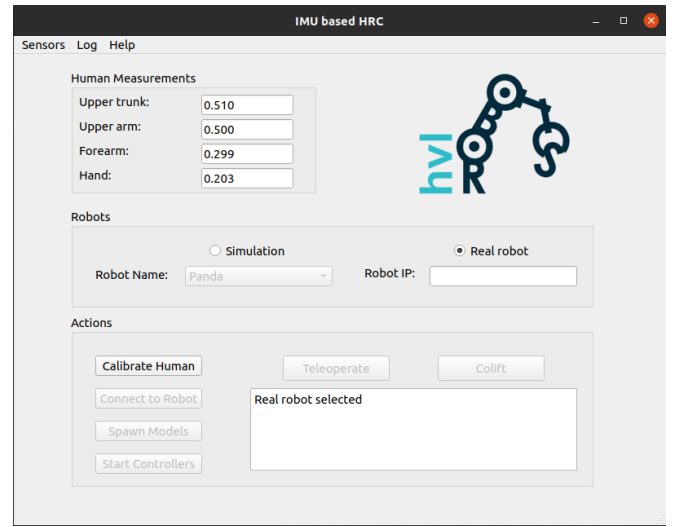


Fig. 3: Main Screen

To provide an easy to use platform, a Graphical User Interface (GUI) is provided. The main window has 3 selections on the toolbar and 3 group boxes in the main layout. Each selection both on the toolbar and in the layout is setting a parameter in a ROS node/launch or a YAML file. The system then calls the respective scripts with proper arguments.

**Human Measurements Groupbox:** This group box is where the user enters upper-body human measurements. The default values are provided based on [39]. In fact, accuracy within a couple of centimetres is not critical because human motions are mapped relative to the robot motions. However, in position-critical applications, it is important to use the measured values rather than default ones.

**Robots Groupbox:** It is possible to control either a simulated robot selected from the dropdown menu or a real robot connected via Ethernet. Both simulated and the real robot cannot work at the same time in this version of the package. Therefore, based on the selection, the other option is disabled.

**Actions Groupbox:** All the actions such as calibration, human-robot initial pose initiation, human-robot motion mapping, teleoperation and cooperation. The actions which cannot

be executed at the same time as some other actions or require some actions to be done beforehand are disabled in default. Also in this way, the user does not need to remember the orders of the actions since the buttons are automatically activated as the requirements are met.

### B. Sensor Selection

In this paper, we used Xsens Awinda wireless Inertial Measurement Units as the main Inertial Measurement Unit system. The 3D orientation output is provided by the Xsens device firmware [40]. The Xsens node can be started directly from the GUI.

In addition to that, the package is not sensor-specific, which means that any sensor providing orientation data as `sensor_msgs/Imu` can be easily implemented in the *Sensors* dialog box as shown in fig. 4. Sensors dialog is a one-time-set additional dialog window that can be opened from the toolbar → sensors → custom IMU sensors.

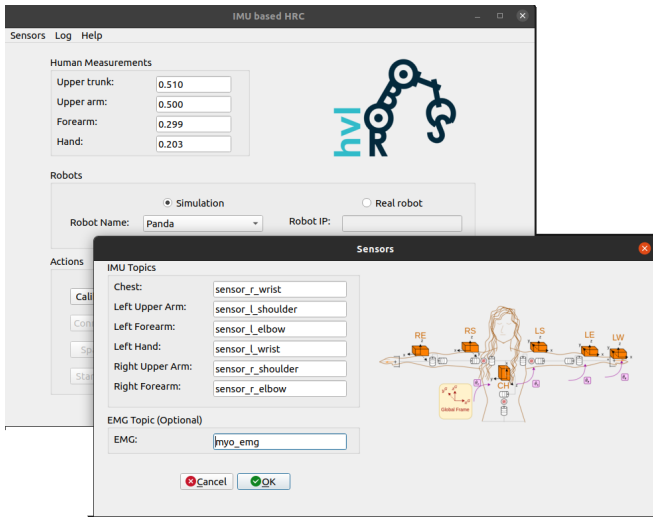


Fig. 4: Sensor selection dialog window

If it is desired to control the gripper, there is an EMG sensor topic slot. A MYO armband EMG sensor can be worn by either arm to control gripper motion by clenched punch and release gestures. Since there are some state changes based on the gripper position in cooperative lifting example, it is a necessity only for this use case, otherwise, it is optional.

### V. EXAMPLE CASE-1: TELEOPERATION IN SIMULATION

The package provides example usages of estimated upper-body human motions and gestures with various robots in different environments. RViz [41] is the main visualization tool in the ROS environment. Most of the ROS-i [42] packages provide a robot model which can be visualized on RViz by setting the *robot description* parameter. Our package provides a *human description* additionally which can be visualized in the same space and rooted from the same parent world frame. The human description is an automatically created XACRO

file based on the human measurements entered in the main user interface (fig. 3).

To manipulate the visualized robot in the task space, MoveIT [43] is a commonly used framework that consists of several ROS packages. The robot goal is achieved by planning the optimal trajectory, depending on the planning criteria, within MoveIT. Our package provides the end robot goal pose based on two arm motions. Although the main objective of the MoveIT platform is not achieving a hard real-time manipulation, it still gives satisfactory results for preliminary tests, especially in simulated environments.

Additionally, some ROS-i packages provide Gazebo simulated robot models which include the inertia and collision properties of the robot. Therefore, Gazebo simulated cases give more realistic approaches. For this purpose, we provide a custom human Gazebo model in this package. As an example use case of a Gazebo simulated Franka Emika Panda robot teleoperated with human upper-body motions as shown in fig. 5 is included in the package as an auxiliary code.

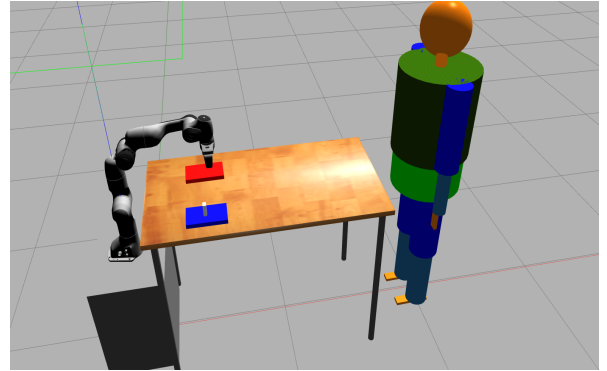


Fig. 5: A teleoperation example using Panda to manipulate objects on the table in Gazebo

### VI. EXAMPLE CASE-2: HRC IN REAL WORLD

As an example of how to use the proposed package in real-world applications, we provide the auxiliary code of a cooperative lifting scenario with Universal Robots UR5e manipulator as shown in fig. 6 [23]. The robot is connected to the master PC with an Ethernet cable. The robot IP is specified in the "Robots Groupbox" in fig. 3. The real-time robot commands are computed using Universal Robots Real-Time Data Exchange (UR-RTDE) [44] protocol. UR-RTDE allows sending various joint and end-effector commands via C++ and Python API. We provided how to utilize the generated robot end-effector pose using *servo control* in the package.

The co-lift example of the proposed package has been validated and the results are presented in our related study [23]. In fig. 7, the real-time motion data of both robot end-effector and human hands from a full co-lift cycle is shown. The robot response to human merged hands input is visible particularly in APPROACH state, which is belong to HUMAN LEADING role in HRC. The actual robot motion curve represented in red straight line follows the same character as the merged



hands motion curve represented in green plus-signed line. Also the merged hands curve is seen as an even combination of both hands since the multiplier coefficients  $\hat{s}$  and  $\hat{k}$  in eq. (5) are selected 1 for this demonstration. The same human-robot motion match is not visible in other states as in APPROACH state because; 1) there is not human-to-robot motion transfer in IDLE state, 2) the robot is not directly driven by human motions in COLIFT state but it decides its own motions in a certain degree by taking a part in SHARED CONTROL, 3) the robot motion is completely independent from the human hand motions in RELEASE state since the robot has the full leadership role. Note that the merged hands position is no longer updated since it is not needed after the APPROACH state.

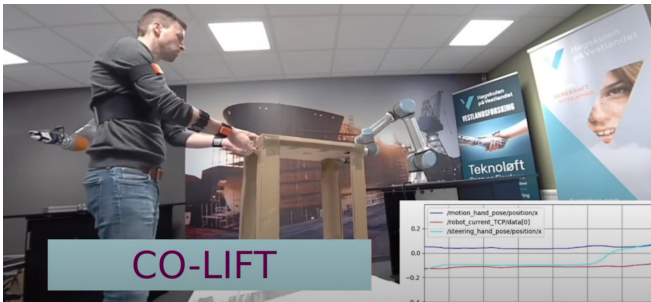


**Fig. 6:** A co-lift experiment using IMUs for human motion estimation and an EMG-sensor to open/close the robot gripper. A frame of the real-time human hand motions and robot end-effector pose is shown on the right bottom corner.

Source: <https://www.youtube.com/watch?v=0BLS0e2amw4>

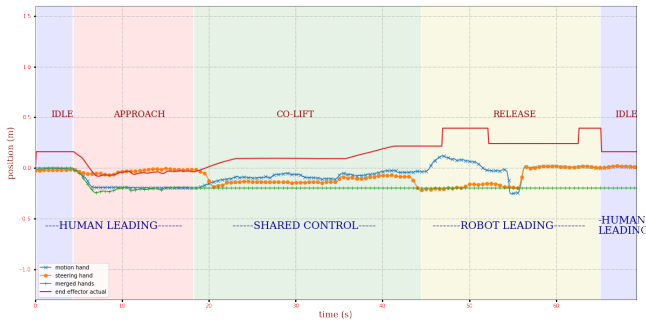


**Fig. 7:** Motion of the hand positions calculated as stated in eq. (5) and the actual robot end-effector in a full cycle co-lift example. Lines show position change on z-axis - which is chosen as in opposite direction of the gravity vector- for motion hand  $\hat{P}_{hm}$  (blue cross), steering hand  $\hat{P}_{hs}$  (orange dot), merged hands  $\hat{P}_h$  (green plus). The actual end-effector pose is shown in red straight line.

(The figure is taken from [23] with authors' permissions.)

## VII. CONCLUSION AND FUTURE WORK

In this study, we presented an open-source generic framework for HRI based on IMU estimated human motions for

HRI applications. Our target is to provide a base where human motions are required to manipulate a robot arm and/or cooperate with it and construct a bridge platform to be used easily in HRI applications and in further HRI research. We aim to facilitate usability by providing an interactive GUI. For more advanced access, the source code is also provided.

The main purpose of this package is to provide a robot goal pose based on human motions. Additionally, there are more information available as ROS topics than only the robot goal pose, such as individual arm poses, upper-body human joint angles, elbow heights etc. Therefore, the package promises a wide range of further research opportunities in various areas.

The package is in the early stage of the development process. It currently contains the core utilities and a few example use cases. Most of the advanced functionalities are available in the source code but the GUI connection of some functionalities are still in progress. There are several planned improvements that could facilitate the use of the package even further. We will add supports for more robots and example tasks to provide a variety in using the system for different applications. Human-to-robot workspace scaling by changing the contribution of main/secondary hands in merged hand motion calculations, changing the hand directions etc. can be defined in the source code but they are not interactable via GUI yet. Connecting those extra functionalities to the GUI application as well as mapping a different human gesture to a robot action assignment option via GUI is also in our future plans. Moreover, the human model is created using only revolute joints. The translational motions due to muscle contractions and soft tissue artifacts are neglected in this version. We will include Bayesian filtering based stochastic approaches to enhance human motion estimation such as in [45], [46].

Overall, the proposed package plays a bridging role between the human motions and the robot actions. It can readily be used for basic applications where upper body human motions are required to be mapped to robot end-effector pose. We believe that this package has the potential to play a key role in HRI applications both in industry and research areas.

## REFERENCES

- [1] E. Eric, A. Geuna, M. Guerzoni, and M. Nuccio, "Mapping the evolution of the robotics industry: A cross country comparison," 2018.
- [2] J. IQBAL, Z. H. KHAN, and A. KHALID, "Prospects of robotics in food industry," *Food Science and Technology*, vol. 37, no. 2, pp. 159–165, May 2017. [Online]. Available: <https://doi.org/10.1590/1678-457x.14616>
- [3] A. Grau, M. Indri, L. L. Bello, and T. Sauter, "Industrial robotics in factory automation: From the early stage to the internet of things," in *IECON 2017-43rd Annual Conference of the IEEE Industrial Electronics Society*. IEEE, 2017, pp. 6159–6164.
- [4] —, "Robots in industry: The past, present, and future of a growing collaboration with humans," *IEEE Industrial Electronics Magazine*, vol. 15, no. 1, pp. 50–61, 2020.
- [5] M. Indri, A. Grau, and M. Ruderman, "Guest editorial special section on recent trends and developments in industry 4.0 motivated robotic solutions," *IEEE Transactions on Industrial Informatics*, vol. 14, no. 4, pp. 1677–1680, Apr. 2018. [Online]. Available: <https://doi.org/10.1109/tii.2018.2809000>

- [6] T. Dhanabalan and A. Sathish, "Transforming indian industries through artificial intelligence and robotics in industry 4.0," *International Journal of Mechanical Engineering and Technology*, vol. 9, no. 10, pp. 835–845, 2018.
- [7] J. Ribeiro, R. Lima, T. Eckhardt, and S. Paiva, "Robotic process automation and artificial intelligence in industry 4.0 – a literature review," *Procedia Computer Science*, vol. 181, pp. 51–58, 2021. [Online]. Available: <https://doi.org/10.1016/j.procs.2021.01.104>
- [8] B. Siciliano and O. Khatib, "Physical Human-Robot Interaction," in *Springer Handbook of Robotics*. Springer, 2016, ch. 69, pp. 1835–1874.
- [9] E. Kyrkjebø, B. L. Rodriguez, G. Ateş, J. Møgster, D. Schüle, M. Drewniak, and A. Ziebinski, "The potential of physical human-robot cooperation using cobots on agvs in flexible manufacturing," *MIC Journal (Submitted)*, 2022.
- [10] S. Liu, L. Wang, and X. V. Wang, "Sensorless haptic control for human-robot collaborative assembly," *CIRP Journal of Manufacturing Science and Technology*, vol. 32, pp. 132–144, Jan. 2021.
- [11] L. Rozo, S. Calinon, D. G. Caldwell, P. Jimenez, and C. Torras, "Learning physical collaborative robot behaviors from human demonstrations," *IEEE Transactions on Robotics*, vol. 32, no. 3, pp. 513–527, Jun. 2016. [Online]. Available: <https://doi.org/10.1109/tro.2016.2540623>
- [12] P. Evrard, E. Gribovskaya, S. Calinon, A. Billard, and A. Kheddar, "Teaching physical collaborative tasks: object-lifting case study with a humanoid," in *2009 9th IEEE-RAS International Conference on Humanoid Robots*. IEEE, Dec. 2009.
- [13] A. Mörtl, M. Lawitzky, A. Kucukyilmaz, M. Sezgin, C. Basdogan, and S. Hirche, "The role of roles: Physical cooperation between humans and robots," *International Journal of Robotics Research*, vol. 31, no. 13, pp. 1656–1674, 2012.
- [14] M. İ. C. Dede, O. W. Maarroof, G. Ateş, M. Berker, İ. Işıkay, and Ş. Hanalioğlu, "Unilateral teleoperation design for a robotic endoscopic pituitary surgery system," in *International Workshop on Medical and Service Robots*. Springer, 2016, pp. 101–115.
- [15] G. Ateş, L. Brunetti, and M. Bonfè, "Improved usability of a low-cost 5-DOF haptic device for robotic teleoperation," in *ROMANSY 22 – Robot Design, Dynamics and Control*. Springer International Publishing, May 2018, pp. 213–221. [Online]. Available: [https://doi.org/10.1007/978-3-319-78963-7\\_28](https://doi.org/10.1007/978-3-319-78963-7_28)
- [16] G. Ateş, "Teleoperation system design of a robot assisted endoscopic pituitary surgery," Master's thesis, 2018.
- [17] D. S. Drew, "Multi-agent systems for search and rescue applications," *Current Robotics Reports*, pp. 1–12, 2021.
- [18] T. Kot and P. Novák, "Application of virtual reality in teleoperation of the military mobile robotic system taros," *International journal of advanced robotic systems*, vol. 15, no. 1, p. 1729881417751545, 2018.
- [19] P. Xu, Q. Zeng, G. Zhang, C. Zhu, and Z. Zhu, "Design of control system and human-robot-interaction system of teleoperation underwater robot," in *International Conference on Intelligent Robotics and Applications*. Springer, 2019, pp. 649–660.
- [20] E. Appleby, S. T. Gill, L. K. Hayes, T. L. Walker, M. Walsh, and S. Kumar, "Effectiveness of telerehabilitation in the management of adults with stroke: A systematic review," *PloS one*, vol. 14, no. 11, p. e0225150, 2019.
- [21] P. Merriaux, Y. Dupuis, R. Boutteau, P. Vasseur, and X. Savatier, "A study of vicon system positioning performance," *Sensors*, vol. 17, no. 7, p. 1591, Jul. 2017. [Online]. Available: <https://doi.org/10.3390/s17071591>
- [22] A. Pfister, A. M. West, S. Bronner, and J. A. Noah, "Comparative abilities of microsoft kinect and vicon 3d motion capture for gait analysis," *Journal of medical engineering & technology*, vol. 38, no. 5, pp. 274–280, 2014.
- [23] G. Ateş, M. F. Stølen, and E. Kyrkjebø, "Force and gesture-based motion control of human-robot cooperative lifting using imus," in *Proceedings of the 2022 ACM/IEEE International Conference on Human-Robot Interaction*, ser. HRI '22. IEEE Press, 2022, p. 688–692.
- [24] M. Kok, J. D. Hol, and T. B. Schön, "An optimization-based approach to human body motion capture using inertial sensors," *IFAC Proceedings Volumes (IFAC-PapersOnline)*, vol. 19, pp. 79–85, 2014.
- [25] N. Ahmad, R. A. R. Ghazilla, N. M. Khairi, and V. Kasi, "Reviews on various inertial measurement unit (imu) sensor applications," *International Journal of Signal Processing Systems*, vol. 1, no. 2, pp. 256–262, 2013.
- [26] Y. Tian, X. Meng, D. Tao, D. Liu, and C. Feng, "Upper limb motion tracking with the integration of imu and kinect," *Neurocomputing*, vol. 159, pp. 207–218, 2015.
- [27] L. Yao, Y.-W. A. Wu, L. Yao, and Z. Z. Liao, "An integrated imu and uwb sensor based indoor positioning system," in *2017 International Conference on Indoor Positioning and Indoor Navigation (IPIN)*. IEEE, 2017, pp. 1–8.
- [28] Z. Zheng, T. Yu, H. Li, K. Guo, Q. Dai, L. Fang, and Y. Liu, "Hybridfusion: Real-time performance capture using a single depth sensor and sparse imus," in *Proceedings of the European Conference on Computer Vision (ECCV)*, 2018, pp. 384–400.
- [29] D. Roetenberg, H. Luinge, and P. Slycke, "Xsens MVN : Full 6DOF Human Motion Tracking Using Miniature Inertial Sensors," *Hand, The*, no. January 2009, pp. 1–7, 2009.
- [30] M. El-Gohary, L. Holmstrom, J. Huisinga, E. King, J. McNames, and F. Horak, "Upper limb joint angle tracking with inertial sensors," in *2011 Annual International Conference of the IEEE Engineering in Medicine and Biology Society*. IEEE, Aug. 2011. [Online]. Available: <https://doi.org/10.1109/iembs.2011.6091362>
- [31] A. Filippeschi, N. Schmitz, M. Miezal, G. Bleser, E. Ruffaldi, and D. Stricker, "Survey of motion tracking methods based on inertial sensors: A focus on upper limb human motion," *Sensors*, vol. 17, no. 6, p. 1257, Jun. 2017. [Online]. Available: <https://doi.org/10.3390/s17061257>
- [32] M. Quigley, J. Faust, T. Foote, J. Leibs *et al.*, "Ros: an open-source robot operating system."
- [33] G. Ateş and E. Kyrkjebø, "Human-robot cooperative lifting using IMUs and human gestures," in *Towards Autonomous Robotic Systems*. Springer International Publishing, 2021, pp. 88–99. [Online]. Available: [https://doi.org/10.1007/978-3-030-89177-0\\_9](https://doi.org/10.1007/978-3-030-89177-0_9)
- [34] M. Shuster, "A survey of Attitude Representation," pp. 439–517, 1993. [Online]. Available: <http://www.ladispe.polito.it/corsi/Meccatronica/02JHCOR/2011-12/Slides/Shuster{ }Pub{ }1993h{ }J{ }Repsurv{ }scan.pdf>
- [35] M. Ben-Ari, "A tutorial on euler angles and quaternions," *Weizmann Institute of Science, Israel*, vol. 524, 2014.
- [36] N. Trawny and S. I. Roumeliotis, "Indirect kalman filter for 3d attitude estimation," *University of Minnesota, Dept. of Comp. Sci. & Eng., Tech. Rep.*, vol. 2, p. 2005, 2005.
- [37] F. L. Markley, Y. Cheng, J. L. Crassidis, and Y. Oshman, "Averaging quaternions," *Journal of Guidance, Control, and Dynamics*, vol. 30, no. 4, pp. 1193–1197, 2007.
- [38] M. V. Liarokapis, P. K. Artemiadis, and K. J. Kyriakopoulos, "Functional anthropomorphism for human to robot motion mapping," in *2012 IEEE RO-MAN: The 21st IEEE International Symposium on Robot and Human Interactive Communication*. IEEE, Sep. 2012. [Online]. Available: <https://doi.org/10.1109/roman.2012.6343727>
- [39] R. Contini, R. J. Drillis, and M. Bluestein, "Determination of body segment parameters," vol. 5, no. 5, pp. 493–504, Oct. 1963. [Online]. Available: <https://doi.org/10.1177/001872086300500508>
- [40] Xsens, "MTw Awinda User Manual," Tech. Rep., 2018, mW0502P, Revision L, 3 May 2018. [Online]. Available: [https://www.xsens.com/hubfs/Downloads/Manuals/MTw\\_Awinda\\_User\\_Manual.pdf](https://www.xsens.com/hubfs/Downloads/Manuals/MTw_Awinda_User_Manual.pdf)
- [41] ROS-Open-Source, "Rviz," <http://wiki.ros.org/rviz>, 2021, [Online; accessed 09-December-2021].
- [42] Open-source, "Ros-industrial," (Date last accessed 21-November-2021). [Online]. Available: <https://rosindustrial.org/>
- [43] —, "Moveit! motion planning framework," (Date last accessed 21-November-2021). [Online]. Available: <https://moveit.ros.org/>
- [44] U. Robots. Real-time data exchange guide. Date created 10-January-2019, Date last accessed 21-November-2021. [Online]. Available: <https://www.universal-robots.com/articles/ur/interface-communication/real-time-data-exchange-rtde-guide/>
- [45] M. Mihelj, J. Podobnik, and M. Munih, "Sensory fusion of magnetoinertial data based on kinematic model with jacobian weighted-left-pseudoinverse and kalman-adaptive gains," *IEEE Transactions on Instrumentation and Measurement*, vol. 68, no. 7, pp. 2610–2620, 2018.
- [46] C. Xu, J. He, X. Zhang, C. Yao, and P.-H. Tseng, "Geometrical kinematic modeling on human motion using method of multi-sensor fusion," *Information Fusion*, vol. 41, pp. 243–254, 2018. [Online]. Available: <https://www.sciencedirect.com/science/article/pii/S1566253517300301>



**IEEE**

IEEE  
**Industrial  
Electronics**  
Society



PROUDLY PRESENTS THE

# BEST PAPER PRESENTATION

TO

“A FRAMEWORK FOR HUMAN MOTION ESTIMATION USING IMUS IN HUMAN-ROBOT INTERACTION”

**Gizem Ateş, Martin Stølen, Erik Kyrkjebø**

WESTERN NORWAY UNIVERSITY OF APPLIED SCIENCES

at the

2022 IEEE International Conference on Industrial Technology  
Shanghai, China  
22 – 25 August 2022

PROF. MARIUSZ MALINOWSKI  
IES PRESIDENT

PROF. VALERIY VYATKIN ICIT 2022  
GENERAL CHAIR

PROF. LUIS GOMES ICIT 2022  
GENERAL CHAIR

PROF. MO-YUEN CHOW ICIT 2022  
GENERAL CHAIR

PROF. XINPING GUAN ICIT 2022  
GENERAL CHAIR



# DESIGN OF A GAMIFIED TRAINING SYSTEM FOR HUMAN-ROBOT COOPERATION

---

Gizem Ateş & Erik Kyrkjebø

Design of a Gamified Training System for Human-Robot Cooperation. Published in Proceedings of the 2nd International Conference on Electrical, Computer, Communications and Mechatronics Engineering (ICECCME) IEEE, November 16-18, 2022 DOI:[10.1109/ICECCME55909.2022.9988661](https://doi.org/10.1109/ICECCME55909.2022.9988661)

*“In reference to IEEE copyrighted material which is used with permission in this thesis, the IEEE does not endorse any of Western Norway University of Applied Sciences’s products or services. Internal or personal use of this material is permitted. If interested in reprinting/republishing IEEE copyrighted material for advertising or promotional purposes or for creating new collective works for resale or redistribution, please go to [http://www.ieee.org/publications\\_standards/publications/rights/rights\\_link.html](http://www.ieee.org/publications_standards/publications/rights/rights_link.html) to learn how to obtain a License from RightsLink. If applicable, University Microfilms and/or ProQuest Library, or the Archives of Canada may supply single copies of the dissertation.”*



# Design of a Gamified Training System for Human-Robot Cooperation

Gizem Ateş

*Dept. of Computer Science, Electrical Eng.  
and Mathematical Sciences  
Western Norway University of Applied Sciences  
Førde, Norway  
gizem.ates@hvl.no*

Erik Kyrkjebø

*Dept. of Computer Science, Electrical Eng.  
and Mathematical Sciences  
Western Norway University of Applied Sciences  
Førde, Norway  
erik.kyrkjebo@hvl.no*

**Abstract**—Human-Robot Cooperation (HRC) is a field which focuses on employing the best skills of both the robot and the human working together to achieve a common or shared task more efficiently. In most cases, both the human and the robot should know the status of each other and interchange data accordingly. There are several successfully researched HRC systems in the literature proposing solutions to various industrial problems yet few of them are used actively in real-world tasks. One of the major reasons for this gap is that the developed HRC systems do not offer an effective training procedure. The availability of a versatile training setup to get the optimal efficiency is important in addition to evaluating the developed HRC system's usability. Recent studies show that serious games offer effective training outcomes in various sectors such as the military, disaster drills, aviation, health etc. This paper presents an open-source gamified modular training design for HRC applications. It shows how the HRC system can be trained using serious games, what game elements can be utilized and how the learning curve of the user can be measured to evaluate the usability and efficiency. The proposed design is demonstrated through a real-world Cooperative Lifting (co-lift) scenario. The main motivation is to constitute a baseline for effective training of the HRC systems so that the gap between research and successful innovation in the HRC field becomes more narrow.

**Index Terms**—Human-robot cooperation, gamified training, serious games, cooperative lifting, inertial measurement unit (IMU)

## I. INTRODUCTION

Humans and robots have different strengths. Robots are excellent for precision, accuracy and repeatability; humans are excellent in decision making and problem-solving. Human-Robot Cooperation (HRC) field aims to bring upon the best skills of both the robot and the human in a cooperative and/or collaborative work to optimize the task efficiency [1]. This is particularly useful for small and middle-size companies where some automation is needed but fully automated systems are not profitable because there is no mass production [2]. There is an increasing trend in using collaborative robots in industrial settings [3]. An in-depth review of the use cases

of the collaborative robots in industrial settings is presented in [4]. The study shows that an overwhelmingly big portion of the use cases is in assembly tasks where the robot and the human work side by side, one after another, but not in active collaboration. It also shows the future trend in HRC towards using Human-Robot Interaction (HRI) methodologies to increase applicability and productivity. The lack of testing is stated as a principal problem in using this research in real industrial settings.

Testing and training are fundamental steps of any research to be publicly used. Particularly in HRC systems, the human is not only an external user of the system but is a part of it. Therefore, training becomes an essential step of the development process and should not be taken separately. Despite the necessity of training being addressed in several studies [3]–[5], there are few studies proposing different training strategies and no developed HRC system presents a training method for its usage.

A virtual simulation environment for real-time cooperation between industrial robotic manipulators is presented in [6]. The study focuses on safety and aims to increase awareness of robot collaborations and their acceptability. Another study highlights the effectiveness of interactive training compared to reading manuals [7]. It presents a computer-assisted training system to familiarize the manual operations of CNC milling using Virtual Reality (VR) technology. The virtual training system consists of 5 modules one of which is performance evaluation and based on the user tests, the interactively trained group outperforms the reading manual group. In [8], a virtual training environment is presented for effective human-robot team performance evaluation. The study focuses on Unmanned Aerial Vehicles (UAVs) and the level of trust is measured during task allocation between the human autonomous UV function. Another trust assessment in human-robot collaboration is presented in [9] to measure the performance of the HRC systems. The assessment is carried out in a Mixed Initiative Team Performance Assessment System (MITPAS) simulation environment.

This work was funded by the Research Council of Norway through grant number 280771.

Serious games are defined "as an experience designed using game mechanics and game thinking to educate individuals in a specific content domain [10]". In serious games, the main purpose is not entertainment but education, practice, training etc. Serious games draw considerable interest in enhancing learning and training outcomes since 2013 [11] in various fields such as military, aviation, disaster drills, crisis management, health etc. [12]. The value of game-based mechanics in generating meaningful learning experiences has been more visible through gamification [13]. Gamification is adding game mechanics into non-game environments. Several game elements are well defined in the literature [14]. The use of game elements and gamification methods in training increase the efficiency of the training outcome. There are some applications of using serious games in the HRC field such as in fatigue assessment [15], rehabilitation [16], constructing better communication with individuals who has Autism Spectrum Disorder [17] etc. Within our research, only one study [6] used serious games in HRC training. A serious game is designed in virtual reality that simulates in real-time the cooperation between industrial robotic manipulators.

HRC applications can be categorized based on applications such as cooperative assembly, manipulation, lifting etc. Cooperative Lifting (co-lift) is a common HRC application where (a) robot(s) and (a) human(s) carry a common object together. In some literature, co-lift is only referred as the action of carrying [18] and some defines co-lift as a sequence of several steps [19]. The communication channel between the human and the robot can be verbally [20], haptic [18] or via human motions [19].

Human motion tracking and prediction is an important part of HRC and particularly co-lift applications. Informing the robot about human motion is critical for safe and reliable interaction [21], [22]. There are several motion capture device used in robotics applications [23] such as optical devices with [24] and without [25] markers, inertial devices [19], acoustic devices [26], radio frequency transceivers [27], etc. Although visual-based human tracking methods are quite precise when it is well-calibrated, they lack mobility and suffer from occlusion, loss of line of sight, and light changes. Therefore, the non-visual-based tracking methods have gained interest and Inertial Measurement Unit (IMU) is one of the most common motion tracking systems in this regard [28].

According to the literature survey, several publications are addressing the necessity of testing and training in HRC applications [3]–[5]. However, a few studies were found related to this issue and those are focusing the trust and safety only rather than training the users for the end application. The majority of the related studies are developed either in simulation only or in virtual reality. Although VR technologies have benefits regarding reducing the cost of training in complex environments it is still tedious to create adequate realistic scenarios in VR and still cannot fill the gap sufficiently today. The novelty of this paper is the methodological design of an HRC training setup using serious games, successful implementation in a real-world example and its open-source code. As an example use

case, a co-lift scenario is demonstrated using the proposed methodology. The example scenario is developed using Robot Operating System (ROS) meta-operating system [29] and all the resources used in this paper are open-source. This paper brings novelty to the literature with the systematic and modular design of a gamified HRC training architecture and presents a template freely customizable for various HRC tasks.

The paper consists of 5 sections: the relevant background is presented in section I, the systematic overview of the proposed training setup is explained in section II, an experimental setup for an example use case is given in section III, the contributions and major findings are discussed in section IV and the overall evaluation and the future work is presented in section V.

## II. METHODOLOGY

The methodology focuses on designing a modular and gamified training setup. The system overview and the modules are given in fig. 3. As an example case, a co-lift task defined in [19] is taken where a human and a robot approach a table whose initial position is unknown to the robot, lift it together and place it in a predefined location. In different stages of the task, the robot follows human motions, the human follows the robot motions or they actively change leadership and follow each other synchronously as illustrated in fig. 1. Designing such an experimental task is aimed at utilizing human cognitive skills and robot accuracy in different parts of the task. The goal is to complete the co-lift starting with picking up the table, carrying it to two desired positions and then placing it as quick and smooth as possible.

In section II-A the gamification process as well as the co-lift task criteria are presented and in section II-B the network and the roles of different units are explained.

### A. Gamification and game elements

Gamification of the HRC training can be defined as a modelling process of the HRC task and all the task objectives as inputs and the game score as output. This process for the proposed HRC scenario is linked with game elements as described in table I. The correspondence of each game element class is explained in this subsection.

1) *Theme*: A theme adds interest and creates engagement within a learning game. It can be a form of introductory backstory or accompanying narrative running through the game. For the proposed HRC scenario, the backstory is the purpose of the research and also the use cases/values of the HRC scenario in the future.

2) *Achievement*: Achievements are the mechanisms connecting the target outcomes of the HRC task that the user should be capable of after the training. The game score is calculated based on the user's achievement and how quickly they completed each achievement. In the proposed co-lift scenario the user is supposed to go through four different states as IDLE, APPROACH, CO-LIFT, and RELEASE as defined in [19] and illustrated in fig. 1. During the state changes the human and the robot exchange the leadership



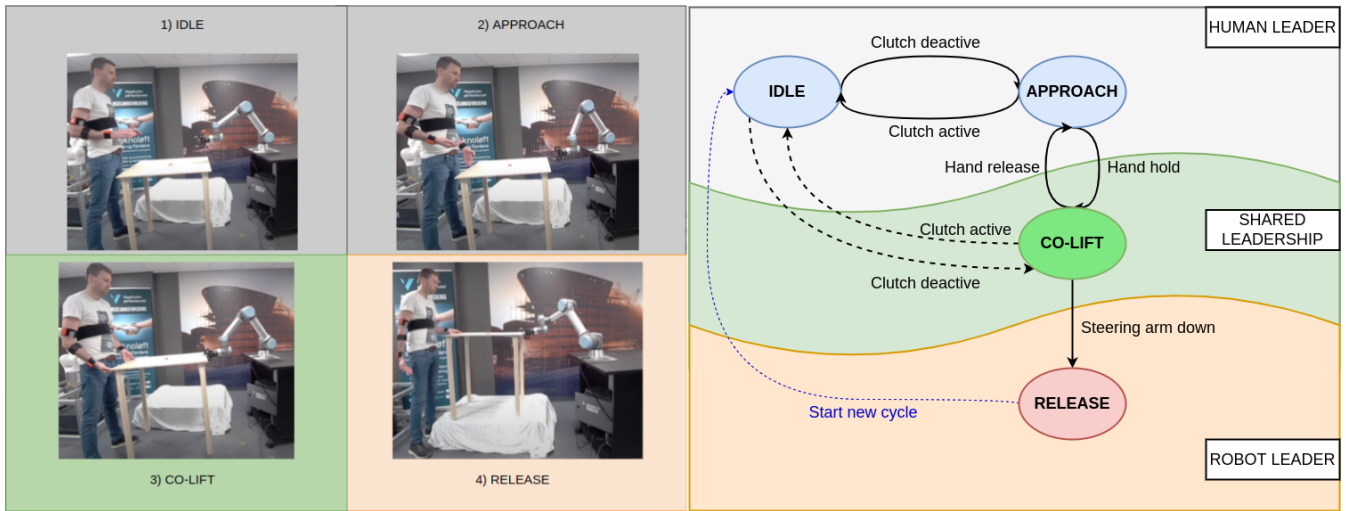


Fig. 1. HRC roles and states in the example co-lift scenario based on [19]. Human Leading role has two states: IDLE: Both chest-to-wrist (hand) motions are actively calculated yet no motion command is sent to the robot. This is a safe state that the human can enter with the clutching gesture at any time. APPROACH: Combined(merged) pose from two hands is actively calculated to produce soft real-time end-effector goal pose commands. The robot follows the human actively. Shared Leadership role has one state: CO-LIFT: The robot applies a directional compliant force and the human decides the direction of this force with elbow gestures. Robot Leading role has one state: RELEASE: The robot takes the lead in the operation, and moves to a predefined release pose. The human follows the robot's motions.

TABLE I  
OVERVIEW OF THE INCLUDED GAME ELEMENTS

Classifier	Game elements	Description
theme	e.g. backstory	Additional information about the purpose of the research and/or being trained HRC system to add interest and create engagement within a learning game.
achievement	e.g. score	A mechanism to show the user his or her progress and achievements within the system linked to the
challenge	e.g. missions, quests	Ask the user to perform a certain activity under predefined conditions such as grabbing the table, pressing physical buttons releasing the table without any crashes etc.
feedback	e.g. notifications, guidance	The system provides the user with additional information, hints or gives encouraging statements through the visual feedback unit.
time constraint	e.g. countdowns	Users are given a certain amount of time in which they ought to complete a full HRC cycle.
self expression	e.g. spaces for open creativity	Freedoms where the user can tweak the usage of the HRC system to improve their personal performance such as the initial pose of their hands, the way how they grab the table etc.
aesthetics	e.g. visual, aural, haptic etc.	The sensory phenomena that the player encounters in the game

roles dynamically within the 3 different roles of cooperation as Human Leading, Robot Leading, and Shared Leadership. The aim is to improve the user's skills in those transitions and quantitatively measure the user confidence/skill in each state. The states and roles are summarized in fig. 1:

The achievements show the progress of the user within the trial as well as between trials. The achievement progress is also linked with the learning curve of each user. Other than achievement class, the contribution of the other components to game score is given in challenges time constraints subsections.

3) *Challenge*: Challenges and conflicts are accepted as the central game element and make the game interesting [14]. The challenge can be a physical obstacle, combat with another player, or a puzzle that has to be solved. In the co-lift scenario, grabbing the table successfully, and requiring the table to be

moved to different locations are defined as challenges.

4) *Feedback*: Feedback stimulates a self-correcting training experience. It enables the learner to understand their errors better and avoid mistakes in real HRC applications. The feedback given to the user is the simulated human model, game score and HRC state. The simulated human model is important because it has been observed in the pilot tests that the users lose the perception of their body posture when they overly focus on what the robot should do. The simulated human model feedback shows how the system registers their motions - almost like a mirror. The score is a continuous and instant feedback type where the user can see own progress. The HRC states data in the feedback provides two benefits; required guidance and it directs the user to stay in the theme and not deviate from the task.

5) *Time constraint*: Time constraint is a special type of challenge in a serious game especially if the serious game is a training simulator to be used in real-world applications. In our HRC task, the time constraint is directly connected to the score element. The game is supposed to be finished in 10 minutes. The user starts with 600 points and loses 1 point every second.

6) *Self-expression*: Self-expressions are the parameters and preferences of the game which are up to the user. Expression category is linked to autonomy in some literature [14] and it can contain any customizable feature that a user can get such as an avatar, virtual goods etc. It is stated that self-expression is a motivational game element since the user takes ownership of one's action [30]. In the gamified HRC training, expressions can be used in investigating the effect of some parameters for optimal use cases. In the co-lift task, the initial poses of the user's hands, and the way how the user grabs the table are not restricted but only guided before the trials. These are open questions in the relevant HRC study and user self-expressions are believed to help decide the most optimal usage.

7) *Aesthetics*: Aesthetics are the visual and audio language of the game, the artwork and the style in a gamified system. They play an engaging and immersive role in the game. In an HRC scenario, the real robot can be perceived as an aesthetic element. However, it is still important to have additional aesthetic elements which serve in focusing the HRC task. In the proposed system, the portable physical buttons have built-in LEDs which are activated when the button is pressed. Also, it is commonly known that ROS is a terminal-based environment which can be perceived as non-appealing to many users. Therefore, in addition to RViz visualization tool in ROS, we have developed a GUI system where the user can easily follow the whole process to increase the aesthetics.

### B. The network and data flow between units

The training system consists of 4 main units: human commander, robot commander, task environment and visual feedback as shown in fig. 3.

1) *Human Commander*: The human commander is the human motion tracking unit where the postures and gestures of the human body produce a set of pose commands in soft real-time. In the current setup, human motion tracking and estimation are executed using an IMU-based approach developed in [31]. A total of 5 IMUs are attached to the human body as shown in fig. 2. The pose changes of the two hands with respect to the chest-fixed frame are used in creating relative motion mapping with the robot.

The raw orientation data from each IMU in a global frame is obtained. Then, individual IMU orientations in their respective sensor frame is calculated as in eq. (1).

$$q_{joint} = (q_{prevLink}^{GS})^* \otimes q_{currentLink}^{GS} \quad (1)$$

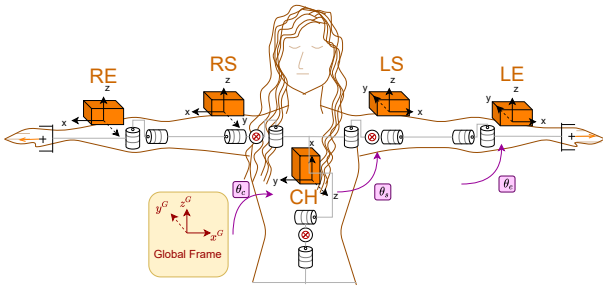


Fig. 2. Human model and IMU placement on right/left elbow (RE/LE), right/left shoulder(RS/LS) and chest (CH) according to [31].

Afterwards, the joint angles in both arms starting from the chest to the left wrist is calculated as in eq. (2).

$$q_c = q_{CH} \quad q_{ls} = q_c^* \otimes q_{LS} \quad q_{le} = q_c^* \otimes q_{ls}^* \otimes q_{LE} \quad (2)$$

where the asterisk denote quaternion conjugate,  $q_c, q_{ls}, q_{le}$  are human joint angles;  $q_{CH}, q_{LS}, q_{LE}$  are IMU-readings of chest, left-shoulder, and left-elbow, respectively. To create a robot command, both hand poses are used to construct a merged hand pose data. The merged hand pose is calculated as in eq. (4) and it is initially set to zero as shown in eq. (3).

$$\left[ \hat{P}_{handLeft,t=0} \times \hat{P}_{handRight,t=0} \right]^{-1} = \hat{P}_{r,t=0} \quad (3)$$

$$\hat{H}(t) = \hat{P}_{h,t=0}^{-1} \times \hat{P}_{h,t} \Rightarrow \hat{P}_{r,t} = \hat{H}(t) \times \hat{P}_{r,t=0} \quad (4)$$

where  $\hat{P}_{handLeft,t=0}$ ,  $\hat{P}_{handRight,t=0}$  and  $\hat{P}_{r,t=0}$  are Homogeneous Transformation Matrix (HTM) representing human left hand, human right hand.  $\hat{H}$  is a HTM to be used in mapping merged hands motion to robot pose with respect to robot's initial pose.

The same calculation applies to the human right side. The human chest is modeled as a ball joint with 3 degrees of freedom (DoF)s, and each arm is modeled with 5 DoF (i.e. 3 DoF shoulder and 2 DoF elbow), while wrist motions are ignored. The 13 DoF biomechanical model of the human is constructed as a pair of kinematic chains for both arms using the measured body link lengths and calculated joint angles. Additionally, a low-cost EMG sensor on the right forearm is used to create gripper commands.

"Posture and gesture info" which is referred to in fig. 3 contains filtered IMU data (angular velocity, linear acceleration and magnetization surrounding as well as 3D orientation) and the transformations of each body link with respect to a base frame. From the transformations, the chest-to-wrist poses from each arm are used to create a goal command for the robot's end-effector and the whole transformation chain is used in visualizing the simulated human body on the visual feedback unit.

2) *Robot Commander*: The robot commander is the unit taking the goal pose for the end effector and executing the required motion commands for the joints.

"Goal pose" in fig. 3 contains only the end-effector goal pose. The robot commander takes the goal pose and projects the current position forward in time with the current velocity. Therefore, the end-effector does not necessarily reach zero velocity at each pose but rather smoothens the motion at the goal regarding the next goal pose. Although the robot joint states are available, we do not provide them in the main data flow because they are not used in any main units currently. However, depending on the task, for instance, if the robot simulation is required in the visual feedback unit, the joint states data can be activated to create a robot model.

3) *Task Environment*: The task environment unit includes all the physical objects that the robot and the human interact with and have a role in the task. The importance of this unit is that the task goals are engaged with physical objects with which the interaction is assigned as points to the game score. In the co-lift task, the task goals are linked to the duration of completion and smoothness. Also, one extra IMU is attached to the table to measure the orientation and the acceleration changes of the table during the co-lift process. Additionally, there are two physical portable buttons representing two locations where the table should be carried before being released. The high jerk and the fluctuations of the table orientation

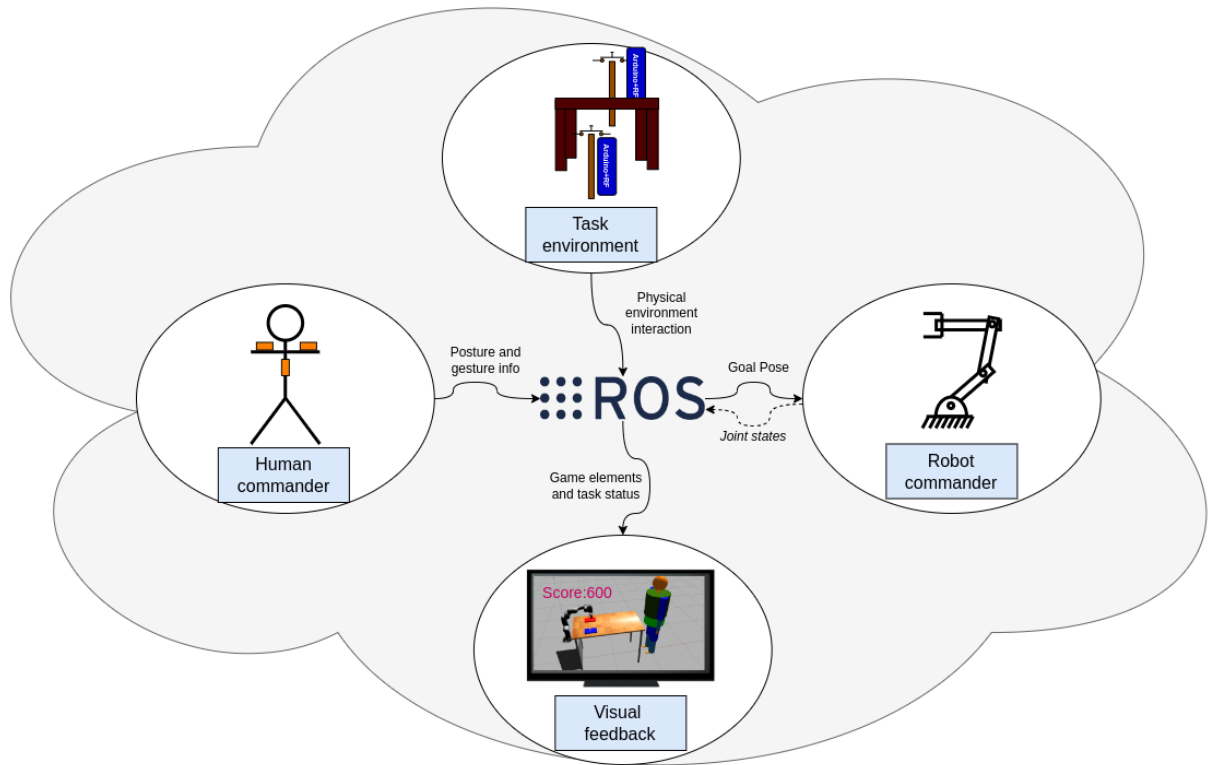


Fig. 3. Overview of the system architecture demonstrating the 4 main units (human commander, robot commander, task environment and visual feedback) connected to ROS network and the data transmitted/received via these units.

are minus points whereas each reached button gives positive points.

”Physical environment interaction” data in fig. 3 contains the button states to measure the timing when they are pressed and the IMU measurements attached to the carried table.

4) *Visual Feedback*: The purpose of the visual feedback unit is to provide dynamic progress feedback to the user as game score as well as to inform the user about the current state of the task.

”Game elements and the task status” data in fig. 3 includes all types of variables affecting the game score and the relevant guidance about the task. The importance of this unit is to give feedback to stimulate a self-correcting training experience. In the current setup, the visual feedback unit shows a simulated human model, game score and state transition indicators depending on the task state. Additionally, a robot model can be visualized in this unit but we disable this feature in our task because we want to keep the user focused on the real robot rather than the simulated one.

### III. EXPERIMENTAL

In this section, the technical specifications of the experimental setup for the proposed gamified HRC training scenario are presented. In this setup, 5 Xsens Awinda IMUs and one base station as the human commander, Universal Robots UR5e collaborative robot with UR-RDTE (Real-time Data Exchange Protocol) as robot commander, 2 handcrafted portable physical

buttons with Arduino controller and 1 regular table on which an extra Xsens Awinda wireless IMU attached as task environment and a display for visual feedback. In this section, the connection of those units to the ROS network and the technical details are presented. However, the proposed training setup is modular, open-source and easily configurable. The general procedure to configure each unit with another type of setup is also mentioned in the respective subsections.

The system is set in ROS Noetic environment. A laptop PC which has Ubuntu 20.04 LTS installed is set to be the ROS master and handles all of the communication between each unit. The open-source code for the training setup can be found by the following link: [https://github.com/frdedynamics/hrc\\_training](https://github.com/frdedynamics/hrc_training).

The base station in the human controller communicates with 5 Xsens Awinda wireless IMU sensors wirelessly. The communication frequency between the base station and each sensor is set to 100 Hz. The base station is connected to the ROS master PC via USB. The IMU data is converted to the goal pose for the robot end-effector in the human controller nodes. Additionally, a wireless Myo Gesture Control Armband which has 8 EMG sensors is connected to control the robot gripper. The armband has a dedicated USB dongle and it communicates with the ROS master via serial port. Although an IMU-based human motion estimator is used as the human commander in this setup, it can be replaced by any type of human motion tracking/estimating unit as long as the human

body motions are translated as a respective robot command.

The robot controller commands a Universal Robots UR5e collaborative robot. The computer and the robot are connected to the same local area network and they communicate with each other wirelessly. The robot controller transmits servo control commands at 125 Hz while utilizing the real-time data exchange protocol [32] as suggested in [33]. This command type is specific for Universal Robots E-series and CB-series robots [32]. However, thanks to the modularity of the proposed network system, the robot controller unit can be replaced with another robot which takes given pose commands and executes them in real-time.

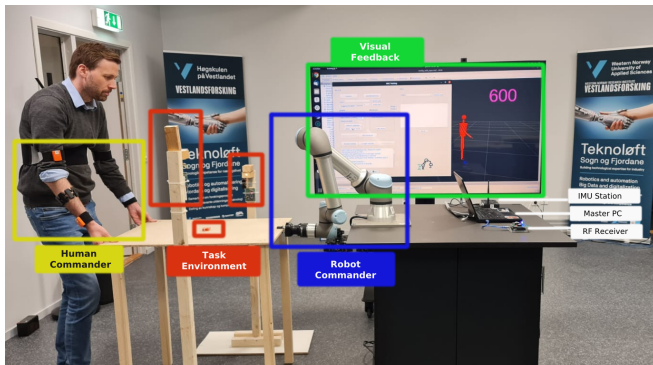


Fig. 4. Experimental setup of co-lift scenario in real-world with the components of 4 main units highlighted.

The task environment consists of the carried table and 2 portable physical buttons as shown in fig. 4. Both the table and the buttons are custom-made to meet the task requirements. The table is 80 cm tall and weighs 2 kg. There is an additional Xsens Awinda wireless IMU which is connected to the same base station as the human commander IMUs. This IMU provides orientation information in quaternions and acceleration information up to  $160 \text{ m/s}^{-2}$ . The physical buttons are crafted using wooden blocks of two different heights 110 cm and 130 cm. Each button is equipped with Arduino Nano, an NRF24L01+ single Chip 2.4GHz Transceiver from Nordic Semiconductors as Radio Frequency (RF) transmitters, a limit switch and a regular LED. The Arduino Uno and the RF module are connected via Serial Peripheral Interface (SPI) protocol. An additional Arduino Uno is connected to the master PC via USB and takes upon the receiver role. The receiver Arduino is connected to the ROS system via `rosserial`, which is a protocol for wrapping serial data from another device and multiplexing multiple topics and services [34], and provides the button states information with time stamps.

#### IV. DISCUSSION

The main purpose of this paper is to design a systematic gamified training architecture for HRC applications. The paper introduces a novel gamification methodology in HRC training and proposes how serious games and game elements can be used for this purpose.

It is focused on the conceptual design and easy reproducibility of the architecture in this paper. The results are provided as an open-source ROS package. The system has 4 main units - human commander, robot commander, task environment and visual feedback - and each unit can be modified/replaced with a coherent mechanism. For instance, an IMU-based human motion tracking system is used in the human commander but another technology or methodology to generate a robot goal pose based on human motions can be used. Similarly, UR5e is used as the robot in the example scenario yet another robotic system can be used as long as the controller of the robot can execute real-time actions given a goal pose.

There are 3 main reasons for choosing ROS as the main development environment. Firstly, ROS is a widely used open-source environment in which the number of users more than doubled between July 2019 - July 2020 [35]. The developed solution can reach many users easier. Second, games and gamified systems are not common subjects in ROS. This study introduces how the ROS environment can be utilized to develop serious games systematically. Third, the ROS environment is highly modular and supported by various robot, sensor and actuator manufacturers. Therefore, it aligns well with the modularity aim of this study.

During the experimental co-lift scenario, it is observed that the task environment and the visual feedback units are crucial for gamification. Depending on the task and HRC system, the size of those units may vary. In the co-lift scenario the task environment is prioritized over the virtual feedback to keep the focus and immersion in reality rather than virtuality. The simulated robot model is initially deactivated and two physical buttons are designed to represent the goal poses instead of virtual elements on the visual feedback unit - which is used only for guidance when needed. Therefore, it is important to have both units in a gamified HRC training system and configure the sizes of those units according to the HRC task requirements.

#### V. CONCLUSION AND FUTURE WORK

As the benefits of human-robot teams are being more visible, the number of researches to develop new HRC systems is increasing. However, only a few applications are actively taking a part in real-world tasks. The cause of this problem is identified as a lack of training both in research for user tests and in the industry for the end-users to excel in using the developed system. Without effective training for users, the evaluation of HRC systems' efficiency, usability and profitability is unfairly evaluated.

This paper provides a baseline for HRC training in a systematic and gamified approach. The importance of training in HRC system development is highlighted and the gap in the literature is elicited. A methodology to develop a gamified HRC training setup is presented and the proposed design is demonstrated in a real-world co-lift scenario. This paper is aimed to be a building block between research and successful innovation for various HRC applications.

As future work, multiple users are going to be trained in the HRC system presented in [19] to evaluate the system according to usability, learnability and eligibility scales.

#### CREDITING AND ACKNOWLEDGMENT

Gizem Ateş: Conceptualization, Methodology, Investigation, Writing - original draft. Erik Kyrkjebø: Conceptualization, Writing - review & editing. The authors thank Sondre Venås for help with experiments.

#### REFERENCES

- [1] A. Vysocky and P. Novak, "Human-robot collaboration in industry," *MM Science Journal*, vol. 9, no. 2, pp. 903–906, 2016.
- [2] G. Michalos, S. Makris, J. Spiliotopoulos, I. Misios, P. Tsarouchi, and G. Chryssolouris, "Robo-partner: Seamless human-robot cooperation for intelligent, flexible and safe operations in the assembly factories of the future," *Procedia CIRP*, vol. 23, pp. 71–76, 2014.
- [3] P. Tsarouchi, S. Makris, and G. Chryssolouris, "Human-robot interaction review and challenges on task planning and programming," *International Journal of Computer Integrated Manufacturing*, vol. 29, no. 8, pp. 916–931, Feb. 2016. [Online]. Available: <https://doi.org/10.1080/0951192x.2015.1130251>
- [4] E. Matheson, R. Minto, E. G. Zampieri, M. Faccio, and G. Rosati, "Human-robot collaboration in manufacturing applications: A review," *Robotics*, vol. 8, no. 4, p. 100, 2019.
- [5] J. Arents, V. Abolins, J. Judvaitis, O. Vismanis, A. Oraby, and K. Ozols, "Human-robot collaboration trends and safety aspects: A systematic review," *Journal of Sensor and Actuator Networks*, vol. 10, no. 3, p. 48, 2021.
- [6] E. Matsas and G.-C. Vosniakos, "Design of a virtual reality training system for human-robot collaboration in manufacturing tasks," *International Journal on Interactive Design and Manufacturing (IJIDeM)*, vol. 11, no. 2, pp. 139–153, 2017.
- [7] F. Lin, L. Ye, V. G. Duffy, and C.-J. Su, "Developing virtual environments for industrial training," *Information sciences*, vol. 140, no. 1–2, pp. 153–170, 2002.
- [8] E. De Visser, R. Parasuraman, A. Freedy, E. Freedy, and G. Weltman, "A comprehensive methodology for assessing human-robot team performance for use in training and simulation," in *Proceedings of the human factors and ergonomics society annual meeting*, vol. 50, no. 25. SAGE Publications Sage CA: Los Angeles, CA, 2006, pp. 2639–2643.
- [9] A. Freedy, E. DeVisser, G. Weltman, and N. Coeyman, "Measurement of trust in human-robot collaboration," in *2007 International symposium on collaborative technologies and systems*. IEEE, 2007, pp. 106–114.
- [10] K. M. Kapp, *The gamification of learning and instruction: game-based methods and strategies for training and education*. John Wiley & Sons, 2012.
- [11] D. Checa and A. Bustillo, "A review of immersive virtual reality serious games to enhance learning and training," *Multimedia Tools and Applications*, vol. 79, no. 9, pp. 5501–5527, 2020.
- [12] T. Susi, M. Johannesson, and P. Backlund, "Serious games: An overview," 2007.
- [13] E. Pesare, T. Roselli, N. Corriero, and V. Rossano, "Game-based learning and gamification to promote engagement and motivation in medical learning contexts," *Smart Learning Environments*, vol. 3, no. 1, Apr. 2016. [Online]. Available: <https://doi.org/10.1186/s40561-016-0028-0>
- [14] M. Sillaots, T. Jesmin, and A. Rinde, "Survey for mapping game elements," in *Proceedings of the 10th European Conference on Game Based Learning ECGBL*, 2016, pp. 617–626.
- [15] V. Kanal, J. Brady, H. Nambiappan, M. Kyrarini, G. Wylie, and F. Make-don, "Towards a serious game based human-robot framework for fatigue assessment," in *Proceedings of the 13th ACM International Conference on Pervasive Technologies Related to Assistive Environments*, 2020, pp. 1–6.
- [16] K. d. O. Andrade, G. Fernandes, J. Martins, V. C. Roma, R. C. Joaquim, and G. A. Caurin, "Rehabilitation robotics and serious games: An initial architecture for simultaneous players," in *2013 ISSNIP Biosignals and Biorobotics Conference: Biosignals and Robotics for Better and Safer Living (BRC)*. IEEE, 2013, pp. 1–6.
- [17] V. Silva, F. Soares, J. S. Esteves, and A. P. Pereira, "Building a hybrid approach for a game scenario using a tangible interface in human robot interaction," in *Joint International Conference on Serious Games*. Springer, 2018, pp. 241–247.
- [18] A. Mörtl, M. Lawitzky, A. Kucukyilmaz, M. Sezgin, C. Basdogan, and S. Hirche, "The role of roles: Physical cooperation between humans and robots," *International Journal of Robotics Research*, vol. 31, no. 13, pp. 1656–1674, 2012.
- [19] G. Ateş, M. F. Stølen, and E. Kyrkjebø, "Force and gesture-based motion control of human-robot cooperative lifting using imus," in *Proceedings of the 2022 ACM/IEEE International Conference on Human-Robot Interaction*, ser. HRI '22. IEEE Press, 2022, p. 688–692.
- [20] P. Gustavsson, A. Syberfeldt, R. Brewster, and L. Wang, "Human-robot collaboration demonstrator combining speech recognition and haptic control," *Procedia CIRP*, vol. 63, pp. 396–401, 2017.
- [21] V. V. Unhelkar, P. A. Lasota, Q. Tyroller, R.-D. Buhai, L. Marceau, B. Deml, and J. A. Shah, "Human-aware robotic assistant for collaborative assembly: Integrating human motion prediction with planning in time," *IEEE Robotics and Automation Letters*, vol. 3, no. 3, pp. 2394–2401, 2018.
- [22] J. Mainprice and D. Berenson, "Human-robot collaborative manipulation planning using early prediction of human motion," in *2013 IEEE/RSJ International Conference on Intelligent Robots and Systems*. IEEE, 2013, pp. 299–306.
- [23] M. Field, Z. Pan, D. Stirling, and F. Naghdy, "Human motion capture sensors and analysis in robotics," *Industrial Robot: An International Journal*, 2011.
- [24] W. Sheng, A. Thobbi, and Y. Gu, "An integrated framework for human-robot collaborative manipulation," *IEEE transactions on cybernetics*, vol. 45, no. 10, pp. 2030–2041, 2014.
- [25] C. Morato, K. N. Kaipa, B. Zhao, and S. K. Gupta, "Toward safe human robot collaboration by using multiple kinects based real-time human tracking," *Journal of Computing and Information Science in Engineering*, vol. 14, no. 1, 2014.
- [26] D. Vlastic, R. Adelsberger, G. Vannucci, J. Barnwell, M. Gross, W. Matusik, and J. Popović, "Practical motion capture in everyday surroundings," *ACM transactions on graphics (TOG)*, vol. 26, no. 3, pp. 35–es, 2007.
- [27] S. Amendola, L. Bianchi, and G. Marrocco, "Movement detection of human body segments: Passive radio-frequency identification and machine-learning technologies," *IEEE Antennas and Propagation Magazine*, vol. 57, no. 3, pp. 23–37, 2015.
- [28] A. Filippeschi, N. Schmitz, M. Miezal, G. Bleser, E. Ruffaldi, and D. Stricker, "Survey of motion tracking methods based on inertial sensors: A focus on upper limb human motion," *Sensors*, vol. 17, no. 6, p. 1257, Jun. 2017. [Online]. Available: <https://doi.org/10.3390/s17061257>
- [29] ROS-Open-Source, "ROS (Robot Operating System)," <http://wiki.ros.org/2022>, [Online; accessed 24-June-2022].
- [30] A. Suh, C. Wagner, and L. Liu, "The effects of game dynamics on user engagement in gamified systems," in *2015 48th Hawaii international conference on system sciences*. IEEE, 2015, pp. 672–681.
- [31] G. Ateş and E. Kyrkjebø, "Human-robot cooperative lifting using IMUs and human gestures," in *Towards Autonomous Robotic Systems*. Springer International Publishing, 2021, pp. 88–99. [Online]. Available: [https://doi.org/10.1007/978-3-030-89177-0\\_9](https://doi.org/10.1007/978-3-030-89177-0_9)
- [32] U. Robots. (2021) Real-time data exchange guide. [Online]. Available: <https://www.universal-robots.com/articles/ur-interface-communication/real-time-data-exchange-rtde-guide/>
- [33] —, "The URScript Programming Language," Tech. Rep., 2016. [Online]. Available: <https://www.universal-robots.com/download/manuals-cb-series/script/script-manual-cb-series-sw33/>
- [34] ROS-Open-Source, "rosserial," <http://wiki.ros.org/rosserial>, 2022, [Online; accessed 24-June-2022].
- [35] —, "ROS metrics," <https://wiki.ros.org/Metrics>, 2021, [Online; accessed 24-June-2022].





# EXPLORING HUMAN-ROBOT COOPERATION WITH GAMIFIED USER TRAINING: A USER STUDY ON COOPERATIVE LIFTING

---

Gizem Ateş Venås, Martin Fodstad Stølen & Erik Kyrkjebø

Exploring Human-Robot Cooperation with Gamified User Training: A User Study on Cooperative Lifting. Submitted to **Frontiers in Robotics and AI**. (*Submitted*)





# Exploring Human-Robot Cooperation with Gamified User Training: A User Study on Cooperative Lifting

Gizem Ateş Venås<sup>ID</sup>, Martin Fodstad Stølen<sup>ID</sup>, and Erik Kyrkjebø<sup>ID</sup>

*Department of Computer Science, Electrical Engineering and Mathematical Sciences, Førde, Norway*

Correspondence\*:  
Gizem Ateş Venås  
gizem.ates@hvl.no

## 2 ABSTRACT

3 Human-robot cooperation (HRC) is becoming increasingly relevant with the surge in collaborative  
4 robots (cobots) for industrial applications. Examples of humans and robots cooperating actively  
5 on the same workpiece can be found in research labs around the world, but industrial applications  
6 are still mostly limited to robots and humans taking turns. In this paper, we use a cooperative  
7 lifting task (co-lift) as a case study to explore how well this task can be learned within a limited  
8 time, and how background factors of users may impact learning. The experimental study included  
9 32 healthy adults from 20 to 54 years who performed a co-lift with a collaborative robot. The  
10 physical setup is designed as a gamified user training system as research has validated that  
11 gamification is an effective methodology for user training. Human motions and gestures were  
12 measured using Inertial Measurement Unit (IMU) sensors and used to interact with the robot  
13 across three role distributions: human as the leader, robot as the leader, and shared leadership.  
14 We find that regardless of age, gender, job category, gaming background, and familiarity with  
15 robots, the learning curve of all users showed a satisfactory progression and that all users could  
16 achieve successful cooperation with the robot on the co-lift task after seven or fewer trials. The  
17 data indicates that some of the background factors of the users such as occupation, past gaming  
18 habits etc. may affect learning outcomes, which will be explored further in future experiments.  
19 Overall, the results indicate that the potential of the adoption of HRC in the industry is promising  
20 for a diverse set of users after a relatively short training process.

21 **Keywords:** HRC, IMU, human motion tracking, co-lift, user training, gamification

## 1 INTRODUCTION

22 Robotics has been a game changer in mass manufacturing by allowing various processes to be automated to  
23 produce a large number of items with the same quality, and often with a significantly shorter production time.  
24 For small and mid-size enterprises (SMEs) with smaller production volumes, the benefits of introducing  
25 industrial robots into production lines have not been as apparent and many have been reluctant to automate  
26 production processes (Insight, 2022). The introduction of collaborative robots (cobots) that can work next  
27 to human workers in the factory without fences has opened up a new potential in automation. However,  
28 robots and humans are still only taking turns when working on products, and the potential for Human-Robot

29 Cooperation (HRC) where humans and robots can cooperate to work on the same product simultaneously  
30 has not been adopted by the industry (Michaelis et al., 2020).

31 A HRC system aims to combine the superior skills of humans (problem-solving, decision-making etc.)  
32 and robots (precision, accuracy, repeatability etc.) to accomplish the task more efficiently and accurately.  
33 There are several factors in HRC usability such as safety, trust, user's experience, effectiveness, efficiency,  
34 learnability, flexibility, robustness and utility (Lindblom et al., 2020; Simone et al., 2022). Although safety  
35 is the most important factor, it is not sufficient for achieving optimal usability from an HRC system. This  
36 study focuses on three integral components of HRC system usability: 1) a robust communication method  
37 characterized by reliability, adequate precision, and accuracy; 2) dynamic role allocation between the  
38 human and robot within the HRC framework; and 3) human operator proficiency in utilizing the system.

39 A human-robot team must have a reliable communication method to achieve successful HRC. The human  
40 input can be via joystick, voice, haptic and/or motion commands. The robot actions should be predictable  
41 and easily understood by human operators to ensure safe, intuitive and effective cooperation and build trust  
42 (Lindblom and Wang, 2018; Lee and See, 2004). Moreover, it is not straightforward to assign a leader to a  
43 human-robot team to achieve the task in the most optimal way. The robot and the human excel in different  
44 skills. Therefore, either their leadership roles should be allocated in a flexible manner depending on the  
45 task requirement/state, or prescribed optimally beforehand, to maximize system performance regardless  
46 of dynamic or static role assignment (Mörthl et al., 2012). Lastly, the human operator should have enough  
47 competence and training to understand system capabilities and usage and to handle system drawbacks and  
48 failures. In order for SMEs to benefit from using cobots for industrial applications, it is crucial that human  
49 operators receive proper training in using HRC systems Michaelis et al. (2020).

50 User training is perhaps not addressed sufficiently in the context of HRC. Werner et al. show the  
51 importance of user training in Human-Robot Interaction (HRI) via an experiment on 25 elderly people who  
52 get help from a bathing robot which they communicate via gestures Werner et al. (2020). A few studies  
53 suggested three methodological approaches for user training in HRI. One methodology is the development  
54 of adaptive human-machine interfaces (HMIs) for industrial machines and robots. This approach involves  
55 measuring the user's capabilities, adapting the information presented in the HMI, and providing training  
56 to the user (Villani et al., 2017). By adapting the interface to the user's needs and abilities, the cognitive  
57 workload can be reduced, and the user can interact more effectively with the robot. The Wizard-of-Oz  
58 (WoZ) technique is another methodology used in human-robot interaction. In this technique, a remote  
59 supervisor drives the robot using a control interface to simulate an artificially intelligent robot (Tennent  
60 et al., 2018). Another approach is to use virtual/physical simulators mostly due to safety reasons (Mitchell  
61 et al., 2020), yet it increases the overall development cost of a novel HRC system. The current examples  
62 found in the literature are limited to mostly medical, surgical and military applications (Azadi et al., 2021;  
63 Dubin et al., 2017; Prasov, 2012) and the main training purpose is to train the user for the specific task  
64 rather than the user learning the HRC system itself.

65 Serious games (SG), gamification methods and game-based learning (GBL) can be used to develop  
66 supplemental training materials that are interesting and interactive, making it simpler for learners to apply  
67 their newfound knowledge (Susi et al., 2007; Anil Yasin and Abbas, 2021; Klefodimos and Evangelidis,  
68 2018). Several studies merged gamification and simulation in user training within various fields (Checa and  
69 Bustillo, 2020; Wang et al., 2016). According to Kapp (2012), "a serious game is an experience created  
70 using game mechanics and game thinking to educate people in a specific content domain". In serious games,  
71 learning, training, and other objectives come first rather than pure entertainment. The effectiveness of the  
72 training outcome can be increased by gamification techniques and game elements (Pesare et al., 2016). SG

73 and GBL have been popularly used in various training purposes since 2013 (Checa and Bustillo, 2020)  
74 such as in fatigue assessment (Kanal et al., 2020), rehabilitation (Andrade et al., 2013), constructing better  
75 communication with individuals who has Autism Spectrum Disorder (Silva et al., 2018) etc. Although it  
76 is not common in user training in HRC applications, one successful study used a serious virtual reality  
77 game that simulated the cooperation between industrial robotic manipulators (Matsas and Vosniakos, 2017).  
78 There is still room for merging SG, GBL and gamification in user training in HRI and HRC (Jones et al.,  
79 2022).

80 Cooperative lifting (co-lift) scenario is a common example in HRC where humans and robots lift and  
81 carry heavy, flexible, or long objects together while exploiting human cognitive skills and robot accuracy  
82 in different parts of the task. The co-lift task was chosen as the experimental study scenario for HRC in  
83 this article due to the fact that material manipulation applications (e.g., handling, positioning, polishing)  
84 have been found to be the most common tasks in the industry with more than 20% of the total number  
85 of tasks (Parra et al., 2020). There are several studies on co-lift and manipulation between a human and  
86 a robot in the literature. In Mörtl et al. (2012), the authors used haptic data to dynamically assign the  
87 leader roles between the human and robot in a co-lift scenario. A recent study presented in Liu et al. (2021)  
88 estimated the external forces applied by the human operator during the collaborative assembly of a car  
89 engine. In Ramasubramanian and Papakostas (2021), the human operator and a collaborative robot on a  
90 mobile platform carried a long stick between two locations in the work environment. In Nemeč et al. (2017),  
91 speed and disturbance rejection were adjusted for transporting an object through learning by demonstration.  
92 While these studies cover important topics for HRC and co-lift tasks, they present solutions only in the  
93 active carrying phase. It is important to address the before (approach) and after (release) phases of the  
94 active co-lift phase as shown in Figure 1 elaborating with the human input method so that the chain or  
95 repeated HRC tasks can automatically restart without any interrupts.

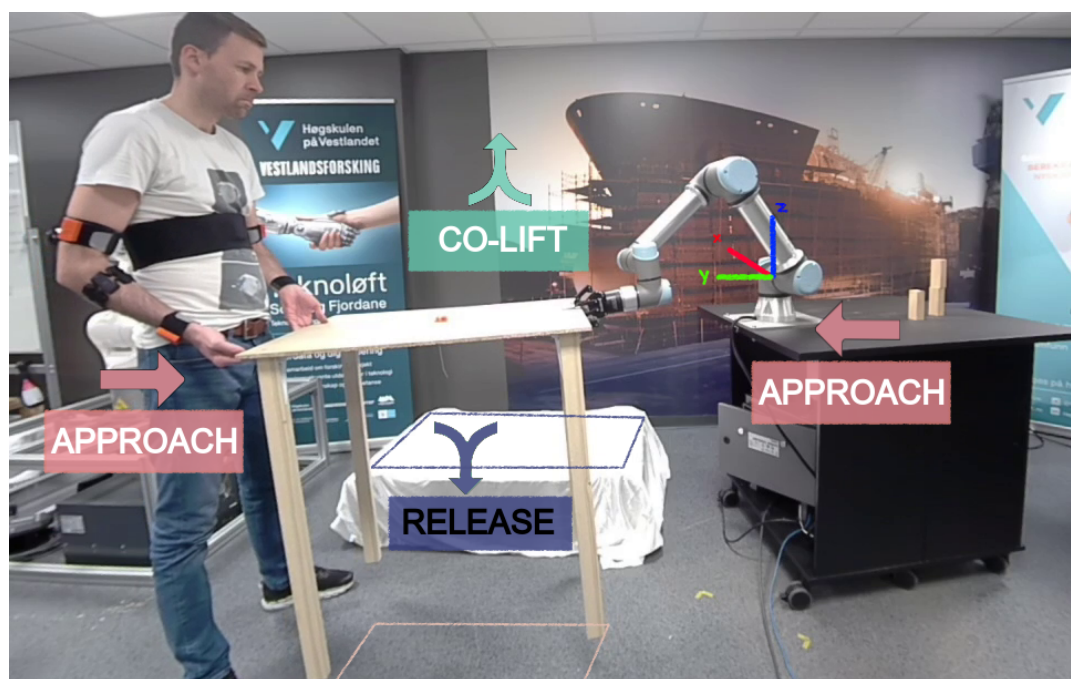


**Figure 1.** The full-cycle of co-lift task and its states (APPROACH, CO-LIFT and RELEASE) and the pick and place locations of the common object. The system uses IMUs for human motion estimation and an EMG-sensor to open/close the gripper (Ates et al., 2022).

96 In this paper, a novel human-motion-based HRC system using Inertial Measurement Unit (IMU)s as the  
97 motion capturing system (Ates et al., 2022) in a co-lift scenario is tested using a gamified user training  
98 approach. The objective is to conduct a quantifiable empirical unbiased observation on the quality of  
99 HRC and the effect of user training. We evaluated if users can quickly learn to cooperate with a robot  
100 irrespective of age, gender, technical background, interest in gaming etc. It is suggested in the literature  
101 that the performance of HRC could be affected by the worker's previous experience with robotics (Simone  
102 et al., 2022), their personality Walters et al. (2005) as well as their gaming background (Tanaka et al.,  
103 2016). We aim to observe if there are significantly important factors in the learning rate in terms of how  
104 quickly and consistently a user cooperates with a robot. We investigate the learning process of 32 human  
105 users and analyze both quantitative data from IMUs and qualitative data from pre- and post-surveys. A  
106 detailed discussion is provided based on user learning curves and the different background factors that  
107 influence learning. Although the results are solely dependent on the specific type of application, these  
108 findings should be considered for the evaluation of the effective convenience of the cobots, including an  
109 analysis of the variation in the workers' performance, and consequently, of the entire HRC system.

## 2 METHODS

### 110 2.1 Cooperative Lifting

111 The operation is divided into different states, and the roles of the human and robot change throughout the  
112 states as shown in Figure 2. The system starts in the IDLE state, where no motion is transferred from the  
113 human to the robot. The human can then use a clutching gesture to transit between IDLE and APPROACH  
114 states, where motion control commands are sent to the robot based on the pose information of the human's  
115 hands. In the CO-LIFT state, the human and robot share leadership and perform complex motions specific  
116 to the application scenario. The human can then gesture the robot to enter the RELEASE state, where the  
117 robot takes charge of the position and velocity control of the object to place it accurately in a predefined  
118 position.

### 119 2.2 Human Motions to Robot Actions

120 Studies on human motion tracking and estimation can be categorized based on the type of motion tracker  
121 devices used: visual-based (Morato et al., 2014; Sheng et al., 2015), and nonvisual-based (Kok, 2014;  
122 Roetenberg et al., 2009), and hybrid solutions (Sugiyama and Miura, 2009). The visual-based solutions are  
123 widespread in motion tracking since they provide highly accurate human motion tracking but often fail in  
124 industrial usage due to occlusion, loss in line-of-sight, intolerant to lightning changes, and lack of mobility  
125 (Rodríguez-Guerra et al., 2021). Common alternatives to non-visual systems are IMU-based solutions  
126 which are stand-alone systems without no permanent installations. They often cost considerably less than  
127 their visual alternatives but are prone to drift for long-term usage. While several solutions to eliminate the  
128 drift problem have been proposed (Kok et al., 2017; M. and J., 2015; Ludwig and Burnham, 2018), there  
129 are still a few examples using IMU-based solutions particularly in real-time in HRC applications. Although  
130 IMUs are selected as the main motion tracking devices, the selected human motion tracking technology is  
131 not the most critical point in this study.

#### 132 2.2.1 Human Motion Estimation (HME)

133 In this study, we used 5 IMUs as the motion-tracking system. After acquiring the 3D orientations from  
134 individual IMUs, the biomechanical model of the human body is placed in the calculations. In order to  
135 measure the full upper-body motions we placed the IMUs as shown in Figure 3. Nonetheless, the selected

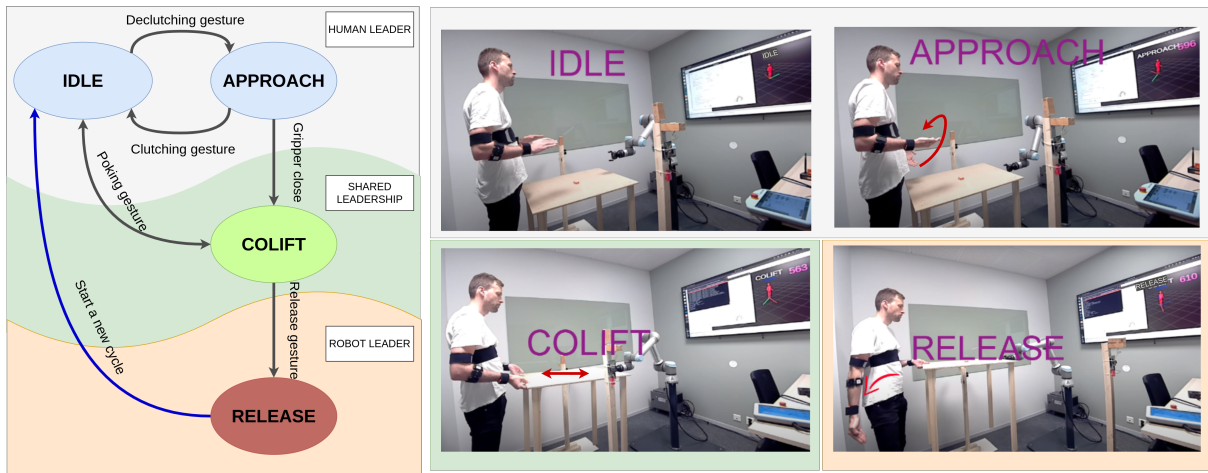


**Figure 2.** HRC roles and states in the experimental co-lift scenario. Human Leading role has two states: IDLE: Both chest-to-wrist (hand) motions are actively calculated yet no motion command is sent to the robot. APPROACH: Combined (merged) pose from two hands is actively calculated to produce soft real-time end-effector goal pose commands. The robot follows the human actively. Shared Leadership role has one state: CO-LIFT: The robot applies a directional compliant force and the human decides the direction of this force with elbow gestures. Robot Leading role has one state: RELEASE: The robot takes the lead in the operation, and moves to a predefined release pose. The human follows the robot’s motions. The steering arm is assigned for transition gestures and the red arrows show the respective transition gestures between states. Rotating the right palm up/down is assigned as the de-clutching/clutching gesture, clenching the right fist is the gripper close gesture (not highlighted in the fig.), pushing/pulling the table is the poking gesture, and releasing the right arm down is the release gesture.

136 motion capture technology is not critical and any type of human-motion estimation method would work as  
 137 long as the human input is appropriate to create a real-time goal pose command for the robot.

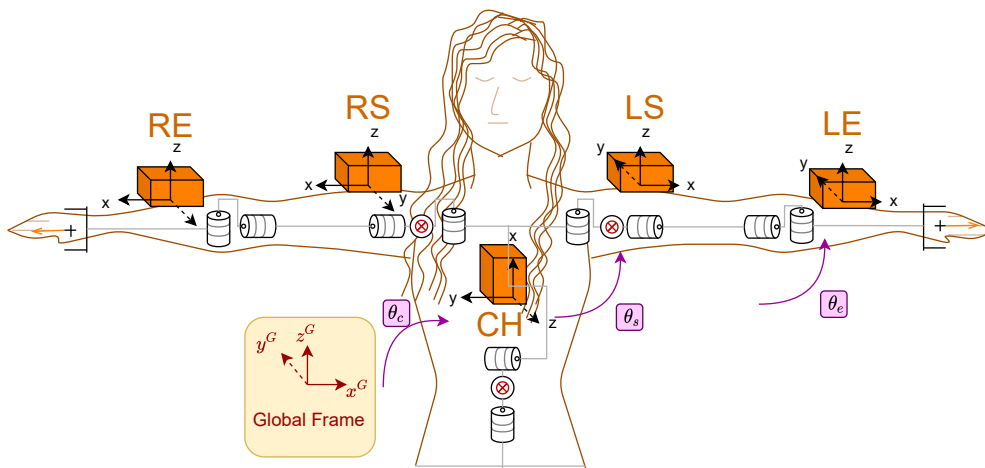


**Figure 3.** Human model and IMU placement on right/left elbow (RE/LE), right/left shoulder(RS/LS) and chest (CH) (Ates et al., 2022)

With this model, we measure 13 degrees of freedom (DoF) upper-body motions including the chest, upper and lower arm motions on both arms but neglected the wrist motions. Our human model is a collection of estimated individual joint angles, where a joint angle can be found by calculating the rotation between two

consecutive links with attached IMUs. The kinematic chain for such a human model from the base (chest) to the tip (left hand) can be written as:

$$q_c = q_{CH}^{GS} \quad q_s = q_c^* \otimes q_{LS}^{GS} \quad q_e = q_c^* \otimes q_s^* \otimes q_{LE}^{GS} \quad (1)$$

138 where  $q_c$ ,  $q_s$  and  $q_e$  are the quaternions representing joint angle rotations,  $q_{CH}^{GS}$ ,  $q_{LS}^{GS}$  and  $q_{LE}^{GS}$  are the IMU  
139 orientation from global to the sensor's frame which are the raw orientation readings from the IMUs. The  
140 same procedure is applied to the right arm. The lower body is taken as the fixed reference frame.

## 141 2.2.2 Human Biomechanical Model

142 In human motion and gesture estimation, the first step is to define the human model. This model can be a  
143 silhouette as in Bradski and Davis (2000) or a biomechanical model as in Roetenberg et al. (2009); Cerveri  
144 et al. (2005). Since the human body contains more complex joints and links than ordinary actuators and  
145 link elements, it is not possible to model the human body with 100% accuracy. As a result of that, the total  
146 degrees of freedom (DoF) of the human model is not exact. For example, the human arm is modeled as 4  
147 DoF in Theofanidis et al. (2016), 9 DoF in Phan et al. (2017) and 7 DoF in Ghosal (2018).

## 148 2.2.3 Human to Robot Motion Translation

149 Human-to-robot motion translation converts estimated human motions and gestures into the desired goal  
150 pose for the robot manipulator in real-time. The human arm motion is not directly mimicked by the robot.  
151 Depending on the states explained in more detail in Section 2.1, different human-to-robot motion mapping  
152 methods are applied. This subsection presents how a robot manipulator goal pose command is created  
153 based on given human arm motions. The human arm is modelled as 5 DoF and the robot used in this study  
154 is a 6 DoF (RRRRRR) manipulator with a spherical wrist configuration.

155 In the case of active command cooperation, two arm motions of the human are merged to create one  
156 end-effector goal pose. In the case of passive command cooperation, two elbow poses are used.

### 157 2.2.3.1 Active command cooperation scenario

The relative motions of both human arms are merged and translated into a single goal pose for the robot as introduced in Ateş and Kyrkjebø (2021). The merged hands pose is calculated based on the relative motions of each arm. We refer to the arms as the motion arm and steering arm. The steering arm is also responsible for clutching and state transitions. In our setup, the steering arm is the right arm but this can be changed in the merged hand pose equation (Equation (2)).

$$\hat{P}_{h,t}^- = \hat{s} \cdot (\hat{P}_{hm,t=0}^{-1} \times \hat{P}_{hm,t}) + \hat{k} \cdot (\hat{P}_{hs,t=0}^{-1} \times \hat{P}_{hs,t}) \quad (2)$$

158 where  $\hat{P}_{h,t}^-$  is the merged hand pose at  $t = 0^-$ ,  $\hat{P}_{hm,t=0}$  is the motion hand's pose,  $\hat{P}_{hs,t=0}$  is the steering  
159 hand's pose. The multiplication with their inverse at  $t = 0$  simply sets the pose readings to zero for relative  
160 motion mapping.

161 Also, different weights for each arm motion can be defined by the scaling factors  $\hat{s}$  and  $\hat{k}$  in Equation (2)  
162 in the code but for these experiments, they both set to the same multiplier.

The robot goal pose based on the merged hand pose is

$$\hat{H}(t) = \hat{P}_{h,t=0}^{-1} \times \hat{P}_{h,t} \qquad \hat{P}_{r,t} = \hat{P}_{r,t=0} \times \hat{H}(t) \qquad (3)$$

163 where  $\hat{H}(t)$  is the transformation of the merged hand pose from the initial to the current pose.

164 **2.2.3.2 Predefined command cooperation scenario**

165 When the human and the robot are both in the leadership role (i.e. carrying the object together, defined  
 166 as COLIFT state in Sect.2.1) the predefined command cooperation method is applied. There the human  
 167 uses elbows to show the direction where the robot should go with a poking gesture (i.e. by pulling/pushing  
 168 the object). The motion type is predefined such that the robot goes upwards, downwards, left and right  
 169 in the xz-plane. The flowchart of how the predefined command cooperation in the active lifting phase is  
 170 implemented is given in Figure 4.

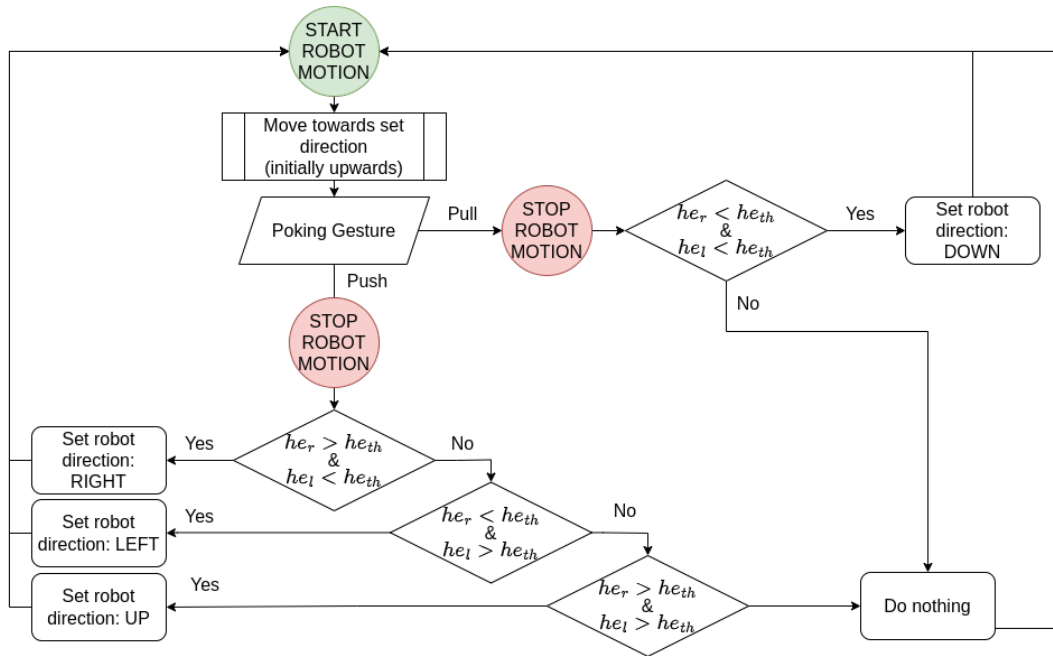


Figure 4. Predefined command cooperation in the active lifting phase (i.e. COLIFT state)

171 **2.3 Gamification**

172 Gamification methods in HRC user training are explained in detail in our previous study (Ates and  
 173 Kyrkjebø, 2022). The time constraint is directly connected to the score element. The game (i.e. each trial)  
 174 is supposed to be finished in 10 minutes. The user starts with 600 points and loses 1 point every second.  
 175 There are 2 buttons within the common workspace that represent physical waypoints and are defined as  
 176 achievement elements. Each successful button press gives an additional 60 points. The game elements used  
 177 in this study and their role is listed below:

- 178 • **Themes** create interest and engagement in educational games. It could be some sort of introductory  
 179 backstory or a narrative that accompanies the entire game. For the proposed HRC scenario, the  
 180 background story is presented as the research objectives.

- 181 • **Achievements** are the mechanisms connecting the target outcomes of the HRC task that the gained  
182 user skills.
- 183 • The **game score** is calculated based on the user's performance, which only depends on how quickly  
184 they complete each achievement in this study. Additional parameters can be enabled such as the  
185 measurements taken from the IMU on the carried table regarding the tilting, deviation and trembling  
186 of the table.
- 187 • **Challenges** and conflicts are central elements in any game and they can be physical obstacles, battles  
188 with other players, or puzzles that need to be solved. In this study, the physical targets are set to be  
189 challenging elements.
- 190 • In an entertainment game, **feedback** is usually immediate and continuous which can be delivered  
191 through, reward points, additional 'powers' within the game or direct messages. In this study, both  
192 immediate and direct message feedback types are used through three main elements: simulated  
193 human model, game score and HRC state. No *guided* feedback is implemented but the procedure was  
194 supervised by a human expert and objective guidance to all users are provided as needed.
- 195 • **Time constraint** is a particular type of challenge in serious games, which is a powerful tool to push  
196 user limits. In this study, the time constraint is directly connected to the score element.
- 197 • **Self-expressions** are the parameters and preferences of the game which are up to the user. The user  
198 could ask to change the speed and the responsiveness of the robot. Moreover, in the proposed HRC  
199 case, the initial poses of the user's hands, and the way the user grabs the table are not restricted but only  
200 guided before the trials. These are open questions in the relevant HRC study and user self-expressions  
201 are believed to be helpful in deciding the most optimal usage.
- 202 • **Aesthetics** are the game's visual, aural and artistic elements in a gamified system. They play an  
203 engaging and immersive role in the game. In an HRC scenario, the real robot can be perceived as an  
204 aesthetic element. Nonetheless, it is still important to add aesthetic elements to help the user engage  
205 in the task. In this study, the physical buttons incorporate LEDs that are activated when the button is  
206 pressed. Additionally, a graphical user interface is developed for the procedures that the user is able to  
207 see throughout the experiment.

### 3 USER EXPERIMENTS

208 This section explains how the cooperative lifting operation is set up for user experiments using human  
209 motion and gesture information, and gaming elements. The technical setup is explained in detail, along  
210 with the user recruitment and selection procedure, the experimental procedure that all participants perform  
211 in the experiments, and the learning criteria users are evaluated by. The experimental procedure was carried  
212 out in 4 stages: pre-survey, video tutorial, physical human-robot experiment, and post-survey.

#### 213 3.1 Technical setup

214 The majority of the physical experimental part is suggested in our previous study (Ates and Kyrkjébo,  
215 2022). The human-robot experimental system was set up in ROS master PC which is a standard laptop with  
216 ROS Noetic installed. The ROS master handles all communication between the Xsens Awinda wireless  
217 IMU system, physical buttons connected to Arduino Uno microcontrollers transmitting wirelessly via  
218 NRF24L01+ RF transmitters, and the Universal Robot UR5e cobot which is connected to the same local  
219 network as shown Figure 5.



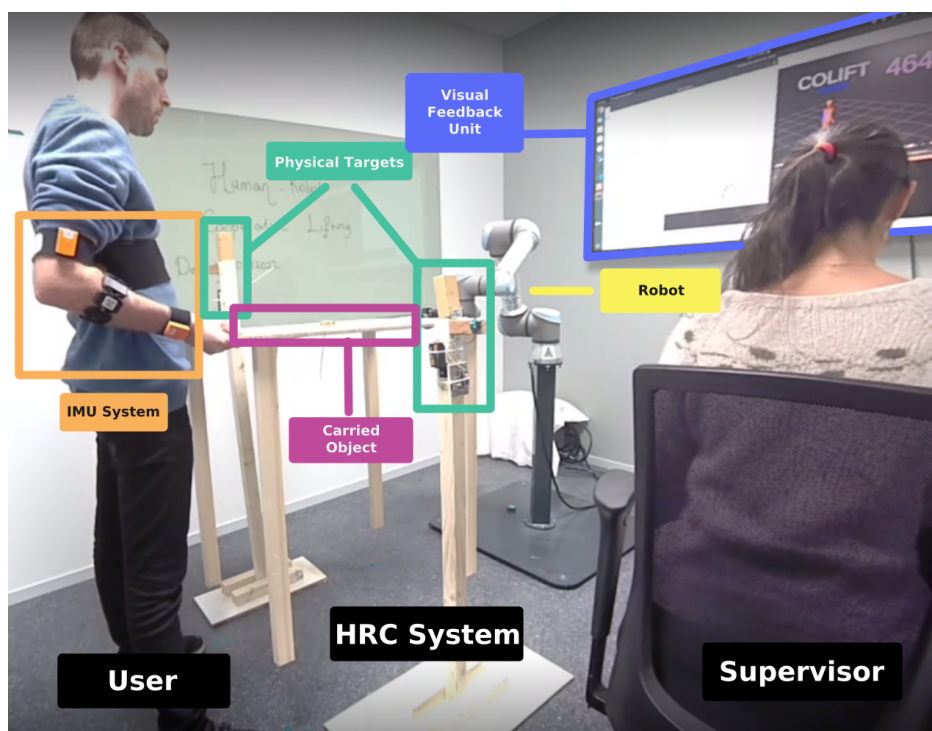


**Figure 5.** Experiment room and the units of the training system

## 220 3.2 User recruitment and selection

221 The user experiments took place at Western Norway University of Applied Sciences, Campus Førde in  
 222 autumn 2022. The announcements for recruitment to the experiment were distributed through social media,  
 223 flyers at the University, and through the local newspaper. A total of 40 healthy participants between ages of  
 224 20-54 were recruited in total, 8 of which were used as pilot users to optimize experimental parameters such  
 225 as the number of trials, the robot interaction force threshold during in co-lift state, human-robot directions  
 226 (mirrored mapping), and some additions to the GUI. Data from the pilot experiments are not included  
 227 in the paper. In total, 32 participants did ten or more trials on the human-robot colift system, and were  
 228 assigned a 5-digit random ID and stored anonymously according to Norwegian Centre for Research Data  
 229 standards <sup>1</sup>. Users with severe physical disabilities were excluded from participating in the experiments.

## 230 3.3 Pre- and post-survey

231 All participants were asked to fill in a pre-survey and a post-survey form online using Microsoft Forms.  
 232 In the pre-survey, users were asked general personal questions, related to interest in robotics and familiarity  
 233 with robots. In the post-survey, the users were asked to assess several elements of the system such as  
 234 the visual feedback, leadership roles between them and the robot, difficulty of the task in four states,  
 235 intuitiveness of the system and fatigue. The answers are collected either as short texts or a selection from a  
 236 Likert scale depending on the question.

237 User's heights and arm lengths are measured before the physical experiment. The user was asked to keep  
 238 the shoes on during the height measurement since we are interested in the effective height the user while  
 239 s/he was performing the task. Arm length measurement was the length between right wrist to right shoulder  
 240 origin.

<sup>1</sup> [www.nsd.no/](http://www.nsd.no/)

241 After the pre-survey, a tutorial video<sup>2</sup> was made available to users to show them the task and how the  
 242 system works. The video was uploaded on Youtube as *Unlisted* and the access link was only shared  
 243 by the subjects before the physical experiments. To minimize the bias, users who had completed the  
 244 experiment were asked not to discuss the details of the procedure with other participants. After the physical  
 245 experimental procedure, the post-survey was applied.

246 To analyse if any background factors played a role in how well users can learn to cooperate with robots,  
 247 we divided participants into two samples based on the survey responses. For the gender and job category,  
 248 the samples were *Woman - Man* and *IT/Engineering - Other*. For other categories, samples were divided  
 249 into *Low - High* based on the numerical selection on the scale in the respective survey question. For  
 250 the majority of the categories, the integer mid-point of the Likert scale was selected as the threshold for  
 251 dividing into samples. However, for some questions, the participants' answers were weighed on only one  
 252 side of the threshold such as for physical tiredness and mental tiredness, and we used the mean of the  
 253 answers instead of dividing participants into two samples.

254 We applied a two-tailed t-test for each category with respect to each learning criterion. The null hypothesis  
 255 was the same for all categories: "*There is no difference between sample- $\mathcal{X}$  and sample- $\mathcal{Y}$  in learning*  
 256 *criteria  $\mathcal{L}$* ". We analyzed the samples with respect to the learning criteria where the null hypothesis was  
 257 rejected with 10% significance level.

258 The t-test formula  $t$  for unequal sizes and variances between samples and the degree of freedom calculation  
 259  $df$  in Equation (4) was used.

$$t = \frac{(\bar{x} - \bar{y}) - (\mu_x - \mu_y)}{\sqrt{\frac{s_x^2}{n_x} + \frac{s_y^2}{n_y}}}, df = \frac{\left(\frac{s_x^2}{n_x} + \frac{s_y^2}{n_y}\right)^2}{\frac{\left(\frac{s_x^2}{n_x}\right)^2}{n_x - 1} + \frac{\left(\frac{s_y^2}{n_y}\right)^2}{n_y - 1}} \quad (4)$$

260 where  $\bar{x}$ ,  $\bar{y}$  are the calculated means,  $s_x$ ,  $s_y$  are standard deviations and  $n_x$ ,  $n_y$  are the size of the sample- $\mathcal{X}$   
 261 and sample- $\mathcal{Y}$ , respectively. The term  $(\mu_x - \mu_y)$  is the difference of hypothetical means of two samples,  
 262 which is zero in our case based on the null hypothesis ( $H_0 : \mu_x = \mu_y$ ). The denominator is the estimated  
 263 standard deviation ( $SE_{\bar{x}-\bar{y}}$ ) of the distribution of differences between independent sample means for  
 264 unequal variances.

265 To calculate the effect size, we used both Cohen's  $d$  and Hedge's  $g$  because of the difference in variance  
 266 between samples. To decide which one to use for particular categories, we set a threshold such that the  
 267 difference between two standard deviations was less than the minimum of the two standard deviations.  
 268 Therefore, the effect size calculation was

$$\begin{cases} d = \frac{(\bar{x} - \bar{y})}{\sqrt{\frac{s_x^2 + s_y^2}{2}}} & \text{if } |s_x - s_y| < |(\min(s_x, s_y))| \\ g = \frac{(\bar{x} - \bar{y})}{\sqrt{\frac{((n_x - 1) \cdot s_x^2 + (n_y - 1) \cdot s_y^2)}{n_x + n_y - 2}}} & \text{otherwise.} \end{cases} \quad (5)$$

<sup>2</sup> [https://youtu.be/\\_JZ-ENtVb7w](https://youtu.be/_JZ-ENtVb7w)

### 269 3.4 Experimental procedure

270 For the experimental procedure, we designed a co-lift operation that deliberately challenged participants  
 271 to cooperate with the robot to achieve the goal of the operation. In the experiments, the human and the robot  
 272 would pick a table whose location was not known to the robot, move it via two goal posts whose locations  
 273 were also unknown to the robot, and place the table on a predefined final position known to the robot. The  
 274 participants were scored based on the elapsed time, if they reached the goal posts, and if the overall co-lift  
 275 operation was successful. Every participant started at 600 points, and lost one point each second. They  
 276 gained 60 points for each successful goal post requiring that participant and the robot could cooperatively  
 277 lift and move the table to trigger the physical buttons. When the last goal post was successfully reached,  
 278 the user could gesture that the system should enter into the RELEASE state, and the robot would take the  
 279 lead in placing the table on the final position to end the experiment and the score countdown.

280 All users started with the same robot speed. In the APPROACH state the `servoL` parameters for the  
 281 robot were selected as acceleration =  $0.5m/s^2$ , velocity =  $0.3m/s$ , blocking time =  $0.002s$ , lookahead time  
 282 =  $0.1s$ , and gain = 300. In the COLIFT state, the `forceMode` parameters were dependent on the direction,  
 283 and the compliant force  $F$  upwards was set to  $3 \cdot F$ , downwards to  $0.5 \cdot F$ , and sideways to  $1.5 \cdot F$ . The  
 284 maximum allowed end-effector speed along the compliant axes was  $0.8m/s$  for horizontal directions and  
 285  $0.5m/s$  for vertical directions. For non-compliant axes, the maximum allowed deviation along any axis  
 286 was  $0.3m/s$ . The angular compliance limits along all axes were set to  $0.17rad/s$ . In the RELEASE state,  
 287 the `moveL` end-effector speed was set to  $0.25m/s$  with acceleration =  $1.2m/s^2$  in asynchronous mode.  
 288 After the user felt comfortable in using the system with the current parameters, s/he could ask to speed up  
 289 the robot in selected directions.

290 Experiments took a place in a distraction-free room where only the experiment conductor (supervisor)  
 291 and the participant were present during the experiments. The visual feedback unit and the robot were  
 292 visible to the participant from the same perspective as shown in Figure 5.

### 293 3.5 Learning evaluation

294 To evaluate learning, we compared user scores of 10 trials using 6 different criteria:

- 295 • **Highest:** The best score for the participant.
- 296 • **Average 3 (*avg\_3*):** Average of 3 best scores.
- 297 • **Average of last 5 (*avg\_last\_5*):** Average of last 5 trials.
- 298 • **Variation of highest 3 (*var\_3*):** Variation of 3 best scores.
- 299 • **Deviation from baseline (*delta\_learning*):** Difference between average of first two trials (*avg\_first\_2*)  
 300 and last 2 (*avg\_last\_2*) trials.
- 301 • **Learned trial (*trial\_no\_avg\_reached*):** The trial number for which the participant reached the *avg\_3*  
 302 score.

303 To eliminate the chance effect, the 3 best scores of the participants were averaged in *avg\_3*, and to evaluate  
 304 the level of how well the participant had learned the cooperation, the average score of the last 5 trials were  
 305 calculated in *avg\_last\_5*. The standard deviation of the highest 3 scores were calculated in *var\_3* to analyze  
 306 if a particular high score was due to luck, or a more consistent learned cooperation. The average of the  
 307 first two trials *avg\_first\_2* were compared to the average of the last two trials *avg\_last\_2* to get a measure in  
 308 *delta\_learning* of how much the participants had improved during trials. How fast the participant gets used

309 to the system was calculated in (*trial\_no\_avg\_reached*). We avoided using a single criterion and/or single  
310 trial score to evaluate learning to obtain a broader perspective on user learning.

## 4 RESULTS

311 A total of 32 healthy adults participated in the experimental study, with 10 female and 22 male participants  
312 between 20 and 54 years old. The users had different occupational backgrounds (health, IT, management,  
313 craftsmanship, pedagogy, unemployed, etc.) at different levels (students, employees) and had different  
314 previous experiences from interacting with robots (both on a technical and a social level). The presentation  
315 of the results is divided into two aspects. First, the measures of the system based on the motion and gesture  
316 data collected during the experiments is presented in Section 4.1. Second, how the participants were able to  
317 learn to use the system with respect to the various background factors collected in the pre- and post-survey  
318 is presented in Section 4.2.

### 319 4.1 HRC System Measures

320 In total nine metrics related to the HRC system are presented in Figure 6. One participant (User ID:35764)  
321 has been selected to illustrate the data from the experimental trials. The participant is a female health  
322 worker, more than 30 years old, has no current or past gaming habits, programming background and  
323 education in robotics, but stated that she has a cleaner type of robot at home/work in the user survey.  
324 The participant is not selected based on any particular background factor other than to visualize the data  
325 collected during the experiments. The user score data from all participants is provided for comparison as  
326 open access data for reproducibility (Venås, 2023).

327 From Figure 6, we see that the user score increases from the 1<sup>st</sup> to the 10<sup>th</sup> trial. The duration of the  
328 first trial is about 400 seconds whereas the last is just over 60 seconds. There are quite a few transitions  
329 between the IDLE and the APPROACH states in the first trial.

330 Since the participant is not familiar with the system, she has a difficult time making the robot move in the  
331 desired direction and resets the hand motions several times by going back to the IDLE state. This type of  
332 several hand-reset behaviours is seen in trials 2, 3 and partly 4, but decreases as the participant learns/gets  
333 familiar with the system. From the 6<sup>th</sup> trial the user reached a consistent level of performance.

334 Another point to highlight is the changes in the duration of the IDLE+APPROACH and COLIFT states.  
335 The duration of the IDLE+APPROACH state shows how comfortably the participant controls the robot's  
336 motion using two-arm motions when the participant is the leader of the system. The first attempt to grab the  
337 table took around 160 seconds, whereas she managed to reduce it to under 10 seconds in later trials. The  
338 duration of the COLIFT state shows two things: 1) how comfortably the user controls the robot's motion  
339 using instant gestures when the user cooperates with the robot, and 2) how well the grasping has succeeded.  
340 By default, the robot moves upward when the grasp on the table is complete. If the grasping is too abrupt,  
341 the robot will not automatically start moving upwards (as seen in trials 1, 2, 5 and 10) because it registers  
342 an initial poking gesture. The user needs to adjust the elbows' poses adequately and poke the robot so that  
343 the initial upward motion starts again.

344 Some minor details to remark are the number of poking attempts during the COLIFT state, the magnitude  
345 of poking force, and the table acceleration over different trials. The table acceleration is pretty smooth  
346 overall for this user except for trial 5. In the first trials, there are significantly more poking attempts than in  
347 the last trials (except for trial 10). The poking force is well above the threshold which could be related to  
348 uncertainty about the system responsiveness. After the 6<sup>th</sup> trial, there is more consistent poking behaviour.

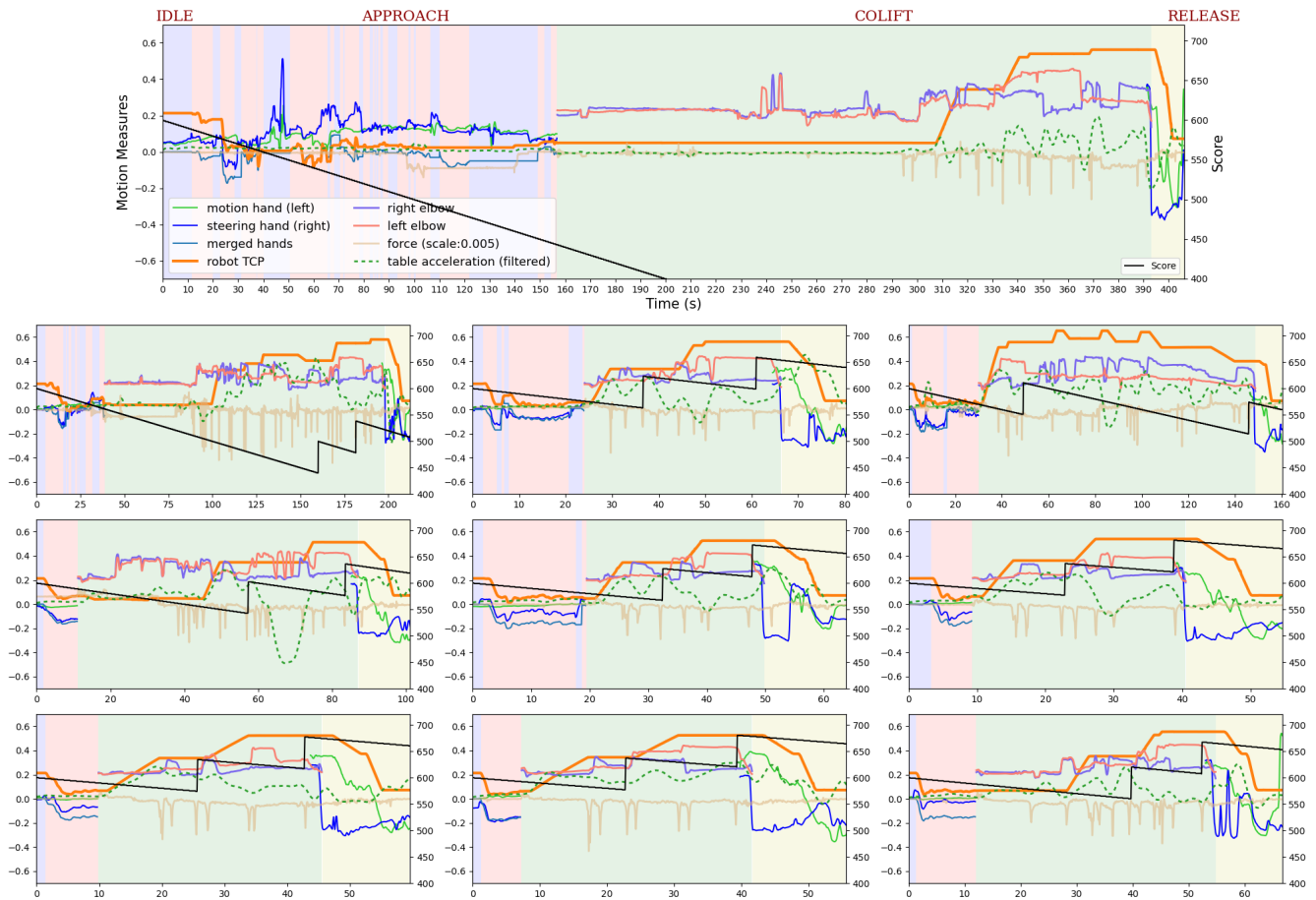


**Figure 6.** The figure shows the experimental measurements of user ID:35764 during the 10 trials. The largest figure on the top is the first trial, and the rest of the trials are presented row by row from the top left to the bottom right. The experiments start with the IDLE state highlighted with purple background colour, followed by the APPROACH, COLIFT, and RELEASE states, which are highlighted with pink, green, and yellow background colours, respectively. The user’s two hand motions, calculated merged hands motion, and two elbow heights are measured from the participant’s side. The hand motions are visible shown in the IDLE, APPROACH and RELEASE states, and the elbow motions are shown only in the COLIFT state. The end-effector (TCP) motion and the exerted force are measured from the robot’s side, and the table acceleration and user score are measured as training parameters.

349 Note that the slight inconsistency in the 10<sup>th</sup> trial with regards to the upwards trend in the score and  
 350 consistent poking behaviour is discussed in Section 5.1.

## 351 4.2 User Learning Evaluation

352 We divided the user sample into two groups for 18 different user parameters such as age, gender,  
 353 occupation, body size, robot familiarity, gaming habits etc. and observed their scores over 10 trials. The  
 354 data is provided in Figure 7 as learning curve plots.

355 The goal of the analysis was to identify any differences in learning curves between the sample groups  
 356 if any significant difference. The null hypotheses are the same for all categories: "There is no difference  
 357 between sample- $\mathcal{X}$  and sample- $\mathcal{Y}$  in learning criteria  $\mathcal{L}$ ": . We investigate the list of samples with respect  
 358 to the learning criteria where the null hypothesis is rejected with 10% significance level.

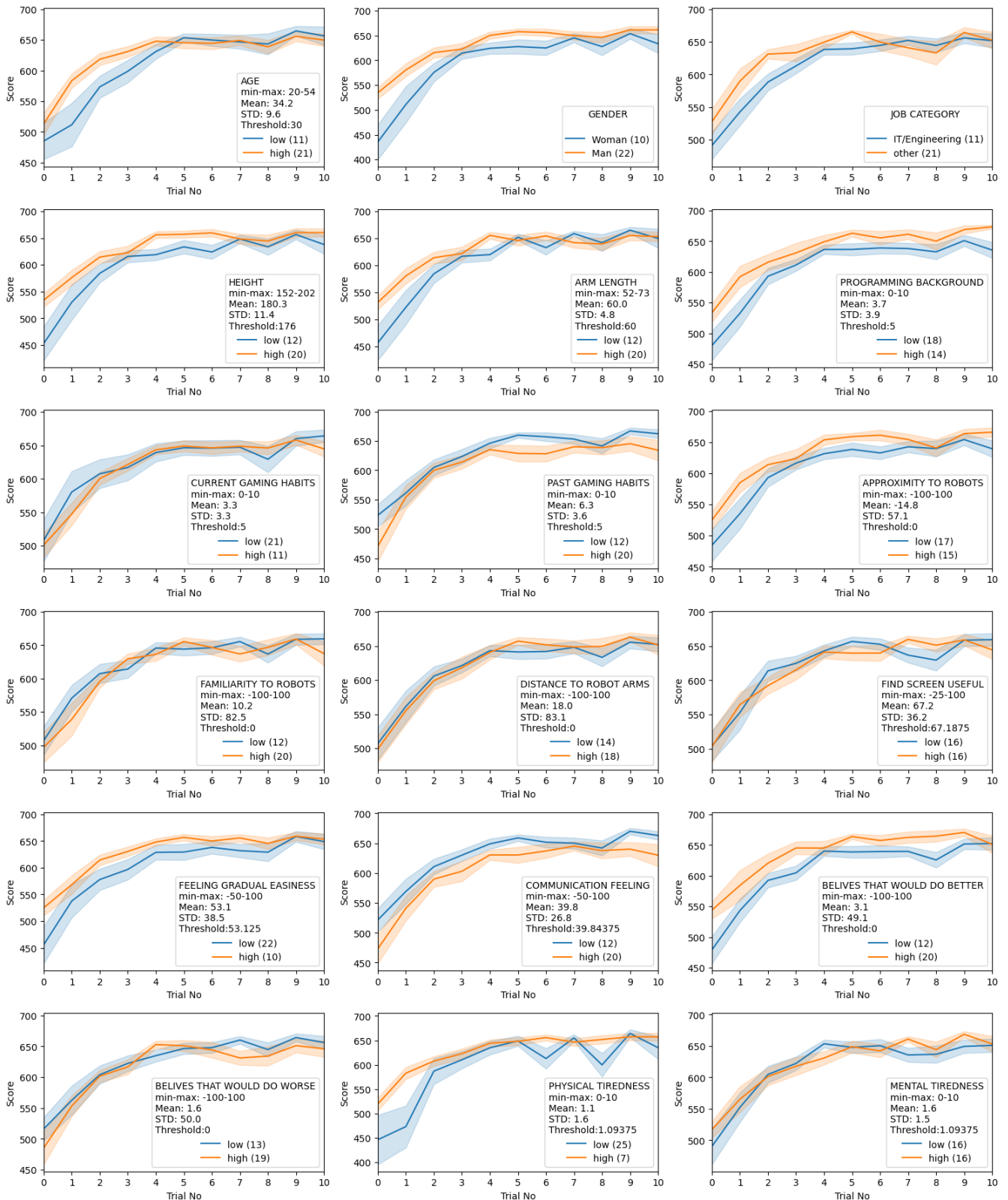


**Figure 7.** Participant background data on learning curves. Each plot shows the score of participants divided into two sample groups for the respective background variable. The plots show the aggregation of all participant scores in each sample group for each trial; the middle line shows the mean, and the shadow region shows the standard error.

359 As seen in Figure 7, all groups in each category have a similar learning curve which is increasing steep  
360 until around trial 3, keeps increasing with a relatively fixed gradient between trial 3 and trial 7, and  
361 reaches a plateau after trial 7. We designate those regions as 1) steep learning, 2) steady learning and 3)  
362 plateau. There is no user background factor that can be identified as significantly positive or negative in the  
363 progress of learning from this perspective. This supports a hypothesis of "everyone can cooperate" - or  
364 more precisely "everyone can *learn* to cooperate" - with robots.

365 Investigating the results more closely, there seems to be a drop in the score as the trial number increases  
366 in the majority of subplots in Figure 7 around 8<sup>th</sup>. This reverse learning effect is discussed in more detail  
367 in Section 5.2. Note also that the physical tiredness parameter seems to be one where there is more of a  
368 difference between the two sample groups. Although none of the users stated that they experienced severe  
369 physical tiredness or fatigue (see the mean and standard deviation, and the number of users in the sample  
370 group "low"), those who have lower physical tiredness have more fluctuating scores in the plateau region.

371 For most of the background factors, the two sample groups have relatively similar start levels, whereas,  
372 for some background factors, one sample group has a higher start score (*gender, job category, height,*  
373 *arm length, programming background, past gaming habits, proximity to robots, feeling gradual easiness,*  
374 *communication feeling, beliefs on would do better and physical tiredness*). While the higher start score  
375 in *gender, height, programming background, past gaming habits, proximity to robots and communicate*  
376 *feelings* is also reflected in higher end-scores, the higher start score for the *job category, arm length, feeling*  
377 *gradual easiness, beliefs on would do better and physical tiredness* converges to the same end score as  
378 the other sample group. The sample groups divided by age start and end in relatively similar scores, yet  
379 the steep learning region in higher age groups are even steeper. Lastly, there are no significant differences  
380 between the sample groups of *current gaming habits, robot and robot arm familiarity, visual feedback*  
381 *screen usage and mental tiredness* for the start and the end scores. Further details on the quantitative  
382 results for each background factor towards the learning criteria based on the results of the t-tests, respective  
383 p-values and effect sizes are given in Section 5.2.

## 5 DISCUSSION

384 The learning progress of the different sample groups towards the different learning criteria, and the main  
385 findings regarding the results of the t-tests, respective p-values and effect sizes, are given in Table 1.

386 Note that in Figure 7, we can see subtle decreases in the score around trial numbers 7,8 and 9. According  
387 to our observations and user feedback, this could come from several reasons. First, participants were new to  
388 the HRC control scheme and how to use both arms to control the robot. Therefore, the participants focused  
389 in their first trials (on average four trials) to get used how to control the robot and their own body motions  
390 and gestures, rather than trying to solve the task as quickly as possible. However, as user confidence  
391 increased (particularly in the learned plateau), more risk-taking behaviour was observed, and users asked  
392 for more speed and tried new approaches to accomplish the task faster. This behaviour was observed more  
393 in users with competitive traits and those who had acquaintances enrolled in the experiment.

394 Note also that the majority of the users requested to continue the experiment after the 10<sup>th</sup> trial and  
395 achieve even better performance. The data from these trials were not included in the analysis for fair  
396 analysis but can be seen in Figure 8.

### 397 5.1 Observed User Behaviours

398 Relevant observations made by the supervisor during experiments are discussed in this section.

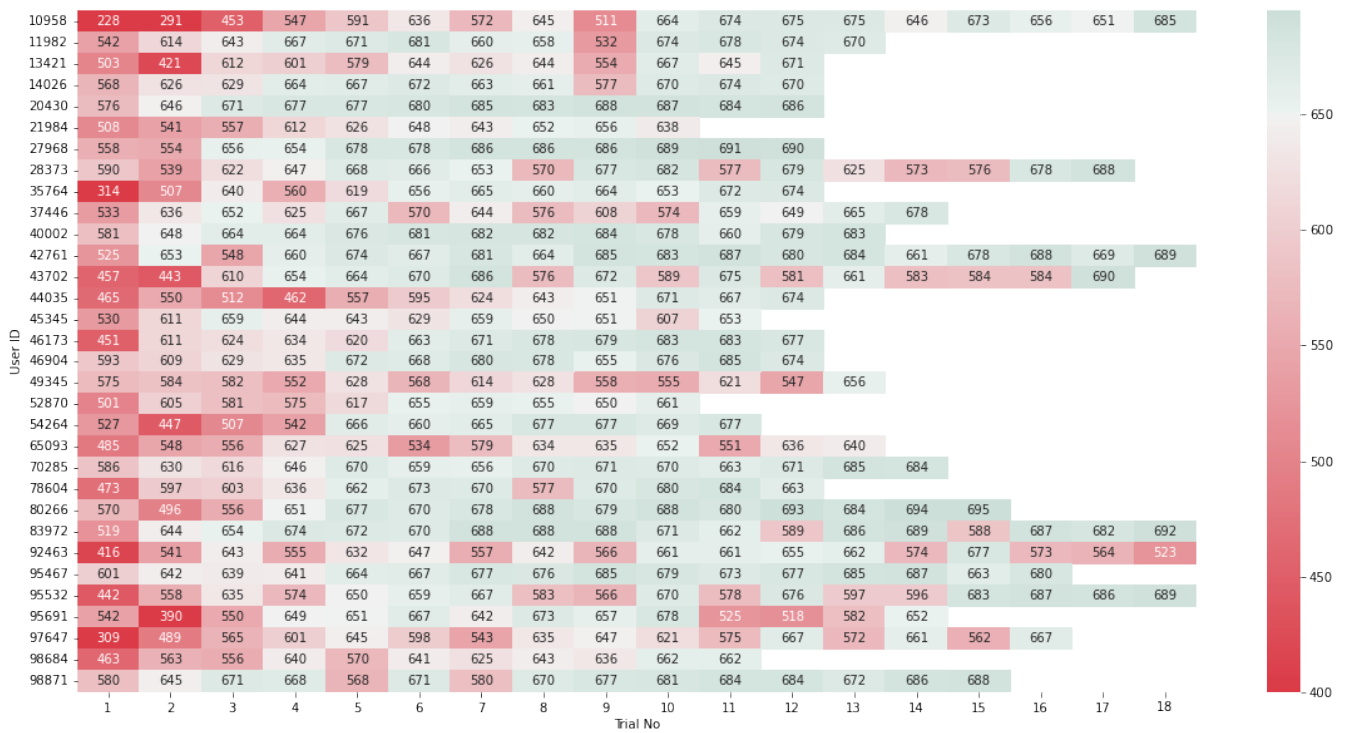


**Figure 8.** User score data on each trial. The results are colour-coded from red to green to visualize the training results from low to high.

399 First, the user’s comfort with the experiment and the setting is important for performance. User comfort  
 400 most likely differ between users who work in similar environments to where the experiment took place and  
 401 those who had never been at campus. Observations on how the user felt after the first trial were noted during  
 402 the experiments, and any discomfort can also be a compounding factor in the metrics related to feeling  
 403 gradual easiness, communication quality, beliefs that would do better or worse. This will be discussed  
 404 more in later sections.

405 A risk-taking behaviour as the user comfort increases can be seen in the measurements figure of the  
 406 example user Figure 6. The 10<sup>th</sup> trial ends up with a lower score than 7-8-9<sup>th</sup> trials. The reason was that  
 407 the user learned how to smoothly transit from the APPROACH state to COLIFT state without any harsh  
 408 grasping after trial number 5 (see the robot TCP line). However, in the 10<sup>th</sup> trial, the user was too quick  
 409 lift the table before the robot’s grasp was completed, which violated the grasp action, and the robot didn’t  
 410 start moving upwards which cost the user a few points. This type of behaviour was also seen for other  
 411 participants as well as in different stages of the task such as elbow height adjustments, releasing before  
 412 the goal post buttons were pressed etc. Another observation linked to user learning was the change in the  
 413 poking force magnitude. Two distinct behaviour was observed between users: 1) they would interact with  
 414 higher forces because they thought of the robot as a sturdy machine, and 2) they would interact with lower  
 415 forces because of fearing to damage the robot. As seen in the force (scale 0.005) line of Figure 6, this  
 416 particular user started with a relatively high poking force (trials 1 and 2) but lowered it in the later trials  
 417 (6,7,8 and 9). Even though the user experienced a problem in trial 10, she did not increase the magnitude of  
 418 the interaction force – she had learned the necessary level of force required to transition into the next state.



419 Participants also implemented instructions differently. For instance, some users preferred using both  
 420 hands equally in the APPROACH state, whereas some chose one hand (unintentionally, regardless of which  
 421 was their dominant hand) and kept the other hand stationary.

422 **5.2 Background factors vs Learning criteria**

423 Regardless of age, gender, job category, gaming background, and robot familiarity, the learning curves  
 424 of all users are positively inclined in Figure 7. The user scores were evaluated in for 6 different learning  
 425 criteria, and the significant participant background factors were calculated with a two-sample t-test as  
 426 shown in Section 3. In total 34 [background parameter, learning criteria] pairs were found to be significant  
 427 with a p-value less than 0.1 and effect size bigger than 0.5 as shown in Table 1

428 We have avoided using a single learning criteria or single trial score to evaluate learning. Based on  
 429 our observations during the experiments, some users changed behaviour after some trials which caused  
 430 deviations and glitches in their score curves. The most common deviation was because of the "reverse  
 431 learning" effect. Some users who experienced that they learned to use the system well in early trials  
 432 pushed their limits to achieve a better high-score. Although participants were informed that there was no  
 433 competition between users, some users with highly competitive traits prioritized a higher score over a  
 434 consistent learning curve. On the other hand, other participants aimed to achieve the task with as little risk  
 435 for failure as possible, and declined increasing the speed even though observations indicated that they could  
 436 have managed this change well. Therefore, we have analyzed data using all 6 learning criteria towards the  
 437 all background factors for the participants.

**Table 1.** Statistics table across user background and learning criteria. In total 34 background variables gave significant results out of 144 t-tests

Category	Learning Criteria	$\bar{x}$	$\bar{y}$	$s_x$	$s_y$	$n_x$	$n_y$	t-score	p-value	effect size ( $d \wedge g$ )
Programming background	highest	674.00	683.43	12.46	9.21	18	14	-2.46	0.02	Large(-0.86)
Programming background	avg_3	660.41	674.10	16.76	12.06	18	14	-2.68	0.01	Large(-0.94)
Physical Tiredness	avg_first_2	551.08	459.71	54.23	109.76	25	7	2.13	0.07	Large(1.32)
Past Gaming Habits	highest	671.25	682.25	12.26	9.96	12	20	-2.63	0.02	Large(-0.99)
Past Gaming Habits	avg_3	657.33	671.83	18.49	12.14	12	20	-2.42	0.03	Large(-0.93)
Height	avg_first_2	491.38	554.92	99.86	50.55	12	20	-2.05	0.06	Large(-0.8)
Gender	var_3	56.22	22.09	50.47	30.89	10	22	1.98	0.07	Large(0.82)
Gender	avg_first_2	473.10	557.45	98.81	49.63	10	22	-2.56	0.03	Large(-1.08)
Gender	delta_learning	167.55	96.23	89.71	52.90	10	22	2.34	0.04	Large(0.97)
Feeling Gradual Easiness	var_3	21.03	58.56	27.38	53.28	22	10	-2.10	0.06	Large(-0.89)
Communication Feeling	highest	669.25	683.45	12.45	8.03	12	20	-3.53	0.00	Large(-1.36)
Communication Feeling	avg_3	657.89	671.50	16.94	13.76	12	20	-2.36	0.03	Large(-0.88)
Believes that would do better	avg_3	674.28	661.67	11.64	16.95	12	20	2.49	0.02	Large(0.87)
Believes that would do better	avg_last_5	663.85	639.12	16.42	29.75	12	20	3.03	0.01	Large(1.03)
Believes that would do better	avg_last_2	667.62	638.80	21.71	36.73	12	20	2.79	0.01	Large(0.96)
Arm Length	avg_first_2	489.67	555.95	97.99	51.27	12	20	-2.17	0.05	Large(-0.85)
Arm Length	delta_learning	163.75	91.38	75.35	58.23	12	20	2.86	0.01	Large(1.07)
Age	trial_no_avg_reached	7.91	6.57	1.22	2.01	11	21	2.33	0.03	Large(0.8)
Age	delta_learning	155.77	99.00	73.64	66.58	11	21	2.14	0.05	Large(0.81)
Programming background	avg_last_5	639.51	659.81	29.74	21.65	18	14	-2.23	0.03	Medium(-0.78)
Programming background	avg_first_2	506.39	562.86	86.24	53.34	18	14	-2.27	0.03	Medium(-0.79)
Past Gaming Habits	avg_last_5	636.20	655.71	33.14	22.29	12	20	-1.81	0.09	Medium(-0.69)
Mental Tiredness	trial_no_avg_reached	6.44	7.62	1.67	1.93	16	16	-1.86	0.07	Medium(-0.66)
Job Category	highest	682.91	675.62	9.17	12.69	11	21	1.86	0.07	Medium(0.66)
Job Category	delta_learning	90.00	133.45	47.20	80.70	11	21	-1.92	0.06	Medium(-0.66)
Height	avg_3	659.92	670.28	14.87	16.06	12	20	-1.85	0.08	Medium(-0.67)
Height	delta_learning	153.71	97.40	87.68	55.16	12	20	2.00	0.06	Medium(0.77)
Gender	avg_3	658.43	670.02	15.42	15.55	10	22	-1.96	0.07	Medium(-0.75)
Communication Feeling	trial_no_avg_reached	6.17	7.55	2.21	1.47	12	20	-1.93	0.07	Medium(-0.74)
Believes that would do better	var_3	17.63	41.83	24.66	45.82	12	20	-1.94	0.06	Medium(-0.66)
Believes that would do better	avg_first_2	564.17	511.25	53.15	84.74	12	20	2.17	0.04	Medium(0.75)
Familiarity with Robots	highest	674.76	681.93	12.13	10.95	17	15	-1.76	0.09	Medium(-0.62)
Familiarity with Robots	avg_3	661.57	671.87	17.94	12.38	17	15	-1.91	0.07	Medium(-0.67)
Familiarity with Robots	avg_first_2	510.03	554.97	92.21	50.98	17	15	-1.73	0.10	Medium(-0.6)

## 438 5.2.1 User Body Size

439 The system is designed such that it does not require to be tuned between users to be easily integrated into  
 440 industrial applications at a later stage. Since the human-to-robot motion mapping is a relative mapping,  
 441 users with different body sizes should be equally able to use the system. From Figure 7, we see that the  
 442 body size parameters *height* and *arm length* give similar progression of learning. However, according to  
 443 Table 1 body size makes a difference in some learning criteria. Participants who are taller and have longer  
 444 arms started with a better score (*avg\_first\_2*), while shorter participants showed a faster learning behaviour  
 445 (*delta\_learning*). In the end, there were no significant differences in the learning criteria except for the  
 446 average of the best 3 scores *avg\_3*. Note the effect of this user parameter is highly related to the model of  
 447 the human and human-to-robot motion mapping method used in Section 2, and thus we cannot generalize  
 448 that larger body sizes performs better. The takeaway from this experiment is that taller participants with  
 449 longer arms performed better in *this* experiment, and that body size *could* play a role in HRC learning  
 performance.

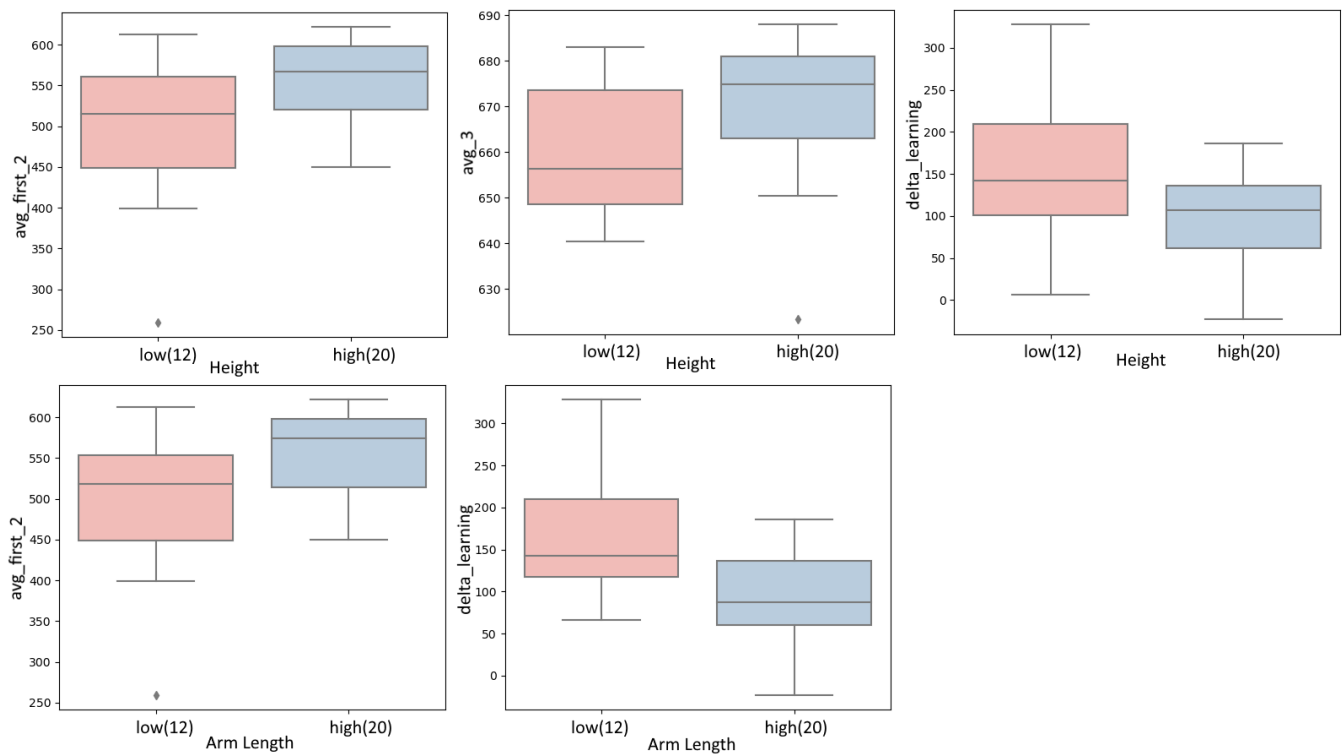


**Figure 9.** Body measures effect on learning. The pink group bar represents the lower measures and the blue group bar represents the higher measures of the respective numeric user factor (for this and the upcoming similar barplots).

450

## 451 5.2.2 Robot Familiarity and Anticipation

452 According to the t-test results in Table 1, users who had commercial robots at home or at work performed  
 453 slightly better on some learning criteria than those who were not that familiar with robots. However,  
 454 having a theoretical background in robotics does not seem to be significant for learning. The participants'  
 455 anticipation of the task had a bigger effect than assumed before the experiments. In total, 30 users out of 32  
 456 thought the first trials were hard, but that it got easier in later trials. Therefore, we took the mean of the given  
 457 answers and applied this threshold to divide the participants into two sample groups. Those participants

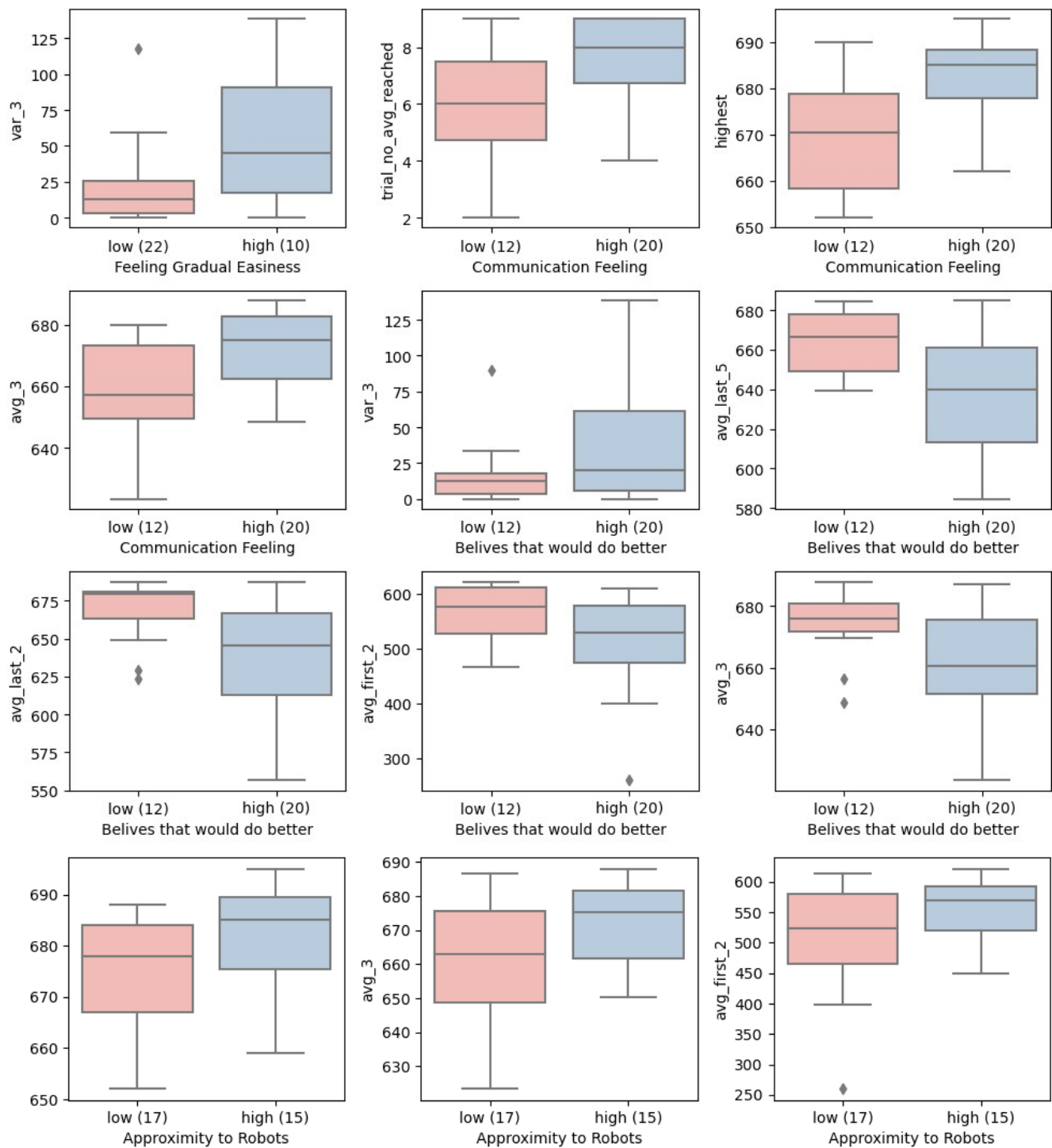


**Figure 10.** Robot familiarity and proximity effect on learning

458 who felt continuous difficulty achieved more consistent scores than those who felt the operation became  
 459 gradually easier. This could be related to higher risk-taking from users that felt the operation became  
 460 gradually easier. Another explanation could be that participants who felt a gradual easiness performed  
 461 worse in the start trials, and then performed much better in later trials. However, the t-test does not return

462 any significant results either for *avg\_first\_2* or *avg\_3*, which suggests that the risk-taking factor could play  
463 the bigger role.

464 Similarly, the experience of having established a good communication with the robot is relatively  
465 high among all users; only one user partly disagrees with this. Therefore, we took the mean of the given  
466 answers and applied this threshold to divide the users into two sample groups with different levels of  
467 communication with the robot. The feeling of good communication with the robot seems to have a positive  
468 impact in reaching higher scores (*highest* and *avg\_3*), but it takes longer to reach the plateau of learning  
469 according to the *trial\_no\_avg\_reached* learning criteria. Those who stated that they experienced a very good  
470 communication reached their consistent level of learning on average at the 8<sup>th</sup> trial, whereas those who  
471 agreed or partly agreed with having established a good communication reached their level of learning on  
472 average at the 6<sup>th</sup> trial. A possible reason for reaching the learning plateau slower could be that participants  
473 who commented positively towards having a good communication during the tests are observed to be more  
474 experimental and taking higher risks when they were about to reach the learning plateau.

475 In all, (13/32) people expected to perform better, (14/32) people expected to perform worse, (2/32)  
476 did not give any opinions, and (3/32) provided conflicting opinions (i.e. agreeing or disagreeing to both  
477 questions). There seems to be an ambiguity in the self-reported success/failure beliefs due to conflicting  
478 answers. However, it is observed in the results of the t-test that those who believed they could have  
479 done better get significantly lower scores in 3 out of 6 learning criteria. Although *delta\_learning* was not  
480 found to be significantly different for this background factor, both the *avg\_first\_2* and *avg\_last\_2* were  
481 significantly different. This is an indication that users learned what could be objectively characterized as a  
482 good performance during the training. The results show that people who need more training could identify  
483 themselves based only on their own performance.

### 484 5.2.3 Age, Gender and Job Category

485 The age parameter was significant for 2 different learning criteria, *trial\_no\_avg\_reached* and  
486 *delta\_learning*. Although the difference is not large, the higher age group seem to converge on a learning  
487 state faster than the younger age group. However, when it comes to the plateau of learning, younger  
488 participants achieved a higher plateau of learning compared to older participants. In all, age seems not to  
489 be a significant factor if enough training is provided.

490 Job category and gender should be looked at together because these two parameters are highly dependent  
491 on our group of participants. We registered people from 5 job categories; IT/engineering, health, craft, non-  
492 technical office job and unemployed. We analyzed data to see if IT/engineering-related jobs outperformed  
493 other jobs grouped together. Unfortunately, there were no women participants enrolled in IT/engineering  
494 jobs in the participant group, and thus the job category and the gender factor became indistinguishable  
495 in the learning criteria. From the analysis, we see that participants from IT/engineering jobs achieved  
496 significantly higher scores than other jobs. The amount of learning (*delta\_learning*) among men was also  
497 lower compared to the amount of learning among women. Although the baseline (*avg\_first\_3*) of men were  
498 higher than women, and women performed learned more *delta\_learning*, men seem to learn enough from  
499 their baseline so that the difference in the average of highest 3 scores *avg\_3* is also significant in favour of  
500 men. Except for 3 outliers, men performed more consistently than women (See (*var\_3*)).

### 501 5.2.4 Gaming Habits

502 The programming background seems to be advantageous both for the baseline (*avg\_first\_2*) and for getting  
503 higher scores (*highest*, *avg\_last\_5* and *avg\_3*). The current gaming habits do not seem to be a significant

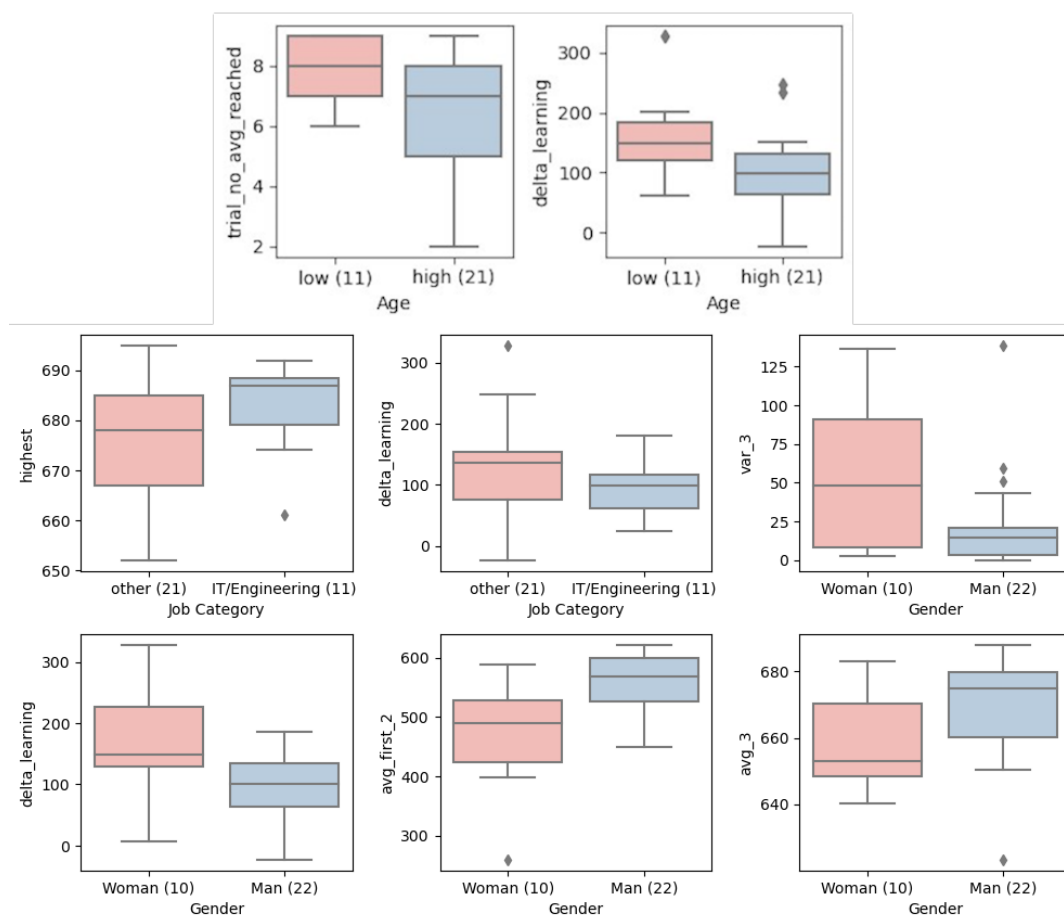


**Figure 11.** Job category and gender effect on learning. The blue group bar represents IT/Engineering related occupations in *Job Category* metric and male users in *Gender* metric. The pink and blue group bars represent other occupations registered such as teacher, craftsperson, nurse, consultant, unemployed etc. in *Job Category* metric and female users in *Gender* metric.

504 factor, which aligns with another relevant study in the literature (Tanaka et al., 2016), whereas past gaming  
 505 habits seem to be advantageous in the same 3 learning criteria as for the programming background. We can  
 506 note that the 3 users who were actively playing video games reported some confusion about the motion  
 507 directions of the robot during the experiments. They reported that the mirrored motion of the robot was  
 508 confusing since they were more used to a third-person or first-person view of controlling avatars. On the  
 509 other hand, several users who did not have a lot of gaming experience reported the mirrored motion of  
 510 the robot was intuitive, as the robot mimicked his/her motions. This should be taken into account when  
 511 designing HRC systems that will be used by operators with different backgrounds in gaming.

## 512 5.2.5 Physical and Mental Fatigue

513 Neither mental nor physical tiredness was reported to be a challenging factor during the physical tasks  
 514 as shown in Figure 7. Therefore, we took the mean of the given answers to the respective question and  
 515 applied this threshold to divide the participants into two sample groups. The participants who experienced  
 516 relatively low physical tiredness had a better start to the trials, and the users who experienced relatively  
 517 high mental tiredness seemed to reach the learning plateau slower.

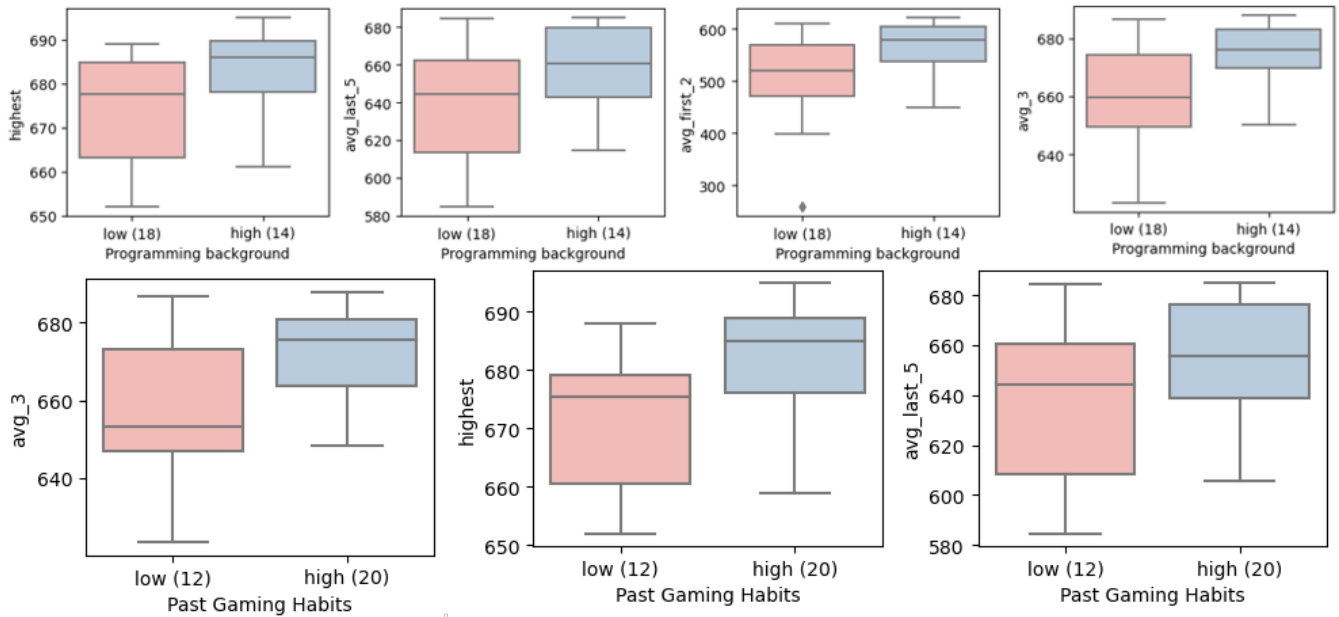


**Figure 12.** Programming skills and gaming habits effect on learning

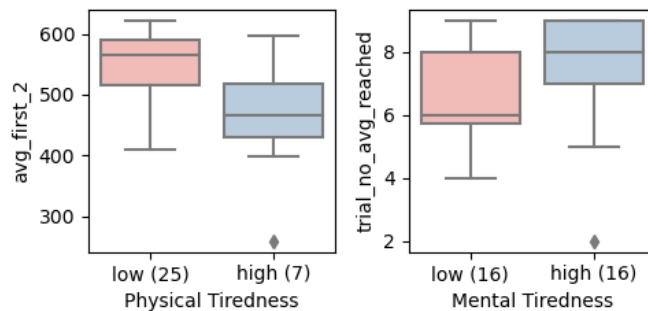


**Figure 13.** Mental and Physical tiredness effect on learning

518 **5.3 Independence of User Parameters**

519 As seen in the detailed comparisons, some parameters related to user background are not independent.  
 520 For example gender and job category. To analyse which parameters were dependent for our participant  
 521 group, we ran the Chi-Square test and the resultant dependent parameters list is given in Table 2. This  
 522 suggests that we should be very careful to draw any individual conclusions on the link between learning  
 523 criteria and the background factors in Table 2 without acknowledging the possible dependency on other  
 524 background factors.

**6 CONCLUSION AND FUTURE WORK**

525 This study investigates if anyone can learn to cooperate with robots through an experimental study with  
 526 32 participants performing a co-lift task, and which background factors such as age, gender, job, gaming  
 527 habits, programming skills, familiarity with robots etc. impact learning. The co-lift experimental setup  
 528 used IMUs for upper-body motion estimation and gesture recognition, and a gamified experimental setup  
 529 to increase user motivation. The results show that all users achieved a satisfactory level of cooperation  
 530 with robots for the co-lift task regardless of background factors within seven or fewer trials. The rate

**Table 2.** Chi-Square of independence: list of dependent parameters

category-1	category-2	$\chi^2$	p
Gender	Job Category	5.56	0.02
Gender	Height	20.52	0.00
Gender	Arm Length	8.73	0.00
Height	Arm Length	14.22	0.00
Programming background	Gender	4.89	0.03
Programming background	Job Category	7.65	0.01
Programming background	Past Gaming Habits	7.62	0.01
Past Gaming Habits	Gender	4.69	0.03
Past Gaming Habits	Job Category	4.07	0.04
Familiarity with Robots	Gender	5.93	0.01
Familiarity with Robots	Job Category	6.22	0.01
Familiarity with Robots	Height	5.23	0.02
Familiarity with Robots	Programming background	12.43	0.00
Familiarity with Robots	Past Gaming Habits	9.11	0.00
Familiarity with Robots	Current Gaming Habits	4.07	0.04
Believes that would do worse	Mental Tiredness	4.66	0.03

531 of learning progression, level of achievement and how consistent the cooperation could be repeated for  
 532 subsequent trials varied between different user groups, but the main conclusion is that all groups benefited  
 533 from training irrespective of background factors and that all participants could achieve a satisfactory level  
 534 of cooperation through training.

535 We believe that the results show that the focus for HRC systems developers should not only be on  
 536 optimizing the technical setup for human-robot cooperation but also focus on better user training to increase  
 537 HRC uptake in the industry. The results presented in this paper show that all users benefit from training to  
 538 better cooperate with a robot and that achieving a satisfactory level of cooperation for any user irrespective  
 539 of background can be done within a fairly short time and a limited number of training runs. This suggests  
 540 that the user's background is not the hindering factor when it comes to the adoption of HRC in the industry.

541 Finally, our study is limited to the co-lift task for HRC. Note that while the implementation of this task in  
 542 this study was designed to be as generic and representative as possible for HRC tasks, we recognize that  
 543 other HRC tasks that require other specific skills may give different results. However, we believe that the  
 544 conclusions from this study apply to a wide range of HRC applications. Note also that the purpose of this  
 545 study was not to reach a strict conclusion between user background factors and specific learning criteria,  
 546 but rather to observe the learning process of the individuals and to investigate which background factors  
 547 play a role in learning to better accommodate future implementation of HRC in industrial applications.

## CONFLICT OF INTEREST STATEMENT

548 The authors declare that the research was conducted in the absence of any commercial or financial  
 549 relationships that could be construed as a potential conflict of interest.

## AUTHOR CONTRIBUTIONS

550 **Gizem Ateş Venås:** Conceptualization, Methodology, Investigation, Writing - original draft. **Martin**  
 551 **Fodstad Stølen:** Conceptualization, Writing - review & editing. **Erik Kyrkjebø:** Conceptualization,  
 552 Writing - review & editing.

## FUNDING

553 This work was funded by the Research Council of Norway through grant number 280771.

## ACKNOWLEDGMENTS

554 The authors thank Sondre Venås for help with the experiments.

## DATA AVAILABILITY STATEMENT

555 Replication Data for this study can be found in the Venås (2023).

## REFERENCES

- 556 (2014). An optimization-based approach to human body motion capture using inertial sensors. *IFAC*  
557 *Proceedings Volumes (IFAC-PapersOnline)* 19, 79–85. doi:10.3182/20140824-6-ZA-1003.02252
- 558 Andrade, K. d. O., Fernandes, G., Martins, J., Roma, V. C., Joaquim, R. C., and Caurin, G. A. (2013).  
559 Rehabilitation robotics and serious games: An initial architecture for simultaneous players. In *2013*  
560 *ISSNIP Biosignals and Biorobotics Conference: Biosignals and Robotics for Better and Safer Living*  
561 *(BRC)* (IEEE), 1–6
- 562 Anil Yasin, A. and Abbas, A. (2021). Role of gamification in engineering education: A systematic literature  
563 review. In *2021 IEEE Global Engineering Education Conference (EDUCON)* (IEEE)
- 564 Ateş, G. and Kyrkjebø, E. (2021). Human-robot cooperative lifting using imus and human gestures. In  
565 *Annual Conference Towards Autonomous Robotic Systems* (Springer), 88–99
- 566 Ates, G. and Kyrkjebo, E. (2022). Design of a gamified training system for human-robot cooperation. In  
567 *2022 International Conference on Electrical, Computer, Communications and Mechatronics Engineering*  
568 *(ICECCME)* (IEEE). doi:10.1109/iceccme55909.2022.9988661
- 569 Ates, G., Stolen, M. F., and Kyrkjebo, E. (2022). Force and gesture-based motion control of human-robot  
570 cooperative lifting using IMUs. In *2022 17th ACM/IEEE International Conference on Human-Robot*  
571 *Interaction (HRI)* (IEEE). doi:10.1109/hri53351.2022.9889450
- 572 Azadi, S., Green, I. C., Arnold, A., Truong, M., Potts, J., and Martino, M. A. (2021). enRobotic surgery:  
573 The impact of simulation and other innovative platforms on performance and training. *J. Minim. Invasive*  
574 *Gynecol.* 28, 490–495
- 575 Bradski, G. R. and Davis, J. (2000). Motion segmentation and pose recognition with motion history  
576 gradients. *Proceedings of IEEE Workshop on Applications of Computer Vision 2000-Janua*, 238–244.  
577 doi:10.1109/WACV.2000.895428
- 578 Cerveri, P., Pedotti, A., and Ferrigno, G. (2005). Kinematical models to reduce the effect of skin artifacts  
579 on marker-based human motion estimation. *Journal of Biomechanics* 38, 2228–2236. doi:10.1016/j.  
580 jbiomech.2004.09.032
- 581 Checa, D. and Bustillo, A. (2020). A review of immersive virtual reality serious games to enhance learning  
582 and training. *Multimedia Tools and Applications* 79, 5501–5527
- 583 Dubin, A. K., Smith, R., Julian, D., Tanaka, A., and Mattingly, P. (2017). A comparison of robotic  
584 simulation performance on basic virtual reality skills: Simulator subjective versus objective assessment  
585 tools. *Journal of Minimally Invasive Gynecology* 24, 1184–1189. doi:10.1016/j.jmig.2017.07.019
- 586 Ghosal, A. (2018). Resolution of redundancy in robots and in a human arm. *Mechanism and Machine*  
587 *Theory* 125, 126–136. doi:10.1016/j.mechmachtheory.2017.12.008



- 588 [Dataset] Insight, F. B. (2022). Industrial automation market size, share covid-19 impact analysis, by  
589 component (hardware, software), by industry (discrete automation, process automation), and regional  
590 forecast, 2022-2029
- 591 Jones, C., O'Donnell, C., Semmens, R., and Novitzky, M. (2022). The effectiveness of virtual reality  
592 for training human-robot teams. In *SoutheastCon 2022* (IEEE). doi:10.1109/southeastcon48659.2022.  
593 9764021
- 594 Kanal, V., Brady, J., Nambiappan, H., Kyrarini, M., Wylie, G., and Makedon, F. (2020). Towards a serious  
595 game based human-robot framework for fatigue assessment. In *Proceedings of the 13th ACM Int. Conf.  
596 on Pervasive Tech. Related to Assistive Environments*. 1–6
- 597 Kapp, K. M. (2012). *The gamification of learning and instruction: game-based methods and strategies for*  
598 *training and education* (John Wiley & Sons)
- 599 Kleftodimos, A. and Evangelidis, G. (2018). Augmenting educational videos with interactive exercises and  
600 knowledge testing games. In *2018 IEEE Global Engin. Education Conf. (EDUCON)* (IEEE)
- 601 Kok, M., Hol, J. D., and Schön, T. B. (2017). Using inertial sensors for position and orientation estimation.  
602 *Foundations and Trends® in Signal Processing* 11, 1–153. doi:10.1561/20000000094
- 603 Lee, J. D. and See, K. A. (2004). Trust in automation: Designing for appropriate reliance. *Human Factors:*  
604 *The Journal of the Human Factors and Ergonomics Society* 46, 50–80. doi:10.1518/hfes.46.1.50\_30392
- 605 Lindblom, J., Alenljung, B., and Billing, E. (2020). Evaluating the user experience of human–robot  
606 interaction. *Human-Robot Interaction: Evaluation Methods and Their Standardization* , 231–256
- 607 Lindblom, J. and Wang, W. (2018). Towards an evaluation framework of safety, trust, and operator  
608 experience in different demonstrators of human-robot collaboration. In *Advances in manufacturing*  
609 *technology XXXII* (IOS Press). 145–150
- 610 Liu, S., Wang, L., and Wang, X. V. (2021). Sensorless haptic control for human-robot collaborative  
611 assembly. *CIRP Journal of Manufacturing Science and Technology* 32, 132–144. doi:10.1016/j.cirpj.  
612 2020.11.015
- 613 Ludwig, S. A. and Burnham, K. D. (2018). Comparison of Euler Estimate using Extended Kalman Filter,  
614 Madgwick and Mahony on Quadcopter Flight Data. In *2018 International Conference on Unmanned*  
615 *Aircraft Systems, ICUAS 2018*. doi:10.1109/ICUAS.2018.8453465
- 616 M., E.-G. and J., M. (2015). Human Joint Angle Estimation with Inertial Sensors and Validation with A  
617 Robot Arm. *IEEE Transactions on Biomedical Engineering* 62, 1759–1767
- 618 Matsas, E. and Vosniakos, G.-C. (2017). Design of a virtual reality training system for human–robot  
619 collaboration in manufacturing tasks. *International Journal on Interactive Design and Manufacturing*  
620 *(IJIDeM)* 11, 139–153
- 621 Michaelis, J. E., Siebert-Evenstone, A., Shaffer, D. W., and Mutlu, B. (2020). Collaborative or simply  
622 uncaged? understanding human-cobot interactions in automation. In *Proceedings of the 2020 CHI*  
623 *Conference on Human Factors in Computing Systems* (New York, NY, USA: Association for Computing  
624 Machinery), CHI '20, 1–12. doi:10.1145/3313831.3376547
- 625 Mitchell, D., Choi, H., and Haney, J. M. (2020). Safety perception and behaviors during human-robot  
626 interaction in virtual environments. *Proceedings of the Human Factors and Ergonomics Society Annual*  
627 *Meeting* 64, 2087–2091. doi:10.1177/1071181320641506
- 628 Morato, C., Kaipa, K. N., Zhao, B., and Gupta, S. K. (2014). Toward safe human robot collaboration by  
629 using multiple kinects based real-time human tracking. *Journal of Computing and Information Science*  
630 *in Engineering* 14

- 631 Mörtl, A., Lawitzky, M., Kucukyilmaz, A., Sezgin, M., Basdogan, C., and Hirche, S. (2012). The role of  
632 roles: Physical cooperation between humans and robots. *International Journal of Robotics Research* 31,  
633 1656–1674. doi:10.1177/0278364912455366
- 634 Nemeč, B., Likar, N., Gams, A., and Ude, A. (2017). Human robot cooperation with compliance adaptation  
635 along the motion trajectory. *Autonomous Robots* 42, 1023–1035. doi:10.1007/s10514-017-9676-3
- 636 Parra, P. S., Calleros, O. L., and Ramirez-Serrano, A. (2020). Human-robot collaboration systems:  
637 Components and applications. In *Int. Conf. Control. Dyn. Syst. Robot.* vol. 150, 1–9
- 638 Pesare, E., Roselli, T., Corriero, N., and Rossano, V. (2016). Game-based learning and gamification to  
639 promote engagement and motivation in medical learning contexts. *Smart Learning Environments* 3,  
640 1–21
- 641 Phan, D., Kashyap, B., Pathirana, P., and Seneviratne, A. (2017). A constrained nonlinear optimization  
642 solution for 3d orientation estimation of the human limb. 1–4. doi:10.1109/BMEiCON.2017.8229138
- 643 Prasov, Z. (2012). Shared gaze in remote spoken hri during distributed military operation. In *Proceedings*  
644 *of the seventh annual ACM/IEEE international conference on Human-Robot Interaction (ACM)*. doi:10.  
645 1145/2157689.2157760
- 646 Ramasubramanian, A. K. and Papakostas, N. (2021). Operator - mobile robot collaboration for synchronized  
647 part movement. *Procedia CIRP* 97, 217–223. doi:10.1016/j.procir.2020.05.228
- 648 Rodríguez-Guerra, D., Sorrosal, G., Cabanes, I., and Calleja, C. (2021). Human-robot interaction review:  
649 Challenges and solutions for modern industrial environments. *IEEE Access* 9, 108557–108578
- 650 Roetenberg, D., Lunge, H., and Slycke, P. (2009). Xsens MVN : Full 6DOF Human Motion Tracking  
651 Using Miniature Inertial Sensors. *Hand, The* , 1–7doi:10.1.1.569.9604
- 652 Sheng, W., Thobbi, A., and Gu, Y. (2015). An integrated framework for human–robot collaborative  
653 manipulation. *IEEE Transactions on Cybernetics* 45, 2030–2041. doi:10.1109/tcyb.2014.2363664
- 654 Silva, V., Soares, F., Esteves, J. S., and Pereira, A. P. (2018). Building a hybrid approach for a game  
655 scenario using a tangible interface in human robot interaction. In *Joint International Conference on*  
656 *Serious Games (Springer)*, 241–247
- 657 Simone, V. D., Pasquale, V. D., Giubileo, V., and Miranda, S. (2022). Human-robot collaboration: an  
658 analysis of worker’s performance. *Procedia Computer Science* 200, 1540–1549. doi:10.1016/j.procs.  
659 2022.01.355
- 660 Sugiyama, J. and Miura, J. (2009). Development of a vision-based interface for instructing robot  
661 motion. In *RO-MAN 2009 - The 18th IEEE International Symposium on Robot and Human Interactive*  
662 *Communication (IEEE)*. doi:10.1109/roman.2009.5326272
- 663 Susi, T., Johannesson, M., and Backlund, P. (2007). Serious games: An overview
- 664 Tanaka, A., Smith, R., and Hughes, C. (2016). Video game experience and basic robotic skills. In  
665 *2016 IEEE International Conference on Serious Games and Applications for Health (SeGAH) (IEEE)*.  
666 doi:10.1109/segah.2016.7586262
- 667 Tennent, H., Lee, W.-Y., Hou, Y. T.-Y., Mandel, I., and Jung, M. (2018). PAPERINO. In *Companion of*  
668 *the 2018 ACM Conference on Computer Supported Cooperative Work and Social Computing (ACM)*.  
669 doi:10.1145/3272973.3272994
- 670 Theofanidis, M., Lioulemes, A., and Makedon, F. (2016). A motion and force analysis system for human  
671 upper-limb exercises (Petra 2016)
- 672 [Dataset] Venås, G. A. (2023). Replication Data for: Exploring Human-Robot Cooperation with Gamified  
673 User Training: A User Study on Cooperative Lifting. doi:10.18710/CZGZVZ
- 674 Villani, V., Sabattini, L., Czerniaki, J. N., Mertens, A., Vogel-Heuser, B., and Fantuzzi, C. (2017). Towards  
675 modern inclusive factories: A methodology for the development of smart adaptive human-machine

- 676 interfaces. In *2017 22nd IEEE International Conference on Emerging Technologies and Factory*  
677 *Automation (ETFA)* (IEEE). doi:10.1109/etfa.2017.8247634
- 678 Walters, M., Dautenhahn, K., te Boekhorst, R., Koay, K. L., Kaouri, C., Woods, S., et al. (2005). The  
679 influence of subjects' personality traits on personal spatial zones in a human-robot interaction experiment.  
680 In *ROMAN 2005. IEEE International Workshop on Robot and Human Interactive Communication, 2005.*  
681 (IEEE). doi:10.1109/roman.2005.1513803
- 682 Wang, R., DeMaria, S., Goldberg, A., and Katz, D. (2016). A systematic review of serious games in  
683 training health care professionals. *Simulation in Healthcare: The Journal of the Society for Simulation*  
684 *in Healthcare* 11, 41–51. doi:10.1097/sih.0000000000000118
- 685 Werner, C., Kardaris, N., Koutras, P., Zlatintsi, A., Maragos, P., Bauer, J. M., et al. (2020). Improving  
686 gesture-based interaction between an assistive bathing robot and older adults via user training on the  
687 gestural commands. *Archives of Gerontology and Geriatrics* 87, 103996. doi:10.1016/j.archger.2019.  
688 103996



# APPENDIX



## CONSENT FORM

---

The consent form which is signed by each human subject in the data collection step and sent to the Norwegian Centre for Research Data (NSD)<sup>1</sup> is provided in this chapter.

---

<sup>1</sup><https://www.nsd.no/>

# Are you interested in taking part in the research project

*“Experiments on physical human-robot interaction in a cooperative lifting scenario”?*

## Purpose of the project

You are invited to participate in a research project where the main purpose of this experiment is to investigate the applicability, intuitiveness, learnability, compatibility, and efficiency of human-robot interaction in a sample cooperative lifting scenario. The experiment relies on the hypothesis that while robots are durable, precise, and repeatable, humans have excellent problem-solving skills and are creative in their decision-making. The theory is that the humans and the robots can be an efficient team and this efficiency can be increased with training. Also, it is aimed to examine the relation of individuals' particular features such as age, body size, related background etc. with the performance and the learning curve of human-robot interaction. It is hoped that the study will show the possibility of a human-robot team tested by various users.

You are expected to carry a wooden table with a robot arm as shown in Figure-1 with the best of your ability. There will be 4 states named IDLE, APPROACH, COLIFT and RELEASE. The functionality of the system in different states will be explained in a tutorial video.

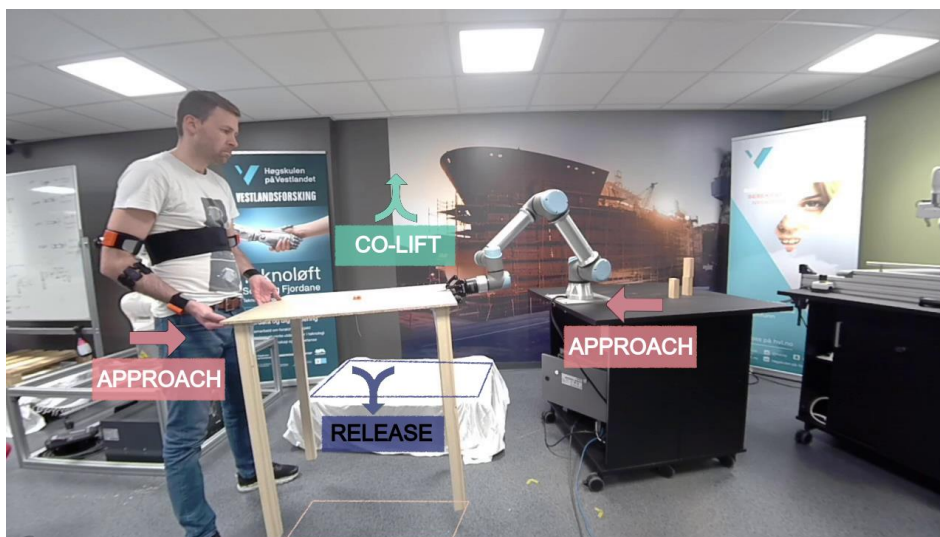


*Figure 1: Experiment Overview*

Human-robot interaction can be assimilated to human-car interaction. You need to have a proper training before having a driving license and use a car effectively. Therefore, this experiment includes repetitive trials to train you in a short period of time.

This project is a part of a doctoral thesis under the Teknoløft project which is funded by the Research Council of Norway through grant number 280771. The data collected during this experimental procedure is going to be used in academical publications within the same project.

## Which institution is responsible for the research project?

Western Norway University of Applied Sciences is responsible for the project (data controller).

## Why are you being asked to participate?

You are asked to be a participant because you are between 18 and 50 years old and have no reduced mobility of either arm (for example a cast or an inhibiting injury). Your contact details are not required but you can enter if you want to get updates about the publications where your data is being used.



## **What does participation involve for you?**

The procedure consists of 2 surveys and 1 experimental activity. You can answer questions both in English and Norwegian.

### Pre-survey:

You will be asked several questions about your personal information as well as your opinions about robots and technology. This will take about 5 minutes.

### Experimental activity:

You will be equipped with 6 sensors to measure your body motions. The robot will move according to your motions and the behaviour of the robot will change in different states of the experiment. All the details of the robot movement, the game concept and the details about scoring will be explained in the tutorial video. The experimental activity consists of 10 repetitive trials. Each trial will take approximately 1-4 minutes (less in the last trials). The total procedure will take approximately 1 hour.

### Past-survey:

You will be asked several questions about your experience with the experiment. This will take about 5 minutes.

The participants will be paid 200 Norwegian Kroner as SAMAN gift card. Additionally, the person who brought the most participants will earn an additional gift card.

## **Participation is voluntary**

The participation in the project is COMPLETELY VOLUNTARY. If you choose to participate, you can withdraw your consent at any time without giving a reason. All information about you will then be made anonymous. There will be no negative consequences for you if you choose not to participate or later decide to withdraw.

## **Your personal privacy – how we will store and use your personal data**

During the surveys, you will be answering some questions about your age, gender, anticipation to robots, technical background, occupation etc. Also, your height and arm length will be measured before the experiment. During the experimental activity, the data consist of body postures and motion data only – there will be no personal data registered.

Additionally, we would like to record a video during the experimental activity for data comparison if needed. This will apply **only if you agree**. The privacy steps in storing the video data will be the same as other types of data.

We will only use your personal data for the purpose(s) specified here and we will process your personal data in accordance with data protection legislation (the GDPR). Here is the list of people who will have access to your data and how your data will be stored.

- All the data will be processed and secured by Gizem Ates (HVL - PhD Candidate).
- The data will be accessible for Erik Kyrkjebø (Main Supervisor), Martin Fodstad Stølen (Co-Supervisor) Janina Ramona Juranek (Adviser at the HVL research and innovation department) and Raquel Motzfeldt Tirach (HVL Robotics Lab Engineer).
- The data will be collected by HVL owned password secured laptop (used by Gizem Ates) and stored on the HVL-secured OneDrive account (Gizem Ates's HVL enterprise account).
- The survey data will be directly stored on the HVL-secured OneDrive account (Gizem Ates's HVL enterprise account). Experimental activity data will be first stored on HVL-200310 laptop locally. Afterwards, it will be backed-up in the same OneDrive account.
- Participants will not be recognizable in publications and no identifiable personal data will be publicly available.

## What will happen to your personal data at the end of the research project?

The planned end date of the project is December 2024. Afterwards, the data will be anonymized and archived according to HVL's Open Data policy (archive reference 20/07537-4).

## Your rights

So long as you can be identified in the collected data, you have the right to:

- access the personal data that is being processed about you
- request that your personal data is deleted
- request that incorrect personal data about you is corrected/rectified
- receive a copy of your personal data (data portability), and
- send a complaint to the Norwegian Data Protection Authority regarding the processing of your personal data

**Note:** Please note that after the academical articles are published, we cannot withdraw the publications made based on the collective data in which yours also included after they have been published. However, we can delete your data from the future publications if you contact us.

## What gives us the right to process your personal data?

We will process your personal data based on your consent.

Based on an agreement with Western Norway University of Applied Sciences Data Protection Services has assessed that the processing of personal data in this project meets requirements in data protection legislation.

## Where can I find out more?

If you have questions about the project, or want to exercise your rights, contact:

- Gizem Ates ([Gizem.Ates@hvl.no](mailto:Gizem.Ates@hvl.no) , tel:46279880) Erik Kyrkjebø ([Erik.Kyrkjebo@hvl.no](mailto:Erik.Kyrkjebo@hvl.no) )
- Our Data Protection Officer: Trine Anikken Larsen ([Trine.Anikken.Larsen@hvl.no](mailto:Trine.Anikken.Larsen@hvl.no))

If you have questions about how data protection has been assessed in this project, contact:

- Data Protection Services, by email: ([personverntjenester@sikt.no](mailto:personverntjenester@sikt.no)) or by telephone: +47 53 21 15 00.

Yours sincerely,

Project Leader  
(Researcher)  
Gizem Ates

---

## Consent form

I have received and understood information about the project **Experiment on physical human-robot interaction in a cooperative lifting scenario** and have been given the opportunity to ask questions. I give consent:

- to participate in pre- and post- surveys,
- to participate in *human-robot cooperative lifting* activity,
- for information about me to be published in a way that I **cannot** be recognised,
- for my personal data to be anonymously archived after the project ends for research purposes only

I accept video recording during the experimental activity:

- Yes
- No
- Anonymously only (All participants will be given a unified clothing to anonymize them during the video recording. Participants' faces will not be recorded).

I give consent for my personal data to be processed until the end of the project.

-----  
(Signed by participant, date)



## USER SURVEYS

---

The pre- and post-surveys which are used in the multi-user co-lift experiments.



# PRE-SURVEY

The survey will take approximately 6 minutes to complete.

Thank you for joining "experiments on physical human-robot interaction in a cooperative lifting scenario". This survey is the first step where we ask some personal questions about you. As explained in the consent form, your answer will be anonymized. Noone else than the people written on the consent form will have an access to your answers.

So, if we are confident, let's start!

\* Required

## Personal Information

1. Experiment ID number: \*

2. How old are you? \*

3. What is your gender? \*

- Woman
- Man
- Non-binary
- Prefer not to say

4. What is your occupation? If you are a student, please state your department also. \*

5. What is your height? If you don't know for sure, we can measure it later.

6. How did you find us? Remeber: the participant who brings the most amount of participants will get double gift card :)

## Interest

7. How often do you play video games? \*

0	1	2	3	4	5	6	7	8	9	10
---	---	---	---	---	---	---	---	---	---	----

Never

Almost every day

8. How often did you use to play video games when you were a kid? \*

0	1	2	3	4	5	6	7	8	9	10
---	---	---	---	---	---	---	---	---	---	----

Never

Almost everyday

9. Have you done any programming? How often do you use programming in your life? \*

0	1	2	3	4	5	6	7	8	9	10
---	---	---	---	---	---	---	---	---	---	----

Not at all

Very Often



## Anticipation on robots

10. Please read each statement and choose the option that suits you best. \*

	Completely disagree	Disagree	Partly disagree	No opinion	Partly agree	Agree	Completely agree
I am quite into robotics field and I have close interaction with robots.	<input type="radio"/>	<input type="radio"/>	<input type="radio"/>	<input type="radio"/>	<input type="radio"/>	<input type="radio"/>	<input type="radio"/>
I have a robot (cleaner or another device) at home/work so I have some interaction with robots.	<input type="radio"/>	<input type="radio"/>	<input type="radio"/>	<input type="radio"/>	<input type="radio"/>	<input type="radio"/>	<input type="radio"/>
I haven't touched an industrial robot arm before.	<input type="radio"/>	<input type="radio"/>	<input type="radio"/>	<input type="radio"/>	<input type="radio"/>	<input type="radio"/>	<input type="radio"/>
I enjoy watching fun videos about robots.	<input type="radio"/>	<input type="radio"/>	<input type="radio"/>	<input type="radio"/>	<input type="radio"/>	<input type="radio"/>	<input type="radio"/>
I think robotics technology has developed a lot and it amuses me.	<input type="radio"/>	<input type="radio"/>	<input type="radio"/>	<input type="radio"/>	<input type="radio"/>	<input type="radio"/>	<input type="radio"/>
I think robotics technology has developed a lot and it scares me.	<input type="radio"/>	<input type="radio"/>	<input type="radio"/>	<input type="radio"/>	<input type="radio"/>	<input type="radio"/>	<input type="radio"/>
I think robots will take over human jobs and	Completely disagree	Disagree	Partly disagree	No opinion	Partly agree	Agree	Completely agree

and  
THEREFOR  
E many  
people will be  
unemployed.

I think robots  
will take over  
human jobs  
and BUT  
many new  
jobs  
opportunities  
will be  
formed.

I think think  
robots will  
take over  
heavy human  
jobs and the  
average life  
quality will  
increase.

I prefer  
humans and  
robots work  
together  
instead of  
removing  
either of them  
from the  
picture.

I believe  
there are  
many jobs  
that humans  
cannot be as  
good as  
robots.

I believe  
there are  
many jobs  
that robots  
will never be  
as good as  
humans.

I believe that  
robots will  
take over the  
world and  
destroy  
humankind  
one day.

## Problems and Solutions

### 11. When I am given a task/problem

- I read instructions before I attempt solving it.
- I start solving first and check the instructions meanwhile.
- I try solving first. I check the instructions if I can't solve it myself.
- I try solving first. I give up if I can't solve it. Challenge is not my cup of tea.

### 12. What do you think about accomplishing this task?

- I am very sceptical. I don't think I can accomplish it or it will take very long.
- With enough given enough time, I can accomplish it.
- I believe that I can do it.

---

This content is neither created nor endorsed by Microsoft. The data you submit will be sent to the form owner.

 Microsoft Forms



# POST-SURVEY

Thank you for joining "experiments on physical human-robot interaction in a cooperative lifting scenario". This survey is the last step where we ask your experience. As explained in the consent form, your answer will be anonymized. Noone else than the people written on the consent form will have an access to your answers.

So, if we are confident, let's finish it!

\* Required

## Overall experience

1. Experiment ID number: \*

2. Please read each statement and choose the option that suits you best. \*

	Completely disagree	Disagree	Partly disagree	No opinion	Partly agree	Agree	Completely agree
Tutorials were clear and enough.	<input type="radio"/>	<input type="radio"/>	<input type="radio"/>	<input type="radio"/>	<input type="radio"/>	<input type="radio"/>	<input type="radio"/>
The screen was useful to give a feedback.	<input type="radio"/>	<input type="radio"/>	<input type="radio"/>	<input type="radio"/>	<input type="radio"/>	<input type="radio"/>	<input type="radio"/>
I am surprised that a robot can be controlled without using any cameras that good.	<input type="radio"/>	<input type="radio"/>	<input type="radio"/>	<input type="radio"/>	<input type="radio"/>	<input type="radio"/>	<input type="radio"/>
	Completely disagree	Disagree	Partly disagree	No opinion	Partly agree	Agree	Completely agree

I was thinking that I would do better.

I was thinking that I would do worse.

I think this study can be useful for human-robot cooperation use cases.

The first trials were more difficult but the last ones were quite easy.

The duration of the experiment was too long.

It feels like the robot has some sort of intelligence.

It feels like the robot and I had a good communication.

It feels like robot and I established a connection.

3. One more time about robots: \*

Completely disagree    Disagree    Partly Disagree    No opinion    Partly agree    Agree    Completely agree

I think robotics technology has developed a lot and it amuses me.

Completely disagree    Disagree    Partly Disagree    No opinion    Partly agree    Agree    Completely agree

I think robotics technology has developed a lot and it scares me.

○ ○ ○ ○ ○ ○ ○ ○

I think robots will take over human jobs and THEREFORE many people will be unemployed.

○ ○ ○ ○ ○ ○ ○ ○

I think robots will take over human jobs and BUT many new jobs opportunities will be formed.

○ ○ ○ ○ ○ ○ ○ ○

I think think robots will take over heavy human jobs and the average life quality will increase.

○ ○ ○ ○ ○ ○ ○ ○

I prefer humans and robots work together instead of removing either of them from the picture.

○ ○ ○ ○ ○ ○ ○ ○

I believe there are many jobs that robots will never be as good as humans.

○ ○ ○ ○ ○ ○ ○ ○

I believe there are many jobs that humans cannot be as good as

Completely disagree ○ Disagree ○ Partly Disagree ○ No opinion ○ Partly agree ○ Agree ○ Completely agree ○

good as  
robots.

I believe that  
robots will  
take over the  
world and  
destroy  
humankind  
one day.

## Physical and cognitive load

4. How difficult was the task? Please consider 1 task only, not the overall experiment. \*

0	1	2	3	4	5	6	7	8	9	10
---	---	---	---	---	---	---	---	---	---	----

Easy Difficult

5. How difficult was the task? Please consider 10 trials together, not an individual trial. \*

0	1	2	3	4	5	6	7	8	9	10
---	---	---	---	---	---	---	---	---	---	----

Easy Difficult

6. How intuitive was the system to use? \*

0	1	2	3	4	5	6	7	8	9	10
---	---	---	---	---	---	---	---	---	---	----

Not intuitive at all Very intuitive

7. How tired do you feel? (Physically) \*

0	1	2	3	4	5	6	7	8	9	10
---	---	---	---	---	---	---	---	---	---	----

Not at all Very tired

8. How tired do you feel? (Mentally) \*

0	1	2	3	4	5	6	7	8	9	10
---	---	---	---	---	---	---	---	---	---	----

Not at all Very tired



Your opinions on...

9. What was the **state that you think was the easiest?**

10. What was the **state that you think was the hardest?**

11. What was the **state that you enjoyed** at most?

12. Has your opinion about **robots** changed after taking part in this research experiment? Please briefly explain.

13. Has your opinion about **human-robot cooperation** changed after taking part in this research experiment? Please briefly explain.

14. Do you have any opinions where this study (fully or partly) be useful?

15. Is there anything that we could improve?

16. Any last thoughts?

---

This content is neither created nor endorsed by Microsoft. The data you submit will be sent to the form owner.



## USERS' MOTION DATA

---

The data given in this section is the real-time motion data of 32 users collected from the user, the robot and the table during the multi-user co-lift experiments.

5 types of measures of human motions are presented; motion hand (left hand for this case), steering hand (right hand in this case), merged hands (human input to the system, which is the combination of two hand motions), right elbow height and left elbow height. 2 types of robot motions are presented: the TCP motion (end-effector motion) and the exerted force in the y-axis, which is towards the robot. The human motion data are in the z-direction of the global reference frame, which is from the ground to the zenith. From the table motion measurements, only one type of data is presented and it is the acceleration of the table in the x-axis (which is towards the human's left on the horizontal plane).

Additionally, the score data is shown as well as the task states are indicated with respective background colours: IDLE-blue, APPROACH-pink, COLIFT-green, and RELEASE-yellow. Commonly, in the initial part of the plots, the IDLE and APPROACH colours are transitioned often but labelled separately. The reason is to show the intended usage of the system which starts with IDLE, goes through APPROACH and COLIFT and finalizes with RELEASE.

Notes: User 28373 - the battery of the 2nd button was out at trials 9 and 10. Therefore, additional 60 points were added to each trial at the end of the experiments. Later on, the button is fixed.

User 49345 trial-1 corrupted motion data - most probably related to the particular rosbag at that particular time when the RAM was pretty full.

User 97647 trial-2 corrupted motion data - most probably related to the particular rosbag at that particular time when the RAM was pretty full.

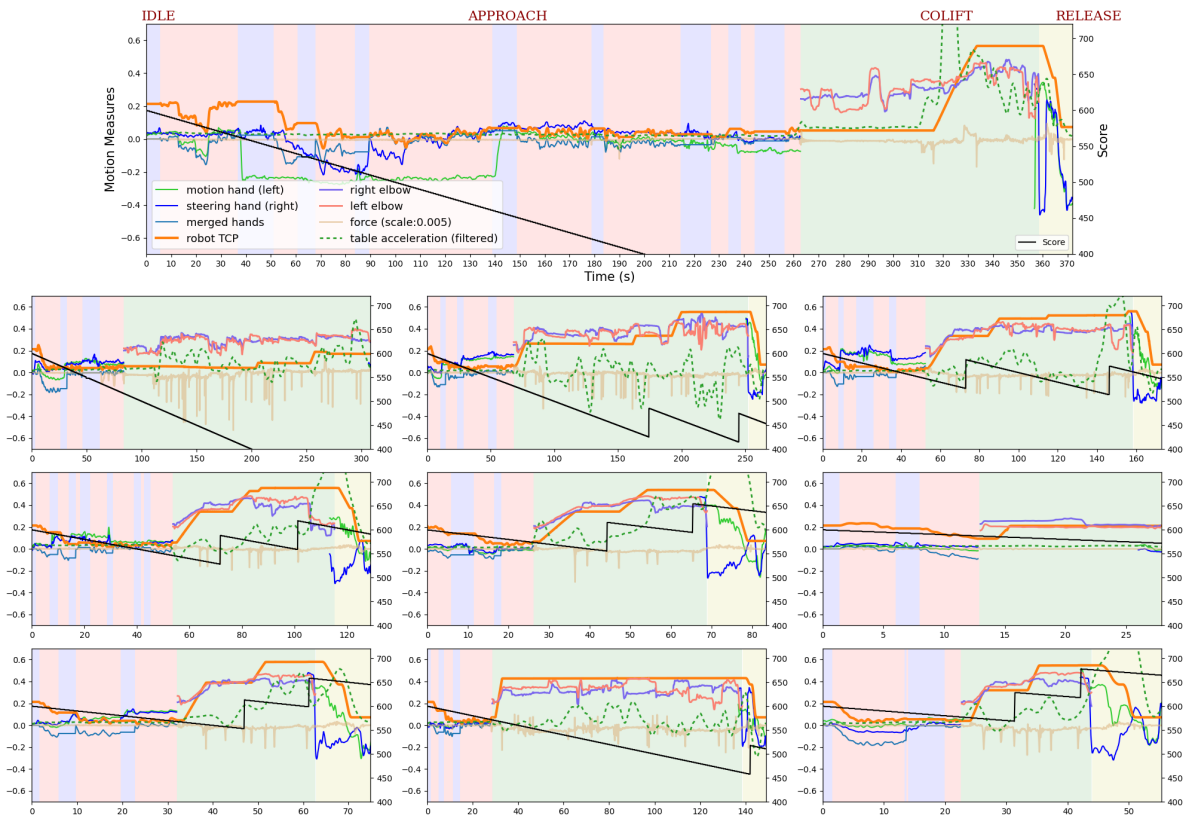


Fig. 1: User ID: 10958

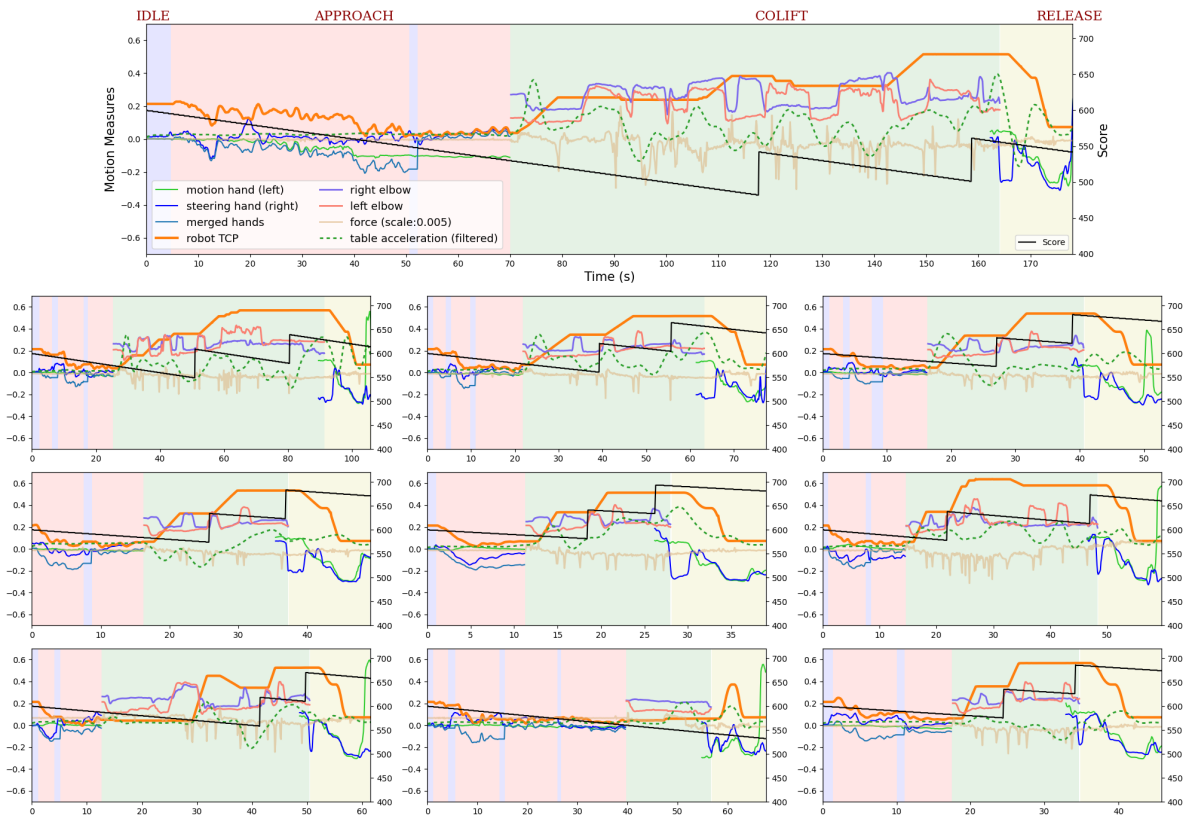


Fig. 2: User ID: 11982

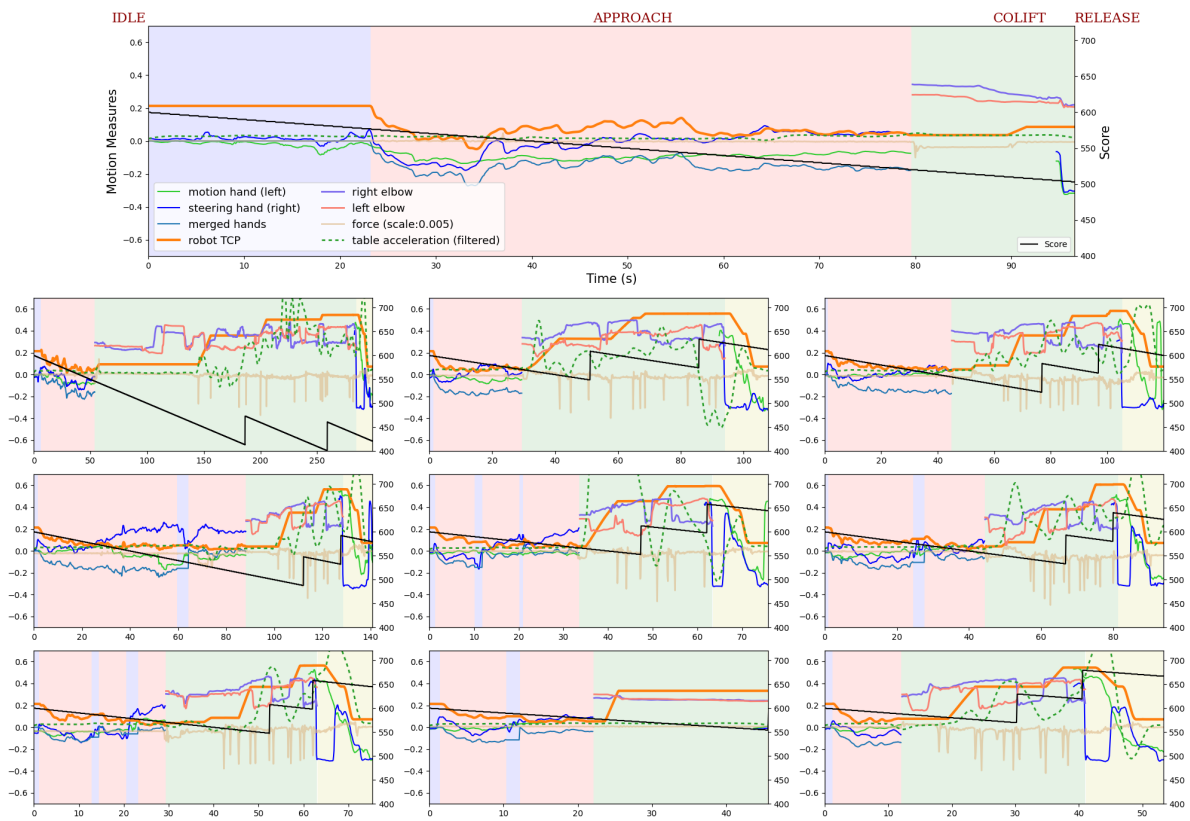


Fig. 3: User ID: 13421

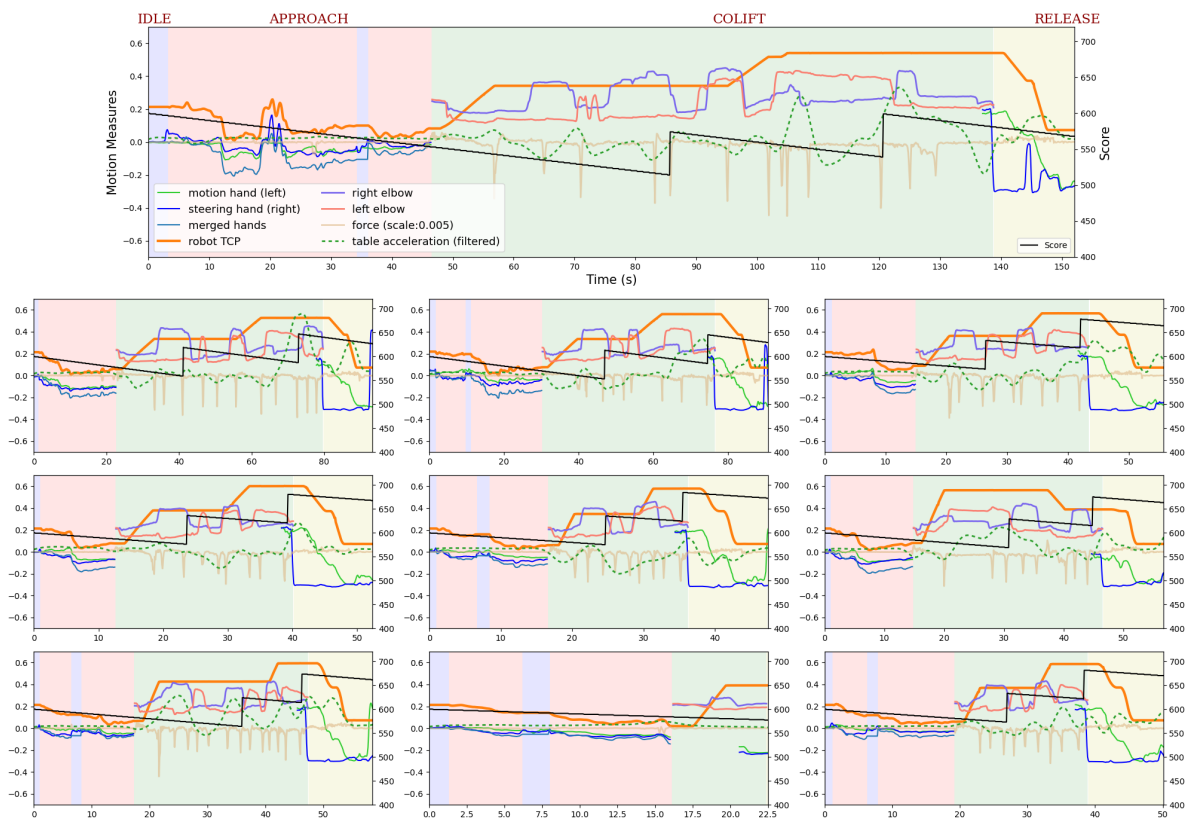


Fig. 4: User ID: 14026

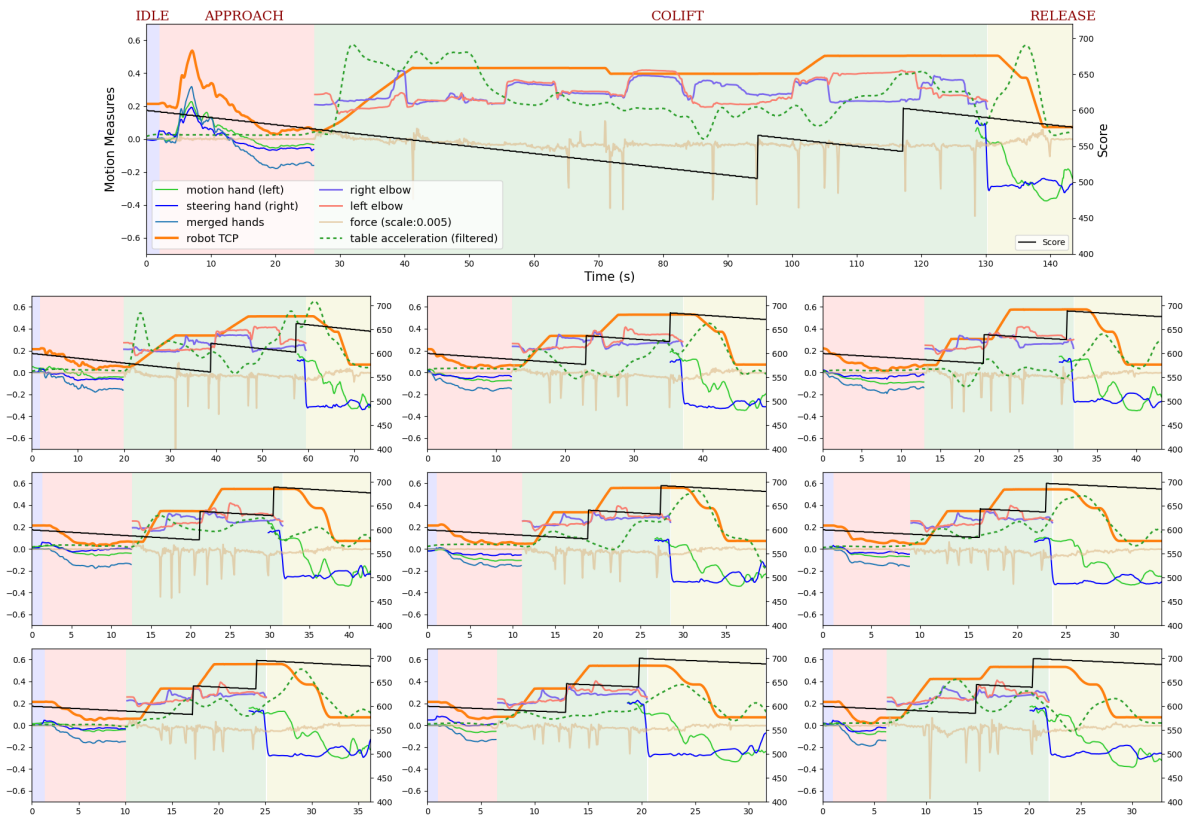


Fig. 5: User ID: 20430

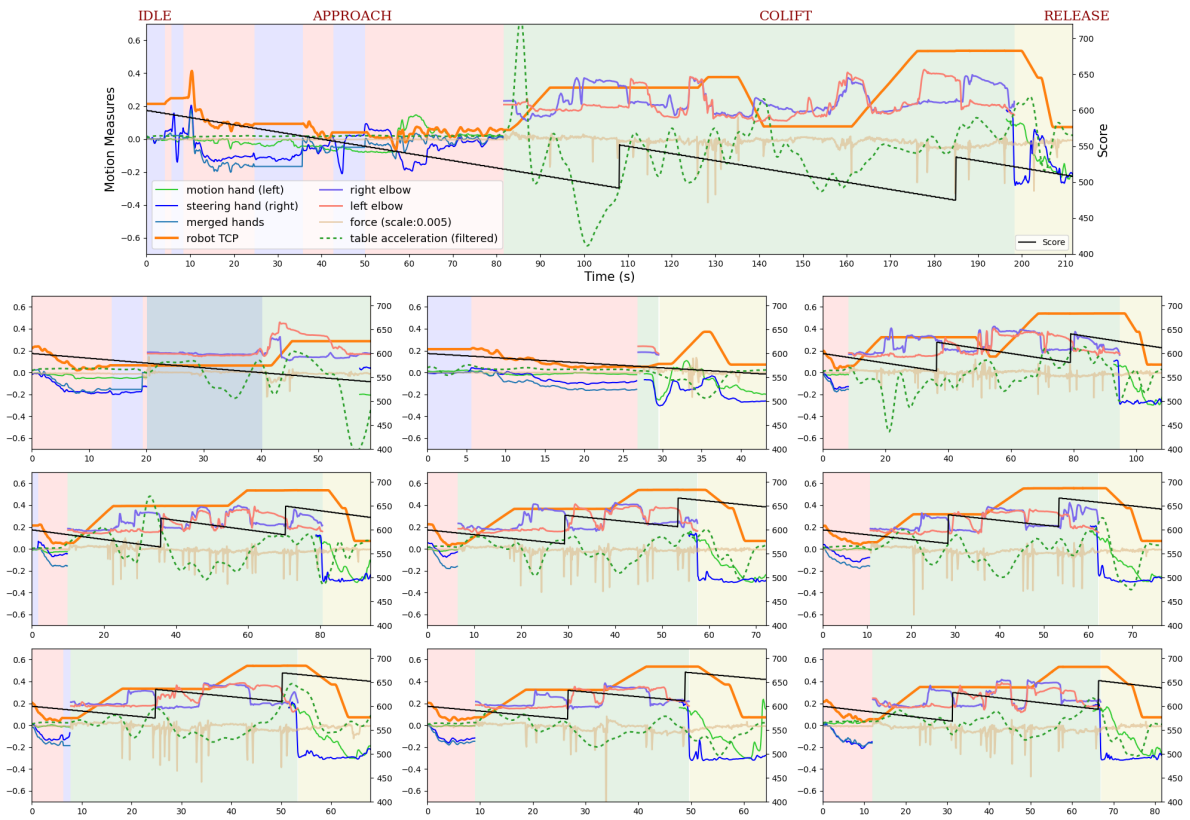


Fig. 6: User ID: 21984

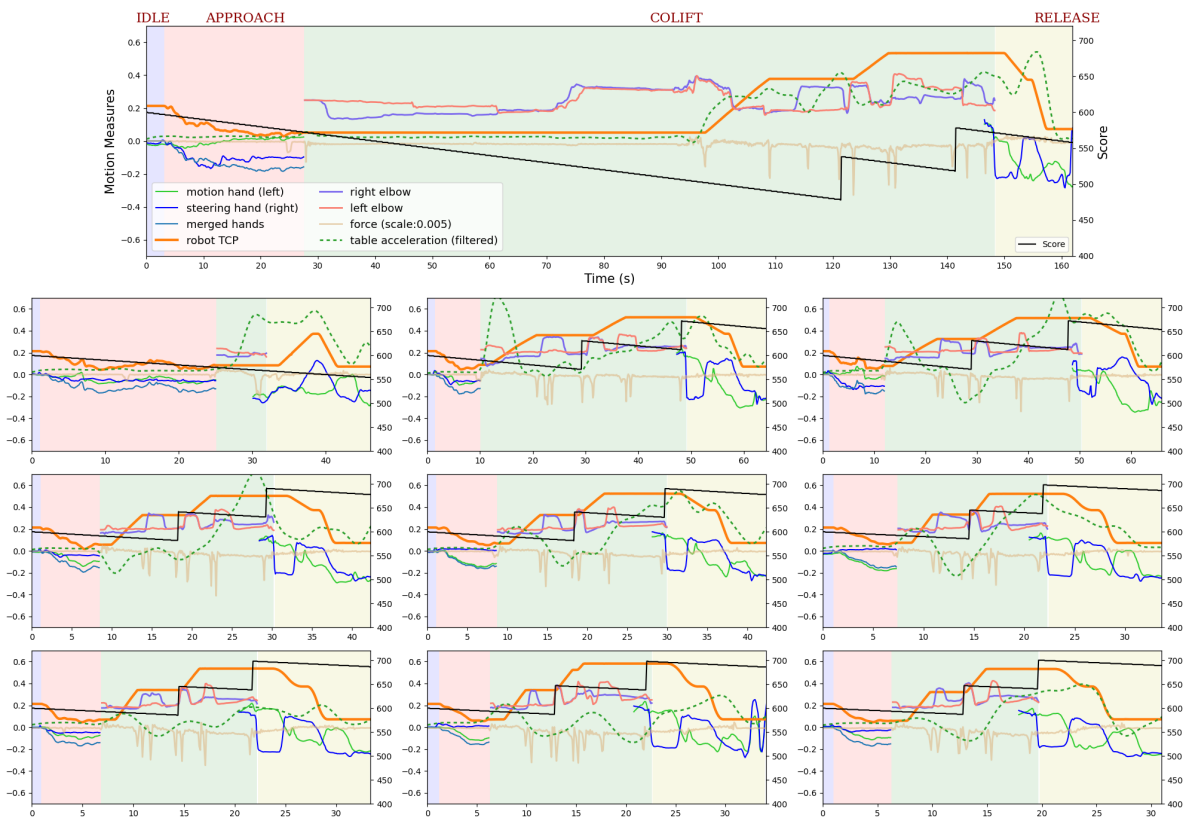


Fig. 7: User ID: 27968

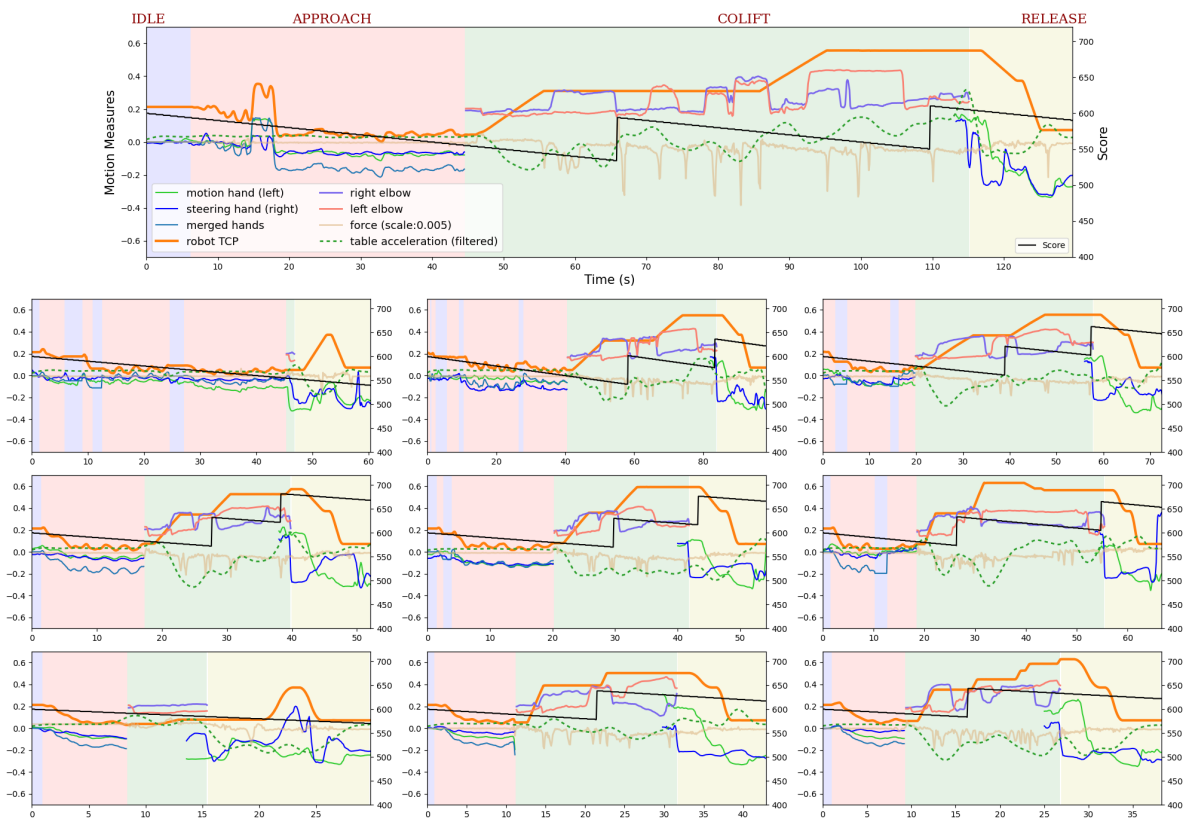


Fig. 8: User ID: 28373

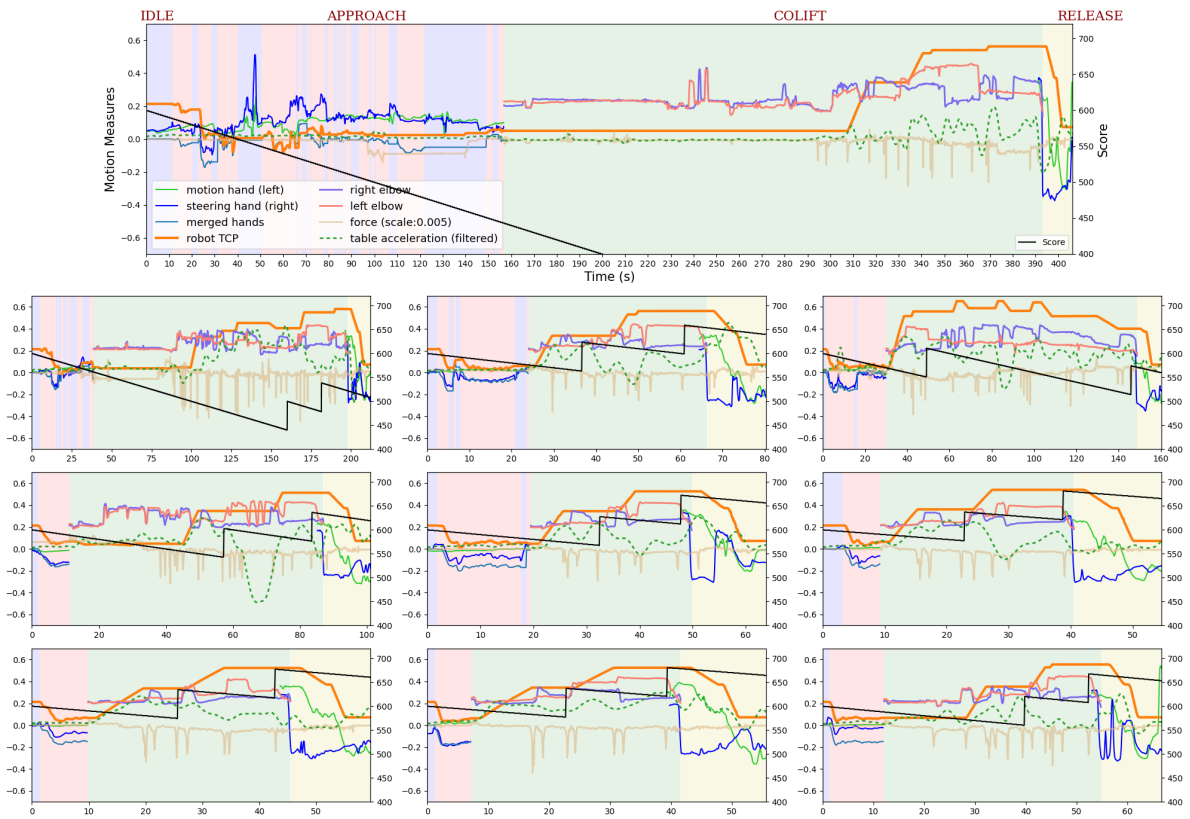


Fig. 9: User ID: 35764

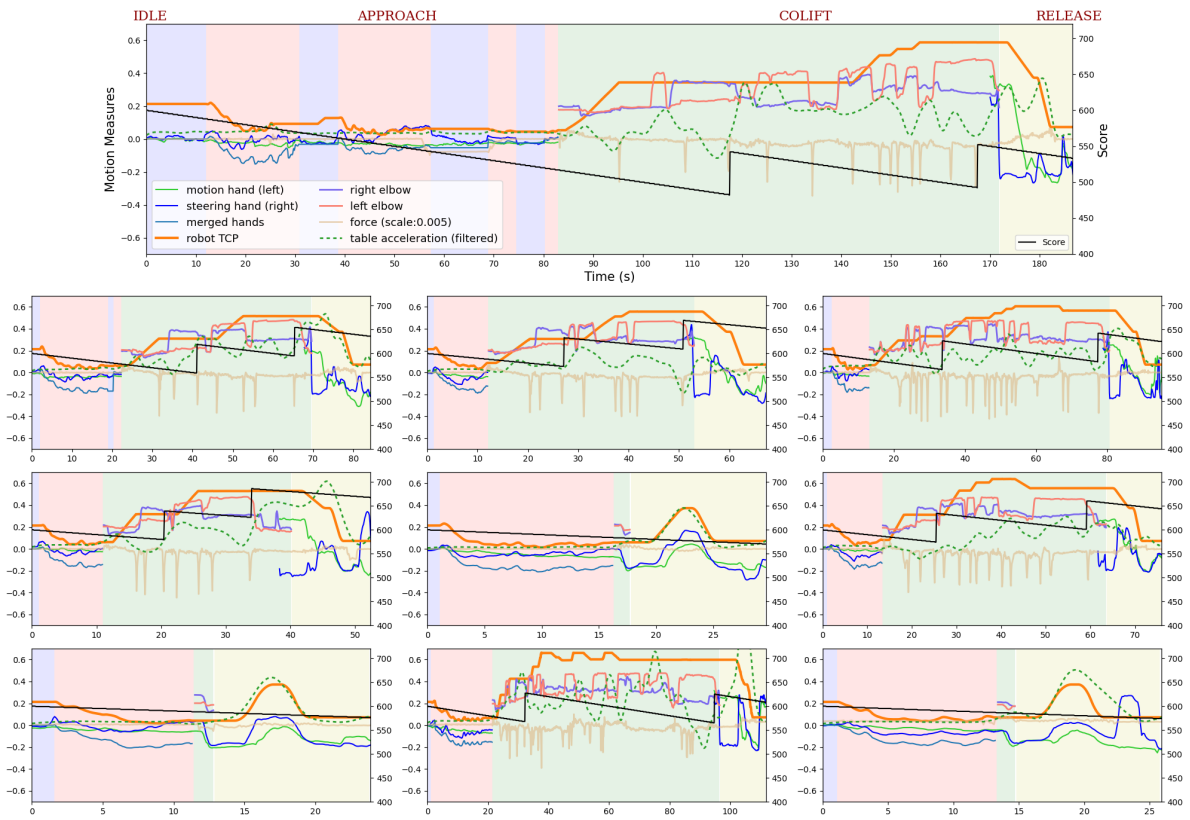


Fig. 10: User ID: 37446



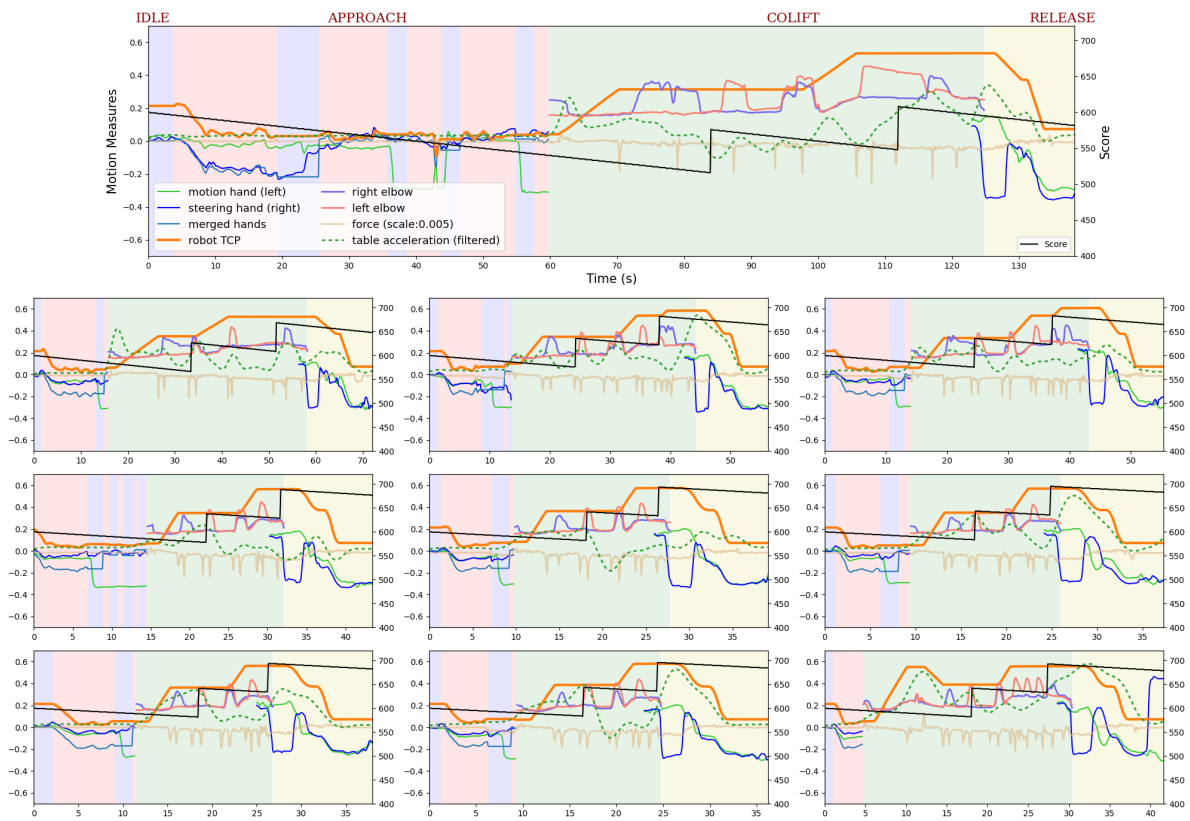


Fig. 11: User ID: 40002

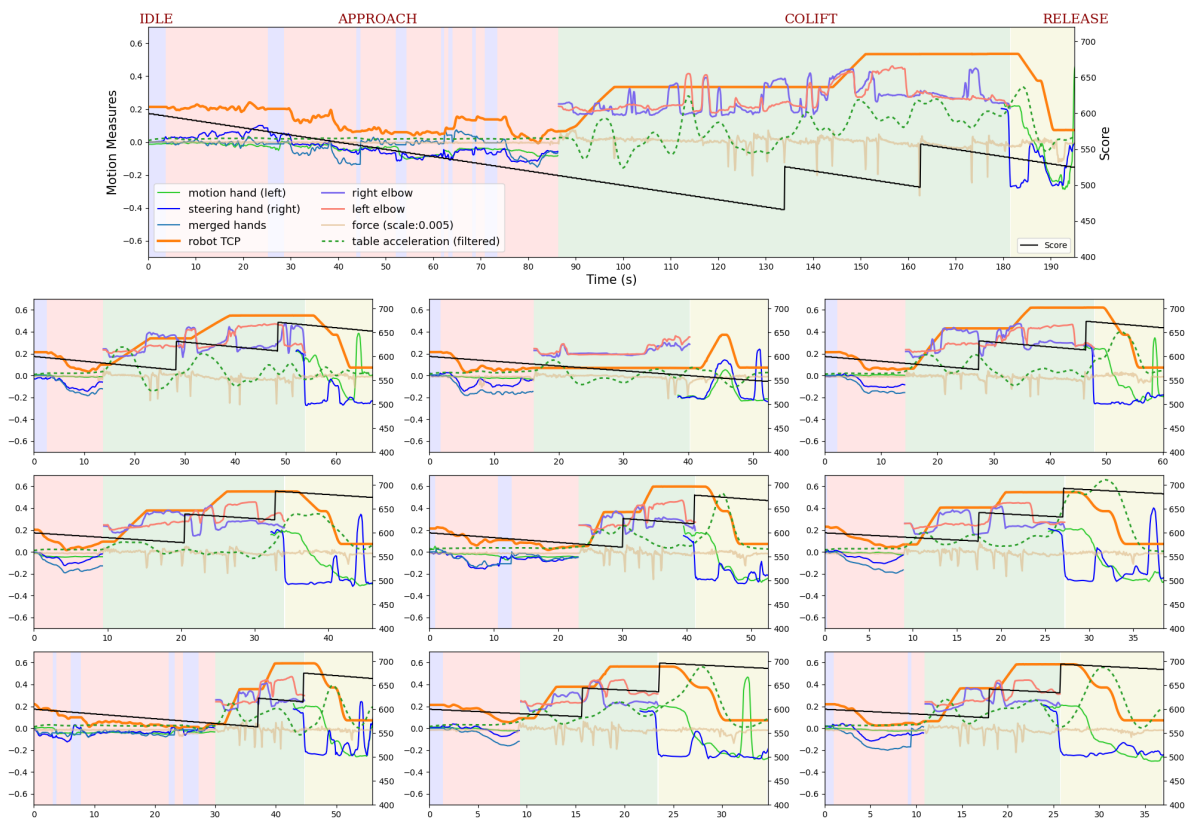


Fig. 12: User ID: 42761

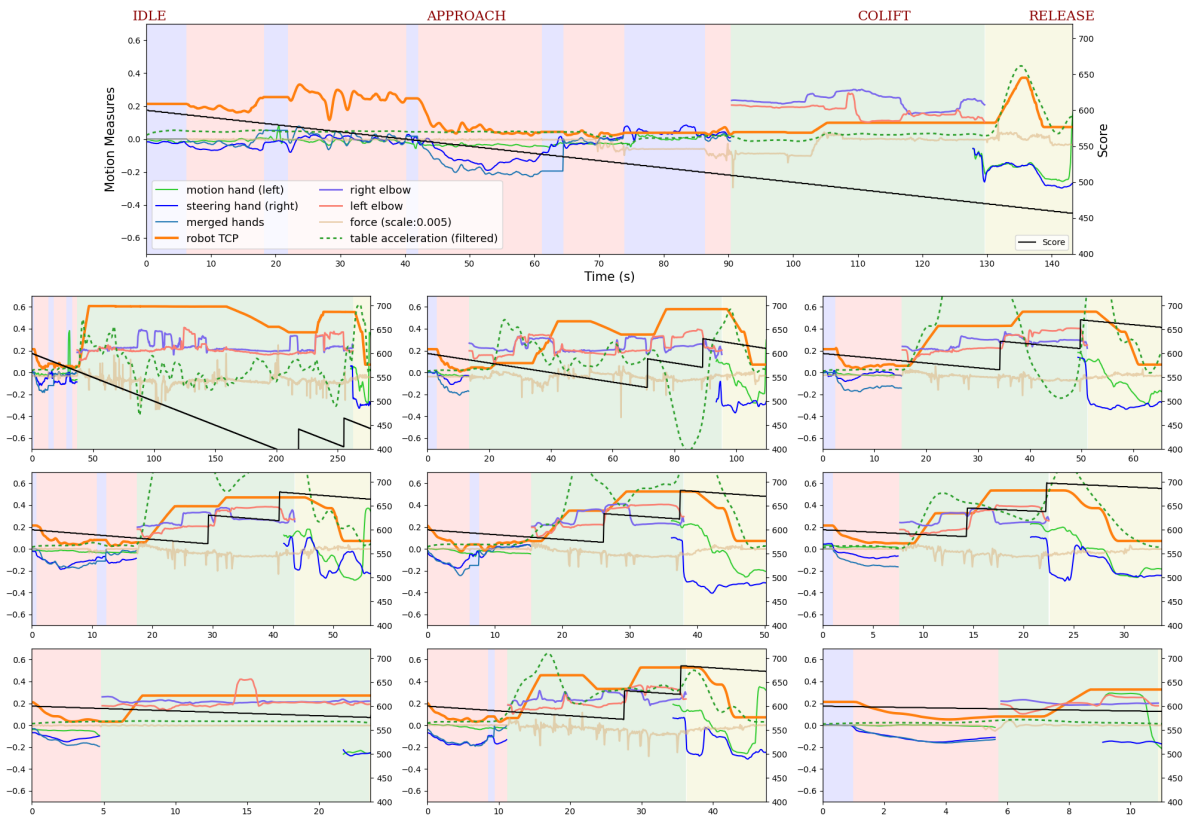


Fig. 13: User ID: 43702

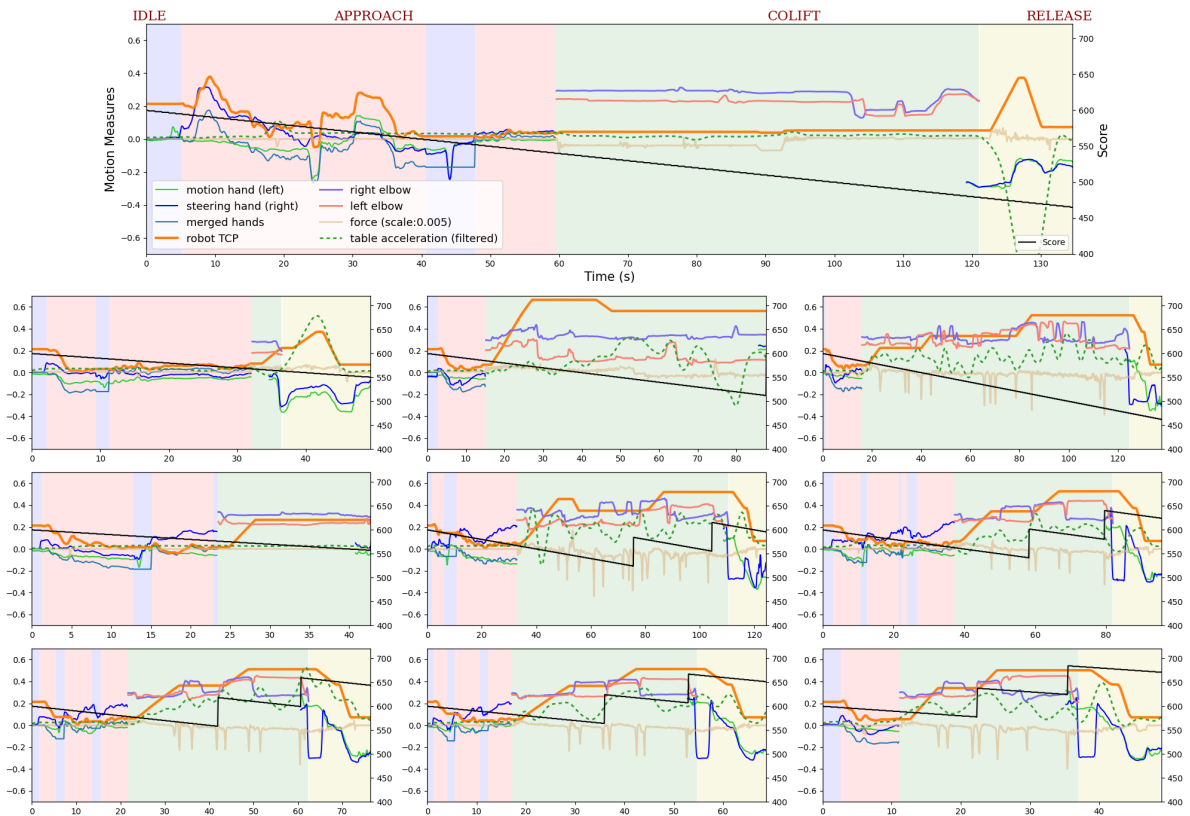


Fig. 14: User ID: 44035

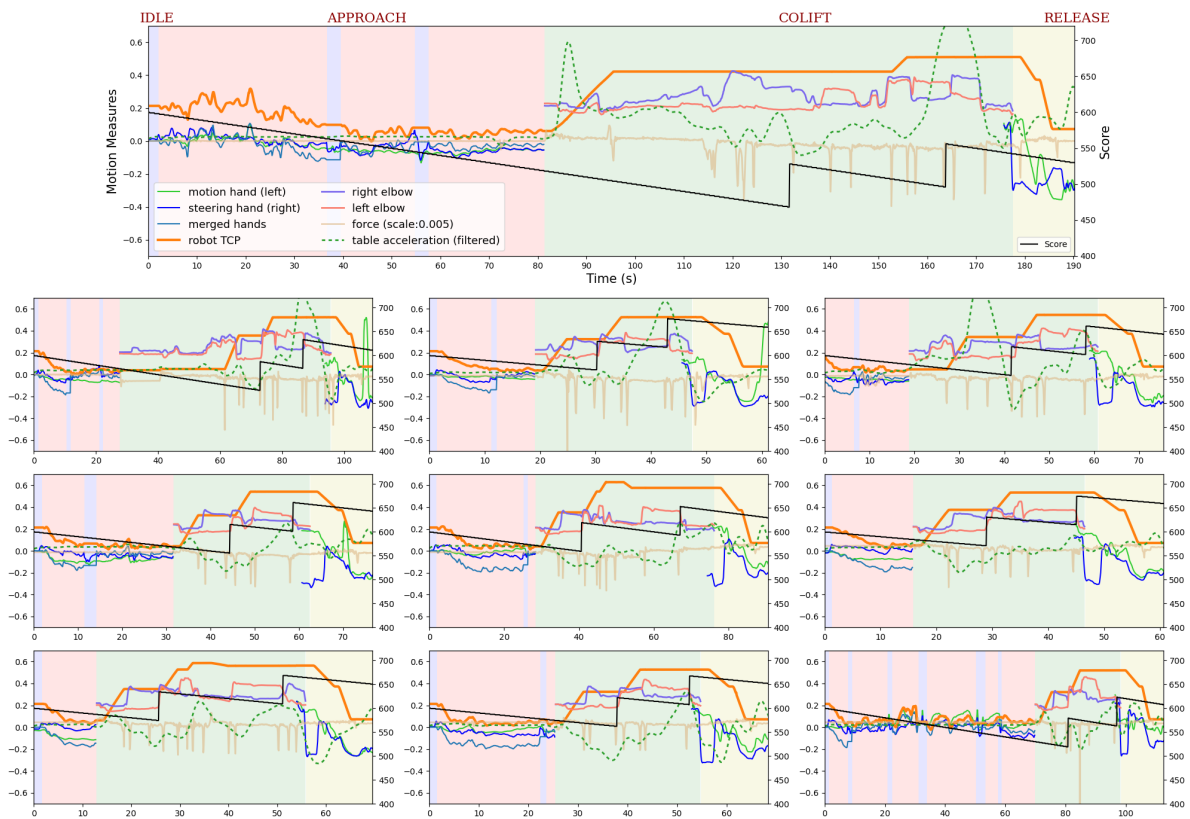


Fig. 15: User ID: 45345

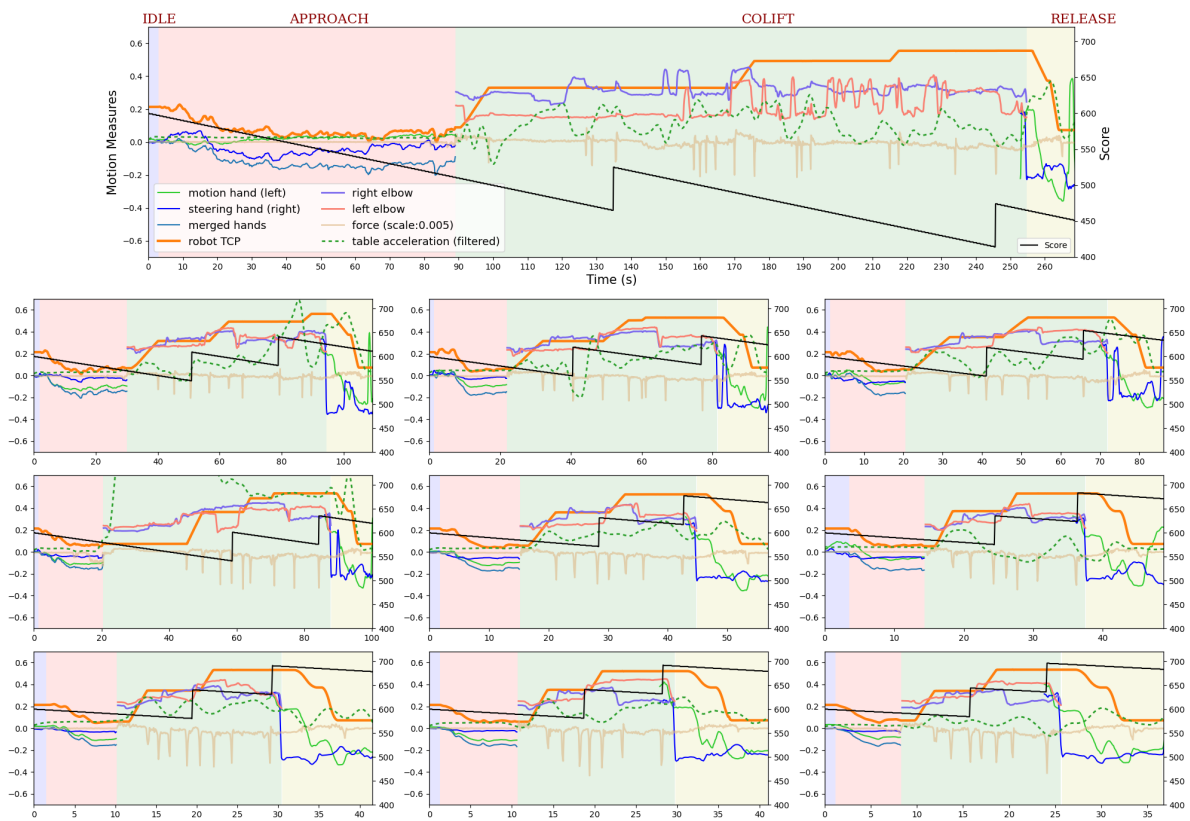


Fig. 16: User ID: 46173

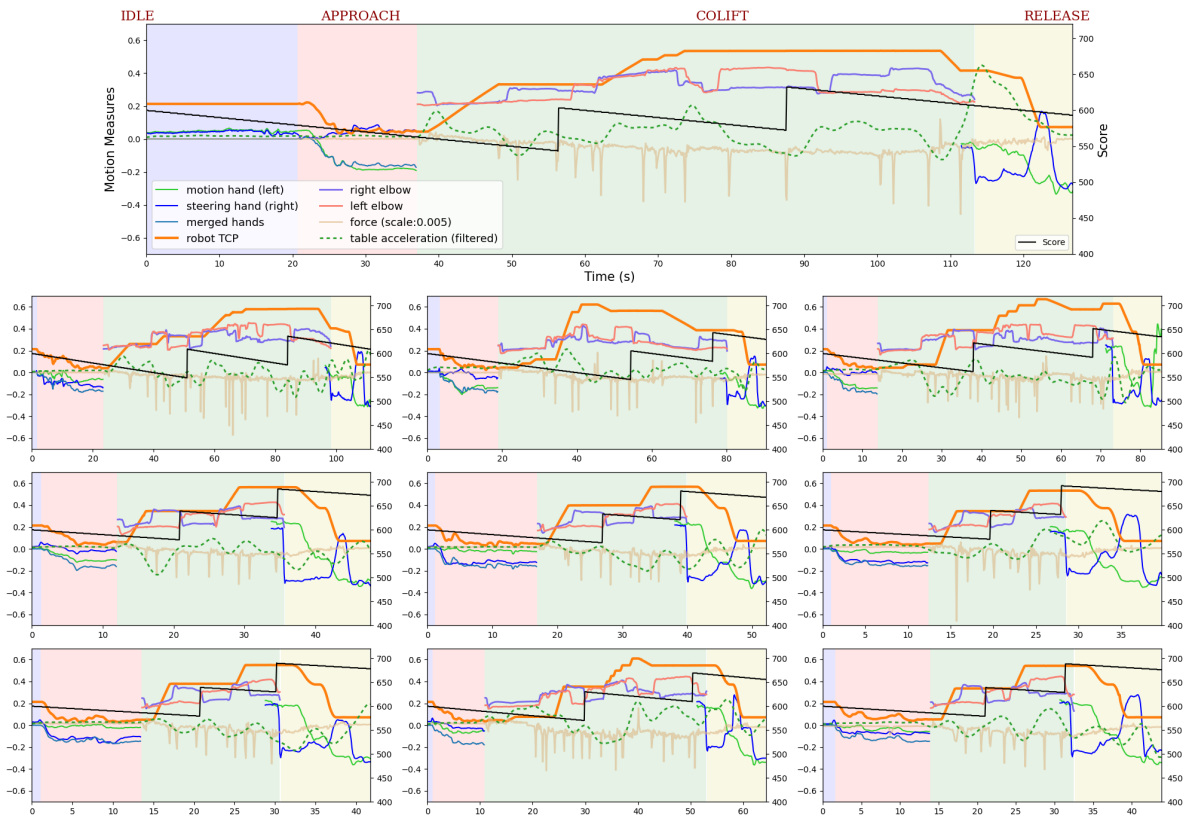


Fig. 17: User ID: 46904

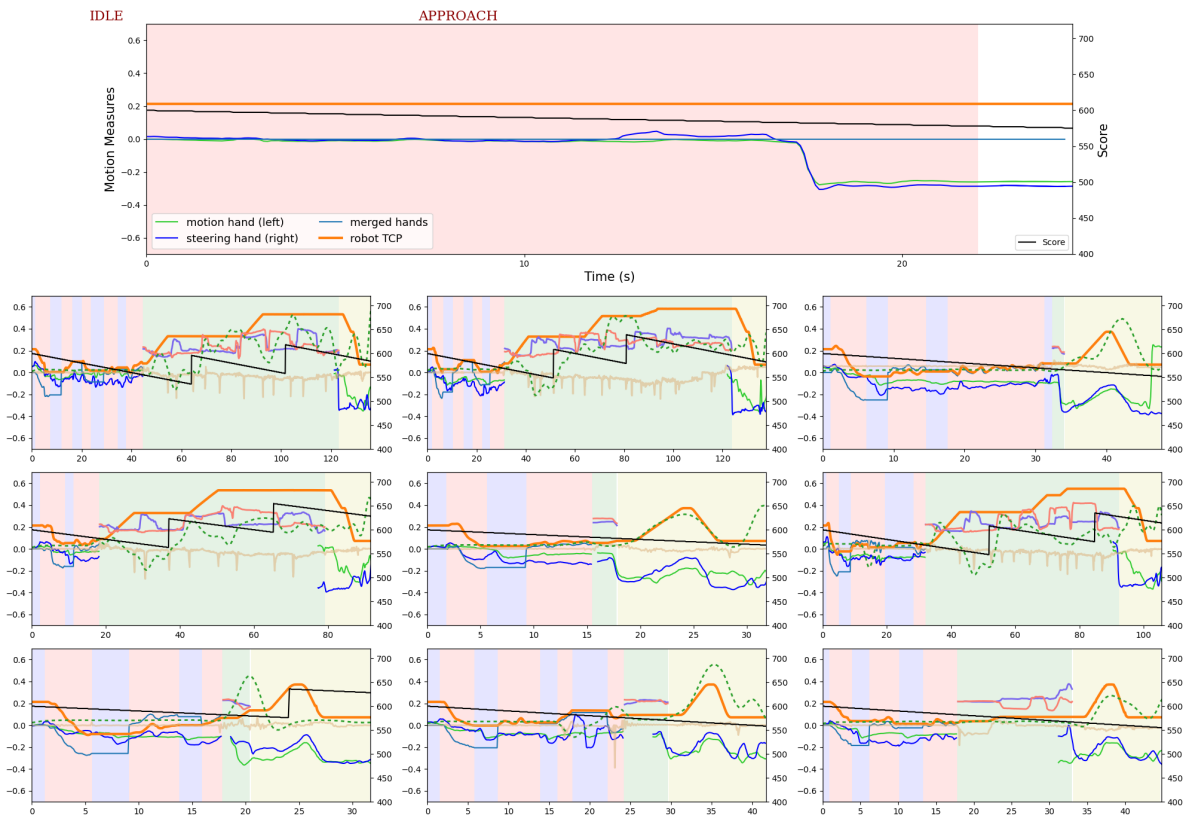


Fig. 18: User ID: 49345

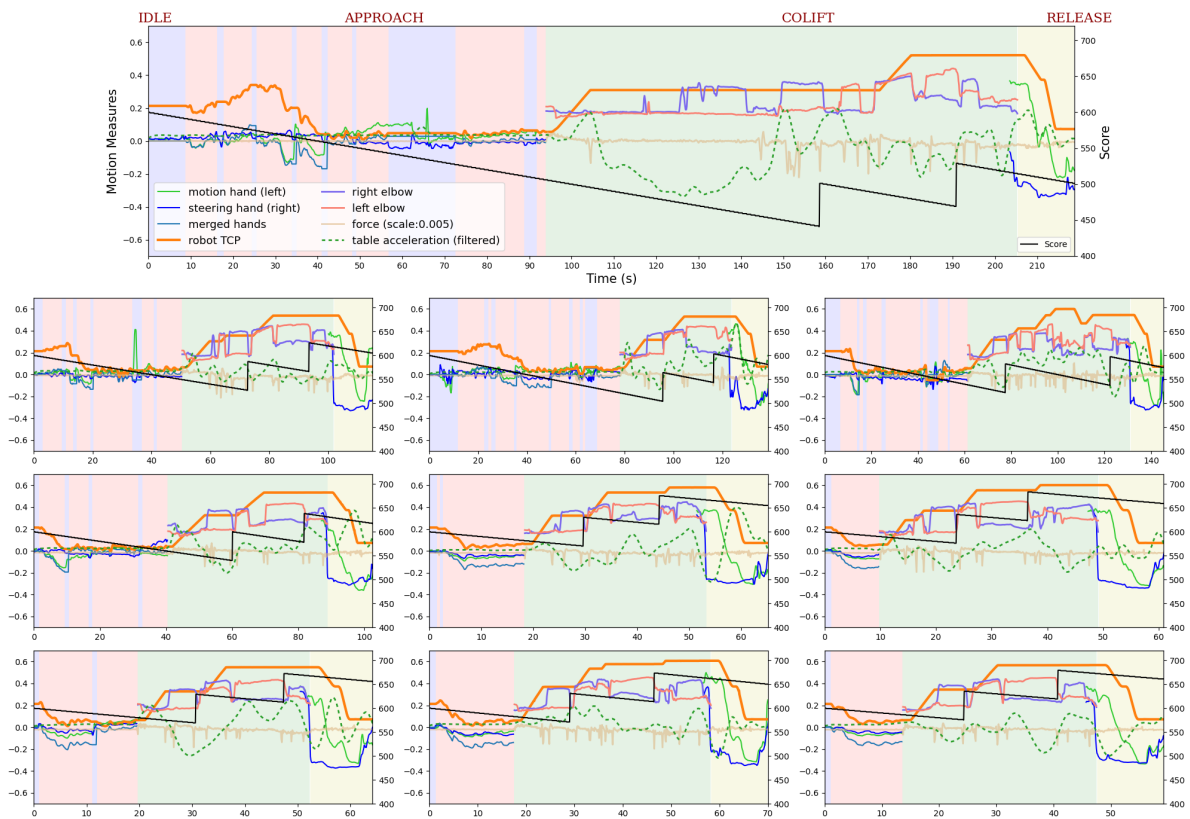


Fig. 19: User ID: 52870

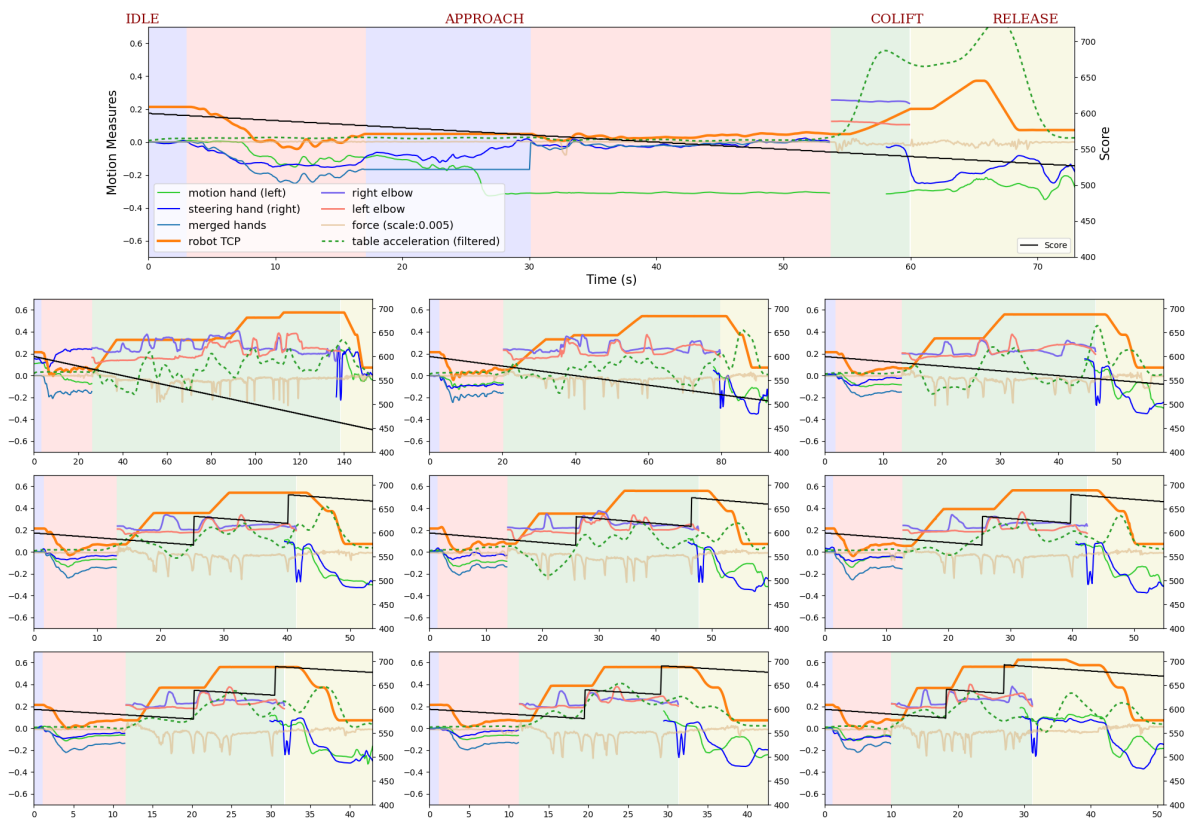


Fig. 20: User ID: 54264

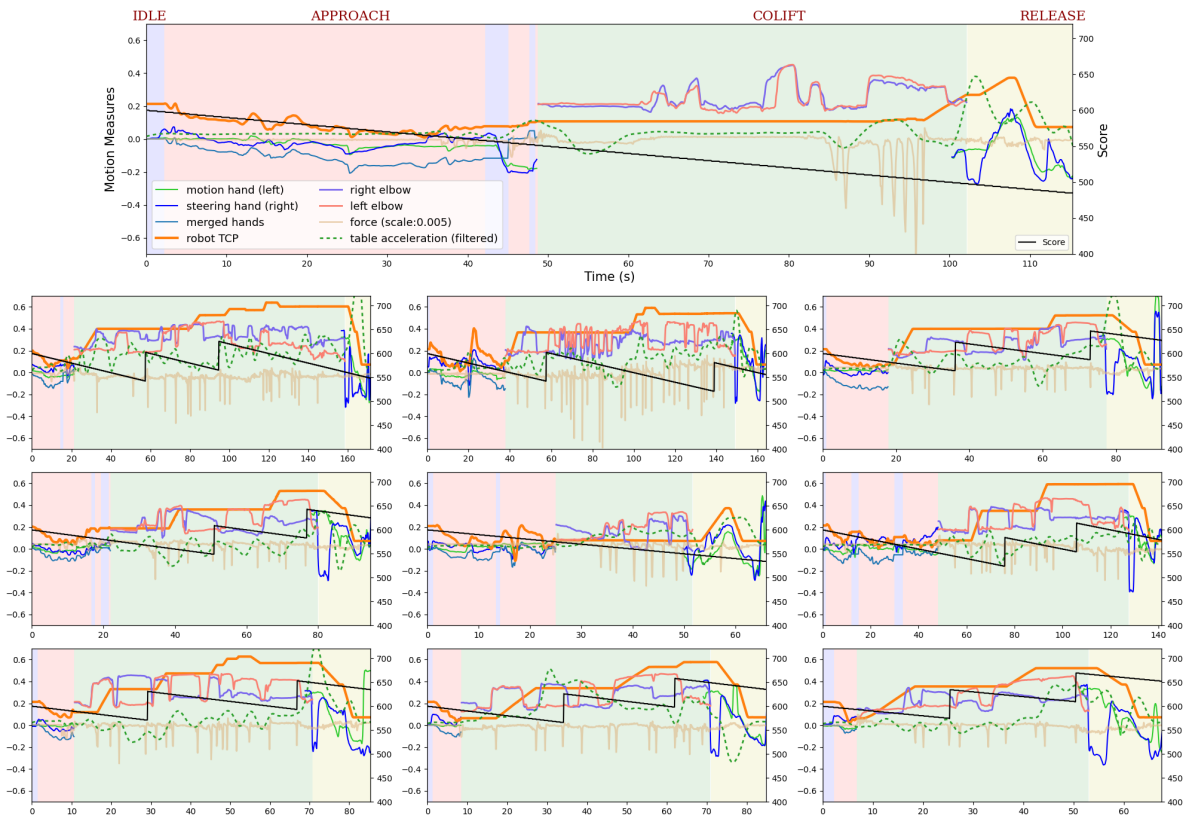


Fig. 21: User ID: 65093

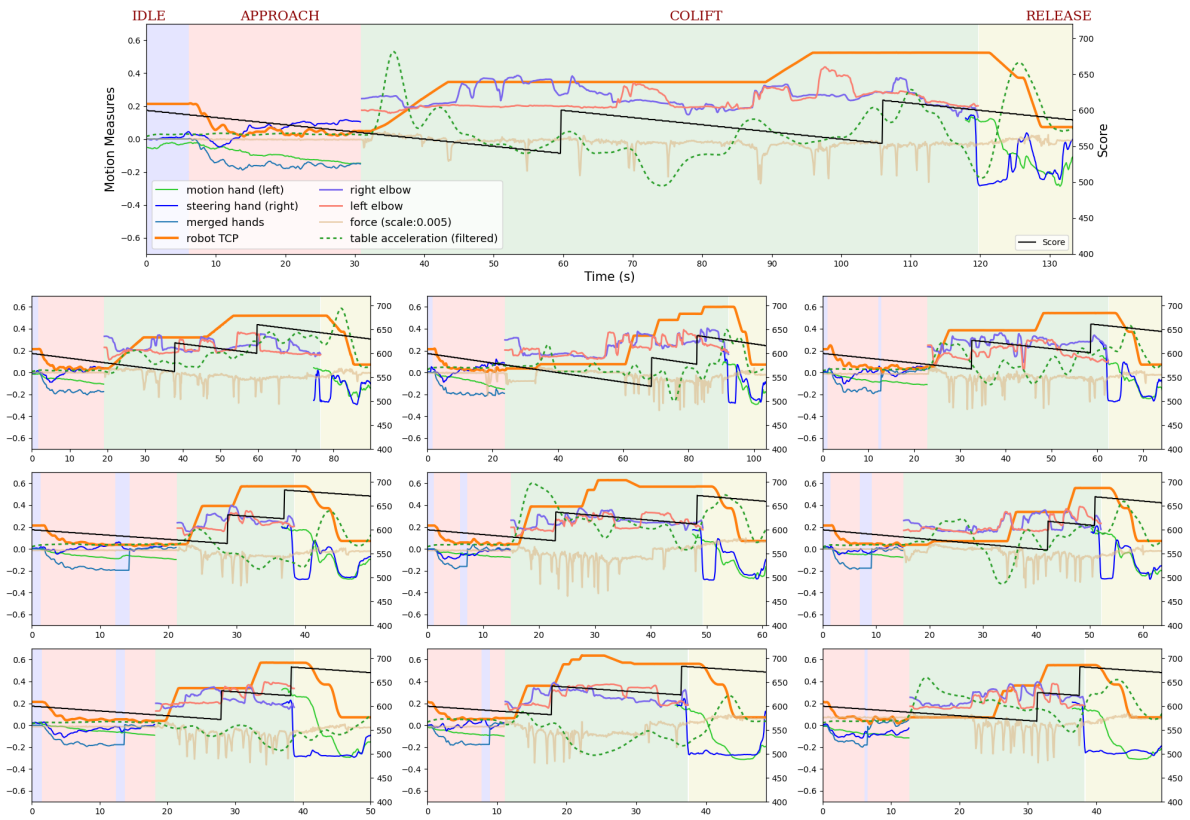


Fig. 22: User ID: 70285

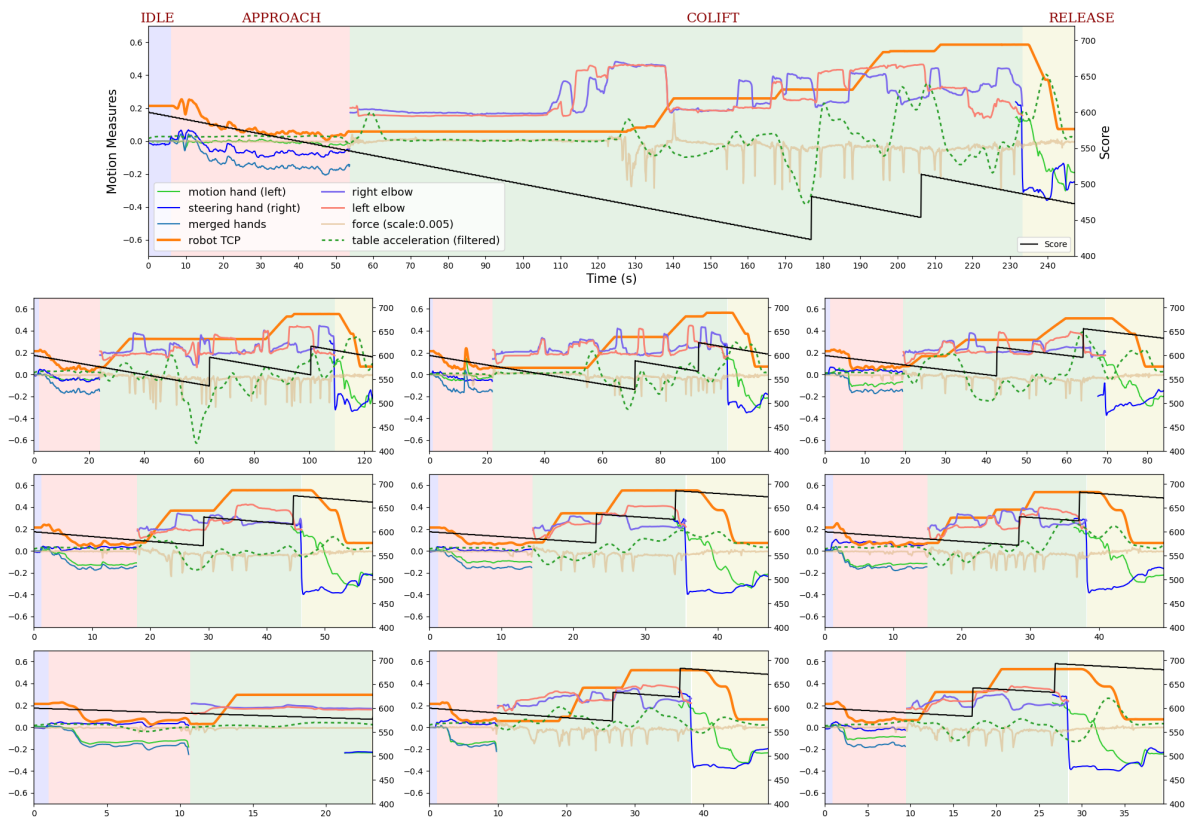


Fig. 23: User ID: 78604

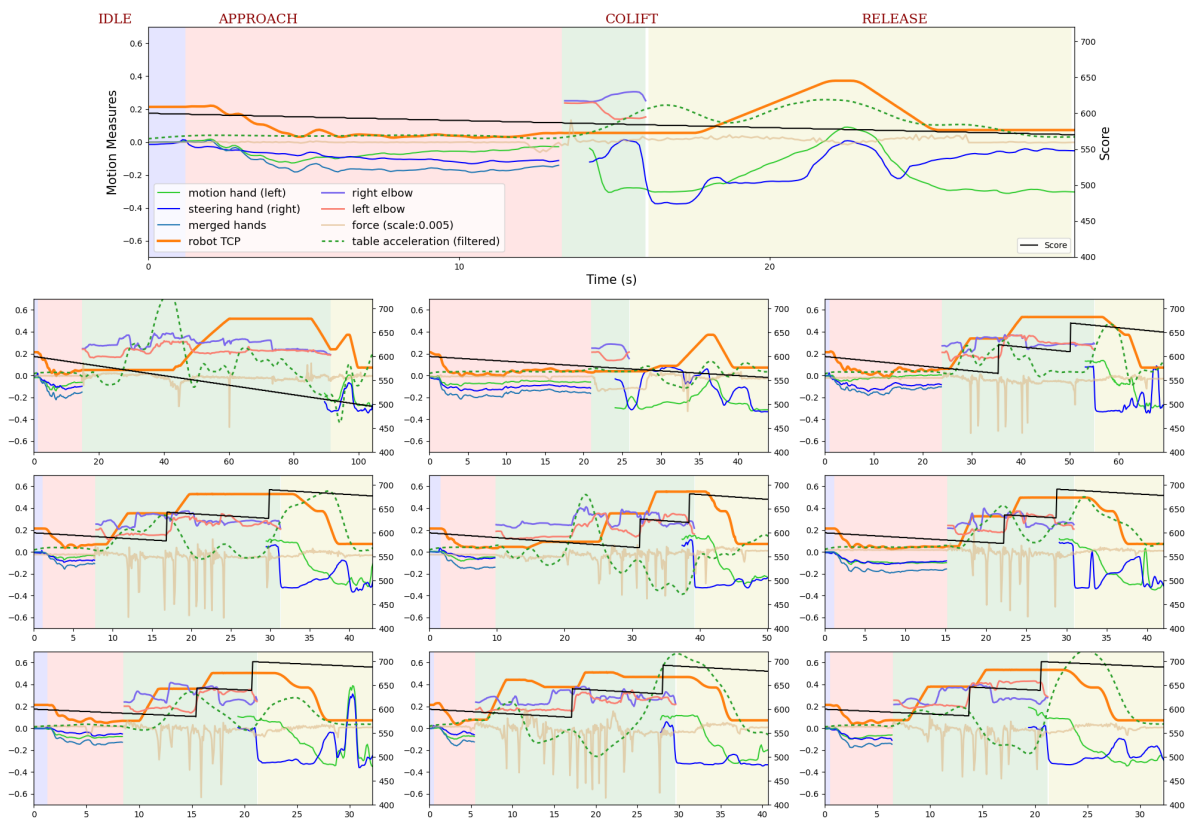


Fig. 24: User ID: 80266

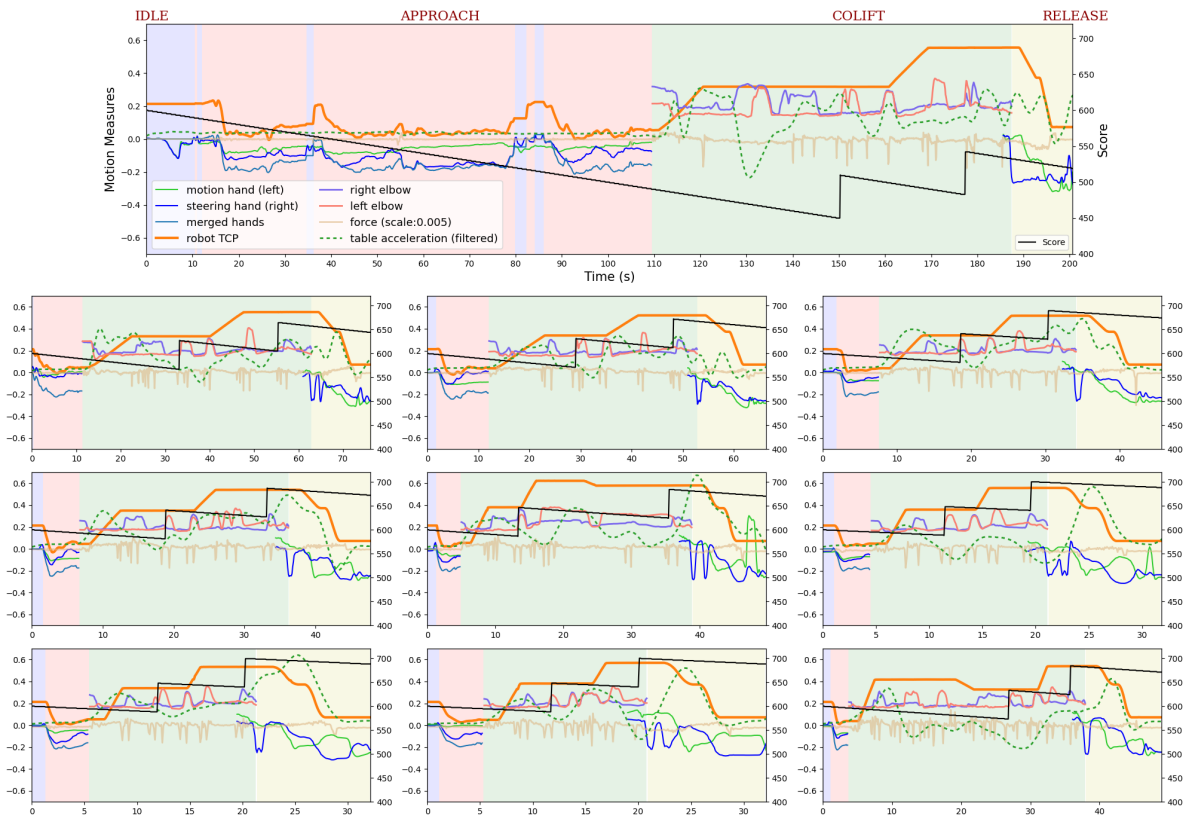


Fig. 25: User ID: 83972

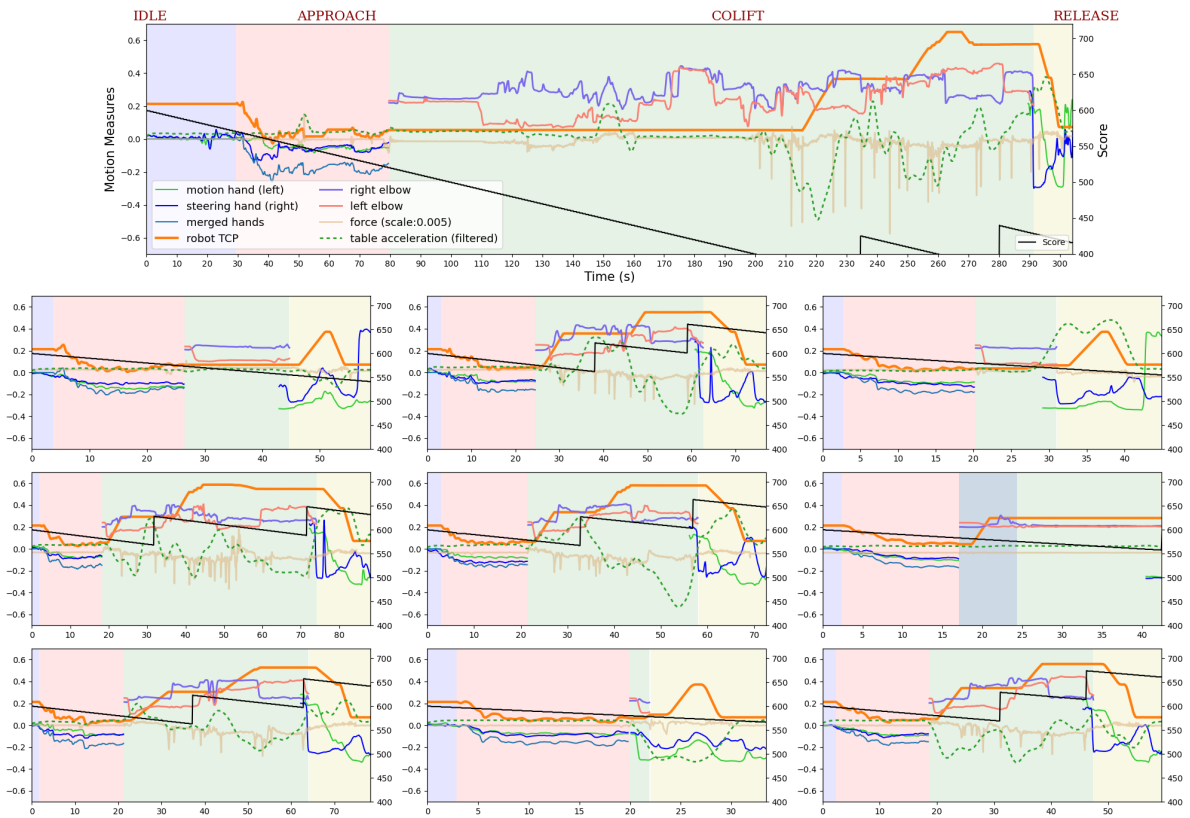


Fig. 26: User ID: 92463



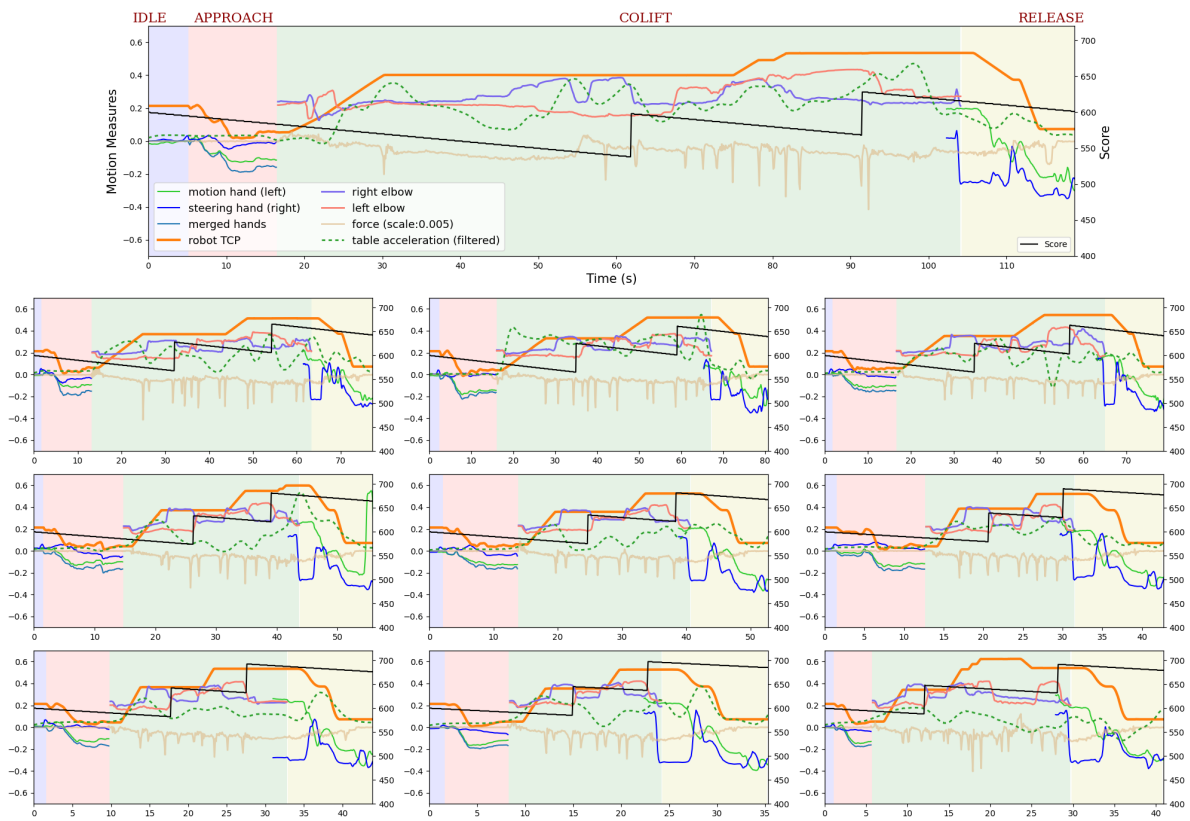


Fig. 27: User ID: 95467

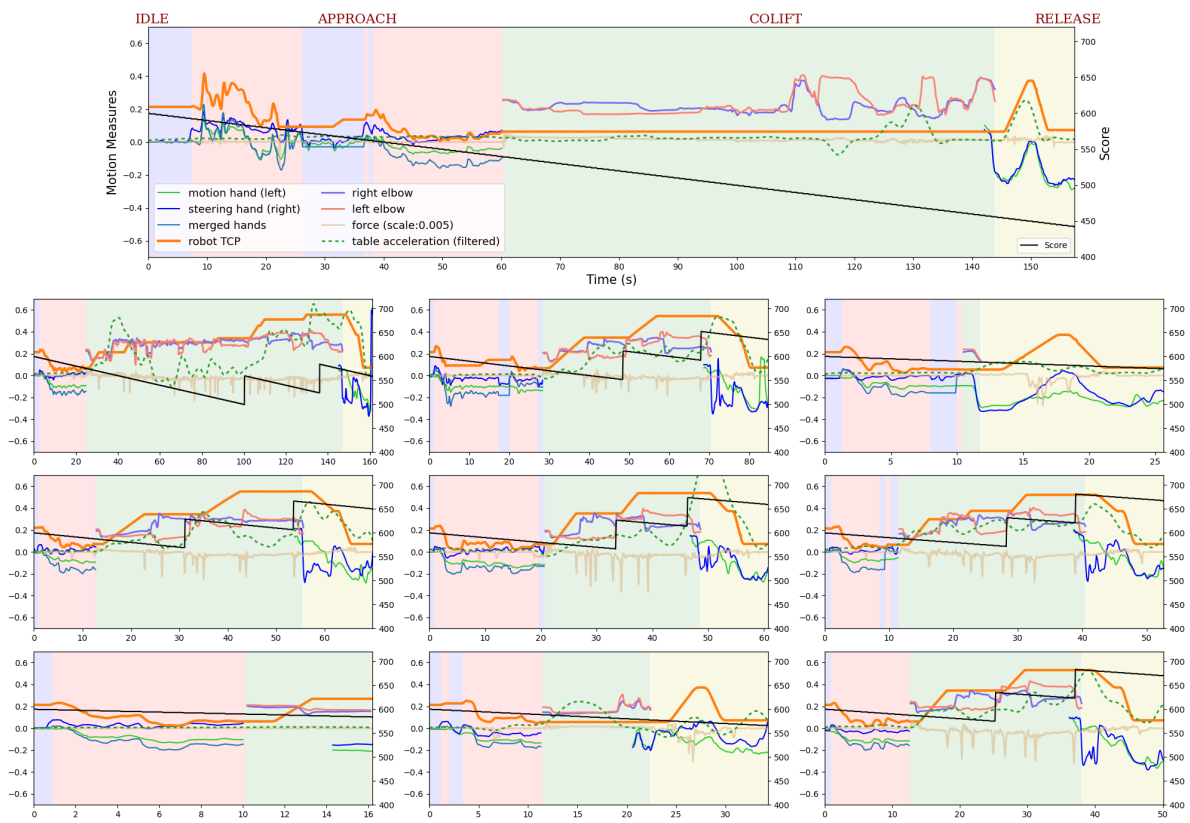


Fig. 28: User ID: 95532

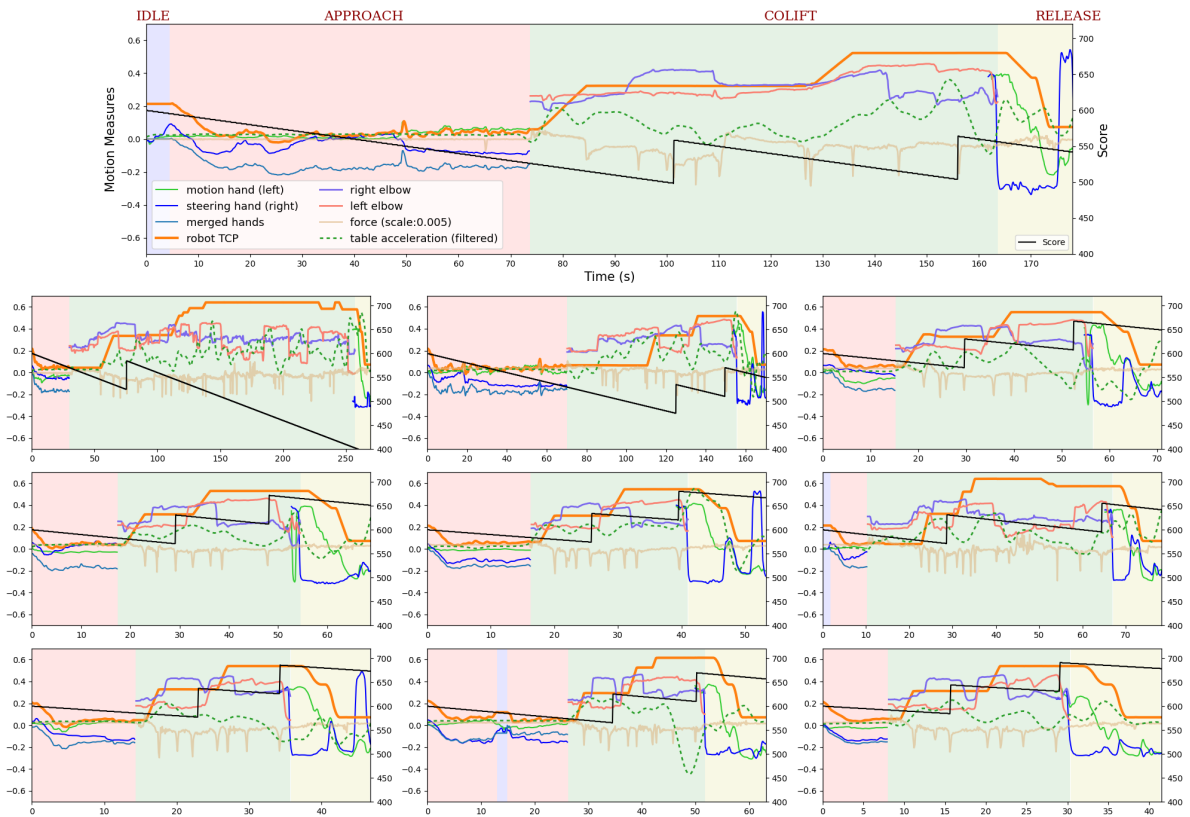


Fig. 29: User ID: 95691

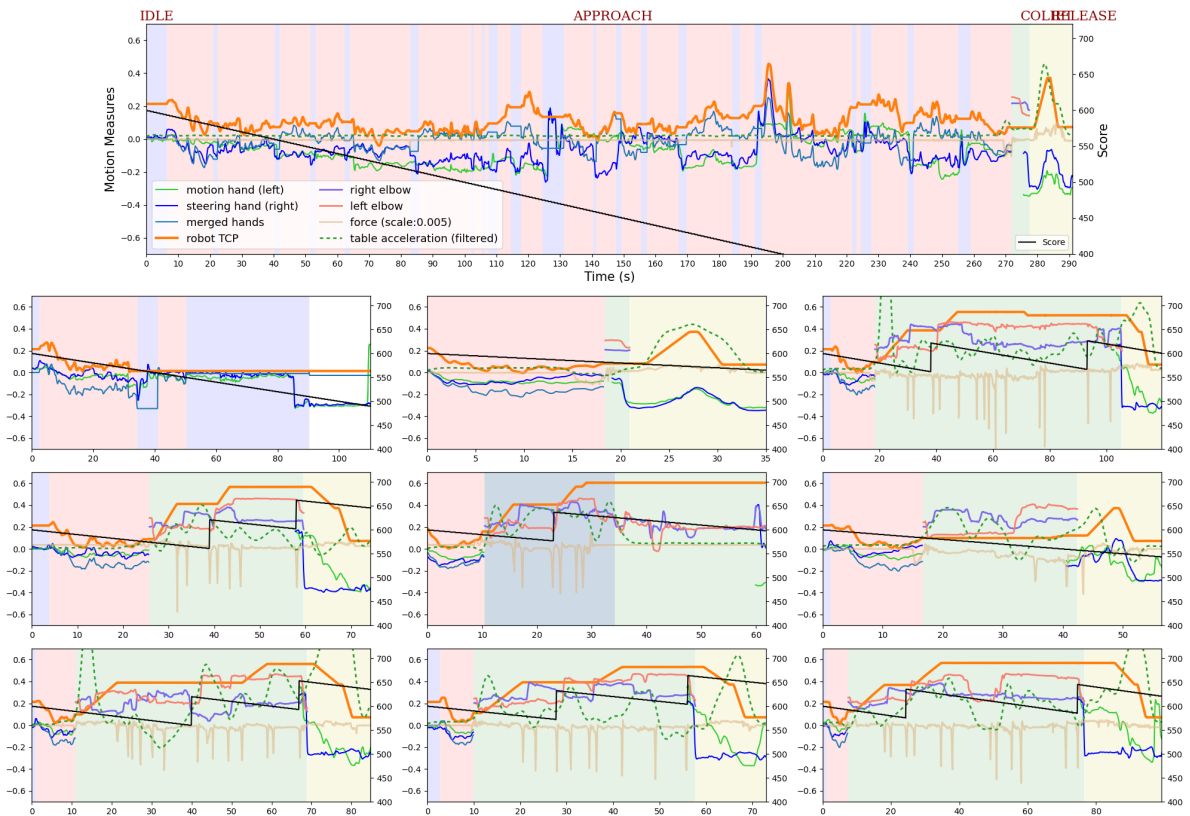


Fig. 30: User ID: 97647

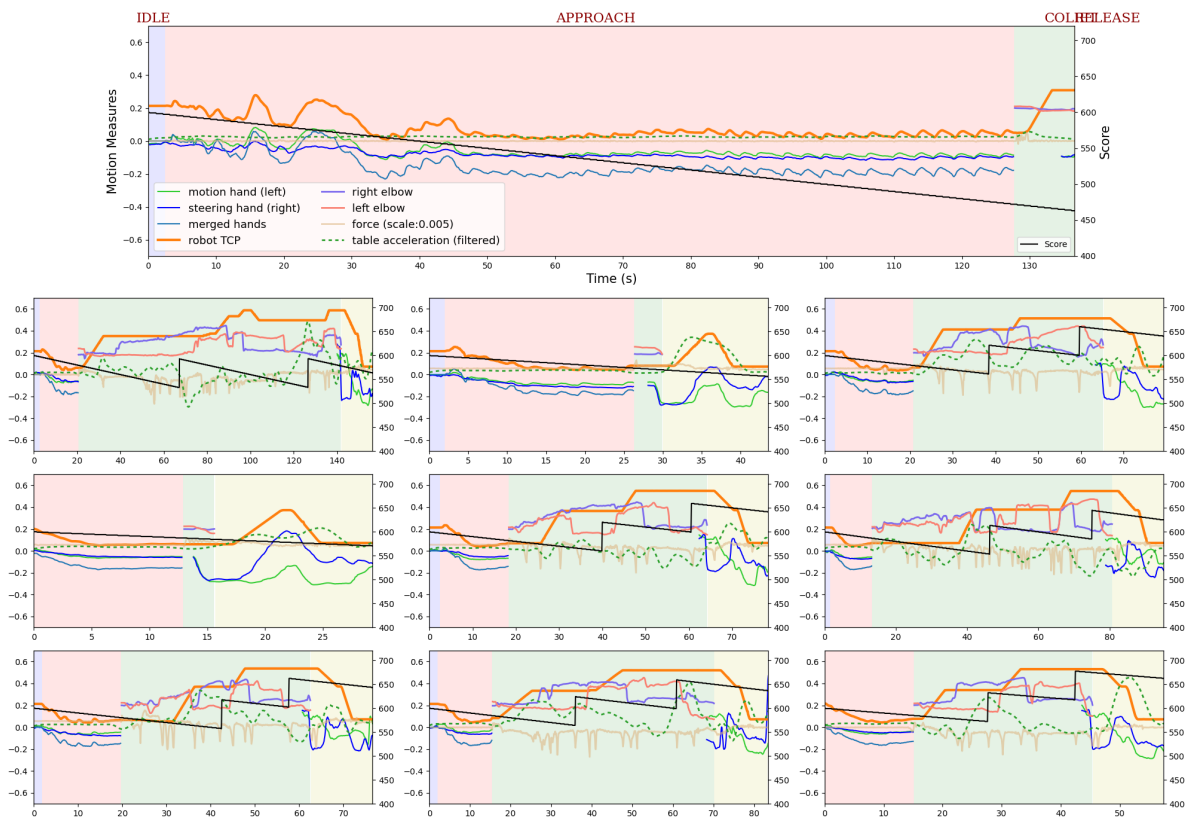


Fig. 31: User ID: 98684

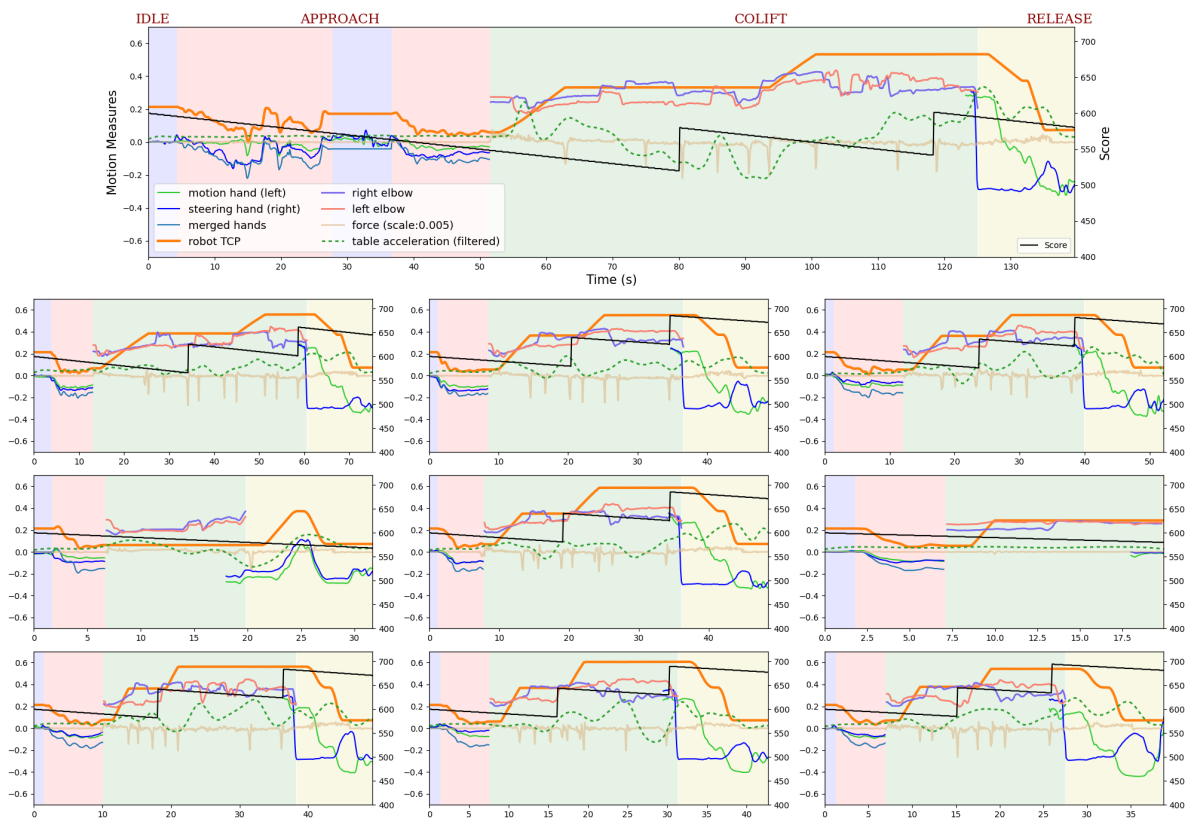


Fig. 32: User ID: 98871



